SunGrant
INITIATIVE

Science for Biomass Feedstock Production and Utilization

Proceedings of the 2012 Sun Grant National Conference

Volume 2

VOLUME 2

4. MODELING AND METRICS

1 BIOMASS CHARACTERIZATION

1.1 VARIATION IN BIOMASS COMPOSITION AND ENZYMATIC SACCHARIFICATION FOR BIOFUEL PRODUCTION AMONG CULTIVARS OF SHRUB WILLOW

Michelle J. Serapiglia[1], Michele Humiston[2], Haowen Xu[3], David Hogsett[3], Ramón Mira De Orduña[2], Arthur J. Stipanovic[4], Lawrence B. Smart[1,]*

Abstract

Variations in biomass composition based on genotypic differences or environmental influences are highly likely to have significant impact on the effectiveness of pretreatment and subsequent sugar release by enzymatic hydrolysis in the process of biochemical conversion to liquid biofuels. We have characterized extensive variation in biomass composition among willow genotypes produced by breeding and in response to site conditions. To evaluate whether the variation in composition affects conversion processes, biomass from 10 genetically diverse, high-yielding cultivars of shrub willow (*Salix* spp.) were pretreated with a hot-water process under two levels of severity, hydrolyzed using commercial enzyme formulations with cellulase and xylanase activities, and sugar release quantified by HPLC. Among the cultivars selected for analysis, cellulose content expressed as percent dry weight ranged from 39% to 45%, and lignin content ranged from 20% to 23%. Differences in the effectiveness of the pretreatment process were observed among the different willow genotypes. The two pretreatment levels impacted polysaccharide accessibility differently among the cultivars. At the high severity pretreatment the cultivar, 'SV1', was the least recalcitrant, with sugar release representing up to 60% of total biomass. Correlations with sugar release and cellulose composition along with ethanol yield were identified. Further analysis of biomass chemical composition and wood properties will be necessary to define traits for the breeding and selection of shrub willow cultivars that are less recalcitrant to conversion.

Keywords: ethanol, hydrolysis, willow

Introduction

In order to promote local production of renewable energy and reduce greenhouse gas emissions, there has been increased interest and demand for research and development of the production of transportation fuels, such as ethanol and butanol, from lignocellulosic biomass. Currently, more than 95% of the ethanol produced in the United States is derived from corn grain, diverting it from food and feed markets. Corn ethanol also has a marginal return on energy investment, estimated at 1:1.53 (Shapouri et al., 2002), which should be much better for conversion processes utilizing lignocellulosic biomass from perennial energy crops, including grasses and short-rotation woody crops, such as hybrid poplar (*Populus* spp.) and shrub willow (*Salix* spp.).

Yields of shrub willow are greater than 11 odt ha^{-1} yr^{-1} on marginal land not suitable for conventional food crops, making it a good resource as a dedicated energy crop (Volk et al., 2011). With high genetic diversity, there is potential for long-term genetic improvement of willow

[1] *Department of Horticulture*

[2] *Food Science and Technology, Cornell University, New York State Agricultural Experiment Station, NY*

[3] *Mascoma Corporation, NH*

[4] *Department of Chemistry, SUNY College of Environmental Science and Forestry, NY*

* *Corresponding author*

feedstock crops. It has been shown that shrub willow have wide phenotypic variation for biomass composition (Serapiglia et al., 2009), but it is not known how this relates to sugar release and biofuel conversion efficiency.

Evaluation of how biomass compositional characteristics will impact sugar release from enzymatic saccharification and subsequent conversion to ethanol will be influential in the future selection and breeding of shrub willow for improved conversion efficiency. The goal of this project is to determine if biomass compositional characteristics in genotypes of shrub willow affect the release of sugars from enzymatic saccharification and the conversion efficiency to ethanol.

Materials and Methods

Source Material and Biomass Collection

Three-year post coppice willow stems from 10 cultivars of willow planted in the 2006 Yield Trial in Constableville, NY were harvested in December 2009 (Table 1). Whole stems (with bark) were chipped and dried to a constant weight at 60ºC and ground in a Wiley mill through a 20-mesh screen. Further fine milling down to a 0.5 mm particle size was performed using an analytical mill (MF 10, IKA, Wilmington, NC).

Table 1. Shrub willow genotypes studied in the 2006 Constableville Yield Trial

Clone ID/Cultivar epithet	**Species/Pedigree**	**Source**
‘SV1’	*Salix* x *dasyclados*	University of Toronto
‘SX61’	*S. sachalinensis*	University of Toronto
‘SX64’	*S. miyabeana*	University of Toronto
00X-026-082	*S. eriocephala*	Bred in 2000
‘Fish Creek’	*S. purpurea*	Bred in 1998
‘Millbrook’	*S. purpurea* x *S. miyabeana*	Bred in 1999
‘Canastota’	*S. sachalinensis* x *S. miyabeana*	Bred in 1999
‘Preble’	*S. viminalis* x (*S. sachalinensis* x *S. miyabeana*)	Bred in 2001
‘Fabius’	*S. viminalis* x *S. miyabeana*	Bred in 1999
‘Owasco’	*S. viminalis* x *S. miyabeana*	Bred in 1999

High-resolution Thermogravimetric Analysis

All willow samples were analyzed using a thermogravimetric analyzer (model 2950, TA Instruments, New Castle, DE) with associated software (TA Universal Analysis 2000) according to Serapiglia et al (2009). Each biomass sample was analyzed with three instrumental replicates to determine cellulose, hemicellulose, lignin, and ash content expressed as percent of dry biomass.

Hot-Water Pretreatment

The willow biomass was pretreated in 316 stainless steel tube reactors fitted with 316 stainless steel caps (Swaglok®) to prevent evaporation of the liquid fraction at a solid loading of 20% (w/w) with water. All samples were pretreated at 200°C in a fluidized sand bath (Techne ® Precision) with two different residence times of 5 and 9 min, allowing for 5 min of heat-up time. The pretreatments were conducted at a logR_0 severity of 3.6 and 3.9 (Eq. 1). Severity was defined as (Eq. 1)

Equation 1. $R_0 = t \cdot e^{\frac{T-100}{14.75}}$

where t is in minutes and T in degrees Celsius.

Enzymatic Hydrolysis

Enzymatic hydrolysis was performed according to an established NREL protocol (Selig et al., 2008). Wet biomass equivalent to 200 mg dry was used. The following was added to all samples: 5 mL of 0.1M sodium citrate buffer (pH 5), 500 µL of 100 µg mL^{-1} natamycin, 100 µL of Cellic® CTec2, and 20 µL HTec2 from Novozymes (Wilmington, DE). All samples were brought to 10 mL total volume using deionized water, then incubated in a water bath at 50ºC for 48 h with shaking at 200 RPM.

Sugar quantification

All monomeric sugars were quantified by HPLC using a Shimadzu Prominence System (Columbia, MD) with a RID-10A refractive index detector. Following filtration (0.2 µm nylon membrane, Millipore), a 20 µL sample was injected and separated using a mobile phase of water and an Aminex HPX-87P column (BioRad, Hercules, CA) preceded by a de-ashing pre-column (BioRad, Hercules, CA) at 85°C.

Ethanol Production by SSF

Fermentation testing was performed in a simultaneous saccharification and fermentation (SSF) process on the pretreated biomass at a 20 mL scale in sealed serum bottles using unwashed, never-dried pretreated material at a final concentration of 50 g L^{-1} (oven dried basis). Hydrolysis was accomplished through the addition of 60 µL Cellic ® CTec2 and 6 µL HTec2 from Novozymes (Wilmington, DE). An engineered, xylose-fermenting strain of *S. cerevisiae* (Mascoma Corporation, Lebanon NH) was inoculated at 0.5 g L^{-1} dry cell weight (DCW) and the SSF was carried out at 35˚C with moderate shaking. A medium comprised of 12 g L^{-1} corn steep liquor and 0.5 g L^{-1} diammonium phosphate, buffered by 50 mM acetate and adjusted to an initial pH of 5.5, was used. Penicillin G was added at a final concentration of 30 µg mL^{-1} to inhibit potential bacterial contaminants. After 73 and 120 h of fermentation, samples were withdrawn, filtered, acidified and analyzed via HPLC for ethanol, organic acids and monomer sugars using the Aminex HPX-87H column (Sluiter et al., 2008).

Results

Cellulose, hemicellulose, lignin, and ash content as percent of the total biomass were significantly different ($p < 0.05$) among the genotypes examined (Fig. 1). Cellulose had the widest variation among the genotypes ranging from 38 to 45%. 'SV1' had the greatest cellulose content with low lignin, hemicellulose, and ash content. Following pretreatment with the higher severity of 3.9, the greatest sugar yield was observed for 'SV1' (Fig. 2). Sugar released from the two different pretreatment severities varied depending upon cultivar. Following the 3.6 severity pretreatment, 'Fabius' released the largest amount of sugar and only marginally greater sugar release was observed when the pretreatment severity was increased to 3.9. For 'SX61', there was no significant difference between the two pretreatments. A correlation between cellulose content and the amount of sugar released from the higher severity pretreatment was identified with a correlation coefficient of 0.60 and a p-value of 0.06 (Fig. 3). Ethanol yield correlated with sugar released from the higher severity pretreatment with a correlation coefficient of 0.74 ($p = 0.014$).

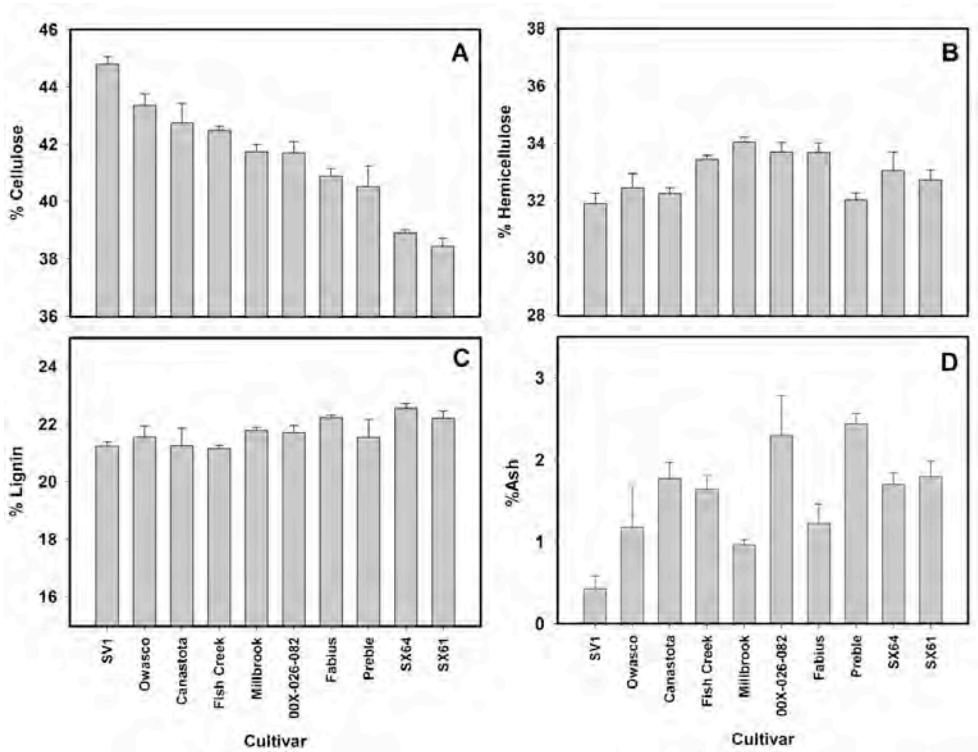

Figure 1. Willow composition as percent dry weight (mean ± SE) at harvest after three years of growth at Constableville, NY as determined by high-resolution thermogravimetric analysis. a cellulose, b hemicellulose, c lignin, and d ash

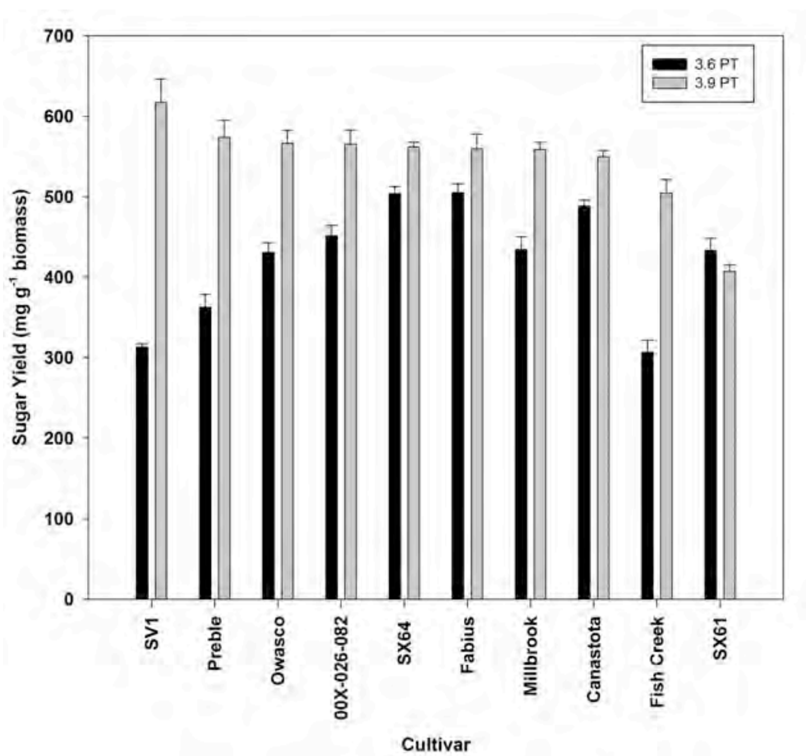

Figure 2. Total sugar released after enzymatic hydrolysis of pretreated biomass (mean ± SE)

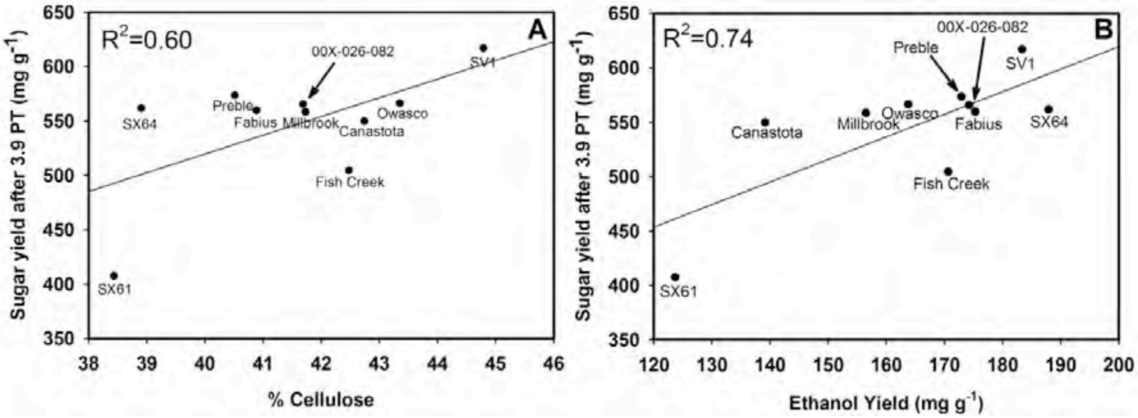

Figure 3. Correlations observed with sugar release following the hot-water pretreatment with a log R_0 severity of 3.9. a total sugar yield vs. % cellulose, b total sugar yield vs ethanol yield.

Discussion

This study examined selected shrub willow genotypes representing significant variation in biomass composition to identify relationships between the compositional differences and sugar release following hot-water pretreatment. Enzymatic hydrolysis was performed with the enzyme load in excess to ensure differences in recalcitrance were being observed. Large differences in sugar yield were observed among all the cultivars.

We found that sugar release following the higher severity pretreatment was dependent on cellulose content in the biomass, based on the observed correlation, similar to what Brereton et al (2010) observed among a larger set of willow genotypes. This suggests that breeding for differences in biomass composition will have an impact on sugar availability for fermentation. ‘SV1’ which has the greatest cellulose content (44.8 %) released the greatest amount of sugar following the 3.9 severity pretreatment, 617 mg g^{-1} biomass or 80% recovery. However, cellulose content alone cannot be the only factor impacting sugar release, since some of the cultivars with low cellulose content had high amounts sugar released, such as ‘Preble’. Other factors influencing recalcitrance and sugar release include cell wall chemistry, such as the free phenolic groups on the lignin monomers (Lapierre et al., 2000) and S:G ratios (Studer et al., 2011), and cell wall structural variability dependent on tissue types (Dinus et al., 2001).

The differences in sugar release between the two different pretreatment severities provide insight into the recalcitrance of the willow genotypes. To reduce costs associated with biomass conversion, it would be highly beneficial to utilize feedstocks that have maximum sugar release even following pretreatments of mild severity. In this study ‘SX64’ and ‘Fabius’ had the greatest sugar yield (70%) after the less severe pretreatment, and there was only marginally greater sugar release (80%) when the biomass was exposed to the more severe pretreatment. These two cultivars are less recalcitrant than ‘SV1’, which required the severe pretreatment to release most of the sugars.

The extent of sugar recovery and sugar yields observed for willow in this study are comparable to the sugar recovery observed for poplar subjected to a similar pretreatment severity (Studer et al., 2011). Further fermentation to ethanol produced relatively low yields compared with reported yields of ethanol production from willow. The greatest ethanol yields observed were from ‘SX64’ and ‘SV1’, attaining 50% of the theoretical ethanol yield. Sassner et al. (2008) reported ethanol yields from simultaneous saccharification and fermentation (SSF) reaching 76% of the theoretical yield. Ethanol yield in this study did correlate with sugar released from the severe pretreatment, indicating that improving sugar release by reducing recalcitrance will improve ethanol yields.

Overall this study has shown that there is significant variation in biomass composition and recalcitrance from specific shrub willow genotypes. Relationships between sugar release and cellulose content were identified, as well as a relationship with ethanol yield. These findings will spur future research and large-scale evaluation of willow germplasm for variation in recalcitrance to promote future breeding efforts aimed at producing new willow cultivars with maximum bioconversion to ethanol.

Acknowledgements

This work was funded by the Northeast Sun Grant Initiative. The authors would like to thank Deidre Willies and Lucas Ellis for their assistance in performing the hot-water pretreatments and fermentation at Mascoma Corp. We are grateful to Novozymes for providing the enzymes for hydrolysis. We also would like to thank Kayla Relyea and Jeffrey Springmeier for their assistance on this project.

References

Dinus RJ, et al. (2001) Genetic modification of short rotation poplar wood: properties for ethanol fuel and fiber productions. Critical Reviews in Plant Science 20**:** 51-69.

Lapierre C, et al. (2000) Genetic engineering of poplar lignins: Impact of lignin alteration on kraft pulping performances. In Lignin : Historical, Biological, and Materials Perspectives, Vol 742, pp 145-160.

Sassner P, et al. (2008) Techno-economic evaluation of bioethanol production from three different lignocellulosic materials. Biomass and Bioenergy 32**:** 422-430.

Selig M, et al. (2008) Enzymatic saccharification of lignocellulosic biomass. national Renewable Energy Laboratory, Golden, CO .

Serapiglia MJ, et al. (2009) Analysis of biomass composition using high-resolution thermogravimetric analysis and percent bark content as tools for the selection of shrub willow bioenergy crop varieties. Bioenergy Research 2**:** 1-9.

Shapouri H, et al. (2002) The energy balance of corn ethanol: an update. Agricultural Economic Report No. 814. USDA, Economic Research Service Office of the Chief Economist, Office of Energy Policy and New Uses, Washington, DC.

Sluiter A, et al. (2008) Determination of Sugars, Byproducts, and Degradation Products in Liquid Fraction Process Samples. National Renewable Energy Laboratory, Golden, CO.

Studer MH, et al. (2011) Lignin content in natural Populus variants affects sugar release. Proceedings of the National Academy of Sciences, USA**:** Advance online publication. doi: 10.1073/pnas1009252108.

Volk TA, et al. (2011) Yields of willow biomass crops across a range of sites in North America. Aspects of Applied Biology 112**:** 67-74.

1.2
CHEMICAL AND ELEMENTAL COMPOSITION OF BIG BLUESTEM AS AFFECTED BY ECOTYPE AND PLANTING LOCATION ALONG THE PRECIPITATION GRADIENT OF THE GREAT PLAINS

Ke Zhang[5], Loretta Johnson[6], Richard Nelson[7], Wenqiao Yuan[8], Zhijian Pei[9], Donghai Wang [1,]*

Abstract
Three big bluestem ecotypes from central Kansas (Cedar Bluffs and Webster populations), eastern Kansas (Konza and Top of the World populations), and Illinois (12Mile and Fults populations), as well as the Kaw cultivar, were harvested from four reciprocal garden planting locations (Colby, Hays, and Manhattan, KS; and Carbondale, IL) and evaluated for their chemical (glucan, xylan, arabinan, lignin and ash) and elemental (carbon, oxygen, hydrogen, nitrogen and sulfur) compositions. The objective of this research was to study the effects of ecotype and planting location on the chemical and elemental compositions of big bluestem along the Great Plains precipitation gradient (~1200 to 400 mm mean annual precipitation). All the populations revealed a large variation in cellulose (31.8–36.5%), hemicellulose (24.96–29.74%), lignin (14.4–18.0%), carbon (47.3–51.3%), and nitrogen (4.91–6.44%). Planting location had significant effects on both chemical and elemental compositions of big bluestem. Ecotype had significant effects on glucan, xylan, lignin, and ash contents as well as on carbon, oxygen, and hydrogen elemental fractions. In addition, the interaction between ecotype and planting location had significant effects on glucan, lignin, and hydrogen. Planting location had a greater effect on chemical and elemental compositions than the ecotype and interaction between location and ecotype. The total sugar content of the big bluestem (regardless of ecotype) increased as the Great Plains precipitation gradient increased from west to east. Annual precipitation, growing degree days and potential evapotranspiration in 2010 explained up to 97%, 88% and 80% of the variation in compositions respectively.

Keywords: Big bluestem; chemical composition; elemental composition; ecotype; reciprocal common garden

Introduction
With the rapid increase in worldwide consumption of nonrenewable fossil fuels, the production of renewable fuels from biomass is attracting more research attention. lignocellulosic biomass could play an important role in biofuel production because of low production inputs and potentially low competition with food production. A recent analysis indicated that over 25 million hectares of land classified by the USDA as rangeland/grassland within land capability class 3–6 soils (more marginal/less productive soils) could be utilized for bioenergy crop production in select states in the central Great Plains (Kansas, Nebraska, Oklahoma, and South Dakota) (USDA, 2010).

Big bluestem (*Andropogon gerardii*) is a dominant warm-season (C4) perennial native grass that

[5] *Department of Biological and Agricultural Engineering, Kansas State University, KS*

[6] *Department of Biology, Kansas State University, KS*

[7] *Center for Sustainable Energy, Kansas State University, KS*

[8] *Department of Biological and Agricultural Engineering, North Carolina State University, NC*

[9] *Department of Industrial and Manufacturing System Engineering, Kansas State University, KS*

** Corresponding author*

comprises as much as 80% of the plant biomass in prairies in the midwestern grasslands of North America (Gould and Shaw, 1983; Knapp *et al*., 1998). Big bluestem is adaptable in most native prairie ecosystems and can represent as much as three times the biomass as switchgrass in midwestern grasslands (Epstein *et al*., 1998). This research helps lay the foundation for the potential development of big bluestem as a bioenergy feedstock on these range/grasslands.

In this research, three big bluestem ecotypes with two populations comprising each ecotype and the widely planted KAW cultivar were harvested from each of four reciprocal garden planting locations. Results from this research will provide basic data that will potentially enable more efficient plant breeding for bioenergy production by providing scientific knowledge about the role of the genetic and environmental factors that influence the development of big bluestem varieties for use as a bioenergy crop.

Materials and Methods

Moisture content of ground big bluestem samples was determined by drying about 2 g of each sample in a forced-air oven at 105 °C for 4 h (Sluiter *et al*., 2008). Extractives and chemical composition of the big bluestem were determined by following NREL laboratory analytical procedures (Sluiter *et al*., 2008; Sluiter *et al*., 2005).

The elemental composition of the big bluestem samples was measured with CHNS/O Elemental Analyzer (PerkinElmer 2400 Series II, PerkinElmer Inc., Waltham, MA

Analysis of variance (ANOVA) test were analyzed using SAS (SAS Institute, Inc., Cary, NC). In general, fully balanced ANOVA tests were performed following the general linear models (GLM) procedure.

Results and Discussion

Both ecotype and planting location had significant effects on chemical and elemental compositions of the big bluestem ($P < 0.05$), except the effect of ecotype on xylan + arabinan, nitrogen, and sulfur contents. The chemical composition of the seven big bluestem populations and three ecotypes from four planting locations varied significantly when specific constituents were considered. For all of the big bluestem samples, the average and range of the chemical composition across planting locations and ecotypes are 34.5% ±2.4 from 29.6–39.5% for glucan, 23.6% ±2.0 from 19.2–26.8% for xylan, 3.5% ±0.7 from 2.1–4.8% for arabinan, 16.8% ±1.8 from 12.0–19.3% for lignin, and 4.3% ±0.7 from 3.1–5.6% for ash.

Effects of Planting Location and Planting Location on Chemical Composition

Fig. 1 shows the big bluestem populations planted in Illinois generally had higher cellulose (glucan) contents, with an average of 36.5% compared with the average of populations planted in Colby, KS (31.8%); Hays KS (33.8%); and Manhattan, KS (36.0%). The average cellulose content of big bluestem planted in Illinois was 4.7% higher than those from Colby in western Kansas, indicating that the same big bluestem populations would yield ≈15% more cellulose if planted in Illinois instead of western Kansas. Table 1 shows the linear regression results between composition and environmental factors associated with the planting locations. The 2010 annual precipitation explained 37–97% of the variation in biomass composition based on coefficients of determination (R^2). In addition to the sharp difference in precipitation from the westernmost planting location (Colby) to the easternmost planting location (Illinois), the difference in potential evapotranspiration between east and west is also responsible for composition differences. The 2010 growing degree days explained 17–88% of the variation in chemical concentrations. The potential evapotranspiration explained 55–80% of the variation in biomass composition (Table 1). The higher precipitation gradient in Illinois is almost one and a half times higher than Colby, which provides a better environment for biomass accumulation. A similar tendency was also observed for hemicellulose (xylan and arabinan). The highest and the lowest hemicellulose contents in the four planting locations, respectively, are Illinois with an average of 29.7% and Colby with an average of 25.0% (Fig. 1). The difference in hemicellulose content was about 19% among the four locations. The total structural polysaccharides content of big bluestem planted in Illinois was about 15% higher than that planted in Colby; however, this increase was associated with higher lignin content. The average lignin contents of all planting locations exhibited a decreasing trend with the ecotype from east to west. In fact, 2010 growing degree days and 2010 precipitation explained 88% and 74% of the variation in lignin concentrations, respectively (Table 1). Big bluestem in Colby had average of 14.4% lignin, which is significantly lower than samples planted in Illinois, with average of 18.0% (Fig. 1). Taking into account the adverse effects of lignin in hydrolysis, further research is needed to determine the sugar yield and fermentation efficiency of all samples to determine the overall location effects. The range of ash contents among 28 samples was quite different in four locations. Ash contents of big bluestem from Illinois (with an average of 4.8%; data not shown) were higher than those populations in the other three planting locations in Kansas. Results suggest that big bluestem planted in Kansas with lower ash content would be best suited for the thermoconversion of biomass to biofuel (Monti *et al*., 2008).

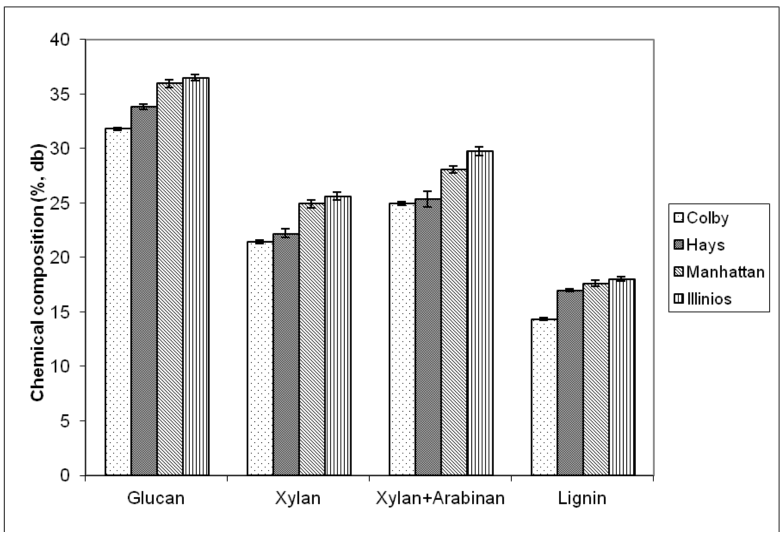

Fig. 1. Effects of planting location on chemical composition of big bluestem.

Table 1. Effects of environmental conditions on chemical composition and elemental fractions of big bluestem analyzed by linear regression models.

Composition (% db)	PPT[a] 2010 (cm)	PPT[a] since 1961 (cm)	GDD[b] 2010 (cm)	avg.GDD[b] (cm)	PET[c] (cm)	Aridity index
Glucan	0.94	0.84	0.93	0.8	0.72	0.81
Xylan	0.97	0.93	0.78	0.66	0.8	0.88
Xylan+ Arabinan	0.88	0.99	0.63	0.67	0.91	0.96
Lignin	0.74	0.63	0.96	0.88	0.55	0.63
Ash	0.37	0.65	0.08	0.17	0.67	0.64
Carbon	0.7	0.96	0.42	0.57	0.95	0.96
Hydrogen	0.69	0.69	0.9	0.96	0.64	0.69
Oxygen	0.79	0.99	0.61	0.76	0.98	0.99
Nitrogen	0.37	0.34	0.74	0.82	0.32	0.36
Sulfur	0.61	0.52	0.91	0.87	0.46	0.52

[a] PPT: Precipitation
[b] GOD: Growing degree days
[c] PET: Potential evapotranspiration

The composition results also showed a significant variation among the different ecotypes at $P < 0.001$ and F values from 3.36 to 28.5, except xylan+arabinan, with $P = 0.935$ and $F = 0.14$ (Table 2). Based on F value, ecotype had more significant effects on glucan and lignin, with F values of 28.5 and 16.2, respectively. Hays ecotype and KAW had significantly higher glucan contents than East KS and Illinois ecotypes. KAW had the highest glucan content among all the ecotypes (Fig. 2). This could be explained by the fact that the KAW cultivar, as the native released cultivar, was selected and bred for carbohydrate accumulation. Of these 28 samples, the highest carbohydrates content was found in KAW at the Illinois location, which indicates combined effects of ecotype and planting location. Although xylan content differs significantly among the different ecotypes, the average values of xylan of the different ecotypes are similar (Fig. 2), indicating no clear effect of ecotype on the average xylan contents within the ecotypes from west to east. This result is probably because glucan and xylan contents were not solely affected by ecotype. The highest and lowest lignin contents of big bluestem were Central KS ecotype and Illinois ecotype, respectively. Results suggest that the Central KS ecotype showed higher lignin content (17.5%) than the Illinois ecotype (15.7%) because of adaptation to drought necessitated by a dry growing environment. The high lignin content may result in relatively lower efficiency of degradation in bioconversion.

Table 2. Effects of ecotype (E), location (L), and interaction between ecotype and planting location on the chemical and elemental composition of big bluestem.

Composition /elements (%)	Source of variation	Location	Ecotype	L×E
Glucan	*F*	73.56	28.51	3.59
	P	<0.001	<0.001	0.002
Xylan	*F*	58.98	3.36	1.811
	P	<0.001	0.028	0.096
Xylan+ Arabinan	*F*	63.70	0.14	1.12
	P	<0.001	0.935	0.369
Lignin	*F*	48.98	16.23	2.61
	P	<0.001	<0.001	0.018
Ash	*F*	7.23	9.62	1.39
	P	<0.001	<0.001	0.224
Carbon	*F*	80.77	11.50	1.69
	P	<0.001	<0.001	0.123
Oxygen	*F*	86.66	5.98	1.67
	P	<0.001	0.002	0.129
Hydrogen	*F*	45.27	2.94	3.24
	P	<0.001	0.044	0.005
Nitrogen	*F*	12.02	2.60	1.13
	P	<0.001	0.065	0.359
Sulfur	*F*	29.52	0.46	1.15
	P	<0.001	0.706	0.347

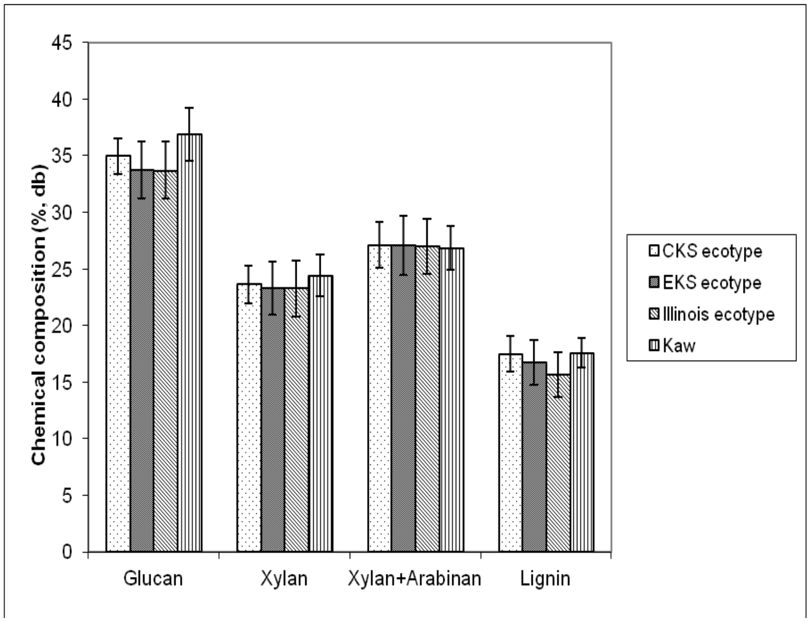

Fig. 2. Effects of ecotype on chemical composition of big bluestem.
Table 2. Effects of ecotype (E), location (L), and interaction between ecotype and planting location on the chemical and elemental composition of big bluestem.

Variations in the glucan, xylan, xylan+arabinan, lignin, and ash contents among the 28 samples were analyzed by two-way ANOVA for examining the genetic and environmental effects on chemical composition of the big bluestem. In general, ANOVA analysis revealed that ecotype and location had significant effects on chemical composition including glucan, xylan, lignin, and ash contents as well as xylan + arabinan content (Table 2). Location had larger *F* values (7.2–73.6) than ecotype (0.14–28.5) and interactions (1.12–3.59), showing that location effects were always highly significant with larger *F* values, at times approaching two orders of magnitude larger; however, significant interactions between location and ecotype have been found only for glucan, with $P < 0.002$ and an F value of 3.59, and lignin, with $P = 0.018$ and an *F* value of 2.64, indicating that the glucan and lignin contents of big bluestem were significantly affected by the combined effects of ecotype and growing locations.

Effects of Ecotype and Planting Location on Elemental Composition

Table 3 shows the carbon, hydrogen, nitrogen, oxygen, and sulfur fractions and H/C ratio of the big bluestem samples. The range of elemental fractions is 47.1–51.4% for carbon, 4.93–6.45% for hydrogen, 40.7–46.1% for oxygen, 0.61–1.27% for nitrogen and 0.78–0.98% for sulfur. The variations of the elements are 10.1% for carbon, 30.8% for hydrogen, 13.2% for oxygen, 10.8% for nitrogen, and 25.6% for sulfur. The average ratio of H/C is 1.44 with variation of 23.6%. Two-way ANOVA analysis shows through larger F values that location had more effects than ecotype and ecotype-location interaction on elemental composition of big bluestem (Table 2). Location had significant effects on all of the elemental fractions, with *F* values from 12.0 to 80.8 and $P < 0.001$. Ecotype had significant effects on carbon, oxygen, and hydrogen with *F* values from 2.94–11.50 and *P* values from 0.001–0.044. Ecotype-location interaction had a significant effect only on carbon content. The linear regression results between composition and environmental factors showed that precipitation explained 37–79% of variation in elemental fractions based on coefficients of determination (R^2) from 0.37–0.79 in growing year 2010 (Table 1). Growing degree days and the potential evapotranspiration also explained a large variation in the elemental composition of the big bluestem samples.

Because the carbon content is the most important factor related to its bioconversion yield and heat content, the histogram showed a parabolic trend with ecotype from west to east, indicating that the middle-location ecotype (EKS ecotype) had the lowest carbon content of the three ecotypes (Fig. 3). In general, the carbon content of the big bluestem (average of 50.8%) planted in Illinois is higher than its counterparts planted in the Kansas locations (average of 49.2% for Manhattan, 47.7% for Hay, and 47.8% for Colby). Decreased longitude of planting location resulted in increased carbon content, which was similar to the trend of environmental effect on chemical composition. Also noteworthy is that the big bluestem in Colby had significantly lower nitrogen content (average of 0.65%) compared with other locations (average of 0.9%) (Fig.4). Low nitrogen fraction in biomass could be an advantage for the combustion process with low NOx emission (Obernberger and Thek, 2004). However, planting location had no clear effect on hydrogen and sulfur (Fig. 5).

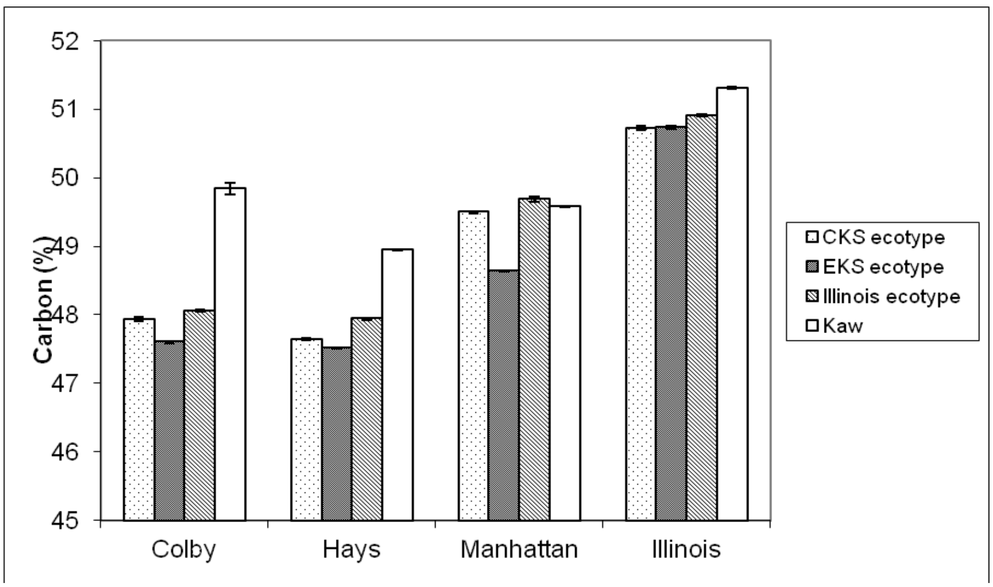

Fig. 3. Effects of planting location on carbon content of big bluestem.

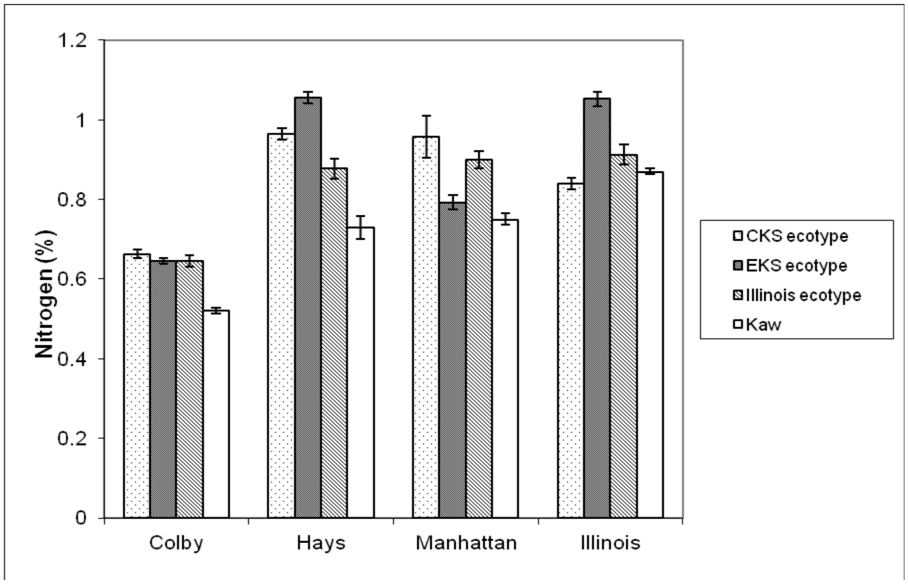

Fig. 4. Effects of planting location on nitrogen content of big bluestem.

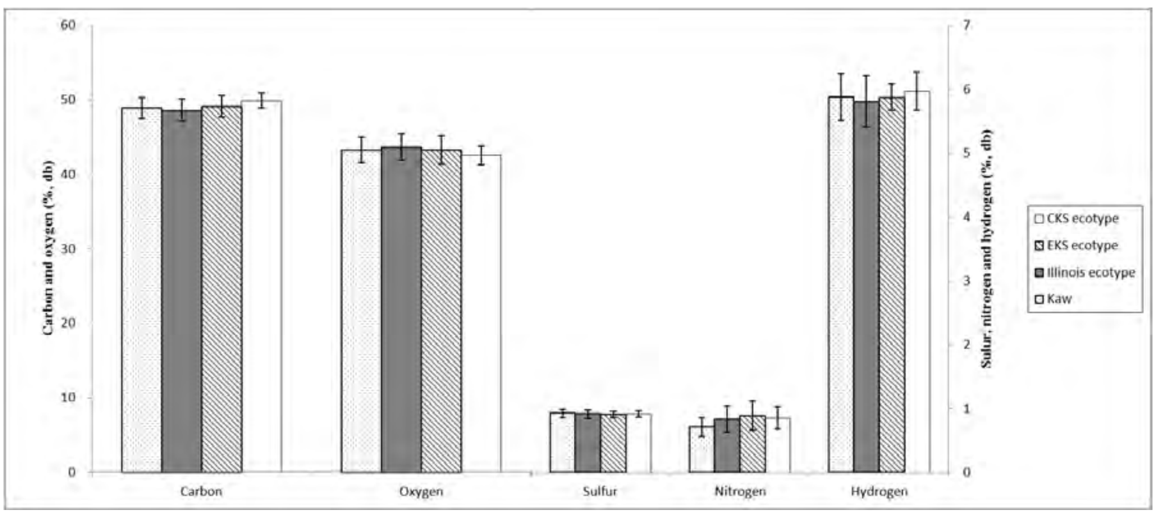

Fig. 5.Effect of ecotype on carbon, oxygen contents hydrogen, nitrogen, and sulfur

Conclusions

Planting location had significant effects on both chemical and elemental compositions of big bluestem. Ecotype had significant effects on glucan, xylan, lignin, and ash contents, and C, O, and H elemental fractions, whereas planting location significantly affected all measured variables. The ecotype-location interaction had significant effects on glucan, lignin, and hydrogen contents. In general, big bluestem planted in Illinois had higher cellulose, hemicellulose, and lignin contents than the populations planted in the Kansas locations. Besides environmental effects, the Illinois ecotype had the lowest lignin contents for all four locations. Carbon content increased with eastward movement. Carbon content of the big bluestem planted in Illinois was higher than those planted in the Kansas locations. Up to 97%, 88% and 80% of the variation in compositions can be explained by annual precipitation, growing degree days and potential evapotranspiration in 2010 respectively. The results show that big bluestem could potentially serve as suitable energy grass in the Midwest with similar or better chemical and elemental compositions compared with other biomass crops and grasses.

References

Gould, F., Shaw, R., 1983. Grass Systematics. 2nd ed. Texas A&M Univ. Press, College Station, TX.

Knapp, A., Briggs, J., Blair, J., Turner, C., 1998. Patterns and controls of aboveground net primary production in tallgrass prairie. In Grassland dynamics: long-term ecological research in tallgrass prairie, A.K. Knapp, J.M. Briggs, D.C. Hartnett, and S.L. Collins Eds., Oxford University Press, New York. 193–221.

Lloyd, T., Wyman, C., 2005. Combined sugar yields for dilute sulfuric acid pretreatment of corn stover followed by enzymatic hydrolysis of the remaining solids. Bioresource Technol. 96 (18), 1967–1977.

McMillan, C., 1959. The role of ecotypic variation in the distribution of the central grassland of North America. Ecological Monographs. 29, 285–308.

Monti, A., Virgilio, N., Venturi, G., 2008. Mineral composition and ash content of six major energy crops. Biomass and Bioenergy. 32(3), 216–223.

Obernberger, I., Thek, G., 2004. Physical characterisation and chemical composition of densified biomass fuels with regard to their combustion behavior. Biomass and Bioenergy. 27, 653–669.

Sluiter, A., Hames, B., Hyman, D., Payne, R., Scarlata, C., Sluiter J., Templeton, D., Wolfe J., 2008. Determination of Total Solids in Biomass and Total Dissolved Solids in Liquid Process Samples. NREL/TP–510–42621.

Sluiter, A., Hames, B., Ruiz, R., Scarlata, C., Sluiter, J., Templeton, D., 2005. Determination of Ash in Biomass. NREL/TP–510–42622.

USDA – NASS. The 2009 Cropland Data Layer, November 2010. Washington, D.C.: U.S. Department of Agriculture, National Agricultural Statistics Service. Available at: http://www.nass.usda.gov/research/Cropland/SARS1a.htm.

1.3
DISTRIBUTION OF ENERGY CONTENT IN CORN PLANTS AS INFLUENCED BY CORN RESIDUE MANAGEMENT

Keri B. Cantrell[1,], Jeffrey M. Novak[1], James R. Frederick[2], Douglas L. Karlen[3], Donald W. Watts[1]*

Abstract
Economic, environmental, climate change and energy independence issues are contributing to rising fossil fuel prices and creating a growing interest in the development and utilization of biomass feedstocks for renewable energy. Potential feedstocks include perennial grasses, timber, and annual grain crops with a current focus being placed on corn (*Zea mays L.*) stover. As part of the Sun Grant Regional Partnership corn stover project, a field study incorporating stover removal management practices was initiated in 2008 on plots composed of Coxville/Rains-Goldsboro-Lynchburg soil associations in South Carolina. In addition to annual yield and soil quality responses being reported elsewhere in this conference, studies were also conducted to measure any variations in the distribution of gross energy, as measured by an isoperibol calorimeter, in various corn stover fractions — whole plant, bottoms, tops, and cob (n = 20). Cobs were found to be the most energy dense with an average value of 18.54 MJ/kg-db. The top half of the corn plant, considered to be the biomass above the ear shank , was more energy dense than the bottom half — 18.42 vs. 18.06 MJ/kg-db. Gross energy content of the whole plant, including the cob, was determined to be 18.62 MJ/kg-db. Over the four years, partial to total removal (*i.e.*, 25 to 100%) of the above-ground plant biomass was dependent on rainfall and could supply between 30.3 and 162.1 GJ/ha. At 162.1 GJ/ha, the quantity of corn stover biomass (whole plant) available in a 3254 km^2 area (32 km radius) could potentially support a 500 MW power plant.

Keywords: higher heating value; residue removal; crop management; Zea mays, Renewable Energy Assessment Project (REAP); bioenergy; combustion

Introduction
Demand for renewable bioenergy feedstocks has grown and developed worldwide with prominent crops being corn stover, sugarcane bagasse, miscanthus, and switchgrass. This demand has also increased concerns regarding the sustainable use of current land and water resources as well as competition for those resources to provide both food and fuel (Pimentel *et al.* 2009). Replenishing and preserving soil organic carbon is necessary to sustain crop productivity and soil structure, and returning crop residues, like corn stover, is an acknowledged management strategy for sustaining soil organic carbon (Wilhelm *et al.* 2007). However, uncertainty remains as to the amount of corn stover that must be returned to prevent subsequent decreases in soil health and crop productivity. Furthermore, research is also limited regarding the impact that stover removal has on the stover quality when targeted for energy generation purposes.

The objective of this investigation was to quantify the gross energy distribution in various fractions of corn stover when harvested for bioenergy production. Specifically, this was accomplished annually by using an isoperibol calorimeter to quantify gross energy content and yield in various plant fractions.

---

[1] *Coastal Plains Soil, Water, and Plant Research Center, USDA-ARS, SC*

[2] *Pee Dee Research and Education Center, Clemson University, SC*

[3] *National Laboratory for Agriculture and the Environment, USDA-ARS, IA*

* *Corresponding author*

Materials and Methods

Twenty experimental plots (137.6 m^2) on a Coxville/Rains-Goldsboro-Lynchburg soil association were established in March, 2008 at the Clemson University Pee Dee Research and Education Center in Florence, SC. These plots contained four replications of five levels of corn stover residue removal treatment: 0, 25, 50, 75, and 100% removal rates. Each plot was surface stripped tilled using a Paratiller that also broke the hard pan at 40 cm depth. Corn (*Zea mays L.*) was planted mid-April in all plots using regional recommended standard production practices for the southeastern Coastal Plain. Corn was harvested in early September of each year in its entirety across each plot with the stover biomass collected using a canvas tarp technique attached to the combine. The wet residue was weighed, and specific portions, by weight according to the removal treatment, were returned and spread manually across each plot. Residue removal treatments were repeated on the same plots in 2009, 2010, and 2011.

Approximately two weeks prior to combine harvest, corn plant samples were collected from a total 5 m^2 area in rows. These corn plant samples were processed into the following plant parts: whole plant (WP); top (T)—representing biomass above the ear shank including the cob; bottom (B)—representing biomass below the ear shank; and cobs only. Whole plant biomass yields were based on samples from a 2 m^2 area; T and B biomass yields were determined from a separate 2 m^2 area; and cob biomass yields were based on samples collected from 1 m^2 area. All biomass were dried at 60 °C and then weighed to obtain biomass yields (kg ha^{-1}). A portion of dried corn stover samples were ball milled and analyzed for energy density or higher heating value (HHV) using a LECO AC500 Isoperibol Calorimeter (Leco Corp., St. Joseph, MI) following ASTM D5865 (ASTM 2006). Subsequent bioenergy yields removed (GJ ha^{-1}) were calculated as the product of removal rate, energy density (MJ kg^{-1}), and biomass yield. Biomass yields and HHV results are reported for 2009 and 2010; WP results are reported also for 2011. Rainfall data, collected at daily intervals, was obtained from an on-site weather station.

Data were analyzed by Proc GLMMIX (General Linear Mixed Model) with plot replications as the random effect using Version of 9.2 of Statistical Analysis System (SAS Institute Inc., Cary, NC). Significant differences between plant parts and removal rates were based on a F-test ($P < 0.05$).

Results and Discussion

Corn stover HHVs (MJ kg^{-1}) and residue collections (kg ha^{-1}) were analyzed for statistical differences by year due to differences in rainfall and its timing. Rainfall during the months of April through August totaled 663 mm for 2009, 671 mm for 2010, and 244 mm for 2011. Rainfall for the month of May varied significantly across the years: 176 mm for 2009; 63.8 mm for 2010; and 22.9 mm for 2011. This difference in rainfall distribution caused notable changes in the WP biomass collected: The total WP dry residue collected decreased from 2009 to 2011 by an average 29.3 % (Table 1).

Table 1. Biomass, energy content (HHV), and energy yield for whole corn plants across all years

Year	Removal Rate	Total dry residue collected		HHV		Bioenergy Yield Removed	
		kg ha^{-1}		MJ kg^{-1}		GJ ha^{-1}	
		Mean	Std Dev	Mean	Std Dev	Mean	Std Dev
2009	0	9269.7	753.9	18.86	0.93	0.0	0.0
	25	9170.9	1013.9	18.80	0.85	43.0	3.7
	50	8764.4	509.5	18.11	0.48	79.3	4.7
	75	9368.6	319.4	18.56	0.67	130.4	6.9
	100	8819.6	282.2	18.38	0.75	162.1	8.6
2010	0	8627.9	146.7	18.55	0.22	0.0	0.0
	25	8476.0	629.4	17.88	0.66	37.9	2.5
	50	8322.4	1006.0	17.95	0.58	74.7	9.7
	75	8304.9	805.8	18.28	0.34	114.0	12.6
	100	7953.9	976.2	18.66	0.34	148.4	18.2
2011	0	6739.4	805.7	19.08	0.17	0.0	0.0
	25	6328.5	757.2	19.12	0.31	30.3	4.0
	50	6261.3	732.6	18.99	0.48	59.4	6.1
	75	6808.0	1131.2	18.97	0.46	96.9	17.0
	100	5937.5	245.9	19.14	0.07	113.6	4.5

Focusing on the effects of corn stover removal on the HHV of the various plant fractions, it was found removal did not significantly affect HHV in WP and T plant fractions (Tables 1-3). However, stover removal did statistically impact HHV for Cob and B fractions (Table 2).

Table 2. Biomass, energy content (HHV), and energy yield for various plant parts in 2009

Part	Removal Rate	Total dry residue collected		HHV		Bioenergy Yield Removed	
		kg ha^{-1}		MJ kg^{-1}		GJ ha^{-1}	
		Mean	Std Dev	Mean	Std Dev	Mean	Std Dev
Cob	0	1389.0	90.0	17.30	0.87	0.0	0.0
	25	1228.3	81.5	17.36	0.94	5.3	0.2
	50	1265.8	193.4	18.92	0.09	12.0	1.8
	75	1280.8	185.4	18.42	0.78	17.7	2.7
	100	1239.4	236.3	18.49	0.59	22.9	4.4
Top (Above Earshank)	0	2841.6	284.2	18.20	1.56	0.0	0.0
	25	2658.9	369.8	18.72	0.50	13.1	1.8
	50	2771.6	236.0	18.50	0.16	25.6	2.1
	75	2737.8	270.8	18.55	0.45	38.1	3.5
	100	2492.9	437.5	18.34	0.35	45.6	7.4
Bottom (Below Earshank)	0	3822.8	412.4	18.39	0.44	0.0	0.0
	25	3384.0	292.1	18.74	0.51	15.9	1.5
	50	3686.4	265.9	16.96	0.99	31.4	4.1
	75	3565.0	222.9	18.18	0.73	48.6	3.5
	100	3319.6	360.9	17.45	1.04	56.7	4.2

For cob fractions in 2009, 0 to 25 % removals generated cob fractions with lower HHV, 17.33 ± 0.04 vs. 18.61 ± 0.27 MJ kg^{-1}. The mixed effects of stover removal were noted with the B fractions: both 50 and 100 % stover removal resulted in the lowest HHV value for B, 17.21 ± 0.35 vs. 18.44 ± 0.28 MJ kg^{-1}. Continued stover removal did not impact HHV for any fraction tested (Table 1 and 3).

Table 3. Biomass, energy content (HHV), and energy yield for various plant parts in 2010

Part	Removal Rate	Total dry residue collected		HHV		Bioenergy Yield Removed	
		kg ha^{-1}		MJ kg^{-1}		GJ ha^{-1}	
		Mean	Std Dev	Mean	Std Dev	Mean	Std Dev
Cob	0	1415.9	199.1	19.07	0.24	0.0	0.0
	25	1406.8	241.3	18.71	0.21	6.6	1.2
	50	1346.1	266.4	19.10	0.44	12.9	2.8
	75	1480.2	243.4	19.12	0.28	21.2	3.4
	100	1155.2	172.8	18.89	0.61	21.9	3.8
Top (Above Earshank)	0	3060.0	166.7	18.29	0.34	0.0	0.0
	25	3016.1	419.9	18.24	0.17	13.7	1.8
	50	3079.3	239.9	18.20	0.27	28.0	2.2
	75	3024.4	285.7	18.60	0.42	42.2	4.0
	100	3079.9	283.7	18.67	0.32	57.6	6.1
Bottom (Below Earshank)	0	4008.5	161.8	18.39	0.36	0.0	0.0
	25	3532.5	511.5	18.41	0.35	16.2	2.2
	50	3669.1	310.9	18.28	0.38	33.5	3.0
	75	3745.4	297.3	18.02	0.56	50.7	5.2
	100	3408.0	284.4	17.85	0.73	60.9	6.8

Even though stover removal did not impact WP HHV, removal did impact overall bioenergy yield: greater stover removals resulted in greater bioenergy available for off-farm purposes (Tables 1-3). For WP stover removal, decreases in bioenergy yield removed (GJ ha^{-1}) across years was directly proportional to the decreases in total dry residue collected (Table 1). With increases in available energy per area, larger power plants can be supported (Figure 1). Assuming a 30 % electrical conversion efficiency (McKendry 2002), WP stover removal at 100 % during productive years (*e.g.*, 2009) within a 32 km radius (*i.e.*, harvested from 3254 km^2 area) would provide sufficient biomass to maintain a 500 MW electrical generation system. To obtain this power from lower biomass yielding years (*e.g.*, 2011), the radius would need to expand to 40 km (5085 km^2 area).

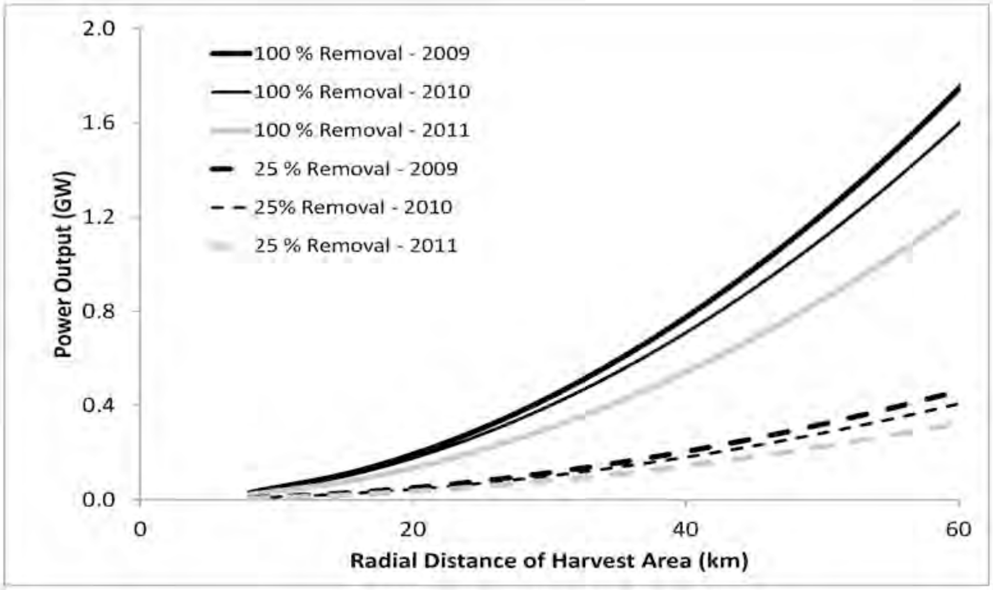

Figure 1. Relative power plant size* supported by combustion of removed whole plant corn stover yields within a defined radius. *Calculations assume 30% conversion efficiency.

References

ASTM. *Petroleum Products, Lubricants, and Fossil Fuels: Gaseous Fuels, Coal, and Coke*. W. Conshohocken, PA: ASTM International, 2006.

McKendry, P. "Energy Production from Biomass (Part 2): Conversion Technologies." *Bioresource Technology* 83, no. 1 (2002): 47-54.

Pimentel, David, Alison Marklein, Megan A. Toth, Marissa N. Karpoff, Gillian S. Paul, Robert McCormack, Joanna Kyriazis, and Tim Krueger. "Food Versus Biofuels: Environmental and Economic Costs." *Human Ecology* 37, no. 1 (2009): 1-12.

Wilhelm, Wally W., Jane M.F. Johnson, Douglas L. Karlen, and David T. Lightle. "Corn Stover to Sustain Soil Organic Carbon Further Constrains Biomass Supply." *Agronomy Journal* 99 (2007): 1665-1667.

1.4
DISTRIBUTION OF STRUCTURAL CARBOHYDRATES IN CORN PLANTS AS INFLUENCED BY CORN RESIDUE MANAGEMENT

Spyridon Mourtzinis[1,], Keri B. Cantrell[2], Francisco Arriaga[3], Jeff M. Novak[2], James. R. Frederick[4], Doug Karlen[5]*

Abstract

As part of the Sun Grant Regional Partnership corn stover project, continuous corn (*Zea mays*) field studies incorporating stover removal management practices (0 and 100% removal) were established in both Alabama and South Carolina. Plots in both states were representative of major soil types in their respective region: Alabama plots were Compass and Decatur soils; South Carolina plots were Coxville/Rains-Goldsboro-Lynchburg association. In addition to grain and biomass yield and soil quality responses being reported elsewhere in this conference, these two sites investigated variations in the distribution of carbon and structural carbohydrates among five plant fractions: whole plant; above the first ear excluding cobs (top); below the first ear (bottom); cob; and above the first ear including cobs (above ear). Using a combination of wet chemistry methods and near infrared spectroscopy (NIRS), the distribution of carbon and structural carbohydrates varied between the sites. Stover removal was not a significant factor on carbohydrate concentrations on any plant fraction and soil type. When compared to the above ear fractions, bottom plant partitions revealed greater carbon, lignin and cellulose concentrations. However, holocellulose concentration was consistently greater in cobs, tops and above ear fractions at every location. Data from this study suggests that Goldsboro and Lynchburg soils have greater potential in producing corn biomass with desirable portions of structural carbohydrates for bioenergy, when compared to Decatur and Compass. Furthermore, the plant portions cob, top and above the first ear have the most desirable characteristics for biofuel production at every location.

Keywords: Corn; Carbohydrates; Cellulose; Distribution; Residue Removal

[1] Department of Agronomy and Soils, Auburn University, AL

[2] USDA-ARS, Coastal Plains Soil, Water, and Plant Research Center, SC

[3] Dept. of Soil Science, University of Wisconsin, WI

[4] Pee Dee Research and Education Center, Clemson University, SC

[5] USDA-ARS, National Laboratory for Agriculture and the Environment, IA

* Corresponding author

Table 1. Corn stover composition as affected by stover harvest (removal) and distribution of major plant components for three locations in the Southeast.

Location	South Carolina								
	Corn Residue			Plant Fraction					
Factor	Removed	Retained	‡Pr > F	Whole Plant	Bottom	Top	Cob	Above Ear	§Pr > F
	%					%			
Carbon	47.72	47.64	0.7019	47.28	47.34	47.16	48.72	47.94	0.0017
Cellulose	40.17	39.73	0.3729	41.19	43.59	37.05	39.6	38.33	0.0325
Hemicellulose	34.31	35.04	0.6009	30.8	25.12	35.96.	39.96	37.96	0.0002
Lignin	6.29	5.67	0.3081	6.58	9.24	5.49	4.52	5.00	0.002
Ash	3.17	3.40	0.2569	3.99	4.16	3.44	2.08	2.76	>.0001
Holocellulose	74.48	74.41	0.9620	71.75	68.67	72.75	79.75	76.25	0.1275
Lignin + Ash	9.46	9.08	0.6065	10.59	13.42	8.50	6.61	7.78	0.0002
Difference †	65.02	65.33	0.8853	61.11	55.05	63.75	73.04	68.39	0.0259
Location	Alabama-Compass								
	%					%			
Carbon	45.99	46.06	0.2221	46.02	45.83	45.78	46.45	46.11	0.0063
Cellulose	40.60	40.73	0.5138	40.87	43.22	40.54	38.55	39.68	>.0001
Hemicellulose	23.63	23.77	0.6004	23.11	17.53	23.07	29.04	25.95	>.0001
Lignin	5.95	5.92	0.7237	6.12	7.85	5.32	5.13	5.24	>.0001
Ash	2.93	2.97	0.2754	2.98	3.31	3.42	2.18	2.81	>.0001
Holocellulose	64.24	64.51	0.2229	64.03	60.82	63.69	67.59	65.68	>.0001
Lignin + Ash	8.88	8.89	0.9667	9.10	11.16	8.75	7.32	8.05	>.0001
Difference †	55.35	55.61	0.3608	54.93	49.66	54.94	60.27	57.63	>.0001
Location	Alabama-Decatur								
	%					%			
Carbon	46.35	46.43	0.4250	46.4	46.47	45.86	46.89	46.37	>.0001
Cellulose	39.79	39.90	0.5471	40.1	42.14	39.43	38.48	39.06	>.0001
Hemicellulose	24.63	24.51	0.7031	23.87	17.22	24.2	30.29	27.21	>.0001
Lignin	6.02	5.99	0.7448	6.25	8.15	5.36	5.18	5.29	>.0001
Ash	3.46	3.47	0.9381	3.52	4.09	4.17	2.32	3.23	>.0001
Holocellulose	64.42	64.41	0.9774	63.98	59.37	63.65	68.75	66.28	>.0001
Lignin + Ash	9.49	9.46	0.8224	9.75	12.23	9.52	7.48	8.51	>.0001
Difference †	54.93	54.94	0.9546	54.24	47.14	54.16	61.28	57.81	>.0001

†Difference = Holocellulose - Lignin - Ash.
‡The Pr > F values represent the probability of a larger F by chance between residue retained and residue removed within locations.
§ The Pr > F values represent the probability of a larger F by chance between plant fractions within locations.

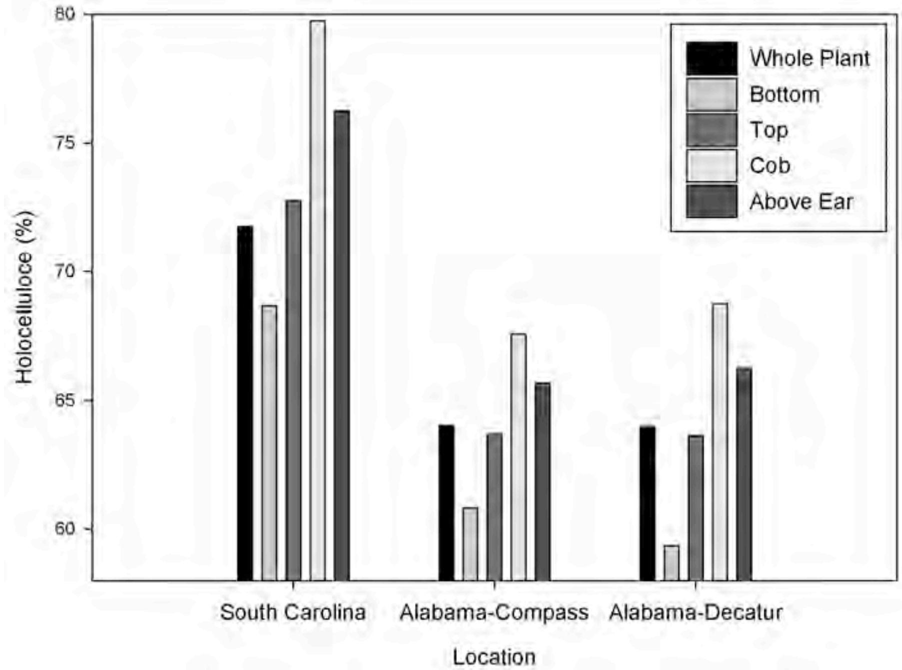

Figure 1. Holocellulose content of five corn plant fractions for three locations in the Southeast.

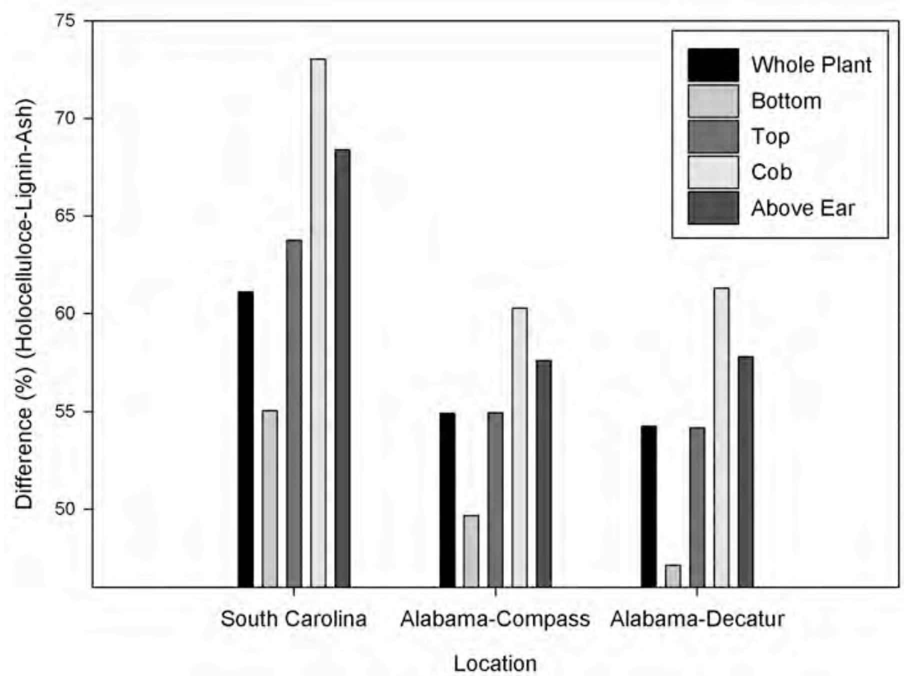

Figure 2. Difference of structural carbohydrates (Difference=Holocellulose-Lignin-Ash) as affected by stover harvest (removal).

1.5
ISOLATION AND CHARACTERIZATION OF LIGNIN THROUGH AN IONIC LIQUID FRACTIONATION APPROACH

N. Labbé[1], L. Kline[1]

Abstract
An integrated biorefinery will rely on the various components of lignocellulosic biomass to produce fuels, chemicals, and products to be economically and sustainably viable. Over the past decade, numerous pretreatment processes have been developed and optimized with the unique goal of reducing the recalcitrance of the biomass and making the cellulose fraction more accessible for biofuel production. These approaches did very little to preserve the lignin fraction of the feedstock as a potential stream for production of value-added products. An ionic liquid approach is a possible method to fractionate lignocellulosic biomass and generate a source of lignin with unique properties for the hardwood Yellow poplar (*Liriodendron tulipifera)*. Advanced technologies such as Fourier transform infrared spectroscopy and pyrolysis-gas chromatography/mass spectrometry coupled with multivariate analysis will be used to monitor not only the changes the biomass undergoes during the ionic liquid fractionation process but also to characterize the properties of the isolated lignin.

Keywords: Biomass recalcitrance, activation, ionic liquid, fractionation, lignin

Introduction
Lignin is the second most abundant source of renewable and sustainable carbon behind cellulose. In recent years, the emphasis in biorefinery processes applied to lignocellulosics has been the isolation and conversion of polysaccharides into biofuels. Lignin is often regarded as a low value by-product, usually existing as a partially hydrolyzed, impure lignin stream utilized as an energy source for other processes. Ionic liquids (ILs) have shown to fully or partially dissolve biomass and its constituents such as cellulose, hemicellulose, and lignin, while also allowing for regeneration of these constituents with the addition of a co-solvent (Swatloski *et al*., 2002; Fort *et al*., 2007; Stark, 2011; Wang *et al*., 2011). ILs have proven to reduce recalcitrance and increase the hydrolyzability of biomass and cellulose (Dadi *et al*., 2006; Fu *et al*., 2011; Labbé *et al*., 2012). With a less recalcitrant biomass, an ionic liquid approach can also be used for fractionation of biomass with enzymatic hydrolysis and solubilization of cellulose and hemicellulose components, thus freeing the lignin and allowing for the study of its structure with minimal degradation, a process necessary for the development of higher grade co-products such as carbon fibers.

Methods

Batch Activation and Recovery from Ionic Liquid
Yellow poplar (*Liriodendron tulipifera*), ground using a Wiley Mill (Thomas Scientific, Swedesboro, NJ) through a 40-mesh screen (0.425 mm), was obtained from the Center for Renewable Carbon at the University of Tennessee. The material was then extracted following the NREL (National Renewable Energy Laboratory) analytical procedure to remove non-structural material called extractives to prevent any interference with later subsequent analytical procedures (NREL, 2008a). The ionic liquid 1-Ethyl-3-methylimidazolium acetate (EmimAce, purum ≥ 95%) used in this study was purchased from Iolitec Inc. (Tuscaloosa, AL). The activation process utilizing EmimAce was similar to previously published work (Labbé *et al*., 2012), but completed at a larger scale in a 1L batch reactor for 72 hours, known as the activation time. Deionized water was used as the anti-solvent and wash used in all experiments.

[1] *Center for Renewable Carbon, University of Tennessee, TN*

** Corresponding author*

Fractionation of the Lignin-rich Component via Enzymatic Hydrolysis

Enzymatic hydrolysis of the cellulosic and hemicellulosic components was completing using Celluclast 1.5L, a *Trichoderma reesei* cellulase (70.3 FPU/mL), Novozym 188, a β-glucosidase, and the Novozymes Biomass conversion kit, a series of cellulases and hemicellulases produced specifically for the conversion lignocellulosic materials, were obtained from Novozymes, Inc. (Franklinton, NC). Experiments were performed similarly to conditions set forth by the protocol developed by US-DOE-NREL (NREL, 2008b). The hydrolysis reaction was maintained for a maximum of 96 hours with sample aliquots taken to monitor sugars released (cellobiose, glucose, xylose, galactose, arabinose, and mannose) approximately every 24 hr. The lignin-rich fraction was washed using a fine porosity vacuum filtration in and allowed to dry at 40°C for 12 hours prior to subsequent characterization described below.

FTIR and Multivariate Statistical Analysis

FTIR spectroscopy was completed using the Spectrum One FTIR spectrometer from Perkin Elmer (Waltham, MA) with a diamond attenuated total reflectance (ATR) attachment. Spectra were collected similarly to methods seen previously (Labbé 2012). The index of crystallinity, a spectral parameter that corresponds to the direct measurement of crystallinity, was estimated as the ratio of corrected peak heights for bands located at 1422 and 899 cm^{-1}. A carbonyl bond generally associated with the C=O stretch of acetyl groups present in hemicellulose is found at approximately 1735 cm^{-1}, so the area under this peak was used to monitor carbonyl groups in the samples (Kataoka and Kondo, 1998). The ratio of syringyl to guaiacyl (S/G) units was based off previous methods, as the intensity of peaks located at 1327 and 1267 cm^{-1} (Rutkowska *et al*., 2009).

Principal component analysis (PCA) is a mathematical technique that identifies major and minor differences between multivariate data sets, in particular infrared spectra. PCA transforms this multivariate dataset to a new dataset that is dependent on new variables, known as principal components (PC). Projection of these principal components to a two-dimensional form called the scores plot, allows for visual interpretation of the degree of correlation that exists within the multivariate data set. The first principal component is associated with the majority of variability between the spectra, with each successive component associated with a decreasing proportion of variability. The relationship between the original variables (wavenumber in the FTIR spectra) and each principal component is given in the loadings plot (Martens and Naes, 1989).

Wet Chemical Compositional Analysis of Yellow Poplar and Lignin-rich Fraction

The quantification of cellulose, hemicellulose, lignin, and ash in the Yellow poplar and lignin-rich fraction was performed using the protocols developed by US-DOE-NREL using three replicates (NREL, 2008c). This protocol was repeated for the biomass material before and after activation to monitor any changes in the chemical composition during the dissolution in EmimAce for 72 hr. The purity of each recovered lignin after enzymatic hydrolysis was assessed in this way, assuming the major impurities were to be trace polysaccharides, moisture, and ash.

Pyrolysis-Gas Chromatography/Mass Spectrometry (Py-GC/MS)

The Frontier EGA/Py-3030 D pyrolyzer was used for the thermo-chemical conversion of the biomass samples. Approximately 200 μg samples were weighed in stainless steel cups and pyrolyzed for 12s at 450^{o}C temperature to initiate the fragmentation of the biomass or lignin components. A Perkin Elmer Clarus 680 Gas Chromatography (with Elite 17 MS capillary column, helium carrier gas at 80:1 split ratio) coupled with Clarus SQ 8C Mass Spectrometer was used for chromatographic separation of the pyrolysis vapors and the identification of the evolved components. Peak areas in the chromatogram were normalized based on the sample weight. The National Institute of Standards and Technology (NIST) library was used for the purpose of matching the mass spectral fragmentation pattern to tentatively identify the evolved products.

Results and Discussion

Recovery of the Yellow poplar after activation in EmimAce followed by precipitation and washing with water was equal to 96% based on the total solids content of the biomass as a percent of the original material.

Application of commercial enzymes to the air-dried IL-activated Yellow poplar resulted in a cellulose conversion rate of 96% using the concentrations of soluble cellobiose and glucose within 96 hr of reaction time. The saccharification also led to 93% conversion of hemicellulose to xylose, galactose, arabinose, and mannose.

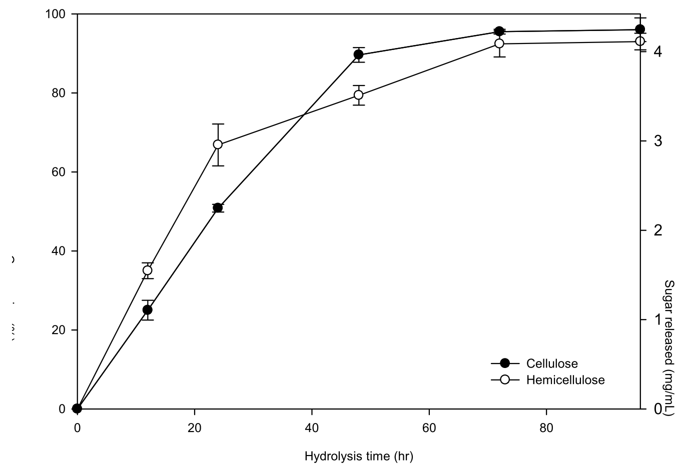

Figure 1. Calculated enzymatic conversion of carbohydrate components via HPLC analysis of sugar soluble sugars of the activated biomass.

FTIR spectra were collected and analyzed for the extractives-free biomass, Yellow poplar activated in EmimAce for 72 hr, and the lignin-rich fraction obtained after enzymatic hydrolysis of the carbohydrate components and some visual differences between spectra were noticeable (Fig 2a). Principal component analysis (PCA) was performed to identify those statistical differences in the spectra that will correspond to the physico-chemical changes within the activated biomass and lignin-rich fraction (Chen 1998, Labbé 2006, Kline 2010). The scores plot obtained for the original biomass and the IL-activation poplar compared to the lignin-rich fraction is shown in Fig 2b. There are three distinct clusters formed for each sample type, with the extractives-free and IL-activated poplar separating along the second principal component (PC2). Figure 2c shows the loadings associated with PC2, thus identifying and quantifying the contribution of these variables (wavenumbers) to the chemical changes between the original and IL-activated biomass. Peaks of interest in PC2 include a negative peak at 1735 (C=O) and 1251 cm^{-1} (C-O), assigned to acetyl group vibrations. As shown previously, the cleaving of these acetyl groups from the hemicellulose component is a key characteristic of the biomass activation and subsequent reduction in recalcitrance (Labbé *et al*., 2012). The deacetylation of the IL-activated Yellow poplar was confirmed by calculating the area under the band located at 1730-1740 cm^{-1}, relative to that band found for the unmodified biomass (extractives-free). A 69% decrease in the relative percent of acetyl groups was found for the biomass activated in EmimAce for 72 hr (Fig 3). A reduction in the crystallinity of cellulose and biomass regenerated from ionic liquid has been reported in literature (Labbé *et al*., 2012 Dadi *et al*., 2006; Lee *et al*., 2009). The index of crystallinity of the IL-activated Yellow poplar was shown to decrease by 50% relative to the unmodified biomass. The classification of the lignin-rich fraction recovered after enzymatic saccharification of the IL-activated poplar is shown by the separation of its cluster from the unmodified and IL-activated Yellow poplar along PC1 (Fig 2b). The presence of positive loadings peaks at 1591 and 1502 cm^{-1} (C=C stretching of aromatic ring in lignin) confirms the removal of carbohydrates from the biomass towards a more lignin-rich fraction (Fig 2c). As seen in Figure 3, the measured S/G ratio of the IL-activated Yellow poplar was seen to slightly decrease by only 1.1% relative to the unmodified biomass. This further supports the idea that the ionic liquid activation results in minimum changes to the native structure of the lignin.

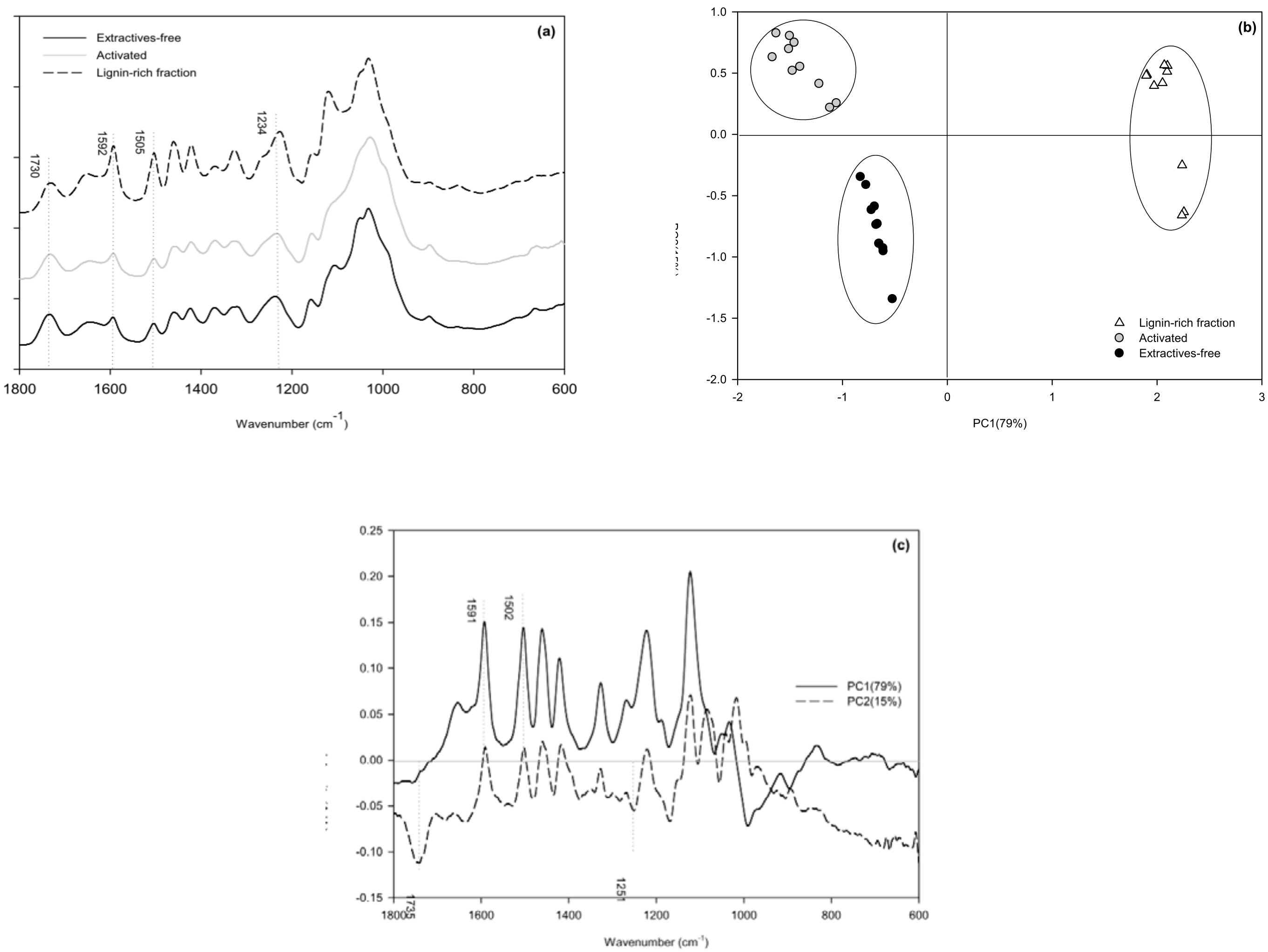

Figure 2. (a) FTIR spectra of extractives-free poplar, activated Yellow poplar, and the lignin-rich fraction; (b and c) PCA scores and loadings plots.

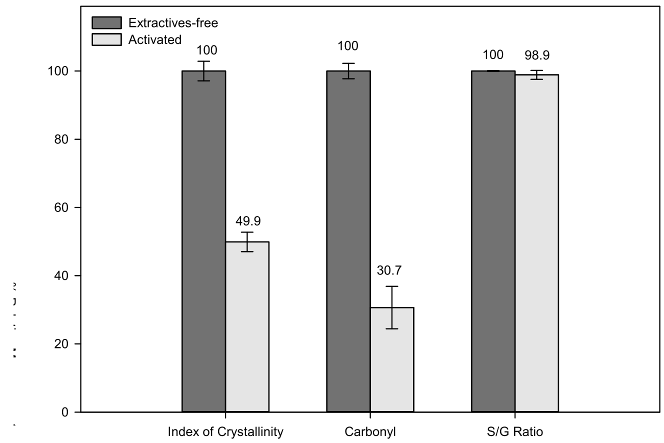

Figure 3. Relative peak measurements for Index of crystallinity (FTIR spectral peak height: 1422 vs 899 cm^{-1}), peak area for the carbonyl groups (1730 cm^{-1}), and S/G ratio (spectral peak height; 1327 vs 1267 cm^{-1}) for activated biomass relative to the unmodified Yellow poplar.

The chemical composition of the Yellow poplar remained relatively constant after 72 hr in EmimAce (Fig 4). There was a <1% change in all chemical components presented, indicating a portion of the mass loss (4% dry basis) is likely attributable to the cleavage of acetyl groups from the hemicellulose component as described above. The carbohydrate component decreased from 66.9 to 8.2% in the lignin-rich fraction when compared to the unmodified biomass, demonstrating a relatively pure lignin product.

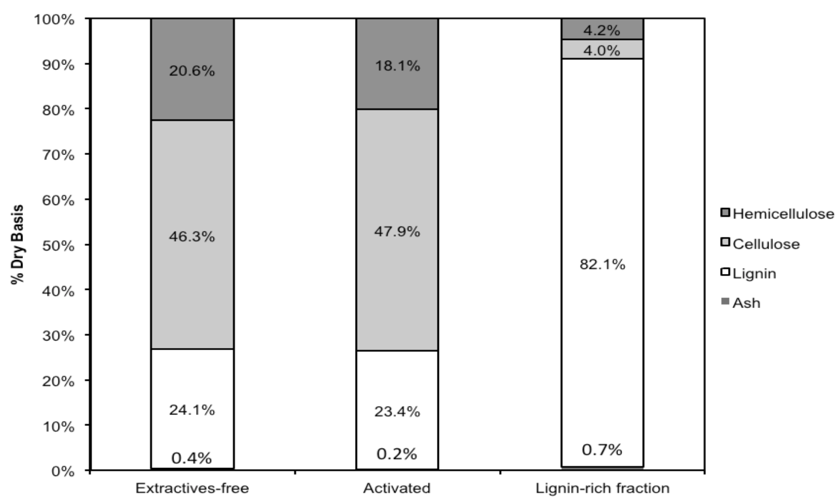

Figure 4. Chemical composition of the extractives-free Yellow poplar, IL- activated poplar in EmimAce for 72 h, and the lignin-rich fraction resulting after saccharification of the activated biomass on a weight percent (%dry basis).

To further classify the IL-activated biomass and lignin-rich fraction from the unmodified, extractives-free Yellow poplar, py-GC/MS was performed to characterize the thermo-chemical conversion of each sample (Fig 5a). One of main pathways responsible for the decomposition of the cellulose and hemicellulose components is depolymerization, forming furans after dehydration of carbohydrates as well as various anhydrosugars such as levoglucosan (Lu *et al.*, 2010). Visual inspection of the chromatograms show a decrease in these peaks associated with the cellulosic and hemicellulosic degradation when comparing the lignin-rich fraction to the unmodified Yellow poplar, corresponding with the lower carbohydrate content found in the classical techniques results described above. Due to the large number of peaks for the many evolved components, multivariate analysis on the sample chromatograms was utilized to identify those significant changes in compounds prior to and after activation and subsequent enzymatic hydrolysis of carbohydrates. As seen in Figure 5b, the scores plot for the py-GC/MS chromatograms shows a cluster for the extractives-free biomass positive along PC1, followed by a cluster for the IL-activated biomass, then the lignin-rich fraction negative along PC1. Since positive loadings peaks associated with the cellulosic and hemicellulosic components, such as levoglucosan and furfural, are positive (Fig 5c), and the data points for the extractives-free biomass are positive along PC1 (Fig 5b), carbohydrates are shown to be more prevalent in the unmodified and IL-activated biomass. Pyrolysis of lignin produces monomeric phenolic compounds and oligomers of different degrees of polymerization (Lu 2010). Since peaks associated with lignin thermo-chemical degradation products (guaiacol, isovanillin, coniferylaldehyde, and phenol,2,6-dimethoxy) are negative in the loadings plot and the data points for the lignin-rich fraction are negative along PC1 in the scores plot, it can be concluded that the enzymatic conversion of the carbohydrate constituents was successful in producing a more lignin-rich fraction. In the same manner, the positive acetic acid loadings peak corresponds to the deacetylation of the hemicellulose component in Yellow poplar during activation in EmimAce.

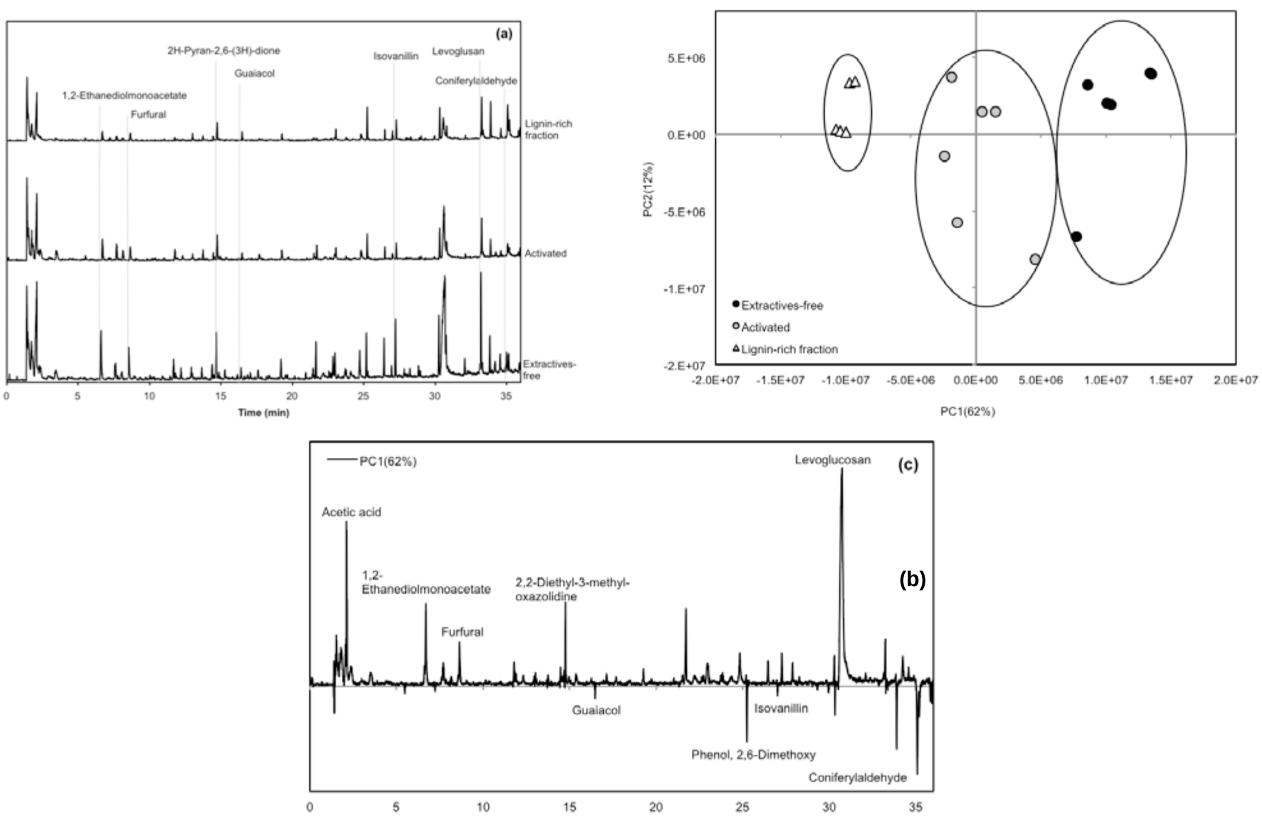

Figure 5. (a) Chromatograms from py-GC/MS of the extractives-free Yellow poplar, Yellow poplar activated in EmimAce for 72 h, and the lignin-rich fraction resulting after saccharification of the activated biomass; (b and c) PCA scores and loadings plot of unmodified Yellow poplar, Yellow poplar activated by EmimAce for 72 h, and the lignin-rich fraction obtained after saccharification of carbohydrates with tentative peak assignments.

Conclusions

An ionic liquid approach has been shown to successfully activate biomass at large bench top scale, opening the structure of the cell wall, decreasing the cellulose crystallinity, and cutting the acetyl groups from the hemicelluloses component. The process takes place under mild conditions with low energy inputs. By providing a less recalcitrant biomass, this IL activation process is of particular interest because it allows for the selective production of two clean fractions, saccharides and lignin, via enzymatic hydrolysis. By incorporating fractionation processes such as this into the biorefinery, this novel lignin allows for increased applications in the production of valuable chemicals and products from lignocellulosic biomass.

Acknowledgements

This research was initially funded by the Southeastern Sun Grant Initiative through the Fellowship program. The project was also financially supported by the US Department of Agriculture, CSREES Wood Utilization Research.

References

Chen, L., Carpita, N.C., Reiter, W.-D., Wilson, R.H., Jeffries, C., McCann, M.C. (1998). A rapid method to screen for cell-wall mutants using discriminant analysis of Fourier transform infrared spectra," *Plant Journal* 16(3), 385-392.

Dadi, A.P., Schall, C.A., Varanasi, S. (2007). Mitigation of cellulose recalcitrance to enzymatic hydrolysis by ionic liquid pretreatment. *Applied Biochemistry and Biotechnology*. 136, 407-421.

Fort D.A., Remsing, R.C., Swatloski, R.P., Moyna, G., Rogers. R.D. (2007). Can ionic liquids dissolve wood? Processing and analysis of lignocellulosic materials with 1-n-butyl-3-methylimidazolium chloride. *Green Chemistry.* 9, 63-69.

Fu, D., Mazza, G. (2011). Optimization of processing conditions for the pretreatment of wheat straw using aqueous ionic liquid. *Bioresource Technology.* 102, 8003-8010.

Kataoka, K., Kondo, T. (1998) FT-IR microscopic analysis of changing cellulose crystalline structures during wood cell formation. *Macromolecules* 31, 760-764.

Kline, L.M., Hayes, D.G., Womac, A.R., Labbé, N. (2010) Simplified determination of lignin content in hard and soft woods via uv-spectrophotometric analysis of biomass dissolved in ionic liquids. *Bioresources* 5(3), 1366-1383.

Labbé, N., Harper, D., Rials, T. (2006). Chemical structure of wood charcoal by infrared spectroscopy and multivariate analysis. *Journal of Agricultural and Food Chemistry.* 54(10), 3492-3497.

Labbé, N., Kline, L.M., Moens, L., Kim, K., Kim, P.C., Hayes, D.G. (2012). Activation of lignocellulosic biomass by ionic liquid for biorefinery fractionation. *Bioresource Technology* 104, 701-707.

Lee, S.H., Doherty, T.V., Linhardt, R.J., Dordick, J.S. (2009). Ionic liquid-mediated selective extraction of lignin from wood leading to enhanced enzymatic cellulose hydrolysis. *Biotechnology and Bioengineering*. 102, 1369-1376.

Lu, Q., Zhang, Z-F., Dong, C-Q., Zhu, X-F. (2010). Catalytic upgrading of biomass fast pyrolysis vapors with nano metal oxides: An analytical py-GC/MS study. *Energies*. 3, 1805-1820.

Martens, H., Naes, T. 1989. *Multivariate Calibration.* New York: Wiley.

NREL (2008a). “Determination of extractives in biomass.” *Biomass Program Analysis Technology Teach Laboratory Procedure, National Renewable Energy Lab* (NREL/TP-510-42629).

NREL (2008b). “Enzymatic saccharification of lignocellulosic biomass.” *Biomass Program Analysis Technology Teach Laboratory Procedure, National Renewable Energy Lab* (NREL/TP-510-42629).

NREL (2008c). “Determination of structural carbohydrates and lignin in biomass.” *Biomass Program Analysis Technology Teach Laboratory Procedure, National Renewable Energy Lab* (NREL/TP-510-42629).

Rutkowska, E.W., Wollboldt, P., Zuckerstätter, G., Weber, H.K., Sixta, H. (2009) “Characterization of structural changes in lignin during continuous batch kraft cooking of *Eucalyptus globulus*, Bioresources 4(1), 172-193.

Stark, A. (2011) Ionic liquids in the biorefinery: a critical assessment of their potential. *Energy and Environmental Science*. 4, 19-32.

Swatloski, R.P., Spear, S.K., Holbrey, J.D., Rogers, R.D. (2002). Dissolution of cellulose with ionic liquids. *Journal of American Chemical Society.* 124, 4974-4975.

Wang, X., Li, H., Cao, Y., Tang, Q. (2011). Cellulose extraction from wood chip in an ionic liquid 1-allyl-3-methylimidazolium chloride (AmimCl). *Bioresource Technology.* 102, 7959-7965.

1.6
Comparison of Lignin and Carbohydrate Analysis Using Pyrolysis-Molecular Beam Mass Spectrometry, Pyrolysis-Gas Chromatography Mass Spectroscopy and Wet Chemistry

Tina P. Thomas[1, 2], Will Rottmann[3], Maud Hinchee[3], Robert Sykes[4], Jung-Der Chung[5], Parastoo Azadi[1, 2] and C.J.Tsai [6]

Extended Abstract

Biomass Characterization

Cell wall mainly consists of cellulose, hemicelluloses and lignin. Cellulose is a homogenous polymer made up of β-1, 4-glucan chains in a linear fashion (McKendry, 2002). It is the most abundant polysaccharides, accounting for 40-50% of biomass. Hemicelluloses are heterogeneous polymers of pentoses, hexoses, and some uronic acids (Saha, 2003). It is the second most abundant polysaccharides which comprises 20-35% of biomass. Lignin, the major impediment to lignocellulosic biomass utilization, is made up of *p*-hydroxyphenyl (H), guaiacyl (G) and/or syringyl monomers, depending on the species, via a complex suite of ether and carbon-carbon linkages (Bocchini et al., 1997). Lignocellulosic materials in plants have conventionally been determined by acid hydrolysis and then measured by gravimetric method for lignin content, and by chromatographic method for carbohydrates. Determination of lignin structure relies on thioacidolysis degradation followed by chromatographic and mass spectrometric analysis. Although well established, these procedures are time and labor-intensive and require large amount of tissues. Analytical tools have been developed to improve the throughput and speed of lignin and carbohydrate analyses while reducing the input sample size (Agblevor et al., 1994; del Río et al., 2007; Fahmi et al., 2007; Rodrigues et al., 1999).

Analytical pyrolysis, which thermally degrades polymers into smaller fragments, can be coupled with various mass spectrometry (MS) techniques to provide both a "fingerprint" and an in-depth structural analysis of biomass. Pyrolysis Gas Chromatograph Mass Spectrometry (py-GCMS) has been used and shown to be a reliable analytical technique for the characterization of biomass. In this method, samples were pyrolyzed and the analytes separated by GC and fragmented by MS according to its molecular weight. It requires less than 1 mg of biomass and ~ 1 hr/sample run time, dependent on the type of column used in GC. A related method, pyrolysis Molecular Beam Mass Spectrometry (py-MBMS), couples a pyrolyzer to a specialized MS for direct analysis of pyrolyzed biomass without chromatography separation. As such, it affords an even higher throughput, more than 200 samples per day, and is highly amenable to screening of large number of samples.

In the current study, we compared the py-MBMS, py-GCMS and wet chemistry methods for analysis of total lignin content, monolignol (S-, G- and H-subunit) composition and carbohydrates (C5 and C6 sugars). *Populus*, *Eucalyptus* and *Pinus* wood samples, including reaction wood, with a wide range of lignin and carbohydrate contents and monolignol composition were used for the comparison. The results showed that lignin and monolignol contents can be determined using py-MBMS that requires less than 2 minutes run time per sample. Samples which have varying lignin content and/or S/G ratio can be easily discerned using multivariate analysis. The data analysis showed that S/G ratio data from py-MBMS are comparable with those obtained by py-GCMS, although the former may not reliably detect the H units, commonly found in conifers and grasses, due to matrix effects. Thus, biomass samples with different cell wall composition can be easily identified by py-MBMS, whereas py-GCMS is recommended when a higher-resolution analysis of the lignin structure is desired. Using both analytical tools, we were able to identify different monomeric lignin compounds and their corresponding fragmentation patterns from a range of species and tissues for profiling or in-depth analysis of lignin composition.

Glycosyl composition analyses, mainly hemicelluloses, were performed by GCMS on the monosaccharide methyl glycosides produced from the sample by acidic methanolysis, followed by trimethylsilyl (TMS) derivatization. This was then compared with the hemicellulose peaks (C5) obtained from py-MBMS. Comparable results were obtained for most of the *Populus* wood samples tested. The analysis also showed clear hemicellulose compositional differences between straight wood and tension wood samples of *Populus*. Composition analysis using TMS derivatives has its own advantage in separating out monosaccharides with similar molecular weight, such as C5 (arabinose, xylose and ribose) and C6 (rhamnose and fucose, glucose, mannose and galactose) sugars that may not be resolved by the pyrolysis techniques. Thus, further investigation is required for mono, oligo and polysaccharide determination by pyrolysis techniques.

This study shows that py-MBMS is well-suited as a high throughput screening platform, and that a multi-pronged approach is necessary for in-depth analysis of biomass samples with unusual characteristics. Cellulosic determination has to be further compared with different wet chemistry methods for more precise determination. The py-MBMS and py-GCMS facility is supported by the Bioenergy Systems Research Institute and the Complex Carbohydrate Research Center at the University of Georgia, and offers analytical services for biomass characterization to the bioenergy community.

References

Agblevor F, Evans R, Johnson K. Molecular-beam mass-spectrometric analysis of lignocellulosic materials: I. Herbaceous biomass. Journal of Analytical and Applied Pyrolysis (1994) 30:125-144.

Bocchini P, Galletti G, Camarero S, Martinez A. Absolute quantitation of lignin pyrolysis products using an internal standard. Journal of Chromatography A (1997) 773:227-232.

del Río JC, Gutiérrez A, Rodríguez IM, Ibarra D, Martínez ÁT. Composition of non-woody plant lignins and cinnamic acids by Py-GC/MS, Py/TMAH and FT-IR. Journal of Analytical and Applied Pyrolysis (2007) 79:39-46.

Fahmi R, Bridgwater A, Thain S, Donnison I, Morris P, Yates N. Prediction of Klason lignin and lignin thermal degradation products by Py–GC/MS in a collection of *Lolium* and *Festuca* grasses. Journal of Analytical and Applied Pyrolysis (2007) 80:16-23.

McKendry P. Energy production from biomass (part 1): overview of biomass. Bioresource technology (2002) 83:37-46.

Rodrigues J, Meier D, Faix O, Pereira H. Determination of tree to tree variation in syringyl/guaiacyl ratio of *Eucalyptus globulus* wood lignin by analytical pyrolysis. Journal of Analytical and Applied Pyrolysis (1999) 48:121-128.

Saha BC. Hemicellulose bioconversion. Journal of industrial microbiology & biotechnology (2003) 30:279-291.

2 BIOMASS LOGISTICS

2.1
SENSING MISCANTHUS STEM BENDING FORCE AND SWATHED BIOMASS VOLUME TO PREDICT YIELD

Sunil K. Mathanker[1,], Alan C. Hansen[1], Tony E. Grift[1], K. C. Ting[1]*

Abstract

Real time yield sensing has the potential to control the working of harvesting machinery and to generate yield maps. Miscanthus, a promising bioenergy crop, can be harvested using traditional hay and forage equipment with minor modifications. A push bar is used on harvesting machines to bend and deflect miscanthus stems prior to cutting. It is hypothesized that the force exerted by the push bar to bend the miscanthus stems is a good predictor of the biomass yield. To measure the exerted bending force, load cells were mounted on the push bar of a disk mower-conditioner. Similarly, it was hypothesized that the swathed biomass volume, formed as a result of mower-conditioner operation, is also a good predictor of the biomass yield. To measure the swathed biomass volume, a LIDAR (Light detection and ranging) sensor was used to scan the swath cross-sectional profile. The tests were conducted for three yield levels and repeated thrice. Both sensing systems were able to sense low, medium, and high yield levels. Further analysis is underway to correlate the sensed data with the yield. Further studies are needed to improve the calibration of the sensing systems, to test the systems at varied ground speeds, and to extend the concept to other crops: corn stover, energycane, sweet sorghum, sugarcane, and willow. It is expected that the integration of developed yield sensing systems with the existing harvesting machinery would improve their work rate and reduce the biomass harvesting cost.

Keywords: yield sensing, yield maps, miscanthus, harvesting, mowing, baling, biomass, bioenergy

Introduction

To reduce dependence upon fossil fuels and to provide an alternative to liquid transportation fuels, the Energy Independence and Security Act (2007) mandates production of 16 billion gallons of cellulosic ethanol by 2022 (US DOE, 2011). To achieve this goal, there is a need to improve the biomass to ethanol conversion efficiency. Similarly, there is a need to increase biomass productivity and reduce biomass delivery cost.

To increase the biomass productivity many bioenergy crops are being investigated. Miscanthus is emerging as a promising bioenergy crop because of its higher productivity and low input requirement (Heaton et al., 2008). Currently, traditional hay and forage machinery are being investigated to harvest miscanthus and there is scope for efficiency improvements. Miscanthus harvesting consists of mowing with a disk mower-conditioner and then baling with a square baler. The miscanthus stems are tall and hard to cut (Huisman and Kortleve, 1994; Johnson et al., 2012; and Liu et al., 2012). The stiff miscanthus stems do offer the possibility to use them as a yield proxy.

A push bar is used to bend the miscanthus stems to facilitate the cutting. The bending force exerted by the push bar or the bending resistance offered by the miscanthus stems while harvesting depends on the miscanthus stem diameter, stem density, and stiffness of the stem rind. It could be hypothesized that the miscanthus stem bending force is proportional to the biomass

---

[1] *Department of Agricultural and Biological Engineering, University of Illinois at Urbana-Champaign, IL*

* *Corresponding author*

yield. Similarly, after the crop has been windrowed by a mower-conditioner then the swathed biomass volume could also be a good predictor of the biomass yield. The swathed biomass volume per unit area would be higher for high yield levels and lower for low yield levels.

Considering the potential of the miscanthus, it was selected as a target crop to evaluate real time yield sensing to control the harvesting machinery such that the material flow rate through the machine becomes a constant. For example, the operator can reduce the ground speed to account for higher incoming biomass or increase the ground speed to account for lower incoming biomass. However, there are no yield sensing methods to sense the miscanthus yield in real time (Maughan et al., 2012). A real time yield sensor capable of sensing the biomass yield just in front of the machine could be an invaluable tool to improve the machine work rate. The objectives of this study were to evaluate two yield monitoring concepts under field conditions, 1) a bending force measurement system and 2) a swath volume measurement system.

Materials and Methods

The experiments were conducted in a fourth year miscanthus plantation at the Bioenergy Farm, University of Illinois at Urbana-Champaign, Urbana, IL USA (40.0686 N, 80.2015 W). A self-propelled disk head mower-conditioner (Model H8080, New Holland, PA) was used for mowing and conditioning the miscanthus crop. The disk mower-conditioner operation consisted of bending the miscanthus stems with a front mounted push bar (fig. 1), cutting the bent stems with the rotating blades mounted on the disks, conveying the severed stems through the conditioning rollers, and finally releasing the conditioned biomass while forming a swath. Three S type 445 N load cells (Transducer Techniques, Temecula CA) were mounted in between the mower-conditioner push bar and another metal pipe (fig. 1). The combined load cell output was sampled at 300 Hz and averaged at one second intervals. Similarly, a LIDAR (Model LMS 291, SICK, Waldkirch, Germany) sensor scanned the swathed biomass profile at one second intervals. The LIDAR scan range was set to 180^0 with a resolution of 0.5^0. A RTK GPS (Real time kinematic, Global positioning system) was used to record the latitude and longitude of these data points.

(a) (b)

Figure 1. Sensing systems to measure (a) the miscanthus stem bending force; (b) the swathed biomass volume.

After the mowing operation, a square baler (Model BB9080, New Holland, PA) was used to collect the swathed biomass. The square baler was equipped with a yield monitoring system. It recorded the GPS the locations where the bale formation was completed and also the bale weight. The tests were conducted for three yield levels: low yield (< 14 t ha^{-1}), medium yield (14-20 t ha^{-1}), and high yield (> 20 t ha^{-1}) and repeated three times.

Results and Discussion

The miscanthus stem bending force and the swathed biomass volume sensing systems were mounted on a disk mower-conditioner (fig. 1). The bending force and the swath cross-sectional profile were recorded at one second intervals. Figure 2 shows the locations of these data points (blue dots) in the miscanthus fields. The red squares show the locations where a specific bale formation was completed. The corresponding number shows the bale identification number assigned by the yield monitor fitted to the baler.

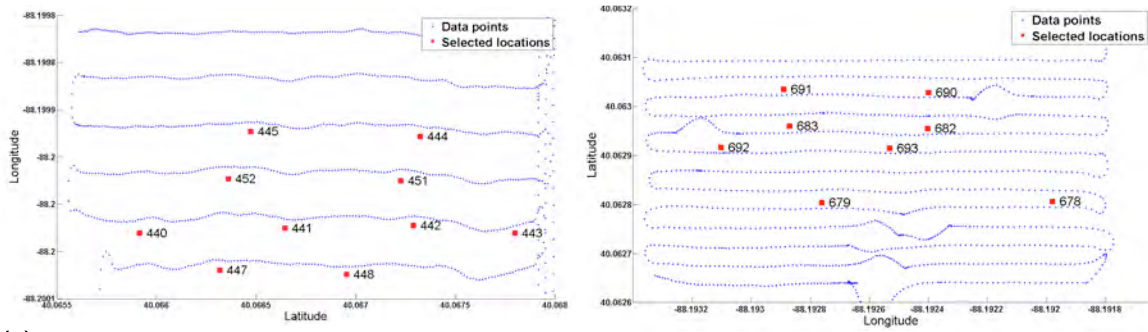

(a) (b)

Figure 2. Field locations of bending force and swathed biomass volume data points (blue dots) and bale locations (red squares): (a) plot 1, and (b) plot 2.

A bale completed in a single row was treated as one test. The area from which a bale was formed varied from 200 m^2 for high yield levels to 500 m^2 for low yield levels. A bale was assumed to be formed from a low yield level area, if the distance between consecutive bale locations was more than 65 m. Similarly, if the distance was less than 50 m then from a high yield level area and if the distance was between 50 to 65 m then from a medium yield level area. The distance between two consecutively numbered bales was calculated using their respective GPS locations. This distance multiplied by the effective cutting width of the disk mower-conditioner gave the field area from which the biomass was collected to form that specific bale. The bale weight divided by the area gave the yield per unit area.

The sensed cross-sectional swath profile at each one second interval was used to calculate the profile area. The distance between two consecutive profile scans and their profile areas were then used to calculate the biomass volume using the trapezoidal formulae. The calculations were performed using ‘trapz’ function in Matlab (Mathworks, Natick MA). These calculated individual biomass volumes were then added to obtain the total biomass volume between the two consecutive bales. Similarly, bending force recorded at each one second interval between the selected consecutive bales were added to determine the accumulated bending force exerted by the miscanthus stems in forming that specific bale. The consecutive bale locations selected for analysis are given in table 1.

Table 1. Selected bale identification numbers representing selected yield levels.

Test no.	Consecutive bale numbers		
	Low yield (< 14 Mg ha^{-1})	Medium yield (14 - 20 Mg ha^{-1})	High yield (>20 Mg ha^{-1})
1.	440 – 441	447 – 448	682 – 683
2.	444 – 445	662 – 663	690 – 691
3.	451 – 452	678 – 679	692 – 693

Figure 3a shows the sensed swathed biomass volume and corresponding yield. It is evident that the sensed swathed biomass volume correlated with the yield levels. The low yield levels could easily be distinguished from the medium and the high yield levels. Figure 3b shows the sensed bending force and corresponding yield. It is evident that the higher yield levels exerted higher bending forces and it was possible to distinguish low yield levels from the medium and the higher yield levels. More sensed data is being analyzed in detail to develop a correlation model.

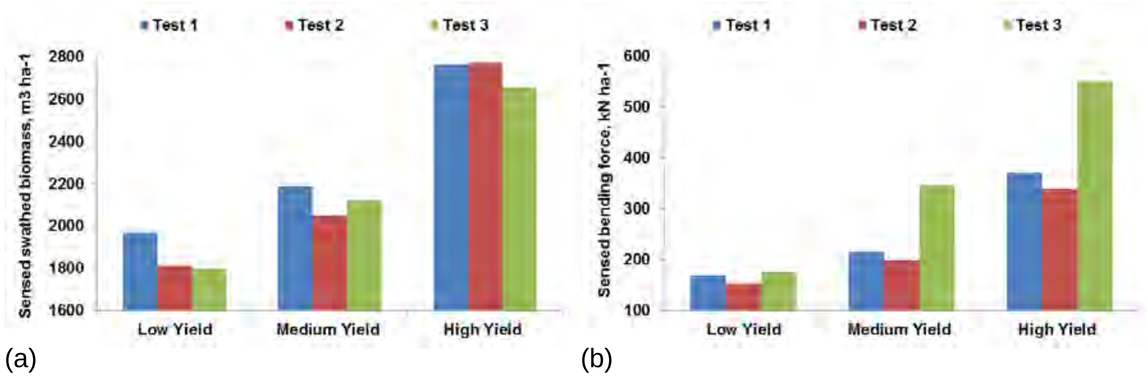

Figure 3. Yield levels and corresponding sensed (a) swath biomass volume and (b) bending force.

The sensed stem bending force and the sensed swathed biomass volume could be used to control a mower-conditioner and a baler. Load cells mounted on the push bar can detect the biomass yield 1.5 m in front of the rotating cutting disks of the mower-conditioner. This sensed bending force can be used to adjust the ground speed of the mower-conditioner so as to match its designed throughput rate to the incoming biomass rate. It would result in higher ground speed in low yielding sections of a field plot. The sensed bending force can also be used to adjust conditioning rollers to obtain the uniform conditioning. It would reduce the potential choking of balers experienced in baling miscanthus. Similarly, the LIDAR sensor can be mounted in front of a baler and the sensed swathed biomass volume can be used to adjust the ground speed. In conclusion, use of the developed yield sensing systems could result in a higher work rate and reduced biomass harvesting cost.

In addition, the sensed data in conjunction with the GPS locations could be used to generate yield maps. The stem bending force sensing system could be extended to other thick stemmed crops: corn stover, energycane, sugarcane, sweet sorghum, and willow. The swathed biomass volume sensing system could be applied to any hay, forage, and bioenergy crop requiring baling: alfalfa, corn stover, prairie grass, switchgrass, and willow. However, there are challenges that still need to be overcome such as more accurate calibration methods, determination of correlation between the sensed data and the biomass yield for varied yield levels, and the effect of ground speed on the sensing accuracy.

Conclusions

A miscanthus stem bending force sensing and a swathed biomass volume sensing concepts were developed to predict miscanthus yield in real time. The results indicated that low, medium and high levels of miscanthus yield could be sensed under field conditions. Efforts are underway to correlate the sensed data with the miscanthus yield. Further studies are needed to develop the sensing systems and to extend them to other crops: corn stover, energycane, sweet sorghum, sugarcane, switchgrass, and willow. Integration of the yield sensing systems with existing harvesting machinery could improve machine work rate and reduce biomass harvesting costs.

Acknowledgement

The authors would like to thank Tim Mies and Justin Maughan for fabricating the fixtures for sensor mountings, Phillip Johnson for help in integrating the LabVIEW program, and Andy Wycislo in harvesting the miscanthus crop. This study was funded by the Energy Biosciences Institute (EBI) within a program titled “Engineering Solutions for Biomass Feedstock Production.”

References

DOE. (2010). 2010 Annual energy outlook 2010. Washington, DC: U.S. Department of Energy, Energy Information Administration, Office of Integrated Analysis and Forecasting. http://www.eia.gov/oiaf/archive/aeo10/index.html Accessed 04.08.11.

Heaton, E. A., F. G. Dohleman, and S. P. Long. 2008a. Meeting U.S. biofuel goals with less land: The potential of Miscanthus. *Global Change Biol.* 14(9): 2000-2014.

Huisman, S. A., and W. J. Kortleve. 1994. Mechanization of crop establishment, harvest, and post-harvest conservation of Miscanthus sinensis giganteus. *Ind. Crops and Products* 2(4): 289-297.

Liu, Q., S. K. Mathanker, Q. Zhang, and A. C. Hansen. 2012. Biomechanical properties of miscanthus stems. *Trans. of the ASABE*, 55(4): (In press)

Maughan, J. D., S. K. Mathanker, S. K., T. E. Grift, and A. C. Hansen. 2012. Yield monitor and mapping systems for hay and forage harvesting: A review. ASABE Meeting Paper No. 121338184. St. Joseph, Mich.: ASABE.

Johnson, P. C., C. L. Clementon, S. K. Mathanker, T. E. Grift, and A. C. Hansen. 2012. Cutting energy characteristics of miscanthus stems with varying oblique angle and cutting speed. *Biosystems Engineering*, 112:42-48.

2.2
EVALUATION OF A MODULAR SYSTEM FOR LOW COST TRANSPORT AND STORAGE OF HERBACEOUS BIOMASS

Stephen Searcy[1,], Brandon Hartley[1], Alex Thomasson[1]*

Abstract
A major challenge for the developing biofuels industry is the delivery of high quality biomass feedstock at the lowest possible cost. Desirable characteristics of a biomass logistics system would be the ability to maximize the dry matter portion of total mass transported while accommodating a range of material moisture content at the time of collection, minimize the number of machines and operators in the system, rapidly load and unload maximum legal truckload quantities, provide an opportunity for distributed storage locations and minimize the total cost of conversion ready feedstocks. Logistics systems based on existing forage or silage systems have difficulty meeting some or all of these characteristics, particularly for high yielding energy crops.

A conceptual system adopting features from cotton, silage and container shipping systems has been evaluated since 2009. The evaluation included both simulation of the anticipated full-scale system and field trials of forming, transporting and storing biomass modules with energy sorghum, switchgrass and corn stover. When compared to the DOE target for logistics costs of $38.59/Mg, the estimated cost was lower for distances up to 80 km. Field results have been promising, with biomass modules of up to 5.2 Mg formed, stored for 3-12 months, loaded on a truck in two minutes or less, and transported for 96 km with no significant degradation. The manually formed modules packages were not able to maintain an anaerobic environment, and degradation occurred. It is expected that negative results for the conceptual system can be overcome with design.

Keywords: logistics, herbaceous, lignocellulosic, module, anaerobic storage, IBSAL, sorghum

Biomass Logistics Challenges
The development of logistics systems to provide feedstocks to a developing biofuels industry has been widely recognized as a challenge that must be overcome if the industry is to develop as desired. USDOE (2011) projects a baseline scenario of 602,000,000 dry tons of a resource at $60.00 per dry ton in 2022. Of that material, a plurality (282 million dry tons) is expected to come from high yielding energy crops. Herbaceous materials are sufficiently distinct from woody biomass and municipal waste to justify the development of unique unit operations that take advantage of material characteristics. Efforts undertaken at Texas A&M University have targeted a logistics system for energy crops grown in the humid southeast region. The following material describes the status of efforts to develop an optimized logistics system for these conditions. Although addressing the specific challenges of energy crops grown in the south, the system has potential application for crop residues in regions where moisture content cannot be controlled at harvest.

Biomass Module Logistics Concept
The logistics concept evaluated was based on successful characteristics of current agricultural materials handling systems. Forage harvesters used for silage are high capacity machines that produce small particle sizes with a minimum of energy, but require support vehicles, resulting in high labor costs and loss of operating efficiency. Anaerobic packaging of chopped biomass in

[1] *Biological and Agricultural Engineering Department, Texas A&M AgriLife Research, TX*

* *Corresponding author*

plastic bags provides storage with low dry matter loss (Shinners, *et al.*, 2011), but the large bags prevent the transport of the biomass in a densified form. The cotton module system provides an effective means of packaging the harvested material for mechanical transport, and decoupled the harvest and ginning operations. In recent years, cotton harvesters that package the harvested material on-board the machine have improved efficiency and reduced labor requirements. The container shipping industry demonstrated the ability to handle and mover large quantities of materials efficiently and at minimal cost. The biomass module concept described here is a combination of the desirable characteristics of these systems.

The system as envisioned will require the design of function-specific machines that do not exist today. This system would include the following machines or unit operations.

- Field drying to reduce moisture content (mow/condition, rake)
- Field chop to small particle size (self-propelled forage harvester)
- Package biomass for anaerobic storage (densification, sealing in air-tight barrier)
- Local transport and loading of modules (transport within field, load on trailers)
- Highway transport (flat-bed semi-trailers)
- Unload at biorefinery (same machine as local transport)

Simulation of Biomass Module System

The proposed biomass module logistics concept was evaluated by computer simulation. Integrated Biomass Supply Analysis and Logistics (IBSAL) is a simulation framework developed by the Oak Ridge National Laboratory to address various biomass logistics systems based on a discrete-event simulation. Previous studies used IBSAL (Sokhansanj et al., 2006; Kumar and Sokhansanj, 2007) to evaluate alternative logistics systems. IBSAL provides elements to model commercially available machines and unit operations. However, several machines not commercially available were required (*i.e.*, a modified forage harvester, a module former, and a module hauler). IBSAL elements to model those conceptual machines were developed.

To determine the potential economic advantages of the biomass module system, it was compared to baling and silage systems in a common scenario. Figure 1 depicts the processes of the three logistics systems. The operations are classified into three categories (*i.e.*, in-field, road-transportation, and in-plant). The in-field operation includes operations from harvesting to field-transportation for delivering crops to local storage sites. The road-transportation covers loading and unloading as well as actual road-transportation. Only the bale system involves a preprocess operation at the plant (i.e., grinding). For this simulation, the field chopping operation was assumed to provide sufficient particle size reduction.

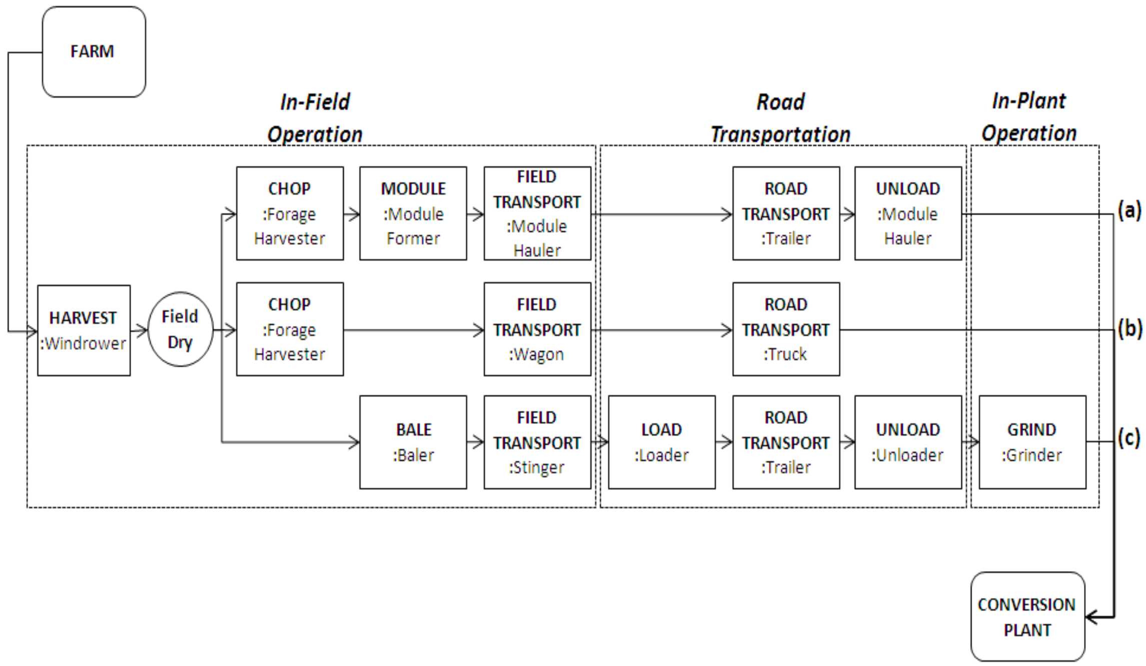

Figure 1. Process diagram for each of biomass logistics systems: (a) biomass module system, (b) silage system, and (c) bale system

The scenario analyzed was supplying 250,000 dry Mg/year of grass-type biomass to a conversion plant near College Station, Texas. Two biomass yield levels were considered (11.2 and 22.4 Mg/ha). The historical weather records for 1992 (near long term mean precipitation of 606 mm) were used. The in-field transportation distance was assumed to be 0.16-0.48 km, and transportation distances of 16, 40, 80, and 161 km were considered. For each set of conditions, the number of machine and labor units was optimized to complete the delivery of the required biomass quantity within the allotted time period at minimum cost.

Logistics costs varied for each system with both yield and transport distance. Table 1 contains the predicted Field and Plant Costs (FPC) and the Transportation Costs (TC). As crop yield increased from 11.2 to 22.4 dry Mg/ha, the total cost decreases in all systems, primarily due to the decrease in FPC. The bale system showed the least impact on the FPC because the grinding operation is not affected by yield.

Table 1. Estimates of costs of biomass logistics systems as a function of transportation distances and crop yield

System	Trans. Distance (km)	Collection & Processing ($/Mg)		Transportation ($/Mg)		Logistics Cost ($/Mg)*	
		11.2 Mg/ha	22.4 Mg/ha	11.2 Mg/ha	22.4 Mg/ha	11.2 Mg/ha	22.4 Mg/ha
Module	16	19.02	12.39	5.28	5.27	**24.30**	**17.66**
	40	19.02	12.39	9.60	9.57	**28.62**	**21.97**
	80	19.02	12.39	16.79	16.75	**35.81**	**29.14**
	161	19.02	12.39	31.17	31.09	50.19	43.49
Silage	16	8.45	4.23	43.12	43.11	51.57	47.34
	40	8.45	4.23	77.67	77.70	86.13	81.93
	80	8.45	4.23	135.23	135.33	143.68	139.56
	161	8.45	4.23	250.46	250.55	258.91	254.78
Bale	16	27.90	24.49	9.70	10.25	**37.60**	**34.73**
	40	27.90	24.49	16.14	17.33	44.03	41.82
	80	27.90	24.49	26.84	29.15	54.74	53.64
	161	27.90	24.49	48.24	52.81	76.14	77.29

*: Bold values meet the DOE goal of $38.59/Mg for logistics costs

The simulation indicated a significant advantage for the biomass module system over bale and silage systems. Based on the DOE target for logistics costs of $38.59/Mg(Hess, *et al.*, 2009), economic feasible was indicated for baling systems with travel distances of 16 km and the module system for distances up to 80 km.

Field Evaluation of Biomass Module Concept

Field studies were conducted in 2009 and 2010 in Burleson County, TX. Two commercial varieties of energy sorghum were used; Ceres ES 5150, a multiple harvests variety, Ceres ES 5200, a single harvest variety. The harvest period was August to January. Two harvest scenarios, twice-cut and once-cut, were followed each year. The logistics unit operations included cutting and windrowing, field curing, raking (2010 only), field chopping and packaging in modules. ES 5150 was harvested under the twice-cut scenario, with the first cutting during August followed by a second harvest in November or later. The ES 5200 harvest began in September and continued through the end of the harvest season each year.

A MacDon M200 self-propelled windrower was used with two different headers: an R80 Rotary Disc header (MD) and an A40-D Auger Header with sickle cutterbar (MA). Once the sorghum was conditioned, a Vermeer R2800 TwinRake was used for windrow manipulation (2010 only). A New Holland FR9080 self-propelled forage harvester (SPFH) with a 3.8 m windrow header (Model 280FP) harvested the windrows.

A modified cotton module builder was used to form the biomass modules. An inner wall was added to shorten the effective operating length of the module builder from 9.75 m to 5.49 m. Creating shorter length modules was done to keep the modules at a manageable weight that could be loaded and transported with a conventional cotton module truck.

Bags made of FeedFresh™ polyethylene plastic (Raven Industries), were designed to fit the inside dimensions of the modified module builder. A bag was placed inside of the module builder before dumping the chopped biomass. Full sized module were 2.13 m to 3.05 m tall. Each load chopped biomass was compressed with the vertical hydraulic system of the cotton module builder. After completing a module, the builder was moved off, leaving the module free standing. A top cover of the same FeedFresh material was placed on top the module and manually sealed with low density polyethylene resin in an attempt to create an air tight seal. Dimensions of the modules were recorded. Module weights were determined by loading with a conventional cotton module truck and transporting each module to a public truck scale.

Evaluation of Field Drying

Two major concerns existed with field drying, the rate of drying and the influence on ash content of the biomass. The ash composition of the standing sorghum stalk fractions were collected at the time of harvest in 2010. Tables 2 and 3 show the average ash composition of the standing crop fractions, and the monthly average for the harvests, respectively. The August cutting of variety ES 5150 was greater than the September and October cutting of ES5200 – energy sorghum – but did not differ from the ash composition of the November cutting. The effect of the variety is confounded with the harvest dates, but appears to have an influence.

Table 2. Average fraction ash composition.

Fraction	Bottom	Middle	Top	Leaf
Ash %	5.8[A]	5.8[A]	7.5[A]	10.7[B]

Numbers connected by the same letters are not significantly different

Table 3. Average monthly ash composition.

Harvest	August	September	October	November
Ash %	9.8[A]	6.5[B]	5.5[B]	7.7[AB]

Numbers connected by the same letters are not significantly different

The August 2010 harvest focused on conditioning the sorghum into various windrow widths – 1.22, 1.83 and 2.44 m – and either invert a single windrow or combine two windrows evaluate impact on drying rate. Several 2.44 m windrows were used as a control without manipulation following conditioning. A 9.4 mm rainfall event was observed two days after conditioning and raking was completed eight days post-cutting, after sampling for the day. The average initial moisture content was 76%, increased slightly to 80% – after rainfall – but dropped to 20% 12 days post-rainfall. The windrow width and windrow manipulation did not significantly impact drying rate. Sample moisture contents were extremely variable throughout the field due to layered drying within the windrows.

An ash analysis was completed on the August harvest. The average ash composition was 10.4%, which compares favorably with the 9.8% ash of the standing crop. Sampling date, raking treatments and their interaction were not significant at the 5% level. The average ash composition of windrows – before and after raking – was not significantly different. A similar analysis was conducted for the September harvest of the ES 5200 variety, with similar results.

Performance of Biomass Modules in Transport

Following storage, modules were loaded with the module truck and taken to the public truck scales to get a post-storage weight. A subset of the modules was then driven on a simulated field–to-plant delivery to evaluate the durability of the modules during transport. One 2009 module and three 2010 modules were transported over a 96 km distance. Module measurements were taken prior to travel and at each 16 km increment of travel.

The percentage of change in module dimension from the pre-transport measurements was determined at each travel increment. The changes in the shape of the module throughout the transport test ranged from -1 to 2%. Prior to conducting the transport test, a settling of the biomass due to road vibration was expected. This pattern did not occur. The rigors of travel did not cause any significant deformations of the modules as they were transported.

Table 4. Module information for modules formed in 2009 and 2010.

Year	Number of Modules	MC range (% w.b.)	DM Content range (Mg)	DM Density range (kg/m³)
2009	7	29.7 - 58.9	3.1 - 5.2	145.8 - 194.1
2010	12	17.2 – 52.6	3.1 – 4.9	125.3 – 188.0

Performance of Biomass Modules During Storage

Modules remained in storage from three to twelve months. Each module was opened, deconstructed, evaluated subjectively for biomass quality and the volume of each quality category was estimated. The moisture content throughout the module was estimated by three different sampling methods, and each was used to estimate the dry matter loss for the module.

Observations of the integrity of the package material indicated that the manual method of sealing the bag was not successful in achieving and maintaining an air-tight package. As a result, degradation of the biomass in the module occurred due to not maintaining the anaerobic environment. Typically, the outer surfaces of the module would have sections of wet, rotted material or a drier, moldy material. Portions of the inner material were found to have essentially the same condition as when the module was formed. Estimates of the portion of the total mass in the original condition ranged from 30 to 87%. Variable moisture levels throughout the module and the inexact nature of estimating the volume of material in each category made estimates of dry matter loss highly variable and suspect.

The inability to maintain the anaerobic environment in the packages resulted in biomass with highly variable moisture levels that would not be acceptable at a biorefinery. The points on the plastic barrier that allowed air transfer were generally at the seam between the top and side walls, and at the seams that were placed under strain. In some instances, handling of the modules caused punctures of the plastic film, but those were minimal. Punctures from birds or other sources were not found to be a problem.

Conclusions and Status of Biomass Module System Development

The biomass module concept has been demonstrated to have potential. Under conservative estimates for the cost and performance of anticipated machines, the use of biomass modules is projected to have a lower cost for delivered material than alternative systems. Field studies using modified cotton equipment proved that the modules can be formed, stored and transported for long distances successfully. The means of forming module package used in the field testing was not able to provide and maintain the desired anaerobic environment, and the resulting biomass degradation was at an unacceptable level.

These results indicate the potential value of the approach of forming anaerobic modules with chopped biomass. The reliance of this proposed system on existing technologies provides confidence in the ability of a successful system to be developed. The design of a new machine to continuously form the modules is the next step in the development of this concept. Other changes needed are redesigns of existing equipment, and are technically feasible with today’s technology.

Acknowledgements
This research was supported by funding made available from U.S. DOE, South Central Sun Grant Program and Texas A&M AgriLife Research. Equipment support was provided by CNH, MacDon, Vermeer and Hlavinka Equipment.

References
Hess, J. R,, Kenney K, L. Ovard, E. Searcy, C. Wright. 2009. Uniform-format solid feedstock supply design report series: commodity-scale production of an infrastructure-compatible bulk solid from herbaceous lignocellulosic biomass, INL/EXT-09-17527. Available at www.inl.gov/bioenergy/uniform-feedstock.

Kumar A., Sokhansanj S., 2007. Switchgrass (Panicum vigratum, L.) delivery to a biorefinery using integrated biomass supply analysis and logistics (IBSAL) model. Biores. Technol. 98,1033-1044.

Shinners, K., A. Wepner, R. Muck and P. Weimer. 2011. Aerobic and Anaerobic Storage of Single-pass, Chopped Corn Stover. BioEnergy Res. 4(1): 61-75.

Sokhansanj S., Kumar A., Turhollow A.F., 2006. Development and implementation of integrated biomass supply analysis and logistics model (IBSAL). Biomass and Bioenergy. 30,838-847.

U.S. Department of Energy. 2011. U.S. Billion-Ton Update: Biomass supply for a bioenergy and bioproducts industry. R.D. Perlack and B.J. Stokes (Leads), ORNL/TM-2011/224. Oak Ridge National Laboratory, Oak Ridge, TN. 227p.

2.3
DETERMINATIONS OF MECHANICAL PROPERTIES OF PELLETIZED BIOMASS AND FUNDAMENTAL MECHANICAL PROPERTIES OF GRANULAR BIOFEEDSTOCK

Hojae Yi[1], Apoorva Karamchandani[1], Virendra M. Puri[1], Daniel Ciolkosz[1]

Abstract
Low bulk density of biomass prevents its optimized usage. Densification is one promising approach that can overcome this issue. Since pelleting machines require relatively low energy input, pelletization is considered a promising densification method. However, the mechanical quality of produced pellets has not been studied using lab/pilot scale pelletizers extensively, which limits scale-up ability to optimize the pelletization process reliably. As the need for renewable bioenergy and bioproducts increases, it is important to establish a foundational knowledge base from which one can engineer efficient supply chain networks and optimum downstream processes. This includes quantification of pellets' quality-related mechanical properties. Since the mechanical properties of densified biomass are a direct consequence of the properties of the raw material, *i.e.* granular biofeedstock, quantitative knowledge of its physical and mechanical properties is essential. The feasibility of relating granular materials' mechanical properties in the low-pressure regime (typically <10 MPa) to the quality attributes of densified compacts was recently established. In this approach, the first step is to determine the fundamental mechanical properties of granular biofeedstock and mechanical properties of densified pellets. Based on the measurements, predictive relationships can be developed and a theoretical explanation for the validity of the relationships can be proposed. The predictive relationship that arises from this approach is a valuable tool for engineering, monitoring, and controlling the quality of densified granular biofeedstock; which is a critical raw material contributing to the expanding bio-based renewable energy industry.

Keywords: Pelletization, Mechanical Properties, Particulate Materials, Biofeedstock, Quality of Pellets

Introduction
For bio-feedstock, densification is an essential step for efficient transportation of biomass from field to point of use. Suboptimized densification poses issues of lower efficiency of the production and lack of quality control, which can translate to significant economic losses. Accordingly, a need exists to implement quality control for efficient utilization of biomass in plants. Toward that end, it is essential to be able to characterize the raw material and final products, namely granulated bio-feedstock and densified biomass, quantitatively. It is well established in the literature that the properties of granular feedstock fundamentally affect the properties of densified biomass (Mittal and Puri, 1999a and b; Pandeya and Puri, 2010 and 2012). However, characterization of granular bio-feedstock and control of quality of densified biomass is not as straightforward as quality control of other materials (de Gennes 1999 and Merrow 2000). It is because of the innate nonlinearity and nonhomogeneity of biomaterials as well as the intrinsic complexity of mechanical behavior of granular materials compared vis-à-vis liquids or solids.

---

[1] *The Department of the Agricultural and Biological Engineering, PA*

* *Corresponding author*

Currently, there have been only a limited number of studies on mechanics of densification of bio-feedstock (Mani *et al.* 2006; Colley 2006; Shaw 2008; Adapa *et al.* 2009; Chevanan *et al.* 2010) However, these studies do not address characteristics of densified biomass in terms of its desired qualities for transportation or downstream bioconversion. Wilson (2010) indicated that a woody pellet's durability depends on the mechanical properties of feedstock rather than its compositional difference. This study is limited to woody materials and did not include comprehensive mechanical property characterization.

Moreover, there is no standardized quality control method of densified biomass with respect to either transportation or bioconversion processes. Because economic competiveness is critical for bioresources, quantification of quality parameters is crucial. This study seeks to bridge this fundamental knowledge gap, which will enable the engineering of densified biomass with optimal characteristics. As a side benefit, but an important one, this will shed light on possible improvements in densification methods. Moreover, standardized quality control will help with improving and maintaining efficiency of the whole processes from harvesting to bioconversion.

The purpose of this study is to determine the low-pressure mechanical properties of ground biofeedstock's as well as the quality attributes of densified biomass created using that feedstock. These quantified properties can then be used develop correlations between mechanical properties of densified biomass and physical and mechanical properties of granular bio-feedstock, using parameters such as size distribution of granules, and granules' shape(s) and density(ies). Once characteristics of densified biomass are identified and the relationship with quantitative mechanical properties of raw bio-feedstock is established, it is possible to establish design parameters for feedstock that result in densified material with desirable traits for transportation and bioconversion processes.

Materials and Methods

Based on the wide availability and current interests in the Northeast United States region three plant species were selected as representative of bio-feedstock sources. These bio-feedstock sources include corn stover (Zea mays), switchgrass (Panicum virgatum) and maple (Acer spp.) and/or oak (Quercus spp.) wood waste. Corn Stover is a reusable waste of a representative field crop, which is widely grown in the northeast and Midwest regions of the US. Switchgrass has been a prime candidate for production of biomass on marginal land. Finally, maple and oak wastes were selected as representative of reusable forest products from the northeast region's hardwood timber industry.

Fundamental physical characteristics of the selected granular bio-feedstock include their density properties and particle sizes. For the density of particulate system, its true or particle density and bulk density of the bulk were characterized. First, particle density was measured by the Quantachrome Multipycnometer using Helium as a pressure medium. The bulk density was measured using with a sample holder of known volume. Particle size distribution was determined using a set of sieves following the ASTM D1921-06 standard (ASTM, 2006).

Determination of the fundamental mechanical properties of granular bio-feed materials is a key to the successful outcome of the proposed study. Because of biological granular material's heterogeneity and nonlinearity, eliminating secondary effects of measurement introduced by the limitations of the instrument is essential. The Penn State's cubical triaxial tester (CTT) is a unique and one of the most relevant instruments for this purpose. The cubical triaxial tester is capable of measuring the true stress-strain behavior of granular materials over a wide range of compression and extension conditions and stress paths without the confounding effect of die-wall friction. A flexible boundary medium pressure CTT was designed and fabricated by Li and Puri (1996). In this tester, the powder sample is contained in a cubical sample chamber, which has dimensions of 25.4x25.4x25.4 mm. Compressed air is used to apply pressure up to 100 KPa on all the six surfaces of cubical sample via the flexible membranes. The use of the flexible membranes eliminates the effect of die-wall friction thereby, permitting the measurement of the true three-dimensional mechanical response.

Data from the CTT will be used to analyze and evaluate the mechanical responses for the determination of the fundamental mechanical properties associated with elastic, elastoplastic, and rate-dependent responses of selected granular bio-feedstock.

First, ground biofeedstock is being processed using Pellet Pros (Model PP 85), a common small-scale pelletizer design that utilizes a flat-plate rotating die design. Axial and diametric strength and friability of the resulting pellets are measured as they are major quality parameters of green compacts in the industry (Pandeya and Puri 2010 and 2012). The axial strength along the long axis of the pellet is determined using an Instron (Model 3345). The diametric strengths of pellets are determined via the splitting test using an Instron according to the ASTM D3967-08 (ASTM, 2008).

Results and Discussion

Since this study is a work in progress, we report preliminary measurements. So far, only ground corn stover and switch grass were pelletized using Pellet Pros (Model PP 85, Complete info of the manufacturer). Figure 1 shows the transformation of bio-feedstock beginning from the raw state to the pelletized stats. The particle density and bulk density of granular corn stover was determined to be 1,460±10 kg/m^3 and 103±1 kg/m^3, respectively. The particle and bulk density of granular switch grass was determined to be 1,360±50 kg/m3 and 141±2 kg/m^3, respectively. The higher particle density of corn stover suggests that corn stover particles may have higher strength than switch grass particles. However, higher bulk density of granular switch grass suggests better initial packing of the ground corn stover.

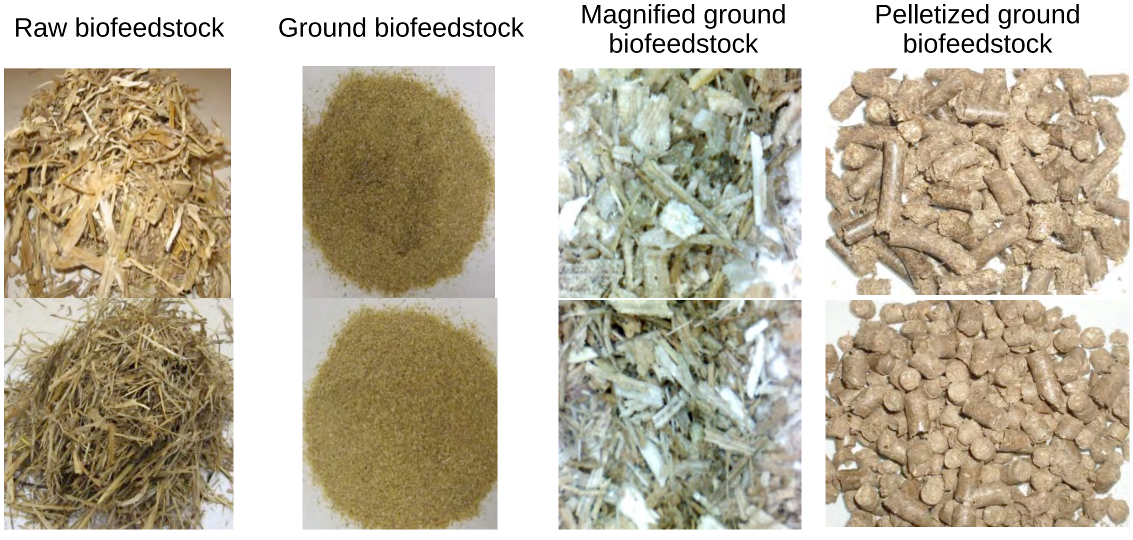

Figure 1. Photographs of biofeedstocks. Pictures of the upper row are corn stover and pictures of the bottom row are switch grass.

The particle size distributions of the ground corn stover and switchgrass is shown in Figure 2. The particle size distributions suggests that particle sizes between ground corn stover and switch grass are almost identical with little larger D_{50} of corn stover. The bulk density of pellet produced with ground corn stover was determined to be 1,270±44 kg/m^3. Compared to the particle density and bulk density of the ground feedstock, one can assess that the pelletization process's compaction is quite substantial.

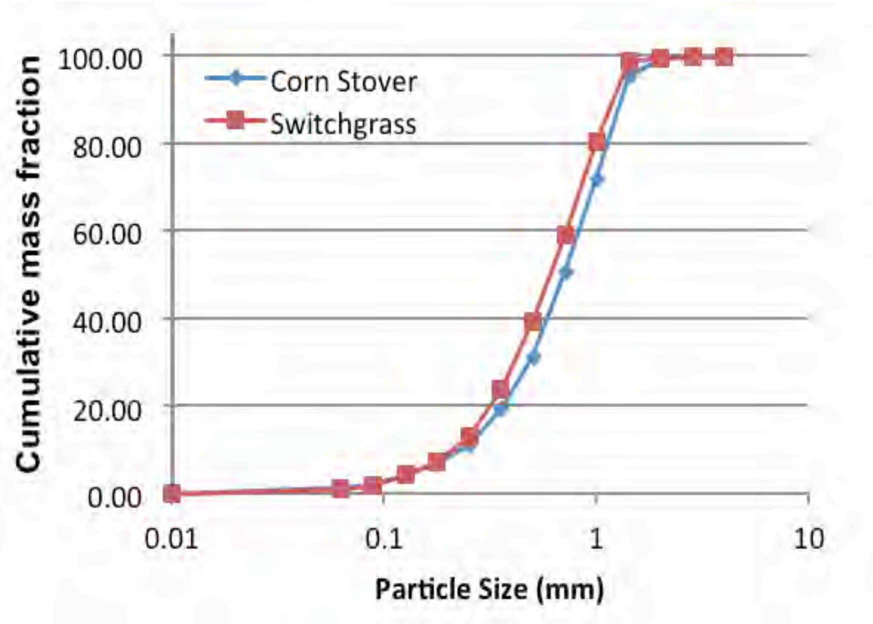

Figure 2. Particle size distributions of the ground corn stover and switchgrass

Axial and diametric strengths were determined with randomly selected corn stover pellets of the mean length of 15.9±3.5 cm and the mean diameter of 5.97±0.05 mm. The axial strength of the corn stover pellet is 10.8±0.8 MPa whereas the diametric strength of the corn stover pellet was 5.4±0.4 MPa. As expected from the nature of pellet formation, we can tentatively conclude that a pellet is weaker in tension than compression from this result.

Concluding Remarks

This study proposes a framework with which one can develop a quantitative equation predicting quality metrics of densified biomass using select mechanical properties of granulated bio-feedstock in early stages of compression. Physical and mechanical properties of those selected bio-feedstock are being measured. Some of the preliminary measurements are reported in this paper.

The higher particle density of corn stover suggests that corn stover particles may have higher strength than switch grass particles. However, higher bulk density of granular switch grass suggests better initial packing of the ground corn stover. We successfully pelletized corn stover with substantial compression with stronger compressional strength than tensile strength.

Based on these quantitative mechanical properties of ground bio-feedstock and quality metrics of pellets, a predictive correlation will be developed and validated. This quantitative correlation will provide a tangible mean to design a densified biomass of desirable quality for transportation and bioconversion processes. Because this relationship is general, the development and validation of this approach can be applied to other raw materials that are grown in other regions of US, North America, and beyond.

References

Adapa, P., Tabil, L., and Schoenau, G. (2009). Compaction characteristics of barley, canola, oat and wheat straw. Biosystems Engineering 104: 335-344.

ASTM Standard D1921, (2006), Standard Methods for Particle Size (Sieve Analysis) of Plastic Materials, ASTM International, West Conshohocken, PA.

ASTM Standard D3967, (2008). Standard Test Method for Splitting Tensile Strength of Intact Rock Core Specimens, ASTM International, West Conshohocken, PA.

Chevanan, N. Womac, A. R., Bitra, V. S. P., Igathinathane, C., Yang, Y. T., Miu, P. I., and Sokhansanj, S. (2010). Bulk density and compaction behavior of knife mill chopped switchgrass, wheat straw, and corn stover. Bioresource Technology 101:207-214.

Colley, Z. J. (2006). Compaction of switchgrass for value added utilization. Master of Science Thesis. Auburn University.

de Gennes, P. G. (1999). Granular matter: a tentative view. Reviews of Modern Physics, 71:S374-S382.

Li, F. and Puri, V.M. (1996). Measurement of anisotropic behavior of dry cohesive and coheionless powders using a cubical triaxial tester, Powder Technology 89:197-207.

Mani, S., Tabil, L. G., and Sokhansanj, S. (2006). Effects of compressive force, particle size and moisture content on mechanical properties of biomass pellets from grasses. Biomass and Bioenergy. 30:648-654.

Merrow, E. W. (2000). Problems and progress in particle processing. Chemical Innovation, 2000 (Jan):35-41.

Mittal, B. and Puri, V. M. (1999a). Correlation between deposition methods, powder compression response and green compact quality: Part I Mechanical properties of powders. Particulate science and technology. 17: 283-300.

Mittal, B. and Puri, V. M. (1999b). Correlation between deposition methods, powder compression response and green compact quality: Part II Compact quality and correlations. Particulate science and technology 17:301-316.

Pandeya, A. and Puri, V. M. (2010). Rate-dependent mechanical properties of dry blended pharmaceutical powder formulations for tableting applications. Powder Technology 207:26-34.

Pandeya, A. and Puri, V. M. (2012). Relationships between tablet physical quality parameters and granulated powder properties. Particulate Science and Technology, 30:482-496.

Shaw, M. (2008). Feedstock and process variables influencing biomass densification. Master of Science Thesis. University of Saskatchewan.

Wilson ,T. O. 2010. Factors affecting wood pellet durability. Master of Science Thesis. Pennsylvania State University.

2.4
IMPROVING BIOMASS LOGISTICS COST WITHIN AGRONOMIC SUSTAINABILITY CONSTRATINTS AND BIOMASS QUALITY TARGETS

Kevin L. Kenney[1,], J. Richard Hess[1], William A. Smith[2], David J. Muth[1]*

Abstract

Equipment manufacturers have made rapid improvements in biomass harvesting and handling equipment. These improvements have increased transportation and handling efficiencies due to higher biomass densities and reduced losses. Improvements in grinder efficiencies and capacity have reduced biomass grinding costs. Biomass collection efficiencies (the ratio of biomass collected to the amount available in the field) as high as 75% for crop residues and greater than 90% for perennial energy crops have also been demonstrated. However, as collection rates increase, the fraction of entrained soil in the biomass increases, and high biomass residue removal rates can violate agronomic sustainability limits. Advancements in quantifying multi-factor sustainability limits to increase removal rate as guided by sustainable residue removal plans, and mitigating soil contamination through targeted removal rates based on soil type and residue type/ fraction is allowing the use of new high efficiency harvesting equipment and methods. As another consideration, single pass harvesting and other technologies that improve harvesting costs cause biomass storage moisture management challenges, which challenges are further perturbed by annual variability in biomass moisture content. Monitoring, sampling, simulation, and analysis provide basis for moisture, time, and quality relationships in storage, which has allowed the development of moisture tolerant storage systems and best management processes that combine moisture content and time to accommodate baled storage of wet material based upon “shelf-life.” The key to improving biomass supply logistics costs has been developing the associated agronomic sustainability and biomass quality technologies and processes that allow the implementation of equipment engineering solutions.

Keywords: biomass feedstock, logistics, harvest, collection, storage, variability analysis

Introduction

The emergent lignocellulosic biofuels industry has adapted agricultural forage and forest logging equipment and practices for the purpose of developing high-tonnage biomass supply systems for biorefining (Hess, Kenney et al. 2009; Searcy and Hess 2010; Perlack and Stokes 2011; Shinners, Digman et al. 2011). High-tonnage biomass logistics development efforts have resulted in much progress with respect to fully understanding and demonstrating the capabilities and limitations of conventional agricultural forage and forestry supply equipment for both herbaceous and woody biomass resources.

Supply system modeling and analyses are instrumental in identifying and quantifying these limitations. Monte Carlo analysis is a common probabilistic analysis method for forecasting a model result based on the uncertainty of model inputs. These techniques have been used in technoeconomic assessments of both biochemical (Aden, Ruth et al. 2002; Humbird, Davis et al. 2011) and thermochemical (Phillips, Aden et al. 2007; Dutta, Talmadge et al. 2011) conversion of

[1] Biofuels and Renewable Energy Technologies

[2] *Biological Systems, Idaho National Laboratory, ID*

* *Corresponding Author*

lignocellulosic biomass to ethanol, as well as feedstock supply system designs (Hess, Wright et al. 2007). A Monte Carlo simulation represents the uncertainty of a result based on aggregated variability of inputs, but it does not distinguish the affects of multiple inputs such that they can be ranked and differentiated according to their impact on the model output.
This is a particular challenge for optimizing biomass supply systems, which, for economic viability must focus on cost reduction, but are also constrained by environmental sustainability and feedstock quality requirements, both of which introduce in-field variabilities that influence and are influenced by logistics parameters. Sustainability and quality constraints underpin the resource supply/demand balance so fundamentally that methodologies are needed to identify not only a system's limitations, but also determine which variables have the greatest potential for cost savings within these constraints.

This paper presents a methodology and approach to quantifying and ranking feedstock supply system variables that affect the delivered feedstock cost according to three statistically-derived parameters: sensitivity, uncertainty, and influence. A discussion of supply chain uncertainty will show that significant variability is introduced when additional metrics—sustainability and quality in this case—impose requirements and limitations on supply chain variables that compete against feedstock cost. Examples of collection efficiency and storage dry matter losses will be presented to support both equipment development and best management practices solutions to reducing uncertainty. This paper further demonstrates and concludes that supply systems that actively manage the uncertainty associated with biomass supply systems will, in the long run, be the most cost-effective and sustainable feedstock logistic systems.

Method for Assessing Uncertainty, Sensitivity and Influence of Feedstock Logistic System Parameters

Analysis Step 1- Defining the model system

A lignocellulosic feedstock logistics system that supplies 800,000 dry matter tons of corn stover to a 60M-gal/yr biochemical ethanol biorefinery was modeled in Microsoft Excel using the methodology documented by Sokansanj and Turhollow (Sokhansanj, Turhollow et al. 2002). The logistics system included raking and baling (large 4x4x8-ft square bales) after grain harvest, collection of bales from the field to a roadside storage stack, transportation of bales to a biorefinery over a 350-day/yr delivery schedule, and preprocessing of bales at the biorefinery to a hammer-milled bulk material ready for insertion into a pretreatment reactor (Hess, Kenney et al. 2009).

Analysis Step 2- Defining Input Parameter Probability Distributions

In order to identify and rank the importance of model input parameters, an analysis was conducted using @RISK, a commercial simulation software package used to solve Excel spreadsheet models for a probable forecasted scenario (@RISK, Palisade Corp., Ithaca, NY; Excel, Microsoft Corp. Redmond, WA). Probability distributions were defined for each model input variable, including biomass resource availability parameters (e.g., grain yield, producer participation, etc.), biomass material property parameters (e.g., moisture content, bulk density, etc.), logistics system parameters (e.g., harvest window, transportation distance, fuel and electricity prices, etc.), machinery performance parameters (e.g., rates, capacities, efficiencies, etc,), and biomass loss parameters (e.g., collection efficiencies, storage losses, etc.). Most input variables were described according to a Pert distribution function, which is commonly used when data to define a distribution is sparse (@RISK, Palisade Corp., Ithaca, NY). A Pert distribution is defined by minimum, mode, and maximum values that are linked in a bell-shaped distribution, and to the extent that the minimum and maximum values are evenly distributed about the mode, this distribution mimics that of a normal distribution. Two input variables—biorefinery daily receiving hours and biorefinery feedstock inventory (i.e, tons of feedstock stored on site)—were defined by a Uniform distribution that assumes all values between the defined minimum and maximum values are equally likely to occur. A Uniform distribution was chosen for these two variables because these parameters are simply a matter of choice.

Minimum, mode and maximum values of the Pert distributions were defined according to our own research data, where available (Hess, Kenney et al. 2009); otherwise, literature data and input from experienced machinery operators, manufacturers and vendors was used. ASABE Agricultural Machinery Management Data (ASABE 2006) was used to define machinery field speeds and efficiencies, repair and maintenance costs, annual operating hours, and estimated lifetime hours. The probability distribution represents either the inherent variability or the uncertainty of the input variables, as determined by the variability in collected field data, published data (e.g., field efficiency and field speed ranges published by ASABE), or range of operating parameters suggested by skilled operators of the equipment. The most likely value included in each distribution is the benchmark value input to the feedstock logistics model (Hess, Kenney et al. 2009).

Analysis Step 3- Perform Deterministic Computations

A Latin Hypercube sampling method was used in the @Risk simulation to generate the input parameter values from the probability distribution functions. This method was chosen over the Monte-Carlo technique, which samples randomly from the distribution function and causes clustering when low probability values are not sampled due to insufficient computational sampling iterations. In contrast, the Latin Hypercube stratified sampling technique systematically samples all segments (stratifications) of the distribution just once, resulting in fewer computational iterations required to produce a representative probability curve.

The analysis was conducted by incrementing each input parameter throughout the defined distribution while randomly varying the remaining parameters according to their own defined probability distributions. Thus, the impact of each parameter on delivered feedstock cost was determined individually, while also capturing the interdependence of the input parameters. Tens of thousands of scenarios were collected in this manner to generate the output shown in Figure 1.

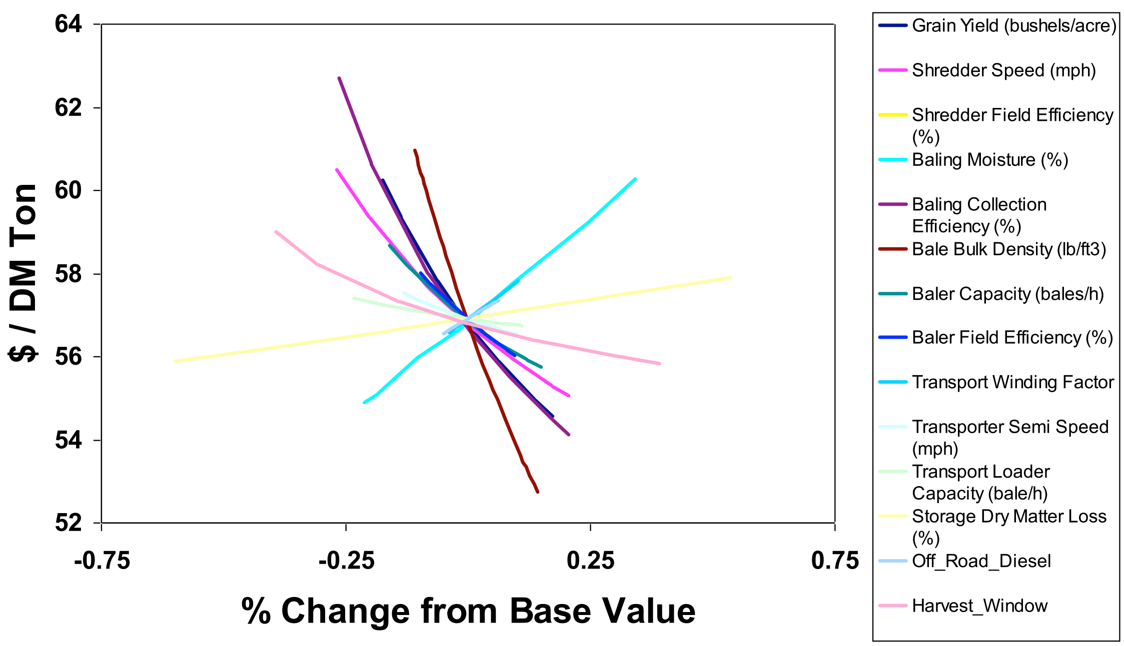

Figure 1. Response of delivered feedstock cost to changes in model input variables.

This @Risk simulation was used to rank input variables based on the statistical relationship between each variable and the delivered feedstock cost. In order to resolve these rankings, the @Risk analysis results were further analyzed to isolate the individual influences with respect to three parameters: sensitivity, uncertainty, and influence (Figure 2). ***Sensitivity,*** a measure of how responsive a unit operation/process cost is to changes in a specific variable, was determined by approximating the slope using a linear regression of each response curve in units of $/ton per % change from the variable's base value.

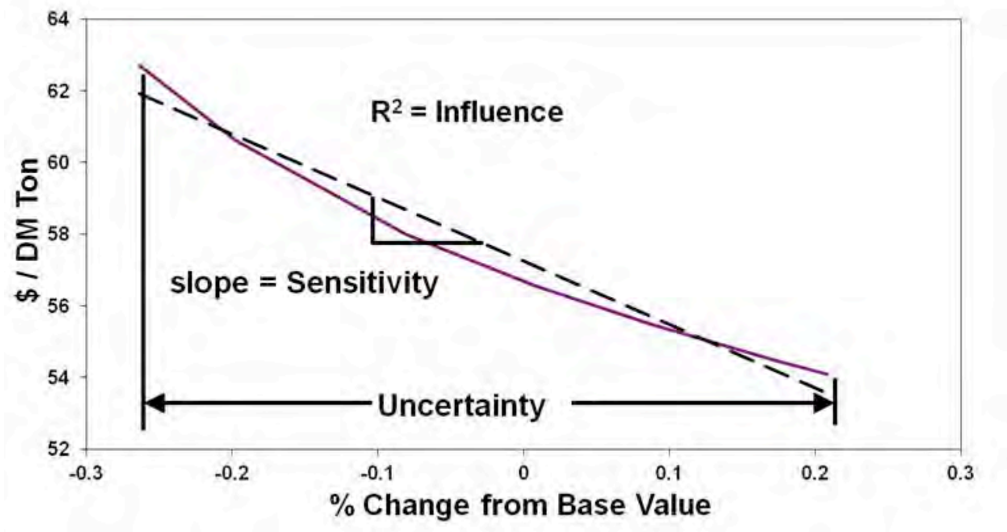

Figure 2. Sensitivity, influence and uncertainty definitions.

Sensitivity alone is not sufficient to rank input variables according to their impact on delivered feedstock cost because while feedstock cost may be highly sensitive to changes in a particular variable, the overall effect may be small if the range of that variable is small. This range or variability of an input variable, termed ***Uncertainty,*** was measured by the horizontal run of the response curve in units of % change from the parameter base value. An additional parameter was included, referred to as ***Influence***, to give preference to those variables that are more influential than others. A parameter's influence is represented by the curvature of the response curve, with greater curvature suggesting greater interdependence (or influence). A parameter's relative influence was estimated as the inverse of the R-squared value derived from a linear regression of the response curve.

Results and Discussion

Independent rankings of input variables according to sensitivity, uncertainty, and influence provided three disparate rankings. Bale bulk density, collection efficiency, and grain yield ranked highest in sensitivity; storage dry matter losses, harvest window, and bale moisture ranked the highest in uncertainty; and harvest window, collection efficiency, and flail shredder field speed ranked highest in influence. A combined normalized ranking was determined by taking the product of sensitivity, uncertainty, and influence and dividing by the highest value (Figure 3). The resulting normalized values show the combined impact of the three parameters—sensitivity, uncertainty, and influence—relative to the input variable of greatest combined effect. The variables shown in Figure 3 were categorized as follows: (1) biomass yield (collection efficiency, grain yield, storage dry matter loss); (2) biomass material properties (bale bulk density, bale moisture); (3) machinery performance (shredder speed, baler capacity, baler field efficiency, semi speed, shredder field efficiency, loader capacity; and (4) system variables (harvest window, transportation distance winding factor—a multiplier applied to the transportation distance input, off-road diesel price).

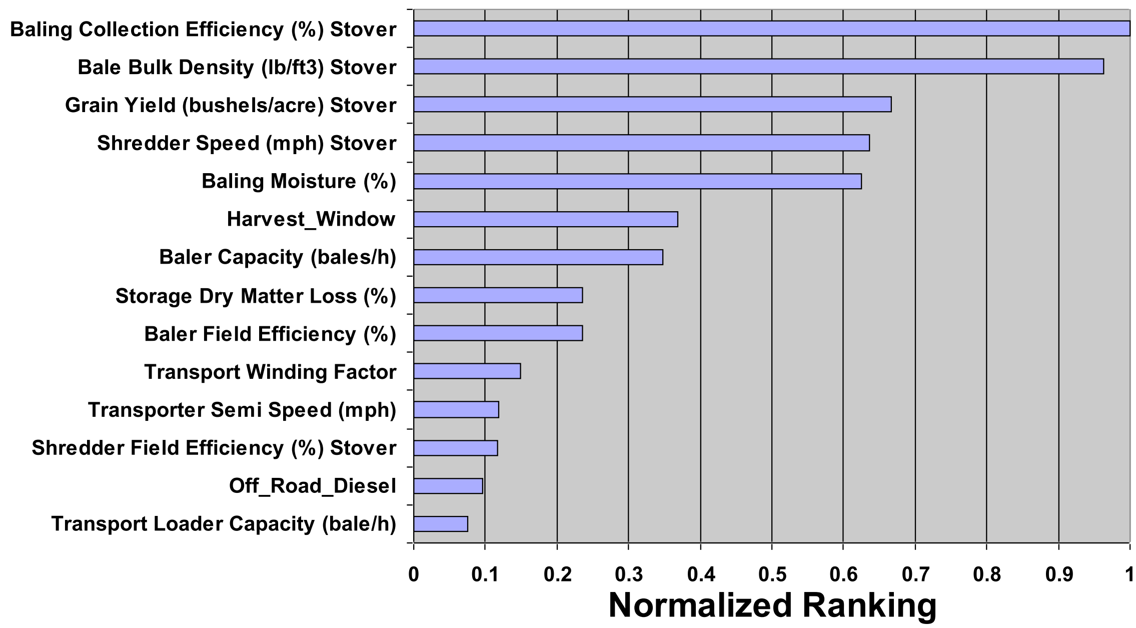

Figure 3. Normalized ranking of model input variables according to combined values of sensitivity, uncertainty, and influence.

Biomass yield variables—those that affect the yield per acre removed--are particularly important since they reside at the front end of the feedstock supply chain and thus have broad impacts that extend through the entire supply chain. In fact, biomass yield affects many of the other variable categories identified in the analysis, including machinery performance and system variables (harvest window and transportation distance). Accordingly, uncertainty of biomass yield variables—particularly collection efficiency and storage dry matter losses—is the focus of the discussion that follows.

Increasing harvest/collection efficiency by responding to in-field variability

Collection efficiency (the ratio of biomass collected to the total amount available in the field) ranked second in sensitivity, fifth in uncertainty, second in influence, and highest in overall combined ranking. The probability distribution for collection efficiency used in this analysis was based on a review of reported corn stover collection efficiencies (Richey, Liljedahl et al. 1982; Shinners, Binversie et al. 2003; Schechninger and Hettenhaus 2004; Shinners and Binversie 2004; Prewitt, Montross et al. 2007) from which we chose a most likely value of 43%, a minimum of 19%, and a maximum of 65%. The wide range of reported results show that current machinery itself is capable of high removal rates, but sustainability (Wilhelm, Hess et al. 2010) and quality (Prewitt, Montross et al. 2007) constraints often dictate deliberately conservative collection efficiencies. Therefore, sustainability and quality constraints are two main sources of uncertainty relating to corn stover collection efficiencies, and reducing feedstock involves solving uncertainty around these two issues.

It has generally been reported that corn stover removal rates of 30–40% could be sustainable over most corn acres (Nelson, Walsh et al. 2004; Gregg and Izaurralde 2010; Perlack and Stokes 2011). However, corn stover removal at a rate of 30–40% is often not economically viable. The emerging biorefining industry has estimated minimum removal rates of 2 dry short tons (DST) per acre for system economics to support corn stover removal operations.

Two management strategies have emerged to deal with this challenge and sustainably achieve a 2-DST/acre removal rate. The first is an equipment development strategy—variable rate residue harvesting—and the second is an agronomic strategy—implementing interval removal schemas (Muth and Bryden 2012). Multi-factor sustainability analyses (Figure 4) has shown that advanced variable-rate harvesting systems capable of responding to subfield variability in topography, soil characteristics, and grain yield could achieve average removal rates as high as 75% (7.69 Mg/ha) without violating sustainability requirements (Muth and Bryden 2012). Interval removal schemas allow conventional equipment to be used to collect corn stover one out of every 2 or 3 years, based on soil erosion and soil organic carbon constraints for an individual field.

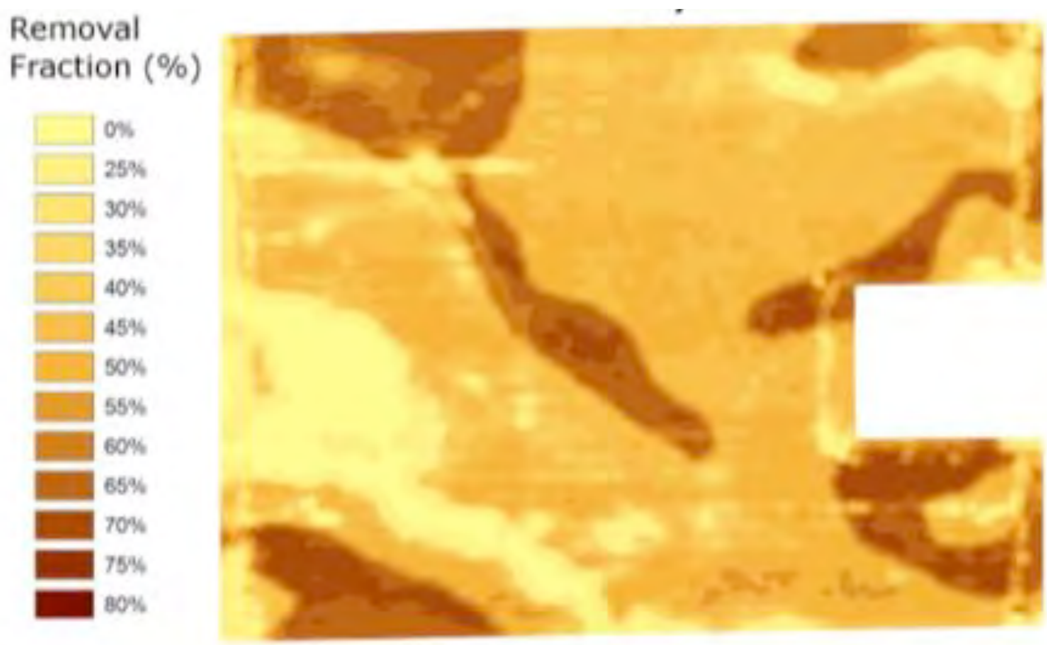

Figure 4. Sustainable sub-field residue harvest plan that varies the removal rate between 0% and 80% (5.6 Mg/ha).

Our own testing has shown that removal rates as high as 80% are attainable with wheel rake, flail shredder, or bar rake windrowers; however, increasing corn stover collection efficiencies with conventional harvest systems tends to reduce stover quality by increasing ash content (Figure 5). The increase in stover ash content—both between equipment and between removal rates—is largely attributed to increased soil entrainment (Prewitt, Montross et al. 2007), but may also be attributed to differences in anatomical composition (Hoskinson, Karlen et al. 2007). Though the dataset is too limited to support specific solutions, it shows that quality is a variable affecting collection efficiency uncertainty, and a priority on low ash content generally necessitates reduced collection efficiencies. The data also shows that an equipment development solution that eliminates a variable from the uncertainty equation, such as a bar rake in this case, is beneficial. Like the sustainability problem, potential solutions exist that include both conventional and advanced harvesting systems. Understanding variable field factors that affect susceptibility of soil to disturbance and entrainment during windrowing may provide a solution for selection and configuration of conventional harvest equipment that can maintain ash content at acceptable levels regardless of removal rate. Ultimately, single-pass harvest systems that eliminate biomass/

ground contact during harvest will provide the best opportunity to remove the quality variable affecting collection efficiencies.

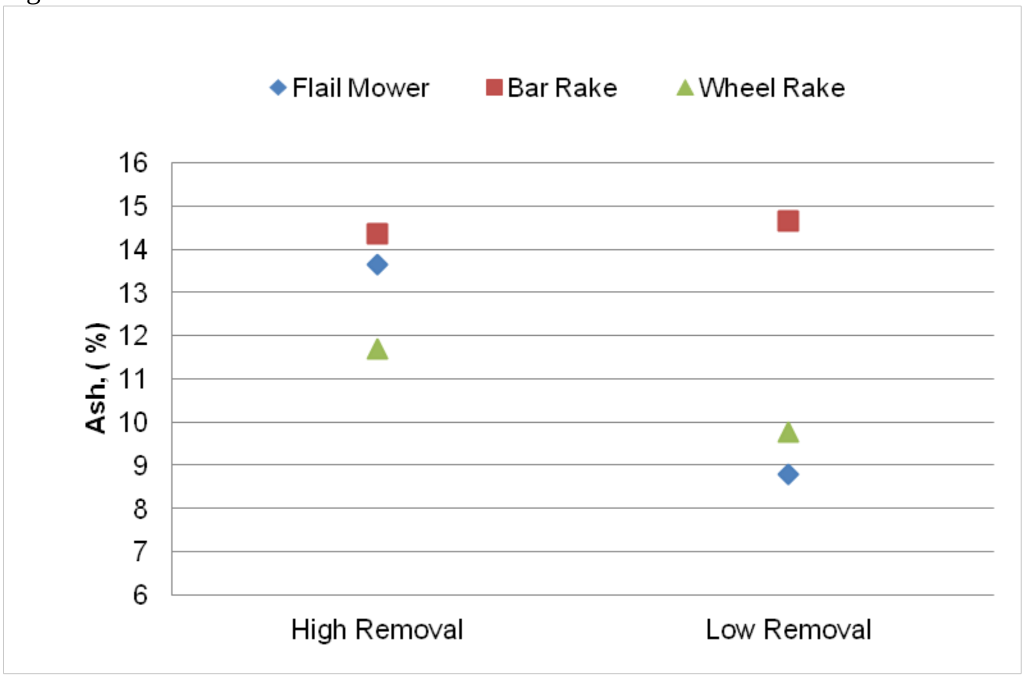

Figure 5. Corn storver large square bale ash content variability due to windrowing machinery and removal rate.

Minimizing Storage Losses by Addressing Moisture Variability

Storage dry matter losses (loss of structural carbohydrates, water-soluble components, lignin, and ash resulting from biological deterioration and/or physical losses in storage) ranked fourteenth in sensitivity, first in uncertainty, twelfth in influence, and eighth in overall combined ranking. The probability distribution for dry matter loss used in this analysis was based on a review (Coble and Egg 1987; Sanderson, Egg et al. 1997; Shinners, Binversie et al. 2007; Shinners, Boettcher et al. 2010) of reported dry matter loss for dry (< 20%, wet basis) aerobic storage, from which we chose a most likely value of 5%, a minimum of 1%, and a maximum of 8%. The range selected actually underestimates the true variability and uncertainty around storage dry matter losses. Storage losses can vary significantly depending on bale moisture, storage method, and environmental conditions during storage; these variables make control and prediction of dry matter loss in storage highly uncertain (Shinners, Binversie et al. 2007; Darr and Shah 2012).

Controlling dry matter losses and reducing uncertainty is highly dependent on moisture management. The ability to field-dry to safe aerobic storage conditions is compromised by often poor, always uncertain, field-drying conditions following the fall grain harvest. This is clearly demonstrated in Midwest corn stover moistures during the 2009 and 2010 feed corn harvest seasons (Figure 6). This annual variability in biomass moisture content presents significant challenges in implementing consistent and reliable storage practices.

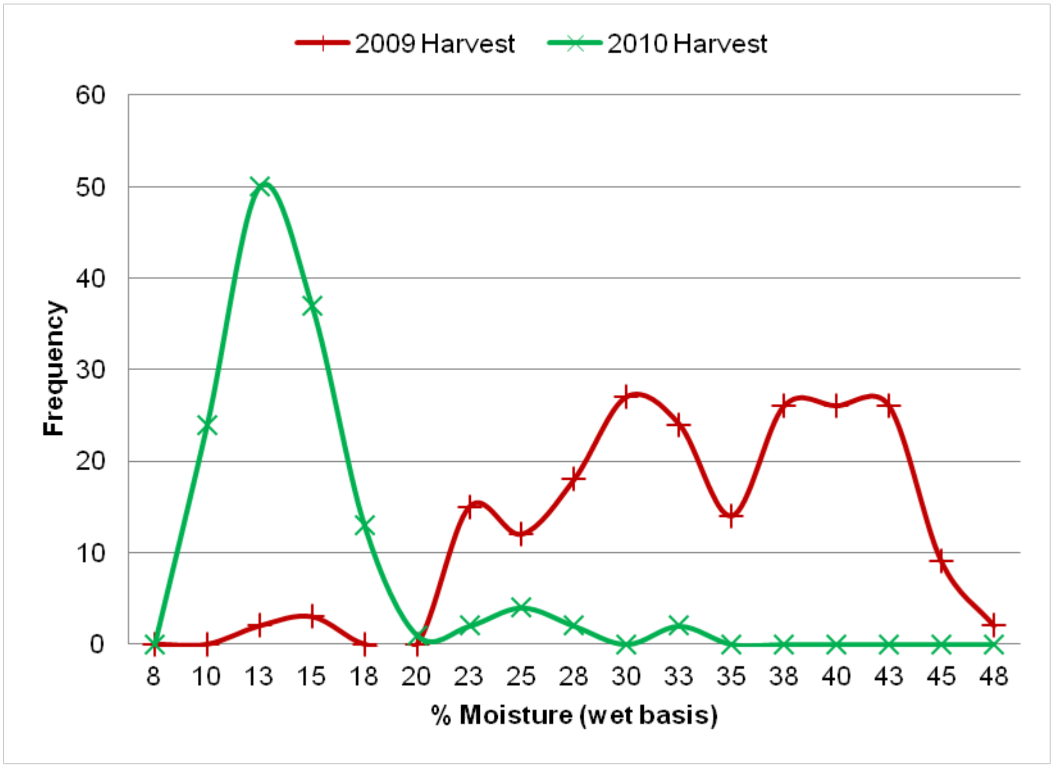

Figure 6. Midwest corn stover harvested in 2009 exceeded moisture limits for stable bale storage, while in 2010 nearly all harvested biomass could be stored stable in conventional stacks.

Proper moisture management does not end in the field. Even with ideal agronomic conditions where the material dries down to safe aerobic storage levels prior to baling, other often subtle differences in storage methods can significantly affect dry matter losses. For example, the orientation of stacks as well as the characteristics of the ground surface on which bales are stacked can greatly affect storage conditions. In a recent INL study, stover bales were found to be more moist on the north-facing side than the south exhibiting up to 40% moisture (wb) differences from side to side (Figure 7). Bottom bales also accumulated more moisture, even when placed on crushed gravel, which was attributed to water running off the tarp and draining towards the stack (Smith, Bonner et al. forthcoming 2012).Thus, bale storage is a dynamic practice with no on-size-fits-all solution. Bales are capable of long-term storage with a proper understanding of the material's condition (moisture content at time of receipt and any past storage information) provided that they are properly managed. The key factors to control are the accumulation of moisture and the timing of this accumulation with respect to environmental conditions in storage.

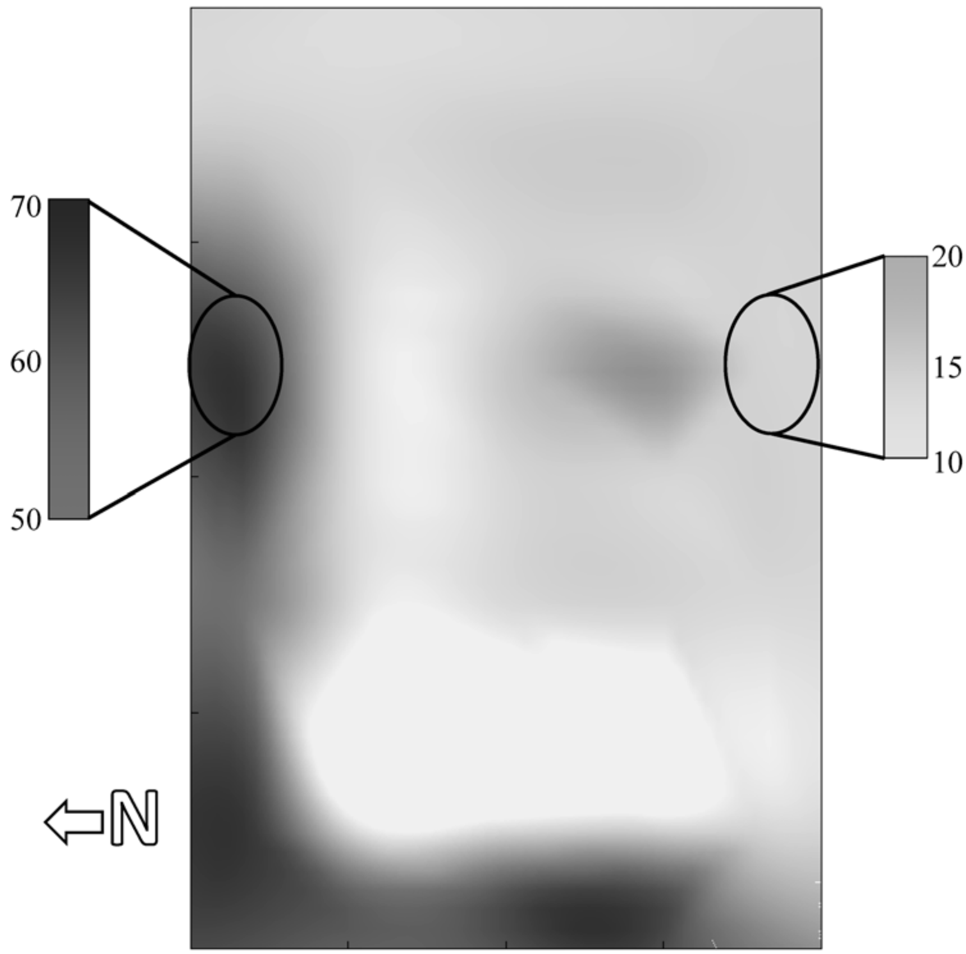

Figure 7. Isopleth moisture distribution of an end view of a stack of 3x4x8-ft large square bales (stacked 1-bale wide x 4-bales high) showing the influence of Northern exposure on bale moisture.

Conclusions

Unlike engineered conversion processes operating within controlled (e.g., low uncertainty) environments of conversion reactors, feedstock logistics processes occur in distributed environments of high uncertainty. An analysis of feedstock cost variability, based on an assessment of sensitivity, uncertainty and influence of feedstock logistics variables, showed that uncertainty dominates when sustainability and quality metrics compete with feedstock cost. This was demonstrated in the case of biomass collection efficiency and storage dry matter losses. Collection efficiency, though a measurement of machinery performance, is strongly dependent on sustainability and quality variables that often constrain collection efficiency to conservative levels. Reducing storage dry matter losses and maintaining feedstock quality through storage are possible through moisture management. Logistics solutions, whether through equipment development or improved methods and practices, must meet cost, sustainability, and quality requirements. Feedstock logistic systems that actively manage uncertainty by balancing these metrics will in the long run be the most cost-effective and sustainable logistic systems.

References

Aden, A., M. Ruth, et al. (2002). Lignocellulosic biomass to ethanol process design and economics utilizing co-current dilute acid prehydrolysis and enzymatic hydrolysis for corn stover. Golden, CO, National Renewable Energy Laboratory.

ASABE (2006). Standards. ASAE D497.5 Feb. 2006, Agricultural machinery management data. St. Joseph, MI., American Society of Agricultural and Biological Engineers.

Coble, C. G. and R. Egg (1987). "Dry matter losses during hay production and storage of sweet sorghum used for methane production." Biomass 14(3): 209-217.

Darr, M. J. and A. Shah (2012). "Biomass storage: and update on industrial solutions for baled biomass feedstocks." Biofuels 3(3): 321-332.

Dutta, A., M. Talmadge, et al. (2011). Process design and economics for conversion of lignocellulosic biomass to ethanol-Thermochemical pathway by indirect gasification and mixed alcohol synthesis. Golden, CO, National Renewable Energy Laboratory. NREL/TP-5100-51400.

Gregg, J. S. and R. C. Izaurralde (2010). "Effect of crop residue harvest on long-term crop yield, soil erosion and nutrient balance: trade-offs for a sustainable bioenergy feedstock." Biofuels 1 (1): 69-83.

Hess, J. R., K. L. Kenney, et al. (2009). Commodity-scale production of an infrastructure-compatible bulk solid from herbaceous lignocellulosic biomass. Uniform-format bioenergy feedstock supply system design report series. Idaho Falls, ID, Idaho National Laboratory. INL/EXT-09-17527.

Hess, J. R., K. L. Kenney, et al. (2009). "Corn stover availability for biomass conversion: situation analysis." Cellulose 16(4): 599-619.

Hess, J. R., C. T. Wright, et al. (2007). "Cellulosic biomass feedstocks and logistics for ethanol production." Biofuels Bioproducts & Biorefining-Biofpr 1(3): 181-190.

Hoskinson, R. L., D. L. Karlen, et al. (2007). "Engineering, nutrient removal, and feedstock conversion evaluations of four corn stover harvest scenarios." Biomass and Bioenergy 31 (2-3): 126-136.

Humbird, D. A., R. Davis, et al. (2011). Process design and economics for biochemical conversion of lignocellulosic biomass to ethanol--Dilute-acid pretreatment and enzymatic hydrolysis of corn stover, National Renewable Energy Laboratory. NREL/TP-5100-47764.

Muth, D. J. and K. M. Bryden (2012) "An investigation of sustainable variable rate residue removal." Journal of Environmental Quality DOI: 10.2135/jeq2012.0067.

Nelson, R. G., M. Walsh, et al. (2004). "Methodology for estimating removable quantities of agricultural residues for bioenergy and bioproduct use." Applied Biochemistry and Biotechnology 113: 13-26.

Perlack, R. D. and B. J. Stokes (2011). U.S. Billion-ton update: Biomass supply for a bioenergy and bioproducts industry. Oak Ridge, TN, Oak Ridge National Laboratory. ORNL/TM-2011/224.

Phillips, S. D., A. Aden, et al. (2007). Thermochemical ethanol via indirect gasification and mixed alcohol synthesis of lignocellulosic biomass. NREL/TP-510-41168.

Prewitt, R. M., M. D. Montross, et al. (2007). "Corn stover availability and collection efficiency using typical hay equipment." Transactions of the ASABE 50(3): 705-711.

Richey, C. B., J. B. Liljedahl, et al. (1982). "Corn stover harvest for energy production." Transactions of the ASAE 25(4): 834-839.

Sanderson, M. A., R. P. Egg, et al. (1997). "Biomass losses during harvest and storage of switchgrass." Biomass & Bioenergy 12(2): 107-114.

Schechninger, T. M. and J. R. Hettenhaus (2004). Corn stover harvesting:grower, custom operator, and processor issues and answers. Report on corn stover harvest experiences in Iowa and Wisconsin for 1997-98 and 1998-99 crop years. Oak Ridge, TN, U.S. Department of Energy, Office of Energy Efficiency and Renewable Energy. ORNL/SUB-04—4500008274-01.

Searcy, E. M. and J. R. Hess (2010). Uniform-format feedstock supply system: A Commodity-scale design to produce an infrastructure-compatible biocrude from lignocellulosic biomass. Idaho Falls, ID, Idaho National Laboratory. INL/EXT-10-20372 Revision 0 (Draft).

Shinners, K. J. and B. N. Binversie (2004). Harvest and storage of wet corn stover biomass. Paper Number: ASAE/CSAE 041159. Presented at the 2004 ASAE/CSAE Annual International Meeting. Ottawa, Ontario, Canada.

Shinners, K. J., B. N. Binversie, et al. (2007). "Comparison of wet and dry corn stover harvest and storage." Biomass and Bioenergy 31(4): 211-221.

Shinners, K. J., B. N. Binversie, et al. (2003). Harvest and storage of wet and dry corn stover as a biomass feedstock. ASAE Paper No. 03-6088. St. Joseph, MI, American Society of Agricultural Engineers.

Shinners, K. J., G. C. Boettcher, et al. (2010). "Harvest and storage of two perennial grasses as biomass feedstocks." Transactions of the ASABE 53(2): 359-370.

Shinners, K. J., M. F. Digman, et al. (2011). Biomass logistics – harvest and storage. Sustainable Production of Fuels, Chemicals, and Fibers from Forest Biomass. J. Zhu, X. Zhang and X. Pan. Washington, DC, American Chemical Society. 1067: 65-86.

Smith, W. A., I. J. Bonner, et al. (forthcoming 2012). "Practical considerations of moisture in baled biomass feedstocks." Biofuels.

Sokhansanj, S., A. Turhollow, et al. (2002). "Engineering aspects of collecting corn stover for bioenergy." Biomass & Bioenergy 23(5): 347-355.

Wilhelm, W. W., J. R. Hess, et al. (2010). "Review: Balancing limiting factors & economic drivers for sustainable Midwestern US agricultural residue feedstock supplies " Industrial Biotechnology 6(5): 271-287.

2.5
DEVELOPMENT AND DEPLOYMENT OF A SHORT ROTATION WOODY CROPS HARVESTING SYSTEM BASED ON A NEW HOLLAND FORAGE HARVESTER AND SRC WOODY CROP HEADER

M.H. Eisenbies[1,], L.P. Abrahamson[1], P. Castellano[1], C. Foster[2], M. McArdle[3], J. Posselius[2], R. Shuren[4], B. Stanton[4], B. Summers[4], T.A. Volk[1], J. Zerpa[4]*

Abstract
While demand for bioenergy sourced from woody biomass is projected to increase, the expansion and rapid deployment of short rotation woody crop (SRWC) systems has been constrained by high production costs and limited market acceptance of chips from first generation harvesting systems because of problems with quality and consistency. For willow and hybrid poplar SRWC systems, harvesting accounts for about 1/3 of the delivered cost. Harvesting and transport combined can account for 45-60% of delivered costs. The objective of this study is to evaluate the performance of a single pass cut and chip harvester base on a New Holland FR forage chopper with a dedicated FB130 short rotation coppice header. The project has examined the use of various in field chip collection equipment in short rotation willow and hybrid poplar biomass crops. The newly designed FB130 header can cut stems up to 10-cm in diameter and results in a superior chip quality and flow of woody biomass through the system. Median harvester speeds on gentle terrain were near 4 km hr^{-1} in mature willow crops and 10 km hr^{-1} in young poplar, which translates to harvesting rates of 0.8 and 2.6 ha hr^{-1} respectively. Harvester delays/stoppages were usually the result of ground conditions, an absence of chip collection equipment, or maintenance. The key challenge in system evolution is to optimize the operation of the harvester and chip collection equipment to minimize down time and maximize machine productivity.

Keywords: Biomass; Short Rotation Woody Crops; Harvest Logistics

Introduction
Biomass for bioproducts and bioenergy can be sourced from forests, agricultural crops, various residue streams, and dedicated woody or herbaceous crops (USDOE, 2011). Woody biomass feedstocks have advantages in the northeastern US where forests occupy 67.4% of the land area (Smith et al., 2009), agricultural production has been in a 20-year decline, and crop residues are limited because of the dominance of dairy in the agricultural sector. Woody biomass is available year-round from multiple sources, so end users are not dependent on a single source of material; this ensures a consistent feedstock supply, reduces the risk of dramatic price fluctuations, and eliminates the needs for complicated and expensive long-term storage of material. As perennial cropping systems, both forests and short rotation woody crops (SRWC), like willow (*Salix spp.*) and hybrid poplar (*Populus spp.*), produce environmental benefits beyond a renewable source of biomass and are less prone to fluctuations in yield due to abnormal weather patterns or pest and disease outbreaks than annual crops.

Shrub willow biomass crops are grown on marginal land using a coppice management system that allows multiple harvests, usually every three years, from a single planting of genetically

[1] *SUNY-ESF, NY*

[2] *New Holland Agriculture, PA*

[3] *6030 E Lake Road, Auburn, NY 13021*

[4] *Greenwood Resources, OR*

improved shrub willow varieties (Abrahamson et al. 2010). Poplar, another commercially available SRWC, is grown using similar crop management systems with adjustments made for site conditions and plant requirements (El Bassam, 2010). The potential to generate usable chipped material during harvesting operations is a key advantage over other woody residues because it facilitates the cost savings projected by advanced uniform format feedstock systems by completing preprocessing steps as close as possible to harvesting and collection steps (Hess et al., 2009).

Despite the extensive benefits associated with SRWC systems, their expansion and deployment has been restricted by higher production costs and lower market acceptance. For willow biomass, crops harvesting is the largest single cost factor (1/3 of the final delivered cost); harvesting, handling, and transportation accounts for 45-60% of its delivered cost (Buchholz and Volk 2011). Cost structures are similar for hybrid poplar. Improving overall efficiency by 25% can reduce the delivered cost of SRWC by approximately \$0.50/MMBtu (\$7.50/ton). Harvesting is also the second largest input of primary fossil energy in the system after commercial N fertilizer, accounting for about one third of the input (Heller et al. 2003).

In early 2003, testing of several types of single-pass, cut and chip systems were evaluated for willow using existing or modified platforms from throughout the world. Technical hurdles encountered included durability, chips lacking a consistent size (< 38 mm) and quality, and irregular feeding of stems from the cutter to the chipper. Since 2008, Case New Holland (CNH) has developed and improved a short rotation coppice header (130 FB) for the FR9000 series forage harvester specifically designed to address previous issues, and can cut and chip a range of SRWC feedstocks. The 130 FB utilizes circular saw blades mounted in a horizontal plane to cut stems, which are transferred into the forage harvester/chipper by three horizontally mounted feedrolls. This FR9000 based harvesting system provides woodchips of a precise and uniform length and size, plus customized size distribution to meet the specific end user needs.

The objective of this study is to evaluate the performance of a single pass cut and chip harvesting system based onFR9000 forage chopper fitted with a dedicated FB130 short rotation coppice header. The performance objectives were the ability to harvest double rows, stems up to 100 mm in diameter, while producing 10 to 45-mm long chips, at a rate up to 2 ha hr^{-1}. Chipped material can be transported directly to the biorefinery without need of further processing.

Methods

Two sites were selected for preliminarily analysis: (1) a 2.6-ha willow trial study located near Constableville, NY (CNY) on October 14, 2011, and (2) an 8.5-ha hybrid poplar operational trial harvest located near Boardman, OR (BOR) on August 11, 2011. As trials, these operations are not wholly representative of a mature harvesting system; the fields consisted of a mix of varieties and silvicultural prescriptions, and the equipment designers were still making engineering modifications to the harvester itself. However, from a research perspective they provide an excellent opportunity to evaluate a range of conditions and system configurations, and provide a foundation for tracking improvements to the overall system.

A framework for the time motion analysis was devised to evaluate system performance (Meyers, 1999; McDonald and Fulton, 2005;). During operations, the harvester and chip collection equipment were instrumented using Trimble GeoExplorer XM, and Juno SB global positioning system (GPS) units recording position and velocity every second, and differentially corrected (Trimble Pathfinder Office 4.10). Instantaneous machine locations (field, headland, chip piles, or transitional zones) were labeled based on field maps (ESRI ArcGIS 10), and a SAS program was developed to aggregates points into “legs”. Each leg captures equipment activities during discrete phases of their operation. For the harvester, these phases consist of (1) harvesting biomass, (2) headland turns, (3) delays and stoppages, and (4) service loops (Figure 1). The operational phases of chip handling equipment consist of (1) receiving chips from harvester (when the machine is operating within 12 m of the harvester), (2) delivering chips to the landing, (3) unloading chips at landing, and (4) returning to harvester. Machine time and motion on these components of the harvest will be subsequently used to evaluate the performance of the harvester and overall system during key operations and transitions. Harvested biomass was determined either using load cells mounted on a dump wagon, or from destructive plots in hybrid poplar. Coordinated Universal Time (UTC) was used to match ancillary information to the GPS time stamps for specific legs.

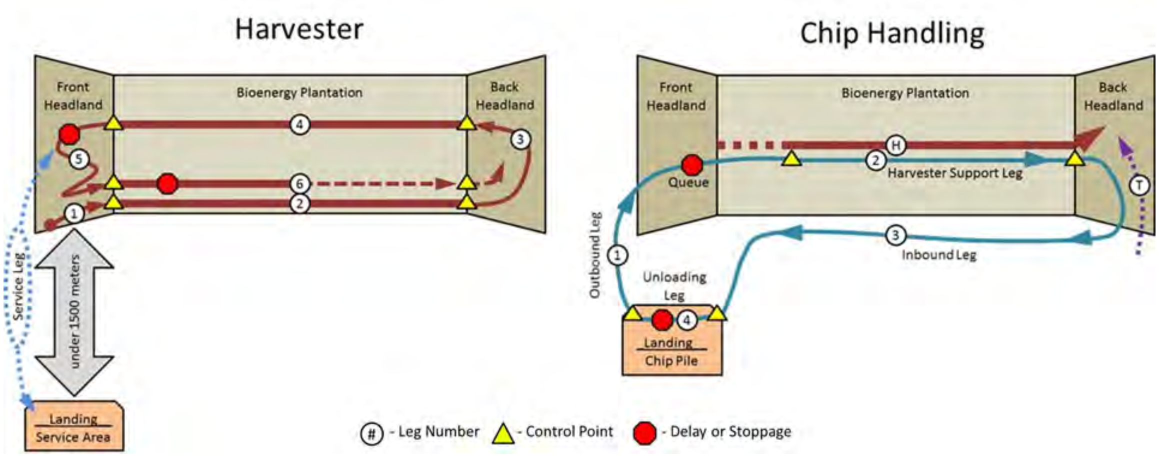

Figure 1: To evaluate system performance during key phases, equipment movement is consolidated into discrete legs based on their location, and relative position.

Results and Discussion

The New Holland harvester was monitored for a total of 6.1 hours at the Constableville, NY site (CNY) and had two tractors (Case IH 4240) equipped with self-unloading, Richardson dump wagons running in support; however, one tractor was down for a period of time. The mean standing biomass of the five year old willow biomass planted at an initial density of 15,400 plants ha^{-1} was approximately 50 Mg ha^{-1} (STDERR 3.4 Mg hr^{-1}) (Table 1). The harvester was monitored for a total of 4.8 hours at the Boardman, OR site (BOR), and had two ten wheeled trucks and a tractor with a manure spreader operating in support. The mean standing biomass of the 1.5 year old hybrid poplar planted at a density of 2,696 or 5,391 plants ha^{-1} was approximately 11 Mg hr^{-1}. There was a small amount of rainfall (< 1 cm) at the New York site.

Table 1. Summary statistics for the trial willow harvest occurring at Constableville, NY (COR) and trial poplar harvest occurring at Boardman, OR (BOR)

		Constableville, NY	Boardman, OR
Standing biomass	Green Mg ha^{-1}	50	11
Harvester Rate	ha hr^{1}	0.73	3.1
Speed	Km hr^{-1}	3.2	5.1
Production Rate	Mg hr^{-1}	36.5	36
[a]In-field delays	Delays ha^{-1}	50	7
Delay time	Min ha^{-1}	26	7
Harvester Efficiency (in field)	Undelayed rate: actual rate	0.84	0.84
Turn Times (undelayed)	Seconds $turn^{-1}$	41	30
Turn Times (with delays)	Seconds $turn^{-1}$	120	168
Chip handling cycle times	Minutes $cycle^{-1}$	21.5	40
[a] speed < 0.65 km hr^{-1}			

The harvesting and production rate of the harvester is dependent on the density of standing biomass. Harvesting rates were 0.73 ha hr^{-1} (3.2 km hr^{-1}) at the CNY, but 3.13 ha hr^{-1} (5.1 km hr^{-1}) at BOR (Table 1). Despite these differences, the chip production rate was virtually identical 36.5 and 36.0 green Mg hr^{-1} respectively. For the purposes of this study, the harvester was considered to be in a delayed state for any cause where speeds dropped below 0.65 km hr^{-1}. The harvester experienced nearly 50 field delays ha^{-1} for a total of 26 min ha^{-1} on the CNY harvest, but only 7 delays ha^{-1} for total of 6.7 min ha^{-1} at the BOR harvest. These differences are largely due to the heterogeneous stem form of clone plantings at the CNY site; willow varieties with spreading stem forms greatly reduced ground speed for the harvester resulting in the operator frequently stopping the machine in order to maintain the RPMs, and wet headland conditions that impeded the progress of chip collection equipment. In spite of these delays, the mean harvester efficiencies for the day were virtually identical 0.84 (undelayed harvester production rate: actual harvester production rate) for both sites.

In the headlands, the harvester may be delayed waiting for a chip collection vehicle and this was exasperated at the CNY site due to wet conditions in the headlands. Mean turn times at CNY site were 120 sec $turn^{-1}$ and 168 sec $turn^{-1}$ at the BOR site excluding outliers. Absent of delays turn times were 41 seconds at the CNY site, and 30 seconds at the BOR site. Delays lasting a few seconds are most often due to the driver dealing with narrow headlands or tight turns; delays lasting several minutes or longer were most commonly either to wait for collection equipment, or to inspect or repair equipment. The hybrid poplar at BOR are planted in regularly spaced blocks that are surrounded by roads for easy turning at either end of the field. The CNY site is representative of a common willow crop grown on marginal agricultural land with irregular field shapes and headlands that may not fully accommodate the large machinery used in these operations.

The longer overall cycle times at the BOR site are due to a haul distance well over a kilometer for the chip handling equipment. Cycle times for the two tractors at the CNY site were 21.5 minutes, and 40 minutes at the BOR site for its support vehicles.

The harvester must remain active due to the high fuel consumption (up to 80 l hr^{-1}) and other costs associated with the harvester. Overall system efficiency, the ability of the system to deliver chips to the landing at the rate they were produced, was evaluated for the CNY site. The harvester’s efficiency is generally affected primarily by crops or field conditions (Figure 2). Overall system efficiency is a product of the proper number of service vehicles; it is generally affected by haul distance, and site conditions, which dictate the type and number of support vehicles.

Another factor that may influence harvester efficiency is stemform. At the CNY site, two willow varieties with a more spreading form factors reduced harvester efficiency between 0.5 and 0.75 (Figure 2); however, when only one tractor was in operation the overall system efficiency remained around 0.5 regardless of harvester efficiency. While two tractors were in operation, mean system efficiency was near 1.0, meaning they were delivering chips to the landing as the same rate the harvester was generating them. System efficiency for individual legs in excess of 1 is an artifact of harvester delays coupled with rapid cycling of the chip handling equipment.

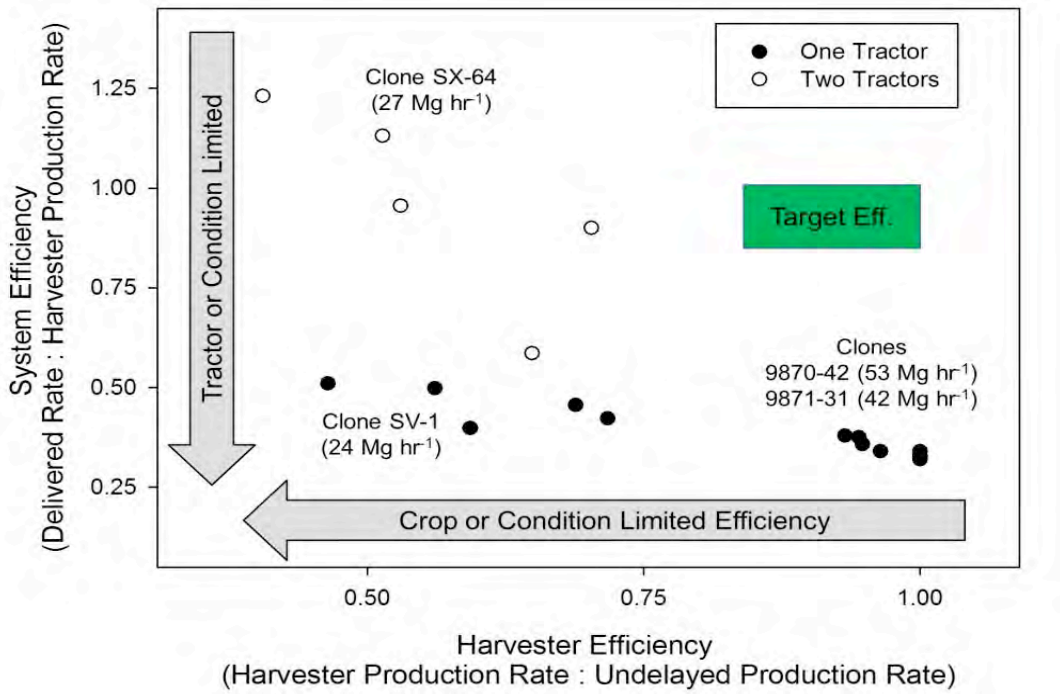

Figure 2: Harvester and system efficiency for four willow varieties in a harvesting trial near Constableville, NY.

Conclusions

The New Holland FR forage chopper with a dedicated FB130 short rotation coppice header mounted on a New Holland FR 9080 forage harvester represents the state of the art of a single pass cut and chip harvester system on a SRWC plantation. Based on preliminary results it is capable of producing over 36 green Mg ha^{-1} but we observed rates as high as 54 Mg ha^{-1} in some willow clones. In the case of willow, clone selection plays a considerable role in the efficiency of the machine, which we attribute to form differences between clones. New Holland is still working to optimize configurations for various woody crops.

While issues such as field configuration and stem form affect the efficiency of the harvester. System efficiency is most affected by the number and type of chip handling equipment operating in support of the harvester. To a degree, driver experience and aggressiveness may also have an influence, but these influences may become easily masked by other factors.

References

Abrahamson, L.P. T.A. Volk, L.B. Smart, K.D. Cameron. 2010. Shrub willow biomass producer's handbook. SUNY-ESF, Syracuse, NY, 27pp.

Buchholz, T. and T.A. Volk. 2011. Identifying opportunities to improve the profitability of willow biomass crops with a crop budget model. Bioenergy Res. 4(2): 85-95.

El Bassam N. 2010. Handbook of Bioenergy Crops. Earthscan. Washington DC. 516pp.

Heller, M.C., G.A. Keoleian, T.A. Volk. 2003. Life cycle assessment of a willow bioenergy cropping system. Biomass Bioenergy 25:147-165.

Hess, J.R., C.T. Wright, K.L. Kenny, and E.R. Searcy. 2009. Uniform-Format Solid Feedstock Supply System. INL/EXT-09-15423. Idaho National Laboratory, Idaho Falls, ID. 12pp.

McDonald, T.P. and J.P. Fulton. 2005. Automated time study of skidders using global positioning system data. Computers and Electronics in Agriculture. 48: 19-37.

Meyers, F.E. 1999. Motion and time study for lean manufacturing. 2nd Ed. Pearson Education. Upper Saddle River, NJ. 334.

Smith, W.B., P.D. Miles, C.H. Perry and S.A. Pugh. 2009. Forest Resources of the United States, 2009. GTR-WO-78, Washington, DC, USDA Forest Service. 336pp.

U.S. Department of Energy. 2011. U.S. Billion-Ton Update: Biomass Supply for a Bioenergy and Bioproducts Industry. ORNL/TM-2011/224. Oak Ridge National Laboratory, Oak Ridge, TN. 227p.

2.6
IMPROVING WOODY BIOMASS FEEDSTOCK LOGISITICS BY REDUCING ASH AND MOISTURE CONTENT

Jason B. Cutshall[1], W. Dale Greene[1,], Shawn A. Baker[1]*

Abstract
We compare a range of likely forest biomass harvesting systems including whole-tree chipping, clean chipping, conventional roundwood, and residue grinding to determine how each system affects woody biomass energy facilities, biomass harvesting firms, and forest landowners. Delivered costs for these systems were evaluated for a range of values for moisture content, ash content, tract size, tons of biomass removed per acre and at grinding decks, truck payload, haul distance, and diesel fuel price. Delivered cost per mmBTU decreased by over 50% for all systems as moisture content decreased from 55% to 30%. Whole tree chipping provided the lowest cost option ($4.39 per mmBTU) at ash content levels less than 1%, and unscreened grinding of clean chip residue produced the least expensive option at 5% ash ($2.87 per mmBTU). Tract size had minimal effects on any operation until the acreage declined below 40 acres. Clean chipping and roundwood systems were considerably more expensive than whole-tree chipping operations on all tract sizes. Costs declined significantly as truck payload increased and/or haul distance decreased. Fuel price increases directly increase cut and haul costs and limit economical haul distances accordingly.

Keywords: forest biomass harvesting, chipping, grinding, moisture content, ash content

Introduction
Higher market prices for fossil fuels as well as proposed policy changes to support renewable energy use and to reduce carbon emissions have recently led to a large number of announced bioenergy projects. Projects recently announced for North America could substantially increase wood energy capacity and potentially consume more than 60 million green tons of woody biomass feedstock (RISI 2011). Woody biomass from forest residues has long been underutilized due to limited access and high costs associated with collection and transportation (Evans 2008). A survey of top state forestry officials identified high harvesting and transportation costs for woody biomass from forests as the top constraint to expanding this new industry (Aguilar and Garrett 2009).

Harvesting systems utilizing whole-tree chippers and grinders convert woody biomass into a suitable feedstock for wood energy facilities. A system harvesting roundwood products typically piles logging slash for later collection by a biomass harvesting system using a grinder or chipper. In this paper we compare a range of likely forest biomass harvesting systems, including whole-tree chipping, clean chipping, conventional roundwood, and residue grinding to determine how each system affects woody biomass energy facilities, biomass harvesting firms, and forest landowners.

Methods
We calculated delivered costs per field ton and per million BTU (mmBTU) for seven harvesting systems. We use the term “field” to reference the moisture content of any material at the time of chipping or grinding and use “green” wood to refer to freshly felled wood with the highest moisture content observed in the field. The harvesting systems included: (1) a whole-tree chipping operation producing fuel chips, (2) a clean chipping operation producing pulp quality

[1] *Center for Forest Business, Warnell School of Forestry and Natural Resources, University of Georgia, GA*

* *Corresponding author*

chips, (3) a horizontal grinding operation processing roundwood logging residues unscreened, (4) a horizontal grinding operation processing and screening roundwood logging residues, (5) a horizontal grinding operation processing clean chipping residues unscreened, (6) a horizontal grinding operation processing and screening clean chipping residues, and (7) a conventional roundwood logging operation.

Production rates, truck payloads, and all physical properties including moisture, ash, and energy content were obtained from Dukes (2012) for screened and unscreened grindings and from Cutshall *et al.* (in press) for whole-tree chips. Hourly operating costs were calculated using the machine rate approach (Miyata 1980) assuming 85% mechanical availability for all machines in each of the seven harvesting systems. Additional assumptions for all machines included: labor rate of $18.00/SMH; labor fringe/overhead expenses of 40% of the base rate of pay; combined interest, insurance, and taxes of 15% of average annual investment; lubrication costs at 37% of fuel expense; and 2,000 scheduled machine hours per year. We evaluated diesel prices ranging from $3.00 to $6.00 per gallon.

We modified a version of the Auburn Harvesting Analyzer (Tufts *et al.* 1985) to determine delivered costs for each system. The model was adapted to evaluate a range of values in lab-derived moisture content, ash content, and energy content (BTU per oven dry pound) among whole-tree chipping and grinding systems based on results obtained from Cutshall *et al.* (in press) and Dukes (2012). Truck payload data from the previous studies were used to obtain ranges in load weights. We added 10% to total costs for a profit margin.

Delivered costs were calculated by adding a stumpage price of $8.00 per field ton for the RW system and $1.00 per field ton for grinding systems. We assumed the CC system to process 10% less material due to bark and limb losses than the RW system resulting in a stumpage price of $8.89 per field ton and the WTC system to process 25% more material than the RW system resulting in a stumpage price of $6.40 per field ton. To further incorporate biomass costs for wood energy facilities, we added an additional $5.00 per field ton to the RW system to represent the cost of chipping roundwood at a facility. We compared delivered cost per mmBTU data at each variable level using analysis of variance with Tukey's range test used for means comparison (Oehlert 2000).

Results

Estimated delivered costs on an energy basis (mmBTU) for whole-tree chipping and screened and unscreened grinding systems were compared by increasing moisture content (MC) from 30% to 55% (wet basis) (Figure 1). Delivered cost per mmBTU decreased by over 50% for all systems as moisture content decreased from 55% to 30%. The system grinding clean chipping residues without using a screen (GCC) had the lowest estimated delivered costs ranging from $2.68 per mmBTU at 30% MC to $4.17 at 55% MC. The grinding system processing and screening clean chipping residues (GCC/S) and the system grinding roundwood logging residues without using a screen (GRW) had marginally higher estimated cut and haul costs per mmBTU, respectively, than the GCC system. The whole-tree chipping system had the highest costs of the "economically feasible" systems. Estimated cut and haul costs for the system grinding and screening roundwood logging residues (GRW/S) were by far the highest. This system was not considered to be an economically feasible option. Dukes (2012) reported that this system averaged 11.7 net tons of truck payload, a 47 minute loading time, and 15.3 tons per productive hour. By comparison, a 780 hp grinder processing and screening clean chip residues averaged 23.5 net tons of truck payload, a 16.9 minute loading time, and 84.7 tons per productive hour.

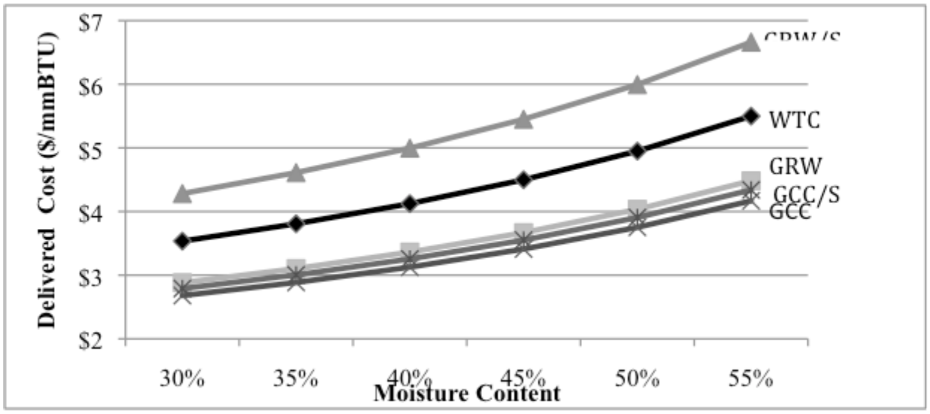

Figure 1. Delivered cost estimates ($/mmBTU) for increasing levels of moisture content

Ash content is another key characteristic affecting net energy content. The whole-tree chipping system produced the lowest estimated delivered cost per mmBTU at the lowest percent ash, $4.39 per mmBTU at 0.5% ash and $4.41 at 1% ash (Table 1). Cutshall *et al.* (in press) reported ash content of less 0.7% in whole-tree chips. The GCC system produced the lowest estimated delivered cost per mmBTU of $2.87 at 5% ash, but this system also produced loads with high ash content (up to 30%). If target ash content is less than 2%, the WTC system was the lowest delivered cost option. If 2% ash is acceptable, then the GCC/S system is the lowest delivered cost option at $3.33 per mmBTU. If ash content of up to 10% is acceptable, then all systems are options with the lowest costs observed for the GCC system.

Table 1. Delivered cost estimates ($/mmBTU) by levels of ash content

	Delivered Cost ($/mmBTU) by Harvesting System				
% Ash	**WTC**	**GRW**	**GRW/S**	**GCC**	**GCC/S**
0.5%	$4.39		$5.27		
1.0%	$4.41		$5.29		
1.5%			$5.32		
2.0%		$3.44	$5.35		$3.33
2.5%			$5.37		
3.0%			$5.40		
4.0%		$3.51			$3.40
5.0%				$2.87	
6.0%		$3.59			$3.47
8.0%		$3.66			$3.55
10.0%		$3.75		$3.03	$3.63
15.0%				$3.20	
20.0%				$3.40	
25.0%				$3.63	
30.0%				$3.89	

Delivered costs per mmBTU for each harvesting system were also compared by increasing net tons of truck payload (Figure 2). The GRW, GCC, and GCC/S systems had the lowest costs for each load size. Costs declined approximately 11% for each system as load size increased except for the GRW/S system which declined 20%.

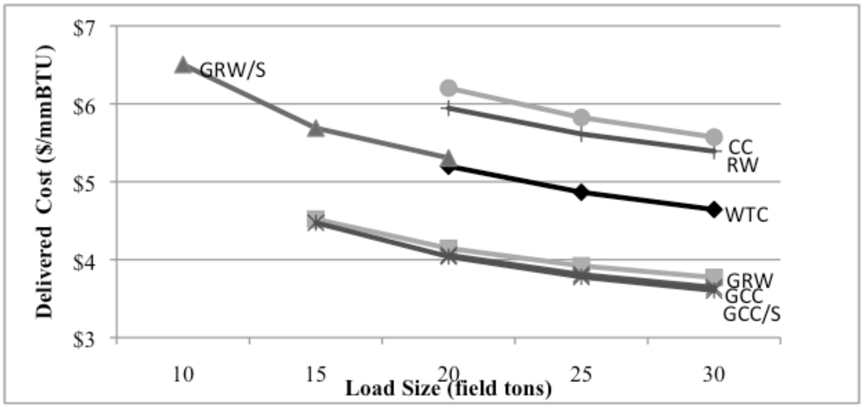

Figure 2. Delivered cost estimates ($/mmBTU) for increasing net tons of truck payload

We compared delivered cost per field ton and per mmBTU for each system (Table 2) under likely conditions and with key assumptions more fully described in Cutshall (2012). The GCC system had the lowest delivered cost per field ton and per mmBTU ($22.48 and $2.71, respectively) and the GRW/S system had highest costs at $46.49 and $4.20, respectively. When factoring in moisture and ash content to derive delivered costs on an energy content basis ($/mmBTU), costs per mmBTU for the GRW and WTC-40% (40% moisture content) systems were lowered relative to their cost per field ton equivalent measure. The RW and CC systems were among the costliest based on field tons and mmBTU.

Table 2. Ranking (lowest=1) of delivered cost estimates ($/field ton and $/mmBTU) for biomass harvesting systems under likely conditions

System	Delivered Cost ($/F-ton)	Rank	Delivered Cost ($/mmBTU)	Rank
GCC	$22.48	1	$2.71	1
GCC/S	$27.04	2	$3.05	3
GRW	$28.07	3	$2.77	2
WTC-50%	$28.94	4	$3.55	5
WTC-40%	$30.36	5	$3.10	4
RW	$31.07	6	$3.81	6
CC	$31.20	7	$3.82	7
GRW/S	$46.49	8	$4.20	8

Systems that collect residues behind clean chip or roundwood operations represent a second pass across the site or at minimum a second operation visiting the logging site. When examining these grinding systems from a holistic standpoint, they may not be as favorable due to costs of both passes. Residue collection systems are also limited by the availability of sites that have received a primary harvest first and by definition have less biomass available to collect since higher value products have already been removed. In this study the WTC systems produced a relatively costly product, but they had the advantages of requiring a single operation and handling large volumes per acre.

Acknowledgments

This study was funded by financial support from the Southeastern Sun Grant Center associated with the US Dept. of Energy and US Dept. of Agriculture.

References

Aguilar, F. and H.E. Garrett. 2009. Perspectives of woody biomass for energy: Survey of state foresters, state energy biomass contacts, and National Council of Forestry Association executives. *Journal of Forestry* 107(6): 297-306.

Cubbage, F.W. and W.D. Greene. 1989. Conventional and biomass harvesting costs by forest tract size. *Biomass* 20(3-4): 219-228.

Cutshall, J.B., W.D. Greene, and S.A. Baker. In Press. Transpirational drying effects on energy and ash content from whole-tree southern pine plantation chipping operations. Accepted for publication in *Southern Journal of Applied Forestry*.

Cutshall, J.B. 2012. Options for reducing moisture and ash content in forest biomass harvesting systems. PhD dissertation, University of Georgia, Athens, GA. 82 p.

Dukes, C. 2012. In-wood screening of wood grindings for biomass feedstock applications. M.S. Thesis. The University of Georgia. 44 p.

Evans, A.M. 2008. *Synthesis of knowledge from woody biomass removal case studies*. Santa Fe, NM. The Forest Guild. 39 p.

Oehlert, G.W. 2000. *A first course in design and analysis of experiments*. W.H. Freeman and Company. New York. 600 p.

RISI. 2011. *Wood Biomass Market Report.* August 2011. 4(8), 7 p.

TAPPI. 1985. *Sampling and preparing wood for analysis*. T 257 cm-85. 5 p.

Tufts, R.A., B.L. Lanford, W.D. Greene, and J.O. Burrows. 1985. Auburn harvesting analyzer. *The Compiler* 3(2): 14–5.

2.7
HARVESTING SYSTEMS AND COSTS FOR SHORT ROTATION POPLAR

B. Rummer[1], D. Mitchell[1,]*

Abstract

The objective of this review is to compare the cost of coppice and longer rotation poplar harvesting technology. Harvesting technology for short rotation poplar has evolved over the years to address both coppice harvest and single-stem harvest systems. Two potential approaches for coppice harvesting are modified forage harvesters and modified mulcher-balers. Both of these systems effectively handle multi-stemmed feedstock. Total harvesting cost to roadside likely ranges from $11 to $15 Mg green. The most significant harvesting constraint with coppice systems is the requirement for dormant season operations. More conventional poplar harvesting at production scales uses forest machines for felling and extraction. The Billion Ton Update report used previous productivity studies to estimate a roadside cost for felling and skidding of about $6 Mg green (unchipped). With chipping cost, single-stem systems are about the same roadside price as coppice harvesting. Other factors such as stand establishment, feedstock storage, and rotation length are more likely to determine an economically optimum management system.

Keywords: coppice, costs, felling, swath harvester

Introduction

Any assessment of the US biomass supply considers purpose-grown woody crops an important component of the future feedstock mix. The Billion Ton Update (US Department of Energy 2011) describes four woody crops—willow, poplar, eucalyptus and pine—as potential bioenergy feedstocks. Under a high yield scenario woody crops may provide as much as 115 Mg (126M dry tons) per year by 2030. Woody crops can be grown in many regions of the country, offer flexibility of supply and storage by having inventory “on the stump”, provide a range of ecosystem values in addition to simple biomass volume, and are responsive to intensive management practices that increase productivity.

Poplar species are the most widely adaptable woody crop considered in the High Yield Scenario. Berguson *et al*. (2010) describe the history of plantings in the Pacific Northwest and Lake States. Many of these plantations were originally established as a source for pulpwood supply with rotation ages of eight or more years. Currently there are more than 15,000 ha (37,000 ac) concentrated near the Columbia River. In Minnesota hybrid poplar has been established on 1000’s of ha of private and industry land. A conservative estimate of plantation yield from these plantings is about 9 Mg ha^{-1} yr^{-1} (4 dry tons ac^{-1} yr^{-1}). Coleman *et al.* (2008) evaluated clonal varieties of poplar, sycamore and eucalyptus in South Carolina and found similar yields.

While it is clear that poplar can be grown for woody feedstock the most significant unknown is the technology and cost for harvesting. Depending on management practice the harvesting system may need to accommodate coppiced, small-stem material or larger single-stem trees. Harvesting methods for coppiced material tend to be derived from agricultural equipment while harvesting methods for single-stem stands are generally purpose-built forest machines. Each approach has advantages and disadvantages, none of these techniques are fully evolved and there is a sense that improved harvesting technology could reduce costs through gains in efficiency.

[1] *Forest Operations Research Unit, AL*

** Corresponding author*

This paper reviews current harvest system technologies for harvesting short-rotation poplar, recognizing the need for technologies to address both single-stem and multi-stemmed management systems. Three harvest systems are identified and production rates and costs are explored for each.

Poplar Harvesting Systems

A review of existing literature shows that many different machines have been tested since the 1980's. Several authors have compiled extensive reviews of equipment (Stokes and Hartsough 1986; Hartsough and Yomogida 1996, Verani *et al*. 2008). Many early trials embraced the idea of agricultural-type continuous forward harvesting, but differed in their approach. Equipment developers tested different cutting mechanisms, different collection and chipping methods, different types of prime movers. System development also led to tests of alternative ways to move material to roadside—chip forwarding, skidding with grapple skidders, or moving large bunches with alternative machines such as front-end loaders.

Functionally two types of systems have evolved: a) chip-at-the-stump or b) chip at roadside. The selection of an appropriate system depends primarily on stem size and is thus determined by the type of SRWC management. Smaller stems are more difficult to handle economically and are therefore more suited to chip-at-the-stump approaches that quickly convert material to mass handling. Larger stems are more amenable to single-stem felling and handling systems including traditional forestry harvesting technology.

Chip-at-the-stump Harvesting

Most of the poplar in the US is managed on longer rotations with the goal of larger diameter single stems that can be utilized for multiple products. An alternative plantation strategy however is coppicing. Coppice systems reduce site prep and establishment costs and maximize utilization of site productivity. However coppice management imposes particular constraints on equipment operation. First, the economics of coppice management depend on minimal mortality of the stools. This means that the cutting mechanism must sever the tree cleanly with little bark damage. Equipment traffic must also minimize stump and root system damage. The coppice produces multiple small diameter stems that must be collected and densified at the point of cutting to allow cost-effective material handling. Coppice felling has to quickly and cleanly cut multiple stems across the row width. This generally leads to some type of swath cutting head, usually with circular saws for a clean cut.

An additional constraint is that coppice systems may require all harvesting during the dormant season. This helps maximize site productivity and stand vigor. Practically this means that operations must be able to proceed during the wettest time of the year in the US South or during winter conditions in the Lake States. Dormant season operation also means that harvesting equipment must be able to move to different applications in other seasons or it must achieve full utilization during a limited operating season. A harvester operating 20-hr shifts for 4 months could log 1600 operating hours for example. Finally, dormant season harvesting means that the feedstock will have to be stockpiled with concomitant storage and handling issues.

The most advanced coppice harvester is the Case New Holland 9080 forage harvester[2] with an FB130 coppice cutter. Abrahamson *et al.* (2010) describe the basic machine and its evolution from agricultural machine to willow harvester. The equipment is continuing to be upgraded to

---

[2] Reference to any specific commercial products does not constitute or imply its endorsement or recommendation by the United States Government. Such reference is solely for the information of the reader.

effectively harvest larger diameter poplar. Production rates of 2 ha (5 ac) per hour in 12 cm (5 in) diameter poplar have been reported in field trials.
A complete coppice system would include the 9080 with tractors and chip wagons to transfer material to roadside. Because the 9080 has no onboard chip storage it requires a coordinated system of shuttle wagons to keep operating. Simple system modeling with 5.5 t (6 ton) capacity trailers, 55 Mg (60 ton) per hour 9080 production rate, and an average 366 m (1200 ft) distance to roadside would suggest that the system requires three tractors, three chip wagons, and the harvester.

The CNH 9080 costs about $575,000 and would have an estimated hourly cost with operator of about $250 per productive hour. Each tractor and wagon with operator could cost about $125 per productive hour for a total system cost of $625 per hour. If the system moves 55 Mg (60 tons) green per productive hour the cost to roadside would be $11.36 per Mg ($10.42 per green ton) chipped. These costs are obviously sensitive to the assumption of production rate. Larger trees, lower volume per acre, too small of trees could all reduce production rate. If the production rate was only 41 Mg (45 green tons) per hour the cost to roadside would increase to $15.24 per Mg ($13.89 per green ton). Spinelli *et al*. (2009) performed similar types of production studies on several sites using a variety of commercially available forage harvesters. More recently, Fiala and Bacenetti (2012) examined a newer version of the heavy duty coppice header. Their trials confirmed a 60 Mg per hour production rate.

An alternative swath cutting system that has been tested in poplar is the Anderson WB55 Biobaler (Savoie *et al*. 2010). This swath cutting machine uses a mulching-type rotary cutter to both sever and chop the feedstock. Unlike the forage harvester the material is collected and compressed into round bales. Cutting and baling can be separated from transport to roadside. This offers the possibility of longer operating season, roadside inventory and storage, and lower capital investment. In one poplar trial the WB55 achieved 19 Mg (21 green tons) per productive hour with a bale weight of about 512 kg (1100 lbs).

The WB55 costs about $125,000 and an appropriately configured towing tractor adds another $150,000. This results in an operating rate of about $117 per hour. This includes operating costs for twine, fuel, and an operator. An additional operation is necessary to collect the bales and transfer them to roadside. This can be done with standard agricultural round bale handling loaders and trailers or with forestry equipment such as a forwarder. Klepac and Rummer (2010) evaluated the Biobaler system and estimated forwarder productivity with bales at 18 Mg (20 green tons) per productive hour, approximately matching the production rate of the Biobaler. Total system cost to roadside would be about $10.39 per Mg ($9.35 per green ton) baled. It is important to note that bales are not quite the same feedstock form as green chips. If the bales need to be reground there will be additional costs to produce feedstock equivalent to the CNH product.

Chip-at-roadside Systems

Longer rotation plantation management yields larger diameter stems. This generally leads to the use of conventional forestry machines that are designed to handle heavier material. McDonald and Stokes (1994) studied a shear feller-buncher working in a 6-year-old sycamore plantation and found average felling production 18 Mg (20 green tons) per hour. Spinelli *et al*. (2002) looked at three different kinds of forestry feller-bunchers working in eucalyptus plantations in California. Production ranged from 18 to 25 Mg (20 to 28 green tons) per hour. These felling studies have highlighted the need to optimize productivity through the interaction of bunch size, tree size, and accumulator capacity.

Typical mechanized forestry operations are most cost-effective using grapple skidders to move bunched wood to roadside. McDonald and Stokes (1994) found a production rate of 25 Mg (27 green tons) per hour at a skid distance of 400 m (1300 ft) when the feller-buncher put two accumulations in each bunch. If the felling operation maximized bunch size with four accumulations skidding productivity increased to 33 Mg (36 green tons) per hour. Spinelli *et al.* (2002) measured skidding productivity at 40 Mg (44 green tons) per hour in their study of eucalyptus stands. Skid distance averaged 250 m (823 ft).

The Billion Ton Update (US Dept of Energy 2011) estimated SRWC harvesting cost based on the assumptions of conventional forestry machines working in poplar. Drawing on exemplar production rates from previous case studies in sycamore, eucalyptus and poplar an average felling production rate of 18 Mg (20 green tons) per hour was selected. Skidding productivity was assumed to be twice felling productivity (suggesting a balanced system of two feller-bunchers working with one skidder). With total hourly costs for two small feller-bunchers and one grapple skidder of $210 per hour, the roadside felling and skidding cost would be $5.83 per Mg ($5.25 per ton) green. The total harvesting cost in the Billion Ton Report including chipping at roadside was about $11 Mg ($10 per ton) green.

Discussion

The three systems described above represent currently feasible approaches to harvesting short rotation poplar. Permutations of each have been tried and may offer advantages in specific situations (i.e. soft soils, longer extraction distance). However the key is that there are technically viable options for harvesting poplar of all sizes. Economically the harvesting costs are similar. Coppice harvesting is in the range of $11 to $15 per Mg green and whole-tree harvesting to chips is only slightly less expensive. Note that the costs presented in this paper only include machine rates and do not include allowances for profit or overhead. Thus they are valid for relative comparison but should not be considered a “market price” for feedstock.

It should also be noted that these cost estimates from previous harvesting trials are only productive hour estimates. There could well be significant issues of equipment utilization, shift schedules and weather delays that would occur at operational scales. Coppice harvesting systems will be more sensitive to these constraints given the tightly linked production functions and operating season constraints.

Harvesting technology is defined to a large degree by tree size and stand conditions. The initial selection of management regime will likely hinge on the economics of stand management, not harvesting cost. If the system will utilize a coppice rotation then swath harvesters will be required. If the system will use longer rotations then small forestry equipment will likely be the technology of choice. Further equipment development opportunities exist to improve efficiency and better match operating functions to specific feedstock requirements. As conversion technology matures and feedstock specifications are better understood these opportunities can be explored.

References

Abrahamson, L., T. Volk, P. Castellano, C. Foster, and J. Posselius. 2010. Development of a harvesting system for short rotation willow and hybrid poplar biomass crops. Presented at the 8th Biennial short rotation woody crops operations working group; short rotation woody crops in a renewable energy future: challenges and opportunities conference: Syracuse, NY. Available at: http://www.esf.edu/outreach/pd/2010/ srwc/program.htm. Accessed April 25, 2012.

Berguson, B., J. Eaton, B. Stanton. 2010. Development of hybrid poplar for commercial production in the United States: The Pacific Northwest and Minnesota experience. Ch. 17. Sustainable Alternative Fuel Feedstock Opportunities, Challenges and Roadmaps for Six U.S. Regions. Soil and Water Conservation Society. pp. 282-299.

Coleman, M. and D. Aubrey. 2008. Coppice culture for biomass production in southeastern United States. In: Biofuels, Bioenergy, and Bioproducts from Sustainable Agricultural and Forest Crops: Proceedings of the short rotation crops international conference. Bloomington, MN. August 19-21, 2008. GTR-NRS-P-31. 9p

Fiala, M. and J. Bacenetti. 2012. Economic, energetic and environmental impact in short rotation coppice harvesting operations. *Biomass and Bioenergy* 42: 107-113.

Hartsough, B, and D. Yomogida. 1997. Compilation of state-of-the-Art mechanization technologies for short rotation woody crop production. Davis, CA: University of California, Biological and Agriculture Engineering Department. 66 p. In cooperation with: Electric Power Research Institute; U.S. Department of Agriculture, Forest Service, Southern Research Station.

Isebrands, J.G. 2007. Best management practices. Poplar manual for agroforestry applications in Minnesota. St. Paul, MN: University of Minnesota. 13 p.

Klepac, J. and B. Rummer. 2010. Harvesting understory biomass with a baler. In: Proceedings of 2010 COFE: 33rd Annual Meeting of the Council on Forest Engineering, June 6-9, 2010. Auburn, AL. p. 1-11.

McDonald, T.P. and B.J. Stokes. 1994. Harvesting costs and utilization of hardwood plantations. In: Proceedings of the International Energy Agency Biomass Agreement, task 9, activity 1 international conference. Mobile, AL: U.S. Department of Agriculture, Forest Service: 5-13.

Savoie, P., D. Sidders, P.L. Hebert, F. Robert, and J. Villeneuve. 2010. Round bale harvest of short-rotation willow and poplar at three sites in Ontario. Research Report: Agriculture and Agri-Food Canada. 20 p.

Spinelli, R, C. Nati, and N. Magagnotti. 2009. Using modified foragers to harvest short-rotation poplar plantations. *Biomass and Bioenergy* 33: 817-821.

Spinelli, R., B. Hartsough, P. Owende, S. Ward. 2002. Productivity and cost of mechanized whole-tree harvesting of fast-growing eucalypt stands. *International Journal of Forest Engineering* 13(2): 49-60.

Stokes, B. and B. Hartsough. 1993. Development and analysis of SRIC harvesting systems. In: Proceedings, First Biomass Conference of the Americas: Energy, environment, agriculture, and industry; 1993 August 30-September 2; Burlington, VT. Golden, CO: National Renewable Energy Laboratory: 302-308. Volume 1.

US Department of Energy. 2011. U.S. Billion Ton Update: Supply for a bioenergy and bioproducts industry. R.D. Perlack and B.J. Stokes (leads), ORNL/TM-2011/224. Oak Ridge National Laboratory, Oak Ridge, TN. 227 p.

Verani, S., G. Sperandio, R. Picchio, R. Spinelli, and G. Picchi. 2008. Field Handbook – Poplar Harvesting. International Poplar Commission Thematic Papers. Working Paper IPC/8. FAO: Rome, Italy. 54p.

2.8
ECONOMIC ANALYSIS OF DRY MATTER AND ETHANOL YIELD FROM STORED SWITCHGRASS

James A. Larson[1,], Burton C. English[1], T. Edward Yu[1], Nicole Labbé[2], Donald D. Tyler[3]*

Abstract

Biomass storage has been identified as a barrier to the development of a sustainable biomass feedstock supply chain. While there exists a developing literature on storage issues for switchgrass, its adverse effect on the composition of switchgrass for the production of biofuel have only been examined on a limited basis. The objective of this research was to evaluate the effects of alternative bale wrap and outdoor storage methods for switchgrass packaged in large round bales on the composition of biomass that potentially influence biofuel yields. Data from a bale storage experiment at Vonore, TN were used for the study. Large round bales (1.8 m [diameter] × 1.5 m [width]) harvested January 2011 were sampled for DM, stored, and sampled again for DM at 314 days (12-December-2011) to evaluate the compositional changes in stored switchgrass. The bale protection treatments were: twine-wrapped without a tarp, mesh-wrapped two times without a tarp, mesh-wrapped three times without a tarp, and mesh-wrapped two times with a tarp. Results indicate that switchgrass composition varied with bale wrap method and protective cover.

Keywords: Biomass, cellulose, hemicelluloses, lignin

Introduction

The storage of lignocellulosic biomass (LCB) such as switchgrass after harvest and before delivery to a biorefinery has been identified as a barrier to the development of a sustainable LCB feedstock supply chain in the southeastern United States (Research and Development Technical Advisory Committee, 2007). A key factor in making switchgrass production a sustainable low input system is a single, late-season harvest (Rinehart, 2006). After a killing freeze, nutrients move from the above ground biomass into the root system and therefore minimize the quantity removed during harvest and the need for their replacement. By contrast, a twice a year harvest system would nearly double nutrient requirements but provide equivalent yields (Sanderson et al., 1999; Thomason et al., 2005; Vogel et al., 2002). The narrow harvest window and the need for LCB feedstock year-round by conversion facilities will require that storage of LCB be one of the functions performed in a feedstock supply chain (Larson et al., 2010). Due to the bulkiness of switchgrass, most of storage is projected to take place outdoors and away from the biorefinery, either on-farm or at a satellite location (Popp and Hogan, 2007). Yet the exposure of switchgrass to rain, ultraviolet rays, and fluctuations in temperature and humidity may result in storage dry matter (DM) losses and reductions in the quality of biomass (Sanderson et al., 1997).

While there is developing literature on issues related to the storage of switchgrass, its adverse effects on the quantity and quality of DM available after extended periods in storage and before conversion to a biofuel have only been examined on a limited basis (Mooney et al., 2012). Mooney et al. (2012) using data from an outdoor switchgrass bale storage experiment conducted

---

[1] *Department of Agricultural and Resource Economics, The University of Tennessee, TN*

[2] *Center for Renewable Carbon, The University of Tennessee, TN*

[3] *Department of Biosystems Engineering and Soil Science, The University of Tennessee West Tennessee Research and Education Center, TN*

* *Corresponding author*

in 2008 and 2009 at Milan, TN, estimated DM losses after 360 days in storage of 6% for covered and 14% for uncovered round bales (1.2 m [diameter]× 1.5 m [width]) wrapped with twine. By comparison, the estimated DM loss for covered rectangular bales (1.2 m × 1.2 m × 2.4 m) wrapped with twine was 19%. Thus, they found that bale type, storage method, and storage time had substantial impacts on switchgrass DM losses and the costs of feedstock for conversion to a biofuel after storage. However, the impacts of harvest and storage method on the composition of switchgrass DM were not evaluated in the Mooney et al. study.

Research has shown that changes in the composition of mature switchgrass from weathering potentially affect the yield of biofuel and thus the cost of biofuel (Adler et al., 2006). The quality of feedstock for producing a biofuel is different for alternative conversions systems: 1) direct combustion, 2) the production of ethanol from a biorefinery, and 3) thermo-chemical conversion through gasification/pyrolysis (Adler et al., 2006; Boateng et al., 2006). Thus, choice of harvest and storage method before switchgrass is delivered to a conversion facility will have an important impact on the quantity and quality of feedstock for conversion to a biofuel. The objective of this research was to evaluate the effects on composition of alternative bale wrap and storage methods for switchgrass packaged in large round bales and stored outdoors. Preliminary switchgrass composition data from an outdoor storage experiment at the University of Tennessee Biomass Innovation Park in Vonore, TN, were used to achieve the aforementioned research objective.

Methods and Data

Alamo switchgrass was harvested 29-Jan-2011 and 30-Jan-2011 from a 3-year old stand on a farm field near Vonore, TN, using a variable chamber baler (bale dimensions 1.8 m [diameter]× 1.5 m [width]). On 1-Feb-2011, bales were weighed using a weigh wagon and core samples using a Penn State forage sampler were extracted from each bale to determine initial DM content. Bales were moved to The University of Tennessee Biomass Innovation Park, Vonore, TN, and were randomly selected into six storage time treatments over a 504 day period. The data analyzed in the present study are for switchgrass that stored 314 days (12-Dec-2011). The bale protection treatments were: twine-wrapped without a tarp, mesh-wrapped two times without a tarp, mesh-wrapped three times without a tarp, and mesh-wrapped two times with a tarp. Each treatment was replicated five times. Upon removal from storage on 12-Dec-2011, bales were sampled for DM using procedures described in Mooney et al (2012) for the Milan, TN, storage study. Bales upon removal from storage were weighed, wrap materials removed, photographed, separated into two halves, and one of the halves photographed again. The photographs from one half bale section were used to identify up to four distinct weathered areas based on observable moisture and decomposition. Biomass samples within each weathered area were collected by drilling into the bales with a Penn State forage sampler. Dry bale weights at destruction were determined using data on the DM content of samples from each weathered area and their relative proportion.

A composite sample of the DM for each of the bale wrap and protective tarp treatments was created and analyzed for the composition that potentially influences the yield of biofuel from switchgrass (three replications per treatment). The components of composition reported in this research were cellulose, hemicelluloses, lignin, extractives, and total ash. The Bioenergy Science and Technology Laboratory in the Center for Renewable Carbon followed the NREL Standard Biomass Analytical Procedures to analyze the samples (Sluiter et al., 2008).

Results

The means for each bale protection treatment on a percentage dry basis for the composition of switchgrass entering storage (1-Feb-2011) and after 314 days in storage (12-Dec-2011) are presented in Figure 1. Confidence intervals ($p<0.05$) for each treatment are also presented in Figure 1. The treatments were used to evaluate whether mesh-wrapped bales with and without a tarp, relative to twine-wrapped bales without a tarp, changed the composition of switchgrass after storage, Several preliminary findings can be drawn from the figure.

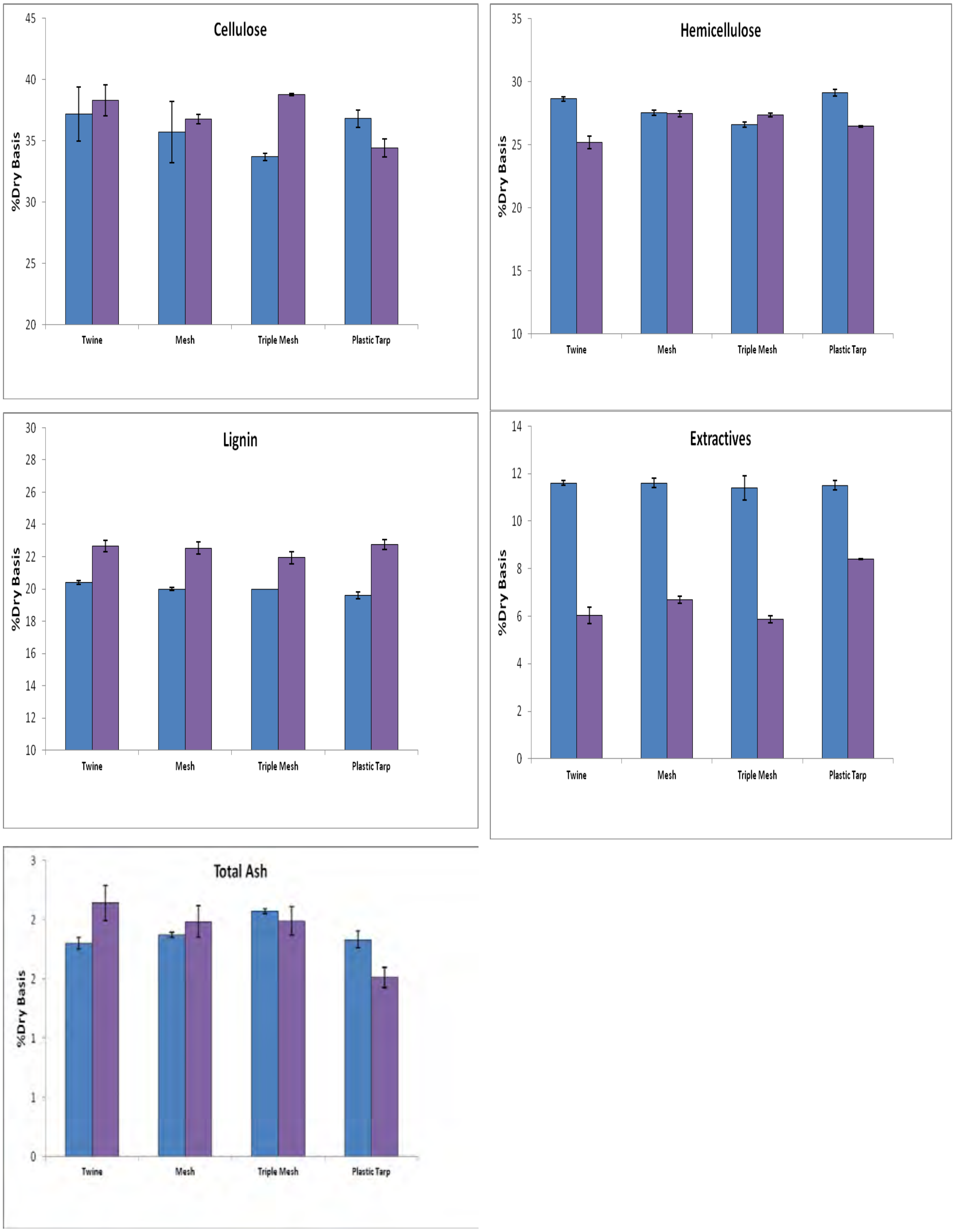

Figure 1. Change in the composition of switchgrass stored outdoors 314 days for alternative large bale wrap and storage cover treatments, Milan, TN, 2011

First, switchgrass bales wrapped two times with mesh and covered with a tarp had significantly lower cellulose and hemicellulose after 314 days in storage. Hemicellulose was also significantly lower in twine wrapped bales after storage. The cellulose content in bales wrapped three times with mesh and stored without a protective cover was significantly higher after 314 days in storage. Cellulose produces glucose and hemicellulose produces mostly pentoses and some hexoses and are indicators of sugars available for the production of ethanol (Sarath et al., 2008). Glucose produces more ethanol than most other sugars (Adler et al., 2006).

Second, lignin content was significantly higher after 314 days in storage for all four bale wrap and storage cover treatments. Lignin potentially interferes with the fermentation process for the production of ethanol (Sarath et al., 2008). The preliminary data presented here indicate that lignin in stored switchgrass was not influenced by choice of bale wrap or storage cover.

Finally, the total ash content of switchgrass stored as uncovered round bales wrapped with twine was significantly larger after 314 days in storage. The total ash content of switchgrass stored as round bales wrapped twice with mesh and covered with a tarp was significantly smaller after 314 days in storage. Total ash content was unchanged for round bales wrapped either two or three times with mesh and not covered with a tarp. Reduced ash (mineral) content is generally associated with increased energy content for conversion to biofuels (Adler et al., 2006).

Conclusions

This study evaluated the effects of alternative bale wrap and storage covers for switchgrass stored outdoors in large round bales for 314 days in an experiment at Vonore, Tennessee. The bale protection treatments were: twine-wrapped without a tarp, mesh-wrapped two times without a tarp, mesh-wrapped three times without a tarp, and mesh-wrapped two times with a tarp. Preliminary results indicate that the composition of stored switchgrass was influenced choice of bale wrap and storage cover method. Large round bales wrapped three times with mesh and stored without a protective tarp had consistent increases in cellulose and hemicellulose during storage when compared to the other treatments. Cellulose and hemicellulose are indicators of potential sugars available for the production of ethanol. The preliminary data described in this paper along with data for other storage times in the experiment will be used to provide a comprehensive evaluation of the costs and returns of alternative methods of packaging and storing switchgrass before delivery to a biorefinery.

References

Adler, P.R, M.A. Sanderson, ,A.A. Boatang, P.J. Weimer, and H.G. Jung. 2006. Biomass Yield and Biofuel quality of Switchgrass Harvested in Fall or Spring. Agronomy Journal 98: 1518-1525.

Biomass Research and Development Technical Advisory Committee. 2007. *Roadmap for Bioenergy and Biobased Products in the United States.* Washington, DC: U.S. Department of Agriculture. Available online at http://www1.eere.energy.gov/biomass/pdfs/obp_roadmapv2_web.pdf

Boateng, A.A., K.B. Hicks, and K.P. Vogel. 2006. Pyrolysis of switchgrass (Panicum virgatum) harvested at several stages of maturity. J. Anal. Appl. Pyrolysis 75:55–64.

Larson, J.A., T. Yu, B.C. English, D.F. Mooney, and C. Wang. 2010. Cost Evaluation of Alternative Switchgrass Producing, Harvesting, Storing, and Transporting Systems and their Logistics in the Southeastern US. *Agricultural Finance Review* 70:184-200.

Mooney, D.F., J.A. Larson, B.C. English, and D.D. Tyler. 2012. Effect of Dry Matter Loss on Profitability of Outdoor Storage of Switchgrass. *Biomass & Bioenergy* 44:33-41.

Popp, M., and R. Hogan, Jr. 2007. Assessment of Two Alternative Switchgrass Harvest and Transport Methods. Presented at Biofuels, Food, and Feed Tradeoffs Farm Foundation Conference, St. Louis, MO, April 12-13.

Rinehart, L, 2006. Switchgrass as a Bioenergy Crop. National Center for Appropriate Technology, Available online at: http://attra.ncat.org/attra-pub/PDF/switchgrass.pdf

Sarath, G., B., R.B. Mitchell, S.E. Sattler, D. Funnell, J.F. Pederson, R.A Graybosch, and K. P. Vogel. 2008. Opportunities and Roadblocks in Utilizing Forages and Small Grains for Liquid Fuels. *Journal of Industrial & Microbiol Biotechnology* 35: 343-354.

Sanderson, M.A., R.P. Egg, and A.E. Wiselogel. 1997. Biomass Losses during Harvest and Storage of Switchgrass. *Biomass & Bioenergy* 12: 107-114.

Sanderson, M., J. Read, and R. Reed. 1999. Harvest Management of Switchgrass for Biomass Feedstock and Forage Production. *Agronomy Journal* 91(1): 5-10.

Sluiter, A., B. Hames, R. Ruiz, C. Scarlata, J. Sluiter, and D. Templeton. 2008. "Determination of Sugars, Byproducts, and Degradation Products in Liquid Fraction Process Samples Laboratory Analytical Procedure (LAP)" Technical Report NREL/TP-510-42623, January 2008. Golden, Colorado: National Renewable Energy Laboratory. Online at: http://www.nrel.gov/biomass/pdfs/42623.pdf.

Thomason, W.E., W.R. Raun, G.V. Johnson, C.M. Taliaferro, K.W. Freeman, K.J. Wynn, and R.W. Mullen, 2004. Switchgrass Response to Harvest Frequency and Time and Rate of Applied Nitrogen. *Journal of Plant Nutrition* 27: 1199-1226.

Vogel, K., J. Brejda, D. Walters, and D. Buxton. 2002. Switchgrass Biomass Production in the Midwest USA: Harvest and Nitrogen Management. *Agronomy Journal* 94(3): 413-420.

2.9
DIRECT HARVEST MOISTURE CONTENT AND COST DIFFERENCES FOR BIOMASS CROPS ACROSS SIX LOCATIONS IN THE SOUTH

Michael P. Popp[1,], Stephen S. Searcy[2], Shahab Sokhansanj[3], James Smartt[1]*

Abstract
The Integrated Biomass Supply Analysis and Logistics (IBSAL) model which sequentially tracks harvest progress for a set of fields with user-defined equipment was modified for this research by allowing: i) rewetting of swathed material in the drying formulae; ii) field queuing rules that are based on equipment availability and weather in addition to moisture content limits; and iii) differential crop yield, harvest time and initial moisture conditions. Using different equipment complements and in-field drying delays between mowing and harvest, harvested moisture content, annual tonnage processed and associated processing cost differences between irrigated forage sorghum and non-irrigated switchgrass were estimated at six different locations across Arkansas and Texas using 10-year daily weather histories. To do this, crop-specific harvest seasons with attendant differences in initial moisture content and starting yields were estimated from available experimental data. Field drying delays ranging from 2 to 6 d with and without use of a rake between mowing and harvest were evaluated. Results showed relatively minor differences in cost of production across location and crop. Hence, extending the hours of annual equipment use with longer harvest windows or with a drier season had minor implications on cost of production. Ultimate harvested moisture content findings, on the other hand, suggest that forage sorghum will prove difficult to dry in the field and hence harvest schedules in the earlier and drier part of the season may be preferred in conjunction with later harvest schedules for switchgrass.

INTRODUCTION
Capital costs needed to harvest and transport copious quantities of biomass for conversion to biofuels (Thorsell et al. 2004; Epplin et al. 2007; Hess, Wright and Kenney 2007; Mapemba et al. 2008; Kumar and Sokhansanj 2007; Sokhansanj et al. 2009; Larson et al. 2010) are a concern to investors interested in meeting federal goals of 16 billion gallons of cellulosic biofuels by 2022 (RFA 2011). Large scale biorefineries, likely to adapt to an integrated supply chain where fields are custom harvested with equipment owned by the biorefinery, are likely to encounter logistics issues associated with bulky, low-density biomass, especially in baled form as handling, storage and other transactions costs associated with small package size would be considerable (Cundiff and Grisso 2008, Popp and Hogan 2007, Stephen et al. 2010, Ebadian et al. 2011). Hence, in-field storage as a standing crop (Ashworth 2010; Douglas 2011; Rocateli 2010) provides an alternative to baling and storage as harvested material from the field would be delivered directly to the biorefinery with limited intermediate storage. As such, moisture condition (MC) limitations for safe storage (MC < 20% w.b.) are less important and in-field drying delays may be scheduled around equipment capacity rather than stochastic delays for meeting MC targets needed for extended storage in baled from.

Further and similar to Larson et al. (2010), this work thus centers around the use of a forage harvester rather than baling biomass as particle size reduction from harvestable plant material to chopped biomass with particle size of < 1/3” is less energy intensive using a forage harvester (~ 2.5 to 5 hp hr/ton as is)

[1] *Department of Agricultural Economics and Agribusiness, University of Arkansas, AR*

[2] *Biological and Agricultural Engineering, Texas A&M University, TX*

[3] *Environmental Sciences Division, Oak Ridge National Laboratory, TN*

* *Corresponding author*

than tub-grinding dried, baled biomass (8 to 21 hp hr/ton as is) (ASABE 2011; Mani, Tabil and Sokhansanj 2004; Buckmaster and Hilton 2005). Field operations commence with a mower conditioner followed by a forage harvester and are modeled with differential in-field drying delays between mowing and harvesting using the IBSAL modeling framework developed by Sokhansanj, Kumar and Turhollow (2006).

Using observed 10-year histories of weather data (NOAA 2008), the specific objectives of this paper were to provide a comparison of processing costs, annual tonnage processed and harvested MC: i) across crops of switchgrass (*Panicum Virgatum)* and forage sorghum (*Sorghum bicolor*); ii) by location (3 locations each in Arkansas and Texas); iii) by harvest period of July through September and October through December for both crops as well as January to February for switchgrass only; and iv) by different in-field drying delays between field operations. Results are deemed useful to biomass logistics managers as annual field capacity estimates of the espoused equipment complement and attendant MC expectations at the biorefinery are available for a range of weather conditions.

DATA AND METHODS

As outlined in Figure 1, a 375-hp, self-propelled forage harvester with a pickup header (panel 3) is used as the base equipment to drive additional equipment needs in the form of two self-propelled mower conditioners (panel 1) and a twin rake (panel 2) intended to enhance drying and field efficiency of the forage harvester. The raking process is not used for forage sorghum since high yield, length and rigidity of stems have been demonstrated to clog equipment at experimental locations in Texas. While trailers equipped with walking floors (panel 4) are pictured, they are not modeled in this analysis as the number of units would depend on a host of factors -- biorefinery size, biomass yields and crop adoption (% of crop land devoted to energy crops) as well as MC given trailer volume and weight limitations.

1. Cut 2. Rake 3. Harvest 4. Unload

Figure 1. Equipment Complement and Operations Sequence.

The cost of equipment is based on 2009 manufacturer suggested retail prices for equipment (JD 2011) discounted by 10% to reflect likely purchase price of equipment. Remaining value calculations for annual capital recovery estimates, repair factors, fuel use, taxes, insurance and housing were performed using ASABE standards (2011). A capital recovery rate of 6% is higher than the recommended 3% by the AAEA to reflect a risk premium associated with as yet unproven investments in biomass conversion facilities (AAEA, 2000).

Table 1 highlights yield potential as well as initial MC assumptions for both crops by expected harvest season. Forage sorghum would yield 8 dry tons per acre from mid-July through mid-December with an initial MC of 75% w.b. regardless of time of cutting within the season. Significant potential for lodging, attendant harvest losses and reduction in processing speed are also deemed to preclude harvest in January and February of the following year. By contrast, harvest of switchgrass can occur as early as July at high initial MC all the way through February as this crop is quite resistant to lodging and dries down after senescence as shown in Figure 2. To approximate yield potential at different times of the year (yield curve) as well as across regions with differences in annual rainfall totals, data from Fayetteville, AR (Ashworth 2010) were fitted with polynomial predicting equations using week of harvest as the explanatory variable to estimate yield and initial MC at different times of the year:

(1) $Yield_x = a_0 + a_1 \cdot x + a_2 \cdot x^2 + a_3 \cdot x^3 + \varepsilon$
(2) $MC = b_0 + b_1 \cdot x + b_2 \cdot x^2 + b_3 \cdot x^3 + \delta$

where $Yield_x$ is the biomass yield in dry tons per acre in week $_x$, x is the harvest starting with 1 for the first week in July and ε/δ are error terms. While initial MC did not vary by location (Figure 3), yields did. Therefore coefficients of the yield curve obtained from Fayetteville, AR, were multiplied by the ratio of expected annual rainfall totals to obtain estimates of yields at different times of the year for the other study locations using the following equation:

(3) $Yield_{x,other} = a_0 \cdot r_{other} / r_{Fay} + a_1 \cdot r_{other} / r_{Fay} \cdot x + a_2 \cdot r_{other} / r_{Fay} \cdot x^2 + a_3 \cdot r_{other} / r_{Fay} \cdot x^3$

where r_{other} and r_{Fay} are the average annual 10-year rainfall as observed in this study for locations other than Fayetteville, AR and Fayetteville, AR, respectively (Table 2). This procedure was deemed appropriate as the only other available yield curve data for lowland Alamo switchgrass in the study region at the time of writing was available for Knox City, TX, a location approximately 130 miles east of Lubbock, TX. Using the above method, estimated yields were similar to the observed data in Knox City, TX with a ten-year average annual rainfall of approx. 26.4" (Figure 2). Finally, a single harvest was modeled primarily for the sake of enhancing stand life of switchgrass and lowering fertilizer needs for forage sorghum.

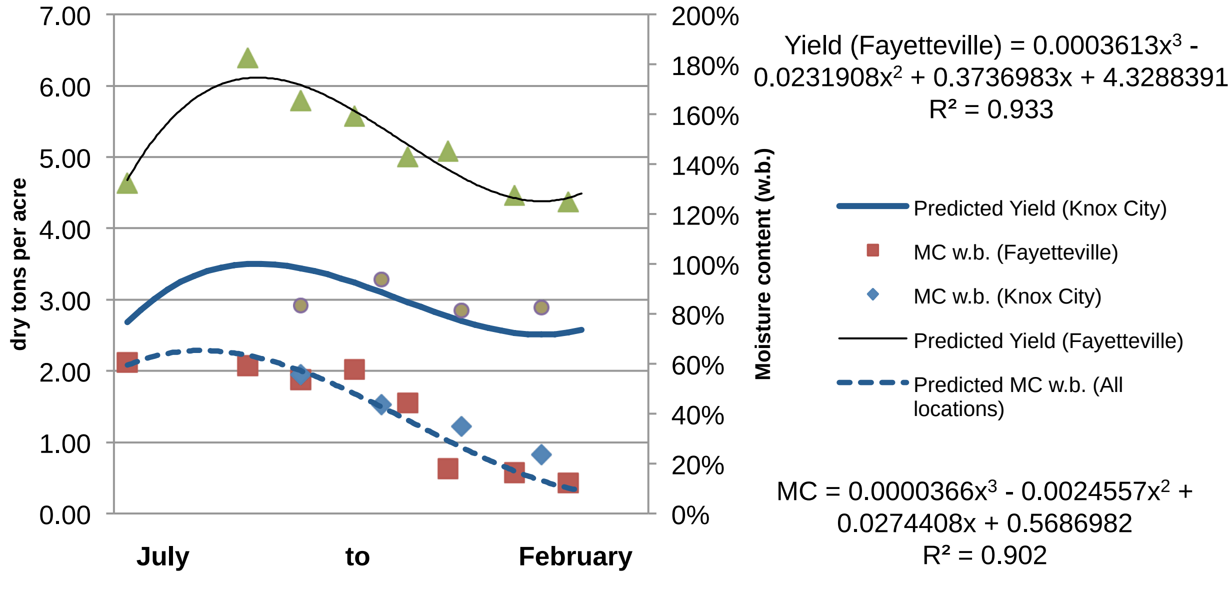

x = week number starting with 1 for the first week of July and ending with 35, the last week in February

Figure 2. Moisture Content (MC) and Yield Tradeoffs in Switchgrass. Source: Ashworth (2010) and Douglas (2011).

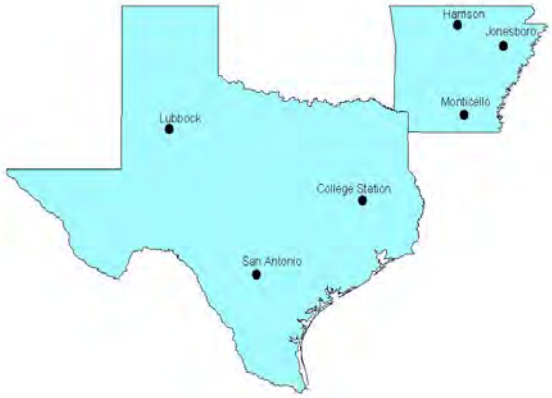

Figure 3. Study Locations for Climate Differences.

Table 1. Expected Yield and Initial Moisture Content of Forage Sorghum and Switchgrass.

Crop	Julian Week	Harvest Moisture Content (w.b.)	Yield (dry ton)
Forage Sorghum	28 - 50	75%	8.00
Switchgrass[a]	26 - 38	63%	5.74
	39 - 50	44%	5.66
	1 - 8	15%	4.47

[a] Yields and moisture content for switchgrass are from the yield curve estimated in Figure 2 for Fayetteville, AR as observed across random plots of experimental trials performed in 2009 and 2010.

To determine a starting point for items or field sizes in IBSAL for comparing weather effects across locations, it was necessary to develop likely estimates of annual acreage harvested for the espoused equipment complement by specifying an expected number of workable field days in a week. Tables 1, 3 and 4 highlight these assumptions by providing equipment details, annual ownership charges as well as processing cost estimates per dry ton related to the forage harvester, mower conditioner and rake. Two 14 ½' wide self-propelled 200-hp disc mowers with twin intermeshed steel conditioning rolls were needed to keep up with the capacity of the forage harvester using 8-hour mowing days. A twin rake, in the case of switchgrass made equipment traffic easier as combined swaths lead to fewer required turn rows and larger turning radii. While other equipment choices are available, the above equipment was readily available for modeling in IBSAL and allowed for MC and cost comparisons across location and differential field drying delays between operations.

Buckmaster and Hilton (2005) reported 2.5 to 4 hph / ton as is for corn stover and haylage, respectively. Using 3.25 hph / ton as is at 65% moisture, 80% field efficiency and a swath density of 3 lb dry matter/cubic foot leads to a volumetric throughput of 21,538 cubic foot per hour or 32.31 dry ton per hour. Shinners et al. (2006) reported an average of nearly 29 dry ton/hour using a 505-hp forage harvester in corn stover. They state that horsepower were underutilized as field speed was curtailed by pickup difficulties. Since all feedstock is not harvested at the same MC we made the added assumption that volumetric throughput does not change significantly across harvest MC of the crop and hence the forage harvester is only expected to slow down/speed up with higher/lower yields per acre. The last footnote to Table 4 provides alternative estimates of fuel use and cost given a higher horsepower forage harvester to address likely impact on throughput capacity of the forage harvester.

Table 4. Investment Cost and Performance Assumptions for Harvesting Equipment Using Five Working Field Days per Week for Forage Sorghum and Switchgrass and Fayetteville Yield Expectations.

Equipment	hp	Capacity in dt / field hr	Pur-chase Price ($)[a]	Disc. Salvage Value ($)[b]	Annual Field Hour Use[c]	Useful Life in Field	Years of Useful Life	R&M Factor[b]	Fuel ($ / field hr)	R&M ($ / field hr)	Labor ($ / field hr)	Op. Int. ($ / field hr)[d]	Crop
Forage Harvester (JD 7250) w pickup	375	32.31	217,445	91,813	1,980	4,000	1.84	0.50	45.38	29.90	16.50	1.04	Switch grass (SG)
200 hp SP mower (JD R450)	200		86,540	21,527	1,320	10,000	6.89	1.00	24.20	9.52	16.50	0.57	
Rot. mow. w steel cond. (JD 994)		24.23	24,973	11,001	1,320	2,000	1.38	1.00	-	13.74	-	0.16	
75 hp MFWD cab tractor (JD 6230)	75		56,319	6,892	660	12,000	16.53	1.00	9.08	5.16	16.50	0.35	
V-twin rake (Vermeer R2800)		96.92	24,938	8,718	660	2,500	3.44	0.60	-	6.58	-	0.07	
Forage Harvester (JD 7250) w pickup	Same as Switchgrass			83,238	1,380	as above	2.64	Same as Switchgrass				0.72	Forage Sorghum (FS)
200 hp SP mower (JD R450)				16,476	920		9.88					0.40	
Rot. mow. w steel cond. (JD 994)				10,317	920		1.98					0.11	

			Annual Capital Recovery[e]		Fixed Cost in $/dt		Var. Cost in $/dt		Total Cost in $/dt		Fuel Use (gal/dt) exl. Lube	
Actual engine hours/field hour	1.1											
Fuel per hp hour (gal)	0.044											
Fuel price ($/gal)	2.50		*SG*	*FS*	*SG*	*FS*	*SG*	*FS*	*SG*	*FS*	*SG*	*FS*
Capital recovery rate	6%	**Chop**	82,876	64,575	1.30	1.45	2.87	2.86	4.17	4.31	0.56	0.56
Labor rate ($/hour)	15.00	**Mow**	52,126	41,357	0.81	0.93	2.67	2.66	3.48	3.59	0.40	0.40
Operating interest	5%	**Rake**	12,055	na	0.19	na	0.39	na	0.58	na	0.04	na
Insurance, Housing and Taxes	2%											
Inflation rate	3%	**Total**	147,056	105,932	2.30	2.38	5.93	5.52	8.23	7.89	1.00	0.96

[a] Purchase prices were taken from the John Deere U.S. Website for Hay & Forage Equipment as available in January 2010 for 2009. The Vermeer rake price was obtained by calling the manufacturer. Purchase price was discounted by 10%. The authors do not endorse John Deere as the manufacturer of choice but merely use them as an example.

[b] Remaining value coefficients, useful life and R&M as percent of purchase price were the ASABE D497.7 Machinery Management Data revised in March of 2011 and were adjusted for inflation to arrive at the salvage value of the equipment if sold at end of useful life in 2009 dollars.

[c] Based on field hours for the forage chopper which in turn depend on crop modeled. The mowers operate at 2/3 the capacity of the forage harvester and hence two units are purchased per forage harvester. The raking operation was assumed to occur at 3 times the field speed of the forage harvester.

[d] Operating interest was prorated on the basis of number of field days and was estimated using half the total annual variable cost required. Variable costs do not change across crop except for added operating interest given the longer harvest window with switchgrass. The cost for forage sorghum was thus one penny less for the chopping and mowing operations.

[e] Raising horsepower requirements on the forage harvester resulted in higher fuel use of (0.82 gal/dt) for chopping and higher total cost/dt of $5.99/dt compared to $4.31/dt in the case of forage sorghum and $5.79/dt vs. $4.17/dt in the case of switchgrass or approximately $1.65/dt higher. With higher fuel prices, this difference would be larger.

Using these performance data, 5,573 and 11,971 acres of forage sorghum and switchgrass, respectively, would be harvested over their respective 23- and 33-week harvest windows by tracking harvest progress on fields approximately 50 acres in size under Fayetteville weather conditions. The annual operating times are much longer than those proposed by Larson et al. (2010) as harvest MC restrictions for safe storage were not imposed. Hence, the delay functions in IBSAL needed to be modified to restrict harvest progress by equipment availability and weather constraints (no harvest on days exceeding ½" of rainfall) rather than harvest MC with an unrestricted supply of equipment. The output would now report on tonnage processed and its estimated harvest MC for one equipment complement at different locations and across different weather years. This information can then be scaled up to allow biorefineries estimates of capital requirements for biomass procurement at different times of year and by crop.

Corn silage drying formulae as well as the switchgrass drying formula available with IBSAL (http://biomass.ubc.ca/research.html) were used to estimate in-field drying of forage sorghum and switchgrass, respectively. Modifications to the drying formulae were made to allow for drying and rewetting as a function of daily precipitation and evaporation (Sokhansanj et al. 2008). In this model, the instantaneous change in surface MC of the biomass is the difference between precipitation and evaporation. The change in the entire biomass is a first order diffusive process.

Moisture content for each field at time of harvest and cumulative tonnage harvested were summarized by harvest season using average and standard deviation of field observations across both crops, by location and drying delay (ranging from 2 d to 6 d between mowing and harvesting) using different actual weather data spanning from 1998 to 2007. This information was used to replace expected annual field hours with actual field hours (tonnage processed/divided by hourly field capacity) for each location and year to arrive at processing cost estimates similar to those provided in Table 4 except that they are now weather, location and in-field-drying delay dependent.

RESULTS

As shown in Figure 4, even at a location with relatively little rainfall, MC varies substantially with a 1d 1d set of delays for switchgrass. January and February MC data are reflective of initial low MC at time of cutting, whereas higher MC observations in the October to December season are reflective of both poorer drying conditions, more frequent rain events and higher initial MC at time of cutting.

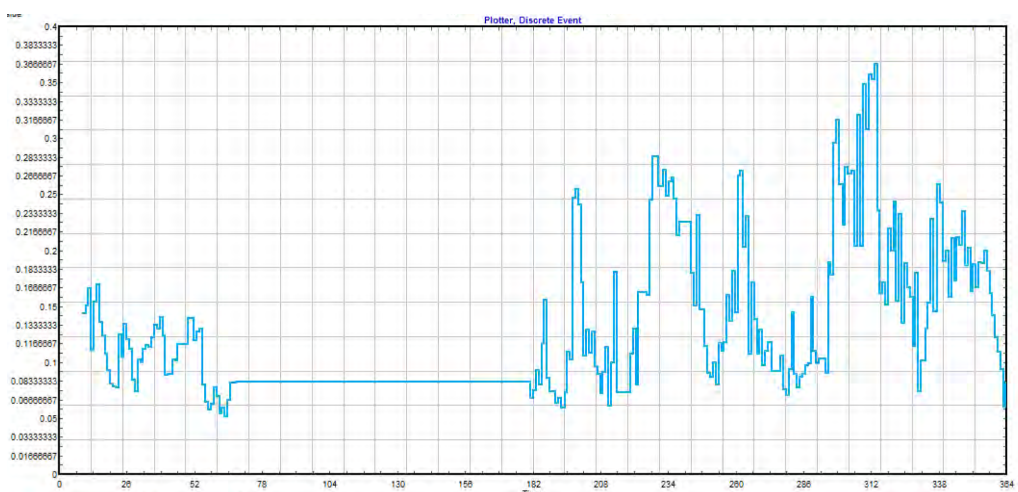

Figure 4. Sample Output of ExtendSim v.8. Moisture Content Results by Day of Year for Switchgrass Harvested in Lubbock, TX Using 1998 Weather Data with a 1 Day Delay Between Mowing and Raking and a 1 Day Delay Between Raking and Harvesting. Flat Lines beyond 1 Day Indicate Lack of Processing on that Day due to Weather Delays or Lack of Harvest.

Tables 5 through 7 summarize information about three locations (remaining locations are available from the author upon request). Jonesboro, AR with similar rainfall and temperature conditions as Fayetteville is the most northeastern location with attendant cooler temperatures and higher rainfall than would typically be observed in Texas. San Antonio, TX provides information for the most southern location with intermediate rainfall and highest annual temperatures, whereas Lubbock, TX provides information for the driest climate with moderate to coldest temperatures depending on season (Table 2).

Table 2. Annual and Seasonal Rainfall Totals and Average Temperatures by Location, 1998 to 2007.

Location		**Rainfall** (in inches)			**Temperature** (in ℉)		
	Annual	Jul. – Sep.	Oct. – Dec.	Jan. – Feb.	Jul. – Sep.	Oct. – Dec.	Jan. – Feb.
Harrison, AR	46.0	11.5	13.8	7.9	76	50	37
Jonesboro, AR	46.2	10.7	15.0	9.4	78	51	38
Monticello, AR	42.0	9.9	13.1	9.1	80	55	41
San Antonio, TX	32.3	9.2	8.7	4.0	82	62	47
College Station, TX	39.0	11.3	16.6	7.2	83	61	46
Lubbock, TX	18.7	5.7	4.8	1.7	78	51	39

As seen in all locations, extending the drying delays beyond 2 days resulted in only small reductions in harvested MC. One of the reasons for this is that the likelihood of rewetting with rainfall events increases with longer delays between cutting and harvest and hence impedes dry down. Cost of processing also increases slightly as fewer tons are harvested with the longer delays given crop losses due to leaching.

The model runs also suggest that primarily the longer production window with switchgrass compared to forage sorghum results in lower processing costs as fixed costs could be spread over higher annual usage although this fact is obscured by not modeling the raking process for forage sorghum. Nonetheless these processing cost differentials between crops are relatively minor in the authors' opinion (see fixed cost per dt in Table 4). The results also suggest that the expectation of five working days per seven day week varies by location as expected. For the drier locations, Lubbock and San Antonio, the average annual capacity for either forage sorghum or switchgrass exceeded expectations. At Jonesboro, however, annual average production was less than budgeted in Table 3 given the higher rainfall compared to San Antonio or Lubbock.

Table 3. Estimated Field Capacity by Production Period Using One 375 HP Forage Harvester for Either Forage Sorghum or Switchgrass Along With Expected Acreage and Tonnage Information Using Fayetteville Yield Expectations for Switchgrass.

Crop	Week of Year	# of weeks	Field Hours per Day/Yr	Expected Field Days per Week/Yr	as is tons per hour[a]	Acres per hour[b]	Field Speed in mph[b]	Acres per day/Yr	Dry tons per day/Yr
Forage Sorghum	28 - 50	23	12	5	129.2	4.04	2.97	48.5	387.7
Total			1,380	115				5,573	44,585
Switchgrass	26 – 38	13	12	5	87.2	5.63	4.15	67.5	387.7
	39 – 50	12	12	5	57.5	5.71	4.21	68.6	387.7
	1 – 8	8	12	5	37.8	7.22	5.32	86.7	387.7
Total			1,980	165				11,971	63,969

[a] Acres per hour are based on 3.25 hp hours per ton at 65% moisture and 80% harvest efficiency. With a dry matter density of 3 lb/cubic foot in the swath, this translates to 21,538 cubic foot processed per hour. In turn, 21,538 cubic foot per hour can be converted to as is tonnage per

hour at different moisture contents assuming that wetter material does not occupy extra space or affect processing speed. The dry matter throughput thus works out to 32.31 tons/hour.

[b] Field speed is calculated using a swath covering 28' and 14' for switchgrass and forage sorghum, respectively. Speed is adjusted for harvest efficiency. Acres per hour = as is tons per hour/as is yield per acre.

What is more significant is the difference in MC across location, crops and harvest delay rule. Average MC in the fall season (Oct – Dec) was 47% or higher across all locations and drying delays for forage sorghum. Given the potentially high cost of drying materials postharvest to safe MC (Table 8), harvest of forage sorghum in late fall comes at a cost disadvantage compared to switchgrass. Even at the wettest and most northeastern location, average MC for switchgrass is half that of expectations for forage sorghum at the driest location. Biorefinery managers may thus curtail harvest of forage sorghum to the earlier season when switchgrass is still achieving yield maximum (mid-August (Fig. 2)) whereas switchgrass would be the primary source later in the year. This recommendation only holds, however, if lower yielding switchgrass can compete economically with forage sorghum and returns of other enterprises (Popp et al., 2008).

Table 8. Natural Gas Cost of Moisture Content (MC) Reduction to 20% w.b. at 1,500 BTU/lb of Water Removed and $3/MM BTU.

% MC	**lbs of Water removed per dry ton**	**Cost** ($/dry ton)
25	133	0.60
30	286	1.29
35	462	2.08
40	667	3.00
45	909	4.09
50	1,200	5.40

ACKNOWLEDGEMENTS

Research funding for this analysis was provided by a 2007 South Central Sun Grant Integrated Award. We also acknowledge the careful review and testing of the drying model by doctoral candidates Mahmoud Ebadian (University of British Columbia) and Heung Jo An (Texas A&M University) and switchgrass data sharing by Dr. C. West (University of Arkansas) and J. Douglas (USDA NRCS, Forth Worth, Texas).

REFERENCES

American Agricultural Economics Association (AAEA). 2000. "Commodity Costs and Returns Estimation Handbook." AAEA. Ames, IA.

ASABE Standards, 2011. ASAE D497.7 American Society of Agricultural Engineers, St. Joseph, MI.

Ashworth, A. J. 2010. "Biomass Production and Nutrient Removal of Switchgrass as a Bioenergy Feedstock". Unpublished MSc Thesis. Department of Crop, Soil and Environmental Sciences, University of Arkansas.

Buckmaster, D. R. and J. W. Hilton. 2005. "Expanded Cycle Analysis—Forage or Biomass Harvest". Paper No: 056054. 2005 ASEA Meeting Presentation, Tampa, Florida.

Douglas, J. 2011. Plant Materials Specialist. USDA Natural Resource Conservation Service. Fort Worth, TX. Personal communication. June 2011.

Ebadian, M., T. Sowlati, S. Sokhansanj, M. Stumborg, L. Townley-Smith. 2011. "A new simulation model for multi-agricultural biomass logistics system in bioenergy production." *Biosystems Engineering* (UK) Forthcoming.

Epplin, F.M., C.D. Clark, R.K. Roberts and S. Hwang. 2007. "Challenges to the Development of a Dedicated Energy Crop". *American Journal of Agricultural Economics* 89(5):1296-1302.

Extend Simulation Model v. 8.0, 2010. Available from: http://www.extendsim.com

Hess, J.R., C.T. Wright and K.L. Kenney. 2007. "Cellulosic Biomass Feedstocks and Logistics for Ethanol Production". *Biofuels, Bioproducts and Biorefining* 1:181-190.

Huang, S. F.M. Epplin, B. Lee and R.L. Huhnke. 2009. "A Probabilistic Estimate of the Frequency of Mowing and Baling Days Available in Oklahoma USA for the Harvest of Switchgrass for Use in Biorefineries". *Biomass and Bioenergy* 33:1037-1045.

JD. 2010. John Deere. USA/Canada Home, Agriculture, Hay and Forage Equipment. http://www.deere.com/en_US/ProductCatalog/FR/category/FR_HAY.html. Accessed January 2010.

Kumar, A. and S. Sokhanshanj. 2007. Switchgrass (*Panicum vigratum*, L.) delivery to a biorefinery using integrated biomass supply analysis and logistics (IBSAL) model. *Bioresource Technology* 98:1033–1044.

Larson, J.A., T-H. Yu, B. C. English and D. F. Mooney. 2010. "Cost evaluation of alternative switchgrass producing, harvesting, storing, and transporting systems and their logistics in the Southeastern USA." *Agricultural Finance* 70(2):184-200.

Mani, S. L. G. Tabil and S. Sokhansanj. 2004. "Grinding Performance and Physical Properties of Wheat and Barley Straws, Corn Stover and Switchgrass." *Biomass and Bioenergy* 27:339-352.

Mapemba, L.D., F. M. Epplin, R.L. Huhnke and C. M. Taliaferro. 2008. "Herbaceous Plant Biomass Harvest and Delivery Cost with Harvest Segmented by Month and Number of Harvest Machines Endogenously Determined". *Biomass and Bioenergy* 32:1016-1027.

Mobini, M., T. Sowlati, S. Sokhansanj. 2011. "Forest biomass supply logistics for a power plant using the discrete-event simulation approach." *Applied Energy* 88(2011):1241-1250.

NOA. 2008. National Climatic Data Center. Integrated Surface Hourly Data. http://www.ncdc.noaa.gov/doclib. Accessed September, 2008 through March 2009.

RFA. Renewable Fuels Association. 2011. Renewable Fuels Standard. Available from http://www.ethanolrfa.org/pages/renewable-fuels-standard as accessed on August 16, 2011.

Rocateli, A.C. 2010. "A New Spin on an Old Crop for Bioenergy: Sorghum". Unpublished MSc Thesis. Department of Agronomy and Soils. Auburn University.

Shinners, K.J., B. N. Binversie, R. E. Muck, P. J. Weimer. 2006. "Comparison of wet and dry corn stover harvest and storage." *Biomass and Bioenergy* 31:211-221.

Sokhansanj, S., S. Mani, S. Tagore, A.F. Turhollow. 2010. "Techno-economic analysis of using corn stover to supply heat and power to a corn ethanol plant - Part 1: Cost of feedstock supply logistics." *Biomass and Bioenergy* 34(1):75-81.

Sokhansanj, S., S. Mani, A. Turhollow, A. Kumar, B. Bransby, L. Lynd, M. Laser. 2009. Large scale production, harvest and logistics of switchgrass (*Panicum vigatum L.*) – current technology and envisioning a mature technology. *Biofuel, Bioproduct & Biorefinery* (2009) 3:124-141.

Sokhansanj, S., A. Kumar and A. Turhollow. 2006. "Development and Implementation of Integrated Biomass Supply Analysis and Locistics Model (IBSAL)". *Biomass and Bioenergy* 30: 838-847.

Sokhansanj, S., A. Turhollow, E. Wilkerson. 2008. Development of the Integrated Biomass Supply Analysis and Logistics Model (IBSAL). Technical Memorandum ORNL/TM-2006/57. Oak Ridge national Laboratory, Oak Ridge , TN 37831. Pp 47.

Stephen, J., S. Sokhansanj, X. Bi, T. Sowlati, C. J. Lim, M. Stumborg, L. Townley-Smith, T. Sauder, T. Kloeck. 2010. "The Impact of Biomass Feedstock Supply Variability on the Delivered Price to a Biorefinery in the Peace River Region of Alberta". *Canada* 105:298-305.

Thorsell, S., F. M. Epplin, R.L. Huhnke and C.M. Taliaferro. 2004. "Economics of a Coordinated Biorefinery Feedstock Harvest System: Lignocellulosic Biomass Harvest Cost". *Biomass and Bioenergy* 27:327-337.

Vermeer. 2010. Personal Communication. January 2010.

Table 5. Estimated Final Harvested Moisture Content, Tonnage and Cost per Dry Ton Processed for San Antonio, TX by Crop and Harvest Delay using an Equipment Complement Centered Around One 375 hp Forage Harvester, 1998 – 2007.

Crop		**Delay[a]**	**Forage Sorghum**			**Delay**	**Switchgrass**			
Harvest Period			Jul - Sep 75 d[b]	Oct - Dec 75 d	Total 150 d		Jan - Feb 60 d	Jul - Sep 90 d	Oct - Dec 75 d	Total 225 d
Tons	Avg.		23,674	25,241	48,527		16,522	27,674	25,265	69,132
Processed	Std. Dev.		3,160	4,086	5,657		1,649	4,127	4,233	6,995
Moisture	Avg.	2 d	41%	51%	46%	1 d 1 d	12%	22%	20%	19%
in % w.b.	Std. Dev.		10%	12%	24%		3%	7%	7%	11%
Cost in $/dt[c]	Avg.		$7.84		*1,502*			$8.16		*2,140*
Field Hours	Std. Dev.		$0.10		*175*			$0.07		*216*
Tons	Avg.		23,863	24,650	48,125		16,814	27,694	24,815	69,031
Processed	Std. Dev.		3,379	4,000	5,796		1,618	4,097	4,469	6,954
Moisture	Avg.	4 d	38%	50%	44%	1 d 2 d	12%	20%	18%	17%
in % w.b.	Std. Dev.		11%	13%	23%		3%	8%	7%	10%
Cost in $/dt	Avg.		$7.85		*1,489*			$8.16		*2,137*
Field Hours	Std. Dev.		$0.10		*179*			$0.07		*215*
Tons	Avg.		24,249	24,095	47,956		17,070	27,608	24,471	68,820
Processed	Std. Dev.		3,442	4,031	5,602		1,627	4,156	4,278	6,694
Moisture	Avg.	6 d	37%	49%	43%	2 d 2 d	12%	20%	16%	17%
in % w.b.	Std. Dev.		12%	14%	23%		3%	8%	7%	10%
Cost in $/dt	Avg.		$7.85		*1,484*			$8.16		*2,130*
Field Hours	Std. Dev.		$0.10		*173*			$0.07		*207*

[a] 2 d, 4 d and 6 d stand for 2, 4 and 6 day delays between mowing and forage harvesting for forage sorghum. 1 d 1 d, 1 d 2 d and 2 d 2 d stand for differential delays between mowing and raking followed by delays between raking and forage harvesting for switchgrass.

[b] Number of days in the period is approximate as different delay times add days to capacity calculations.

[c] Cost is derived by changing budgeted annual field hours with actual annual field hours in Table 4. Field hours represent annual forage harvester hours with mower conditioner and raking hours derived from the forage harvester hours.

Table 6. Estimated Final Harvested Moisture Content, Tonnage and Cost per Dry Ton Processed for Jonesboro, AR by Crop and Harvest Delay using an Equipment Complement Centered around a 375 hp Forage Harvester, 1998 – 2007.

Crop		Delay[a]	Forage Sorghum			Delay	Switchgrass			
Harvest Period			Jul - Sep 75 d[b]	Oct - Dec 75 d	Total 150 d		Jan - Feb 60 d	Jul - Sep 90 d	Oct - Dec 75 d	Total 225 d
Tons	Avg.	2 d	22,747	20,453	42,812	1 d 1 d	13,050	26,358	20,452	59,640
Processed	Std. Dev.		3,357	3,579	3,988		1,769	3,873	3,439	4,924
Moisture	Avg.		49%	57%	53%		14%	28%	26%	24%
in % w.b.	Std. Dev.		12%	12%	26%		3%	9%	7%	14%
Cost in $/dt[c]	Avg.		$7.94		*1,325*			$8.27		*1,846*
Field Hours	Std. Dev.		$0.08		*123*			$0.06		*152*
Tons	Avg.	4 d	22,702	19,941	42,256	1 d 2 d	13,305	26,003	20,256	59,308
Processed	Std. Dev.		3,456	3,566	3,954		1,700	3,920	3,496	4,983
Moisture	Avg.		46%	56%	51%		14%	25%	24%	22%
in % w.b.	Std. Dev.		13%	13%	26%		3%	10%	8%	13%
Cost in $/dt	Avg.		$7.95		*1,308*			$8.27		*1,836*
Field Hours	Std. Dev.		$0.08		*122*			$0.07		*154*
Tons	Avg.	6 d	22,616	19,472	41,702	2 d 2 d	13,561	25,804	19,901	59,011
Processed	Std. Dev.		3,531	3,796	4,035		1,647	3,987	3,453	5,065
Moisture	Avg.		45%	56%	50%		14%	25%	22%	21%
in % w.b.	Std. Dev.		15%	13%	26%		3%	10%	8%	13%
Cost in $/dt	Avg.		$7.96		*1,291*			$8.28		*1,826*
Field Hours	Std. Dev.		$0.09		*125*			$0.07		*157*

[a] 2 d, 4 d and 6 d stand for 2, 4 and 6 day delays between mowing and forage harvesting for forage sorghum. 1 d 1 d, 1 d 2 d and 2 d 2 d stand for differential delays between mowing and raking followed by delays between raking and forage harvesting for switchgrass.

[b] Number of days in the period is approximate as different delay times add days to capacity calculations.

[c] Cost is derived by changing budgeted annual field hours with actual annual field hours in Table 4. Field hours represent annual forage harvester hours with mower conditioner and raking hours derived from the forage harvester hours.

Table 7. Estimated Final Harvested Moisture Content, Tonnage and Cost per Dry Ton Processed for Lubbock, TX by Crop and Harvest Delay using an Equipment Complement Centered around a 375 hp Forage Harvester, 1998 – 2007.

Crop		**Delay**[a]	**Forage Sorghum**			**Delay**	**Switchgrass**			
Harvest Period			Jul - Sep 75 d[b]	Oct - Dec 75 d	Total 150 d		Jan - Feb 60 d	Jul - Sep 90 d	Oct - Dec 75 d	Total 225 d
Tons	Avg.	2 d	25,772	28,568	53,952	1 d 1 d	18,313	30,251	28,243	76,516
Processed	Std. Dev.		1,636	1,997	2,418		808	1,381	2,067	2,418
Moisture	Avg.		35%	47%	42%		10%	17%	17%	15%
in % w.b.	Std. Dev.		9%	13%	22%		4%	7%	8%	10%
Cost in $/dt[c]	Avg.		$7.75		*1,670*			$8.09		*2,368*
Field Hours	Std. Dev.		$0.03		*75*			$0.02		*75*
Tons	Avg.	4 d	26,120	27,934	53,666	1 d 2 d	18,569	30,317	27,838	76,432
Processed	Std. Dev.		1,635	2,136	2,523		797	1,505	2,168	2,384
Moisture	Avg.		33%	46%	40%		10%	15%	16%	14%
in % w.b.	Std. Dev.		10%	14%	22%		4%	7%	8%	9%
Cost in $/dt	Avg.		$7.76		*1,661*			$8.09		*2,366*
Field Hours	Std. Dev.		$0.03		*78*			$0.02		*74*
Tons	Avg.	6 d	26,662	27,310	53,584	2 d 2 d	18,788	30,273	27,541	76,273
Processed	Std. Dev.		1,632	2,125	2,581		787	1,590	2,149	2,495
Moisture	Avg.		30%	46%	38%		10%	14%	14%	13%
in % w.b.	Std. Dev.		11%	15%	22%		4%	7%	8%	8%
Cost in $/dt	Avg.		$7.76		*1,658*			$8.09		*2,361*
Field Hours	Std. Dev.		$0.04		*80*			$0.02		*77*

[a] 2 d, 4 d and 6 d stand for 2, 4 and 6 day delays between mowing and forage harvesting for forage sorghum. 1 d 1 d, 1 d 2 d and 2 d 2 d stand for differential delays between mowing and raking followed by delays between raking and forage harvesting for switchgrass.

[b] Number of days in the period is approximate as different delay times add days to capacity calculations.

[c] Cost is derived by changing budgeted annual field hours with actual annual field hours in Table 4. Field hours represent annual forage harvester hours with mower conditioner and raking hours derived from the forage harvester hours

2.10
EFFECT OF MECHANICAL CONDITIONING ON THIN-LAYER DRYING OF ENERGY SORGHUM (*Sorghum bicolor* (L.) Moench)

Ian J. Bonner[1], Kevin L. Kenney[1]*

Abstract
Cellulosic energy varieties of *Sorghum bicolor* (L.) Moench show promise as a bioenergy feedstock, however, high moisture content at the time of harvest results in unacceptable levels of degradation when stored in aerobic conditions. To safely store sorghum biomass for extended periods in baled format, the material must be dried to inhibit microbial growth. One possible solution is allowing the material to dry under natural in-field conditions. This study examines the differences in thin-layer drying rates of intact and conditioned sorghum under laboratory-controlled temperatures and relative humidity levels (20°C and 30°C from 40% to 85% relative humidity), and models experimental data using the Page's Modified equation. The results demonstrate that conditioning drastically accelerates drying times. Relative humidity had a large impact on the time required to reach a safe storage moisture content for intact material (approximately 200 hours at 30°C and 40% relative humidity and 400 hours at 30°C and 70% relative humidity), but little to no impact on the thin-layer drying times of conditioned material (approximately 50 hours for all humidity levels < 70% at 30°C). The drying equation parameters were influenced by temperature, relative humidity, initial moisture content, and material damage, allowing drying curves to be empirically predicted. The results of this study provide valuable information applicable to the agricultural community and to future research on drying simulation and management of energy sorghum.

Keywords: Sorghum bicolor, biomass storage, crop conditioning, in-field drying, thin-layer drying,

Introduction
As the demand for renewable transportation fuels increases, a proper understanding of the functional attributes of biomass feedstocks is crucial for advancing the processes of material collection, handling, and preservation. Numerous recent reviews have highlighted moisture content of biomass entering storage as a critical factor for material stability (Hess, *et al.*, 2007; Rentizelas *et al.*, 2009; Inman *et al.*, 2010). The deleterious effects of high moisture levels on aerobically stored biomass present a major barrier to the cost effectiveness of lignocellulosic feedstocks harvested at high moisture (Shah *et al.*, 2011; Shinners *et al.*, 2011). In light of the ease and low cost of dry storage to supply biomass logistics systems, high-moisture energy crops must undergo an initial drying process if they are to be successfully integrated into an aerobic year-round supply system.

Energy sorghum (specialized varieties of forage sorghum; *Sorghum bicolor* (L.) Moench) has received positive attention as a dedicated lignocellulosic energy crop for its large biomass yields and flexible growing conditions (McBee *et al.*, 1988; Rooney *et al.*, 2007). Unfortunately, high moisture content at the time of harvest (50% to 90% wet basis) is a key barrier to the use of energy sorghum in model feedstock supply systems (Zegada-Lizarazu and Monti, 2012). In-field drying is commonly used for other

[1] Idaho National Laboratory, Biofuels & Renewable Energy Technologies, ID

* Corresponding author

herbaceous materials (Thompson *et al.*, 1985; Pordesimo *et al.*, 2006), but the thick stalk of sorghum limits moisture removal, causing drying times to be lengthy and creating solicitude about prolonged exposure to environmental conditions. The practice of conditioning plants with mechanical rollers at the time of harvest to damage the stem and allow moisture to more readily escape has been shown to significantly reduce in-field drying times of herbaceous crops (Frost and Binnie, 1999; Seo *et al.*, 2000; Savoie *et al.*, 2002), which can decrease in-field dry-matter loss (Rotz and Muck, 1994). However, information on the impact of conditioning on sorghum drying rates is limited.

In this study, thin-layer drying of energy sorghum was conducted at 20°C and 30°C with relative humidity levels of 40%, 55%, 70%, and 85%. By conducting drying experiments at fixed temperature and relative humidity on a monolayer of test material, many of the complex interactive variables encountered in field conditions (*i.e.*, precipitation, diurnal temperature and humidity, solar radiance, wind speed, and material bed thickness) are removed, allowing the impact of a few key variables on a material's drying characteristics to be better understood (Jayas *et. al.*, 1991; Sander 2007). The objectives of the study were to model the thin-layer drying curves of intact and conditioned energy sorghum, determine the time required to reach moisture contents suitable for safe storage, and examine the influence of physical parameters on the drying equation constants.

Nomenclature

Acronyms and Abbreviations		Symbols	
Con	Material condition class, intact or conditioned	k, n	Model parameters, unitless
db	Dry basis moisture content	M	Instantaneous moisture content, dry basis
Dmg	Ratio of heavily damaged stalks, cm^3/cm^3	M_e	Equilibrium moisture content, dry basis
MR	Moisture ratio, unitless	M_i	Initial moisture content, dry basis
r.h.	Relative humidity	M_p	Predicted moisture content, dry basis
RMSE	Root mean square error	M_s	Safe storage moisture content, dry basis
SD	Standard deviation	N	Number of observed data points
SEE	Standard error of the estimate	R^2	Coefficient of determination
T	Temperature, °Celsius	t	Time, hours

Methods and Materials

Two Conviron PGR-15 Plant Growth Chambers (Winnipeg, Manitoba Canada) were used to dry four experimental samples simultaneously with an even upward airflow (average of 0.027 $\pm$ 0.008 m/sec though the material bed). Each chamber housed two weather resistant balances ($\pm$ 0.2 g) connected to a Campbell Scientific (Logan, UT USA) CR1000 datalogger programmed to record sample mass and drying conditions every five minutes. Drying baskets for each balance (#20 mesh; 63.5 cm x 53.5 cm x 10.5 cm) were placed on 10.5 cm stands to allow air to flow through the material bed. A total of eight environmental conditions were tested on four replicates of intact and conditioned sorghum (20°C and 30°C at 40%, 55%, 70%, and 85% relative humidity, r.h.). Due to unsuitable ambient conditions, the test at 20°C/40% r.h. was not performed on the conditioned material.

Mendel Biotechnology, Inc. (Hayward, CA USA) provided an experimental cellulosic energy variety of forage sorghum (*Sorghum bicolor* (L.) Moench) that was grown in field plots in Stotts City, MO USA and harvested in March, 2010. Whole frozen stalks were cut to approximately 63 cm segments, placed in vacuum sealed bags and allowed to equilibrate to the test temperatures (approximately 6 hours). For tests on conditioned material, the thawed sorghum was manually crushed between two plywood planks with 2 cm teeth separated by 8 cm from center to center. Stalks were arranged in a single parallel layer in each drying basket and dried until a state near equilibrium was reached (ASABE, 2006). Completed samples were dried at 105°C for 24 hours to determine dry mass. Each stalk segment was measured for length and diameter at both ends. Those that were splintered or had exposed pith were noted separately and used to describe the extent of material damage to each replicate on a percent volume basis.

Drying curves were modeled using the Page's Modified equation (Eq. 1; Page, 1949; ASABE, 2006). Values for the equilibrium moisture content (M_e) were applied from a previous examination of energy sorghum's moisture adsorption isotherms (Bonner and Kenney, In Review). In addition to modeling each replicate individually, masses of all four replicates were combined to create a mathematical composite for producing a single set of model parameters for each test condition. The coefficient of determination (R^2; Eq. 2) and root mean squared error (*RMSE*; Eq. 3) were calculated to determine the quality of fit for each model. To calculate the optimized values of k and n, the "solver" function in Microsoft Excel (Redmond, WA USA) was used to perform non-linear regression to minimize the RMSE value. Further analysis of the experimental data and predicted model parameters were conducted using SigmaPlot Version 12.3 (Systat Software, San Jose, CA USA)

$$\text{Page's Modified} \quad MR = (M - M_e)/(M_i - M_e) = \exp\left(-k \cdot t\hat{\ }n\right) \qquad (1)$$

$$R^2 = 1 - \sum(M_e - M_p)^2 / \sum(M_e - \bar{M})^2 \qquad (2)$$

$$RMSE = \sqrt{\,[\,\sum(M_e - M_p)^2 / N\,]} \qquad (3)$$

Results and Discussion

Drying Kinetics

All tests were observed within the falling-rate period of drying. The conditioned material exhibited drastically accelerated drying times and improved extent of drying when compared to the intact material (Figure 1). Drying times of intact material above 40% r.h. were decreased as temperatures increased from 20°C to 30°C (Figure 1). Relative humidity had a large impact on the rate of moisture loss within the first hour of drying for both intact and conditioned materials, causing a difference of approximately 4% db·h^{-1} between the high and low relative humidity tests (Figure 2). Initial drying rates of conditioned material were approximately 2.5% db·h^{-1} higher than intact material and remained elevated (>1% db·h^{-1}) for approximately 25 hours at high and low humidity. The rate of moisture loss for intact material fell below 1% db·h^{-1} within approximately 2 to 5 hours of drying at 85% r.h. and 12 hours of drying at 40% r.h. (Figure 2).

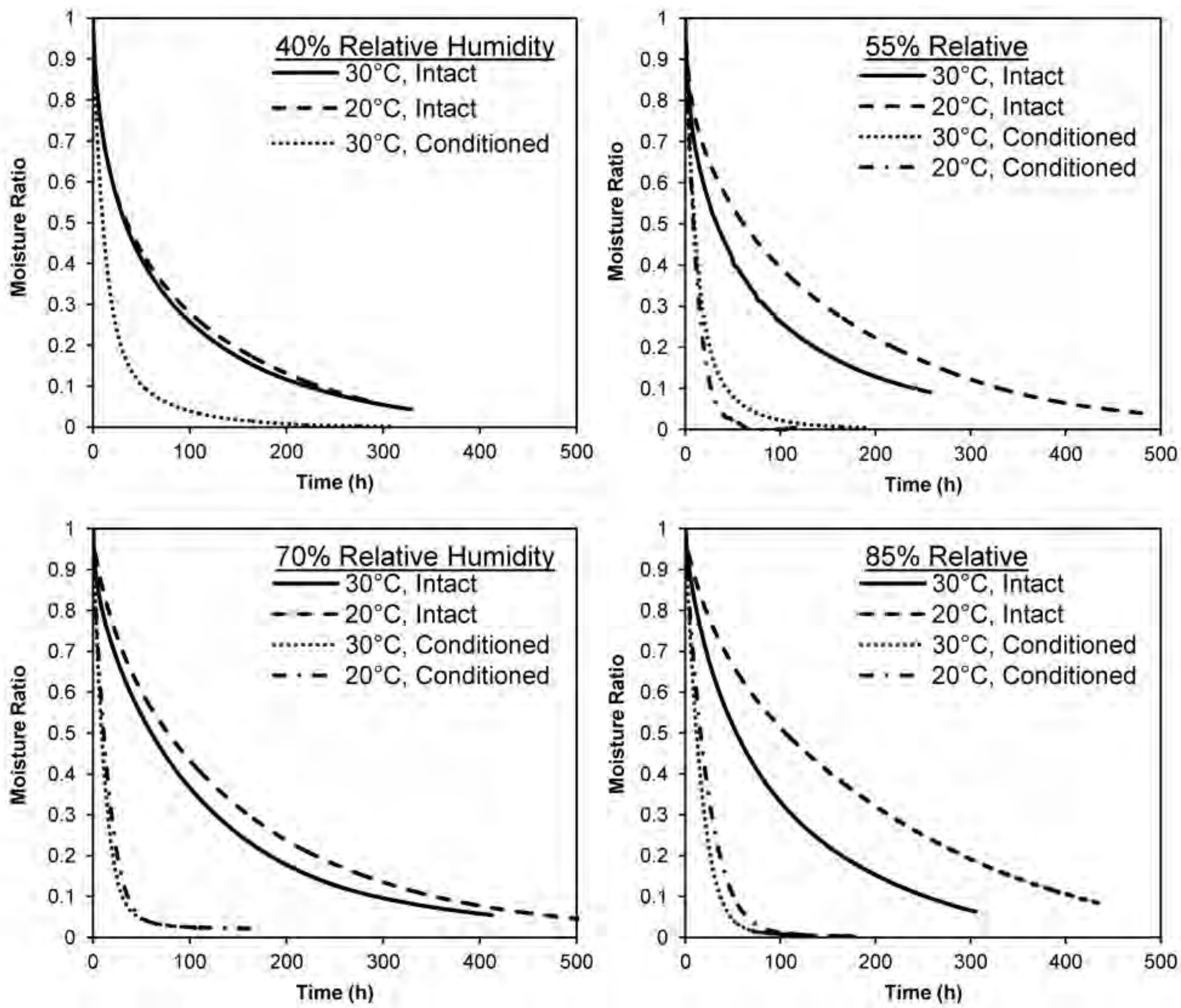

Fig. 1 Experimental thin-layer drying curves for energy sorghum. Each curve is from the combined mass of four replicates.

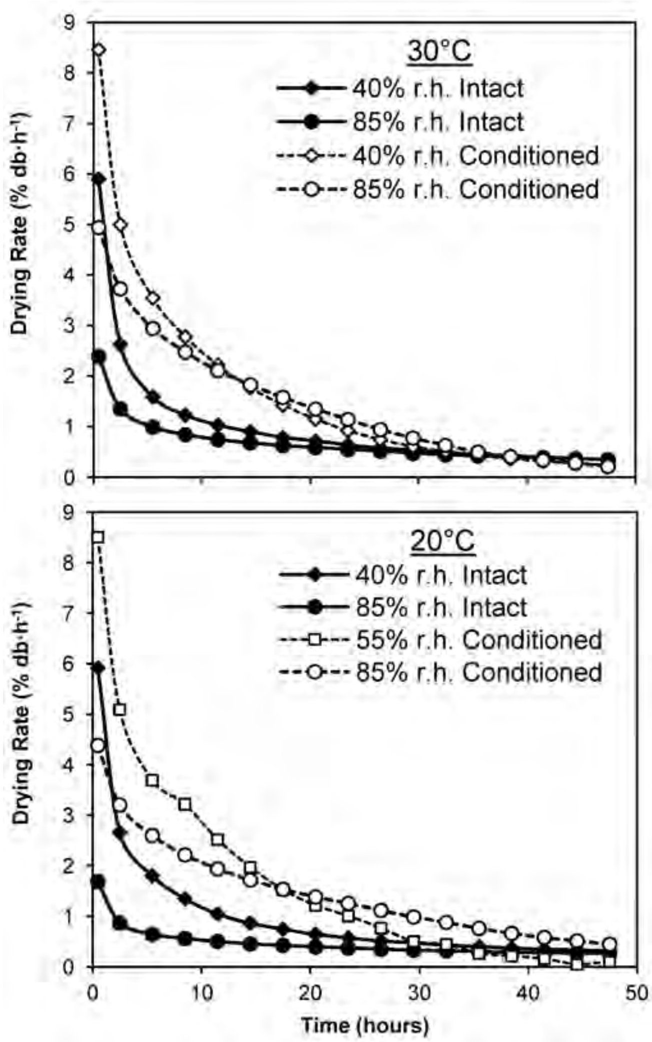

Fig. 2 Hourly rates of moisture loss for the high and low relative humidity tests at 20°C and 30°C for intact and conditioned energy sorghum.

The moisture content suitable for safe storage (M_s) of energy sorghum was previously determined to be approximately 17.5% db as the material undergoes its initial desorption in the range of 20°C to 30°C (Bonner and Kenney, In Review). The time required to reach this value of M_s ranged from 200 to nearly 500 hours for intact sorghum, and 30 to 50 hours for conditioned sorghum. Temperature and relative humidity strongly influenced the drying times of intact material, but had no clear impact on conditioned material (Figure 3). This finding suggests that the process of conditioning not only reduces drying times, but removes the dependency on optimal drying conditions when compared to non-conditioned sorghum.

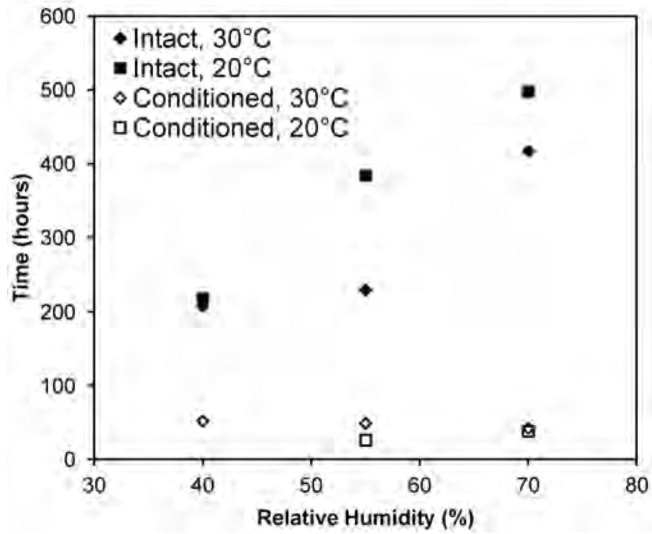

Fig. 3 Drying time required to reach a moisture content suitable for safe storage of intact and conditioned energy sorghum.

When compared with other products, the thin-layer drying behavior of conditioned energy sorghum most closely resembles that of corn cobs (*Zea mays* L.), which reached moisture ration (*MR*) values near zero by 40 hours and 100 hours under similar conditions for cob halves and whole cobs, respectively (McNeill *et al.*, 1985). The reported thin-layer drying of chopped alfalfa (*Medicago sativa* L.; Patil *et al.*, 1992), southern yellow pine chips (*Pinus* spp.; Phanphanich and Mani, 2009), and flax fiber (*Linum usitatissimum* L.; Ghazanfari *et al.*, 2006) all exhibited notably higher rates of drying than conditioned energy sorghum. Of the comparisons made, intact sorghum behaved similarly to plums, figs, and grapes that were sun dried at ambient conditions (Toğrul and Pehlivan, 2004). It is worth noting that these fruits had initial moisture contents of 200% to 400% db, yet reached *MR* near zero in a comparable amount of time to intact sorghum at 30°C and 40% r.h., exemplifying the difficulty of moisture transfer through the stalk's surface. It should also be considered that the longitudinal diffusion distance of the segmented sorghum tested was shorter than a naturally intact stalk, presumably supporting increased drying rates. A recent study on the thin-layer drying of finely-chopped sweet sorghum reported drying from 370% db to equilibrium in approximately 18 hours in a 30°C convection oven; supporting the notion that the extent of physical manipulation can result in more rapid drying rates (Shen *et al.*, 2011).

Modeling and Influence of Parameters

Non-linear regression of the experimental data to Page's Modified equation resulted in high R^2 values and low *RMSE* values for the individual replicates and the combined sample sets, indicating an accurate fit for the thin-layer drying of energy sorghum (Table 1). The predicted values of *MR* were calculated back to percent moisture and compared with the observed drying curves. The intact tests had a mean residual of -0.1% $\pm$ 0.5% db at 30°C ($\pm$ *SD*, *n*=15,619) and -0.2% $\pm$ 1.0% db at 20°C ($\pm$ *SD*, *n*=20,410). The conditioned tests had a mean residual of 0.4% $\pm$ 0.8% db ($\pm$ *SD*, *n*=8,516) and 0.1% $\pm$ 0.6% db ($\pm$ *SD*, *n*=4,832) at 30°C and 20°C, respectively.

Table 1. Mean initial moisture content and fraction of heavily damaged stalks for each temperature and relative humidity (r.h.) combination. Page's Modified equation parameters for the combined replicate masses of intact and conditioned energy sorghum.

Test		Material Characteristics[a]		Page's Modified Equation Parameters[b]			
Drying Condition	Sorghum Condition	% Initial Moisture (kg/kg)	% Heavily Damaged (cm^3/cm^3)	*k*	*n*	R^2	*RMSE*
30°C / 40% r.h.	Intact	91.7 (12.0)	36.3 (12.3)	0.0749	0.6332	0.9991 (0.0023)	0.0057 (0.0049)
30°C / 55% r.h.	Intact	75.7 (12.3)	41.0 (10.5)	0.0895	0.5891	0.9993 (0.0039)	0.0048 (0.0037)
30°C / 70% r.h.	Intact	99.8 (14.4)	18.8 (8.2)	0.0354	0.7320	0.9984 (0.0015)	0.0083 (0.0029)
30°C / 85% r.h.	Intact	89.3 (12.2)	29.3 (3.3)	0.0330	0.7644	0.9996 (0.0007)	0.0043 (0.0026)
20°C / 40% r.h.	Intact	91.3 (7.4)	27.7 (5.6)	0.0866	0.5946	0.9989 (0.0010)	0.0061 (0.0031)
20°C / 55% r.h.	Intact	99.9 (10.8)	36.1 (8.2)	0.0431	0.6774	0.9921 (0.0024)	0.0176 (0.0033)
20°C / 70% r.h.	Intact	107.7 (16.9)	21.2 (3.7)	0.0241	0.7738	0.9992 (0.0008)	0.0060 (0.0032)
20°C / 85% r.h.	Intact	88.9 (12.4)	29.3 (7.6)	0.0163	0.8093	0.9962 (0.0022)	0.0136 (0.0040)
30°C / 40% r.h.	Conditoned	99.9 (6.9)	68.4 (15.2)	0.1408	0.7059	0.9944 (0.0038)	0.0107 (0.0041)
30°C / 55% r.h.	Conditoned	103.6 (15.7)	56.6 (11.8)	0.1249	0.7738	0.9970 (0.0030)	0.0092 (0.0041)
30°C / 70% r.h.	Conditoned	98.4 (9.1)	70.6 (8.2)	0.1025	0.8960	0.9917 (0.0070)	0.0179 (0.0066)
30°C / 85% r.h.	Conditoned	95.0 (8.3)	91.0 (4.5)	0.0581	1.0146	0.9994 (0.0015)	0.0052 (0.0023)
20°C / 55% r.h.	Conditoned	95.7 (15.5)	82.9 (5.8)	0.0878	0.9827	0.9994 (0.0004)	0.0047 (0.0013)
20°C / 70% r.h.	Conditoned	88.3 (7.1)	89.2 (7.5)	0.0785	0.9274	0.9918 (0.0037)	0.0169 (0.0030)
20°C / 85% r.h.	Conditoned	103.8 (16.0)	94.4 (4.9)	0.0433	1.0080	0.9995 (0.0003)	0.0047 (0.0016)

[a] Mean values presented with one standard deviation in parenthesis. *n* =4

[b] Parameters calculated from the combined replicate sets. Value in parenthesis is one standard deviation of the replicate values. *n* =4

Numerous studies that employ empirical equations to describe the thin-layer drying of various products have made correlations between the model parameters and environmental conditions and/or material properties (McNeill *et al.*, 1985; Patil *et al.*, 1992; Sinicio *et al.*, 1995; Babalis and Belessiotis, 2004). To determine if any such physical relationship could be established for the thin-layer drying equations of energy sorghum, multiple-linear regression was performed using all individual test replicates to determine the most suitable representation of the model parameters k and n. The parameter n was able to be predicted from a linear combination of material condition (*Con;* where intact is represented by a value of "0" and conditioned by a value of "1"), temperature (°C), relative humidity (decimal basis), initial moisture content (dry decimal basis), and ratio of heavily damaged stalks (*Dmg,* decimal basis; R^2=0.811, *SEE*=0.070, Constant Variance Test P=0.282; Eq. 4). The parameter k was able to be predicted separately for intact and conditioned material from a combination of relative humidity, initial moisture content, and the value of n (R^2=0.792, *SEE*=0.017, Constant Variance Test P=0.255 for conditioned material; R^2=0.783, *SEE*=0.020, Constant Variance Test P=0.423 for intact material; Eq. 5 and 6).

$$n = 0.213 + (0.0944 \cdot Con) - (0.00363 \cdot T) + (0.42 \cdot r.h.) + (0.275 \cdot M_i) + (0.198 \cdot Dmg) \quad (4)$$
$$k_{conditioned} = 0.334 - (0.0566 \cdot r.h.) - (0.0243 \cdot M_i) - (0.201 \cdot n) \quad (5)$$
$$k_{intact} = 0.317 - (0.021 \cdot r.h.) - (0.0628 \cdot M_i) - (0.275 \cdot n) \quad (6)$$

To check the appropriateness of the predictive equations for k and n, the composite material properties for each data set were applied and compared to the observed MR drying curves. Of the fifteen conditions predicted, each provided drying curves similar to the observed with the exception of the 20°C intact material at 55% r.h. and 85% r.h. (Table 2). The accuracy of fit for the majority of test conditions suggests that the predictive equations may be useful for understanding how subtle changes to material damage, initial moisture content, and relative humidity impact the drying rates of intact and conditioned sorghum within the conditional bounds of this experiment. Further research on the role of initial moisture content, precise extent of damage, and drying temperature is recommended to validate the equations presented and better define the relationship between such variables and drying rates of energy sorghum.

Table 2. Parameters of fit for the predicted moisture ratio drying curves using the empirically related equations for the model parameters *k* and *n.*

Sorghum Condition	Fit Parameters	Drying Conditions			
		20°C / 40% r.h.	20°C / 55% r.h.	20°C / 70% r.h.	20°C / 85% r.h.
Intact	R^2	0.9939	0.8661	0.9950	0.8420
	RMSE	0.0142	0.0725	0.0154	0.0880
Conditioned	R^2	NA	0.9863	0.9834	0.9599
	RMSE	NA	0.0234	0.0241	0.0432
		30°C / 40% r.h.	30°C / 55% r.h.	30°C / 70% r.h.	30°C / 85% r.h.
Intact	R^2	0.9960	0.9604	0.9719	0.9993
	RMSE	0.0120	0.0360	0.0351	0.0055
Conditioned	R^2	0.9730	0.9938	0.9790	0.9992
	RMSE	0.0235	0.0133	0.0285	0.0059

Conclusions

Conditioning of energy sorghum stalks was determined to drastically accelerate drying times when compared to intact stalks. Conditioned stalks dried at $\leq$ 70% r.h. reached moisture contents suitable for dry storage in approximately 50 hours, while intact stems under the same conditions required 200 to 500 hours. The Page's modified equation was suitable for representing the thin-layer drying of intact and conditioned energy sorghum. Temperature, relative humidity, percent heavily damaged stalks, act of conditioning, and initial moisture content were reliable surrogates for predicting drying model parameters, allowing theoretical drying curves to be generated. The results of this study indicate that damage severity within conditioned materials does not heavily influence drying times. Further research on the topic of mechanical conditioner choice and severity settings would be recommended to find an optimized performance balance. Expansion of the study's results to simulated thick-bed drying would enhance the understanding of in-field drying performance. Overall, the process of conditioning energy sorghum to accelerate drying has clear benefits if the value of energy sorghum justifies the additional expense of handling within the feedstock logistics system.

Acknowledgements

The authors would like to thank Mendel Biotechnology, Inc. for supplying the sorghum used in this experiment, and Chris Anderson at Mendel for his collaborative support and time. We would also like to thank Amber Hoover of the Idaho National Laboratory for her support in data interpretation, and Mark Delwiche of the Idaho National Laboratory for ensuring proper function of the test chambers.

This work is supported by the U.S. Department of Energy, under DOE Idaho Operations Office Contract DE-AC07-05ID14517. Accordingly, the U.S. Government retains a nonexclusive, royalty-free license to publish or reproduce the published form of this contribution, or allow others to do so, for U.S. Government purposes.

U.S. Department of Energy Disclaimer

References

ASABE Standards. 2006. S448.1. "Thin-Layer Drying of Agricultural Crops." St. Joseph, Mich.: ASABE.

Babalis, S.J., Belessiotis, V.G. "Influence of the drying conditions on the drying constants and moisture diffusivity during the thin-layer drying of figs" *Journal of Food Engineering* 65 (2004): 449-458.

Beuchat, L.R. "Microbial stability as affected by water activity." *Cereal Foods Worlds* 26 (1981): 345-349.

Bonner, I.J., Kenney, K.L. "Moisture Sorption Characteristics and Modeling of Energy Sorghum (*Sorghum bicolor* (L) Moench)." Manuscript submitted for publication (2012).

Frost, J.P., Binnie, R.C. "The effect of mechanical treatment on the drying rates of Italian and perennial ryegrass." *Grass and Forage Science* 54 (1999): 144-154.

Ghazanfari, A., Emami, S., Tabil, L.G., Panigrahi, S. "Thin-Layer Drying of Flax Fiber: I. Analysis of Modeling Using Fick's Second Law of Diffusion" *Drying Technology* 24 (2006): 1631-1635.

Hess, J.R., Wright, C.T., Kenney, K.L. "Cellulosic biomass feedstocks and logistics for ethanol production." *Biofuels, Bioproducts, and Biorefining* 1 (2007): 181-190.

Igathinathane, C., Pordesimo, L.O., Womac, A.R., Sokhansanj, S. "Hygroscopic Moisture Sorption Kinetics Modeling of Corn Stover and its Fractions." *Applied Engineering in Agriculture* 25-1 (2009): 65-73.

Inman, D., Nagle, N., Jacobson, J., Searcy, E., Ray, A.E. "Feedstock handling and processing effects on biochemical conversion to biofuels." *Biofuels Bioproducts and Biorefining* 4 (2010): 562-573

Jayas, D.S., Cenkowski, S., Pabis, S., Muir, W.E. "Review of Thin-Layer Drying and Wetting Equations." *Drying Technology* 9-3 (1991): 551-588.

Lamond, W.J., Spencer, H.B., Graham, R., Moore, A.B. "Effect of thin layer drying rate and swath structure on the rate of grass swath drying under controlled conditions" *Journal of Agricultural Science* 113 (1989): 59-65.

McBee, G.G., Creelman, R.A., Miller, F.R. "Ethanol Yield and Energy Potential of Stems from a Spectrum of Sorghum Biomass Types." *Biomass* 17 (1988): 203-211.

McNeil, S.G., Overhults, D.G., White, G.M., Ross, I.J. "Thin Layer Drying Characteristics of Corncobs." Paper presented at the Winter Meeting American Society of Agricultural Engineers, Chicago, USA, December 17-20, 1985. *ASAE* Paper No. 85-3565.

Page, G. "Factors influencing the maximum rates of air drying shelled corn in thin-layers." M.S. Thesis, Purdue University, 1949.

Patil, R.T., Sokhansanj, S., Arinze, E.A., Schoenau, G. "Thin layer drying of components of fresh alfalfa." *Canadian Agricultural Engineering* 34-4 (1992): 343-346.

Phanphanich, M., Mani, S. "Drying Characteristics of Pine Forest Residues." *BioResources* 5-1 (2009): 108-120.

Pordesimo, L.O., Saxton, A.M., Sokhansanj, S. "Comparative Field Drying of *Bt* and Non-*Bt* Corn Stover Fractions after Grain Physiological Maturity." *International Journal of Agricultural Research* 1-2 (2006): 194-201.

Rentizelas, A.A., Tolis, A.J., Tatsiopoulos, I.P. "Logistics issues of biomass: The storage problem and the multi-biomass supply chain." *Renewable and Sustainable Energy Reviews* 13 (2009): 887-894.

Rooney, W.L., Blumenthal, J., Bean, B., Mullet, J.E. "Designing sorghum as a dedicated bioenergy feedstock." *Biofuels Bioproducts and Biorefining* 1 (2007): 147-157.

Rotz, C.A., Muck, R.E. "Changes in forage quality during harvest and storage." In *Forage Quality, Evaluation and Utilization*, edited by Fahey, G.C., Jr., Collins, M., Mertens, D.R., Moser, L.E. Madison: American Society of Agronomy, 1994.

Sander, A. "Thin-layer drying of porous materials: Selection of the appropriate mathematical model and relationships between thin-layer models parameters." *Chemical Engineering and Processing* 46 (2007): 1324-1331.

Savoie, P., Tremblay, Y., Dubreuil, S., Khelifi, M. "Effect of mechanical conditioning, windrow handling, and maturity on the drying rate of timothy hay in a wind tunnel." *Canadian Biosystems Engineering* 44 (2002): 2.1-2.8.

Seo, S., Chung, E.S., Kim, J.G., Kang, W.S., Kim, W.H. "Mechanical and Chemical Conditioning Effect on Field Drying Rate and Quality of Grass Hay." *Asian-Australian Journal of Animal Science* 13-8 (2000): 1109-1112.

Shah, A., Darr, M.J., Webster, K., Hoffman, C. "Outdoor Storage Characteristics of Single-Pass Large Square Corn Stover Bales in Iowa." *Energies* 4 (2011): 1687-1695.

Shen, F., Peng, L., Zhang, Y., Wu, J., Zhang, X., Yang, G., Peng, H, Qi, H., Deng, S. "Thin-layer drying kinetics and quality changes of sweet sorghum stalk for ethanol production as affected by drying temperature." *Industrial Crops and Products* 34 (2011): 1588-1594.

Shinners, K.J., Wepner, A.D., Muck, R.E., Weimer, P.J. "Aerobic and Anaerobic Storage of Single-pass, Chopped Corn Stover." *Bioenergy Research* 4 (2011): 61-75.

Sinicio, R., Muir, W.E., Jayas, D.S., Cenkowski, S. “Thin-layer drying and wetting of wheat” *Postharvest Biology and Technology* 5 (1995): 261-275.

Thompson, N, Barrie, I.A., Harvey L.D.J. “The climatic potential for field drying hay in north-west Europe.” *Journal of Agricultural Science* 105 (1985): 167-181.

Toğrul, I.T., Pehlivan, D. “Modeling of thin later drying kinetics of some fruits under open-air sun drying process” *Journal of Food Engineering* 65 (2004): 413-425.

Zegada-Lizarazu, W., Monti, A. “Are we ready to cultivate sweet sorghum as a bioenergy feedstock? A review on field management practices.” *Biomass and Bioenergy* 40 (2012): 1-12.

3 CONVERSION TECHNOLOGY

3.1
FED-BATCH, SIMULTANEOUS SACCHARIFICATION AND FERMENTATION IN A HIGH SOLIDS BIOREACTOR TO MAXIMIZE ETHANOL TITER

Nichole A. Bauer[1], Craig C. Long[1], William R. Gibbons[2,]*

Abstract
The goal of this project was to evaluate fed-batch, solid-state, simultaneous saccharification and fermentation (SSF) as an approach to reduce enzyme use in converting cellulose to ethanol and maximize ethanol titer. Kraft pulp represented a fractionated cellulose feedstock. Based on the literature, average dosages of 34 FPU of cellulase (Celluclast 1.5L) and 135 CBU of β-glucosidase (Novozyme 188) per gram of glucan were determined and set as 100%. Initial SSF trials were conducted in traditional submerged bioreactors, using enzyme dosages of 133% versus 67%. Kraft pulp and additional enzymes were added throughout SSF, achieving 14% final solids loading rate. Companion trials were performed where water was added instead of enzymes during substrate additions, effectively reducing net enzyme dosages to 33% and 17% of literature average. Ethanol yields were similar (77.3-83.4% of theoretical) for trials with 33-133% enzyme dosages, but fell to 36% of theoretical at 17% enzyme dosage. Net enzymes used in 33% dosage trials were 11 FPU cellulase/g glucan and 45 CBU β-glucosidase/g glucan. Fed-batch saccharification and fed-batch SSF were performed in a solid-state bioreactor, and achieved 34.8% solids loading rate. This reduced initial 133% enzyme dosage to 19%. Saccharification trials produced 103.6 g/L glucose, which was 35% of theoretical yield. This was expected, due to feedback inhibition of enzymes. SSF trials conducted with same loading pattern and enzymes dosages, however, only yielded 30.1 g/L ethanol, which represented 20% of theoretical yield. Reducing SLR to 25% increased ethanol titer to 47.1 g/L with a yield of 43.4%. Some ethanol was lost to evaporation, but low water activity inhibited yeast performance in the solid-state reactor.

Keywords: Saccharification, Cellulose, Ethanol, Solid State Reactor, Fed-batch fermentation

Introduction
Submerged bioreactors have traditionally been used for fermentation processes, including large scale systems common in corn ethanol facilities since they allow for precise control of temperature, pH, agitation, aeration, and mass transfer. The chief limitation is viscosity of the fermentation broth, as this limits mixing/mass transfer, and dramatically increases agitation energy requirements (Zhang, Wang et al. 2009). An option for dealing with low bulk density feedstocks is to perform an initial saccharification of a dilute slurry, then remove the non-fermentables through filtration or centrifugation, and finally concentrate liquid through evaporation to achieve a clean solution with the desired sugar concentration for fermentation. Another alternative is solid-state conversion, in which a minimum amount of water is added to the substrate, so simultaneous saccharification and fermentation (SSF) occurs in the liquid film on the solid particles. Many advantages exist to using a solid-state fermentation system: lower production cost, less energy needed and greater fermentation productivity (Gibbons, Westby et al. 1986) with less energy for ethanol recovery (Zhang, Mo et al. 2003). Gibbons et al. (1986a 1986b) used solid state fermentation to convert fodder beet and sweet sorghum pulp to ethanol

[1] *Biology-Microbiology Department, South Dakota State University, SD*

[2] *Biology-Microbiology Department, South Dakota State University, SD*

* *Corresponding Author*

achieving ethanol yields of 78-85% and 85% of theoretical, respectively. Moukamnerd et al. (2010) used a solid state fermentation system to convert raw corn starch to ethanol. Ethanol was recovered continuously, with an ethanol yield of 93%. The purpose of this project was to compare submerged bioreactors versus solid state bioreactors at various solid loading rates of a cellulosic substrate. The goal was to minimize enzyme use, while maximizing ethanol titer.

Materials and Methods

Effects of Enzyme Dosage on Fed-batch Submerged SSF of Kraft Pulp

Trials in triplicate were conducted in 5 L bioreactors to determine if fed-batch additions of kraft pulp could be made without the need for additional enzymes. Table 1 lists the components added to bioreactors for treatments resulting in final enzyme dosages of 17-133% of the literature average (34 FPU of cellulase activity/g glucan, 135 CBU of β-glucosidase activity/g glucan were set as the 100% dosage). Each bioreactor was also charged 10 g condensed corn solubles (CCS) and 20 ml of *S. cerevisiae.* Temperature was set at 35^{o}C and agitation rate was initially set to 900 rpm to achieve adequate mixing until the viscosity dropped, after which it was lowered to 75-100 rpm. Total final volume of all trials was 2,856 ml, resulting in a 14% solids loading rate (SLR).

Table 1: Materials for Fed-batch Submerged Fermentation

Materials Used	**Treatment (Effective Enzyme Dosage)**			
	133%	67%	33%	17%
Buffer (ml)	1965	2127	2307	2364
Celluclast 1.5L (ml)	216	108	54	27
Novozyme 188 (ml)	240	120	60	30
Kraft pulp (g)	100	100	100	100
Components added at @ 3, 6, and 24 h				
Kraft pulp (g)	100	100	100	100
Celluclast 1.5L (ml)	54	27	0	0
Novozyme 188 (ml)	60	30	0	0
Buffer (ml)	0	0	114	114

Fed-Batch Saccharification in a Solid-State Bioreactor

To assess performance of a solid-state bioreactor we constructed, initial trials were performed in triplicate using fed-batch saccharification. This reactor has a 16 L internal capacity and variable speed motor (20-60 rpm). The bioreactor was initially loaded with 1,380 ml of sodium citrate buffer, 54 ml of cellulase enzyme, 60 ml of β-glucosidase enzyme, 6 ml of tetracycline solution, and 100 g of kraft pulp. This provided an initial enzyme dosage of 133% and a solid loading rate of 15%. Temperature was set to 50^{o}C with agitation at 60 rpm. Saccharification was performed for 96 h with 100 g additions of kraft pulp at 3, 6, and 9 h, while 200 g were added at 24 and 36 h, resulting in final solids loading rate of 34.8% and a final volume of 2.3 L. No additional enzymes were added, resulting in a final enzyme dosage of 19%.

Fed-batch SSF in a Solid State Bioreactor

Fed-batch SSF trials (96 h) were performed in triplicate following a similar protocol to that described above for fed-batch saccharification. Table 2 lists the materials used for trials with final SLRs of 34.8% to 14%. A 24 h yeast inoculum and CCS (to supply yeast nutrients) were also added initially. Temperature was set to 35°C, with agitation at 60 rpm.

Table 2: Materials for Fed-batch Solid State SSF

Materials	34.8% SLR	27% SLR	25% SLR	21% SLR	14% SLR
Cellulase (ml)	282	70.5	65.28	54.84	36.56
β – glucosidase (ml)	313	78.25	72.45	60.86	40.57
Buffer (ml)	7020	1988.5	2059.52	2201.55	2450.12
Tetracycline (ml)	31	7.75	7.75	7.75	7.75
Yeast (ml)	120	30	30	30	30
CCS (ml)	60	15	15	15	15
Kraft Pulp – initial (g)	521.75	101.25	93.75	78.75	52.5
Kraft Pulp additions - 3, 6, 9 h (g)	521.75	101.25	93.75	78.75	52.5
Kraft Pulp additions - 24 and 36 h (g)	1043.50	202.5	187.5	157.5	105
Final Enzyme Dosages	19%	20%	22%	26%	39%
Total Volume	12L	3L	3L	3L	3L

Secondary Analysis of Fed-Batch, Solid State SSF Samples

To quantify un-hydrolyzed cellulose remaining in the kraft pulp slurry at 0, 24, 48, 72, and 96 h, samples were collected and subjected to an additional saccharification. Each sample of 5 ml of fermentation broth was blended with 89.3 ml of buffer in a 250 ml Erlenmeyer flask, sealed with a rubber stopper. After autoclaving to kill the yeast, the 133% enzyme dosage was added to the cooled slurry and incubated at 250 rpm at 35°C for 72 h. HPLC samples were taken at 0 and 72 h, and the differences in glucose was used to calculate the amount of un-hydrolyzed cellulose.

Samples (100 g) collected at the end of SSF were also diluted with various amounts of buffer (10, 25, 50 or 100 ml) and were incubated an additional 72 h at 35°C to determine if water activity was limiting yeast metabolism. In a separate flask, 49 ml of buffer and 1 g of yeast extract were added to 100 g of fermented pulp to determine if nutrients were limiting.

Samples (5 ml) collected throughout the trials were boiled for five min to denature enzymes, and filtered through 0.2 μm filters into HPLC vials, which were frozen until analysis. Carbohydrates, organic acids, and ethanol were measured in a Waters HPLC, with an Aminex HPX-87H column operated 65°C, and Waters 2410 refractive index detector. The mobile phase was 0.01 N H_2SO_4 at a flow rate of 0.6 ml/min.

Results and Discussion

At a 14% solid loading rate of kraft pulp, enzyme dosages of 33-133% resulted in ethanol titers of ~48-51 g/L and yields of 77.3-83.4% in a submerged bioreactor. Maximum ethanol titer (22.2 g/L) was significantly lower at the 17% enzyme dosage, demonstrating that enzyme dosage could be safely reduced to 33% of the literature average (11.25 FPU cellulase and 45 CBU β-glucosidase per gram glucan). Residual glucose levels in all trials ranged from 0.4-2.2 g/L.

Fed-batch saccharification trials in the solid-state bioreactor were able to achieve a 34.8% SLR and final enzyme dosage of 19% with a glucose titer of 103.6 g/L and yield of 35%. Fed-batch SSF trials under the same conditions only achieved an ethanol titer of 30.1 g/L and yield of 20% of theoretical. Residual carbohydrates in these trials was >60 g/L, suggesting that low water activity inhibited yeast metabolism (Erdei, Barta et al. 2010). Trials at lower SLRs (14-27%) resulted in higher ethanol yields of 35.9-49.3% (Table 3), with low residual glucose concentrations (0-3 g/L). Unhydrolyzed cellulose levels ranged from 25-53 g/L. Further dilution of post-96 h SSF by a factor of 0.8 further increased ethanol yields to ~60% of theoretical.

Table 3: Materials for Fed-batch Solid State SSF

Parameter	**34.8% SLR**	**27% SLR**	**25% SLR**	**21% SLR**	**14% SLR**
Maximum ethanol (g/L)	30.1	42.1	47.1	38.5	30.0
Ethanol yield (%)	20.0	35.9	43.4	42.2	49.3
Unhydrolyzed cellulose (g/L)					

Conclusion

Fed-batch, submerged SSF of kraft pulp at 14% SLR achieved ethanol concentrations of 47-52 g/l and yields of 77-83% at enzyme dosages of 33-133% of the literature average. Fed-batch saccharification in a solid state reactor at 34.8% SLR and 19% enzyme dosage resulted in glucose levels of ~100 g/L; a yield of 35% of theoretical. Fed-batch SSF in the solid-state reactor was limited by ethanol and water loss through evaporation, resulting in low water activity stressing yeast metabolism. At an SLR of 34.8%, maximum ethanol titers were only 30 g/L, with an ethanol yield of only 20% of theoretical. Reducing SLR to 25% increased ethanol titer to 47.1 g/L, with a yield of 43.4%. Higher ethanol yields were obtained upon further dilution and incubation.

References

Erdei, B., Z. Barta, et al. (2010). "Ethanol Production from Mixtures of Wheat Straw and Wheat Meal." Biotechnology for Biofuels **3**: 1-9.

Gibbons, W. R., C. A. Westby, et al. (1986). "Intermediate-scale, Semicontinuous Solid-phase Fermentation Process for Production of Fuel Ethanol from Sweet Sorghum." Applied Environmental Microbiology **51**(1): 115-122.

Zhang, M. J., F. Wang, et al. (2009). "Ethanol Production from High Dry Matter Corncob using Fed-batch Simultaneous Saccharification and Fermentation after Combined Pretreatment." Bioresource Technology **101**(13): 4959-4964.

Zhang, X. Y., H. Mo, et al. (2003). "A Solid-State Bioreactor Coupled with Forced Aeration and Pressure Oscillation." Biotechnology Letters **25**(5): 417-420.

3.2
SIMULTANEOUS FERMENTATION OF GLUCOSE AND XYLOSE BY CO-CULTURE IN A NOVEL BIOREACTOR

Min Hea Kim[1], Meng Liang[1], Qinghua He[2], Jin Wang[1]

Abstract
The use of renewable resources, such as lignocellulosic biomasses, to produce ethanol offers great environmental and economic benefits over fossil fuel. An efficient conversion of glucose and xylose is a prerequisite for a profitable process of ethanol production from lignocellulose. Existing research has shown that, besides recombinant strategy, co-culture is a simple and promising way to co-ferment glucose and xylose for ethanol production, especially in reducing fermentation time and improving ethanol productivity. However, there is a lack of systematic study on the dynamic properties of co-culture systems. In addition, major challenges associated with xylose fermentation, such as catabolite repression on xylose uptake and low ethanol tolerance of the xylose fermenting strain, have not been fully addressed. Therefore, new approaches are needed to help understand and explore the potential of the co-culture strategy. In this work, an innovative fermentation scheme was designed, co-culturing *Saccharomyces cerevisiae* and *Scheffersomyces stipitis* (formerly *Pichia stipitis*) in an in-house developed bioreactor for the glucose and xylose co-fermentation. With this fermentation scheme, we were able to achieve simultaneous complete consumption of glucose and xylose. In addition, the developed novel bioreactor enables us to test different fermentative conditions, such as independent oxygen transfer rate for different strains. Furthermore, the pseudo-continuous mode, i.e. continuous fermentation with cell retention, was proposed to prevent cell washout and to provide an ideal environment for cell adaptation, evidenced by the significantly improved ethanol tolerance of both strains.

Keywords: co-culture; cofermentation; bioethanol; lignocellulosic ethanol

Introduction
Ethanol production from lignocellulosic hydrolysates in an economically feasible process requires complete utilization of both glucose and xylose, the main components of cellulose and hemicellulose. Although successful cycles of metabolic engineering have improved xylose utilization in recombinant *S. cerevisiae*, the ethanol production from xylose is still inferior to those of xylose fermentation by well-known yeast, *Scheffersomyces stipitis* (Jefferies *et al.* 2004). *S. stipitis* has promising potential for converting biomass into ethanol since it can ferment both hexose and pentose sugars under microaerophillic conditions. However, this strain has a slower sugar consumption rate than *S. cerevisiae* and requires oxygen for both growth and maximal ethanol production. In addition, diauxic lag is a practical problem associated with mixed sugar utilization by both *S. stipitis* and engineered strains of *S. cerevisiae* (Kuyper et al. 2005).

In this work, we proposed to use a co-culture of *S. cerevisiae* and *S. stipitis* to achieve simultaneous conversion of glucose and xylose to ethanol. However, it is difficult to establish optimum conditions for a co-culture in a single bioreactor, because the two strains do not have compatible optimum culture conditions. Most existing studies on the co-culture systems for lignocellulosic ethanol production reported that the fermentation of xylose by *S. stipitis* was often

[1] *Department of Chemical Engineering, Auburn University, AL*

[2] *Department of Chemical Engineering, Tuskegee University, AL*

** Corresponding author*

slow with low yield due to the conflicting oxygen requirements (Gutierrez-Rivera *et al.* 2012) between the two strains. In addition, co-cultures of these yeast strains do not ensure the complete conversion of xylose because of the diauxic kinetics of *S. stipitis* (Nakamura *et al*. 2001). Finally, another limiting step of the co-culture process is the low ethanol tolerance of *S. stipitis*. To address these challenges, we designed and customized a novel co-culture bioreactor with an innovative fermentation scheme to offer a promising alternative to overcome the difficulties of the existing co-culture systems and to study the dynamics of co-culture systems.

Materials and Methods

Strain preparation and fermentation conditions

Saccharomyces cerevisiae D5A and *Scheffersomyces stipitis* CBS5773 were used as glucose-fermenting yeast and xylose-fermenting yeast, respectively. The strain was maintained at 4°C on YPD (*S. cerevisiae*) or YPX (*S. stipitis*) agar plates. The pre-culture medium contained (per liter DI water) 20g D-glucose or D-xylose, 1.7g yeast nitrogen base without amino acids and ammonium sulfate and 2.27g urea. The batch culture medium and feed medium contained (per liter DI water) 50g D-glucose, 25g D-xylose, 1.7g YNB w/o AA & AS and 2.27g urea. The *S. cerevisiae* and *S. stipitis* cells were grown through the following three different phases during co-culture experiment.

1. **Pre-culture phase:** *S. cerevisiae* and *S. stipitis* cells were pre-grown for 24h in a rotary shaker (250rpm) at 30°C in a 250mL Erlenmeyer flask containing 100mL of the pre-culture medium defined above.
2. **Batch growth phase:** pre-cultured *S. cerevisiae* and *S. stipitis* cells were inoculated into different chambers of the in-house developed co-culture bioreactor. The total working volume of the bioreactor was 1.65L. The pH was maintained at 5.0 by automatic addition of 1.0N KOH. The initial optical densities *of S. cerevisiae* and *S. stipitis* at 600nm (OD_{600}) were 0.2 and 0.5, respectively. The cells were cultivated and fermented at 30°C with agitation under a constant air flow rate of 483.2 mL/min till the glucose was completely consumed.
3. **Pseudo-continuous fermentation phase:** system was shifted from growth state to fermentation state by reducing the oxygen supply. The aeration rate of *S. stipitis* was further reduced to 4.8ml/min and nitrogen gas of 49.1ml/min was fed into *S. cerevisiae*. The continuous feed-in of the feed medium into the *S. cerevisiae* chamber and continuous withdraw of the effluent from the *S. stipitis* chamber through the cell retention module was started at 0.12mL/min to maintain a dilution rate of $0.004h^{-1}$. Other conditions were remained the same as the batch growth phase. This pseudo-continuous phase was maintained for more than 2 weeks.

Accurate control of OTR

The efficient conversion of xylose to ethanol by *S. stipitis* is highly influenced by OTR and there exists an optimal OTR. Above the optimal OTR, carbon flows preferentially through the tricarboxylic acid cycle which results in faster cell growth at the expense of ethanol production, while below optimal OTR, the imbalance of cofactors (NAD/NADH, NADP/NADPH) will result in the production of xylitol. Hence, a precise control of OTR is important to maximize the ethanol production. In order to achieve an accurate control of the oxygen transfer rate in the co-culture system, we developed and tested a gas mixing apparatus as shown in Figure1 (Left). The initial test runs confirmed that the OTR using gas mixture of air and nitrogen could be accurately controlled at different desired OTRs as shown in Figure1 (Right). The overall flow rate of gas mixture was almost identical to the measured flow rate of combined air and nitrogen gases at each OTR.

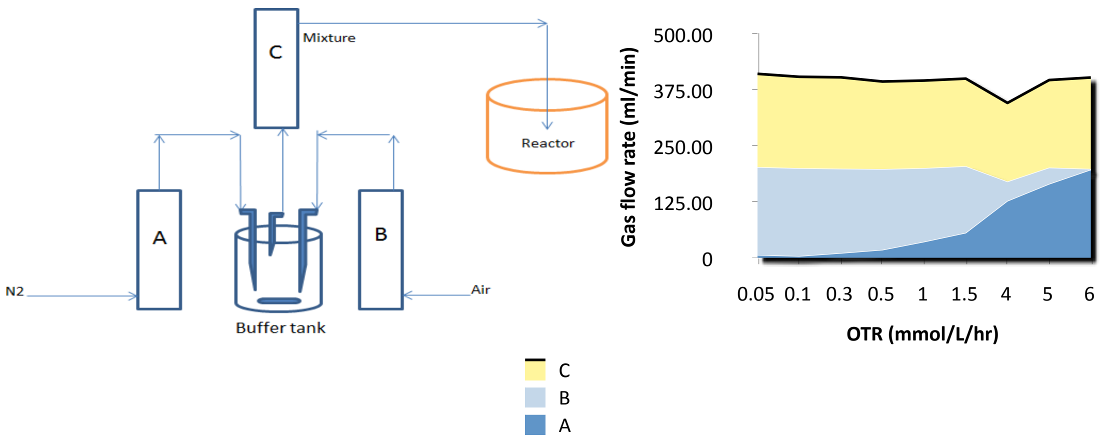

Figure 1. The schematic diagram of gas mixing apparatus for OTR measurements (Left) & the control of OTR in gas mixture for co-culture study (Right) (A: N_2 flow rate, B: Air flow rate, C: Mixture of N_2 and Air flow rate)

Construction of co-culture bioreactor

We have developed a novel two-chambered bioreactor to address the identified challenges associated with co-culture system. The schematic diagram and actual set-up of developed bioreactor for co-culture study are shown in Figure2. This configured co-culture system enables not only confinement of each strain to each chamber, but also exchange of culture medium and extracellular metabolites between the two chambers. Moreover, it enables us to maintain different OTR for each strain by adjusting nitrogen and air flow rates into each chamber. The propellers of the agitator were driven by an external magnetic field and the pH and temperature controllers were implemented to control the co-culture system effectively. In addition to this reactor design, an innovative fermentation scheme, pseudo-continuous fermentation (i.e. continuous fermentation with cell retention), was proposed to carry out the experiment.

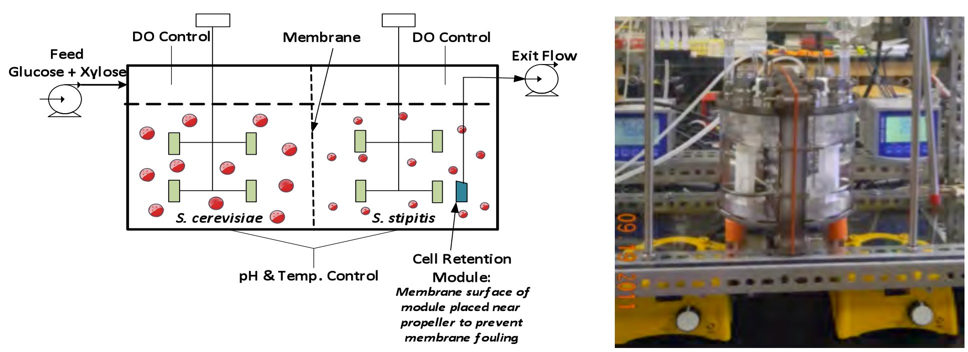

Figure 2. The schematic diagram (Left) and actual set-up of developed bioreactor (Right) for co-culture study

Results and Discussion

Advantages of novel two-chambered co-culture bioreactor

There are several benefits associated with the reactor design and pseudo-continuous fermentation proposed in our co-culture study. The novel two-chambered reactor can provide the independent control of optimal dissolved oxygen required for each strain. With pseudo-continuous operation the diauxic lag of *S. stipitis* and catabolite repression on xylose were eliminated by completing consumption of glucose and xylose by each strain, *S. cerevisiae* and *S. stipitis*, respectively. In addition, while continuously removing cellular wastes and other inhibitors, cell retention is achieved to provide an ideal environment for cell adaptation to tolerate higher ethanol concentration. Furthermore, it allows the wide range of feasible operation to study the properties of the co-culture system.

Preliminary results on co-culture system

The preliminary results from co-culture study showed that the complete consumption of both glucose and xylose was achieved simultaneously by pseudo-continuous fermentation (Figure3, Left) and the diauxic lag of *S. stipitis* often existed in continuous or fed-batch fermentations was eliminated (Figure3, Right).

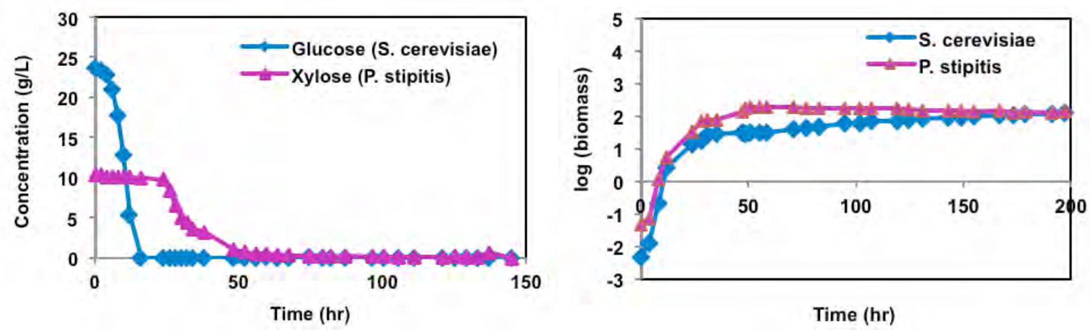

Figure 3. Simultaneous complete consumption of glucose and xylose (Left) & biomass concentration along with time (Right)

The proposed co-culture system also achieved the significant improvement on the ethanol tolerance of both strains by cell adaptation (Figure4). The cell adaptation to environmental changes is achieved by the mechanism that a cell adjusts its intracellular physiological conditions to the surrounding environment to grow (Dinh *et al.* 2008). Hence, it was expected that exposing retained yeast cells to the surrounding environment of slow increase in the level of ethanol stress could be effective for obtaining the ethanol-tolerant strains and the results confirmed this hypothesis.

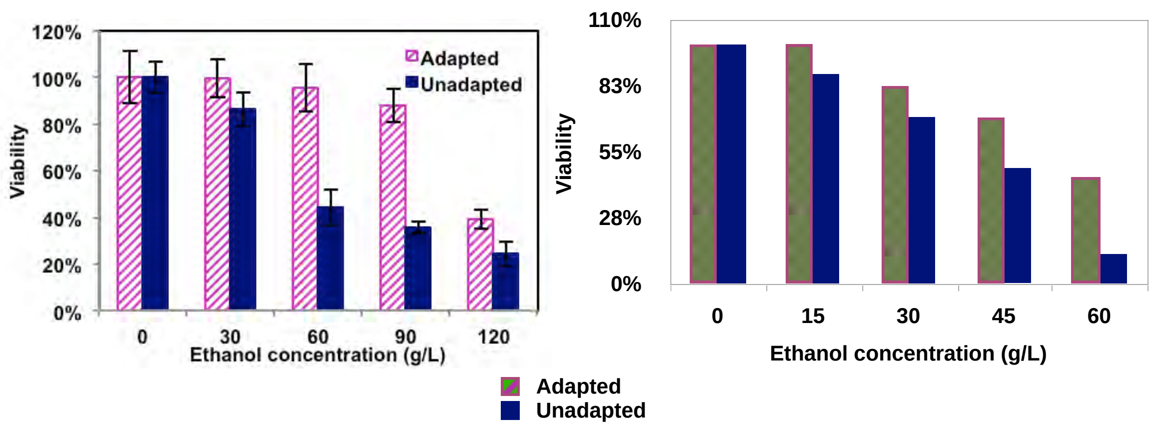

Figure 4. Cell viabilities of *S. cerevisiae* (Left) and *S. stipitis* (Right) after adaptation

References

Dihn, T.N., Nagahisa, K., Hirasawa, T., *et al.* (2008). “Adaptation of *Saccharomyces cerevisiae* cells to high ethanol concentration and changes in fatty acid composition of membrane and cell size,” *PLoS ONE* 3(7), e2623.

Gutierrez-Rivera, B., Waliszewski-Kubiak, K., Carvajal-Zarrabal, O., *et al.* (2012). “Conversion efficiency of glucose/xylose mixtures for ethanol production using *Saccharomyces cerevisiae* ITV01 and *Pichia stipitis* NRRL Y-7124,” *J Chem Technol Biotechnol* 87, 263-270.

Jeffries, T.W., Jin, Y.S. (2004). “Metabolic engineering for improved fermentation of pentoses by yeasts,” *Appl Microbiol Biotechnol* 63,495-509.

Kuyper, M., Toirkens, M.J., Diderich, J.A., *et al.* (2005). “Evolutionary engineering of mixed – sugar utilization by a xylose-fermentation *Saccharomyces cerevisiae* strain. *FEMS Yeast Res* 5, 925-934.

Nakamura, Y., Sawada, T., Inoue, E. (2001). “Mathematical model for ethanol production from mixed sugars by *Pichia stipitis*,” *J Chem Technol Biotechnol* 76, 586-592.

3.3
ENHANCING BUTANOL PRODUCTIVITY THROUGH IMPROVED UTILIZATION OF BIOMASS BY *CLOSTRIDIUM BEIJERINCKII* NCIMB 8052

Victor Ujor[1], Venkat Gopalan[2,], Thaddeus Ezeji[1,*]*

Abstract
Due to our long-standing interest in *Clostridium beijerinckii* NCIMB 8052, a model microorganism for studying acetone-butanol-ethanol (ABE) fermentation, the overarching goal of this study is to address some of the bottlenecks that prevent large-scale industrial production of butanol, a fossil fuel alternative. Key factors that impede effective sugar utilization result from (i) butanol's microbial toxicity and (ii) carbon catabolite repression (CCR) in solventogenic clostridia. We are attempting to address these two limitations. First, we integrated *in situ* vacuum-aided recovery of butanol into *C. beijerinckii* ABE fermentation and increased butanol productivity by 2-fold. Second, we are investigating the use of RNase P (ribozyme)-based gene knock-down methods to down-regulate expression of CcpA, a transcription factor that decreases pentose utilization when glucose is still available. Motivated by a recent report (Wesolowski et al., 2011), we designed a cell-penetrating peptide-morpholino conjugate, with the latter's sequence complementary to the CcpA mRNA. The objective is to generate a bipartite (CcpA mRNA—Peptide-morpholino) complex that is recognized and cleaved by endogenous RNase P, a tRNA processing enzyme. Although preliminary data from this approach showed no significant utilization of pentoses by *C. beijerinckii*, we unexpectedly observed 11% and 18% increases in initial glucose utilization in media containing glucose (40 g/L) + arabinose (20 g/L) and glucose (40 g/L) + xylose (20 g/L), respectively, and a 25% increase in total ABE production in both cases. While we will investigate the bases for these increases, we are also pursuing in parallel variants of the RNase P-based approach.

Keywords: *Clostridium beijerinckii*; butanol; RNase P; vacuum fermentation; carbon catabolite repression

Introduction
Butanol has received attention recently as a potential transportation fuel due to its fuel characteristics such as comparable energy content to that of regular gasoline and its lower vapor pressure than ethanol; the latter trait makes it more attractive compared to ethanol in terms of decreased flammability and increased safety during transport and use in combustion engines. However, butanol is highly toxic to the microbes which produce it. As a result, butanol titers produced during acetone-butanol-ethanol (ABE) fermentation are low. In addition, for ABE fermentation to attain commercial viability, cheap, readily available and easily metabolizable substrates are required. Although lignocellulosic biomass meets the first two criteria above, the third remains elusive. This is largely because pentoses (xylose and arabinose), which account for approximately 38% of the total fermentable sugars in lignocellulosic hydrolysates (LCH) are barely consumed in the presence of glucose, the predominant sugar in LCH. Cumulative evidence indicates that microbes typically consume glucose before other sugars present in a mixed-sugar feedstock due to a phenomenon called carbon catabolite repression (CCR) (Ren *et al*. 2010), which prevents pentose utilization as long as there is availability of glucose, the preferred carbon

[1] The Ohio State University and Ohio Agricultural Research and Development Center (OARDC), OH

[2] Department of Chemistry & Biochemistry and Center for RNA Biology, The Ohio State University, OH

* Corresponding author

source. Delayed and incomplete utilization of pentoses result in lower productivity, poor yield and interference with downstream processing.

This on-going study seeks to address the highlighted impediments to large-scale industrial production of bio-butanol. First, to alleviate butanol toxicity, we have integrated *in situ* vacuum-assisted recovery of butanol into *Clostridium beijerinckii* ABE fermentation to keep butanol concentrations below the toxic threshold, thereby extending sugar utilization, microbial growth and butanol productivity (Mariano *et al*. 2011; 2012). Second, for economically viable *C. beijerinckii*-mediated bioconversion of biomass to butanol, novel metabolic engineering strategies are required to override the intrinsic order of preferential sugar utilization to allow simultaneous fermentation of mixed-sugars. To this end, we are investigating the use of RNase P (ribozyme)-based gene knock-down methods to down-regulate expression of the global carbon catabolite protein A (CcpA) transcription factor, which negatively regulates pentose utilization in the presence of glucose.

Materials and Methods

Vacuum Fermentation

ABE fermentation with *C. beijerinckii* NCIMB 8052 was conducted anaerobically in a 14-L bioreactor (New Brunswick Scientific, New Brunswick, New Jersey) containing 7 L of P2 medium (Mariano *et al*. 2011; 2012). The fermentation was allowed to proceed for 20 h during which ABE concentration approached 8 g/L, before establishing continuous ABE recovery by vacuum during which broth in the bioreactor was boiled at the fermentation temperature (35 °C; at vacuum range 711–737 mm Hg) generating ABE and water vapors (continuous; Mariano *et al*. 2011). Subsequently, fermentations were conducted as described above where vacuum pressure was applied intermittently with 2 h-vacuum fermentations punctuated by 4 h-fermentation (cyclic) at atmospheric pressure, a measure adopted to lower overall fermentation energy cost (Mariano *et al*. 2012).

Knock-down of CcpA

A central focus of this study is to knock-down the expression of carbon catabolite protein A (CcpA) in *C. beijerinckii* NCIMB 8052, with a view to enhancing pentose utilization in the presence of glucose. Our approach entails the delivery of a guide sequence (GS) complementary to the accessible region of CcpA mRNA, and the subsequent cleavage of the mRNA by endogenous RNase P, an enzyme involved in tRNA maturation (Wesolowski et al., 2011). A CcpA-specific guide sequence was designed with the aid of mfold RNA folding software (http://mfold.rna.albany.edu/?q=mfold/RNA-Folding-Form). For preliminary screening to assess the efficacy of the CcpA GS in *C. beijerinckii*, we undertook an expedient approach inspired by Wesolowski et al. (2011) who successfully employed a T cell-derived cell penetrating peptide (TCPP) to deliver morpholino oligonucleotides into bacterial cells and altered gene expression.

Analytical procedures

ABE and acid concentrations were measured using a 7890A Agilent Technologies gas chromatograph (Agilent Technologies Inc., Wilmington, DE) as described elsewhere (Mariano *et al*. 2011; 2012). Sugars were quantified by high performance liquid chromatography (HPLC), using an LC-20AB HPLC unit (Shimadzu, Columbia, MD, USA).

Results and Discussion

The continuous and cyclic vacuum-assisted gas stripping processes produced 132 and 141 g of ABE, respectively, whereas the control resulted in 110 g of ABE. ABE productivity of 0.43 g/L/h was achieved with the continuous system, relative to 0.24 g/L/h in the control; ~2-fold higher (Mariano et al. 2012). Before optimizing vacuum-assisted gas stripping, we assessed whether this process can be operated for long periods. Hence, the gas stripping system was operated for 504 h (21 days) after which the fermentation was intentionally terminated (Ezeji et al., 2012). This result demonstrates that ABE fermentation can be operated in an integrated, continuous one-stage fermentation system and, importantly, product recovery could be sustained for a long period of time (21 days) provided butanol and other microbial metabolites in the bioreactor are kept below a toxic threshold.

Treatment with the TCCP-CcpA GS fusion did not result in significant utilization of pentoses by *C. beijerinckii* NCIMB 8052. Unexpectedly, however, we observed 11% and 18% increases in glucose utilization in media containing glucose (40 g/L) + arabinose (20 g/L) and glucose (40 g/L) + xylose (20 g/L), respectively, during the early stages of fermentation (Fig. 1). Similarly, there was a 25% increase in ABE production in the presence of both arabinose and xylose. We also observed a 17% increase in butanol production with TCCP-CcpA GS treatment (only in the xylose-containing medium); however, acetone production increased 40% and 51% in arabinose and xylose-containing media respectively, accounting for the significant increases in total ABE production.

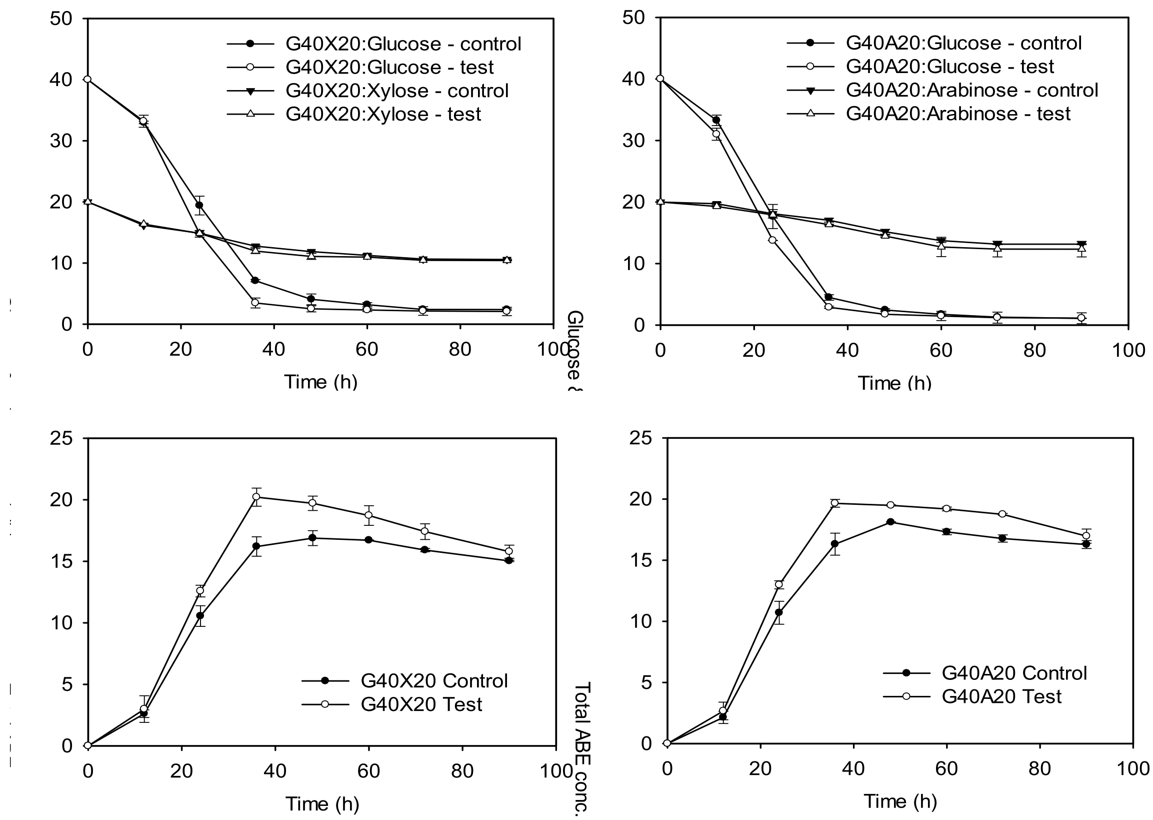

Figure 1. Comparative sugar consumption and total ABE production in batch fermentations of *C. beijerinckii* NCIMB 8052 treated with TCCP-CcpA GS morpholino conjugate, relative to untreated cultures. G40X20: 40 g/L glucose + 20 g/L xylose; G40A20: 40 g/L glucose + 20 g/L arabinose.

Since we did not observe significant increases in pentose utilization, we are uncertain if significant down-regulation of CcpA was achieved. However, it is worth mentioning that the morpholino peptide is lost by replicating cells after some generations. Moreover, all cells are not simultaneously penetrated by the morpholino peptide, which could contribute to phenotypic variability. The mechanism for the observed increases in glucose utilization is unclear; however we are pursuing the cloning of a bacterial RNase P RNA–CcpA GS fusion, and intend to transform *C. beijerinckii* with this customized ribozyme. Such a genetic approach will help address some of the caveats with the morpholino methodology.

References

Mariano, A. P., Qureshi, N., Filho, R. M., and Ezeji, T. (2011). Assessment of *in situ* butanol recovery by vacuum during acetone butanol ethanol (ABE) fermentation. *J. Chem. Technol. Biot*., 87, 334-340.

Mariano, A. P., Filho, R. M., and Ezeji, T. (2012). Energy requirements during butanol production and in situ recovery by cyclic vacuum. *Renew. Energ*., 47, 183-187.

Ezeji, T.C., Qureshi, N., and Blaschek, H.P. (2012) Microbial Production of a Biofuel (Acetone-Butanol-Ethanol) in a Continuous Bioreactor: Impact of Bleed and Simultaneous Product Removal. Bioproc. Biosys. Eng. (in press)

Ren, C., Gu, Y., Hu, S., Wu, Y., Wang, P., Yang, Y., Yang, C., Yang, S., and Jiang, W. (2010). "Identification and inactivation of pleiotropic regulator CcpA to eliminate glucose repression of xylose utilization in *Clostridium acetobutylicum*." *Metab. Eng*., 12, 466-454.

Wesolowski, D., Tae, H. S., Gandotra, N., Llopis, P., Shen, N., and Altman, S. (2011). Basic peptide-morpholino oligomer conjugate that is very effective in killing bacteria by gene-specific and nonspecific modes. *Proc. Natl. Acad. Sci., USA.*, 108, 16582 – 16586.

3.4
SYNTHESIS OF FLUOROGENIC MODEL COMPOUNDS FOR BIOPROSPECTING OF ENZYMES THAT BREAK LIGNIN-HEMICELLULOSE BONDS

Cheng-Wei Tom Chang[1,] Qian Zhang[1] and Nancy Kravit[2]*

Abstract
Separating polysaccharides in wood from lignin is the major difficulty in using forest biomass. The problem is mostly due to ether bonds between lignin and hemicellulose, especially the α- or β-benzyl and phenolic ether bonds. Using an enzyme pretreatment instead of current high stringency chemical procedures is much more environmentally friendly. We have designed and synthesized fluorogenic probes mimicking the structure of lignin-mannan ether bonds. These probes will be assayed for bond hydrolysis, and bioprospected for microbes capable of specifically breaking lignin-mannan ether bonds. We expect to elucidate the synthetic pathways to models of non-glycosidic ether bonds between lignin and hemicellulose. Enzyme activities from 3-5 potential sources can then be tested for their ability to specifically cleave those lignin-mannan ether bonds. The outcomes will increase the efficiency in biofuel production from lignin-hemicellulose based biomass and increase environmental friendliness of biorefineries.

Keywords: wood, lignin, hemicellulose, mannan, mannose, fluorogenic, α-benzyl ether, β-benzyl ether, lignin-carbohydrate complexes (LCC)

Background and Introduction
Separating polysaccharides in wood from lignin is the major difficulty in using forest biomass. The problem is mostly due to ether bonds between lignin and hemicellulose (mannan and xylan), especially the α- or β-benzyl, and, potentially, phenolic ether bonds. Using an enzyme pretreatment instead of current high stringency chemical procedures is much more environmentally friendly. We propose to synthesize model fluorogenic compounds/probes and use them to bioprospect for enzymes that break non-glycosidic ether bonds between lignin and hemicellulose (mannan). The ultimate goal is to enhance the efficiency of utilizing lignin-based biomass for the production of biofuels and other chemicals. The project began at September 2011. All the designed probes have been chemically synthesized. The developed synthetic methodologies can be employed for the preparation of different probes that mimic the ether bonds between lignin and xylan, which is another dominant form of hemicellulose. The preliminary assay of one probe reveals the fluorogenic property upon enzyme treatment that provides a positive proof-of-concept support.

Significance

The Problem
Today, the United States imports vast amounts of petroleum to help satisfy its energy and chemical requirements (~5% of the total output of a petroleum refinery is used by the chemical processing industry as raw material).[1] Alternatively, both fuels and chemicals can be synthesized from biomass in biorefineries. <u>First generation</u> biorefineries use corn starch as a feedstock. Unfortunately, cultivating agricultural crops as a source of biomass is energy intensive and

[1] *Department of Chemistry and Biochemistry, Utah State University, UT*

[2] *Tethys Research LLC, Tethys Research LLC, ME*

* *Corresponding author*

escalates competition between the use of land for food or for fuel.[2] Thus, second generation biorefineries have focused on lignocellulosic sources of biomass, like agricultural waste, energy crops such as switchgrass, and wood waste. It is estimated that 60-80% of the cost of manufacturing chemical products like biofuels from agricultural biomass is incurred in separating fermentable sugars from the rest of the starting biomass.[3] Therefore, decreasing the cost and increasing the efficiency of separation will have a substantial effect on the economic efficiency of using biomass for chemical and biofuel production. The full potential of biomass for fuel and chemical production can only be realized when new cost effective fractionation procedures are developed that maintain the functionality and downstream use of their hemicellulose, cellulose and lignin components.

The solution

Dr. Nancy Kravit, has pioneered a new class of enzymes that cleave non-glycosidic ether bonds between hemicellulose and lignin. Unlike other laboratories that have concentrated on glycosidic lignin-hemicellulose bonds, Dr. Kravit has based her enzyme discovery strategy on wood biosynthesis, which strongly implies that non-glycosidic links are the major type of bonds between lignin and hemicellulose. As a result, her laboratory is the sole source of these novel enzymes called hemicellulose lignin etherases (HLEs). The first member of this class, MLE (mannan:lignin etherase), targets phenolic ether bonds between lignin and mannan, the predominant hemicellulose of softwoods.[4] Our goal is to search for new HLEs targeted to α-, β-benzyl and, probably, phenolic ether bonds between lignin and hemicellulose (Figure 1). These new enzymes will eventually be developed into a biomass pulping process to increase the separation of lignin, hemicellulose and cellulose without the concomitant degradation that occurs with the stringent pretreatment technology currently in use. Because the enzyme(s) will not depolymerize any of the polysaccharides, pretreatment with HLEs will lead to increased yield of polysaccharides for biorefining purposes and clean, undegraded lignin fractions for chemical manufacturing or simply for the biomass boiler. HLE treatment can also be used further downstream (e.g. to brighten paper and decrease the need for chemical bleaching), reducing associated chemical and environmental costs.

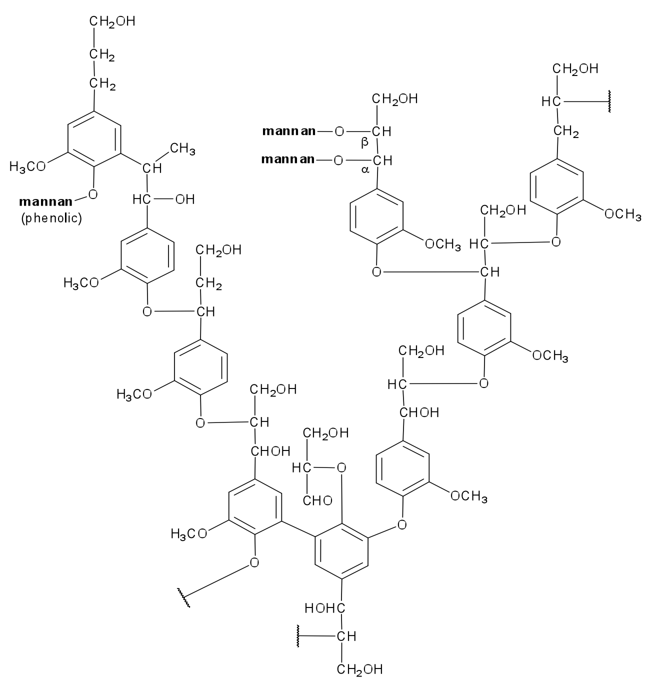

Figure 1. Representative structure of lignin and mannan

Method

To evaluate the activities of MLE and HLE, we have designed and synthesized model fluorogenic probes that mimic ether bonds between α, β benzyl and phenolic carbons of lignin (Figure 2). Probe I has a fluorogenic tag, 6MN (6'-methoxy-2'-(2-methyl)naphthylene), attached to O-6 of mannose that mimics the linkage between α benzyl carbon of lignin and mannan. Probe II has a similar fluorogenic tag, 6MN' (6'-methoxy-2'-hydroxyethylnaphthylene), also attached to C-6 of mannose to mimic the linkage between □-benzyl carbon of lignin and mannan. We chose to use the linkage through *nitrogen* rather than *oxygen* due to the encountered synthetic difficulties, which will be described later. Probe III has a fluorogenic tag, 4MU (4-methylumbelliferone) attached to O-6 of mannose to mimic the linkage between phenolic carbon of lignin and mannan. We prefer to use mannose instead of mannan because natural mannans have very high and heterodisperse molecular weights that make solvent choices difficult. After completion of the synthesis, these probes will be employed to test enzyme activities for the ability to specifically cleave those lignin-mannan ether bonds. If the cleavage occurs, these probes will release fluorescence molecules (6MN or 4MU that can be monitored to offer quantity analysis on the enzyme activities.

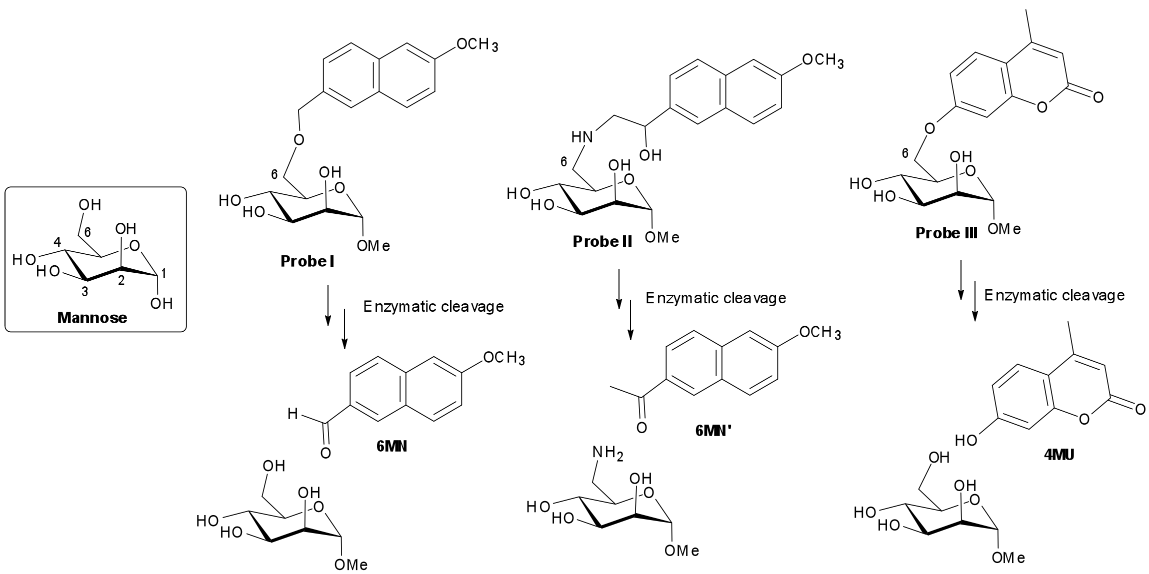

Figure 2. Design of fluorogenic probes

Synthesis and Results

The syntheses of probe I began with the reduction of compound 1 followed by converting the resulting primary alcohol into a good leaving group (trichloroacetimidate group) (Scheme 1). In a separate route, commercially available methylmannoside, 3 was used to synthesize compound 4 with free O-6 hydroxy group. Attaching the methoxynaphthalene moiety onto the 6-OH of compound 4 was carried out under Lewis acid-catalyzed condition to yield compound 5. Finally, debenzoylation of compound 5 furnished the desired probe I. The synthesis of probe III can be readily achieved via a one step process under the Mitsunobo condition (Scheme 2).

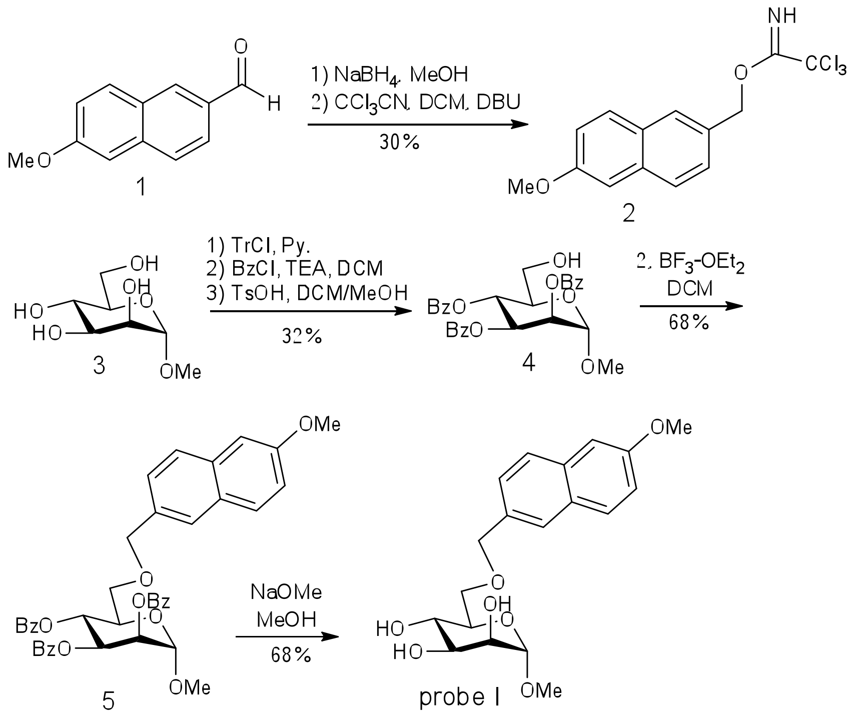

Scheme 1. Synthesis of fluorogenic probe I

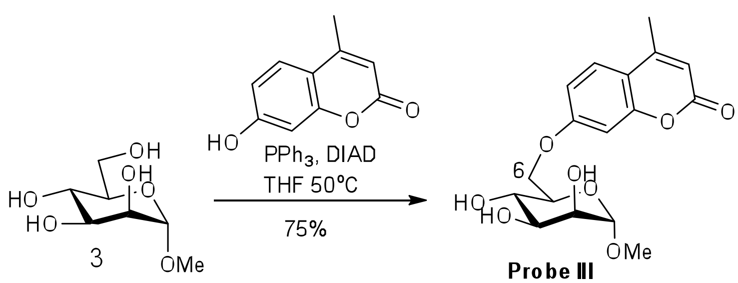

Scheme 2. Synthesis of fluorogenic probe III

The synthesis of probe II started with commercially available 6-methoxy-2-vinylnaphthlene (Scheme 3). Dihydroxylation using $KMnO_4$ followed by selective protection of the secondary hydroxy group yielded compound 8. Several attempts of attached protected mannose derivatives with 6-OH failed to provided the desired product. Therefore, we decided to adopt the nitrogen-linkage rather than oxygen-linkage. Oxidation of the primary hydroxy group using Swern oxidation furnished an aldehyde, 9. In a separate route, compound 10 was synthesized. the 6-N_3 was reduce to 6-NH_2. Both compounds 9 and 11 were used as crude products for reductive amination using $NaBH_3CN$ to give compound 12. Hydrogenolysis of the Bn protecting groups offered the desired probe II.

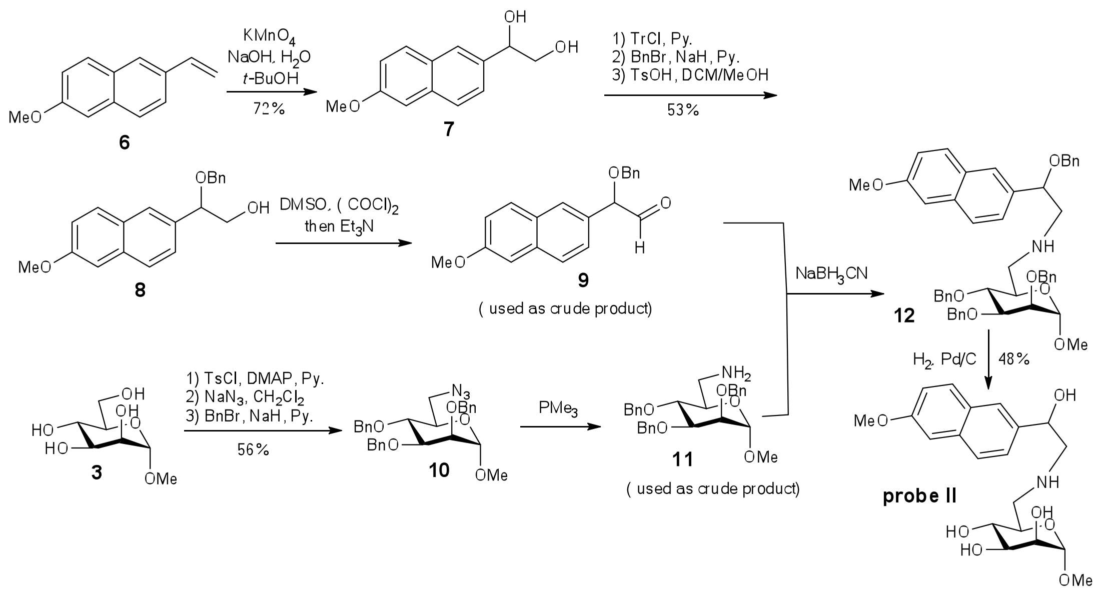

Scheme 3. Synthesis of fluorogenic probe II

Preliminary result from the study of probe III has shown that the mannan:lignin etherase (MLE) can take probe III with phenolic linked mannose as the substrate. This suggests that some hemicelluloses are linked to lignin through phenoic bond (Figure 3).

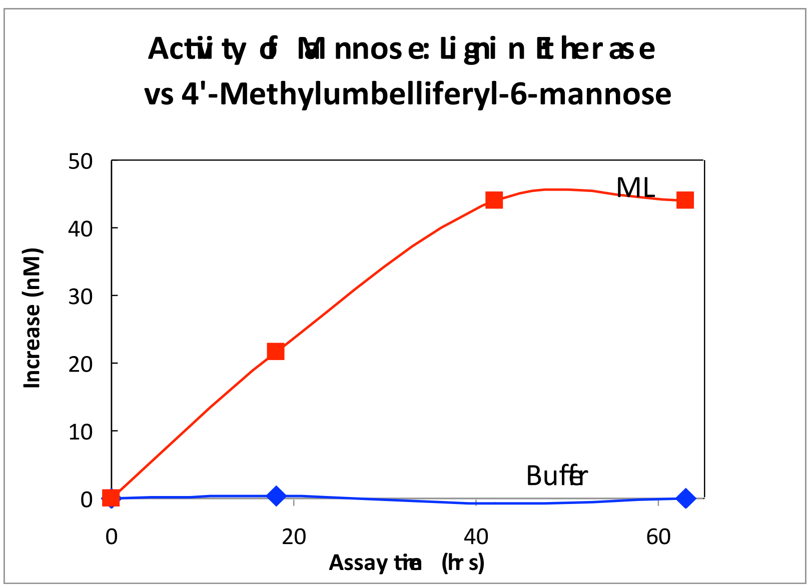

Figure 3. Study of probe III with MLE

Conclusion

Although the project has been commenced for less than a year, significant progress has been made. The proof-of-concept has been demonstrated. The ongoing effort will be directed toward the bioprospecting for enzymes that will increase the efficiency of breaking down lignin-hemicellulose ether bonds.

References

Ragauskas, A. J., Williams, C. K., Davison, B. H., Britovsek, G., Cairney, J., Eckert, C. A., Frederick, W. J. Jr., Hallett, J. P., Leak, D. J., Liotta, C. L., Mielenz, J. R., Murphy, R., Templer, R. and Tschaplinski, T. (2006) "The path forward for biofuels and biomaterials." *Science* 311:484-489.

Rising food prices: policy options and World Bank response. http://siteresources.worldbank.org/NEWS/Resources/risingfoodprices_backgroundnote_apr08.pdf

Hedenstroma, M., Wiklund-Lindstrom, S., Omana, T., Lub, F., Gerberc, L, Schatzd, P., Sundberg, B. and Ralph, J. (2009) "Identification of lignin and polysaccharide modifications in *Populus* wood by chemometric analysis of 2D NMR spectra from dissolved cell walls." *Molec. Plant* 2:933–942.

Dickey, E. E. and Roth, L. (1981) Hemicelluloses and gums. Institute of Paper Chemistry, Appleton, Wis.

3.5 SELECTIVE METABOLISM OF INHIBITORS FOUND IN LIGNOCELLULOSIC HYDROLYSATES

Mark A. Eiteman,[3,] Elliot Altman[4]*

Abstract

Acetic acid, furfural, and 5-(hydroxymethyl)furfural are three inhibitors found in lignocellulosic hydrolysates. Towards our goal of developing microbial strains which do not metabolize sugars but selectively consume only the inhibitors found in these hydrolysates, we have isolated 5 strains which are able to metabolize furfural as the sole carbon source. These isolates are distinct from existing phylogenetic neighbors, and one strain (named ALS1267) phylogenetically close to Pseudomonas aeruginosa is able to metabolize 9 mM furfural in less than 9 hours. We are currently isolating the enzyme associated with the first step in the degradation pathway, furfural dehydrogenase, with the goal of expressing this protein in an E. coli that only degrades acetate.

Keywords: acetic acid, furfural, Escherichia coli, 5-(hydroxymethyl)furfural, Pseudomonas

Introduction

Lignocellulosic biomass can potentially be used to diversify our current fossil-fuel based systems for fuel, power and products, and microbial conversion of carbohydrates into biochemical products is a well-developed practice. Lignocellulosic biomass must first be hydrolyzed into its constituents, however, and a key technical challenge lies in utilizing the resulting complex hydrolysate which typically is composed of a mixture of hexoses and pentoses and microbial inhibitors such as acetic acid and furans. The challenge is thus two-fold: how to convert a (variable) sugar mixture efficiently, and how to overcome the (variable) presence of inhibitors. Although the yeast *Saccharomyces cerevisiae* is the preferred organism for ethanol production, industries have considered *Escherichia coli* for the production of many chemicals such as hydroxypropionate (Lynch, 2011), isobutanol (Atsumi et al., 2008) and isoprene (Bott et al., 2012) because of this organism's metabolic flexibility. Since current technology generates a hydrolysate composed of less than 10% (w/v) sugar, *E. coli* is also sufficiently tolerant to be used for generating the resulting low concentrations of ethanol (<5%) or other fuel products (<10%) attainable from this starting material (Taherzadeh et al., 2001). While formation of inhibitors can be reduced by judicious design of the hydrolysis process or by improvements in the biomass itself, it does not appear feasible to eliminate their generation. Removing inhibitors after hydrolysis by ion exchange or membrane filtration is also not feasible because these technologies significantly impact the overall production cost for a relatively low value product (von Sivers et al., 1994). Most present research focuses on creating a single, "do-it-all" microorganism that is both able to convert varying mixtures of sugars and contend with the fluctuating presence of inhibitors such as acetic acid without loss of yield or productivity.

Another approach for the conversion of lignocellulosic hydrolysate is to use a *consortium of organisms*. This approach involves multiple strains which each are able to consume

[3] BioChemical Engineering, College of Engineering, University of Georgia, GA

[4] Department of Biology, Middle Tennessee State University, TN

* Corresponding author

only one substrate although they are otherwise identical. Because each member of the consortium is able only to consume one substrate, the strains effectively ignore other substrates while they each carry out their one target conversion. An advantage of such substrate-selective uptake is that the system naturally adapts to fluctuations in the feed stream; for example, the proportion of each member of the consortium will respond to a variable feed composition when it is supplied in a carbon-limiting fashion (Eiteman et al., 2008). In addition, because consortium members are the same species, growth incompatibilities (e.g., pH, temperature, nutritional requirements, negative cell-to cell interactions) are generally avoided (Chen, 2011). The approach has been used to generate lactic acid from a mixture of glucose and xylose (Eiteman et al., 2009).

Such a consortium approach can theoretically be extended to detoxify lignocellulosic hydrolysate. That is, microorganisms exist which can even metabolize inhibitors like acetic acid and furfural. Constructing the pathways involved in inhibitor degradation into one or more strains which cannot metabolize any sugar should allow the system to remove the inhibitors selectively prior to a sugar-conversion step.

The goal of this research is to isolate microorganisms which degrade furfural. The isolated strains will be characterized and enzyme activities measured. Ultimately, key enzymes in the furfural-degradation pathway will be introduced into a strain of *Escherichia coli* which is unable to consume any of the sugars so that a lignocellulosic hydrolysate can be detoxified.

Methods

The defined growth medium (FIM) contained (per L): 1.0 g furfural (about 9 mM), 1.50 g KH_2PO_4, 3.092 g $Na_2HPO_4{\cdot}7H_2O$, 0.50 g NH_4Cl, 0.50 g $(NH_4)_2SO_4$, 20 mg $FeSO_4{\cdot}6H_2O$, 90 mg $MgCl_2{\cdot}6H_2O$, 40 mg $CaCl_2{\cdot}2H_2O$, 0.5 mL Vitamin Solution, 5.0 mL Mineral Solution (Freier et al. 1988). The Vitamin Solution comtained (per L): 40 mg biotin, 100 mg p-aminobenzoic acid, 40 mg folic acid, 100 mg calcium D-(+)-pantothenate, 100 mg nicotinic acid, 2 mg vitamin B_{12}, 100 mg thiamine-HCl, 200 mg pyridoxine-HCl, 100 mg thioctic acid, 10 mg riboflavin, and the Mineral Solution contained 1.5 g nitriloacetic acid, 3.0 g $MgSO_4{\cdot}7H_2O$, 0.50 g $MnSO_4{\cdot}H_2O$, 1.00 g NaCl, 100 mg $FeSO_4{\cdot}7H_2O$, 81.7 mg $CoCl_2{\cdot}6H_2O$, 132.4 mg $CaCl_2{\cdot}2H_2O$, 91.7 mg $NiCl_2{\cdot}6H_2O$, 100 mg $ZnSO_4{\cdot}7H_2O$, 10 mg $CuSO_4{\cdot}5H_2O$, 8.0 mg $Al_2(SO_4)_3{\cdot}18H_2O$, 10 mg H_3BO_3, 10 mg $Na_2MoO_4{\cdot}2H_2O$, 10 mg $Na_2WO_4{\cdot}2H_2O$, 1.0 mg Na_2SeO_3. The pH of the medium was adjusted to 7.0 with NaOH and/or H_2SO_4. FIM plates were made with the same medium containing 15 g/L Bacto Agar.

Microorganisms were isolated from samples from the wastewater of a local chemical company and a carpet dyeing company. Replicate liquid samples were transferred with 10× dilution into 3 mL FIM and incubated at 28°C and 37°C. When the OD reached about 0.5, a sample was transferred again with 10× dilution into 3 mL FIM. The process was repeated, and serial dilutions of the fourth solution used to streak FIM plates which were incubated at the isolation temperature for three days. From these plates individual colonies were selected and used to restreak FIM plates.

To determine growth on furfural, bacteria were first grown at their isolation temperature with an agitation of 250 rpm (19 mm pitch) in 250 mL shake flasks with 50 mL FIM. When the OD of a culture reached approximately 0.5, the flask contents were diluted with fresh FIM so that 100 mL having an effective OD of 0.25 was used to inoculate the bioreactor containing 0.9 L FIM. Batch experiments were carried out in a 2.5 L bioreactor (Bioflow III, New Brunswick Scientific Co., Edison, NJ) maintained at the isolation temperature with air sparged at a flow rate of 1.0 L/min, an agitation of 500 rpm, and the pH controlled at 7.0 using 5% (w/v) NaOH and/or 20% H_2SO_4.

To determine growth on 5-(hydroxymethyl)furfural (HMF), bacteria were first grown at their isolation temperature with an agitation of 250 rpm (19 mm pitch) in 250 mL shake flasks with 50 mL FIM (i.e., containing HMF). When the OD of this culture reached approximately 0.5, the flask contents were diluted with fresh FIM so that 5 mL having an effective OD of 0.25 was used to inoculate a second 250 mL shake flask containing 45 mL FIM.

The optical density (OD) measured at 600 nm (DU-650 spectrophotometer, Beckman Instruments, San Jose, CA) was used to monitor cell growth. Concentrations of soluble organic compounds were determined by high performance liquid chromatography using refractive index detection as previously described (Eiteman and Chastain, 1997). Furfural dehydrogenase activity was measured using the method of Koopman et al. (2010).

Results and Discussion

Five aerobic isolates were obtained from an industrial wastewater source which formed colonies in 24 h on FIM plates containing 9 mM furfural as the sole carbon source (Table 1). Each of these strains ultimately exhausted furfural in 1.0 L bioreactors, and in all cases furoate was detected as an intermediate of the degradation. ALS1267 consumed furfural at the highest rate of the five isolates (Fig. 1) and had the greatest activity of furfural dehydrogenase (Table 1). Several of the strains also were able to degrade 5-(hydroxymethyl) furfural (Table 1).

Table 1. Bacteria isolated which metabolize furfural.

Isolate	Time to Consume 9 mM furfural (h)	16S RNA Phylogenetic Identification	Furfural Dehydrogenase Activity (U/OD)	Degrades 5-(hydroxymethyl)furfural?
ALS1131	15	*Pseudomonas mendocina*	1.0	No
ALS1172	28	*Pigmentiphaga* sp. R-4	1.7	No
ALS1267	9	*Pseudomonas aeruginosa* C1	121	Yes
ALS1279	15	*Pseudomonas* sp. BWDY 9	2.8	Yes
ALS1280	21	*Wautersia numazuensis*	3.1	No

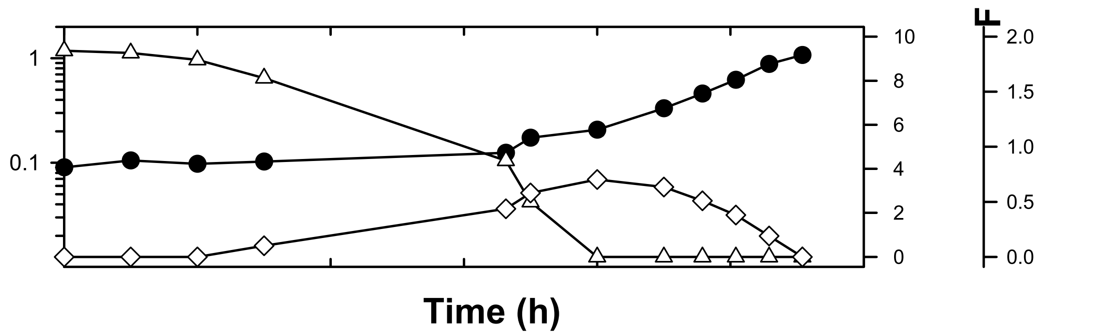

Figure 1. Degradation of furfural by ALS1267: OD (●), furfural (△) and furoate (◇).

16S RNA was also extracted and sequenced from each of the five strains. These sequences were aligned using ClustalW, and the distances and phylogenetic tree were generated using SplitsTree4 (Fig. 2). The results demonstrate that three of the strains, ALS1131, ALS1267 and ALS1279, cluster in the Pseudomonas family, while the other two strains, ALS1172 and ALS1280, are quite distinct.

We have demonstrated (data not shown) that our isolates behave differently than the closest phylogenetic neighbors obtained from culture collections, and ALS1267 is the strain with the greatest furfural dehydrogenase activity. In other work we observed that *E. coli* is inhibited by 10 mM furfural although it can tolerate 100 mM furoate. Our current efforts are to clone the gene that encodes furfural dehydrogenase using two parallel paths. First, plasmid expression libraries are being prepared from ALS1267, to be cloned into *E. coli* using a selective medium. Second, we are purifying the furfural dehydrogenase using standard protocols.

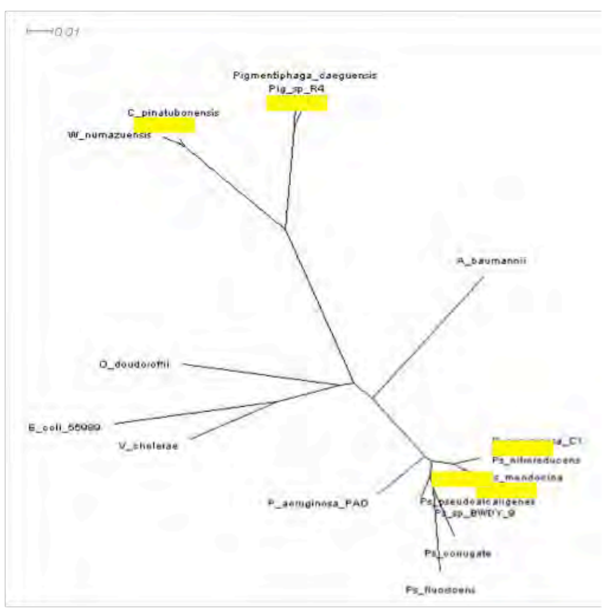

Figure 2. Phylogenetic analysis of five strains isolated for growth on furfural as a sole carbon source.

References

Atsumi, S., T. Hanai, and J. C. Liao. 2008. Non-fermentative pathways for synthesis of branched-chain higher alcohols as biofuels. *Nature* 451:84-90.

Bott, R. R., M. A. Cervin, J. T. Kellis, Jr., J. C. McAuliffe, A. Miasnikov, C. M. Peres, C. L. Rife, D. H. Wells, W. Weyler, G. M. Whited. Isoprene synthase variants for improved microbial production of isoprene. U. S. Patent 8,173,410, May 8, 2012.

Chen Y. 2011. Development and application of co-culture for ethanol produciton by cofermentation of glucose and xylose: a systematic review. *J Industr Micro Biotechnol* 38:581–597.

Eiteman, M. A., M. J. Chastain. 1997. Optimization of the ion-exchange analysis of organic acids from fermentation. *Anal Chem Acta* 338:69–75.

Eiteman, M. A., S. A. Lee, E. Altman. 2008. A co-fermentation strategy to consume sugar mixtures effectively. *J Biol Eng* 2:3.

Eiteman, M. A., S. A. Lee, R. Altman, E. Altman. 2009. A substrate-selective co-fermentation strategy with *Escherichia coli* produces lactate by simultaneously consuming xylose and glucose. *Biotechnol Bioeng* 102:822–827.

Freier, D., C. P. Mothershed, J. Wiegel. 1988. Characterization of *Clostridium thermocellum* JW20. *Appl Environ Microbiol* 54:204-211.

Koopman, F. N. Wierckx, J. H. De Winder, H. J. Ruijssenaars. 2010. Identificaiton and characterization of the furfural and 5-(hydroxymethyl)furfural degradation pathways of *Cupriavidus basilensis* HMF14, *Proc Natl Acad Sci* 107:4919–4924.

Lynch, M. Composition and methods for 3-hydroxypropionate bio-production from biomass. U.S. patent 8,048,624, November 1, 2011.

Taherzadeh, M.J., R. Millati, C. Niklasson. 2001. Continuous cultivation of dilute-acid hydrolysates to ethanol by immobilized *Saccharomyces cerevisiae*. *Appl Biochem Biotechnol* 95:45.

von Sivers, M., G. Zacchi, L. Olsson, B. Hahn-Hägerdal. 1994. Cost analysis of ethanol production from willow using recombinant *Escherichia coli*. *Biotechnol Prog* 10:555-560.

3.6
ACETIC ACID INHIBITION OF LIGNOCELLULOSE-DERIVED SUGAR PLATFORM FERMENTATIONS

Jun Ding[1,2], Mark R. Smith[1], Jana Patton-Vogt[3], Michael H. Penner[1], Alan T. Bakalinsky[1,]*

Abstract
Typical lignocellulose-derived sugar platforms intended for biofuel fermentations contain significant amounts of acetic acid, a documented inhibitor of yeast growth. One approach to circumventing the negative effects of acetic acid in these sugar platforms is to make use of microbial strains that are themselves tolerant of elevated levels of such acids. This study addressed this approach by evaluating a yeast (S. cerevisiae) library of deletion mutants for acetic acid-resistant isolates. The genome-wide collection of mutants was screened in mixed pools for the ability to grow in standard yeast medium containing 120 mM acetic acid, pH 4.8. Survivors were plated on solid medium, confirmed by retesting, and identified by sequencing of mutant-specific oligonucleotide bar code sequences. Resistant mutants were then subjected to quantitative dose-response analysis that related cell yield (A_{600} values) to acetic acid concentration. A total of 25 acetic acid-resistant mutants were isolated among the 4,800 yeast deletion mutants screened. Increases in resistance ranged up to 75% relative to the parent strain based on the concentration of acetic acid that reduced cell yield two-fold. Analysis of the defects shared by the mutants revealed an enrichment in mutants impaired in the processes of endocytosis, ubiquitination, and vesicle/vacuole-mediated transport. The question of how defects in these specific processes relate to acetic acid resistance is discussed.

Keywords: acetic acid, lignocellulose, fermentation, Saccharomyces cerevisiae, inhibition, inhibitors, endocytosis, ubiquitination, vesicle, vacuole

Introduction
Lignocellulosic biomass represents a highly significant potential source of renewable energy (Rubin, 2008). Calculations of the productivity of lignocellulosic feedstocks, based in part on their ability to grow on marginal agricultural lands suggest a major contribution to transportation needs without competing for land needed for food crops (Tilman et al., 2006). Lignocellulosic biofuel production involves biomass collection, deconstruction of cell wall polymers into simple sugars (pre-treatment and saccharification), and conversion of the sugars into biofuels (fermentation). Native lignocellulosic biomass is highly refractory to deconstruction, hence the need for pre-treatments. Pre-treatments (e.g., dilute acid, steam explosion) render the hemicellulose and cellulose components more amenable to sugar production. Such treatments also generate non-sugar compounds that inhibit subsequent fermentation, including organic acids, furfural, hydroxymethyl furfural, and phenolics.

Acetic acid is generated from acetylated hemicellulose during pre-treatment of lignocellulosic biomass (Kim and Holtzapple, 2006). The amount of acetic acid formed can be estimated based on the extent of acetylation and the amount of solids used in the subsequent fermentation. Using corn stover as an example, if one assumes that 2.9% of total solids consist of acetyl groups (Aden et al., 2002), that 100% of these groups are hydrolyzed during pre-treatment, and that a 30% (w/

---

[1] Food Science and Technology, Oregon State University, OR

[2] Biochemistry and Biophysics, Oregon State University, OR

[3] Biological Sciences, Duquesne University, PA

* Corresponding author

w) solids loading is used, the fermentation will contain ~10 grams of acetic acid per liter or ~170 mM or ~ 1% acetic acid. For general application, this calculation may underestimate acetic acid levels because other feedstocks may have greater acetyl contents and overall processing efficiency of lignocelluosic biomass benefits from the highest solids loading possible. One approach to circumventing the negative effects of acetic acid in lignocellulose-derived sugar platforms is to make use of microbial strains that are themselves tolerant of elevated levels of such acids.

A number of studies have documented acetic acid inhibition of fermentation of lignocellulosic hydrolysates (Larsson et al., 1999; Palmqvist et al., 1999; Martin and Jonsson, 2003). Like other weak acids, the toxicity of acetic acid to microbes is pH-dependent and is directly related to the concentration of the undissociated free acid which preferentially enters cells ($pK_a = 4.76$). Upon uptake, the acid dissociates which acidifies the cytoplasm and forces cells to expend energy expelling protons. Inhibitory concentrations of acetic acid have been reported to cause ATP depletion (Mollapour et al., 2008), interfere with nutrient uptake (Bauer et al., 2003; Hueso et al., 2012), repress transcription of genes encoding nutrient transporters (Mira et al., 2010), and trigger programmed cell death, “apoptosis” in *S. cerevisiae* (Ludovico et al., 2002; Guaragnella et al., 2008).

A genome-wide screen for acetic acid-sensitive yeast mutants in a yeast deletion library found about 6% of the mutants to be sensitive (Hillenmeyer et al., 2008). Considering those sensitive strains, about 40% of the deleted genes were found to be involved in unknown cellular processes, about 16% in transport, and from 7-11% in the gene ontology process categories of “organelle organization”, “stress response”, “RNA metabolic process”, and “vesicle-mediated transport”. While screens for sensitive mutants are informative with respect to identifying cellular processes required for tolerance, it is difficult to identify critical target genes for possible overexpression analysis from the ~350 whose deletion led to sensitivity in the above study (the yeast genome contains approximately 6,000 genes, with approximately 4,800 being non-essential and thus capable of being deleted as part of a deletion library).

Piper and colleagues have done considerable work on organic acid resistance in yeast (Mollapour et al., 2008; Bauer et al., 2003; Mollapour and Piper, 2007). Their efforts uncovered a mechanism in yeast to cope with acetic acid stress based on selective targeted degradation of the glycerol channel Fps1 that was also found to mediate acetic acid uptake (Mollapour and Piper, 2007). Deletion of *FPS1* resulted in a 40% increase in acetic acid resistance. Assuming loss of this channel does not result in unexpected deleterious phenotypes that might compromise ethanol productivity, incorporating this deletion into a commercial production strain represents one promising means for increasing resistance to acetic acid.

Here we report the results of screening a genome-wide collection of deletion mutants of *S. cerevisiae* for acetic acid-resistant isolates. Among the total 4,800 mutants screened, 25 acetic acid-resistant mutants were found. Among these 25 mutants, a significant enrichment in frequency was observed for defects in the processes of endocyotosis/ubiquitination and vesicle/ vacuole-mediated transport, and in protein kinase function, relative to the frequency of these same processes/functions among the entire collection of 4,800 mutants.

Methods

Screening of yeast deletion library for acetic acid-resistant mutants

A *S. cerevisiae* deletion library (YSC1054Y, Open Biosystems, Inc.) consisting of about 4,800 haploids constructed in strain BY4742 (*MATα his3Δ1 leu20 lys2Δ0 ura3Δ0*), that each harbor a single deletion in a non-essential gene (Winzeler et al., 1999) was screened for acetic acid-resistant mutants. Mutants were grown individually in YEPD (1% yeast extract, 2% peptone, 2%

glucose) in 96-well microtiter plates overnight at 30°C to minimize population bias due to differences in growth rates. Mutants were then grouped into 7 pools consisting of about 700 mutants each., washed by centrifugation, concentrated 10-fold, resuspended in YEPD-20% glycerol, and immediately stored in multiple 200-µl aliquots at -70°C. To initiate screening, the frozen pooled deletion mutants were diluted 100-fold into fresh YNB-4.8 (Difco Yeast Nitrogen Base without amino acids adjusted to pH 4.8 containing 2% glucose and supplemented with 20 µg/ml histidine, 30 µg/ml each of leucine and lysine, and 10 µg/ml of uracil) and incubated overnight at 30°C at 200 rpm. The overnight culture was then diluted 500-fold into fresh YNB-4.8 containing 122.5 mM acetate at pH 4.8. Following growth for 48 hours at 200 rpm and 30°C, aliquots from each pool were plated onto solid YNB-4.8 plates containing 122.5 mM acetate which were incubated for 48-72 hr at 30°C. Mutants growing on these plates were deemed putative acetic acid/acetate resistant isolates and were restreaked to yield isolated colonies on fresh YNB-4.8 + 122 mM acetic acid. Putative mutants were then subjected to an additional plate spot test. BY4742 and the putative resistant mutants were grown 24 hours in YNB-4.8 at 200 rpm and 30°C. Cells were washed twice with sterile water and 3 µL of undiluted and 50-fold diluted cells were spotted in duplicate onto YNB plates containing 52.5 to 105 mM acetic acid. The parent strain BY4742 was spotted in parallel. Genes deleted in the mutants that grew better than BY4742 were identified by sequencing gene-specific oligonucleotide tag sequences within a PCR product generated using primers complementary to sequences shared by all mutants.

Dose-response analysis

Growth of the mutants in YNB-4.8 containing a range of acetic acid concentrations was assessed spectrophotometrically (A_{600}) after 48 h at 30° and 200 rpm. Mutants were grown under non-strict anaerobic conditions in 1-ml aliquots of medium inoculated with a 1:200 dilution of a 24 h YNB-4.8 culture. Acetic acid concentrations that reduced cell yields by 50% (IC_{50} values) were estimated by graphing A_{600} values as a function of acetic acid dose.

Results and Discussion

Table 1 lists the 25 acetic acid-resistant mutants obtained in decreasing order of resistance. A significant enrichment was found for mutants defective in the processes of endocyotosis/ ubiquitination and vesicle/vacuole-mediated transport and in protein kinase function. In other words, loss of these non-essential genes involved in the above processes or functions led to an increased tolerance for acetic acid. Our gene ontology analysis of a previous hunt for acetic acid-resistant mutants of *S. cerevisiae* (Kawahata et al., 2006) also found a significant enrichment for endocytosis/ubiquitination mutants. One potential explanation for why defective endocyotosis/ ubiquitination or vesicle/vacuole-mediated transport could lead to increased resistance is related to the stability of nutrient transporters. Cells take up nutrients required for growth via specific transporters and normally degrade transporters during growth via endocytosis in response to specific extracellular signals. For example, when *S. cerevisiae* is grown in a medium containing a mixture of ammonia and other nitrogen sources, it takes up ammonia preferentially via an ammonia-specific transporter. Upon depletion of ammonia, other nitrogen sources are taken up by different transporters, while the ammonia transporter that is no longer needed, is degraded via endocytosis. This process involves both ubiquitination and vesicle/vacuole-mediated transport. Defects in any of these steps will interfere with transporter turnover. Thus, if high concentrations of acetic acid serve as a signal for aberrant turnover of transporters in wild-type cells, active nutrient transporters could become limiting for growth. However, in mutants impaired in the process of endocytosis or ubiquitination or vesicle/vacuole-mediated transport, turnover of transporters will be less efficient. We speculate that such mutants may retain greater transporter function than a wild-type strain in the presence of acetic acid and thus, will have a growth advantage.

Future work is aimed at determining the validity of this mechanism of acetic acid tolerance with respect to establishing promising genetic approaches for systematically improving the performance of commercial yeast strains for use in lignocellulose-derived sugar platform biofuel fermentations.

Table 1. Genes whose loss resulted in increased acetic acid resistance in *S. cerevisiae* BY4742[a].

Gene	**IC_{50}[b]**	**Gene Ontology Function/Process/Cell Component[c]**
RTS1	85.2	B-type regulatory subunit of protein phosphatase 2A
SIP5	81.4	Protein of unknown function
UBP2[d]	79.6	Ubiquitin-specific protease that removes ubiquitin from ubiquitinated proteins
EDE1[de]	73.8	Key endocytic protein
YNL179c	67.6	Dubious open reading frame unlikely to encode a functional protein
MMS2[d]	66.7	Ubiquitin-conjugating enzyme variant involved in error-free postreplication repair
PPH21	66.4	Catalytic subunit of casein kinase 2, a Ser/Thr protein kinase
MVB12[de]	66.4	ESCRT-1 subunit required to stabilize oligomers of the ESCRT-1 core complex
STP1	66	Transcription factor processed by Ssy1p-Ptr3p-Ssy5p-sensor component Ssy5p in response to extracellular amino acids
YDR344c	65.9	Dubious open reading frame unlikely to encode a functional protein
CKA2[f]	65.8	Catalytic subunit of casein kinase 2, a Ser/Thr protein kinase
CCM1	64.5	Protein required for intron removal of COB & COX1 pre-mRNAs
PRK1[def]	64	Protein serine/threonine kinase, regulates organization and function of actin cytoskeleton and reduces endocytic ability of cell
YLR164w	61.7	Mitochondrial inner membrane protein of unknown function
GAL3	59.3	Transcriptional regulator involved in activation of GAL genes
ALD2	59.2	Cytoplasmic aldehyde dehydrogenase that oxidizes EtOH
FTH1[de]	59	Putative high affinity iron transporter, proposed to play indirect role in endocytosis
YOR024w	54.4	Dubious open reading frame unlikely to encode a functional protein
TOR1[f]	54	PIK-related protein kinase and rapamycin target
SEE1[e]	53.9	Protein with a role in intracellular transport
MEK1[f]	51.9	Meiosis-specific serine/threonine protein kinase
FUI1	51.4	High affinity uridine permease
VAM7[de]	42	Component of the vacuole SNARE complex
LRG1	nd	Putative GTPase-activating protein involved in the Pkc1p-mediated signaling pathway
MED1	nd	Subunit of the RNA polymerase II mediator complex

[a]IC_{50} for BY4742 was 48.5 mM acetic acid; [b]concentration of acetic acid that reduced cell yields by 50% in YNB-4.8; [c]*Saccharomyces* genome database annotations, http://www.yeastgenome.org/; [d]gene involved in process of endocytosis or ubiquitination; [e]gene involved in vesicle/vacuole-mediated transport; [f]gene encodes protein kinase.

References

Aden, A., Ruth, M., Ibsen, K., Jechura, J., Neeves, K., Sheehan, J., Wallace, B., Montague, L., Slayton, A., Lukas, J. (2002). "Lignocellulosic biomass to ethanol process design and economics utilizing co-current dilute acid prehydrolysis and enzymatic hydrolysis for corn stover," *NREL/TP-510-32438, http://www.nrel.gov/docs/fy02osti/32438.pdf*.

Bauer, B. E., Rossington, D., Mollapour, M., Mamnun, Y., Kuchler, K., Piper, P. W. (2003). "Weak organic acid stress inhibits aromatic amino acid uptake by yeast, causing a strong influence of amino acid auxotrophies on the phenotypes of membrane transporter mutants," *Eur. J. Biochem. 270: 3189-3195*.

Guaragnella, N., Antonacci, L., Giannattasio, S., Marra, E., Passarella, S. (2008). "Catalase T and Cu, Zn-superoxide dismutase in the acetic acid-induced programmed cell death in *Saccharomyces cerevisiae*," *FEBS Lett. 582: 210-214*.

Hillenmyer, M. E., Fung, E., Wildenhain, J., Pierce, S. E., Hoon, S., Lee, W., Proctor, M., St. Onge, R. P., Tyers, M., Koller, D., Altman, R. B., Davis, R. W., Nislow, C., Giaever, G. (2008). "The chemical genomic portrait of yeast: uncovering a phenotype for all genes," *Science. 3200: 362-365*.

Hueso, G., Aparicio-Sanchis, R., Montesinos, C., Lorenz, S., Murguia, J. R., Serrano, R. (2012). "A novel role for protein kinase Gcn2 in yeast tolerance to intracellular acid stress," *Biochem. J. 441: 255-264*.

Kawahata, M., Masaki, K., Fujii, T., Lefuji, H. (2006). "Yeast genes involved in response to lactic acid and acetic acid: acidic conditions caused by the organic acids in *Saccharomyces cerevisiae* cultures induce expression of intracellular metal metabolism genes regulated by Aft1p," *FEMS Yeast Res. 6: 924-936*.

Kim, S., Holtzapple, M. T. (2006). "Effect of structural features on enzyme digestibility of corn stover," *Biores. Tech. 97: 583-591*.

Larsson, S., Palmqvist, E., Hahn-Hagerdal, B., Tengborg, C., Stenberg, K., Zacchi, G., Nilvebrant, N.-O. (1999). "The generation of fermentation inhibitors during dilute acid hydrolysis of softwood," *Enzyme Microb. Tech. 24: 151-159*.

Ludovico, P., Rodrigues, F., Almeida, A., Silva, M. T., Barrientos, A., Corte-Real, M. (2002). "Cytochrome c release and mitochondria involvement in programmed cell death induced by acetic acid in *Saccharomcyes cerevisiae*," *Mol. Biol. Cell. 13: 2598-2606.*

Martin, C., Jonsson, L. J. (2003). "Comparison of the resistance of industrial and laboratory strains of *Saccharomyces* and *Zygosaccharomyces* to lignocellulose-derived fermentation inhibitors," *Enzyme Microb. Tech. 32: 386-395*.

Mira, N. P., Palma, M., Guerreiro, J. F., Sa-Correia, I. (2010). "Genome-wide identification of *Saccharomyces cerevisiae* genes required for tolerance to acetic acid," *Microb. Cell Fact. 9: 79, doi: 10.1186/1475-2859-9-79*.

Mollapour, M., Piper, P. W. (2007). "Hog1 mitogen-activated protein kinase phosphorylation targets the yeast Fps1 aquaglyceroporin for endocytosis, thereby rendering cells resistant to acetic acid," *Mol. Cell Biol. 27: 6446-6456*.

Mollapour, M., Shepherd, A., Piper, P. W. (2008). “Novel stress responses facilitate *Saccharomyces cerevisiae* growth in the presence of the monocarboxylate preservatives,” *Yeast 25: 169-177*.

Palmqvist, E., Grage, H., Meinander, N. Q., Hahn-Hagerdal, B. (1999). “Main and interaction effects of acetic acid, furfural, and *p*-hydroxybenzoic acid on growth and ethanol productivity of yeasts,” *Biotech Bioengineer. 63: 46-55*.

Rubin, E. M. (2008). “Genomics of cellulosic biofuels,” *Nature*. *454: 841-845*.

Tilman, D., Hill, J., Lehman, C. (2006). “Carbon-negative biofuels from low-input high-diversity grassland biomass,” *Science*. *314: 1598-1600*.

Winzeler, E. A., Shoemaker, D. D., Astromoff, A., et al., (1999). “Functional characterization of the *Saccharomyces cerevisiae* genome by gene deletion and parallel analysis,” *Science 285: 901-906*.

3.7
INTEGRATING SEPARATION AND CONVERSION – CONVERSION OF BIOREFINERY PROCES STREAMS TO BIOBASED CHEMICALS AND FUELS

Joseph J. Bozell[1], Anton Astner, Darren Baker[1], Diana Cedeno[1], Thomas Elder[1], Omid Hosseinaei[1], Lukas Delbeck[1], Jae-Woo Kim[1], C. J. O'Lenick[1], Timothy Young[1]*

Abstract
The concept of the integrated biorefinery is critical to developing a robust biorefining industry in the United States. Within this model, the biorefinery will produce fuel as a high volume output addressing domestic energy needs, and biobased chemical products as a high value output providing necessary economic support for fuel production. This paper will overview recent developments within two aspects of integrated biorefinery development - the fractionation of biomass into individual process streams and the subsequent conversion of these process streams into chemical products. Solvent based separation of switchgrass, poplar and mixed feedstocks is being developed as a biorefinery "front end" and will be described as a function of fractionation conditions. Control over the properties and structure of the individual biomass components (carbohydrates and lignin) can be observed by adjusting the fractionation process. Subsequent conversion of the process streams from this fractionation leads to low molecular weight aromatics and potentially, drop-in hydrocarbon fuels from the selective chemical and biochemical oxidation of lignin. Alternatively, the carbohydrate stream will provide building blocks for production of new nanostructural materials, serving as templates for catalyst support and delivery.

Keywords: fractionation, catalysis, Co-Schiff base complex, lignin, biorefinery, organosolv

Introduction
The last decade has witnessed the advent of biomass (forest resources, agricultural crops such as switchgrass, corn and soybeans, residues, etc.) as a source of renewable carbon, as evidenced by a huge upsurge in research and commercial interest. The *biorefinery* is widely recognized as the organizing concept to unify the transition of biomass from agricultural and forestry raw materials through intermediate monomeric and biopolymeric building blocks, and ultimately to biobased chemicals and fuels. The petrochemical industry, as the nation's primary consumer of nonrenewable carbon, provides the standard for developing and optimizing the biorefining industry. Petrochemical refining has developed a highly integrated value chain based on nonrenewable carbon, from raw material collection and processing to fuel and chemical production. Coupling chemical and fuel manufacture is of particular importance. Even though chemicals account for only 7-8% of crude oil use in the US, they provide the key economic driver for overall profitability of the petrochemical industry, which reports US sales of over $435 billion.[1] Chemicals provide nearly 50% of the value-added for the industry ($375 billion) despite their low comparative consumption of crude oil.[2]

Incorporation of chemicals is also an ideal operational model for the emerging biorefinery. Although much of the current effort in biorefinery development focuses only on fuel EtOH, analyses reveal that a next generation biorefinery adopting the petrochemical model of simultaneous fuel and HVO production realizes a much higher return on investment.[3-5] However, turning the chemical industry model into a successful and commercially viable biorefining industry requires developing fractionation technology able to provide process streams suitable for chemical and fuel production, and conversion technologies able to transition these process streams to final products. Work in our laboratories has examined both of these aspects of biorefinery development, and this paper summarizes some of our recent results.

---

[1] *Center for Renewable Carbon, University of Tennessee, 2506 Jacob Drive, Knoxville, TN 37996;*
**Corresponding author: jbozell@utk.edu*

Experimental Design for Optimized Separation of Lignocellulosic Biomass

Biomass, as harvested, is difficult to use directly, because it is a complex mixture of several simpler components. Like crude oil, it requires an initial separation and upgrading before it can be converted into high value chemicals or biobased transportation fuels. We have been developing a separation process for biomass using organic solvents can convert this complex starting material into three individual process streams – cellulose, hemicellulose and lignin – each of which can serve as a starting material for the production of biobased chemicals and fuels.[6] Our process heats biomass with a mixture of methyl isobutyl ketone, ethanol, water and an acid promoter. This solvent mixture selectively dissolves the lignin and hemicellulose fractions leaving the cellulose as an undissolved material that can be washed, fiberized, and further purified. The dissolved material is separated into individual lignin and hemicellulose fractions simply by adding NaCl and removing excess solvent (Figure 1).

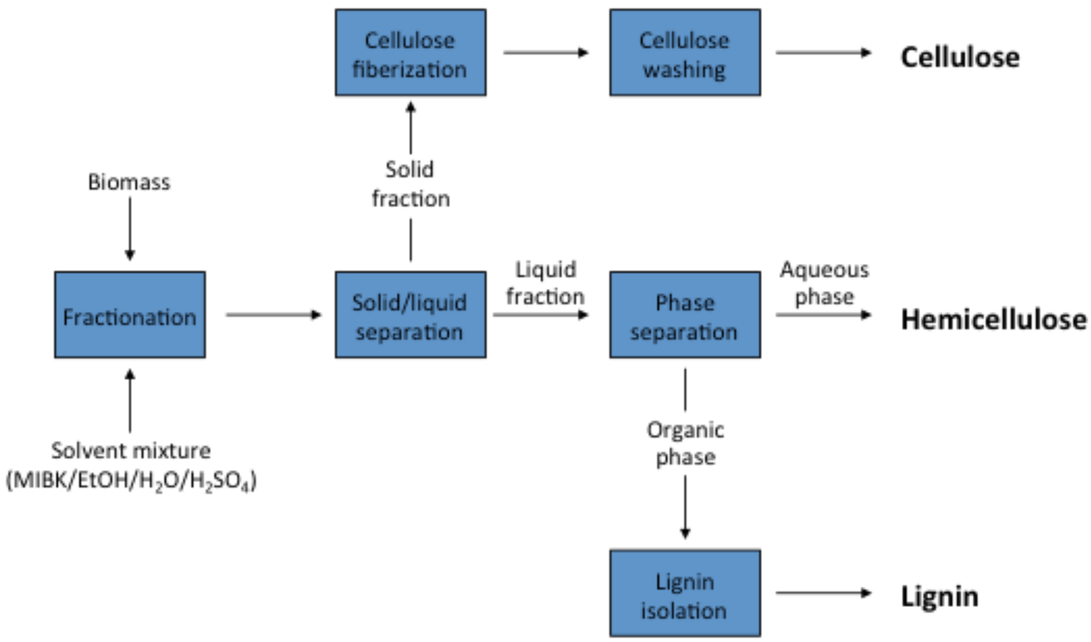

Figure 1 – Schematic of the solvent fractionation process

The process is efficient. Greater than 95% of the components present in the starting feedstock are isolated after fractionation in high purity, which is important for their eventual use as chemical building blocks. Importantly, the process works well on switchgrass and poplar, two renewable feedstocks important to the southeast US. Our recent work has incorporated experimental design for optimization of the process using mixtures of switchgrass and poplar as the raw material supply. Feedstock mixtures are of importance because a wide variety of feedstocks within an economically feasible transportation distance can be utilized. The use of herbaceous and woody mixtures tolerates variations in weather conditions that other annual agricultural crops such as corn cannot and offer mixed feedstock solutions that are beneficial to the sustainable supply required by a viable biorefinery. For example, biomass from mixed feedstocks may require longer transportation distances from source to the plant gate and therefore incur more cost. A recent study[7] found that the delivered cost of raw material was lower when wood and herbaceous biomass were combined rather than delivered as single feedstocks.

The results of our experimental design (Taguchi Robust Product Design)[8] defined conditions optimal for obtaining the highest yield of lignin from the solvent fractionation process. A maximum lignin yield was found upon treatment of the feedstock with the solvent mixture for 90 minutes at 160°C, using 0.1 mol/L sulfuric acid, and a feedstock composition of 90 percent switchgrass, and 10 percent tulip poplar. The results of the design were substantiated by statistical simulation of 5000 additional runs, which predicted a mean for lignin yield of 74.41 wt%, comparable to the lignin yield mean of 78.63 wt% at the maximum found in our investigation.

Selective Cobalt Catalyzed Oxidation of Lignin and Lignin Models

Subsumed within the US Renewable Fuels Standard to develop lignocellulosic biofuels is the inevitable availability of an enormous amount of lignin. Assuming that a commercial biorefinery produces 80 gallons biofuel/ton biomass and that the biomass averages 20 wt% lignin, operation at the legislated levels of the RFS will afford 40 million tons of lignin on an annual basis. This remarkable level of renewable carbon production and availability is an attractive target for downstream chemical processing and conversion to higher value materials. However, the heterogeneous structure of lignin has frustrated efforts to selectively convert this abundant biopolymer into low molecular weight aromatics.[9] Moreover, the structure of lignin is variable. The distribution of substructural units within isolated lignin is a function of both the lignin source and the methodology employed in its isolation.[10, 11] To address this issue of selectivity, we are developing methodologies for conversion of the structural units common to all isolated lignins. Recent work from our laboratories describes oxidation of *para*-substituted phenolics with Co-Schiff base complexes and oxygen that is applicable to the arenes comprising biorefinery lignin.[12] Cobalt-Schiff base complexes have been extensively used to catalyze oxygen activation in the oxidation of phenols.[13-16] However, the use of these complexes for the oxidation of *p*-substituted phenols as models of catalytic conversion of lignin within the biorefinery has not been widely studied. We reported that O_2 in the presence of various Co-Schiff base catalysts [e. g., Co(salen) or Co(*N*-Me salpr)] and pyridine in MeOH at room temperature converted several *p*-substituted lignin models into 2,6-dimethoxybenzoquinone (DMBQ) in high yield.[14] However, oxidation of compounds modeling the less electron-rich G units in lignin proceeded in much lower yield. To expand the utility of this process to a wider range of lignin's substructural units we examined the reactivity of the catalytically active complex in the presence of added aromatic or aliphatic nitrogen bases and found that the yield of quinone from oxidation of several lignin models is strongly affected by the addition of a series of structurally diverse aromatic nitrogen-containing ligands and that oxidation of vanillyl alcohol is markedly improved in the presence of sterically hindered aliphatic nitrogen bases. Importantly, this improvement was realized without compromising the already high yield observed for oxidation of S models. More broadly, this result suggests approaches able to convert all aromatic units available in biorefinery lignin streams. Figures 2 and 3 summarize some of our results.

In addition, we have applied these processes to lignin isolated by our organosolv fractionation process. Under optimal oxidation conditions, 2D NMR (HMQC) revealed that that the main lignin oxidation products were vanillin, DMBQ and syringaldehyde. While the yield of low molecular weight product is low, it is at least comparable with typical yields for other lignin oxidation processes.[17] Figure 4 shows a typical NMR spectrum of the products isolated after lignin oxidation. The formation of DMBQ is in line with our studies with models[12] that show the selective conversion of the aromatic functionality of various phenol lignin models. Interestingly, we learned that the addition of an aromatic base does not change the identity or yield of the products of the reactions. We can infer that the aromatic bases are not coordinating to the cobalt in the Co(salen) catalyst. However, the addition of an aliphatic base such as DIPEA produces drastic changes in the identity of the products of the reaction. We are still evaluating the mechanistic implications of these observations and have carried out preliminary molecular modeling studies on the process.

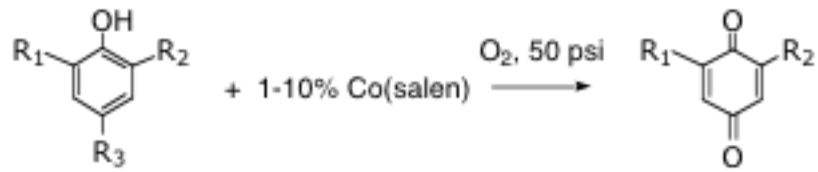

Substrate	Added imidazole	Conjugate acid pK_a	DMBQ yield (%,10:1 L:C)	DMBQ yield (%, 1:1 L:C)	Added pyridine	Conjugate acid pK_a	DMBQ yield (%)
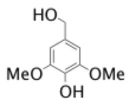		5.03[c]	30	31	2,6-diMePyr	6.65	42
	Im	7.00	<5	5[d]	4-MePyr	6.04	74
	1-MeIm	7.33	29	69	Pyr	5.24	82
	2-MeIm	7.85	67	63	DMAP	4.48	50
	1,2-diMeIm	8.00	72	65	4-CNPyr	1.64	64
	2,4-diMeIm	8.52[e]	71	67			

Figure 3 - Complexes and ligands used in this study

Substrate	Base	Conjugate acid pK_a[a]	yield (%)[b]
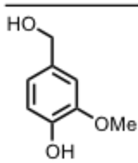	none	-	21
	DABCO	8.19	21
	DIPEA	10.98	55
	DIPA	10.76	51
	TEA	10.60	52
	DBU	13.28	0[c]

Figure 4 – Improved catalytic oxidation of G models

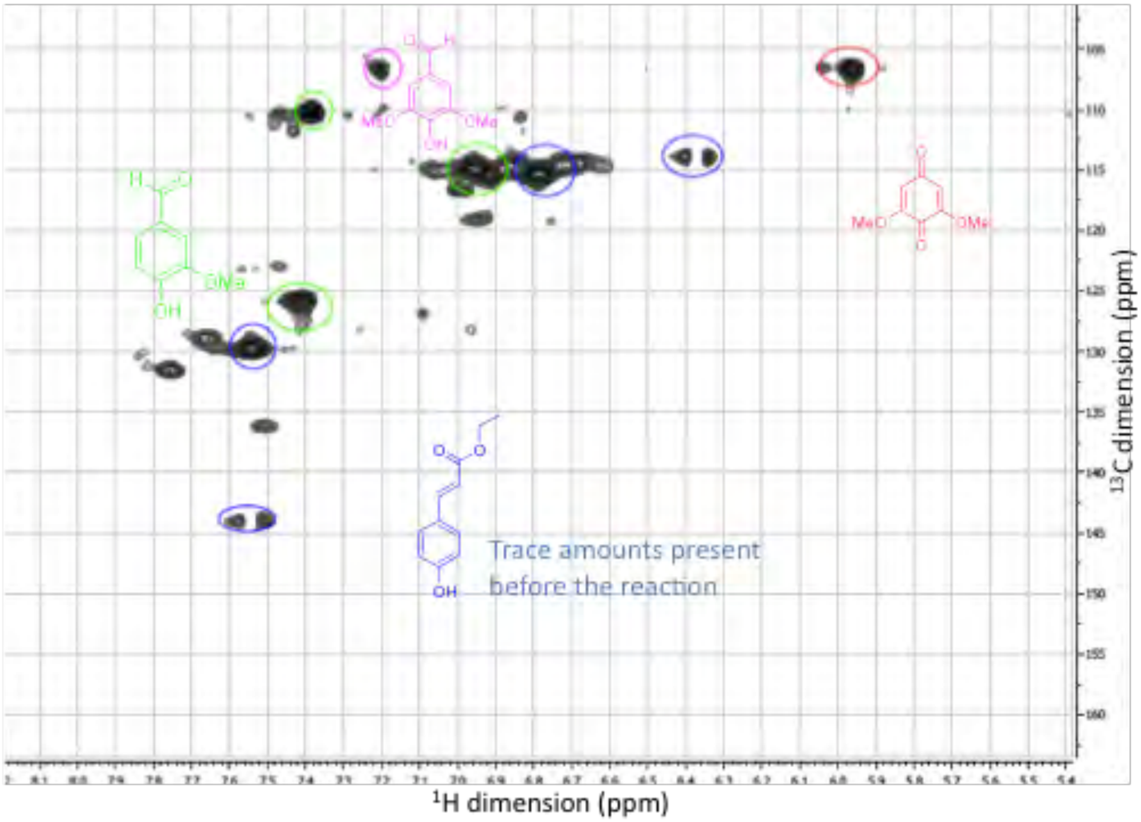

Figure 5 – Typical 2D HMQC spectrum of lignin oxidation products

Conclusions

The ability to integrate production of biobased chemicals with the production of biofuels will play a critical role in development of an integrated biorefinery. Our research has revealed that organosolv fractionation of biomass can serve as a source of high quality lignin. Further, this lignin can be converted to low molecular weight aromatics. The current yield of these processes is low, but ongoing work in our laboratories is examining methodology to extend the lifetime of oxidation catalysts and expand the number of substructural units able to be converted by these processes.

References

Guide to the Business of Chemistry 2006. American Chemistry Council: Arlington, 2006.

Marshall, J., Biorefineries: Curing our addiction to oil. *New Scientist* 2007, 2611 (July 4, 2007), 28-31.

Bozell, J. J., Feedstocks for the future - Biorefinery production of chemicals from renewable carbon. *Clean-Soil Air Water* 2008, 36, 641-647.

Luo, L.; van der Voet, E.; Huppes, G., Biorefining of lignocellulosic feedstock - Technical, economic and environmental considerations. *Bioresour. Technol.* 2010, 101, 5023-5032.

Bozell, J. J., Connecting biomass and petroleum processing with a chemical bridge. *Science* 2010, 329, 522-523.

Bozell, J. J.; Black, S. K.; Myers, M.; Cahill, D.; Miller, W. P.; Park, S., Solvent fractionation of renewable woody feedstocks: Organosolv generation of biorefinery process streams for the production of biobased chemicals. *Biomass Bioenergy* 2011, 35, 4197-4208.

Sultana, A.; Kumar, A., Optimal configuration and combination of multiple lignocellulosic biomass feedstocks delivery to a biorefinery. *Bioresour. Technol.* 2011, 102, 9947-9956.

Taguchi, G., *Taguchi on robust technology development : bringing quality engineering upstream*. American Soc. of Mechanical Engineers Press: New York, NY, 1993; p 136 p.

Zakzeski, J.; Bruijnincx, P. C. A.; Jongerius, A. L.; Weckhuysen, B. M., The Catalytic Valorization of Lignin for the Production of Renewable Chemicals. *Chem. Rev.* 2010, 110, 3552-3599.

Baciocchi, E.; Rosato, G. C.; Rol, C.; Sebastiani, G. V., TiO2-catalyzed photooxygenation of methylaromatic compounds in the presence of Ag2SO4 in CH3CN. *Tetrahedron Lett.* 1992, 33, 5437-5440.

Bozell, J. J.; O'Lenick, C. J.; Warwick, S., Biomass fractionation for the biorefinery: heteronuclear multiple quantum coherence-nuclear magnetic resonance investigation of lignin isolated from solvent fractionation of switchgrass. *J. Agric. Food. Chem.* 2011, 59, 9232-9242.

Cedeno, D.; Bozell, J. J., Catalytic oxidation of para-substituted phenols with cobalt-Schiff base complexes/O2-selective conversion of syringyl and guaiacyl lignin models to benzoquinones. *Tetrahedron Lett.* 2012, 53, 2380-2383.

Caldin, E. F.; Dagnall, S. P.; Mak, M. K. S.; Brooke, D. N., Kinetics of hydrogen-atom transfer from phenols to galvinoxyl in aprotic-solvents. *Faraday Discuss.* 1982, 74, 215-228.

Bozell, J. J.; Hames, B. R.; Dimmel, D. R., Cobalt-Schiff base complex-catalyzed oxidation of para-substituted phenolics - preparation of benzoquinones. *J. Org. Chem.* 1995, 60, 2398-2404.

Kervinen, K.; Korpi, H.; Mesu, J. G.; Soulimani, F.; Repo, T.; Rieger, B.; Leskela, M.; Weckhuysen, B. M., Mechanistic insights into the oxidation of veratryl alcohol with Co (salen) and oxygen in aqueous media: An in-situ spectroscopic study. *Eur. J. Inorg. Chem.* 2005, 2591-2599.

Zombeck, A.; Drago, R. S.; Corden, B. B.; Gaul, J. H., Activation of molecular-oxygen - mechanistic studies of the oxidation of hindered phenols with cobalt-dioxygen complexes. *J. Am. Chem. Soc.* 1981, 103, 7580-7585.

da Silva, E. A. B.; Zabkova, M.; Araujo, J. D.; Cateto, C. A.; Barreiro, M. F.; Belgacem, M. N.; Rodriques, A. E., An integrated process to produce vanillin and lignin-based polyurethanes from Kraft lignin. *Chem. Eng. Res. Des.* 2009, 87, 1276-1292.

3.8 DEVELOPMENT OF AN EFFECTIVE HARDWOOD PRETREATMENT FOR THE PRODUCTION OF ETHANOL IN A REPURPOSED KRAFT MILL

Hasan Jameel[1], *Hou-min Chang*[1], *Richard Phillips*[1]

Abstract

The North American pulp and paper industry is in decline due to falling demand for paper. As a result, it would be very attractive to repurpose a kraft pulp mills to the production of ethanol. The development of a pretreatment process that can be easily implemented in a repurposed kraft mill with minimum capital is described in this paper. Various pretreatments method was studied for hardwoods that would be compatible in a repurposed mill. These pretreatments method included: water autohydrolysis, and sodium carbonate, green liquor (sodium carbonate and sodium sulfide). These results show that a pretreatment based on green liquor is the most effective pretreatment for a repurposed mill. The pulps produced by this process can be enzymatically hydrolyzed to monomeric sugars with a high overall sugar recovery. The use of green liquor for pretreatment ensures that the chemicals used during pretreatment can be recovered efficiently using proven technology and can be easily implemented in a repurposed Kraft pulp mill. A patent for the green liquor pretreatment process has been applied for by N. C. State University. In addition, the use of oxygen delignification and mechanical refining can decrease the enzyme dosage to practical economical levels. Repurposing an existing kraft mill - can reduce capital investment by 70% compared to a Steam Explosion Greenfield Project, and results in a minimum ethanol revenue (MER) of $1.97/gallon of ethanol to achieve a 12% IRR. By comparison greenfield steam explosion has a MER of $2.50/gallon.

Keywords: Repurposing, lignocellulosic, ethanol, pretreatment, enzymatic hydrolysis, hardwood

Introduction

The North American pulp and paper industry is in decline due to falling demand for paper and board products and in some cases, loss of market pulp share to lower cost countries. As a result more than 15 million tonnes of capacity has been permanently closed. Simultaneous to the decline of paper products, interest in biomass to biofuel has accelerated to unprecedented levels. As a result, it would be very attractive to repurpose a kraft pulp mills to the production of ethanol. In concept, repurposing features a number of significant advantages over other approaches to the production of bioethanol:

- A supply chain to grow, harvest, and deliver biomass is already in place, thus avoiding new demand and creating price pressure on the raw material,
- When kraft mills are permanently closed, significant equipment assets are left behind, such as woodyard, digesters, evaporators, power and waste treatment plants, which can be directly repurposed to ethanol production.
- Much of the process equipment in a repurposed kraft mill has little technology risk, since most equipment has been operating for many years

Various pretreatments method was studied for hardwoods that would be compatible in a repurposed mill. These pretreatments method included:

[1] *Department of Forest Biomaterials, North Carolina State University, NC*

* *Corresponding author*

- water prehydrolysis
- sodium carbonate
- green liquor (sodium carbonate and sodium sulfide)

These pretreatments were chosen because they could be easily implemented in a repurposed kraft mill with minimum capital. They also have the potential to decrease the labor requirement and improve the overall energy efficiency.

Materials and Methods

Mixed hardwood chip were provided by a mill in the Southeastern United States and was used in this study.

A lab-scale M/K pulping digester with a capacity of 800 g of oven dry wood was used for the pretreatment studies. Prehydrolysis was carried out with water at 160^{o}C or 170^{o}C for 60 min. Pretreatment with sodium carbonate was carried out at 160^{o}C at a H Factor of 400. The chemical charge was varied between 12-24% sodium carbonate as Na_2O. In the case of the green liquor pretreatment the wood chips were pretreated using a mixture of sodium carbonate and sodium sulfide with a sulfidity of 25%. The Total Titrateable Alkali (TTA) charge as Na_2O on OD wood chips was varied from 4% to 20%.

The portion of the pretreated chips was delignified using oxygen with 5% sodium hydroxide at 110°C. The reaction was one hour at the oxygen pressure level of 100 psi. The PFI refining was performed to improve the digestibility of green liquor pretreated substrates.

An enzyme cocktail of cellulase, xylanase and β-glucosidase (1 FPU:1.2 FXU:1 CBU) was used for enzymatic hydrolysis. The activity loading was based on a cellulase charge between 5 to 40 FPU/g substrate

Results and Discussion

The total carbohydrate content in the initial wood was 66.4%. This value will be used to calculate the overall carbohydrate yield (sugar recovery) from the pretreatment and enzymatic hydrolysis processes. The pretreatments will be evaluated with respect to a) ability of the substrate to be enzymatically hydrolyzed b) overall sugar recovery (monomeric sugar/total sugar in initial biomass)

Prehydrolysis

Prehydrolysis stage uses only water and heat and has the advantage that no recovery is necessary and the vessel used for the pretreatment is compatible with the existing pulping vessel. In prehydrolysis pretreatment, there would be no need for the chemical recovery process.

Results for prehydrolysis at 160^{o}C show the pulp yield was 85.3% on wood after one hour and that 8% of the wood can be recovered as sugar (monomer and oligomer) in the filtrate from prehydrolysis.

After pretreatment the samples were enzymatically hydrolyzed using cellulase, xylanse and β-glucosidase. After enzymatic hydrolysis the sugar yield was measured for different enzyme charges. The results can be summarized as follows:

- Total sugar recovered from pre and enzyme hydrolysis: 43% on wood
- Total sugar recovery: 65% (43% as sugar/66% as sugar in original wood)

Sodium carbonate pretreatment

Sodium carbonate was studied as a pretreatment chemical since it can be recovered using a recovery boiler and its use does not require a caustic plant thereby simplifying the overall operation. At a cellulase dosage of 20 FPU/g, enzymatic hydrolysis sugar yield for samples pretreated at 20% TTA is only 28% (on wood) and the total sugar recovery is about 42% (28% recovered sugar/66% sugar in original biomass).

Green liquor pretreatment

Green liquor which is a mixture of sodium carbonate and sodium sulfide was also used as a pretreatment chemical. Green liquor is readily available in a kraft mill and its use also does not require a caustic plant. The details of the chemical reactions were summarized by Chang [1]. The results indicate that the total sugar recovery with a green liquor pretreatment of 16% TTA is about 77% at 20 FPU/g enzyme charge (51% recovered sugar/66% sugar in original biomass). This is significantly higher than the prehydrolysis and the sodium carbonate pretreatments.

Green liquor pretreatment had the highest sugar recovery for the various options studied. At 20 FPU/gm enzyme charge 77% of the sugar can be recovered with green liquor pretreatment as compared to 42% for the sodium carbonate pretreatment and 65% for prehydrolysis with water.

Post-treatments to improve enzymatic hydrolysis

In spite of the encouraging results it was realized that at these enzyme charges (20 FPU/gm of substrate), these processes would not be viable because of the high cost of enzymes. Enzyme costs have decreased in the last 10 years, but even with the lower costs the enzyme dosages need to be less than 5 FPU/gm of substrate.

Oxygen delignification was utilized as an industrially practical step to selectively reduce the residual lignin content of green liquor pretreated biomass. When oxygen delignification was performed, the enzymatic conversion was improved. The mechanical refining process also significantly improved the enzymatic conversion at all conditions. The enzymatic conversion of refined substrates at 6,000 PFI revolutions was 72% (based on pretreated substrates) at 5 FPU. This result clearly demonstrates the benefit of the refining process, which can decrease the enzyme charge.

Economic Evaluation

The economics of producing bioethanol using a repurposed green liquor process are shown in Table 1 and it is also compared to the greenfield steam explosion process. Total CAPEX per gallon and the minimum ethnaol revenue for the green liquor repurposed case is significantly lower than the steam explosion process. It is realized that there are only limited situaltions that are applicable for this process, however it is an attractive alternative for getting a bioetanol process implemented so that issues with the biorefinery portion of ethanol production can be improved and optimized.

Table 1: Operating cost and ethanol revenue estimates for green field steam explosion and repurposed green liquor

	Greenfield Steam Explosion		Repurpose Green Liquor	
	Quantity	Cost per Unit	Quantity	Cost per Unit
Total Capex, $ Millions		$270,630,000		$87,951,016
Total Capex/gallon		$7.24		$2.25
Total Biorefinery Capex/gallon		$1.04		$0.99
Hardwood	454,545	$72.18	454,545	$72.18
Annual Ethanol, gallons	37,480,000		39,128,000	
Ethanol Yield, gallons/BDt	82.5		86.0	
Biomass Cost/gallon		$0.91		$0.91
Enzyme Cost/gallon		$0.26		$0.45
Energy Credit/gallon		($0.30)		($0.08)
Direct Cost/gallon		$0.87		$1.32
Indirect Cost/gallon		$1.63		$0.68
Cash Cost/gallon		$1.51		$1.70
Total Cost/gallon		$2.27		$2.04
MER, $/gallon		$2.27		$1.97
IRR, %		12		12

Conclusions

Auto hydrolysis at 160 ^{O}C and green liquor (Na_2CO_3 + Na_2S) were effective pretreatments for a repurposed mill. More than 75% of wood polysaccharides can be recovered as monomers when wood is cooked by green liquor and followed by enzymatic hydrolysis at enzyme dosage of 20 FPU/g. Sodium carbonate was not as effective as green liquor as a pretreatment. Oxygen delignification and mechanical refining of green liquor pretreated hardwood were performed in order to evaluate the reduction of enzyme dosage by post-treatment,. Combination of oxygen delignification and mechanical refining could reduce the enzyme dosage to economically feasible levels of 5 FPU/gm.

Our process and financial analysis shows the green liquor pretreatment technology to be the most capital-efficient process for an existing kraft pulp mill. Repurposing an existing kraft mill - can reduce capital investment by 70% compared to a steam explosion greenfield project, and results in a minimum ethanol revenue (MER) of $1.97/gallon of ethanol to achieve a 12% IRR. By comparison greenfield steam explosion has a MER of $2.50/gallon.

Acknowledgements

This work was funded by the Wood-to-Ethanol Research Consortium (American Process, Andritz, Arborgen, Catchlight, Evolution Resources, KBR, Nippon Paper). Enzymes were provided by Novozymes.

References

J. Jin, H. Jameel, H-m. Chang and R. Phillips, (2009) Green Liquor Pretreatment of Mixed Hardwood for Ethanol Production in a Repurposed Kraft Mill", Journal of Wood Chemistry and Technology, 30:1,86-104

3.9
PYROLYSIS OF NORTH-AMERICAN GRASS SPECIES: EFFECT OF FEEDSTOCK COMPOSITION AND LOCATION

Shantanu Kelkar[1,2], Jonathan M. Bovee[1], Kurt D. Thelen[3], Christopher M. Saffron[1,2,4,]*

Abstract

Perennial grasses native to the Midwest are ideal bioenergy crops due to their potential to be productive on marginal lands. Fast pyrolysis is a simple, flexible process for converting these feedstocks into bio-oil, a precursor to liquid hydrocarbon fuels. However, organic acids and oxygenates in bio-oil lead to storage instability and limit its early adoption as a transportation fuel. Biomass constituents such as inorganic salts dramatically alter the speciation of pyrolysis products. Therefore, the objective of this study was to prospect amongst several native grasses for cultivars suitable for pyrolysis to biofuels, by investigating the effects of biomass composition on pyrolysis products.

In this work, the composition of native grasses, including big bluestem, coastal panicgrass, deertongue, indiangrass, Miscanthus, sandreed, sideoats grama and switchgrass grown on four different plots was determined. Pyrolysis of the grasses was studied using analytical pyrolysis-GC/MS. The resulting pyrolysis gas contains hundreds of chemical species. Acetic acid, glycolaldehyde and acetol were major products. Potassium had a significant effect on acetic acid, acetol, levoglucosan and the biochar yield. Plot location did not have a significant effect on biomass composition or pyrolysis products.

Keywords: pyrolysis, grass, bio-oil, switchgrass

Introduction

Native warm-season grasses show potential for fulfilling a portion of the U.S. Department of Energy's annual goal of 60 billion gallons of biofuels, while maintaining food and feed production (U.S. Department of Energy 2011)[1]. Besides Miscanthus and switchgrass, which have been extensively studied, native Midwestern grasses such as big bluestem, coastal panicgrass, deertongue, indiangrass, sandreed and sideoats grama can be grown in monoculture or polyculture plantations. Since these grasses can be grown and harvested on marginal land, they do not carry the burden of competing with food crops and, therefore, are ideal candidates for biofuel production.

Several technologies are being developed to support the conversion of plant biomass to ethanol. *In lieu* of biological methods for biomass conversion, pyrolysis of biomass to bio-oil could provide a means of producing liquid fuel for the U.S. motor fleet. Fast pyrolysis is a thermochemical approach for rapidly converting low-density biomass to a higher density liquid known as bio-oil at yields in excess of 60% by weight. However, chemical species found in bio-oil are reactive, causing instability during storage and limit the early adoption of bio-oil for producing transportation fuels.

---

[1] *Department of Biosystems & Agricultural Engineering, Michigan State University, MI*

[2] *Department of Chemical Engineering & Materials Science*

[3] *Department of Crop & Soil Sciences*

[4] *Department of Forestry*

** Corresponding author*

Biomass constituents such as lignin, ash, and inorganic salts dramatically alter the speciation of pyrolysis products. Previous studies have demonstrated the effect of inorganic minerals (especially alkali and alkaline earth metals) on the distribution of pyrolysis products and on bio-oil production (Mohan, Pittman, and Steele 2006; Patwardhan et al. 2010; Hodgson et al. 2011; Fahmi et al. 2008). Therefore, the objectives of this work were to evaluate the composition of eight grass species and study the effect of their composition on the nature and quality of pyrolysis products. In addition, a switchgrass cultivar, Cave-In-Rock, grown on different plots in Michigan under similar growth conditions was studied to assess the impact of location (latitude) and plot treatments on switchgrass pyrolysis products.

Experimental

All plant species examined are common native warm-season grasses found in Michigan and other Midwestern states and were as follows: big bluestem, coastal panicgrass, deertongue, indiangrass, Miscanthus, sandreed, sideoats grama and switchgrass. In addition, switchgrass was harvested from four plots in Michigan: Grand Valley (latitude 45.42°), Roger City (43.33°), Cass County (42.97°), and Frankenmuth (41.79°). All biomass samples were dried to less than 10% moisture by weight at room temperature and milled to a particle size of less than 0.5 mm. Neutral detergent fiber (NDF), acid detergent fiber (ADF), and acid detergent lignin (ADL) were measured using Van Soest fiber analysis. Analysis of inorganic constituents such as potassium, sodium, magnesium, calcium, and iron was done at Dairyone Labs (Ithaca, NY) using Inductively Coupled Plasma (ICP) Radial Spectrometry after microwave digestion. The higher heating value of biomass was determined using a Parr 1341 Plain Jacket Calorimeter (Parr Instrument Co., Moline, IL). Pyrolysis experiments were conducted at 600 °C using a microscale pyrolysis unit, CDS Pyroprobe 5250 (CDS Analytical Inc, Oxford, PA), and the products were analyze by a Shimadzu QP-5050A gas chromatograph/mass spectrometer (Shimadzu Corp, Columbia, MD). The GC used a Restek Rtx-1701 column (Restek, Bellefonte, PA); column gas flow was 1 ml/min with a split ratio of 1:100. The GC oven temperature program began at 40°C followed by heating at 8°C/min to 270 °C. The mass spectra were recorded in electron ionization mode for *m/z* 28 to 400.

Results and Discussion

Feedstock Composition

The cellulose content for the eight grass species ranged from 35.2 to 50.2% weight of dry biomass (db), hemicellulose ranged from 27.3 to 32.8% db and the total lignin ranged from 13.5 to 23.6% db for the eight grass species. The higher heating values (HHV), measured by bomb calorimetry, were found to be in the range 18.4 to 21.2 MJ/kg on a dry biomass basis. The HHV of the grasses was significantly affected by lignin content and varied inversely with ash. Elemental analysis showed that of the alkali and alkaline earth metals (AAEM), potassium was the most significant, measuring 0.5 to 0.86% db. Calcium constituted between 0.19 to 0.40% db while magnesium varied between 0.1 to 0.2% db. Sodium constituted less than 0.01% db while iron was present in the 45-112 ppm range. Three of the four switchgrass samples grown on different plots showed similar composition with 34.9-36.2% db cellulose and 1.22-1.24% db AAEM. Although the growth conditions such as soil properties, nitrogen supplementation (95 lb/acre) and harvest time (first frost of Fall) were similar, Cass county switchgrass reported the highest cellulose (42%) and the lowest AAEM content (0.68% db). This anomaly is being investigated further as no obvious relationships were observed between the location and its effect on feedstock composition.

Miscanthus and big bluestem were found to have the highest cellulose and lignin content whereas switchgrass and coastal panicgrass had the highest AAEM. Increasing levels of AAEM have been shown to increase the yield of char and gases upon pyrolysis and to decrease the amount of condensable products such as bio-oil (Fahmi et al. 2008). Coastal panicgrass, with the highest

HHV, lowest ash and low Ho:L ratio may be suitable for pyrolysis applications. Sideoats grama and deertongue, with the lowest HHV, highest ash and Ho:L ratio may be better suited for fermentation based processes. [

Analytical Pyrolysis-GC/MS

Analytical pyrolysis of the grass species in this study produced a similar mixture of chemical species upon pyrolysis as presented in Figure 1. Fast pyrolysis yields a reactive mixture of water carboxylic acids, hydroxyaldehydes, hydroxyketones, furancarboxaldehydes, sugars, and phenolics such as guaiacols, catechols, syringols, vanillins and isoeugenol. The major chemical products of fast pyrolysis, as determined by GC/MS analysis, were acetic acid, hydroxyacetone (acetol) and 2-hydroxyacetaldehyde (glycolaldehyde). Production of acetic acid and acetol was accompanied with a decrease in production of levoglucosan. Sideoats grama and sandreed, produced higher levels of acetic acid and acetol, which may be unsuitable for producing reactively stable bio-oil that can be transported and stored for further chemical upgrading. Switchgrass, indiangrass and big bluestem produced less small carbonyl and carboxylate compounds compared to other grasses, which implies that the pyrolysis products may be less chemically reactive, less corrosive to metal surfaces and more stable during storage. Rogers city switchgrass produced the most carboxyl and carbonyl group compounds (Figure 2) while Grand valley switchgrass produced the lowest acid and highest saccharide derivatives such as the anhydrosugar, levoglucosan.

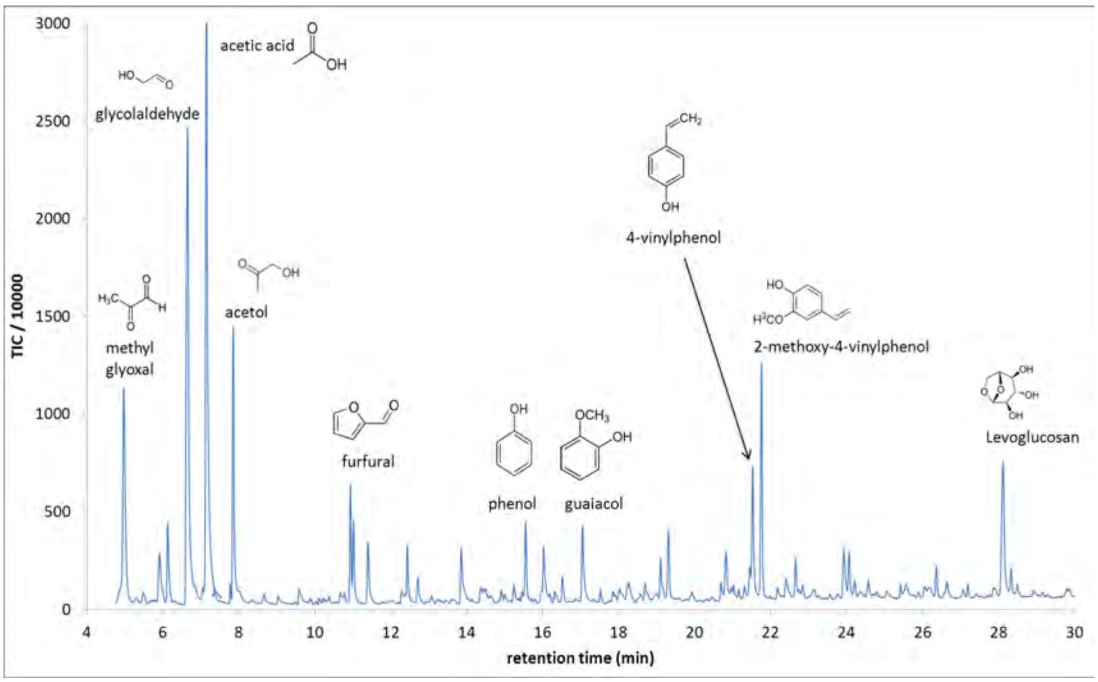

Figure 1. Representative pyrogram (switchgrass pyrolysis) with major chemical species found in products of pyroprobe GC/MS analysis.

List of compounds in condensable product (bio-oil) are listed below as follows: (Retention time) Chemical compound, (4.8) Methyl glyoxal,(5.7) 2,3-Butanedione, (6.4) Glycolaldehyde, (7.0) Acetic acid, (7.9) Acetol, (11.5) Furfural, (13.9) 2-methyl-cyclopenten-1-one, (14.4) Heptanol, (15.3) γ –Crotonolactone, (15.5) Phenol, (17.1) o-Guaiacol, (19.1) p-Methylguaiacol, (19.4) Unknown, (20.7) p-Ethylguaiacol, (21.2) 2,3-Anhydrogalactosan, (21.2) α-D-Glucopyranose, (21.5) γ-Butyrolactone, (21.6) 4-Vinylphenol, (21.8) 2-Methoxy-4-vinylphenol (4-vinylguaiacol), (22.7) 2,6-Dimethoxyphenol (Syringol), (23.9) trans-Isoeugenol, (24.1) Vanillic acid, (26.4) 4-Vinylsyringol, (28.1) 1,6-anhydro-β-glucopyranose (Levoglucosan), (28.3) Methoxyeugenol

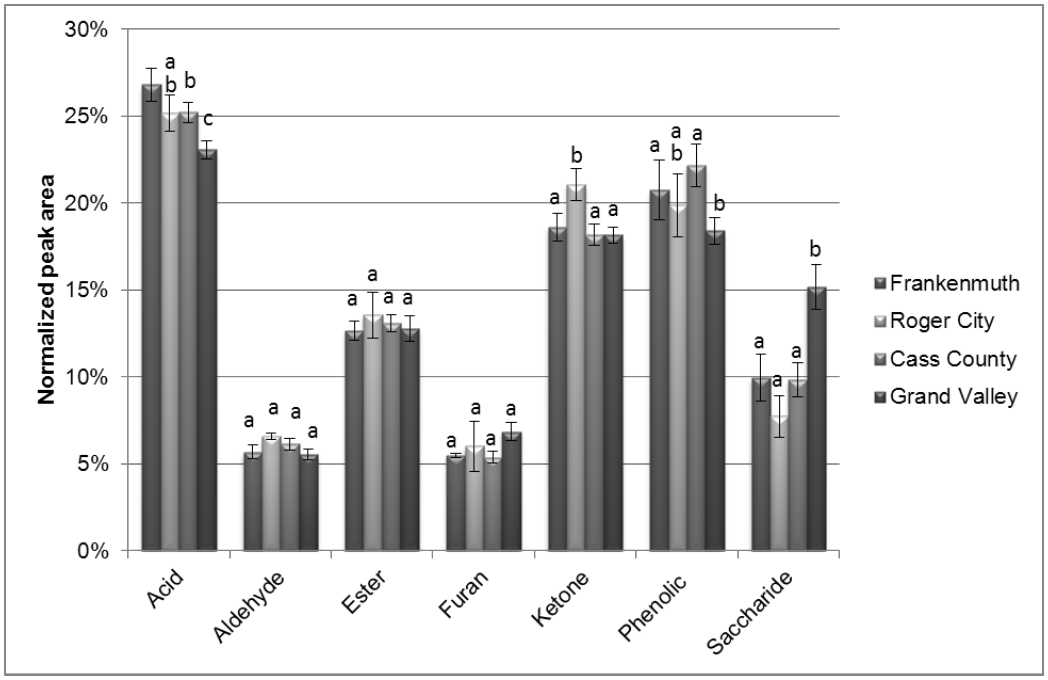

Figure 2. Comparison of pyrolysis products of switchgrass grown on four plots

Effect Of Feedstock Composition On Pyrolysis Products

Increasing hemicellulose levels correlated with the production of acetic acid and acetol as well as char yield. Elemental analysis of the grass species showed potassium to be a major inorganic constituent. Of all the metals analyzed during this study, only potassium was found to have a significant effect on reducing the biomass decomposition temperature and increasing the char yield. Potassium correlated with a decrease in the amount of levoglucosan, a product of cellulose de-polymerization, and an increase in acetic acid and acetol. Levels of calcium, magnesium, sodium and iron did not correlate with the levels of the pyrolysis products for the native North American grass species. Rogers City switchgrass, with the highest potassium level, produced the most carboxyl and carbonyl group compounds. Thus the quantity of potassium may be critical in determining the outcome of biomass pyrolysis. Although Grand valley switchgrass produced the highest amount of anhydrosugars, statistically significant correlations with the feedstock composition were not observed.

Summary

Several grass species were studied as potential feedstocks for conversion to liquid fuels by fast pyrolysis. The quality of bio-oil, the condensable fraction from biomass pyrolysis, was a function of feedstock composition. Potassium increased the carboxyl and carbonyl compounds and biomass with low potassium levels may be suitable as feedstock for thermochemical conversion to biofuels. No obvious relationships were observed between switchgrass grown on different locations and their effect on pyrolysis products.

References

Fahmi, R., A.V. Bridgwater, I. Donnison, N. Yates, and J.M. Jones. 2008. "The Effect of Lignin and Inorganic Species in Biomass on Pyrolysis Oil Yields, Quality and Stability." *Fuel* 87 (7) (June): 1230–1240.

Hodgson, E M, D J Nowakowski, I Shield, A Riche, A.V. Bridgwater, J C Clifton-Brown, and I S Donnison. 2011. "Variation in Miscanthus Chemical Composition and Implications for Conversion by Pyrolysis and Thermo-chemical Bio-refining for Fuels and Chemicals." *Bioresource Technology* 102 (3) (February): 3411–3418.

Mohan, Dinesh, Charles U. Pittman, and Philip H Steele. 2006. "Pyrolysis of Wood/Biomass for Bio-oil: A Critical Review." *Energy & Fuels* 20 (3) (May): 848–889.

Patwardhan, Pushkaraj R, Justinus A Satrio, Robert C Brown, and Brent H Shanks. 2010. "Influence of Inorganic Salts on the Primary Pyrolysis Products of Cellulose." *Bioresource Technology* 101 (12) (June): 4646–4655.

U.S. Department of Energy. 2011. *U.S. Billion-Ton Update: Biomass Supply for a Bioenergy and Bioproducts Industry*. Oak Ridge, TN.

3.10
Catalytic Pyrolysis of Torrefied Biomass for Hydrocarbons Production

Vaishnavi Srinivasan[1], Sushil Adhikari[1], Shyamsundar Ayalur Chattanathan[1], and Sunkyu Park[2]*

Abstract
Fast pyrolysis process is one of the promising techniques that produces high liquid yield. However, pyrolysis liquid (bio-oil) is unstable, and has high oxygen content (~35 wt.%), which restricts its use as a transportation bio-fuel. A number of upgrading techniques have been experimented over the last two decades to improve the quality of the liquid product--primarily to reduce the oxygen content-- but those processes still suffer from several technical challenges. A simple thermal pretreatment process called torrefaction has shown to be effective in reducing the oxygen content in biomass to a certain extent. The main objective of this study was to integrate torrefaction with fast pyrolysis process to produce high quality of bio-oil. In this study, the effects of four pyrolysis temperatures (450, 500, 550 and 600^{o}C), and shape-selective zeolite catalyst (H^+ZSM-5) on hydrocarbon yield were analyzed.

Keywords: Fast pyrolysis, Bio-oil, Torrefaction, Catalyst, Zeolite

Introduction
Biomass has the potential to alleviate the use of fossil based fuel because it is the only currently available carbon-based renewable source for liquid fuels production. Previous studies (Czernik and Bridgwater 2004; Thangalazhy-Gopakumar *et al.* 2010) have shown that fast pyrolysis is an effective process that deals with the conversion of solid biomass to liquid fuel in short residence time. This fuel is dark brown liquid and a complex mixture of water, acids, phenolic compounds, oxygenated hydrocarbons, and solid char. The present form of bio-oil has to be altered to use it as a liquid transportation fuel. The high oxygen content (approximately 35 wt.%, dry basis) imparts several negative attributes to the bio-oil such as instability, low heating value, and also makes it immiscible with the current hydrocarbon fuels. These disadvantages hinder bio-oil from becoming a feasible solution for an alternate liquid fuel. This calls for the need to develop an upgrading technique to improve the quality and stability of the liquid product.

Recently, a simple thermal pretreatment of biomass called torrefaction has attracted some interest mainly because pretreated biomass contains high energy but requires less energy for grinding. This is the main advantage because pyrolysis process requires very fine particles to increase liquid yield (Shen *et al.* 2009). Torrefaction is a thermochemical process operated at 200-300°C in the absence of oxygen. During torrefaction, biomass undergoes partial decomposition with the release of volatiles, which results in overall mass loss. In addition to these, there is a significant loss of oxygen from the biomass, which results in an increase of the calorific value. A handful studies have focused on the influence of torrefaction on the quality of the liquid fuel (Meng *et al.* 2012; Ren *et al.* 2012; Uslu *et al.* 2008). However, none of them have focused in the combined effect of catalyst and pretreatment on the bio-oil quality. Therefore, the main objective of this paper was to study the combined effect of catalyst and torrefaction on hydrocarbons yield through catalytic fast pyrolysis of torrefied biomass. Further, the influence of temperature and catalytic loading ratio on the various product yields was studied. The governing hypothesis is that the

[1] *Department of Biosystems Engineering, Auburn University, AL*

[2] *Department of Forest Biomaterials, North Carolina State University, NC*

* *Corresponding Author*

pretreated biomass (low in oxygen content) would produce more aromatic compounds as compared to raw biomass.

Experimental Setup

Fast Pyrolysis- Pyroprobe/GC-MS

Pretreatment of biomass was done at 225°C for 30 min. Physical and chemical characterization was performed for both raw and torrefied pine. Fast pyrolysis experiments were carried out using a commercial pyrolyzer (CDS Analytical Inc., Model 5200). Fast pyrolysis of raw and torrefied pine was carried out at 650°C, whereas catalytic fast pyrolysis was carried at four different temperatures (450,500,550, and 600˚C) and with three different biomass:catalyst ratios (1:04, 1:09, and 1:14) for torrefied biomass and at 450˚C with 1:09 biomass:catalyst ratio for raw biomass as a control. All the temperatures specified for pyroprobe experiment is filament temperature but the actual sample temperature was lower. ZSM-5 (Zeolyst, Inc. SiO_2/Al_2O_3 = 50, surface area = 425 m^2/g) was calcined in air at 550˚C for 2 h in a furnace to convert into H^+ZSM form prior to use. The biomass heating rate was kept constant at 2000˚C/s throughout the study. Helium gas was used as the inert pyrolysis gas as well as the carrier gas for the GC/MS system. A known amount of (approximately 1 mg) reactant mixture was taken for each run. Experiments were carried out in triplicates, and the average values are reported. Bio-oil compounds were analyzed with an Agilent 7890 GC/5975 MS using a DB 1701 column. Compounds were identified using NIST (National Institute of Standards and Technology) mass spectral library. Compounds which appeared consistently with high probability were selected and quantified. Quantification was done by injecting calibration standards into the GC/MS system. The slope of the calibration line was taken as the quantification factor in the calculation. A split ratio of 5:1 was set for injection. Ultrahigh purity (99.999%) helium gas supplied from Airgas Inc. was used as carrier gas, and its flow was maintained at 1.25 mL/min.

Results and Discussion

Effect of torrefaction on the product distribution from fast pyrolysis (without catalyst) of biomass at 650°C is shown in Figure 1. The products were grouped into different categories such as aromatic hydrocarbons (AH), phenolics (PH), guaiacols (G), naphthalenes (Naph), furans (FN), and anhydrous sugars (AS). Aromatic hydrocarbon group included BTX, benzene derivatives, idane and indene; phenolics included phenols, cresols and catechols; guaiacols included guaiacols and homoguaiacol; anhydrous sugars included levoglucosans and straight chain compounds; naphthalenes included naphthalene and its derivatives and the group furans included furan and its derivatives. The compositions of the products from the pyrolysis of torrefied biomass were significantly different from that of raw pine. Phenolics group included phenols and cresols. The guaiacols produced were found to be higher from the pyrolysis of torrefied pine. However, phenolics yield remained almost constant from pyrolysis of raw and torrefied pine. Hydrocarbons, one of the important compounds in any liquid fuel, was found to be very minimal from the pyrolysis of raw pine, while it was found a significant increase when torrefied pine was used. Moreover, other oxygenated hydrocarbons mainly furans were significantly higher from the pyrolysis of raw pine as reported in another study (Meng *et al.* 2012). These results indicated that the pretreatment favored the production of lignin derivative- phenols more than hemicellulose derivative – furans.

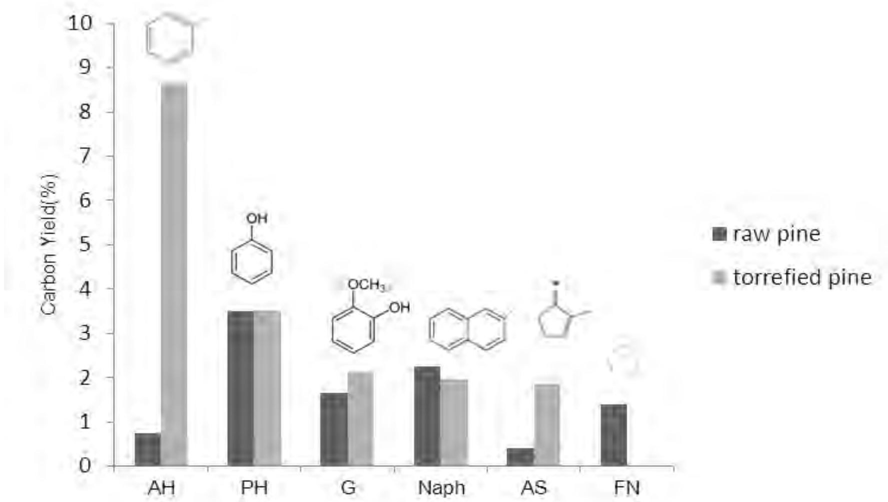

Figure 1. Product distribution from the fast pyrolysis of torrefied and raw pine at 6500C in a pyroprobe

Increase in reaction temperature from 450°C to 550°C increased the total carbon yield significantly for all three biomass to catalyst ratios. Total carbon yield was highest from the pyrolysis results at 550°C with 1:14 biomass to catalyst ratio. Catalytic fast pyrolysis of raw pine resulted in ~14 (wt%) of total carbon. The carbon distribution on each group is given in Table 1. The product distribution with temperature for 1:09 catalyst ratio is shown in Figure 2. The three main components of biomass, cellulose, hemicellulose, and lignin, decompose at various temperatures and produce different compounds. Thermal decomposition of hemicellulose gives furan derivatives and few low molecular weight compounds such as formic acid, acetol (Patwardhan *et al.* 2011). However, low molecular weight compounds were not observed in this study. The yield of furan derivatives is high at low temperature probably because of the primary degradation and decrease with increase in temperature due to the secondary vapor phase reactions (Branca *et al.* 2003). Phenols and guaiacols are mainly derived from the decomposition of lignin (Murwanashyaka *et al.* 2001). From the figure, it can be seen that the phenols increases while guaiacols decreases with the temperature. Similar trend was observed from the pyrolysis results with 1:4 and 1:14 biomass to catalyst ratios. This can be due to the demethoxylation reactions of guaiacols at high temperatures to give phenols.

Table 1. Product distribution from catalytic fast pyrolysis of raw pine at 450°C with 1:9 biomass to catalyst ratio

	Raw Pine	Torrefied Pine
	Average (wt% carbon)	Average (wt% carbon)
Aromatic Hydrocarbon (AH)	5.66±0.23	10.2±1.36
Phenols (PH)	3.51±0.65	1.08±0.025
Guaiacols (G)	1.65±0.02	1.07±0.12
Naphthalene (Naph)	2.25±0.97	5.66±0.31
Anhydrous sugars (AS)	0.42±0.005	-
Furans (FN)	1.39±0.03	2.31±0.11
Total Carbon Yield	14.88±1.12	20.32±1.26

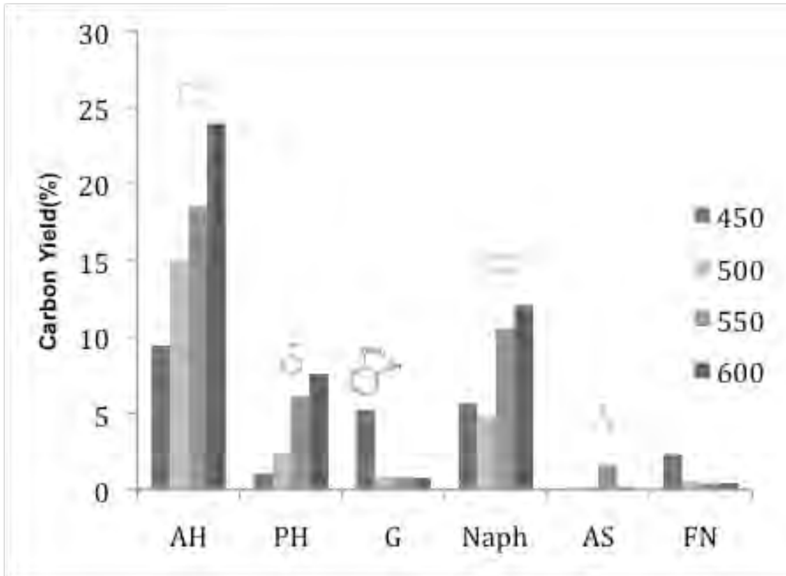

Figure 2. Effect of temperature on product distribution of catalytic fast pyrolysis of torrefied pine with 1:09 biomass: catalyst ratio

Figure 3 shows the effect of catalyst to biomass ratio on the product composition at 600°C. The aromatic hydrocarbons were most affected by catalyst to biomass ratio and, significantly, increased with the catalyst to biomass ratio. Among the aromatic hydrocarbons, benzene, toluene, and styrene were primary compounds, and few alkyl substituted aromatics such as benzene-1-ethyl-2-methyl, benzene 1, 2, 3 trimethyl, and benzene 1, 2, 3, 4 tetra methyl were also seen in traces. Naphthalene compounds also followed the same trend with increase in catalyst to biomass ratio. This can be due to the size selectivity of zeolite catalyst as the kinetic diameter of naphthalene (6Å) is very similar to ZSM-5 pore size (~6.2Å) (Carlson *et al.* 2009). It was also observed that the thermally stable oxygenates mainly furans and its derivatives were formed as catalyst to biomass ratio decreased. The oxygenated compounds can diffuse into the pores of the H^+ZSM-5 catalyst, and can result in aromatics through decarbonylation, dehydration, and oligomerization reactions (Carlson *et al.* 2010).

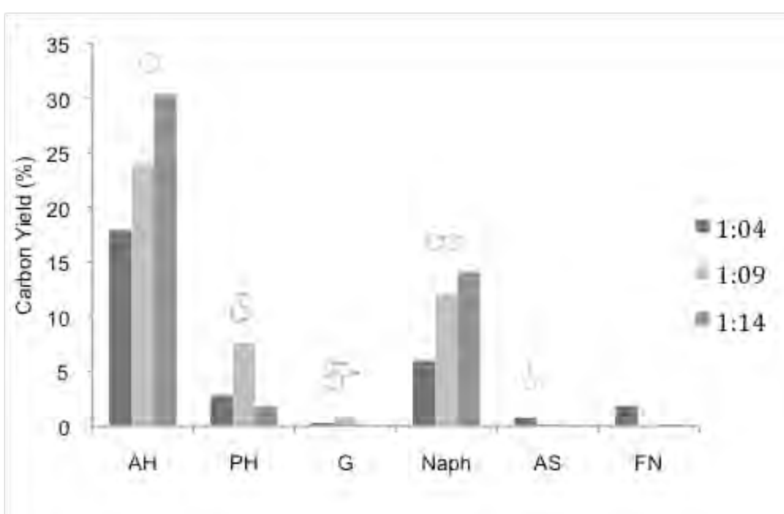

Figure 3. Product distribution for the catalytic pyrolysis of torrefied biomass at 600°C with different biomass to catalyst ratios

Conclusion

Simple pretreatment process, torrefaction, has shown to be effective in improving the quality of bio-oil produced from catalytic fast pyrolysis. Torrefaction also resulted in more of lignin derivatives –guaiacols, phenols and less of hemicellulose derivatives mainly furans. Interestingly, guaiacols and furans were found to be a possibly intermediates in the formation of aromatics. Aromatic hydrocarbons were significantly produced as a result of torrefaction, and temperature and catalyst enhanced their production. Presence of catalyst resulted in the formation of naphthalenes due to its size selectivity. All these results indicated that the combined effect of pretreatment and shape selective catalyst (H^+ZSM-5) resulted in highly de-oxygenated and stable liquid product.

References

Branca, C., Giudicianni, P., and Di Blasi, C. (2003). "GC/MS characterization of liquids generated from low-temperature pyrolysis of wood." *Industrial & Engineering Chemistry Research*, 42(14), 3190-3202.

Carlson, T., Tompsett, G., Conner, W., and Huber, G. (2009). "Aromatic production from catalytic fast pyrolysis of biomass-derived feedstocks." *Topics in Catalysis*, 52(3), 241-252.

Carlson, T. R., Jae, J., Lin, Y.-C., Tompsett, G. A., and Huber, G. W. (2010). "Catalytic fast pyrolysis of glucose with HZSM-5: The combined homogeneous and heterogeneous reactions." *Journal of Catalysis*, 270(1), 110-124.

Czernik, S., and Bridgwater, A. V. (2004). "Overview of Applications of Biomass Fast Pyrolysis Oil." *Energy & Fuels*, 18(2), 590-598.

Meng, J., Park, J., Tilotta, D., and Park, S. (2012). "The effect of torrefaction on the chemistry of fast-pyrolysis bio-oil." *Bioresource Technology*, 111(0), 439-446.

Murwanashyaka, J. N., Pakdel, H., and Roy, C. (2001). "Step-wise and one-step vacuum pyrolysis of birch-derived biomass to monitor the evolution of phenols." *Journal of Analytical and Applied Pyrolysis*, 60(2), 219-231.

Patwardhan, P. R., Brown, R. C., and Shanks, B. H. (2011). "Product distribution from the fast pyrolysis of hemicellulose." *ChemSusChem*, 4(5), 636-643.

Ren, S., Lei, H., Wang, L., Bu, Q., Chen, S., Wu, J., Julson, J., and Ruan, R. "The effects of torrefaction on compositions of bio-oil and syngas from biomass pyrolysis by microwave heating." *Bioresource Technology*(0).

Shen, J., Wang, X.-S., Garcia-Perez, M., Mourant, D., Rhodes, M. J., and Li, C.-Z. (2009). "Effects of particle size on the fast pyrolysis of oil mallee woody biomass." *Fuel*, 88(10), 1810-1817.

Thangalazhy-Gopakumar, S., Adhikari, S., Ravindran, H., Gupta, R. B., Fasina, O., Tu, M., and Fernando, S. D. (2010). "Physiochemical properties of bio-oil produced at various temperatures from pine wood using an auger reactor." *Bioresource Technology*, 101(21), 8389-8395.

Uslu, A., Faaij, A. P. C., and Bergman, P. C. A. (2008). "Pre-treatment technologies, and their effect on international bioenergy supply chain logistics. Techno-economic evaluation of torrefaction, fast pyrolysis and pelletisation." *Energy*, 33(8), 1206-1223.

3.11
Char-based Ni Catalysts for Syngas Cleanup and Conditioning in Biomass Gasification

Wenqiao Yuan[3,], Duo Wang[4], Donghai Wang[5]*

Abstract
A newly developed nano-Ni on char catalyst was studied for syngas cleaning and upgrading in an updraft biomass gasifier. The nano-Ni/char catalyst was prepared by mechanically mixing nano-sized NiO powders with char particles and its performance was compared with Ni/char and Ni/γ-Al_2O_3 catalysts in terms of syngas composition enhancement and tar removal. The SEM/EDX analysis showed that nano-NiO particles uniformly distributed on the surface of char particles, with 66.3% Ni dispersion rate and 128.5 m2/g-Ni surface area. The effect of cracking temperature (650°C to 850°C), nickel oxide loading (5% to 20%), and gas residence time (0.1 to 1.2 s) on catalyst performance was studied. Nano-Ni/char catalyst showed better catalytic reactivity than Ni/char, also, nano-Ni/char showed higher reactivity than Ni/γ-Al_2O_3 at a relatively low temperature (~700°C).

Keywords: biomass gasification, nanocatalyst, syngas cleanup, tar removal

Introduction
Biomass gasification technology has been developed extensively to convert carbon-containing biomass fuel into high quality fuels (Sims et al., 2010). As the main product in the process of biomass gasification, syngas can be burned directly to provide heat and electricity for us. They can also be further converted to a wide variety of liquid transportation fuels and chemicals, such as synthetic diesel (Dunn et al., 2004), mixed alcohols (Bao et al., 2009), and dimethyl ether (Mao et al., 2009). However, in addition to the main syngas composition gasification gas contains also impurities like tar, which is a major obstacle of the widespread application of syngas. In order to reduce the tar content of syngas, such as physical treatment (Jansen et al., 2002), thermal cracking (Narvpaez et al., 1996), plasma-assisted cracking (Nair et al., 2003), and catalytic reforming (Baker and Mudge, 1984) have been reported in the literatures, among which catalytic reforming is considered the most promising in large scale applications due to its fast reaction rate and reliability and also its ability to increase the quantity of useable gases such as CO and H_2 in syngas.

Various types of catalysts for tar removal during biomass gasification, such as calcined rocks (Yu et al., 2009), zeolites (Dou et al., 2003), iron ores (Tamhankar et al., 1985), alkali metals (Suzuki et al., 1992), Ni-based catalysts (Park et al., 2010), and precious metals (Furusawa et al., 2005) have been under rigorous investigation since the 1990s. Nickel is a promising catalyst for steam reforming of tar derived from biomass gasification due to high catalytic reactivity and syngas composition adjustment ability. Nickel catalysts are usually supported by metal oxides (e.g., Al_2O_3 and MgO) or natural materials (e.g., dolomite, olivine, activated charcoal and brown coal char) (Wang et al., 2005; Courson et al., 2002; Lee et al., 2009; Le et al., 2009). Different support and catalytic preparation methods lead to the difference of the particle size and dispersion of nickel-based catalysts, which affect the catalytic activity significantly for tar reforming. Ni/γ-Al_2O_3 catalysts prepared by complicated preparation steps involving impregnation and

[3] *Department of Biological and Agricultural Engineering, North Carolina State University, NC*

[4] *School of Energy Research, Xiamen University, Xiamen, Fujian, China*

[5] *Department of Biological and Agricultural Engineering, Kansas State University, KS*

* *Corresponding author*

calcinations exhibit high catalytic reactivity for tar reforming (Wang et al. 2010a), not surprisingly, Ni/char catalysts prepared by mechanically mixing method simply also show definitely catalytic reactivity (Want et al., 2011). Therefore, considering both catalytic reactivity and economic reasons, a suitable catalyst support and preparation method will be a key factor for tar removal and syngas reforming and applied for industrial producing extensively.

In previous studies (Wang et al., 2010b, 2011), NiO supported by chars were investigated. The Ni/coal char catalyst removed 99% tars in the syngas but the increase of H_2 in syngas was lower than reported results using Ni/γ-Al_2O_3 catalysts. This pioneering study explored the use of a new nano-sized Ni catalyst, called nano-Ni/char, for biomass gasification tar removal and syngas enhancement. The catalyst was prepared by mechanically mixing coal char particles with nano-scale NiO powder. Use of nano-NiO particles is expected to significantly improve the surface area of active NiO, and enhance the adhesion of NiO particles to the char surface. The objective of this study was to test the performance of the new nano-Ni/char catalyst for tar removal and syngas composition enhancement. The new catalyst was tested in a laboratory-scale updraft biomass gasifier. Micro-sized NiO on coal char made by mechanical mixing method (called Ni/char) and conventional NiO on γ-Al_2O_3 prepared by the impregnation and calcination method (called Ni/γ-Al_2O_3) were also studied for comparison.

Materials and Methods

Catalysts preparation

The coal char used in this study was obtained from Royal Oak Enterprises, Inc. (Omaha, AR). Char granules were crushed and sieved to obtain particles in the size range of 40 to 60 meshes (0.3 to 0.45 mm). The micro-sized NiO powder was purchased from Fisher Scientific (Catalog number: AC41558-5000, Pittsburgh, PA) and the nano-NiO was obtained from MTI corporation (Item number: NP-NiO, Richmond, CA). Ni/char and nano-Ni/char catalysts were prepared by mechanically mixing NiO, nano-NiO particles and char in a transparent glass beaker at desired ratios. Commercial γ-Al_2O_3 balls (Delta Adsorbents Company, Roselle, IL) with a diameter of 1/8 inch and surface area of 355 m^2/g were used as the support of Ni/γ-Al_2O_3. $Ni(NO_3)_2 \cdot 6H_2O$ (Fisher Scientific, Pittsburgh, PA) was used as the Ni precursor. The Ni/γ-Al_2O_3 catalysts were prepared by incipient wetness impregnation and calcination following a previously published method (Wang et al., 2010a). All Ni catalysts were scanned with a HITACHI S-3500N scanning electron microscope (SEM; Hitachi, Ibaraki, Japan) and an EDX (energy dispersive X-ray) measurement was conducted.

Catalytic testing

The system consists of three subsystems: (1) an updraft biomass gasifier system, which provided a constant flow of raw syngas at a specific flow rate to the reforming unit via control of a flow control valve and vacuum pump; (2) tar reforming unit; and (3) tar collection unit, a detailed description of this system can be found in the literature (Wang et al., 2011). The gasification system provides an overall air rate of 5-50 cfm depending on the voltage to the 15-W blower (Delibang, Zhejiang, China). In gasification tar reforming experiments, a small fraction of the syngas was directed to the reforming tube, and syngas flow rate was adjusted and measured with a gas valve and a gas flow meter (Brooks Instrument, Hatfield, PA). The tar reforming system was comprised of a quartz, 1-in.-diameter, 24-in.-long reactor tube with a complete vacuum-sealing assembly (MTI Corporation, Richmond, CA) and a Thermolyne Economy solid-tube furnace (Fisher Scientific, Pittsburgh, PA). The catalyst bed was placed in the center of the tube and horizontally supported by two alumina foam blocks (MTI Corporation, Richmond, CA). Table 1 shows the experimental parameters of tar reforming. Reaction temperatures were in the range of 650°C to 850°C at steps of 50°C, and Ni loadings ranged from 0% to 20% at steps of

5%. Gas residence times were set at 0.1, 0.3, 0.6, 0.9 and 1.2 s by adjusting the syngas flow rate in the reforming tube through the flow control valve.

Table 1. Experimental parameters of tar reforming.

Condition	Parameter
Gasification agent	Air
Biomass feed	Pine sawdust
Catalytic bed temperature, °C	650 to 850
Gas residence time, s	0.1 to 1.2
Ni loading in catalysts	0 to 20%
Gas flow rate, l/min	9.12
Run time per sample, min	15
Char particle size, mesh (mm)	40 to 60 (0.45mm to 0.3mm)
Catalyst bed length, cm	9

The tar sampling unit was comprised of four 250-mL flasks dipped into an insulation box filled with dry ice. Each sampling ran for over 100 liters of syngas carried tars flowed through the cold flasks and were quenched and collected. All tars and water vapor were collected in the flasks, which were then dried at 105°C in an oven for 2 h. The residue was considered as tars. Other researchers have used similar or slightly modified forms of this method (Narváez, et al., 1997; Leppala et al., 1991). It must be noted that only heavy tars (boiling point above 105°C) were measured in this study considering that heavy tars are more damaging and difficult to remove than light tars in catalytic cracking. Syngas was collected from the sampling port or the outlet of the vacuum pump with a 500-mL Tedlar sampling bag. Analysis of syngas was carried out by an SRI 8610s gas chromatograph equipped with a thermal conductivity detector (SRI Instruments, Torrance, CA).

Results and Discussion

SEM observation of catalysts

As shown in Figs. 1d/1e, nano-NiO particles uniformly distributed on the surface of char, similar to or even better than Ni/γ-Al_2O_3 catalyst prepared by impregnation (Figs. 1c/1d). The micro-sized NiO particles covered smaller areas and were less uniformly distributed on the char support (Figs. 1a/1b) than nano-Ni/char or Ni/γ-Al_2O_3 catalysts, indicating that NiO particle size played a significant role in catalyst preparation. The smaller size of nano-NiO particles could probably have helped the adhesion of NiO to char particles and also increased the surface area and spread of Ni on the support, making Ni more uniformly distributed on char support.

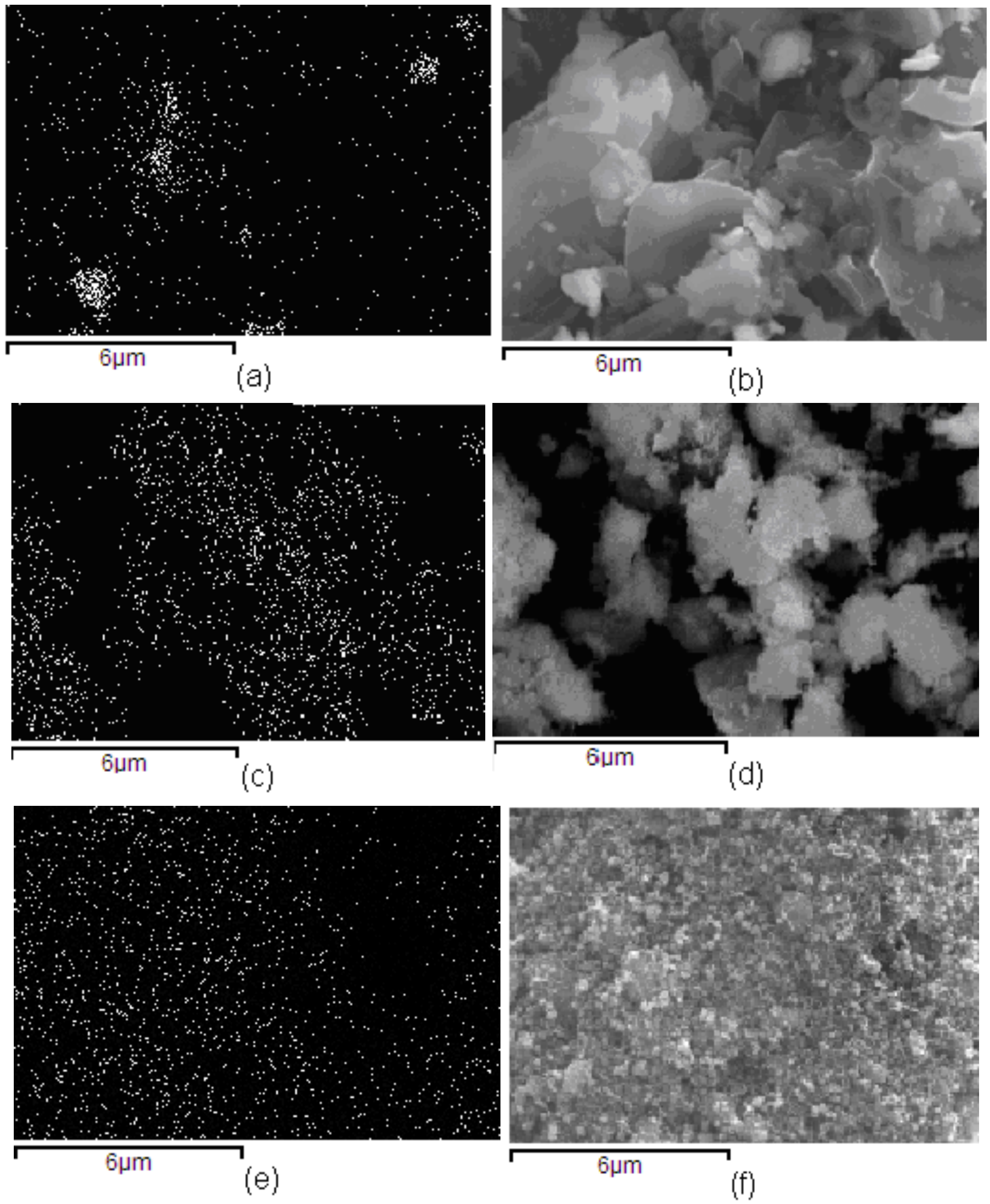

Fig. 1. EDX/SEM images of Ni/Char (a/b), Ni/γ-Al_2O_3 catalysts (c/d) Nano-Ni/Char (e/f), (15% NiO loading, white dots or areas are Ni).

Catalytic performance

Tar removal

The effect of reforming temperature on tar removal and syngas composition were investigated for the temperature range of 650°C to 850°C while the Ni loading and gas residence time were fixed at 15wt% and 0.3 s, respectively. As shown in Fig.2a, tar removal rate increased with increasing reaction temperature in all cases. Under the same reaction conditions, nano-Ni/char catalyst showed the highest tar removal rate at all temperatures, ranging from 91% to 99%. The Ni/char catalyst also achieved higher than 90% tar removal rates, even at relatively low temperatures (<800°C) where the Ni/γ-Al_2O_3 was not very effective. However, when temperatures were at 800°C or higher, Ni/γ-Al_2O_3 was as effective as nano-Ni/char and better than Ni/char in tar removal. It indicates that the Ni/γ-Al_2O_3 catalyst requires higher reaction temperature, while Ni/char and nano-Ni/char can work effectively at lower temperatures. If 95% tar removal is the target, a reaction temperature of 750°C is needed for nano-Ni/char, and a minimum of 800°C is required for the other two catalysts. The higher catalytic performance of Nano-Ni/char and Ni/char at a relatively low temperature could be explained by the fact that char itself decomposes heavy tars into small hydrocarbons at low temperatures (Gilbert et al., 2009), but γ-Al_2O_3 lacks of the ability. It is also well known that nickel catalysts have low catalytic activity when reaction temperature is under 750°C (Li, et al., 2008).

The effect of Ni loading on tar removal and syngas reforming was studied with Ni/char, nano-Ni/char and Ni/γ-Al_2O_3 catalysts at 0.3 s gas residence time and 800°C reaction temperature. As shown in Fig. 2b, tar removal rate of all catalysts steadily but slightly increased when Ni loading increased from 5% to 15%. The nano-Ni/char catalyst showed better performance than Ni/char and Ni/γ-Al_2O_3 catalyst when Ni loading was in the range of 5 to 15 wt.% probably due to better adhesion and more uniform distribution of NiO particle on char particles. However, the performance of nano-Ni/char decreased when nickel loading further increased up to 20 wt.%. This is due to nickel dispersion rate decreased significantly with increasing nickel loading (Bartholomew and Boudart, 1976). It can also be seen that Ni/γ-Al_2O_3 with 5 wt% Ni loading for tar removal is significantly lower than Ni/char and nano-Ni/char. This could be attributed to the different ways the catalysts were prepared. In γ-Al_2O_3 supported catalysts, NiO is also formed inside the support via the impregnating and calcining methods. NiO inside of the support is not as active as on the surface causing loss of active nickel. On the other hand, all NiO particles stay on the surface of chars in the mechanical mixing processing, leading to more efficient use of nickel.

Fig. 2c shows tar removal affected by gas residence time. It can be seen that tar removal rate remained high when gas residence time was greater than 0.3 s, but decreased sharply below 0.3 s. When gas residence time is equal to or longer than 0.3 s, the three catalysts had similarly high tar removal rate at the same temperature (800) and Ni loading (15%), indicating that 0.3s is sufficient for tar removal for all the catalysts.

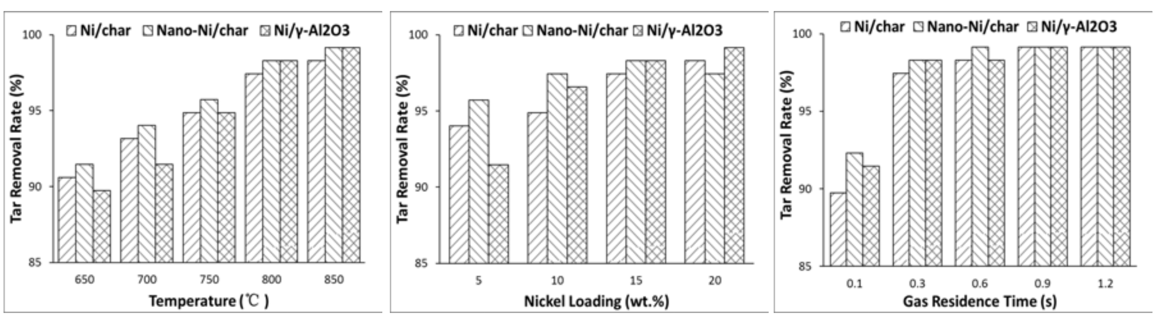

(a) (b) (c)

Fig. 2. Effect of catalytic reaction tempretature, nickle loading and gas residence time on tar removal.

H_2 enhancement

Fig. 3a shows H_2 concentrations affected by temperature using Ni/Char, nano-Ni/char, Ni/γ-Al_2O_3 and no catalyst systems. As expected, H_2 concentration increased with increasing temperature for all the catalysts. When temperature was below 750, H_2 concentrations in syngas reformed by Ni/char and Nano-Ni/char were higher than by Ni/γ-Al_2O_3. was increased with linear increment from 29.86 to 34.82 vol.% and from 29.04 to 39.17 vol.%, respectively. However, for Ni/γ-Al_2O_3 catalyst, H_2 concentration had a slow increase before 750°C, then increased rapidly from 30.90 to 44.94 vol.%. At a previous study (Wang et al. 2011), it has been verified that the heavy tars decompose into the small hydrocarbons (small hydrocarbons mean several C1-C5 gas presented in the syngas, which has been used by Corella) at a relatively low temperature (~700°C) while char as catalysts, and the same phenomenon will not happen by Al_2O_3 catalysts (Wang et al., 2010a). In terms of Le et al. (2009), the light tars are easier react with steam or CO_2 to produce H_2 than heavy tars by nickel catalyst. Therefore, H_2 concentration in syngas is higher for Ni/char and Nano-Ni/char catalysts than Ni/γ-Al_2O_3 catalyst while the temperature was under 750°C. Compared with the Ni/char and nano-Ni/char catalyst, higher H_2 concentration was achieved by Ni/γ-Al_2O_3 catalyst when the temperature was over 800°C, which is due to Ni/γ-Al_2O_3 catalyst prepared by the impregnation method better than Ni/char and nano-Ni/char catalyst prepared by mechanically mixed method for favoring water gas shift reactions (WGS) ($CO+H_2O \rightarrow CO_2+H_2$) at a relatively high temperature. The similar phenomenon was also found by Kinoshita et al. (1995) who reported that H_2 concentration kept stability up to 700°C, then increased rapidly, which showed Ni/γ-Al_2O_3 catalyst favored the WGS strongly at the condition of higher than 700°C reaction temperature. Several other authors (Lv et al., 2004; Kimura et al., 2006) also reported Ni-based catalyst favored the WGS reactions significantly in the syngas reforming process.

The effect of Ni loading on syngas composition is shown in Fig. 3b. With the increase of nickel content from 5% to 20%, H_2 concentration significantly increased from 29.79 to 34.33 vol.% for Ni/char and from 27.29 to 38.70 vol.% for Ni/γ-Al_2O_3 catalyst, which suggests that it is mainly Ni that enhanced H_2 generation. H_2 concentration almost reached the highest value up to 37.39 vol.% for Ni/γ-Al_2O_3 with 15 wt% nickel loading, meanwhile, CO concentration significantly decreased with the nickel loading increased. It again indicated nickel catalyst strongly favored WGS reactions as section 3.2.1 discussed. However, for nano-Ni/char catalyst, H_2 concentration increased significantly from 31.03 to 36.73 vol.% when Ni loading increased from 5 to 15 wt.%, then decreased to 33.83 vol.% with Ni loading further increased to 20 wt.%.

Fig. 3c shows the change of concentrations of H_2 at various gas residence times. It can be found that H_2 concentration increased sharply when gas residence time increased from 0.1 s to 0.3 s. After 0.3 s, increase of H_2 concentration slowed down, similar to the trend of tar removal rate. H_2 concentration closed to reach the highest value at 0.9 s gas residence time, 37.42 vol.% of Ni/char, 42.35 vol.% of nano-Ni/char and 49.23 vol.% of Ni/γ-Al_2O_3 catalyst, respectively.

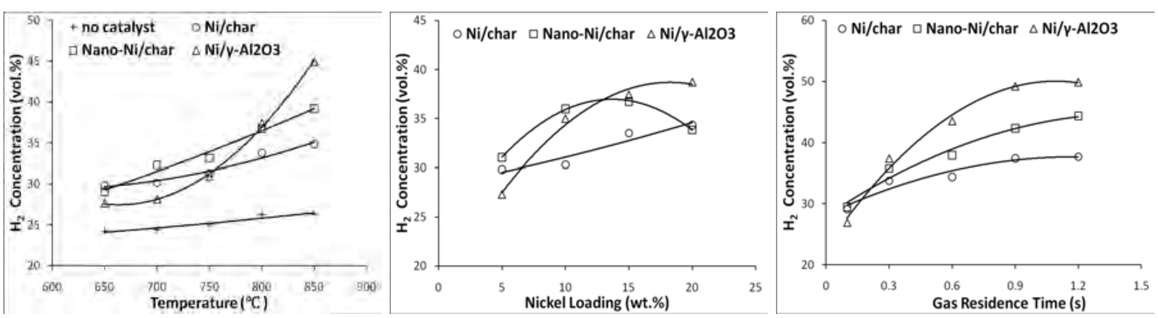

(a) (b) (c)

Fig. 3. Effect of catalytic reaction tempretature, nickle loading and gas residence time on H_2 concentration in syngas.

Conclusions

Char and two sizes of NiO particles were mechanically mixed at various ratios and tested in a laboratory-scale updraft biomass gasifier. Ni/γ-Al_2O_3 catalysts were prepared by using the impregnation and calcining method as a baseline for comparison. SEM/EDX analysis showed that nano-Ni particles uniformly distributed at the surface of char which even obtained better distribution than Ni/γ-Al_2O_3 catalyst prepared by impregnation method. Nano-Ni/char and Ni/

char catalysts showed promising results for tar removal and H_2 enhancement of biomass syngas. Using char as the catalyst support also possesses several advantages, such as being more economical, reduced use of NiO in reforming, and energy and time saving in catalyst preparation.

Acknowledgements

The authors thank the U.S. Department of Transportation and Sun Grant (DTOS59-07-G-00053) and the U.S. Department of Energy (DE-EE0000620) for their financial support. Part of this work was also supported by the startup fund of North Carolina State University.

References

Baker, E.G., Mudge, L.K., 1984. Mechanisms of catalytic biomass gasification. Journal of Analytical and Applied Pyrolysis. 6(3), 285-297.

Bangala, D.N., Abatzoglou, N., Chornet, E., 1998. Steam reforming of naphthalene on Ni-Cr/ Al_2O_3 catalysts doped with MgO, TiO_2, and La_2O_3. AIChe Journal. 44(4), 927-936.

Bao, J., Sun, Z., Fu, Y., Bian, G., Zhang, Y., Tsubaki, N., 2009. Mixed alcohol synthesis from syngas on K-Co-Mo/C catalyst prepared by a sol-gel method. Topics in catalysis. 52(6-7), 789-794.

Bartholomew, C.H., Farrauto, R.J., 1976. Chemistry of nickel-alumina catalysts. J. Catal. 45(1), 41-53.

Courson, C., Udron, L., Ski, D.W., Petit, C., Kiennemann, A., 2002. Hydrogen production from biomass gasification on nickel catalysts: Tests for dry reforming of methane. Catalysis Today. 76(1), 75-86.

Dou, B., Gao, J., Sha, X., Baek, S.W., 2003. Catalytic cracking of tar component from high – temperature fuel gas. Applied Thermal Engineering. 23(17), 2229-2239.

Dunn, B.C., Covington, D.J., Cole, P., Pugmire, R.J., Meuzelaar, H.L.C., Ernst, R.D., Heider, E.C., Eyring, E.M., 2004. Silica xerogel supported cobalt metal Fischer-Tropsch catalysts for syngas to diesel range fuel conversion. Energy and Fuel. 18(5), 1519-1521.

Furusawa, T., Tsutsumi, A., 2005. Comparison of Co/MgO and Ni/MgO catalysts for the steam reforming of naphthalene as a model compound of tar derived from biomass gasification. Applied Catalysis A: General. 278(2), 207-212.

Gilbert, P., Ryu, C., Sharific, V., Swithenbank, J., 2009. Tar reduction in pyrolysis vapours from biomass over a hot char bed. Bioresource Technology. 100(23), 6045-6051.

Jansen, J.C., Jönsson, K., Hagman, M., 2002. Biological detoxification of tar-water. Water. Sci. Technol. 46(4-5), 59-65.

Kimura, T., Miyazawa, T., Nishikawa, J., Kado, S., Okumura, K., Miyao, T., Naito, S., Kunimori, K., Tomishige, K., 2006, Development of Ni catalysts for tar removal by steam gasification of biomass. Applied Catalysis B: Environmental. 68,160-170.

Kinoshita, C.M., Wang, Y., Zhou, J., 1995. Effect of reformer conditions on catalytic reforming of biomass-gasification tars. Ind. Eng. Chem. Res. 34(9), 2949-2954.

Le, D.D., Xiao, X., Morishita, K., Takarada, T., 2009. Biomass gasification using nickel loaded brown coal char in fluidized bed gasifier at relatively low temperature. Journal of Chemical Engineering of Japan, 42(1), 51-57.

Lee, I.G., Ihm, S.K., 2009. Catalytic gasification of glucose over Ni/activated charcoal in supercritical water. Ind. Eng. Chem. Res. 48(3), 1435-1442.

Leppala, H.J., Simell, P., Kurkela, E., 1991. Catalytic conversion of nitrogen compounds in gasification gas. Fuel Process Technol. 29(1-2), 43-56.

Li, J., Yan, R., Xiao, B., Liang, D.T., Du L., 2008. Development of Nano-NiO/AlO catalyst to be used for tar removal in biomass gasification. Environ. Sci. Technol. 42(16), 6224–6229.

Lv, P., Chang, J., Wang, T.J., Fu, Y., Chen, Y., 2004. Hydrogen-Rich gas production from biomass catalytic gasification. Energy Fuels. 18, 228-233.

Mao, D., Xia, J., Chen, Q., Lu, G., 2009. Highly effective conversion of syngas to dimethyl ether over the hydrid catalysts containing high-silica HMCM-22 zeolites. Catalysis Communications. 10(5), 620-624.

Nair, S.A., Pemen, A.J.M., Yan, K., Van Heesch, E.J.M., Ptasinski, K.J., Drinkenburg, A.A.H., 2003. Chemical processes in tar removal from biomass derived fuel gas by pulsed corona discharges. Plasma Chemistry and Plasma Processing. 23(4), 665-80.

Narváez, I., Corellar, J., Orío, A., 1997. Fresh tar (from a Biomass Gasifier) elimination over a commercial steam-reforming catalyst. Kinetics and effect of different variables of operation. Ind. Eng. Chem. Res. 36(2), 317-327.

Narvpaez, I., Orío, A., Aznar, M.P., Corella, J., 1996. Biomass gasification with air in an atmospheric bubbling fluidized bed. Effect of six operational variables on the quality of produced raw gas. Ind. Eng. Chem. Res. 35(7), 2110-2120.

Park, H.J., Park S.H., Sohn, J.M., Park, J., Jeon, J.K., Kim, S.S., Park, Y.K., 2010. Steam reforming of biomass gasification tar using benzene as a model compound over various Ni supported metal oxide catalysts. Bioresource Technology. 101(1), 101-103.

Pis, J.J., Mahamud, M., Pajares, J.A., Parra, J.B., Bansal, R.C., 1998. Preparation of active carbons from coal part 3: Activation of char. Fuel Processing Technology. 57, 149-161.

Sims, R.E.H., Mabee, W., Saddler, J.N., Taylor, M. 2010. An overview of second generation biofuel technologies. 101, 1570-1580.

Suzuki, T., Ohme, H., Watanabe, Y., 1992. Alkali metal catalyzed carbon dioxide gasification of carbon. Energy Fuels. 6(4), 343-351.

Tamhankar, S.S., Tsuchiya, K., Riggs J.B., 1985. Catalytic cracking of benzene on iron oxide-silica:catalyst activity and reaction mechanism. Applied Catalysis. 16(1), 103-121.

Wang, D., Yuan, W., Ji., W. 2010. Effective syngas cleanup and reforming using Ni/γ-Al_2O_3 catalyst. International Journal of Agricultural and Biological Engineering. 3(2):39-45.

Wang, D., Yuan, W., Ji, W., 2010. Use of biomass hydrothermal conversion char as the Ni catalyst support in Benzene and gasification tar. Transactions of the ASABE. 53(3), 795-800.

Wang, D. Yuan, W., Ji, W., 2011. Char and char-supported nickel catalysts for secondary syngas cleanup and conditioning. Applied Energy. 88(5), 1656-1663.

Wang, T.J., Chang, J., Wu, C.Z., Fu, Y., Chen, Y., 2005. The steam reforming of naphthalene over a nickel–dolomite cracking catalyst. Biomass and Bioenergy. 28(5), 508-514.

Wojcieszak, R., Zieliński, M., Monteverdi, M., Bettahar, M.M., 2006. Study of nickel nanoparticles supported on activated carbon prepared by aqueous hydrazine reduction. Journal of Colloid and Interface Science. 299(1), 238-248.

Yu, Q.Z., Brage, C., Nordgreen, T., Sjostrom, K., 2009. Effects of Chinese dolomites on tar cracking in gasification of birch. Fuel. 88, 1922-1926.

Zhao, H., Draelants, K.J., Baron, G.V., 2000. Performance of a nickel-activated candle filter for naphthalene cracking in synthetic biomass gasification gas. Ind. Eng. Chem. Res. 39(9), 3195-3201.

3.12
GASIFICATION OF SOUTHERN FOREST RESOURCES

Thomas Elder[1], Leslie H. Groom[1], Nicole Labbé[2], Priyanka Bhattacharya[2]*

Abstract

Southern pine and mixed hardwoods have been gasified using a pilot scale system, with varying process conditions. The unit consumes 35-70 pounds of wood chips per hours as a function of the gas flow rate. The synthesis gas, composed of carbon monoxide, carbon dioxide, hydrogen and methane has an energy content of approximately 6 MJ/m^3. Gas samples have been collected for catalytic upgrading to produce synthetic gasoline and diesel.

Keywords: gasification, southern pine, mixed-hardwoods, catalysis

Introduction

The large scale gasification of biomass for the production of energy and chemicals dates back to at least World War II (Vera and Jurado 2009), during which it was widely practiced in Europe. Given the renewed interest in fuels from sustainable, domestic resources, gasification is again receiving attention at a range of scales.

The current paper is concerned with the operation and performance of a pilot-scale unit, using woody biomass from the southern United States (Elder and Groom 2011). Similar downdraft gasifiers have been used for work reported by Diebold et al. (2006), Gautam et al. (2011b) and Wei et al. (2009). Hardwood chips at 10-19% moisture content were gasified with at temperatures from 750 to 950°C and gas flow rates 35-55 scmh. Carbon monoxide and heating value decreased with moisture content while tar production increased (Wei et al. 2009). It has also been reported that the use of pelletized wood resulted in higher tar levels than chips (Gautam et al. 2011a).

Methods

The gasifier used in this work is a computer controlled, open-top, downdraft unit manufactured by Community Power Corporation of Littleton, Colorado. The gasifier itself is approximately 47 inches tall and 14 inches in diameter (Figure 1), with combustion air added at five levels, and operating at 800-900°C. The gas exits at about 600°C, is cooled with a shell and tube heat exchanger to about 100°C, and filtered. The gas produced is analyzed for carbon monoxide, carbon dioxide, hydrogen, methane and oxygen with a NOVA 7500P5 infrared gas analyzer. Temperatures, pressures and gas composition are collected in real time. The flow rate through the gasifier was varied from 40-70 scmh. Upon reaching operating temperature, the gasifier was equilibrated for an hour, with data collected for the next three hours. Southern pine and mixed southern hardwoods (oak, hickory, sweetgum, maple) have been used as the furnish. The wood has been chipped and pre-dried to approximately 15% moisture content.

Gas samples have been compressed to be used Fischer-Tropsch synthesis for conversion to liquid fuels, using a bench scale high-pressure, high-temperature reactor.

[1] *USDA-Forest Service, Southern Research Station, LA*

[2] *Center for Renewable Carbon, The University of Tennessee, TN*

** Corresponding author*

Figure 1. Gasifier

Results

The composition of the synthesis gas produced with varying flow rate is as shown in Table 1. The pine samples have slightly higher levels of carbon monoxide, while the hardwoods are somewhat higher for the other gases. The energy value of the gas as a function of flow rate is as shown in Figure 2. The values of ~6 MJ m^{-1} are fairly consistent except at the highest flow rate, where the hardwoods are higher. This is in agreement with the gas composition results indicating that the syngas from the pine has lowered levels of hydrogen and methane in comparison to the hardwoods. The efficiency of the gasifier with flow rate is shown in Figure 2. It can be seen that there is an abrupt increase in efficiency at the higher flow rates, which depending on the objectives of a given run, may be an important factor to control.

Table 1. Syngas composition

Flow rate (scmh)	CO %		CO_2 %		H_2 %		CH_4 %	
	pine	hardwood	pine	hardwood	pine	hardwood	pine	hardwood
40	20.9±0.8	20.2±0.6	11.9±0.5	13.1±0.4	18.6±0.4	19.1±0.7	3.9±0.5	4.0±0.6
55	21.2±0.7	20.5±0.5	11.9±0.6	12.8±0.3	18.6±0.3	19.2±0.3	3.6±0.6	3.6±0.3
62	21.3±0.5	20.7±0.7	11.8±0.4	12.9±0.5	18.9±0.3	19.1±0.4	3.6±0.5	3.7±0.5
70	20.9±.5	20.8±0.6	12.1±0.4	13.0±0.5	18.6±0.3	19.3±0.4	3.3±0.4	3.6±0.4

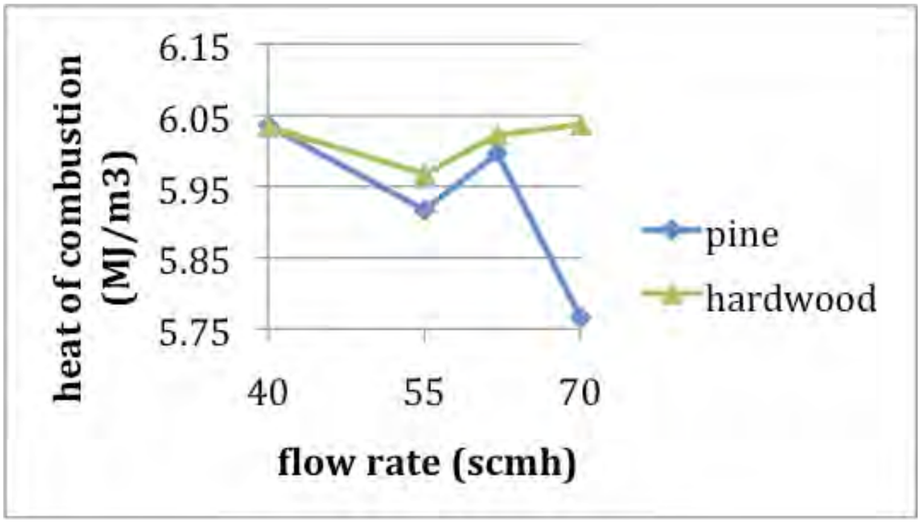

Figure 2. Energy values of syngas

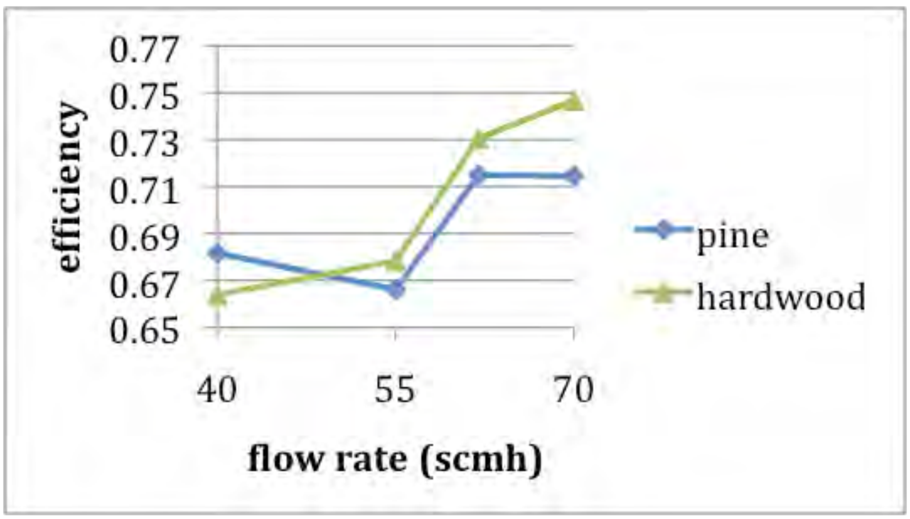

Figure 3. Efficiencies of gasifier

References

Diebold J.P., K. Browne, D. Duncan, M. Fields, T. Smith, and M. Walker (2006). "The BioMax 15: the automation, integration and pre-commercial testing of an advanced down-draft gasifier and engine/gen set". In: *Science in thermal and chemical conversion of biomass*, Ed. A.V. Bridgwater and D.G.B Boocock, 894-907, UK: Cpl Press.

Elder, T. and L. Groom (2011). "Pilot-scale gasification of woody biomass," *Biomass and Bioenergy* 35:3522-3528.

Gautam, G., S. Adhikari, S. Thangalazhy-Gopakumar, C. Brodbeck, S. Bhavnani, and S. Taylor (2011a). "Tar analysis in syngas derived from pelletized biomass in a commercial stratified downdraft gasifier," *BioResources* 6:4652-4661.

Gautam, G., S. Adhikari, C. Brodbeck, S. Bhavnani, O. Fasina, and S. Taylor (2011b). "Gasification of wood chips, agricultural residues and waste using a downdraft commercial gasifier," *Trans of ASABE* 54:1801-1807.

Vera, D. and F. Juarado (2009). "Biomass gasification systems integrated with fuel cells and microturbines" In: *Biomass Gasification. Chemistry, Processes and Applications*. Ed. J-P. Badeau and A. Levi, 231-270, New York, Nova Science Publishers.

Wei L. J.A. Thomasson, R.M. Brick, R. Sui, J.R. Wooten and E.P. Columbus (2009). "Syn-gas quality evaluation for biomass gasification with a downdraft gasifier". *Transactions ASABE* 52:21-37

3.13
Effects of Biomass Feedstocks, Gasifier Design and Conditions on Physiochemical Properties of Biochar

Ajay Kumar[1,], Kezhen Qian[1], Krushna N. Patil[1], Raymond L. Huhnke[1]*

Abstract

Biochar is a low-value byproduct of biomass gasification and pyrolysis with many potential applications, such as for soil amendment, synthesis of activated carbon and carbon-based catalysts. Considering the high-value applications, biochar can provide economic benefit to the biorefinery. However, the properties of biochar depend heavily on biomass feedstocks, gasifier design and operating conditions. The effects on biochar properties must be better understood so that different biochars can be made suitable for various applications. This paper summarizes the results of the physiochemical properties of biochar derived from gasification of switchgrass and forage sorghum at three equivalence ratios: 0.20, 0.25 and 0.28. The surface area results showed all biochar samples were less than 10 m^2/g. The highest volatile content was obtained at an equivalence ratio of 0.28 while the lowest was at 0.25. As expected, ash content of biochar was much higher than that of the original biomass. Biochar ash content increased with the equivalence ratio. All samples showed large peaks in FTIR spectra where the silicon band vibration occurs. FTIR spectra showed that aliphatic structure was available in biomass but not in biochar.

Key words: biochar, gasification, fluidized bed, property

Introduction

Traditionally, biochar is produced by heating biomass in the absence of O_2, called slow pyrolysis. Biochar is also a byproduct of gasification and fast pyrolysis (Mohamed, Alauddin, Lahijani, & Mohammadi, 2010). Although the target product of gasification and fast pyrolysis are syngas and bio-oil, respectively, a large quantity of biochar is often produced. Currently, biochar is disposed of or combusted because high-value use of biochar is currently not available. Identifying high-value applications of biochar can provide economic benefits to the biorefinery.

As soil amendment, biochar can increase soil fertility and agricultural productivity (Meyer, Glaser, & Quicker, 2011). Making activated carbon from biochar is another potential application (Oleszczuk, Hale, Lehmann, & Cornelissen, 2012). Activated carbon is a form of carbon with high surface area and large amounts of pore space which is available for catalysis of chemical reactions and for physical sorption such as purification of waste water (Lima & Marshall, 2005). Recently, researchers have found that the raw biochar has relative high catalyzing activity in syngas cleaning (Abu El-Rub, Bramer, & Brem, 2008; Wang, Yuan, & Ji, 2011). Developing biochar-based catalyst for syngas cleaning may become another novel high-value application.

Properties of biochar depend heavily on biomass feedstocks, gasifier design and operating conditions. The property of biomass such as the mineral content, element component, and fiber structure may affect the resulted biochar. The effects on biochar properties must be understood so that different biochar can be made suitable for various applications. For example, biochar with high ash content and low porosity may not be suitable for producing activated carbon (Dąbrowski, Podkościelny, Hubicki, & Barczak, 2005). Although some studies on investigation property of biochar made through pyrolysis and gasification are available (Brewer, Schmidt-Rohr, Satrio, & Brown, 2009; Cantrell, Hunt, Uchimiya, Novak, & Ro, 2012), the biochars used in these studies were not made at same reaction conditions or with same feedstocks. Effects of reaction conditions on properties of biochar are mostly unknown, which limits the use of biochar

[1] *Biosystems & Agricultural Department, Biobased Products & Energy Center, Oklahoma State University, OK*

* *Corresponding author*

for novel and high-value applications. Our objective was to study the physiochemical properties of switchgrass and sorghum biochar made through gasification at three air-to-biomass flowrates.

Materials and Methods

Material

Two types of biomass feedstocks, switchgrass (Kanlow) and forage sorghum were obtained from Oklahoma State University Agronomy Research Station. Large round bales of switchgrass and sorghum were chopped by a Haybuster tub grinder. Particle size was less than 1.5 mm. Proximate analysis of the feedstocks are showed in table 1.

Table 1. Proximate analysis of feedstocks

Proximate	Switchgrass	Forage Sorghum
Moisture (wt% wb)	9.7	9.39
Volatile matter (wt%)	70.36	68.1
Ash (wt%)	4.62	5.05
Fixed carbon (wt%)	15.02	17.46

Fluidized bed gasification

The two feedstocks were gasified in a lab-scale fluidized bed gasifier at three equivalence ratios (ER) of 0.20, 0.25 and 0.28. ER is defined as the ratio of total air and biomass supplied to gasifier (Sharma, Kumar, Patil, & Huhnke, 2011). A screw feeder injected the biomass into the gasifier. Silica sand was used as fluidizing bed material. Detailed information on the performance of the gasifier using switchgrass is available in Sharma et al. (2011).

Biochar property analysis

The biomass and resulting biochar were analyzed by proximate, energy content, Brunauer–Emmett–Teller BET, Fourier transformed infrared spectroscopy (FTIR). Proximate analysis was determined using a thermogravimetric analyzer (TGA). The energy content or higher heating value (HHV) was determined using a bomb calorimeter (Parr instrument 6200). The surface areas were measured via N_2 adsorption using a surface area analyzer (Quantachrome). The data were analyzed by BET theory. The biochar functional structural analysis was performed using (FTIR) (Nicolet ATR FTIR 6700) and all biochar samples were analyzed without any pretreatments. The FTIR spectral peaks were analyzed by characteristic vibrations data (Silverstein, Webster, & Kiemle, 2005).

Results and Discussion

The proximate and surface area data of raw material and biochar are shown in table 2. The gasification process resulted in the clear differences between raw material and biochar. Moisture content of the raw material was around 9% (wet basis) while the biochar was no more than 4%. The biochar contained 10-20% volatile matter while the raw material contained 70%; therefore, the raw material lost most of the volatile matter during gasification. The ash contents of biochar were much higher than raw biomass, indicating the ash component in biomass remained in biomass during gasification. The high ash content in biochar may prevent its use for many applications. The surface areas of the biochar from both feedstocks were relatively low (< 5 m^2/g). This is considered a disadvantage for fluidized bed gasification biochar because low surface areas are not suitable for making activated carbon or catalysts.

Table 2. Proximate analysis, higher heating value (HHV) and BET surface area of biochar made at different conditions

Biomass	ER*	Moisture (wt% wb)	Volatile (wt%)	Ash (wt %)	Fixed carbon (wt%)	Higher Heating value (MJ/Kg)	BET surface area (m^2/g)
Switchgrass	0.20	0.69	12.69	51.61	34.99	7.40	1.3
	0.25	4.01	16.86	57.70	21.42	4.03	5.2
	0.28	1.83	12.11	64.07	21.98	6.70	2.0
Forage Sorghum	0.20	1.99	14.24	53.89	30.76	4.18	1.0
	0.25	1.94	20.01	45.94	32.10	9.42	0.7
	0.28	0.01	11.36	54.87	31.77	4.63	-

*Equivalence Ratio.

The heating value of the biochars ranged from 4-10 MJ/Kg, which is also low compared to raw biomass or other combustible fuels such as coal. In addition to the gasification process effect on the property difference between biomass and biochar, the different ER ratios also affected biochar properties. Biochar from gasification at 0.25 ER had the highest volatile matter content while the lowest volatile content was measured at 0.28 ER. Ash content of the biochar increased as ER ratio increased, i.e. switchgrass and sorghum biochar ash content increased from 51% to 64% and 53% to 55%, respectively. It was observed that the heating value of biochar correlates with the fixed carbon content. The biochar with the highest fixed carbon had the highest heating values. There was no obvious trend in the BET surface areas among these biochars.

Figure 1 shows the FTIR spectra of selected four biochars, switchgrass and sorghum. All of the six samples showed a large peak at 1000 cm^{-1}, where the silicon band vibration occurs. This peak indicates that the biomass and biochar contain relatively high levels of silica. There are broad peaks at around 3400 cm^{-1} (O-H stretching) found in switchgrass, sorghum, char of sorghum but not in char of switchgrass. Around 2950-2800 cm^{-1}, FTIR peaks are found in switchgrass and sorghum spectra but was not noticeable in biochars derived from sorghum and switchgrass. These peaks are associated with the aliphatic C-H stretching which suggests the raw material has more aliphatic structure than gasified char. The peaks around 780 cm^{-1} correlated with aromatic C-H bending which clearly was seen in the switchgrass biochar but not in sorghum biochar. Another difference between the sorghum biochar spectra and switchgrass biochar spectra is that only sorghum biochar had peak around 1375 cm^{-1}, which corresponds to O–H bending of phenols.

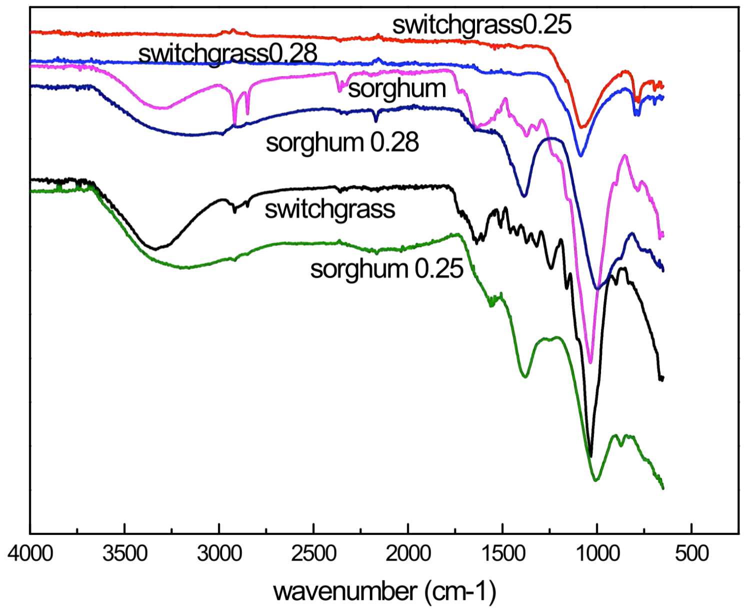

Figure 1. FTIR spectra of switchgrass, sorghum, switchgrass char and sorghum char

Conclusion

The moisture and volatile content of biochar were much lower than the raw material. The fixed carbon content increased in the biochar compared with raw material. ER ratio effected biochar property in that. Biochar from 0.25 ER gasifier operation had the highest volatile matter content while 0.28 ER ratio resulted in biochar having the lowest. Ash content increased with the ER ratio, indicating that higher conversion of biomass carbon into gaseous products with increase in ER. Surface areas of all biochars were all less than 10 m^2/g, which must be increased if used to make activated carbon. The FTIR spectrum showed the variation in the structure of switchgrass, sorghum and chars from both feedstocks. The FTIR spectra of sorghum and switchgrass were similar. The raw biomass showed aliphatic structure, which were not noticeable in biochars.

References

Abu El-Rub, Z., Bramer, E. A., & Brem, G. (2008). Experimental comparison of biomass chars with other catalysts for tar reduction. *Fuel, 87*(10–11), 2243-2252. doi: 10.1016/j.fuel.2008.01.004

Brewer, C. E., Schmidt-Rohr, K., Satrio, J. A., & Brown, R. C. (2009). Characterization of biochar from fast pyrolysis and gasification systems. *Environmental Progress & Sustainable Energy, 28*(3), 386-396. doi: 10.1002/ep.10378

Cantrell, K. B., Hunt, P. G., Uchimiya, M., Novak, J. M., & Ro, K. S. (2012). Impact of pyrolysis temperature and manure source on physicochemical characteristics of biochar. *Bioresource Technology, 107*(0), 419-428. doi: 10.1016/j.biortech.2011.11.084

Dąbrowski, A., Podkościelny, P., Hubicki, Z., & Barczak, M. (2005). Adsorption of phenolic compounds by activated carbon—a critical review. *Chemosphere, 58*(8), 1049-1070. doi: 10.1016/j.chemosphere.2004.09.067

Lima, I. M., & Marshall, W. E. (2005). Adsorption of selected environmentally important metals by poultry manure-based granular activated carbons. *Journal of Chemical Technology and Biotechnology, 80*(9), 1054-1061. doi: 10.1002/jctb.1283

Meyer, S., Glaser, B., & Quicker, P. (2011). Technical, Economical, and Climate-Related Aspects of Biochar Production Technologies: A Literature Review. [Review]. *Environmental Science & Technology, 45*(22), 9473-9483. doi: 10.1021/es201792c

Mohamed, A. R., Alauddin, Z. A. B. Z., Lahijani, P., & Mohammadi, M. (2010). Gasification of lignocellulosic biomass in fluidized beds for renewable energy development: A review. *Renewable & Sustainable Energy Reviews, 14*(9), 2852-2862. doi: DOI 10.1016/j.rser.2010.07.026

Oleszczuk, P., Hale, S. E., Lehmann, J., & Cornelissen, G. (2012). Activated carbon and biochar amendments decrease pore-water concentrations of polycyclic aromatic hydrocarbons (PAHs) in sewage sludge. *Bioresource Technology, 111*(0), 84-91. doi: 10.1016/j.biortech.2012.02.030

Sharma, A., Kumar, A., Patil, K., & Huhnke, R. (2011). Performance evaluation of a lab-scale fluidized bed gasifier using switchgrass as feedstock. *Transactions of the ASABE, 54*(6), 2259-2266.

Silverstein, R. M., Webster, F. X., & Kiemle, D. J. (2005). *Spectrometric identification of organic compounds* (7 ed.): John Wiley & Sons.

Wang, D., Yuan, W., & Ji, W. (2011). Char and char-supported nickel catalysts for secondary syngas cleanup and conditioning. *Applied Energy, 88*(5), 1656-1663. doi: 10.1016/j.apenergy.2010.11.041

Zhang, A., Bian, R., Pan, G., Cui, L., Hussain, Q., Li, L., . . . Yu, X. (2012). Effects of biochar amendment on soil quality, crop yield and greenhouse gas emission in a Chinese rice paddy: A field study of 2 consecutive rice growing cycles. *Field Crops Research, 127*(0), 153-160. doi: 10.1016/j.fcr.2011.11.020

3.14 Lignin as a Material Platform for Bio-derived Macromolecules and Fibers

Meghan E. Wilt[1], Maryam Mazloumpour[1], Orlando Rojas[2], Julie A. Willoughby[1,]*

Abstract

The abundance of lignin, the second major component of wood and annual plants, provides an ample feedstock for conversion to viable macromolecule materials. Our research focuses on the production of high-value added materials derived from lignin including micro- and nano- fibers, surfactants for fuel emulsions, and resin-coated proppants. Our initial work evaluated the compatibility of silicon-containing plasticizers with a commercial kraft lignin, Indulin AT. Lignin's highly branched molecular structure limits it use as a carbon fiber precursor due to its inherent brittle nature. Lignin's rich carbon content and abundance in nature highly motivates the elimination of this challenge. Utilizing an inherently flexible poly(dimethylsiloxane) (PDMS) co-polymer, we successfully electrospun core-sheath (lignin-PDMS) microparticles and microfibers. Tuning the morphology of the resultant materials is enabled through control of solvent, viscosity, and surface tension of the initial formulation. Preliminary thermal analysis data indicates an interaction between the silicon-containing component and Indulin AT. This work represents a key starting point for fundamental understanding on the interfacial compatibility between these two components. Future work aims to convert the particles and fibers to ceramic-carbon materials through pyrolysis.

Keywords: interfacial properties, thermal stability, fibers, particles, Indulin AT, silane, silicone

Introduction

As lignin is a highly branched poly(aromatic) molecule comprising phenylpropanes units[1], it can be used for the production of cost-effective carbonaceous materials if properly exploited. This is especially true as its barriers as a macromolecule feedstock becomes irrelevant if converted to a carbon fiber form.[1-3] Both traditional technical and organosolv lignins have been studied for the production of carbon fibers.[4-9] Unit operations for lignin-based carbon fiber processing encompass solution spinning and thermal extrusion techniques. A main issue with spinning lignin fibers is their inherent brittle nature. To circumvent this problem, lignin-synthetic polymer fibers have been produced from polyethylene terephthalate (PET), polyethylene oxide (PEO) and polypropylene (PP).[4,10-15] Plasticizing lignin fibers with silicone precursors is a novel approach to make the lignin fiber processing feasible and impart the advantages of silicon-containing materials. Silicon- containing materials have high heat stability, low surface energy and intrinsic backbone flexibility; attributes that often result in high performing, cost-effective products as compared to their hydrocarbon counterparts. The current study focuses on combining silicone materials with lignin feedstock to create precursors for polymeric derived ceramics (PDC)-carbon materials. The study objectives include 1) determine a silicon- containing polymer for blending with a kraft lignin, Indulin AT, 2) evaluate thermal properties of the silicone-lignin blend and 3) examine the feasibility of electrospinning a silicone-lignin solution.

Preparation and Characterization of Silicone Lignin Blends

Silicone polyamide (SiPA) was obtained from Dow Corning Corporation (Midland, MI). While the amide component will not contribute to the conversion of PDCs, it solidifies the silicone to

[1] *Department of Textile Engineering, Chemistry and Science, North Carolina State University, NC*

[2] *Department of Forest Biomaterials, North Carolina State University, NC*

* *Corresponding author*

make electrospinning feasible. Indulin AT from MeadWestvaco (Charleston SC) was used as the lignin source. A lignin and SiPA blend at equal weight ratios was heated in a 100°C oven followed by compounding with a mortar and pestle (Indulin_SiPA). The cooled Indulin_SiPA blend was solubilized in tetrahydrofuran (THF, Sigma Aldrich) at 10 and 20 weight percent solutions.

The surface tension of each solution was measured using the Wilhelmy plate method via a tensiometer instrument (DCAT11) from Future Digital Scientific Corporation equipped with SCAT11 software (cf. Table 1). The mass concentrations of lignin and silicone polyamide did not have a significant impact on the surface tension of the solution. THF's surface tension was the dominating factor contributing to the Indulin_SiPA solution surface tension since little variance in the values was observed between all samples. The kinematic viscosity of the electrospinning solutions was measured using a u-tube viscometer (*cf.* Table 1). The mass concentration of lignin did not have a significant impact on the viscosity of the solution. However, the mass concentration of silicone polyamide affected significantly the viscosity of the solution; for example, the 20 wt% Indulin_SiPA blend was over ten times more viscous than the corresponding lignin solution at the same solids level.

Table 1. Surface tension of the lignin and SiPA blend in THF

Sample	Surface Tension (mN/m)	Kinematic Viscosity (cSt)
Tetrahydrofuran	26.0	0.6
10% Indulin AT	25.1	0.7
20% Indulin AT	25.4	0.8*
10% SiPA	25.6	8.0
20% SiPA	25.3	29.2
20% Indulin AT_SiPA	25.4	11.8

Thermal Characterization was completed through the use of differential scanning calorimetry (DSC) and thermogravimetric analysis (TGA) using TA® instruments with heating and cooling rates of 5°C/minute. DSC evaluated the miscibility of the blended polymers and associated glass transition temperatures. Figure 1 shows the heat flow versus temperature data for Indulin AT, SiPA, and the 50:50 (wt) Indulin_SiPA blend. The broad endothermic curve from 100 to 250°C for Indulin AT is indicative of its branched, 3-dimensional structure. The moisture removal from lignin starts at 100°C. With further heating, the DSC profile shows a broad endothermic peak at 177 °C due to endothermic volatilization.[16] SiPA, shows its first temperature transition around -100° C, the polymer's glass transition temperature (T_g). Pure silicone (polydimethylsiloxane) has a comparatively lower Tg, ~123°C. The higher T_g of SiPA is attributed to the intramolecular hydrogen bonding occurring between amide blocks. The second exothermic peak observed at -94°C corresponds to the crystalline temperature (T_c) of polydimethylsiloxane block with the last distinct endothermic peak at -51 °C attributed to the corresponding melting transition (T_m) of silicone. As the fraction of amide component is small, the exothermic peak observed at ~185°C is appropriately less significant than the silicone counterpart. However, this small fraction is enough for the SiPA to be solid at room temperature. Blending Indulin AT with SiPA significantly changes the heating capacity behavior of both components. The endothermic peak at ~-51°C is retained after compounding; however, no glassy or crystalline point is recorded for SiPA. Meanwhile the second sharp peak is recorded at 172°C which is attributed to the preservation of pyrolysis peak of Indulin AT, after this point a sharp exothermic transition occurrs; likely attributed to thermal decomposition.

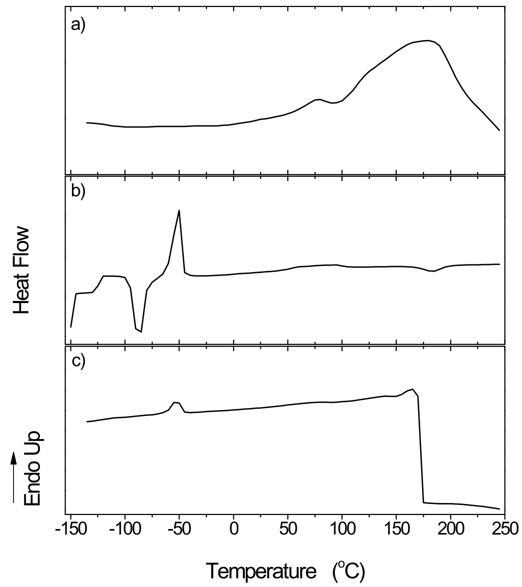

Figure 1. Differential scanning analysis of a) Indulin AT, b) silicone polyamide (SiPA), and c) Indulin AT_SiPA, 50:50 weight percent blend.

Figure 2 depicts the percent weight loss of the Indulin AT and the Indulin_SiPA as a function of temperature. Higher weight loss for silicone polyamide versus lignin is attributed to the amide component. Significant weight loss of a compound at temperatures above its melting transition makes melt spinning difficult. As this processing method for spinning fibers is commercially viable compared to electrospinning, future effort will focus on new silicone chemistries that enable *in situ* crosslinking during processing.

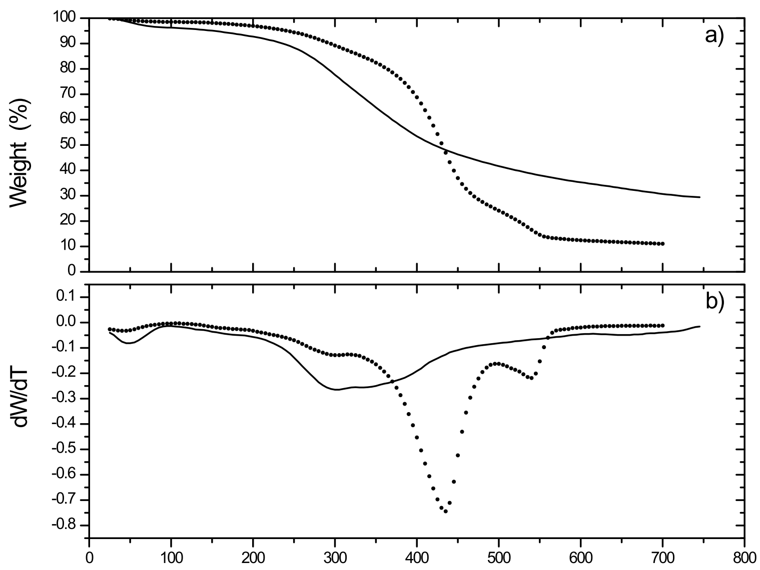

Figure 2. a) Percent weight loss as a function of temperature for Indulin AT (solid line) and 50:50 weight percent blend of Indulin AT and SiPA (dotted line) and b) differential weight loss as a function of temperature for Indulin AT (solid line) and 50:50 weight percent blend of Indulin AT and SiPA (dotted line).

Electrospinning Silicon Containing Materials with Lignin

The polymer solutions were electrospun using a standard electrospinning setup consisting of a syringe pump, a high-voltage power supply, and a ground collector. Scanning electron microscopy-energy disperse X-ray spectroscopy (SEM-EDX) was used for high resolution morphology imaging and elemental analysis of the fibers. Figure 3 illustrates the SEM micrographs of electrospun lignin, silicone polyamide, and Indulin_SiPA. Based on the solution properties for each material, namely viscosity, the process conditions for each run were varied until fiber formation was observed (cf. Figure 3c). We note the formation of short rod-like fibers with the Indulin_SiPa. Although not shown, we are also able to form Indulin_SiPA particles similar to the ones depicted for SiPA shown in Figure 3b. The elemental analysis for each imaged material is listed in Table 2 and indicates the distribution of silicon, carbon, and oxygen in the expected range.

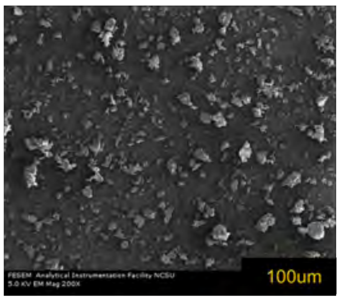

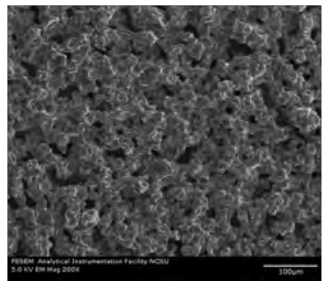

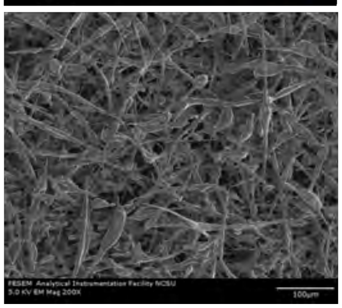

d).

Run Needle Tip to Plate Distance (cm) Flow Rate (uL/minute) Voltage (kV)

A 20 30 20

B 15 90 20

C 20 98 30

Figure 3. Scanning electron microscopy images for electrospinning of a) 10 weight percent lignin in THF (Run A), b) 10 weight percent silicone polyamine (SiPA) in THF (Run B), c) 20 weight percent of lignin_SiPA in THF (Run C), and d) electrospinning parameter conditions for each run.

Table 2. Elemental analysis of formed microparticles and rods via scanning electron microscopy-energy disperse X-ray spectroscopy

Element	Lignin in THF (10% solids)	Silicone Polyamide in THF (10% solids)	Lignin + Silicone Polyamide in THF (20% solids)
Carbon	81.6	21.0	50.8
Oxygen	13.6	12.6	16.4
Silicone	0.8	66.4	30.1
Sulfur	2.0	0.0	0.0
Sodium	1.7	0.0	0.8

Conclusions

We have shown the feasibility of producing silicone lignin microparticles and fiber-like rods. Future work will focus on optimizing the silicone chemistry and interfacial properties between the lignin and silicone compound.

Acknowledgements

The funding for this research was provided by NC State College of Textiles, American Chemical Society and The Southeastern Sun Grant Center at the University of Tennessee, project 2011-2079/8500022319 "Biorefinery LIgnins as Stabilizers of Emulsions for Power Generation". We gratefully acknowledge their support. We would also like to thank MeadWestvaco and Dow Corning Corporation for the respective samples of Indulin AT and silicone polyamide.

References

Gandini A, Coelho D, Gomes M, Reis B, Silvestre A. Materials from renewable resources based on furan monomers and furan chemistry: Work in progress. Journal of Materials Chemistry 2009;19(45):8656-64.

Kadla JF, Kubo S, Venditti RA, Gilbert RD, Compere AL, Griffith W. Lignin-based carbon fibers for composite fiber applications. Carbon 2002;40(15):2913-20.

Wang JS, Manley RS, Feldman D. Synthetic-polymer lignin copolymers and blends. Progress in Polymer Science 1992;17(4):611-46.

Dallmeyer I, Ko F, Kadla JF. Electrospinning of technical lignins for the production of fibrous networks. J Wood Chem Technol 2010;30(4):315-29.

Kubo S, Uraki Y, Sano Y. Preparation of carbon fibers from softwood lignin by atmospheric acetic acid pulping. Carbon 1998;36(7-8):1119-24.

Ma Xiaojun, Zhao Guangjie. Preparation of carbon fibers from liquefied wood. Wood Sci Technol 2010 FEB;44(1):3-11.

Uraki Y, Nakatani A, Kubo S, Sano Y. Preparation of activated carbon fibers with large specific surface area from softwood acetic acid lignin. Journal of Wood Science 2001;47(6):465-9.

Uraki Y, Kubo S. Fibrous carbons from woody biomass. Mokuzai Gakkaishi 2006;52(6):337-43.

Kubo S, Kadla JF. Lignin-based carbon fibers: Effect of synthetic polymer blending on fiber properties. Journal of Polymers and the Environment 2005 APR;13(2):97-105.

Ruiz-Rosas R, Bedia J, Lallave M, Loscertales IG, Barrero A, Rodriguez-Mirasol J, Cordero T. The production of submicron diameter carbon fibers by the electrospinning of lignin. Carbon 2010 MAR;48(3):696-705.

Lallave M, Bedia J, Ruiz-Rosas R, Rodriguez-Mirasol J, Cordero T, Otero JC, Marquez M, Barrero A, Loscertales IG. Filled and hollow carbon nanofibers by coaxial electrospinning of alcell lignin without binder polymers. Adv Mater 2007 DEC 3;19(23):4292,+.

Brewer CM, Bujalski DR, Parent VE, Su K, Zank GA. Insights into the oxidation chemistry of SiOC ceramics derived from silsesquioxanes. J Sol Gel Sci Technol 1999 MAR;14(1):49-68.

Segatelli MG, Radovanovic E, Nunes Pires AT, Goncalves MdC, Pagotto Yoshida IV. Influence of multiwall carbon nanotubes on the structural and morphological features of si-C-O ceramics derived from a hybrid polymeric precursor. Mater Chem Phys 2010 DEC 1;124(2-3):1216-24.

Narisawa M, Sumimoto R, Kita K, Mabuchi H, Kim Y, Sugimoto M, Yoshikawa M. Investigation of curing process on melt spun polymethylsilsesquioxane fiber as precursor for silicon oxycarbide fibers. Advanced Synthesis and Processing Technology for Materials 2009;66:1-4.

Narisawa M, Sumimoto R, Kita K, Kado H, Mabuchi H, Kim Y. Melt spinning and metal chloride vapor curing process on polymethylsilsesquioxane as si-O-C fiber precursor. J Appl Polym Sci 2009 DEC 5;114(5):2600-7.

Ball R, McIntosh A.C, Brindley J. Feedback processes in cellulose thermal decomposition: implications for fire-retarding strategies and treatments. Combust Theor Model,2004, 8 (2), pp. 281–291.

3.15
SOLVENT SYSTEMS FOR ENHANCED FURFURAL AND HYDROXYMETHYLFURFURAL PRODUCTION FROM CELLULOSIC BIOMASS

Charles M. Cai[1,2], Taiying Zhang[1], Rajeev Kumar[1,2], Charles E. Wyman[1,2,]*

Abstract

Cellulosic biomass derived reactive intermediates (RIs) such as furfural and hydroxymethylfurfural (HMF) and levulinic acid are potential building blocks for sustainable production of drop-in hydrocarbons such as jet fuel. Currently, limited process yields hinder their competitiveness as a fuel precursor. However, significant yield improvements are possible by using organic solvents like tetrahydrofuran (THF) and methyl isobutyl ketone (MIBK). MIBK is an effective extracting solvent in a biphasic reaction and THF's miscibility in water allows for both a single phase and biphasic reaction. Although literature is abundant on the production of these RIs from pure sugars, information on solvent system performance with cellulosic biomass is limited. In this study, we confirm the capability of these solvents to enhance RI production from raw maple wood and assess their feasibility for an industrial process. The major C6-sugar product was HMF for a biphasic solvent reaction and levulinic acid for a single phase solvent reaction. The major C5-sugar product for all reactions was furfural. Furthermore, both solvents demonstrated a high affinity to furfural – MIBK achieved 95% extraction efficiency with furfural and THF improved the solubility of furfural in water by more than double.

Keywords: Furfural, HMF, 5-HMF, levulinic acid, organic solvent extraction, cellulosic biomass, hydrolysis, dehydration, tetrahydrofuran, methyl isobutyl ketone

Introduction

Declining petroleum supplies around the world has led to the increasing necessity to secure domestic oil supplies and develop an economic and highly effective renewable replacement for fossil fuels (Lugar and Woolsey 1999). Increased public awareness on the imbalance of atmospheric CO_2 emissions from the extensive use of non-renewable fossil fuels has put pressure on industrialized countries to demand the gradual integration of biomass-derived fuels into their transportation sectors (Dautzenberg *et al*. 2011). Lignocellulosic biomass is the most abundant resource of organic carbon on Earth and is the only renewable resource that is cheap enough to replace fossil fuels and sustain our energy demands in the transportation sector (Wyman 2007). It is composed of three major polymeric components: cellulose, hemicellulose, and lignin. Cellulose is crystalline in structure and is comprised of linear β-1,4 linked glucose units known as glucan. Hemicellulose is amorphous in structure and is primarily comprised of polymeric chains of β-1,4 linked xylose units known as xylan, a major hemicellulose in most hardwood species, agricultural residues, and energy crops (Laine 2005). Lignin is a cross-linked heterogeneous complex covalently bonded to hemicellulose involving polymers of phenyl propanol units called monolignols (Onnerud *et al*. 2002). Only the maximum utilization of these three components in lignocellulosic biomass will allow the economic production of "drop-in" biofuels to sustain our current and future energy demands.

The major routes to converting cellulosic biomass into biofuels include gasification of biomass to syngas and subsequent Fischer-Tropsch synthesis, pyrolysis and liquefaction of biomass to bio-

[1] *Center for Environmental Research and Technology*

[2] *Department of Chemical and Environmental Engineering. University of California Riverside, CA*

**Corresponding author*

oils, aqueous phase catalytic processing of sugars dehydration compounds, and sugar hydrolysis by pretreatment followed by enzymatic hydrolysis of solids residue for microbial fermentation (Yang and Wyman 2008). Process yields, production costs, and feedstock availability are key limitations to these routes and the best process must achieve the highest product yield from biomass sugars, while using the simplest process, and be the least selective towards feedstock types. For biological conversion pathway, raw biomass needs to be pretreated to allow the maximum accessibility and utilization of the sugars. Pretreatment technologies such as dilute acid pretreatment assist to recover the pentose sugars from hemicellulose and to disrupt the recalcitrant nature of the cellulose fraction. Other pretreatment techniques use organic solvents to help remove the lignin fraction (Zhao 2009). Acid neutralization must follow dilute acid pretreatment and the presence of non-sugar byproducts can inhibit downstream biocatalysts.

Alternatively, reactive intermediates (RIs) such as furfural and hydroxymethylfurfural, which are formed during the acid catalyzed pretreatment of cellulosic biomass, can be hydrogenated and hydrodeoxygenated into alkanes by the action of heterogeneous catalysts (Xing *et al*. 2010 and Huber *et al*. 2005). These RIs can be formed at sufficiently high concentrations from raw biomass with an acid catalyst and heat in aqueous conditions (Zeitsch 2000). Fig. 1 depicts the hydrolysis and dehydration pathways for glucan and xylan to form RIs.

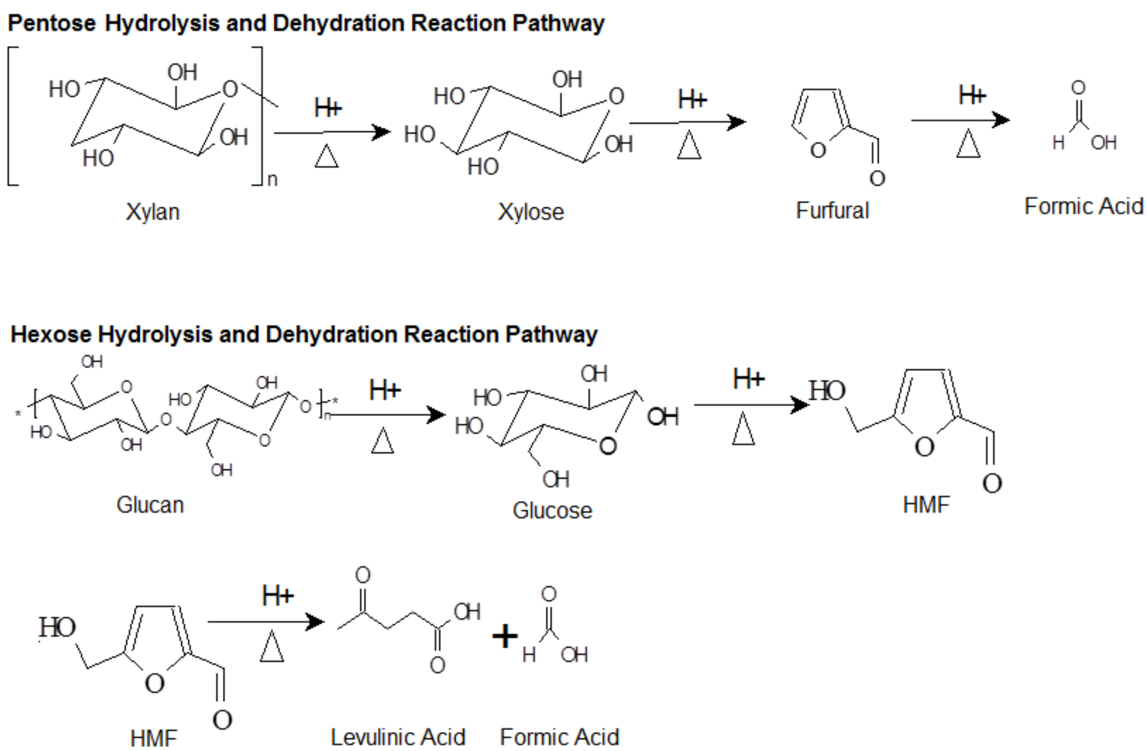

Fig. 1 Hydrolysis and dehydration reaction pathway for glucan and xylan.

In the pentose pathway, xylan is first hydrolyzed into xylose, which is then dehydrated with the removal of three water molecules to form furfural. Further dehydration of furfural at high temperatures will produce formic acid. Similarly for the hexose pathway, glucan is hydrolyzed into glucose, which then dehydrated to form HMF. HMF is highly unstable in an aqueous environment and the reaction will proceed to form equimolar amounts of levulinic acid and formic acid until the HMF is consumed (Karinen 2011).

Furfural is a heterocyclic aldehyde that is made from agricultural raw materials rich in pentosans and is useful as a furanic precursor. The maximum mass yield of furfural that can be obtained from xylan is 0.7273. Since pentosan hydrolysis occurs at a much faster rate than the formation of furfural from a pentose sugar, the kinetics of hydrolysis can be mostly disregarded in the optimization of furfural production. It is also safe to approximate that all the pentosan content in most biomass types except softwoods is xylan (Zeitsch 2000). Furfural can degrade under an aqueous environment by self-resinification or condensation with a pentose-to-furfural intermediate, so removing furfural from the catalytically active phase by vaporization can prevent these loss reactions from occurring (Zeitsch 2000). Currently, furfural is produced predominantly in China from various agricultural wastes at reported yields of less than 50% with the higher yields owing to the continuous removal of furfural by steam stripping (Win 2005). Continuous distillation following steam stripping allows for product purity of up to 99.5% (Win 2005).

HMF is the 6-carbon analog of furfural with an additional alcohol group on a branched carbon. It can be produced by dehydration from either fructose or glucose with higher yields from the former (Karinen 2011). The maximum mass yield of HMF from glucan is 0.7785. Due to the less stable ring structure of fructose than glucose, the formation of HMF is faster from fructose. Further hydrolysis of HMF in the aqueous phase leads to levulinic acid and formic acid, which are stable species with no further hydrolysis products (Kuster 1990). Levulinic acid is also considered an important platform chemical for biofuel synthesis (Dautzenberg 2010).

Improving the yields of furfural and HMF requires the removal of the species from the catalytically active aqueous phase. Extraction of the furans can be done with the use of organic solvents such as methyl isobutyl ketone (MIBK), tetrahydrofuran (THF), acetone, and alcohols in a stirred biphasic reactor (Amiri 2010). Solvents like MIBK and alcohols are immiscible in water and can serve as extracting solvents in a biphasic reaction. On the other hand, THF and acetone are naturally miscible in water and must be salted out of solution to form a separate phase. It has been shown with milled rice straw that a biphasic reaction with the aforementioned solvents can increase furfural and HMF yields over a single phase aqueous reaction system by up to three times (Amiri 2010). However, research on the optimization of furan production from raw cellulosic biomass is insufficient when compared to studies performed using pure sugars.

The present study assesses the capability of a single phase solvent system and a two phase solvent system for the production of furfural, HMF, and levulinic acid from raw maple wood. Key observations unique to each system will be noted and used for the future optimization of yields with the selected solvent system.

Materials and Methods

Maple wood was provided by Mascoma Corp., NH, and was air dried at 55˚C for one day before reaction. Solid content was measured to be higher than 95% before the maple wood was further milled down to 1 mm size particles. The composition of the resulting maple wood was then determined to be 17.1 ± 0.1wt.% xylan, 41.5 ± 0.5% glucan, 23.5 ± 0.3% Klason-lignin (k-lignin), and 17.9% other unidentified material by following NREL (National Renewable Energy Laboratory) "Determination of Structural Carbohydrates and Lignin in Biomass" procedure (http://www.nrel.gov/biomass/pdfs/42618.pdf). Due to the high temperature and non-specific nature of the reactions to the feedstock, only accurate quantification of xylan, glucan, and k-lignin was deemed necessary for analysis.

All reactions were performed in a stirred 1L Hastalloy Parr® batch reactor (Parr Instrument Company, IL). The stirring shaft contains twin 6-blade impellers and stirring rate is held constant at 200 rpms. Heating was provided by a fluidized sand bath with a digital PID temperature controller. Temperature inside the reactor was monitored with an inline K-type thermocouple. The reaction temperature was maintained at 170˚C and fine-tuned by raising or lowering the reactor over the sand bath as necessary, as described elsewhere in detail (Lloyd and Wyman, 2005). Reaction volumes were kept at approximately 800 ml to allow sufficient overhead. The solid content of the reaction volume was maintained at 5% w/w with respect to the aqueous phase with 40 g of dry maple wood for the single phase and 20 g for the two phase system reactions, respectively. H_2SO_4 was the acid catalyst used in each reaction. It was prepared by dilution of a 72% w/w stock solution. Histological grade THF (with inhibitor) was purchased from Fisher Scientific (Pittsburgh, PA) and ACS reagent grade MIBK was purchased from Sigma-Aldrich (St. Louis, MO).

For this study, equal parts by volume of THF and water were combined to make the THF solution. MIBK was added by weight to achieve a 1:1 weight ratio with the aqueous layer in biphasic reactions. After sample preparation, the biomass was allowed to soak overnight at 5 ± 3˚C before reaction. A set of control experiments without solvents were also performed in conjunction with the solvent reactions. The control reactions also contained a 5% w/w loading of maple wood and H_2SO_4.

After each reaction, the solids were separated from the liquid by vacuum filtration. Analysis of the liquid fraction was performed on an HPLC (1200 series, Agilent, CA) using an Aminex HPX-87H column (Bio-Rad Laboratories, Hercules, CA). The solid fraction was washed several times with room temperature deionized water and analyzed for composition by following the aforementioned NREL procedure (http://www.nrel.gov/biomass/pdfs/42618.pdf).

Results

In the reactions with maple wood using MIBK, 91% of the total HMF produced was extracted into the solvent phase. This high extraction efficiency minimized the conversion of HMF to levulinic acid and formic acid. As the reaction progressed, most of the glucose released from the solids had been consumed and HMF yields steadily increased. However, levulinic acid and formic acid yields remained minimal. The extraction efficiency of furfural in MIBK is 95% and the formation of furfural was more rapid than the formation of HMF. The observed saturated vapor pressure at 170˚C was 138 psig for the biphasic reaction.

For the maple wood reactions in THF solution, furfural and levulinic acid was the major product. HMF yields were unsubstantial. At 40 min of reaction, the concentration of furfural had stopped increasing as most of the xylose in solution had been converted and degradation reactions began overcoming furfural formation rates. Levulinic acid yields, however, continued to increase linearly over reaction time up to 60 min. The observed saturated vapor pressure for THF solution at 170˚C was 220 psig.

For the aqueous control experiments with maple wood in acid solution, the concentration profile of furfural formation was remarkably similar to the MIBK reactions. Xylose concentrations in solution remained high. Glucose conversion remained minimal resulting in low concentrations of both 5-HMF and levulinic acid. The observed saturated vapor pressure for the aqueous control at 170˚C was 115 psig.

We also explored the solubility of furfural by measuring the furfural concentrations of flasks introduced with increasing amounts of furfural. As furfural has a limited water solubility of 83 g/ L (GESTIS, IFA), we determined that furfural solubility can be significantly improved with THF solution. As shown in Fig. 2, we confirmed the maximum water solubility of furfural to be approximately 83 g/L at room temperature as we were unable to saturate the water solution further.

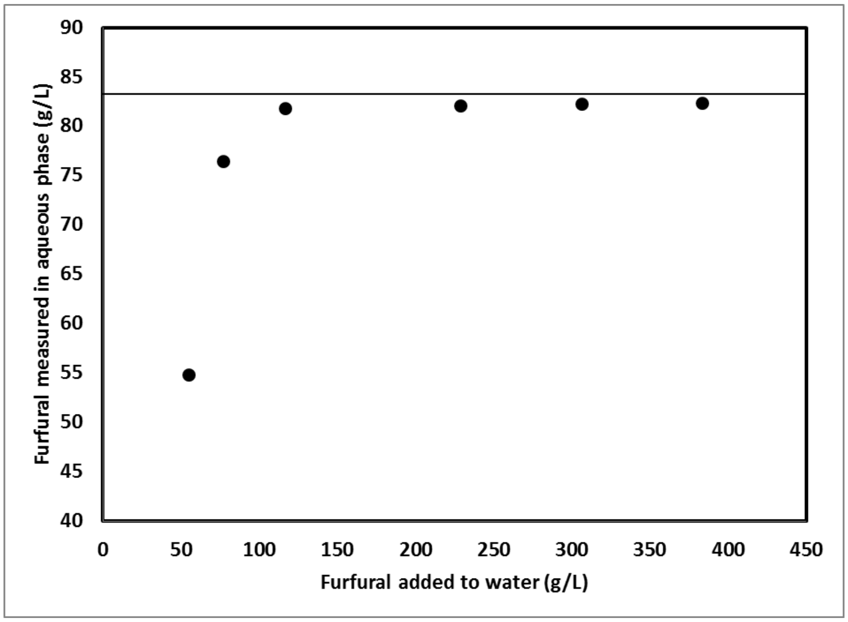

Fig. 2 Addition of furfural to a water solution to determine the highest solubility of furfural in water at room temperature. The solid line represents the theoretical limit of furfural solubility in water of 83 g/L.

When we introduced increasing furfural concentration into the THF solution (Fig. 3), we were able to achieve a maximum furfural solubility of 174 g/L.

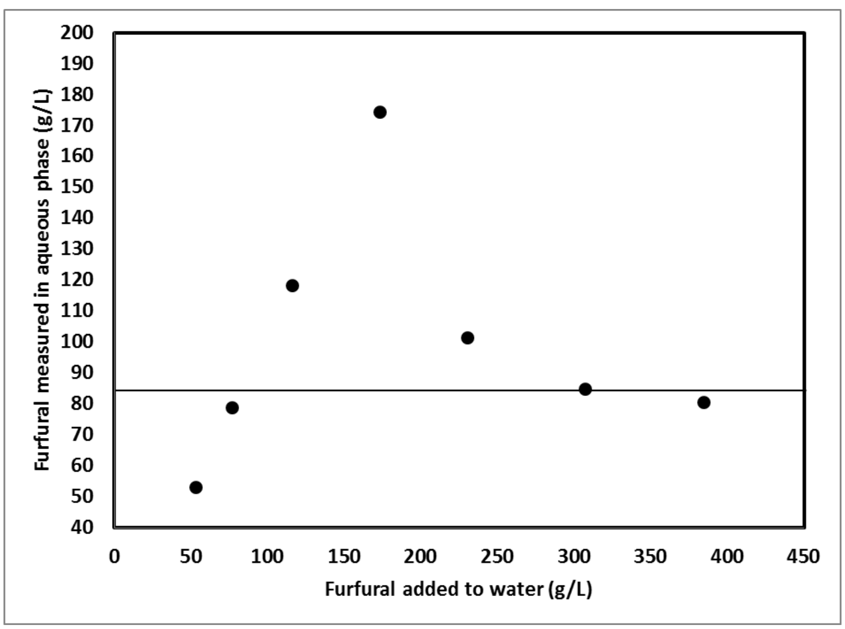

Fig. 3 Addition of furfural to a THF-water solution to determine the solubility characteristics of furfural in the solution at room temperature. The solid line represents the theoretical limit of furfural solubility in water of 83 g/L. The sharp decrease of furfural measured from the aqueous phase after 174 g/L of furfural added is the result of a phase separation of THF from water.

Interestingly, any further increase in furfural to the solution prompted a separation of phases. At 230 g/L furfural concentration, the furfural was able to extract the THF out of solution forming two distinct phases: one aqueous and one with THF.

Discussion

From the results reported in this study, solvent systems have the ability to alter reaction kinetics to favor the production of certain RIs. However, the use of a solvent will increase the overall cost of a process and any perceived improvements must be justified by the additional expense.

Biphasic solvent systems offer the advantage of isolating the product from a catalytically active aqueous phase to minimize degradation reactions. Since HMF will readily hydrolyze to levulinic acid and formic acid in the presence of water, a biphasic solvent system, such as with MIBK, is required to obtain a high yield of HMF. Any products in the organic phase are not only protected, but also free from unwanted contaminants and solids that may interfere with necessary downstream separation steps and catalytic processes for biofuel production. A disadvantage of the biphasic system is the reduction of effective solids loading in a reactor of finite volume. Since about half the reaction volume must now be occupied by the solvent, additional energy must be consumed heating and stirring the liquid solvent, which likely has a higher heat capacity than biomass. Biphasic systems also do not interfere with the aqueous-side reaction kinetics and the optimum reaction times will mirror that of the non-solvent case. Increased operating pressures from the use of a solvent are also a safety concern.

On the other hand, a single phase solvent system does not offer the same kind of isolation effect of a two-phase system, but can potentially accelerate the reaction in other ways. In this study, THF appears to have shortened the optimum reaction time for furfural production. In addition, THF accelerated levulinic acid formation from HMF. This suggests that THF improved the reaction kinetics of sugar conversion to favor the formation of furfural and levulinic acid. Under a single phase system, biomass loading will not be sacrificed to make room for the solvent. As a result, the energy cost of operating a single phase solvent system should be equivalent to that of a non-solvent setup. However, separation of the products by distillation and solvent recovery will be required. Consequently, a modified downstream catalytic system must be developed to be compatible with the high temperature effluent.

The improved solubility of furfural in THF-water solution suggests that furfural has a high affinity towards THF during the reaction. At sufficiently high concentrations, furfural can serve as the extracting solvent to pull THF out of the aqueous phase. The effects of this phenomenon at high temperatures can be explored by molecular simulation in the future. Furthermore, a reaction of furfural in THF solution and acid will determine if their high affinity can help to reduce furfural degradation.

Due to structural differences hemicellulose is more readily hydrolyzed than cellulose. This means the reaction temperature of 170˚C in this study may only be ideal for the hydrolysis of hemicellulose. Optimum HMF and levulinic acid production from cellulosic biomass would require a higher temperature (≥200˚C) reaction without the assistance of heterogeneous catalysts. This suggests that a two stage reaction may be necessary to achieve the highest conversion of both C5 and C6 sugars into furanic products. The first reaction would occur at about 170˚C and the remaining solids containing majorly cellulose and some lignin from the first reaction would then be sent to a second reaction at 200˚C. The products from both stages would then be collected and sent to a catalytic step to be hydrogenated and dehydrated into gasoline grade alkanes.

Conclusions

RIs from cellulosic biomass are important precursors to biofuel production. Solvent systems help to enhance the production of RIs from cellulosic biomass. We have discovered that a single phase solvent system using THF and a biphasic solvent system using MIBK improve the conversion of sugars from maple wood into furanic products. We have also determined that the major C6 product of a biphasic solvent reaction is HMF and the major C6 product of a single phase solvent reaction is levulinic acid. Since not all the maple wood glucan was hydrolyzed at 170˚C, a two stage reaction scheme is recommended to maximize the product yields from both C5 and C6 sugars.

References

Lugar, Richard G. and R. James Woolsey. 1999. The New Petroleum. *Foreign Affairs* 78 (1), 88-102.

Dautzenberg, Geertje, Mirko Gerhardt, and Birgit Kamm. 2010. Bio based fuels and fuel additives from lignocellulose feedstock via the production of levulinic acid and furfural. *Holzforschung* 65, 439-451.

Wyman, Charles E. 2007. What is (and is not) vital to advancing cellulosic ethanol. *Trends Biotechnol* 25(4), 153-157.

Laine, Christiane. 2005. Structures of Hemicelluloses and Pectins in Wood and Pulp. D.Sc. Diss., Helsinki University of Technology.

Onnerud, Hans, Liming Zhang, Goran Gellerstedt, and Gunnar Henriksson. 2002. Polymerization of Monolignols by Redox Shuttle – Mediated Enzymatic Oxidation. *Plant Cell* 14(8), 1953-1962.

Yang, Bin and Charles E. Wyman. 2008. Pretreatment: the key to unlocking low-cost cellulosic ethanol. *Biofuels, Bioproducts and Biorefining* 2(1), 26-40.

Zhao, X, K Cheng, and D. Liu. 2009. Organosolv pretreatment of lignocellulosic biomass for enzymatic hydrolysis. *Appl. Microbiol. Biotechnol*. 82(5), 815-827.

Xing, Rong, Ayyagari V. Subrahmanyam, Hakan Olcay, Wei Qi, Peter van Walsum, Hemant Pendse, and George W. Huber. 2010. Production of jet and diesel fuel range alkanes from waste hemicellulose-derived aqueous solutions. *Green Chemistry* 12(11), 1933-1946.

Huber, George W., Juben N. Chheda, Christopher J. Barett, and James A. Dumesic. 2005. Production of Liquid Alkanes by Aqueous-Phase Processing of Biomass-Derived Carbohydrates. *Science* 308(5727), 1446-1450.

Zeitsch, Karl J. 2000. *The Chemistry and Technology of Furfural and its Many By-Products*. Amsterdam (The Netherlands): Elsevier Science BV.

Karinen, Reetta, Kati Vilonen, and Marita Neimela. 2011. Biorefining: Heterogeneously Catalyzed Reactions of Carbohydrates for the Production of Furfural and Hydroxymethylfurfural. *ChemSusChem* 4(8), 1002-1016.

Win, David T. 2005. Furfural – Gold from Garbage. *AU J. T.* 8(4), 185-190.

Kuster, B.F.M. 1990. 5-Hydroxymethylfurfural (HMF). A review focusing on its manufacture. *Starch/Starke* 42(8), 314-321.

Amiri, Hamid, Keikhosro Karimi, and Shapoor Roodpeyma. 2010. Production of furans from rice straw by single-phase and biphasic systems. *Carbohydrate Research* 345(15), 2133-2138.

3.16
GREEN PROCESSING: A BIOREFINERY PERSPECTIVE

Devin Takara[1], Andrew G. Hashimoto[1], Samir Kumar Khanal[1,]*

Abstract

Pennisetum purpureum, Napier grass, is a naturalized perennial feedstock in Hawaii that highly resembles the former staple crop of the state, sugarcane. Because of its high moisture content, Napier grass presents a unique opportunity for separation into solid and liquid fractions via green processing. The resulting clean fibers can serve as a substrate for biofuel production, while the nutrient-rich juice can serve as a substrate or additive for microbial co-product production. Biomass age is an often overlooked parameter in biomass handling and logistics. As Napier grass matures, changes in its composition and moisture significantly affect fractionation as well as co-product and subsequent biofuel production. This study evaluated the effects of age on biochemical constituents relevant to the conversion of Napier grass into biofuel and biobased products. Samples were hand-harvested at 2, 4, and 8 months of age and passed through a cutting mill for initial size reduction. The material was then screw-pressed under 40 psi of pneumatic backpressure. The reported characteristics of solid fibers and liquid juice will have significant implications on the feasibility of biorefineries in Hawaii and other (sub)tropical regions of the world

Keywords: Biorefinery, biofuel, co-product, green processing, lignocellulose

Introduction

Continuous growth of global energy demands, coupled with political instability in oil-exporting and neighboring countries have raised concerns over fossil-derived resources globally. The U.S. transportation sector, for example, comprises 72% of the nation's oil and liquids consumption, and currently meets about half of this demand through foreign imports. Although recent reports predict an optimistic reduction of 0.9 million barrels of petroleum-based gasoline per day (domestically), these projections are contingent on an increase in biofuel supply, namely ethanol, over the next two decades (U.S. Energy Information Administration 2012).

Presently, there are no large-scale commercial cellulosic biofuel facilities in the U.S. (*EMTS 2012 Data* 2012), even with government subsidies, thus exemplifying a known key issue: the production of biofuels (both ethanol and other advanced types) has not yet been proven to be cost competitive with petroleum-based fuels. One approach to mitigate this issue is through the establishment of biorefineries which seek to convert renewable feedstocks into two or more products; one having a high market value and low volume (i.e. co-product), and the other having high volume, but relatively low value (i.e. biofuel).

Perennial, herbaceous energy crops are excellent feedstocks for green processing biorefineries based on their intrinsically high moisture content and structural sugar constituents. The topic of green processing is described in detail elsewhere (Takara and Khanal 2011) but briefly, the upstream operations omit biomass drying stages and fractionate raw feedstock, via screw-pressing, into a solid and liquid stream. The liquid component can be used to produce a high value co-product, and the solid clean fiber can be converted to (advanced) biofuels through conventional bioprocessing.

In (sub)tropical regions of the world, the high-yielding energy crop *Pennisetum purpureum* (Napier grass) was reported to have significant potential in the large-scale production of

[1] *Department of Molecular Biosciences and Bioengineering, University of Hawaii at Manoa, HI*

* *Corresponding author*

renewable fuel (Tran et al. 2011). But the outputs of biorefineries are inherently tied to the inputs, and an often overlooked property of all lignocellulosic feedstocks is the compositional changes that occur during maturation. To date, little is known about the composition of Napier grass, and the ideal number of harvests permissible per year, particularly with an emphasis on biofuel and bioproduct production. In this study, the biochemical composition of Napier grass over its natural course of maturation in Hawaii was analyzed and correlated to juice collected during green processing operations. A recommended age for crop harvest was reported along with future insight for commercial applications in (sub)tropical regions of the world.

Methods

Green Processing

Napier grass samples from Waimanalo, HI were hand-collected in June, August, and December 2011 corresponding to 2, 4, and 8 months of age; the latter representing full maturity of the feedstock. The Napier grass was immediately transported from the field to the University of Hawaii at Manoa, and was shredded by a commercial cutting mill (Vincent Corporation, Tampa, FL). The moisture content at 105°C was determined after shredding, and the biomass was subsequently dewatered via screw-pressing (Vincent Corporation, Tampa, FL) under 40 psi of pneumatic backpressure (Takara and Khanal 2011). Liquid juice samples were collected and analyzed for total Kjeldahl nitrogen (TKN) and soluble sugar concentrations. Extruded solid fibers were dried and ground.

Biomass Composition

The carbohydrate constituents of solid fibers were determined as per the National Renewable Energy Laboratory analytical procedures described elsewhere (Sluiter et al. 2008). In brevity, the biomass was digested in a two-stage process which used sulfuric acid to hydrolyze structural hemicellulose and cellulose into their monomeric sugars; xylose and glucose, respectively. Although minor sugars (e.g. arabinose and mannose) were present, the concentrations were minuscule and at the lowest limit of our detection capabilities. To minimize the introduction of error, the concentrations of minor sugars were omitted.

The liquid analyses were conducted as per the procedures described by commercial TKN test kits (HACH, Loveland, CO) and Sluiter et al. (2006). Solubilized sugar and TKN of Napier grass juice are properties known to be invaluable for fungal co-product production in biorefinery processes (Nitayavardhana and Khanal 2010).

Results

Carbohydrate Content of Solid Fiber

The results of the age variation investigation of lignocellulosic fiber are summarized in Figure 1. The concentration of structural glucose and xylose, reported as glucan and xylan respectively, were the lowest when the plant was the youngest, i.e. 2 months old. After 4 months, the structural glucose increased by about 8%, correlating with a physical growth spurt observed in the field during harvests: the planted Napier grass more than doubled its height from 5 feet tall at 2 months old to over 10 feet tall at 4 months old. In contrast to structural glucose (i.e. cellulose), changes in hemicellulose were relatively small over the same period.

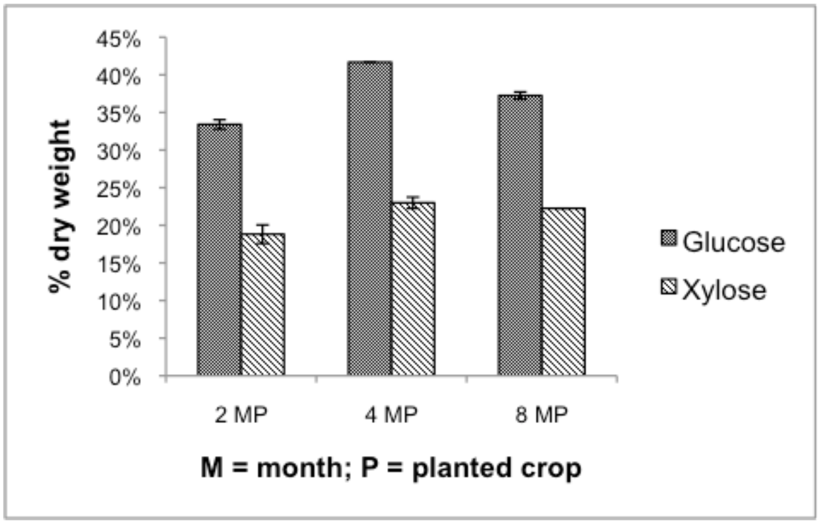

Figure 1. Primary Structural Sugars of Napier grass

At maturity, the glucose content of Napier grass decreased from 42% dry weight (at 4 months old) to 37%. This reduction was most likely a consequence of lignification, the addition of lignin to structural components, as the plant aged. In 8-month old Napier grass, the lignin content was 22% compared to 16% the 2-month old crop.

Moisture Content of Solid Fiber

Determining the moisture content of Napier grass is essential for green processing and the simultaneous generation of co-products in biorefineries. As expected, the moisture in freshly harvested material declined over the natural course of maturation. A near 20% reduction was observed for Napier grass between 2 and 8 months of age. Respectively, the moisture contents for 2, 4, and 8 months old Napier grass were 86%, 75%, and 67%.

Soluble Sugars and TKN of Juice

The results from soluble sugar and total Kjeldahl nitrogen analyses for Napier grass juice are summarized in Table 1. A post-hoc Tukey's comparison confirmed that the values reported in the table are statistically different between each group. Nitrogen appeared to be at its lowest value when the structural carbohydrate content was at its highest (at 4 months old); this was likely a consequence of the rapid feedstock growth.

Table 1. Napier Grass Juice Analysis for Sugar and Nitrogen Content

Age	Glucose (g/L)	Xylose (g/L)	TKN (g/L)
2 MP	5.51 ± 0.02	0.42 ± 0.03	0.92 ± 0.03
4 MP	6.69 ± 0.03	0.65 ± 0.04	0.57 ± 0.02
8 MP	18.99 ± 0.14	1.38 ± 0.07	1.52 ± 0.01

Co-Product

Fungal biomass, in particular, is an attractive co-product for green processing biorefineries since fungi maintain a rather unique ability to utilize numerous organic compounds for growth. Like many microorganisms, however, fungi prefer sugars over other (often more complex) sources of carbon. In (sub)tropical places such as Hawaii, species with a high protein content (e.g. *Rhizopus microsporus*) can be cultivated on Napier grass juice for applications in aquatic and animal feeds

(Nitayavardhana and Khanal 2010). Characteristics of culture media, used to promote increased fungal protein production, require a carbon-nitrogen ratio of 10:1 or less (Leeuwen et al. 2012); conveniently this corresponds with captured juice from 4 month old Napier grass. Thus, feedstock harvested and green processed at this age has the potential to produce the maximum amount of both biofuel and bioproducts (in the form of fungal protein). Although future optimization work and economic analyses are still required to truly forecast and realize the potential of green processing biorefineries on a commercial scale, more than likely, Napier grass and fungal co-products will play a significant role in upcoming commercial ventures.

Acknowledgements

This work was supported by grants from Western Sun Grant Center, Oregon State University and the U.S. Department of Energy, award number DE-FG36-08GO88037. The authors would like to thank Dr. Richard Ogoshi and Dr. Scott Turn for their support.

References

EMTS 2012 Data. 2012. U.S. Environmental Protection Agency (US EPA), July 31 2012 [cited August 1 2012]. Available from http://www.epa.gov/otaq/fuels/rfsdata/2012emts.htm.

Leeuwen, J. (Hans) van, Mary L. Rasmussen, Sindhuja Sankaran, Christopher R. Koza, Daniel T. Erickson, Debjani Mitra, and Bo Jin. 2012. "Fungal Treatment of Crop Processing Wastewaters with Value-Added Co-Products": In *Sustainable Bioenergy and Bioproducts*, ed. Kasthurirangan Gopalakrishnan, J. (Hans) van Leeuwen and Robert C. Brown, 13-44. Springer.

Nitayavardhana, Saoharit, and Samir Kumar Khanal. 2010. Innovative biorefinery concept for sugar-based ethanol industries: Production of protein-rich fungal biomass on vinasse as an aquaculture feed ingredient. *Bioresource Technology* 101(23): 9078–9085.

Sluiter, A., B. Hames, R. Ruiz, C. Scarlata, J. Sluiter, and D. Templeton. 2006. Determination of Sugars, Byproducts, and Degradation Products in Liquid Fraction Process Samples. National Renewable Energy Laboratory.

Sluiter, A., B. Hames, R. Ruiz, C. Scarlata, J. Sluiter, D. Templeton, and D. Crocker. 2008. Determination of Structural Carbohydrates and Lignin in Biomass. National Renewable Energy Laboratory.

Takara, Devin, and Samir Kumar Khanal. 2011. Green processing of tropical Napier grass into biofuel and biobased products: An innovative biorefinery approach. *Bioresource Technology* 102(2): 1587–1592.

Tran, Nghia, Prabodh Illukpitiya, John F. Yanagida, and Richard Ogoshi. 2011. Optimizing biofuel production: An economic analysis for selected biofuel feedstock production in Hawaii. *Biomass and Bioenergy* 35(5): 1756–1764.

U.S. Energy Information Administration. *Annual Energy Outlook 2012: with Projections to 2035* 2012. Available from http://www.eia.gov/forecasts/aeo/pdf/0383(2012).pdf.

3.17
BIOSOLAR CONVERSION OF CO_2 AND H_2O TO LONG-CHAIN ALCOHOLS BY ENGINEERED CYANOBACTERIA

Liping Gu[2], Xianling Xiang[1], Doug Raynie[3], William Gibbons[1], Ruanbao Zhou[1,]*

Abstract
Biorefineries typically release one third of the carbohydrate carbon as CO_2 during fermentation, as well as significant amounts of low grade heat. Ideally, a photosynthetic organism could be engineered to convert these unused resources into high value chemicals. The current microalgae production model suffers from technical challenges including harvest cells, extract oils, and then convert them into a final product. We circumvented these challenges by engineering cyanobacteria to directly produce and secrete linalool ($C_{10}H_{18}O$: a high energy dense long-chain alcohol and "drop-in" biofuel) as a living factory using sunlight and CO_2 as the feedstock. Linalool is a naturally-occurring terpene alcohol, emitted as a volatile compound from many flowers and spice plants. Cyanobacteria, like plants, have both the MVA pathway and the MEP pathway to produce geranyl diphosphate (GPP), the precursor for linalool. However, cyanobacteria lack the linalool synthase that plants use to convert GPP into linalool. In this project, the linalool synthase gene from Norway Spruce was fused to His_6-tag driven by a dual *Pnir–PpsbA1* promoter. The plant linalool synthase was overexpressed in transgenic *Anabaena* in which linalool was produced and secreted as monitored by GC-MS.

Key words: cyanobacteria, genetic engineering, linalool, MEP pathway, GC-MS

Introduction
Current ethanol fermentation technologies release one third of the carbohydrate carbon as CO_2. In addition to negatively affecting the carbon balance of the process, this also represents a substantial loss of the embedded energy in biomass growth, harvest, and transport. It is possible to recapture some of this lost CO_2 using photosynthetic microbes. Engineering cyanobacteria to directly produce and excrete high value chemicals in a one-step system will bypass the expensive, multiple unit operation process currently used for biofuel production from algae.

Linalool is an energy rich 10-carbon alcohol with an energy density of 40 mj/kg, heat of vaporization of 0.19 mj/kg, and octane of 102, being a suitable "drop-in" replacement for petrofuels. However, current prices for linalool (>$19.8/Kg) are high because extraction from linalool-producing plants is costly and productivity is limited. Linalool is naturally produced in some plants from the MEP pathway (Pichersky et al., 1995; Phillips et al., 2008) where the universal isoprenoid intermediate geranyl diphosphate (GPP) is converted to linalool by linalool synthase (LinS) (Cseke et al., 1998). MEP pathway genes are highly conserved among plants and cyanobacteria. All genes required for synthesis of GPP (the immediate precursor used for production of linalool) are found in the *Anabaena* genome. However, no LinS gene is found in cyanobacterial genomes using E-Value 0.001 as cutoff. Therefore, we proposed that shunting the native MEP pathway of *Anabaena* to produce linalool from GPP may be achieved by transferring-in just one gene, a plant linalool synthase (LinS) gene, which encodes an enzyme responsible for conversion of GPP into linalool. Photosynthetic cyanobacteria produce large quantities of phytol

[2] *Department of Biology and Microbiology*

[3] *Department of Chemistry and Biochemistry, South Dakota State University, SD*

* *Corresponding author*

and carotenoid pigments from DMAPP and IPP (Disch et al., 1998; Protean, 1998), suggesting a greater innate MEP pathway flux, and presumptively, more GPP available for linalool production. Due to their high photosynthetic efficiency, cyanobacteria are the best organisms for engineering production of excreted linalool using CO_2 as a feedstock.

Materials and Methods

Strains and Plasmids

NEB10-beta (New England Biolabs) and BL21 (DE3) (Novagen) were used for routine maintenance of plasmid preparation and protein expression. *Anabaena* sp. PCC 7120 and its genetically modified strain were grown in AA/8N medium (Hu et al., 1981), at 30°C, 100 rpm, and 50 μmol photons m^{-2} s^{-1}. All primers and plasmid constructions are listed in Table 1. The LinS-containing plasmid pZR808 was introduced into *Anabaena* by conjugation (Wolk et al., 1984) and the transformants were selected on a nitrate-containing AA/N agar plate (Hu et al., 1981) with 100 μg/mL Neomycin Sulfate.

Table 1. Plasmids/oligonucleotides used in this study

Plasmids	Description	Construction	Reference
pFPN	Kan^r, P_{psbA1}-containing vector		Chaurasia & Apte, 2008; Elhai, 1993
pNIR	Kan^r, P_{nir}-containing vector		Desplancq et al., 2005
pZR703	Kan^r, modified pNIR;	Annealed oligonuclotides ZR64/65 containing a TTS ligated to XhoI-NotI cut pNIR	This study
pZR749	Kan^r, modified pFPN	Annealed oligonuclotides ZR66/67 containing BglII-rbs-MCS-BamHI ligated to BamHI cut pFPN	This study
pZR769	Kan^r, dual P_{nir}-P_{psbA1} promoter vector	MfeI-F1-PpsbA1-MCS-BamHI fragment from pZR749 clockwise ligated to EcoRI-BamHI cut pZR703	This study
pZR780	Kan^r, modified pZR769	pZR769 was subjected to SDM with primers ZR116 and ZR117 to eliminate SmaI-XhoI sites and add SalI site	This study
pZR804	Kan^r, delete a 300bp F1 fragment in pZR780	pZR780 was subjected to SDM with primers ZR135 and ZR136 to delete a 300bp F1 fragment	This study
pZR807	Kan^r, eliminate a BglII site in pZR804	pZR804 was subjected to SDM with primers ZR137 and ZR138 to delete a BglII site around bp4856	This study
pZR808	Kan^r, His_6-LinS containing expression vector	BglII-H_6-LinS-AatII from pTPS-LinS ligated to BglII-AatII cut pZR807	This study & Martin et al., 2004
Primers	Sequence		
ZR64	TCGAGAATGCCTCCGATTTCTAATCGGAGGCATTGC		
ZR65	GGCCGCAATGCCTCCGATTAGAAATCGGAGGCATTC		
ZR66	GATCTAAGGAGATATACATATGAGATCTCCCGGGCCCGGTACCCTGCAGGCATGCCTCGAGGACGTCCCTAGGGCTAGCG		
ZR67	GATCCGCTAGCCCTAGGGACGTCCTCGAGGCATGCCTGCAGGGTACCGGGCCCGGGAGATCTCATATGTATATCTCCTTA		
ZR116	CGGATCCCCCGGTCGACgagaatgcctcc		
ZR117	ggaggcattctcgTCGACcgggGGATCCG		
ZR135	actttatgagaacgCACTGCAGGGATTCCCA		
ZR136	TGGGAATCCCTGCAGTGcgttctcataaag		
ZR137	GGGGATCAAGATATGATCAAGAGAC		
ZR138	GTCTCTTGATCATATCTTGATCCCC		

Notes: His_6-LinS, Hexhistidine-Linalool synthase; Kan^r, kanamycin; MCS, multiple cloning site; SDM, site-directed mutagenesis; rbs, ribosome binding site; TTS, transcriptional termination sequence; Plasmids pFPN, pNIR, pTPS-LinS were gifts from the corresponding investigators.

Linalool extraction and identification by GC-MS

To extract secreted linalool, 6 mL pentane was added to 100 mL culture fluid in a sealed container which was shaken at 250 rpm at 30°C for 10 min. To extract intracellular linalool, ~500 mg (FW) cell pellet was resuspended in 2 ml fresh growth medium and was sonicated at 25% amplitude (Digital sonifer, BRANSON). Then 6 mL pentane was added into this sonicated suspension to extract intracellular linalool. About 5 mL pentane extracts in both cases were then evaporated in darkness to 100μL-200μL at 30°C. One μL samples were analyzed by Agilent 7890 GC/5975 MSD using electron ionization mode with a 30m x 0.32mm x 0.25μm Supelco SPB-5 column. The initial temperature was 40°C, held for 2 min, ramped at 10°C/min to 300°C, and then held for 5 min. Inlet temperature was set at 250°C.

Results

LinS plasmid construction and *Anabaena* transformation

To engineer *Anabaena* to produce linalool, linalool synthase gene (*LinS*) from Norway Spruce (Martin et al., 2004), with N-terminal plastid targeted sequence deletion, was cloned immediately downstream of the engineered translation initiation sequence (Shine-Dalargno sequence) under a dual promoter (*Pnir-PpsbA1*) in shuttle vector pZR807 to generate LinS-containing plasmid pZR808 (Fig. 1 and Table 1). To monitor LinS expression in *Anabaena*, a His_6-tag was also fused to N-terminal LinS (Fig. 1A). Transformants bearing pZR808 after conjugation (Wolk et al., 1984) were verified by PCR (data not shown).

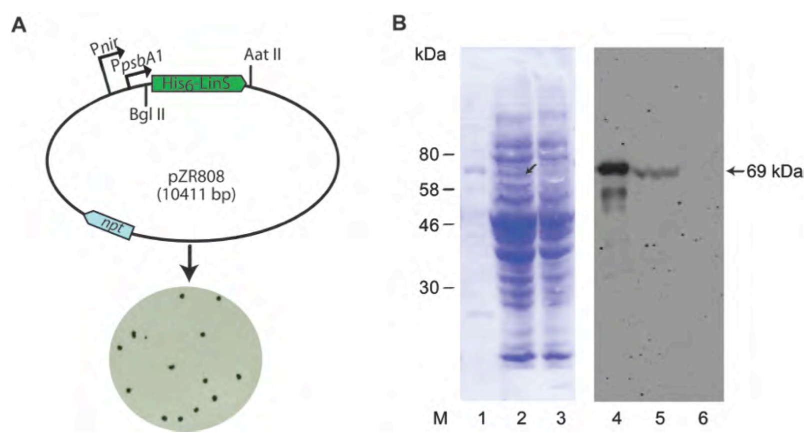

Figure 1. LinS plasmid construction and His_6-LinS protein expression in *Anabaena.*

A. The *his_6-LinS* fragment isolated from pTPS-LinS (Martin et al., 2004) by double digestion with BglII and AatII was ligated to the downstream of a dual promoter P_{nir}-P_{psbA1} engineered in pZR807 to produce pZR808 (Table 1). The green colonies grown on an AA/N selecting plate with 100 μg/ml Neomycin Sulfate were the presumptive transformants that contain pZR808 following conjugative transformation. npt: neomycin phosphotransferae gene, conferring kanamycin resistance for *E. coli*, and neomycin resistance for *Anabaena*. B. Heterologous expression of Norway Spruce's linalool synthase gene (*LinS*) in *Anabaena* (lanes 2 and 5) and in *E. coli* (lanes 1 and 4) detected by Coomassie Blue R-250 staining (*left panel*) and Western blot with anti-His antibodies (*right panel*). An approximately 69 kDa protein was readily detected in the protein extracts of transgenic *Anabaena* (lanes 2 and 5) or transgenic *E. coli* (lanes 1 and 4).

Over-expression of LinS in transgenic *Anabaena*

As shown in Fig. 1B, a ~69 kDa protein was detected in both transgenic *Anabaena* (lane 5) and in *E. coli* bearing pZR808 by Western blot with anti-His antibodies (Zhou & Kroos, 2004) (lane 4). Because this His_6-tagged protein was not detected in the protein extracts from wild-type *Anabaena* (lane 6) and the molecular mass also matches the calculated 68764 Da for His_6-LinS protein, we conclude that His_6-LinS was well expressed in both *E. coli* and *Anabaena.*

Photosynthetic production of linalool by the transgenic Anabaena

GC-MS analysis showed a peak with retention time of 8.2 min from the growth medium of transgenic *Anabaena* (Fig. 2C arrowed), which was confirmed to be linalool as its mass spectrum

(Fig. 2E) matches well with that from linalool standard (Fig. 2D). This peak was neither detected in the medium of wild-type *Anabaena* (Fig. 2B) nor in the total cell extracts of transgenic *Anabaena* (data not shown). Thus, we conclude that we created a transgenic *Anabaena* capable of directly producing and secreting linalool using CO_2 and sunlight. In addition to this finding, we also discovered that N_2-fixing *Anabaena* is innately capable of producing and secreting long-chain alkanes/alkenes (C_9-C_{18}), the major peaks in Fig. 2B and C. This additional finding will serve as a future research thrust to identify the alkane synthetic pathway, and then manipulate it for high energy dense fuels production in *Anabaena*.

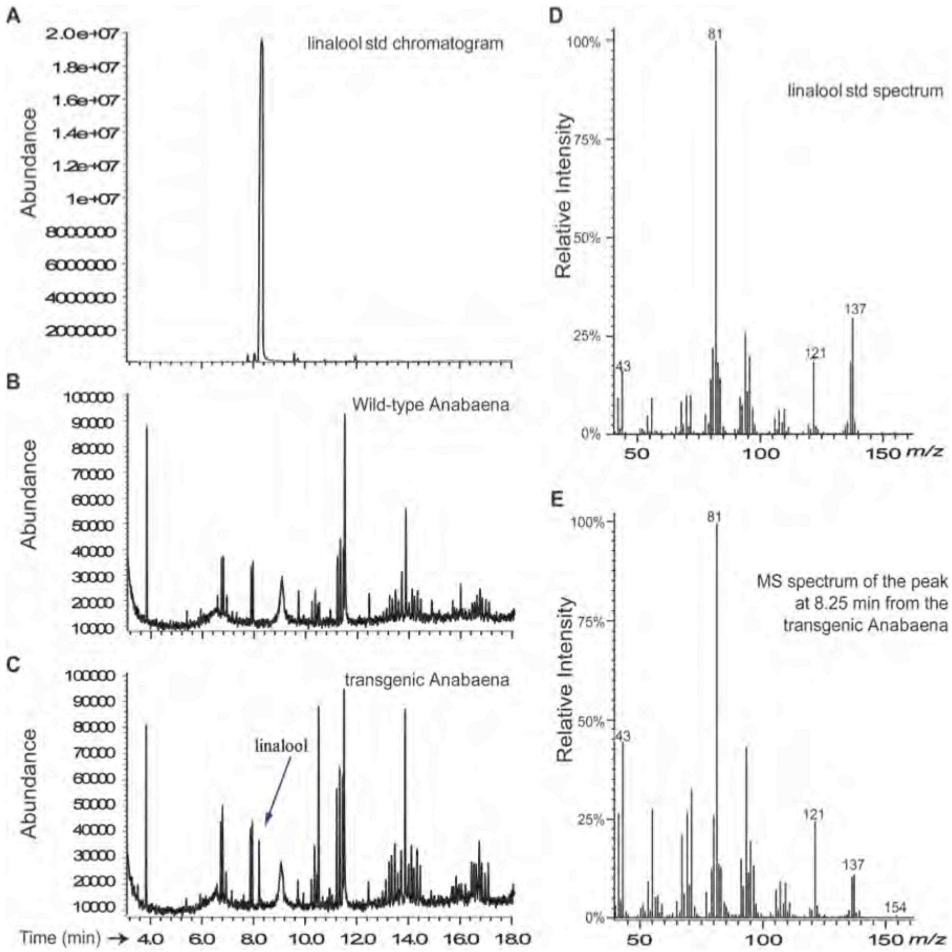

Figure 2. GC-MS identification of linalool production by engineered *Anabaena.*

A peak with retention time of 8.2 min was detected from the transgenic *Anabaena* growth medium (C, arrowed), but neither in the medium of wild-type *Anabaena* (B) nor in the total cell extracts of transgenic *Anabaena* (data not shown). This peak was confirmed to be linalool as its retention time and mass spectra (E) match well with those from linalool standard (A and D, respectively).

Discussion

Cyanobacteria have both MVA pathway and MEP pathway to synthesize GPP (the immediate precursor for production of linalool) using CO_2 as the carbon source. By introducing a plant linalool synthase gene to cyanobacterium *Anabaena*, we demonstrated, for the first time, “proof of concept” in direct turning CO_2 and H_2O into a drop-in fuel. The engineered cyanobacterium *Anabaena* is capable of both synthesis and secretion of linalool, placing linalool in a unique position ideal for commercial applications. In conclusion, the present work provides a great potential to further engineer *Anabaena* to be a living cellular factory of linalool.

Cyanobacteria photosynthetically produce many metabolites from CO_2. However, the majority (80-85%) of fixed carbon is directed toward sugar biosynthesis, about 10% toward fatty acid biosynthesis, and only 3-5% toward MEP pathway (Lindberg et al., 2010). To improve titer of linalool production, we need to maximize the flux of fixed carbon into production of linalool by both altering the competitive pathways and boosting up the MEP pathway. For instance, ADP-GPPase inactivation (Hill et al., 1991) may shunt the carbon flux from glycogen synthesis to linalool production. Alternatively, overexpressing the rate-limiting enzymes in MEP pathway such as DXS (Cordoba et al., 2009) would expect to pull more carbon flux to synthesize precursor GPP.

References

Chaurasia AK, Parasnis A, Apte SK. 2008. An integrative expression vector for strain improvement and environmental applications of the nitrogen fixing cyanobacterium, Anabaena sp. strain PCC7120. *J Microbiol Methods.* 73(2):133-41.

Cordoba E, Salmi M, León P. 2009. Unravelling the regulatory mechanisms that modulate the MEP pathway in higher plants. J Exp Bot. 60(10):2933-43.

Cseke L, Dudareva N, Pichersky E. 1998. Structure and evolution of linalool synthase. *Mol Biol Evol.* 15(11):1491-8.

Desplancq D, Bernard C, Sibler AP, Kieffer B, Miguet L, Potier N, Van Dorsselaer A, Weiss E. 2005. Combining inducible protein overexpression with NMR-grade triple isotope labeling in the cyanobacterium *Anabaena sp. PCC 7120*. *Biotechniques*. 39:405-11.

Disch A, Schwender J, Müller C, Lichtenthaler HK, Rohmer M. 1998. Distribution of the mevalonate and glyceraldehydes phosphate/pyruvate pathways for isoprenoid biosynthesis in unicellular algae and the cyanobacterium Synechocystis PCC 6714. *Biochem J*. 333:381-8.

Elhai J. 1993. Strong and regulated promoters in the cyanobacterium *Anabaena* PCC 7120. FEMS Microbiol Lett. 114(2):179-84.

Hill MA, Kaufmann K, Otero J, Preiss J. 1991. Biosynthesis of bacterial glycogen. Mutagenesis of a catalytic site residue of ADP-glucose pyrophosphorylase from Escherichia coli. J. Biol Chem. 266(19):12455-60.

Hu NT, Thiel T, Giddings TH, Wolk CP. 1981. New *Anabaena and Nostoc* cyanophages from sewage settling ponds. *Virology* 114:236–46.

Lindberg P, Park S, Melis A. 2010. Engineering a platform for photosynthetic isoprene production in cyanobacteria, using Synechocystis as the model organism. Metab Eng. 12(1):70-9.

Martin DM, Fäldt J, Bohlmann J. 2004. Functional characterization of nine Norway Spruce TPS genes and evolution of gymnosperm terpene synthases of the TPS-d subfamily. *Plant Physiol*. 135(4):1908-27.

Phillips MA, León P, Boronat A, Rodríguez-Concepción M. 2008. The plastidial MEP pathway: unified nomenclature and resources. Trends Plant Sci. 13(12):619-23.

Pichersky E, Lewinsohn E, Croteau R. 1995. Purification and characterization of S-linalool synthase, an enzyme involved in the production of floral scent in Clarkia breweri. *Arch Biochem Biophys*. 316(2):803-7.

Proteau PJ. 1998. Biosynthesis of phytol in the cyanobacterium synechocystis sp. UTEX 2470: utilization of the non-mevalonate pathway. *J Nat Prod*. 61(6):841-3.

Wolk CP, Vonshak A, Kehoe P, Elhai J. 1984. Construction of shuttle vectors capable of conjugative transfer from *Escherichia coli* to nitrogen-fixing filamentous cyanobacteria. *Proc Natl Acad Sci U S A.* 81:1561-5.

Zhou, R., L. Kroos. (2004). BofA protein inhibits intramembrane proteolysis of pro-σK in an intercompartmental signaling pathway during Bacillus subtilis sporulation. Proc. Natl. Acad. Sci. USA. 101:6385-6390

3.18
MECHANISTIC MODEL DEVELOPMENT OF FUNDAMENTAL BIOLOGICAL AND PHYSIOLOGICAL PROCESSES GOVERNING LIPID PRODUCTION BY MICROALGAE

Barbara C. Benson[1], Carlos J. Fernandez[2], Joe M. Fox[3]*

Abstract
Microalgae biomass production efficiency depends on optimization of various fundamental processes, such as interception of photosynthetic photon flux density (PPFD), CO_2 uptake through photosynthesis, and biomass production and partitioning into primary organic fractions such as carbohydrates, proteins, and lipids. Quantification of these fundamental processes is essential to optimize microalgae production. Mathematical expressions of the various biological and physiological processes governing microalgae production and their responses to environmental factors are being integrated into a mechanistic model to gain a fundamental understanding of their complex interactions and to optimize the efficiency of microalgae production.

The conceptual components of model development and the quantification of fundamental biological and physiological processes governing lipid production by microalgae will be discussed. These numerical relationships include a complex network of equations. PPFD (how it is attenuated by the aqueous medium and how this relationship is influenced by the availability of PPFD at the culture surface, the depth or thickness of the culture, and the density of the biomass) is the forcing function of the mass balance model. The biomass density is determined by the specific growth rate, which is driven by the PPFD that hits cells within the culture. This latter relationship is influenced by the mixing rate (cell light/dark cycling by self-shading), the dilution rate, and the intrinsic reproductive capacity of the microalgae (partially rhythmic and partially stochastic in nature). Stoichiometry used to quantify carbon assimilation into biomass and biomass partitioning into primary organic fractions such as carbohydrates, proteins, and lipids.

Keywords: biomass production, algae biofuel, biomass conversion, microalgae, growth kinetics, Lipid production, algal biomass, photon flux

Introduction
Microalgae farms could theoretically produce enough biodiesel to replace petroleum-transportation fuel in the US in an area equivalent to 1-3% of available cropland and grazing (Chisti, 2007). Microalgae captures solar energy, absorbs CO_2 and inorganic nutrients, and transforms these into carbohydrates, proteins, and lipids with significant current and potential commercial application, such as biofuel, food and fodder, and high-value cosmetics and nutrient supplements (Huntely and Redalje, 2007). Although algal biomass alone had a global product value of US $ 1.25 billion (Becker, 2007), the economic viability of such microalgae production systems depends on their ability to efficiently produce high-value products. This production

[1] *School of Geosciences, Environmental Science Program, University of Louisiana at Lafayette, LA*

[2] *Crop Physiology, Modeling, Management, Texas AgriLife Research at Corpus Christi, TX*

[3] *Environmental Science, Coastal & Marine System Science, Texas A&M University-Corpus Christi, TX*

** Corresponding author.*

efficiency, in turn, depends on the optimization of various fundamental processes, such as interception of photosynthetic-active solar radiation (PAR), CO_2 uptake for photosynthesis, and biomass conversion and partitioning into carbohydrates, proteins, and lipids. Quantification of responses of these fundamental processes to environmental factors is considered essential to optimize the efficiency of microalgae production systems. Furthermore, this information can be integrated in a mechanistic simulation model to achieve this optimization. The overarching goal of this research is, the improvement of the efficiency of microalgae oil production systems through the quantification and integration of fundamental biological and physiological processes governing the growth and lipid production of microalgae cultures. The main objective is the development of a mechanistic model that simulates biomass production, physiological responses, and the cellular partitioning of the biomass into lipids, proteins and carbohydrates.

While studies on the effects of light availability and microalgae biomass production are common, studies quantifying responses of photosynthesis of microalgae cultures to various factors including photosynthetic photon flux density (PPFD), CO_2 availability, and temperature are scarce. Much less available are studies quantifying respiration of microalgae cultures and its interaction with photosynthesis and the environment. Since carbon plays a dominant role in both plants and microalgae, it would be also acceptable to express biomass production in terms of carbon. This entire process of carbon uptake and carbon loss (respiration) is referred to as carbon economy. All three components are needed to quantify the carbon economy of microalgae cultures.

PPFD decreases with depth as the solar radiation flux is attenuated by turbidity of the aqueous medium. Availability of PPFD at the surface, the depth or thickness of the culture, the mixing rate (cell light/dark cycling frequency), and the dilution rate are important factors determining the performance of microalgae production systems (Zou and Richmond, 1999; Benson et al., 2009). Photoautotrophic cultures depend on photosynthetically available radiation and these systems must be optimized for light utilization (Molina Grima et al., 1994; Acien Fernandez et al., 2000).

The biochemical composition of microalgae in terms of the primary compound carbohydrates, proteins and lipids is highly variable for various genera and appears to be altered by growing conditions (Becker, 2000). Conversion of biomass is highly dependent on biochemical composition and assessment of the carbon economy of microalgae must be accompanied by biochemical analysis of its biomass.

Mathematical expressions of the various biological and physiological processes governing microalgae production and their responses to environmental factors are being integrated into mechanistic simulation models to gain an understanding of their complex interactions and to optimize the efficiency of microalgae-based production systems.

Methods and Materials

To quantify the relationships between the fundamental biological and physiological responses to environmental factors, studies were conducted at the Microalgae Physiology Laboratory located at the Texas AgriLife Research Center in Corpus Christi. This lab houses a new, state-of-the-art, fully automated, controlled-environment system of four 75.6 L flat-plate microalgae bioreactors (FACE 4 Bioreactors) capable of measuring microalgae growth continuously using a carbon balance approach while exposing the culture to accurately controlled levels of environmental factors (Figure 1).

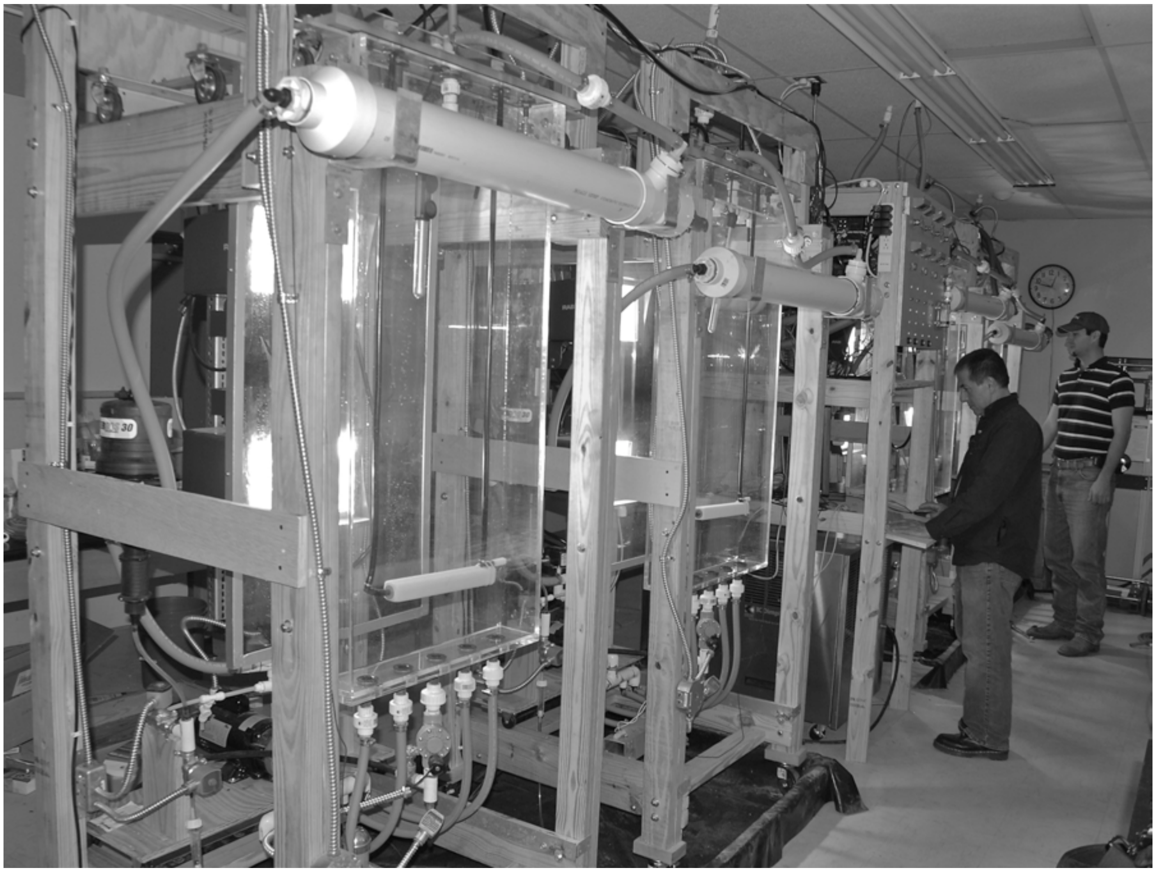

Figure 1. Fully automated controlled-environment microalgae bioreactor system at the Microalgae Physiology Laboratory located at the Texas AgriLife Research and Extension Center in Corpus Christi.

Cultures of *Nannochloropsis salina* were grown at 25 C and exposed to five levels of photosynthetic photon flux densities (PPFD) ranging from 250 - 1250 μmol $m^{-2}s^{-1}$. Upon inoculating the FACE 4 Bioreactors with microalgae, PPFD was measured across the 10.16 cm thick vertical flat plate (51.12 cm X 111.76 cm) bioreactors with various concentrations of microalgae using a Li-Cor (model # LI-1935A) bulb quantum sensor. Nonlinear regression analyses of PPFD data were done to estimate the light attenuation coefficients to be used in the mechanistic model.

The dry weight biomass of the culture was assessed daily. Biomass density was estimated using a regression between total suspended solids (TSS) and optical density (OD) recorded at a wavelength of 750 nm using a UV–vis spectrophotometer (Standard Methods 8111G.4c; APHA, 1998). Growth studies were conducted in a 1L fermenter under optimal conditions and dry weight biomass was assessed every 6 hours. Growth curves were obtained and linear regression analyses of the natural log of biomass concentration during the exponential growth phase indicated the maximum growth rate.

Model Development

The mechanistic model of the microalgal productivity in FACE 4 is being developed using the "STELLA" modeling platform (High Performance Systems, 1996) (Figure 2).

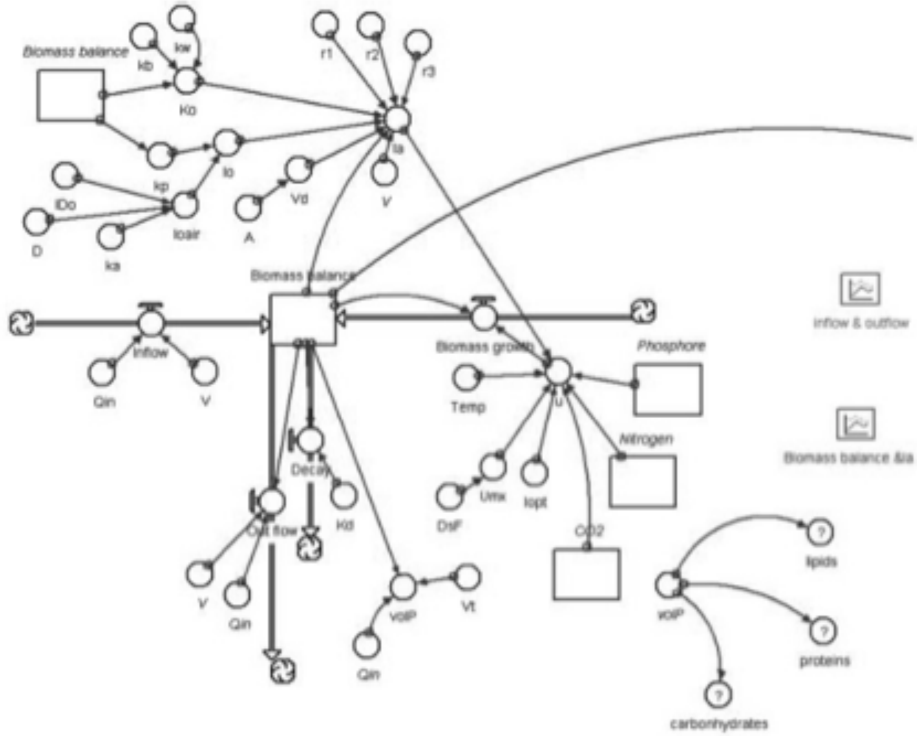

Figure 2. Map of the mechanistic model (developed using the "STELLA" modeling platform) of the microalgal productivity in a fully automated controlled-environment microalgae bioreactor system.

The governing equation for the model was based on a mass balance for FACE 4 modeled as a continuous flow stirred tank reactor (CFSTR) with the concentration of effluent biomass (X_o) for the CFSTR being the equal to the instantaneous biomass concentration of the CFSTR (X). The differential equation around the CFSTR is:

where: Q_i is the inflow of culture media; X_i is the concentration of biomass in the inflow; Q_o is

$$\frac{\partial X}{\partial t}V = (Q_i X_i) - (Q_o X_o) + (\mu X V) \quad (1)$$

the outflow; V is volume of the reactor; and μ is the growth rate in the CFSTR.

The effects of light dynamics on the net specific growth rate was factored into the growth term of equation 1. The dependence of growth rate on light peaks at an optimal level (I_{opt}) thus, Steele's, (1965) growth model was applied which acknowledges that growth is limited by low irradiance and inhibited by high irradiance levels:

$$\mu = \mu_{max}\left(\frac{I}{I_{0pt}}\right)e^{\left(1-\frac{I}{I_{opt}}\right)} \quad (2)$$

where: I_{opt} is the average PPFFR causing the maximum specific growth rate (μ_{max}).

The data collected during studies in a FACE 4 were used to estimate the parameters for the model. The productivity model includes a component that averages PPFD over the depth of the culture (by integrating Lambert Beer's Law over the thickness of the reactor) at the instantaneous biomass concentration in the reactor to determine the average, instantaneous PPFD (I_a). Each module also includes a complex growth rate term, which is the product of a series of influence factors and μ_{max}. These influence factors represent the effect of temperature T, I_a, nutrients P and N, and CO_2 have on growth rate (μ). The light attenuation coefficient (k_{aw}), optimum I_a (I_{opt}) and maximum specific growth rate (μ_{max}) vary for lighting conditions and for different microalgal species. The studies in the experimental unit were performed to determine these three parameters for different light intensities.

The P_v component, which calculates productivity based on the product of the dilution rate D and the biomass concentration in the CFSTR, was incorporated into the productivity model. Once the relationships between P_v and the cellular partitioning into lipids, proteins and carbohydrates are determined they will be used to calculate the different products based on the P_v. The model will also calculate E_o from the P_v.

References

Acien Fernandez, F.G., Sanchez Perez, J.A., Fernandez Sevilla, J.M., Garcia Camacho, F., Molina Grima, E., 2000. Modeling of Eicosapentaenoic Acid (EPA) production from *Phaeodactylum tricornutum* cultures in tubular photobioreactors. Effects of dilution rate, tube diameter, and solar irradiance. Biotech. and Bioeng. 68 (2), 173-183.

Becker, E.W. 1994. Microalgae as a source of protein: research review. Biotechnol. 25:207-210.

Benson B.C., Gutierrez-Wing M. T. Rusch K. A. 2009. Optimiztion of the lighting system for a Hydraulically Integrated Serial Turbidostat Algal Reactor (HISTAR): Economic Implications. Aquaculture Engineering 40: 45-52.

Chisti Y., 2007. Biodiesel from Microalgae. Biotechnol. Adv. 25:294-306.

Huntely, M., Redalie, D., 2007. "CO_2 Mitigation and renewable oil from photoshnthetic microbes: a new appraisal", Mitigation and Adaptation Strategies for Global Change. Vol.12: 573-608.

Molina-Grima, E.M., Garcia Camacho, F., Sanchez Perez, J.A., Contreras Gomez, A., Valdez Sanz, F., 1994. Outdoor turbidostat culture of the marine microalga *Tetraselmis sp*. Aqua. Fish Man. 25, 547-555.

Zou, N., Richmond, A., 1999. Effect of light-path length in outdoor flat plate reactors on output rate of cell mass and of EPA in *Nannochloropsis sp*. J. Biotechnol. 70 (13), 351-356.

3.19
INNOVATIVE ALGAE DEWATERING TECHNOLOGY

A.R. Völkel[1,], H. B. Hsieh[1], N. Chang, K. Melde[1], A. Kole[1]*

Abstract

This paper describes a novel technology for dewatering of bio materials, such as algae, for biofuel production and other applications. This hydrodynamic separation (HDS) technology uses customized fluid flow patterns to focus suspended particulates into a well-defined band near a side wall of a curved channel, and where they can be separated off with a suitably designed flow splitter. The novel and innovative capability of this system is its ability to separate particles of any density, including neutrally buoyant particles such as algae and other biological and/or organic matter, from a liquid without the use of a physical barrier. Advantages of this technology over conventional practice include: small foot print, low energy requirement, rapid process, and continuous flow operation. We explored the dewatering of different algae species including Spirulina, Chlorella Vulgaris, and S. dimorphus. Larger algae or algae that naturally form larger aggregates can be concentrated very efficiently without the use of any added chemicals and harvesting efficiencies up to 97% have been demonstrated. This makes HDS very attractive for the dewatering of algae from concentrations typical for open ponds (<0.1%) to above 1 % dry weight, where the addition of flocculants, which is needed for most other dewatering technologies, is costly and may add constraints to the reuse of the clean stream.

Keywords: Hydrodynamic separation, algae dewatering, bio fuels

Introduction

Algae are one of the potential crops for the production of all kinds of biofuels. Typically cultivated at a concentration of 0.02-0.06% total suspended solids, microalgal cultures requires dewatering to reach a concentration of 5-25% TSS depending on target process objective (Uduman 2010). This dewatering step adds a significant portion to the cost of the entire process, often as high as 25-40%, due to the vast amount of water that needs to be treated. Centrifugation is energy intensive, but also dissolved air flotation (DAF) requires significant amount of energy for aeration plus cost of chemicals. A less energy intensive alternative technology for dewatering is highly desirable.

The Palo Alto Research Center (PARC) has invented, tested and demonstrated at the laboratory scale a novel, low-cost, hydrodynamic separation technology for continuous-flow, barrier-free removal of all types of particles from multiple water matrices (Lean 2008 and 2010, Völkel 2011). Besides using this technology directly to remove already existing larger suspended particles from a liquid stream, it can be used in combination with a flocculation stage to grow smaller particles into larger aggregates before separation.

In the following sections we provide a more detailed description of this novel separation technology followed by specific application examples for removal of selected algae samples.

Hydrodynamic Separation

PARC has developed a novel hydrodynamic separation (HDS) technology for the concentration of suspended particles in fluids. By carefully controlling the flow conditions in a curved channel

[1] *Palo Alto Research Center, 3333 Coyote Hill Rd., Palo Alto, CA 94304;*

* *Corresponding author*

suspended particles are moved through a combination of hydrodynamic forces (drag, shear, etc.) to an equilibrium position near one of the side walls. By placing a flow splitter at the end of the channel a dilute stream, and a concentrated particle stream is obtained (Figure 1).

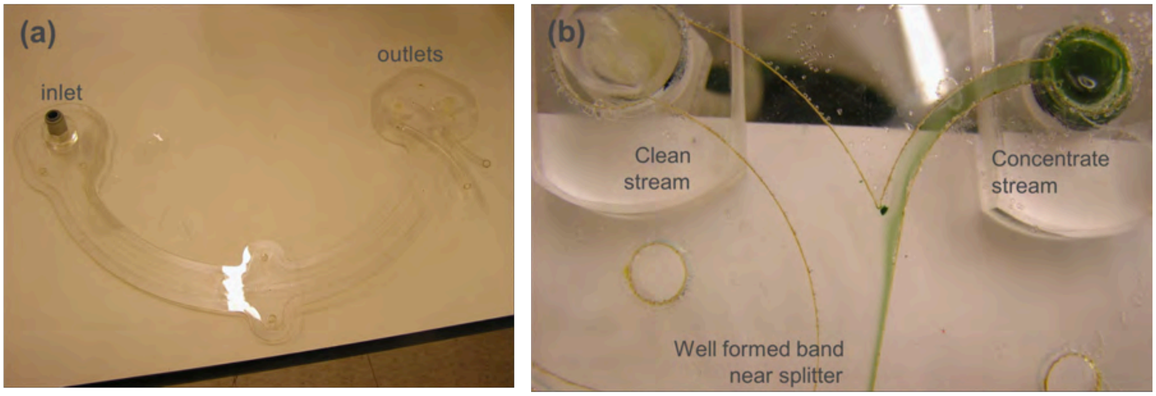

Figure 1: (a) Typical "half-turn" HDS channel for algae dewatering experiment; (b) Flow splitter with well-developed algae (spirulina) band.

The novel and innovative feature of this system is the fact that the separation is predominantly driven by the particle size, even though no physical barrier is involved. This makes this technology especially attractive for separating out organic and/or biological particles (such as algae), which have a density close to water and tend to foul on any mechanical barriers used to filter them.

This technology has been tested on many raw water matrices, including seawater, ballast water, and different types of wastewater and particle concentrations of up to a few % by weight have been demonstrated with a single stage separator. Based on test results with our research prototypes and technical analyses conducted to date, the technology appears compelling on a number of dimensions:

- Highly effective with neutrally buoyant material, making it highly suitable for removal of organic and biological particles as well as oil/water separation.
- Optimal performance for concentrations typically found in algae ponds up to a few weight %.
- Highly modular design allows dewatering of algae at the ponds, even for large area pond systems, without the need of pumping huge quantities of water.
- Direct concentration of algae without the use of chemicals allows recycling of the clean water stream directly back into the algae ponds.

Sample Results

We have explored separation efficiencies for several different algae species at the laboratory scale using HDS technology. For direct (chemical free) separation tests we used a HDS channel that concentrates particles above a size of about 20 μm. Sample characterization and dewatering efficiency were measured using two different analytical approaches:

Particle size distribution (PSD). Particle sizes affect the separation efficiency of HDS and thus are carefully monitored. Horiba LA-950 is a laser-scattering based particle size analyzer and was used for all PSD measurements.

Total suspended solids (TSS). TSS assays are performed confirming to the gravimetric method approved in "Method 2540 D, Total Suspended Solids" by Standard Methods committee in 1997.

Sufficient amount of each sample was carefully filtered through 1.5 µm glass fiber filter with house vacuum and the filter was baked at 105ºC for at least one hour or until the weight change was negligible. The net dry weight of the solids retained is divided by the volume of liquid filtered to calculate the TSS in mg/L or ppm.

Separation test were done with "full-turn" (345º arc length) and "half-turn" (180º arc length) channel and a splitter design with a flow rate ratio of 80:20 of dilute to concentrate stream was used. The total suspended solids (TSS) of the input sample and the two exit streams are measured and the harvesting efficiency η_H=(total mass in concentrate stream)/(total mass in input stream), which provides a measure of how much of the original algae mass is contained in the concentrate stream, is calculated.

Spirulina algae

Spirulina has a cork-screw-like shape with a diameter of 30-50 µm and can be as long as 200-300 µm. Despite its odd shape it is separated very well with HDS. Starting from a concentration of 0.8 g/l a 6-fold concentration increase to 4.6 g/l at over 97 % harvesting efficiency is achieved. Assuming a similar harvesting efficiency at a second stage the algae concentration can be pushed above 1 % by weight at a total harvesting efficiency of > 90% and with more than 90% water recovery rate (Figure 2). Reducing the channel length by half reduces harvesting efficiency by about 5% to about 93%, but leads to a 50% reduction in pressure from about 20 psi to about 10 psi.

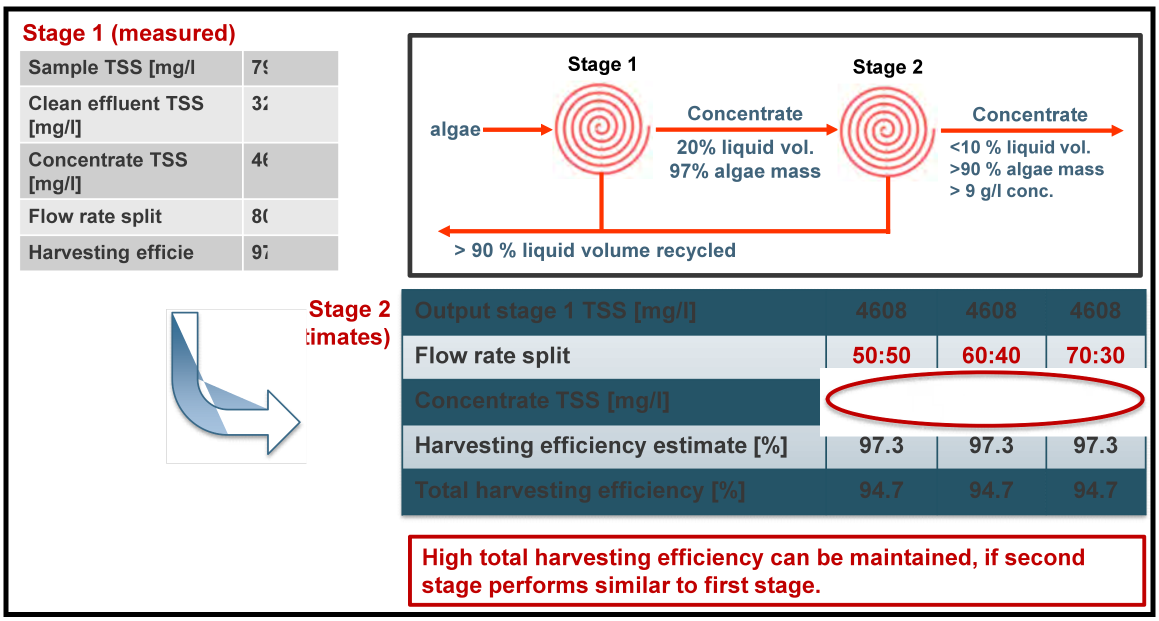

Figure 2: Schematic 2-stage algae dewatering process. Top left table shows experimental results achieved using spirulina algae with a single concentration stage. Bottom right table shows concentration estimates of a second stage with different flow splits.

S. dimorphus algae

Smaller algae can be concentrated with HDS devices by using a polymer, which promotes flocculation into larger aggregates. For a test with the algae species S. dimorphus, which is less than 10 µm in size, we used the bio-degradable flocculent Chitosan [Guibal 2006]. Figure 3 shows a schematic process diagram and PSD curves of the sample at different stages of this process. The aggregates are about 100 µm in size and a low pressure (low shear) HDS channel (1.1 psi) was used to avoid potential floc break-up during separation.

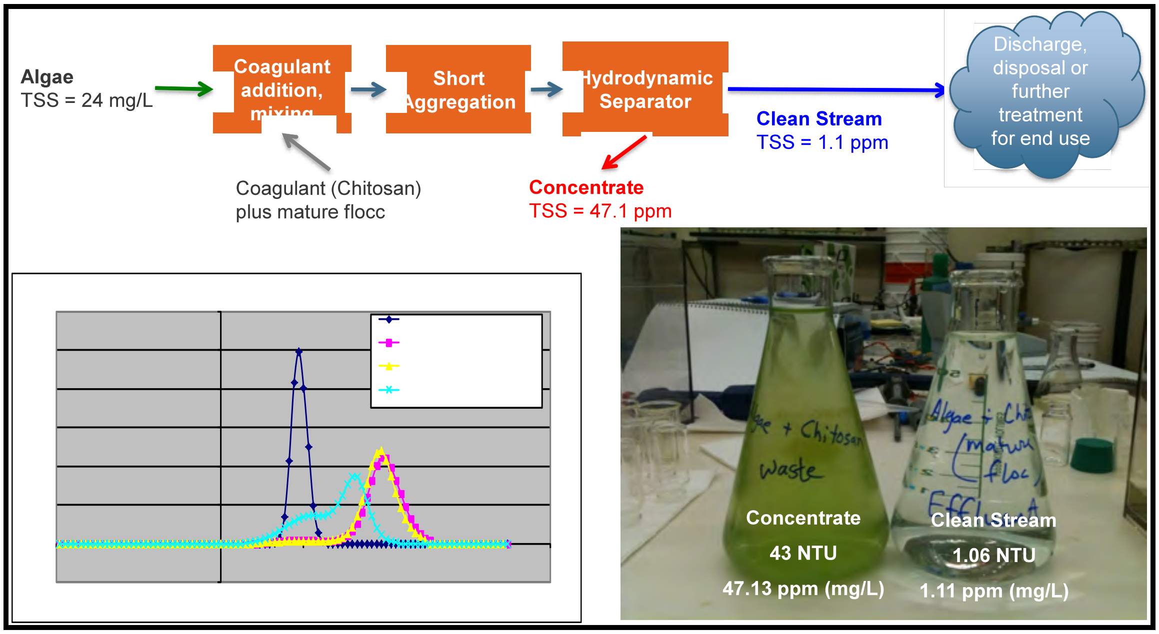

Figure 3: Top: process schematics for separation experiment with S. dimorphus algae. Bottom left: PSD data for dimorphus algae: blue: raw sample; pink: after flocculent addition; yellow: concentrate stream; cyan: dilute stream. Bottom right: output from concentrate (left) and dilute (right) stream.

The separator used for this experiment had a 50:50 flow splitter, resulting in a doubling of the algae concentration, while only a few percent of the algae where lost with the dilute stream. The smaller aggregates that are left with the dilute stream grow further as can be seen by the peak at about 50 [?]m from the PSD measurement in Figure 3. A higher concentration factor may be achieved by using a more optimized splitter design and by cascading multiple HDS in series.

Conclusions

This paper describes a novel approach for the removal of suspended solids from many water matrices. Using purely hydrodynamic forces this technology efficiently removes suspensions by concentrating them into a narrow band that is split off the main stream without the need for physical filtration. Because this is a size and not density dependent particle concentration method it is ideally suited for the dewatering of algae from concentrations typically found in algae ponds up to a few weight %. Depending on the size of the algae separation can be achieved without the extra addition of any chemicals, allowing the direct recycling of the dilute stream back into the algae ponds. Smaller algae can be addressed with the use of a suitable flocculent, such as Chitosan. Added benefits include no moving parts, high scalability, high modularity in construction, and low cost in materials and TCO. In addition, this technology can be used for water treatment processes such as activated sludge recycling in a waste water plant.

References

Uduman N., et al. (2010), “Dewatering of microalgal cultures: A major bottleneck to algae-based fuels”, *J. Renewable Sustainable Energy* 2, 012701.

Lean, M.H., et al. (2008), “Curved Fluidic Structures to Improve Aggregation Kinetics in Municipal Water Treatment”, *Proc. Water Quality Technology Conference*.

Lean, M.H.; et al. (2010), “Innovative system to pre-treat seawater for RO”, *Proc Singapore International Water Convention*.

Völkel, A.R. (2011), “Innovative Technology for Selective Contaminant Removal”, *Proc. TechConnect.*

Guibal E., et al., (2006), “Review of the Use of Chitosan for the Removal of Particulate and Dissolved Contaminants”, *Separation Science and Technology, 41, 2487–2514.*

3.20
COMPARISON OF SYNGAS FERMENTATION REACTORS FOR BIOLOGICAL ALCOHOL PRODUCTION

Mamatha Devarapalli[1], Hasan K. Atiyeh[1,], John R. Phillips[1], James J. Orgill[b], Randy S. Lewis[2], Raymond L. Huhnke[1]*

Abstract
Cellulosic ethanol can be produced by fermenting syngas (CO, H_2 and CO_2) made from gasifying agricultural and forestry biomass feedstocks. Syngas fermentation is constrained by gas-liquid mass transfer limitation due to low CO and H_2 solubility in the fermentation broth. In the present study, the mass transfer capability of continuously stirred tank reactor (CSTR), trickle-bed reactor (TBR) and hollow fiber membrane reactor (HFR) for syngas fermentation was investigated. The volumetric mass transfer coefficient ($K_{tot}A/V_L$) for O_2 in the three reactors was measured experimentally. The highest $K_{tot}A/V_L$ was obtained for the HFR-module 4 (871 h^{-1}) that is made of polydimethylsiloxane (PDMS) followed by the TBR (421 h^{-1}). The highest $K_{tot}A/V_L$ for the CSTR was 114 h^{-1}. Reactor configuration, agitation speed, and gas and liquid flow rates greatly affected the mass transfer characteristics for each reactor.

Keywords: syngas, mass transfer, continuously stirred tank reactor (CSTR), trickle-bed reactor (TBR)

Introduction
Hybrid thermochemical-biochemical technology, such as gasification-fermentation, has the potential to increase the alcohol yield by more than 35%, compared to the saccharification-fermentation process. This is due to the utilization of all components of the biomass (cellulose, hemicellulose, and lignin). In gasification, biomass is converted into synthesis gas (syngas), primarily consisting of CO, CO_2, and H_2. The syngas is then cleaned to remove particulates and tars, which may inhibit its biochemical conversion by microbial catalysts. Syngas fermentation involves complex biochemical reactions to convert H_2, CO and/or CO_2 into liquid fuels using microbial catalysts such as *Clostridium ljungdahlii, Clostridium carboxidivorans, Clostridium ragsdalei, Alkalibaculum bacchi (Liou et al., 2005; Liu et al., 2012; Maddipati et al., 2011; Phillips et al., 1994; Tanner et al., 2008; Wilkins & Atiyeh, 2011)*. The conversion efficiency and productivity of syngas fermentation are affected by gas to liquid mass transfer limitation, low cell density and enzyme inhibition by syngas components. The mass transfer limitation is related to the low solubility of CO and H_2 in the fermentation broth. Additionally, gas-liquid mass transfer depends on reactor configuration. A comparison of continuous stirred tank reactor (CSTR), packed bubble column (PBR) and trickle bed reactor (TBR) showed that TBR had higher mass transfer than PBR and CSTR (Klasson et al., 1990). The use of submerged hollow fiber membrane reactor (HFR) (Munasinghe & Khanal, 2010) or a microsparger in a CSTR also enhanced mass transfer (Bredwell & Worden, 1998). The objective of the present study is to investigate the mass transfer characteristics of continuously stirred tank reactor (CSTR), trickle bed reactor (TBR) and hollow fiber reactor (HFR) at various operating conditions. The overall mass transfer coefficient of O_2 in water was experimentally measured in each reactor and compared.

[1] *Department of Biosystems and Agricultural Engineering, Oklahoma State University, OK*

[2] *Department of Chemical Engineering, Brigham Young University, UT*

[*] *Corresponding author*

Materials and Methods

Trickle Bed Reactor (TBR)

The TBR reactor is made of borosilicate glass (61 cm long × 5.1 cm diameter). The TBR was packed with soda lime glass beads. Two bead sizes (3 mm or 6 mm) were investigated. The beads were held using a metal mesh above a sump that hold 200 ml of deionized water at the bottom of the TBR. A perforated Teflon disk was used to distribute water flowing from the top of the TBR. The gas and liquid flow was counter current. The gas flow rate was controlled using a rotameter. The DI water in the sump was circulated in the TBR using a peristaltic pump (Cole Parmer, Vernon, IL, USA). A dissolved oxygen (DO) probe (New Brunswick, Edison, NJ, USA) was placed in-line in the recirculation loop. Various gas and liquid flow rates were examined.

Various gas (6 to 144 ml/min) and liquid (20 to 1000 ml/min) flow rates were examined at 20 °C and 37 °C. The liquid flow rate was set to the desired value and N_2 was purged through the TBR until the DO reading reached zero. Then, the gas was switched to air at the desired gas flow and DO concentration in % saturation was recorded with time using Biocommand software (New Brunswick, Edison, NJ, USA) until the liquid was completely saturated. The overall mass transfer coefficient ($K_{tot}A/V_L$) was calculated using Eq. 1.

$$\frac{K_{tot}A}{V_L} = \frac{ln\left(1-\frac{C_L}{C_S}\right)}{t} \cdot \frac{V_S}{V_L} \qquad (1)$$

where, K_{tot} is the total mass transfer coefficient (m/h), A is the mass transfer area (m^2), V_S is the total volume of the liquid in the reactor (m^3), V_L is the volume of the liquid between the beads in the TBR (m^3), C_L is the bulk DO concentration in the liquid (mol/m^3), C_S is the saturated DO concentration (mol/m^3) and t is the time (h). V_L was the difference between measured resting and operating liquid volumes in the TBR sump at a given gas and liquid flow rates.

Continuously Stirred Tank Reactor (CSTR)

A 3-L BioFlo110 fermentor (New Brunswick Scientific, Edison, NJ, USA) was assembled with two rushton impellers of 5.1 cm diameter, a baffle ring with 4 baffles 14 cm long and 1.3 cm wide, and a sparger. An external heating blanket was used to control temperature at 37 °C. The reactor was configured as suggested by (Bakker et al., 1994). A mass flow controller (Porter, Hatfield, PA, USA) was used to control the gas flow rate. The CSTR was filled with 2.5 L DI water and purged with N_2 until the DO concentration reached zero. The desired agitation speed and air flow rate were set and the changes in DO concentration with time was recorded using Biocommand software. Agitation speeds from 150 to 900 rpm, and gas flow rates from 60 to 400 ml/min were used. The overall mass transfer coefficient ($K_{tot}A/V_L$) for O_2 was calculated using Eq. 1. For the CSTR, V_L and V_S are the same so V_S/V_L is 1.

Hollow Fiber Reactor (HFR)

A 5-L tank was filled with DI water and deaerated with N_2. The O_2-free water was passed through the shell of the HFR using a peristaltic pump (Masterflex, Vernon Hills, IL, USA). Air was passed through the fiber lumen in the HFR at 25 °C and 101.3 kPa. The inlet and outlet pressures were measured using pressure transducers. The gas flow rate was measured using a rotameter. Hydrophilic HFRs were wetted with water prior to the mass transfer experiment in order to reduce the variability between experiments due to absorption of water into the pores. DO probes were used to measure the inlet and outlet DO concentration for a single pass of the water through the shell side of the HFR. DO measurements were collected for 5 different HFR modules (Table 1) at 25 °C and liquid flow rates between 20 and 80 ml/min. DO measurements for module 4 were obtained at liquid flow rates up to 400 ml/min because it has the highest A/V_L. The % DO saturation at each liquid flow rate was recorded after the HFR reached quasi-steady state (40 min for liquid flow rates 20 - 30 ml/min, 30 min for 30 - 80 ml/min, 20 min for 80-140 mL/min, and 10 min for >140 mL/min).

Table 1 Specifications of HFR modules used in the mass transfer experiments.

Module[a]	(1) PS[b]	(2) PES[b]	(3) PP[c]	(4) PDMS[d]	(5) FPS[c]
Fiber ID (μm)	500	1000	480	200	200
Fiber OD (μm)	660	1300	630	300	280
V_L (mL)	18.6	16.6	9.7	25	237
A/V_L (m^{-1})	4366	2271	4361	10000	9198

[a] PS: polystyrene; PES: polyethersulfone; PP: polypropylene; PDMS: polydimethylsiloxane; FPS: Fresenius polysulfone; [b] hydrophilic, porous; [c] hydrophobic porous; [d] hydrophobic, nonporous

The mass transfer coefficient ($K_{tot}A/V_L$) for O_2 in the HFR was calculated using Eq 2.

$$\frac{K_{tot}A}{V_L} = \frac{C_{L_{Out}} \cdot Q}{V_L \cdot \Delta C_{lm}} \qquad (2)$$

where, K_{tot} is the total mass transfer coefficient (m/h), A is the mass transfer area (m^2), which is the total fiber outer surface area for non-porous HFRs or the total outer pore area for the porous HFRs, V_L is the volume of liquid in the shell of the HFR (m^3), C_{Lout} is the quasi-steady state concentration of O_2 in the liquid outlet (mol/m^3), Q is the liquid volumetric flow rate (m^3/h), and ΔC_{lm} is the log mean O_2 concentration difference between the saturated DO concentration C_S (mol/m^3), and inlet C_{Lin} and outlet C_{Lout} DO concentrations in water (mol/m^3). For HFRs, K_{tot} includes the intrinsic mass transfer coefficient of the membrane for the module used.

Results and Discussion

The effect of bead size, gas and liquid flow rates on $K_{tot}A/V_L$ is shown in Fig. 1. The $K_{tot}A/V_L$ increased with the increase in gas flow rates. However, it decreased with the increase in liquid flow rates. The $K_{tot}A/V_L$ was higher in the TBR with 6 mm beads. It is known that the overall mass transfer coefficient increases with the increase in the gas-liquid interfacial area. The interfacial area with the 3 mm beads was 50% higher than with the 6 mm beads. In addition, the liquid holdup volume between the 6 mm beads (V_L) was almost two times lower than with the 3 mm beads. Lower V_L resulted in higher $K_{tot}A/V_L$. Also, an increase in the liquid flow rate increases the liquid holdup (V_L) between the beads and the thickness of the liquid film around the beads. This causes an increase in the gas-liquid mass transfer resistances and consequently reduces the $K_{tot}A/V_L$. The gas flow rates used did not affect V_L. No significant effect of temperature on $K_{tot}A/V_L$ was measured using statistical analysis using ANOVA model in SAS software with p value > 0.05. The maximum obtained $K_{tot}A/V_L$ values for 3 mm and 6 mm beads at 37 °C were 178 h^{-1} and 421 h^{-1}, respectively.

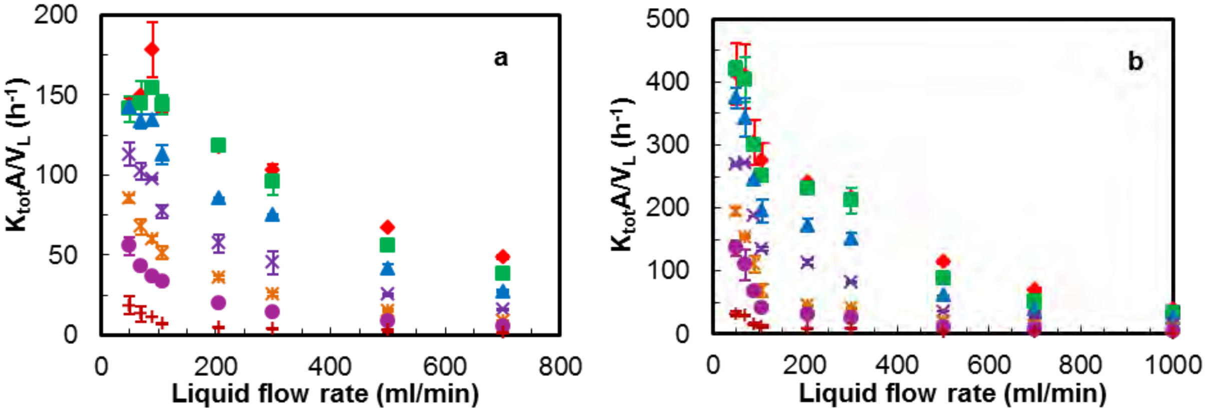

Fig. 1 $K_{tot}A/V_L$ values for (a) TBR with 3 mm beads and (b) TBR with 6 mm beads at various air flow rates (+) 6, (●) 20, (*) 31, (×) 51, (▲) 80, (■) 117, (♦) 144 ml/min. Error bars represent ± 1 standard deviation.

The effect of agitation speed and gas flow rate on $K_{tot}A/V_L$ in the CSTR is shown in Fig. 2. The increase in the gas flow rate or agitation speed increased $K_{tot}A/V_L$. The highest measured $K_{tot}A/V_L$ was 114 h^{-1} at 400 ml/min and 900 rpm. For the HFRs, the specification of the membranes (hydrophilic *vs.* hydrophobic or porous vs. nonporous shown in Table 1) used affected the $K_{tot}A/V_L$ values (Fig. 3). Among all the five modules, the highest $K_{tot}A/V_L$ was obtained with the nonporous polydimethylsiloxane (PDMS) module 4. The hydrophobicity of the PDMS membrane increases the $K_{tot}A/V_L$ because most of the membrane diffusion is gaseous diffusion as opposed to liquid diffusion. The PDMS module 4 has also the largest A/V_L (Table 1). The small increase of $K_{tot}A/V_L$ with liquid flow rate for the PS and PES modules 1 and 2, respectively, indicates that these modules become limited by membrane resistance in this flow regime. The linear increase of $K_{tot}A/V_L$ with flow rate for the FPS module 5 indicates that this module is largely limited by the liquid boundary layer in this flow regime.

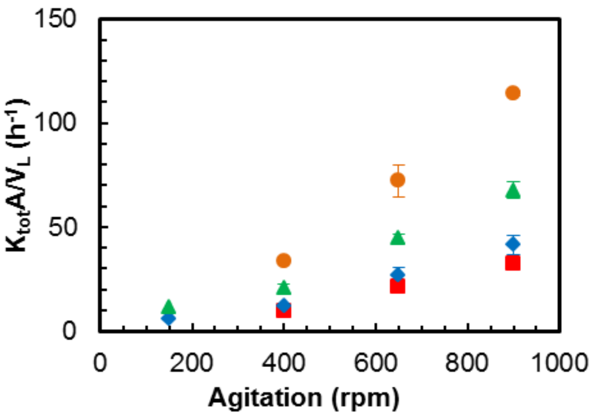

Fig. 2 $K_{tot}A/V_L$ values for CSTR at various air flow rates (■) 60, (♦) 100, (▲) 200 and (●) 400 ml/min. Error bars represent ± 1 standard deviation.

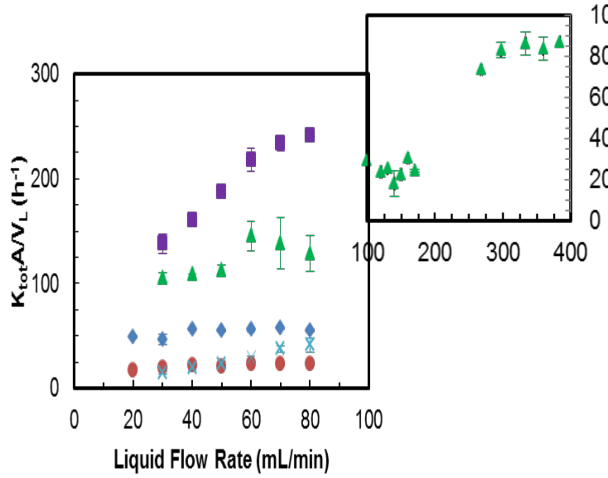

Fig. 3 $K_{tot}A/V_L$ values for HFR at various liquid flow rates and (♦) Module 1, (●) Module 2, (■) Module 3, (▲) Module 4, (×) Module 5 as in Table 1. Error bars represent ± 1 standard deviation.

Conclusion

Among the three reactors tested in this study, highest $K_{tot}A/V_L$ was provided by the HFR followed by TBR and CSTR. In syngas fermentation, mass transfer provided must be balanced with the kinetic requirement. Gas flow rates over the kinetic capacity of the culture can compromise gas conversion efficiencies. To assess these effects, further analysis of the three reactors during syngas fermentation is ongoing.

References

Bakker, A., Smith, J., Myers, K.J. 1994. How to disperse gases in liquids. *Chemical Engineering*, 101(12), 98-104.

Bredwell, M.D., Worden, R.M. 1998. Mass Transfer Properties of Microbubbles. 1. Experimental Studies. *Biotechnology Progress*, 14(1), 31-38.

Klasson, K., Elmore, B., Vega, J., Ackerson, M., Clausen, E., Gaddy, J. 1990. Biological production of liquid and gaseous fuels from synthesis gas. *Applied biochemistry and Biotechnology*, 24(1), 857-873.

Liou, J.S.C., Balkwill, D.L., Drake, G.R., Tanner, R.S. 2005. Clostridium carboxidivorans sp. nov., a solvent-producing clostridium isolated from an agricultural settling lagoon, and reclassification of the acetogen Clostridium scatologenes strain SL1 as *Clostridium drakei* sp. nov. *International Journal of Systematic and Evolutionary Microbiology*, 55(5), 2085-2091.

Liu, K., Atiyeh, H.K., Tanner, R.S., Wilkins, M.R., Huhnke, R.L. 2012. Fermentative production of ethanol from syngas using novel moderately alkaliphilic strains of *Alkalibaculum bacchi*. *Bioresource Technology*, 104, 336-341.

Maddipati, P., Atiyeh, H.K., Bellmer, D.D., Huhnke, R.L. 2011. Ethanol production from syngas by *Clostridium* strain P11 using corn steep liquor as a nutrient replacement to yeast extract. *Bioresource Technology*, 102(11), 6494-6501.

Munasinghe, P.C., Khanal, S.K. 2010. Syngas fermentation to biofuel: Evaluation of carbon monoxide mass transfer coefficient (k_La) in different reactor configurations. *Biotechnology Progress*, 26(6), 1616-1621.

Phillips, J.R., Clausen, E.C., Gaddy, J.L. 1994. Synthesis gas as substrate for the biological production of fuels and chemicals. *Applied Biochemistry and Biotechnology*, 45(1), 145-157.

Tanner, R.S., Wall, J., Harwood, C., Demain, A. 2008. Production of ethanol from synthesis gas. Amer Society for Microbiology. pp. 147.

Wilkins, M.R., Atiyeh, H.K. 2011. Microbial production of ethanol from carbon monoxide. *Current Opinion in Biotechnology*, 22(3), 326-330.

3.21 METABOLIC NETWORK ANALYSIS OF XYLOSE METABOLISM BY *PICHIA STIPITIS*

Meng Liang[1], Min Hea Kim[1], Qinghua He[2], Jin Wang[a]

Abstract

The conversion of pentoses to ethanol is one of the major barriers of industrializing lignocellulosic ethanol processes. As the most promising native strain for pentoses fermentation, *Pichia stipitis* has been widely studied for its xylose fermentation. In spite of the abundant experimental evidence regarding ethanol and by-products production under various aeration conditions, the mathematical descriptions of the processes are relatively rare. In this work, the constraint-based metabolic network model for central carbon metabolism of *P. stipitis* was reconstructed by integrating genomic (*P. stipitis* v2.0, KEGG), biochemical (ChEBI, KEGG) and physiological information available for this microorganisms and other related yeast. The stoichiometry of the metabolic reactions was used in combination with biosynthetic requirements for growth and pseudo-steady state mass balances over intracellular metabolites for the quantification of metabolic fluxes using metabolite balancing. This model was employed to perform an *in silico* characterization of the phenotypic behavior of *P. stipitis* grown on xylose and the model predictions are in general agreement with published experimental results. The effects of single reaction deletions on growth were assessed. In the process, essential biochemical reactions for growth were identified. In addition, flux balance analysis has been applied to the model to elucidate the redox balance of *P. stipitis* for xylose fermentation. The results revealed key metabolic constraints related to redox homeostasis. A comparison of flux distribution involved in redox balance with different oxygenation conditions provides important insights on the role of redox balance in the metabolism of xylose utilization, ethanol and xylitol production.

Keywords: xylose metabolism; Pichia (Scheffersomyces) stipitis; Flux Balance Analysis (FBA)

Introduction

High efficient utilization of xylose is one of the biggest obstacles for commercial production of lignocellulosic ethanol. *Pichia stipitis* (*P. stipitis*, now renamed as *Scheffersomyces stipitis*) has a set of physiological traits that make it potentially valuable candidate for the lignocellulosic ethanol production. Oxygen availability plays a critical role in xylose metabolism of *P. stipitis* due to redox balance (Jeffries & Van Vleet 2009). In spite of the abundant experimental evidence, little is known about the mechanism and metabolic flux distributions of how redox balance affects xylose metabolism. In this work we developed central carbon metabolic model for *P. stipitis* and analyzed xylose metabolism using Flux Balance Analysis (FBA) and Principal Component Analysis (PCA). The combination of FBA and PCA revealed details of metabolism shifts.

Methods

Construction of metabolic model

The metabolic model of *P. stipitis* was constructed following the published protocol (Thiele & Palsson 2010) and was built based on the genomic and biochemical information of the organism available in its

[1] Depart~~ment of Chemical Engineering,~~ Auburn University, AL

[2] Department of Chemical Engineering, Tuskegee University, AL

* Corresponding author

genome project (Jeffries & Van Vleet 2009), KEGG, ChEBI and PubChem. An overview of the metabolic model is shown in Box 1. Cell mass reaction in the model was assembled from the macromolecular components (Senger 2010). The contribution of each component to cell mass and the appropriate coefficients for every building block were estimated from literature data.

Flux Balance Analysis (FBA)

Flux balance analysis was performed using a publicly available COBRA toolbox for Matlab version 2.04 (Schellenberger et al. 2011). The output of the toolbox includes the values of metabolic fluxes. The simulated results were used for further analysis to reveal the intracellular mechanism of xylose metabolism.

Principal Component Analysis (PCA)

Principal component analysis (PCA) is a simple, non-parametric method for extracting relevant information from confusing data sets (Jolliffe 2002). In this work, PCA was carried out with PLS toolbox for Matlab version 3.0 (Eigenvector Research, Inc.). The simulated metabolic fluxes were used as the input for PCA to identify different phenotypes caused by various oxygen supplies. The scores generated by PCA were used to distinguish the distributions of different reactions to the metabolic status changes.

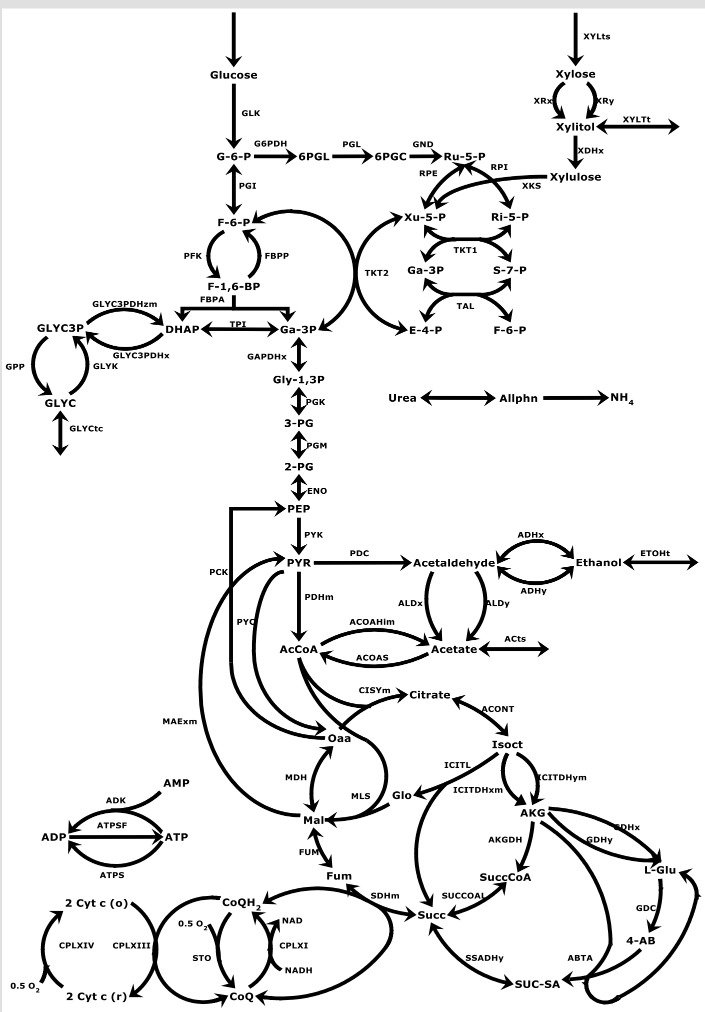

Brief description of the metabolic network model

The model represented cell growth on glucose and xylose. 117 reactions (66 reversible and 51 irreversible) were included. 15 compounds were allowed to exchange with external environment. Reactions were constituted from glycolysis, pentose phosphate pathway, tricarboxylic acid (TCA) cycle, glyoxylate and dicarboxylate metabolism, oxidative phosphorylation, nitrogen metabolism, nicotinate and nicotinamide metabolism, cell mass formation, and synthesis pathways of common byproducts of *P. stipitis*: ethanol, glycerol, xylitol and acetate. Some linear reactions in the model were lumped together for simplification. Transport reactions, including passive diffusion, facilitated diffusion and active transport, were also incorporated. Non-growth associated maintenance energy was set to 3.5 mmol/gDCW/h. The metabolic map (left) represents a brief overview of the metabolic network.

Box 1. Overview of the metaboilc network model

Analysis of *P. stipitis* metabolic network

After the construction of the model, FBA was applied to study the intracellular metabolic flux distributions under various conditions. In this work, the model was constrained to grow on minimal defined medium (Jeffries et al. 2007). The reaction essentiality to cell growth was evaluated as whether its removal was fatal. The results (excluding transport reactions and cell mass reaction) showed differences with different cultivation conditions: 14 and 18 reactions for aerobic and oxygen-limited glucose culture respectively while 16 and 26 for aerobic and oxygen-limited xylose cultivation. 10 reactions in glycolysis, pentose phosphate pathway (PPP) and urea metabolism are essential under all conditions. The bigger differences in xylose metabolism under different aeration conditions confirmed that xylose metabolism is more sensitive to oxygen. The predictions of model with glucose or xylose under aerobic or oxygen-limited condition were shown in **Error! Reference source not found.**. Under aerobic condition the carbon has been used for cell growth and energy generation. Under oxygen-limited condition the cell growth was inhibited and ethanol was produced with by-products (acetic acid, glycerol or xylitol). These results were in good agreement with experimental observation and indicated the constructed model could capture metabolic changes caused by different carbon source and oxygen supply. The carbon flux distribution through PPP was also studied. The result under aerobic glucose culture was 61.66%, which was consistent with the reported value of 57±9% (Fiaux et al. 2003).

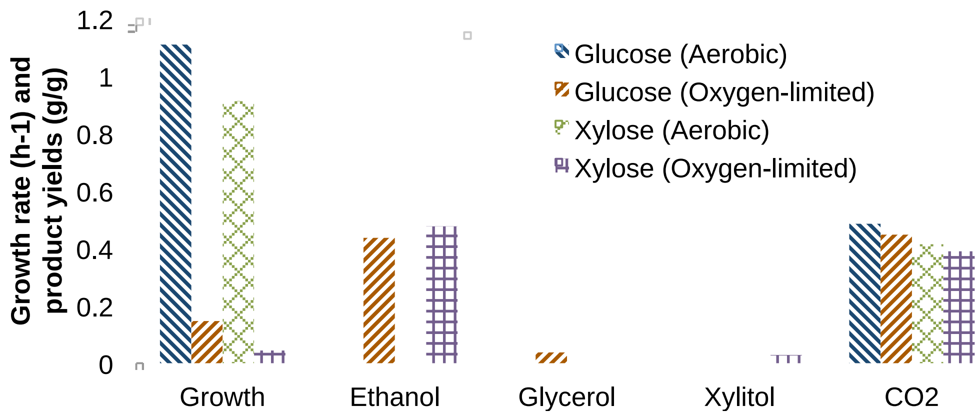

Fig. 1. Growth and products formation under various oxygen conditions

Analysis of redox balance in xylose metabolism

Oxygen plays an important role in cell growth, redox balance, functioning of the mitochondria and generation of energy for xylose transport in *P. stipitis*. But how oxygen influences the intracellular flux distribution and redox balance and which reactions would be most important for redox balance have not been studied systematically. In this work, the oxygen influences, especially on the redox balance, was studied by combining FBA and PCA. The intracellular flux data for PCA were generated by FBA through changing oxygen supply within [0, 20] mmol/gDCW/h with a step of 0.001. The ratio of fluxes through NADPH- and NADH-dependent XR and the ratio through $NADP^+$- and NAD^+-dependent XDH were set to 1.5 and 0.02 respectively. By PCA, six phenotypes have been identified with the constraint on xylose uptake rate of maximal 10 mmol/gDCW/h. The results were shown in Fig. **1**. The main characteristics of the six phenotypes identified were summarized in Table 1.

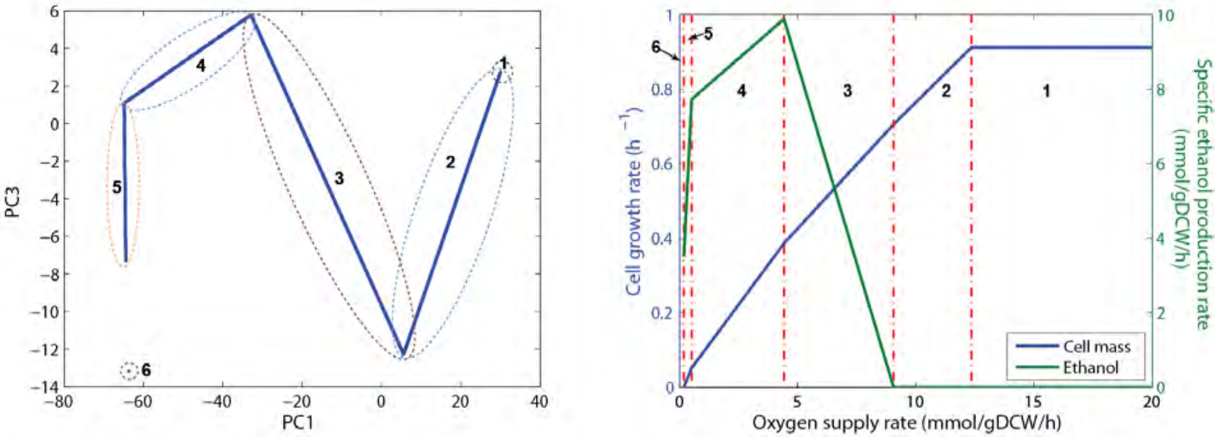

Fig. 1. Phenotypes identified with PCA when oxygen supply changes within [0, 20] mmol/gDCW/h.

Table 1. Characteristics summary of phenotypes.

Phenotype	Growth limitation	Metabolic product(s)	Main metabolic characteristics
1	Xylose	Cell mass	Aerobic growth
2	Xylose, Oxygen	Cell mass, acetic acid	Oxygen-limited and acetic acid production
3	Xylose, Oxygen	Cell mass, ethanol, acetic acid	Ethanol production and declined acetic acid production
4	Xylose, Oxygen	Cell mass, ethanol, xylitol	Declined ethanol production and increasing xylitol production
5	Oxygen	Cell mass, ethanol, xylitol	Declined ethanol and xylitol production.
6	-	-	Cannot maintain metabolism

With the scores for fluxes by PCA, the critical reactions for redox balance and the fluxes most influenced by oxygen supply change for each phenotype were also identified. The importance of identified reactions to redox balance in each phenotype was confirmed by comparison of the NAD(P)H consumption and generation fluxes. The involvement of key reactions to ethanol, xylitol, glycerol and acetic acid in the identified reactions indicated their roles to keep intracellular redox balance.

Conclusion

In this work the central carbon metabolic network of *P. stipitis* has been reconstructed. The validation of the model with experimental observation and flux distribution through PPP showed that the constructed model could capture most of the behaviors of central carbon metabolism. The essential reactions under different conditions were identified. Xylose metabolism by *P. stipitis*, especially redox balance, was studied by combining FBA and PCA. Six phenotypes have been identified and the reactions that satisfied the redox balance also been established. The results showed PCA could be a powerful tool for analyzing output of metabolic model.

References

Fiaux, J. et al. (2003). "Metabolic-flux profiling of the yeasts Saccharomyces cerevisiae and Pichia stipitis." *Eukaryotic Cell* 2(1), 170–80.

Jeffries, T.W. et al. (2007). "Genome sequence of the lignocellulose-bioconverting and xylose-fermenting yeast Pichia stipitis." *Nature Biotechnology* 25(3), 319–26.

Jeffries, T.W. and Van Vleet, J.R.H. (2009). "Pichia stipitis genomics, transcriptomics, and gene clusters." *FEMS Yeast Research* 9(6), 793–807.

Jolliffe, I.T. (2002). *Principal Component Analysis*. 2nd ed., Springer.

Schellenberger, J. et al. (2011). "Quantitative prediction of cellular metabolism with constraint-based models: the COBRA Toolbox v2.0." *Nature Protocols* 6(9), 1290–1307.

Senger, R.S. (2010). "Biofuel production improvement with genome-scale models: The role of cell composition." *Biotechnology Journal* 5(7), 671–85.

Thiele, I. and Palsson, B.Ø. (2010). "A protocol for generating a high-quality genome-scale metabolic reconstruction." Nature protocols 5(1), 93–121.

3.22

BIODIESEL-GLYCEROL CARBONATE PRODUCTION PLANT BY GLYCEROLYSIS

Nghi Nguyen[1], *Yasar Demirel*[1,*]

Abstract

Crude glycerol is the byproduct of the biodiesel production plant and the economic value of glycerol may affect the profitability of the biodiesel production plant. Bioglycerol market values drop considerably as its production rate increases. Thus, conversion of bioglycerol into value-added products can reduce the overall cost, hence, leading to a more economical biodiesel production plant. A recent study (Nguyen, N, Demirel, Y., 2011, Int. J. Chem.React. Eng. 9, A108) suggests that additional production of glycerol carbonate by direct carboxylation may be more economical than the conventional biodiesel production plant. However, direct carboxylation suffer low yield (<35%) leading to high production cost. Consequently, indirect use of carbon dioxide by glycerolysis of glycerol with urea is investigated in this study. The results show that the net present value of the biodiesel-glycerol carbonate production by glycerolysis plant is 27.83 $ million higher than the biodiesel-glycerol carbonate production by direct carboxylation plant at the end of the 12-year project. The stochastic model has predicted that using glycerolysis route for the synthesis of glycerol carbonate production may increase the probability of getting positive net present value by about 15%.

Introduction

Biodiesel is renewable, nontoxic, biodegradable, and essentially free of sulfur and aromatics, hence may be one of the most suitable candidates for future biofuel. Besides, U.S. Department of Energy life cycle analysis on biodiesel shows that biodiesel produces 78.5% less net carbon dioxide emissions compared to petroleum diesel (Sheehand et al., 1998). In 2011, the United States produces approximately 1.1 billion gallons of biodiesel annually and the volume of production is expected to increase to 1.9 billion gallons in 2015 (Urbanchuk, 2011). Major drawbacks of biodiesel production using vegetable oil are the cost of manufacturing and the high cost of oil since it competes with food. Currently, biodiesel production plants depend on government subsidies in order to keep their plants in operation (Urbanchuk, 2011). Thus, seeking for a more economic biodiesel production process to reduce the dependency of government subsidies and promote expansion of biodiesel industry is desirable.

About 1 kg of glycerol is formed for every 10 kg of biodiesel produced (Nguyen and Demirel, 2010). The production cost of biodiesel increases by $0.08/gal for every $0.10/lb reduction in glycerol selling price (Zheng et al., 2008). As a result, economical utilization schemes of bioglycerol can lead to a more economical biodiesel production plant. A recent study suggests that addition of glycerol carbonate production by direct carboxylation route may be more economical than the conventional biodiesel production plant (Nguyen and Demirel, 2011). However, recently, Li and Wang (Li and Wang, 2011) has suggested that direct carboxylation of glycerol and CO_2 is thermodynamically limited and the yield is very low (less than 35%) (George and Patel, 2009). Low yield requires high energy for products separation and reactants recovery leading to high cost of manufacturing. Thus, in this study, synthesis of glycerol carbonate by glycerolysis route is developed and economics of the biodiesel-glycerol carbonate production by direct carboxylation and glycerolysis plants are compared. Economic analysis based on

[1] Department of Chemical and Biomolecular Engineering, University of Nebraska Lincoln, NE

* Corresponding author

deterministic and stochastic models are used to compare the two plants to determine the most feasible process.

Glycerol Carbonate Production by Glycerolysis

The glycerolysis plant contains two sections as shown in Fig. 1. Section 1 (Fig. 1a) produces biodiesel and bioglycerol with methanol, while Section 2 (Fig. 1b) produces bioglycerol carbonate and water. Section 1 utilizes methanol and triglyceride to produce fatty acid methyl ester (FAME) and glycerol using calcined eggshell contains mostly CaO (~99%) as a catalyst (Chakraborty, 2010). Recycled and fresh methanol and oil are mixed in mixer M101 before they are fed into the reactor R101. The reactor effluent, stream S2, containing mixture of catalyst, products, and unreacted reactants, is sent to separator SEP101 to recover catalyst, which will be discarded after 13 cycles (approximately 36 hours in operation) (Bandyopadhyay, 1998). The outlet of separator SEP101, stream S3, enters decanter DEC101 to remove glycerol by phase separation. The top layer, stream S4, of the decanter DEC101 is heated by stream S6 in HX101 to reduce temperature gradient before it is sent to the flash drum, F101. The distillate, containing mostly methanol, is recycled while the bottom, is the primary product.

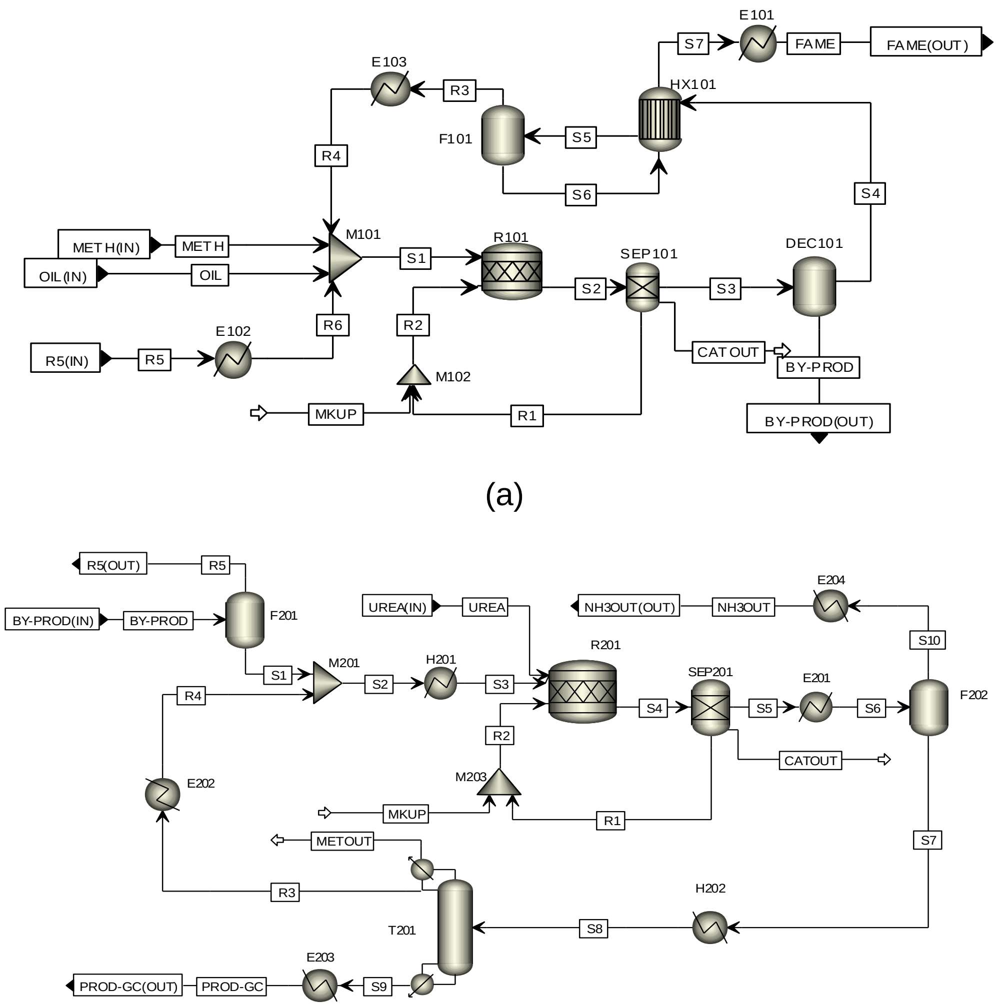

(a)

(b)

Fig. 1. (a) Process flow diagram of Section 1 for biodiesel and bioglycerol production plant; (b) process flow diagram of Section 2 for bioglycerol carbonate production plant.

In Section 2, stream BY-PROD is sent to flash drum F201 to recover methanol. The distillate, stream R5, is recycled to Section 1, while the bottom, stream S1, mixes with recycled glycerol, stream R4, in Mixer M201. Stream S2, containing mostly glycerol, is heated to reaction conditions before entering reactor R201. Fresh urea, stream UREA, is also sent to reactor R201. Separator SEP201 is used to recover the lanthanum oxide from the reactor outlet. After six consecutive runs, lanthanum oxide will be discarded as waste (Wang et al., 2011). The outlet of separator, stream S5, is cooled before sending to flash drum F202 to separate NH_3.

Results and Discussions

Fig. 2 shows the discounted cash flow diagrams generated using the deterministic model based on the 5 year modified accelerated cost recovery system (MACRS) depreciation method. The net present value of the glycerolysis plant is about $30.18 million higher than the direct carboxylation plant at the end of 12-year project.

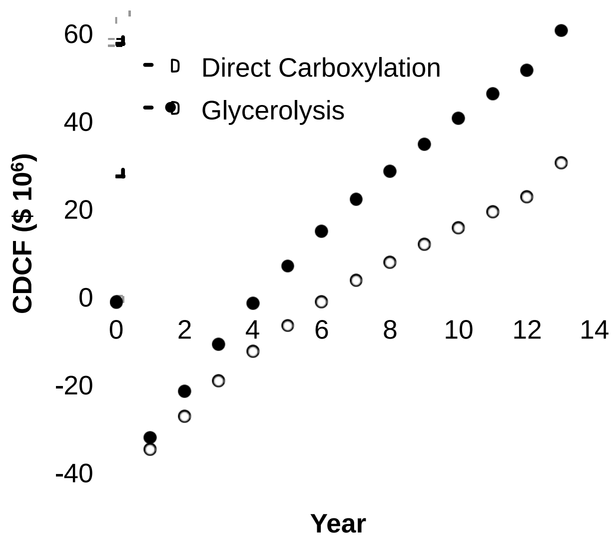

Fig. 2. Comparison of the cumulative discounted cash flow (CDCF) diagrams of the direct carboxylation and glycerolysis routes.

Fig. 3 presents the cumulative probability distributions obtained 1000-point Monte Carlo simulations for the values of NPV and discounted cash flow rate of return (DCFROR) values produced using CAPCOST 2008 software. Fig. 3a shows that there is about 17% chance that the direct carboxylation plant will not be profitable, while there is approximately 2% chance that the glycerolysis plant will not be profitable.

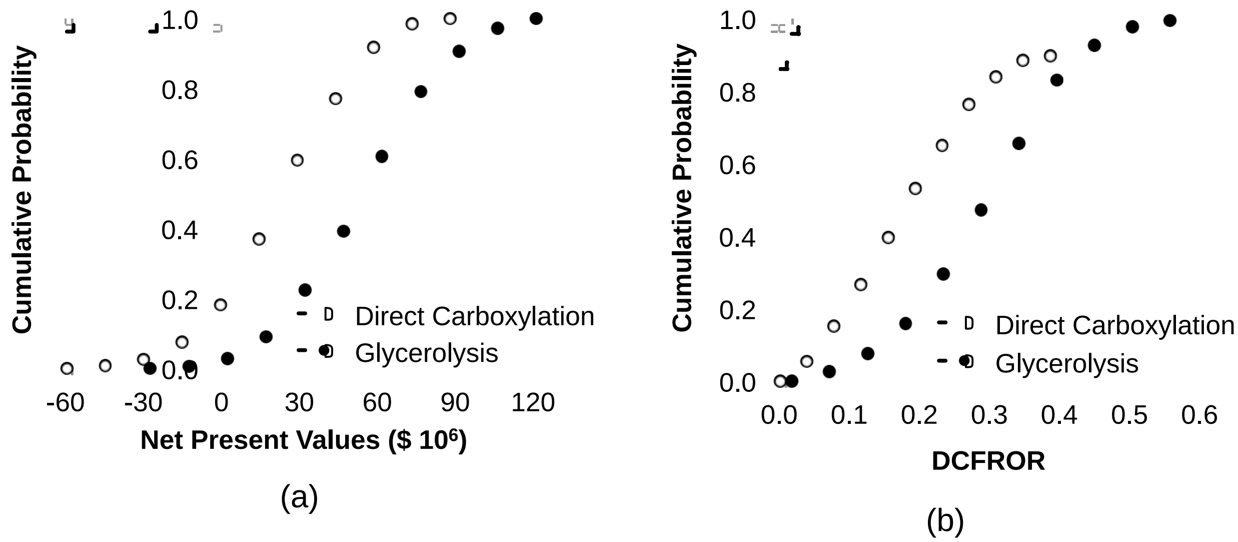

Fig. 3. 1000-point Monte Carlo simulation on; (a) net present values (NPV), (b) discounted cash flow rate of return (DCFROR).

Conclusions

Production of glycerol carbonate using direct carboxylation route suffers low yield requires more complex separation units leading to high operating cost. In contrast, indirect uses of CO_2 by using urea as a CO_2 donor simplify the glycerol carbonate production process, hence, creating a more economical biodiesel-glycerol carbonate production process. Using deterministic model prediction, the net present value of the glycerolysis plant is $30.18 million higher than the direct carboxylation plant at the end of 12-year project. Also, stochastic model has predicted that using glycerolysis route for glycerol carbonate production may increase the probability of getting positive net present value by about 15%.

References

Bandyopadhyay, Santanu, Ranjan Kumar Malik, and Uday V Shenoy. 1998. Temperature-enthalpy curve for energy targeting of distillation columns. Comput. Chem. Eng. 22: 1733-44.

Chakraborty, R, S Bepari, and A Banerjee. 2010. Transesterification of soybean oil catalyzed by fly ash and egg shell derived solid catalysts. Chem. Eng. J. 165: 798-805.

George, Jimil, Yogesh Patel, S. Muthukumaru Pillai, and Pradip Munshi. 2009. Methanol assisted selective formation of 1,2-glycerol carbonate from glycerol and carbon dioxide using ^{n}Bu2SnO as a catalyst. J. Mol. Catal. A Chem. 304: 1-7.

Li, Jiabo, and Tao Wang. 2011. Chemical equilibrium of glycerol carbonate synthesis from glycerol. J. Chem. Thermodynamics 43:731-6.

Nguyen, Nghi, and Yasar Demirel. 2011. A novel biodiesel and glycerol carbonate production plant. Int. J. Chem. Reactor Eng. 9: A108.

Nguyen, Nghi, and Yasar Demirel. 2010. Carboxylation of glycerol in a biodiesel plant. Paper presented at the AIChE Annual. Meeting. Conf. Proc., Nov 7-12, in Utah, USA.

Sheehan, J, V Camobreco, J Duffield, M Graboski, and H Shapouri. 1998. Life cycle inventory of biodiesel and petroleum diesel for use in an urban bus. NREL(May 01), http://www.nrel.gov/docs/legosti/fy98/24089.pdf (accessed August 20, 2011).

Urbanchuk, JM. 2011. Economic impact of removing the biodiesel tax credit for 2010 and implementation of RFS2 targets through 2015. Cardno ENTRIX (Jun 8), http://www.biodiesel.org/docs/fueling-action---tax-incentive/biodiesel-economic-impact-w-summary-2011.pdf?sfvrsn=2 (accessed March 20, 2012).

Wang, Liquo, Yubo Ma, Ying Wang, Shimin Liu, and Youquan Deng. 2011. Efficient synthesis of glycerol carbonate from glycerol and urea with lanthanum oxide as a solid base catalyst. Catal. Commun. 12: 1459-62.

Zheng, Yuguo, Xiaolong Chen, and Yinchu Shen. 2008. Commodity chemicals derived from glycerol, an important biorefinery feedstock. Chem. Rev. 108: 5253-77.

4 MODELING AND METRICS

4.1
ECONOMICS OF RESIDUE HARVEST: REGIONAL PARTNERSHIP EVALUATION

David W. Archer[1], David J. Muth[2], Jacob J. Jacobson[2], Douglas L. Karlen[3]*

Abstract
Economic analyses on the viability of corn (*Zea mays*, L.) stover harvest for bioenergy production have largely been based on simulation modeling. While some studies have utilized field research data, most field-based analyses have included a limited number of sites and a narrow geographic distribution. An Iowa case study is developed illustrating the use of data extracted from a database of geographically distributed field studies for a region-specific economic analysis. The analysis utilizes grain and residue yield and associated management information from two Iowa field research sites that are Sun Grant Regional Partnership locations associated with the Corn Stover Regional Partnership Team and the Renewable Energy Assessment Project (REAP). This information is used with the Biomass Logistics Model, to quantify costs for delivery of corn stover to a biorefinery for three stover harvest strategies. Results show that economics tends to drive residue harvest toward higher removal rates. However, higher removal rates can degrade soil resources. Limiting harvest quantities to leave sufficient residues to protect against excessive erosion and maintain soil organic carbon levels may provide economic incentives for producers to adopt cropping practices, such as no-till and cover cropping, allowing for higher harvest rates and reducing biomass costs to the biorefinery.

Keywords: corn stover, bioenergy, economics, sustainability

Introduction
Economic analyses on the viability of corn stover harvest for bioenergy production have largely been based on simulation modeling (Archer and Johnson, 2012; Graham et al., 2000; Kurkalova et al., 2010). While some studies have utilized field research data, most field-based analyses have included a limited number of sites and a narrow geographic distribution (Hoskinson et al., 2007; James et al., 2010). However, field studies are being conducted at sites across the U.S. (Karlen, 2010). By consolidating information from these studies into a common database, there is an opportunity to utilize these data to conduct economic analysis for a wide range of sites based on field research data. Furthermore, these data provide validation points that can help improve the credibility and reliability of model-based analyses. The objective of this analysis is to demonstrate the use of a newly-implemented field research database to analyze corn stover supply. The methodology is demonstrated as a case study for sustainable biomass supply delivered to an Iowa biorefinery. Expansion of the methodology to other sites is planned for future analyses.

Methods and Materials
The analysis utilized grain and residue yield and associated management information from the Sun Grant Regional Partnership locations associated with the Corn Stover Regional Partnership

[1] *USDA-Agricultural Research Service, Northern Great Plains Research Laboratory, ND*

[2] *Idaho National Laboratory, Idaho Falls, ID*

[3] *USDA-Agricultural Research Service, National Laboratory for Agriculture and the Environment, IA*

** Corresponding author*

Team and other long-term ARS studies contributing to the Renewable Energy Assessment Project (REAP). A common database has been implemented as part of REAP to store data for each of the participating research sites. The database includes nearly 500 data fields with treatment, location, and weather information; soil, greenhouse gas, plant, and biomass measurements; and detailed management information for each site. Data from the ‘Field 70/71’ site at Ames, IA, and a stover harvest study near Emmetsburg, IA (Karlen et al., 2012) were used to demonstrate the potential use of this database for economic analysis of corn stover supply. These data were used to construct crop enterprise budgets for the crop production treatments and as inputs to the Biomass Logistics Model (BLM) (Jacobson and Searcy, 2010) to evaluate three biomass harvest scenarios: cob only harvest; rake and bale stover removal; and chop, rake, and bale stover removal.

Crop Production Budgets

Management data were retrieved from the database for the ‘Field 70/71’ site, and were used to construct crop enterprise budgets for the conservation tillage (CT) and no-till (NT) continuous corn treatments, under standard management (Standard) and the no-till corn plus rye cover crop treatment (NT+Rye). The enterprise budgets were constructed based on the machinery operations and inputs used in the field study. Machinery costs were from 2012 projected costs from Iowa State University Extension budgets (Duffy, 2011). Machinery costs included depreciation, interest, taxes, insurance, fuel, lubricants, and repairs. Seed, fertilizer, and pesticide costs were 2011-2012 prices from USDA National Agricultural Statistics Service (USDA-NASS, 2012) or from North Dakota State University Extension (NDSU, 2012) for items not reported by USDA-NASS. Costs did not include land, labor and management, or crop insurance, drying, hauling, or storage costs as these were expected to be relatively consistent across treatments. Corn grain gross income was calculated using a corn price of \$184 Mg^{-1}, which was the average price received by Iowa farmers for 2007-2011 (USDA-NASS, 2012). Biomass harvest costs were estimated using the BLM.

Biomass Logistics Model

The BLM is part of a simulation toolset developed by Idaho National Laboratory (INL) to estimate delivered feedstock cost, and energy consumed for supply systems delivering biomass to biorefineries for biofuel production (Jacobson and Searcy, 2010). The BLM is engineered to work with various thermochemical and biochemical conversion platforms and accommodates numerous biomass materials (i.e., herbaceous residues, short-rotation woody and herbaceous energy crops, woody residues, algae, etc.). The BLM simulates the flow of biomass through the entire supply chain, tracking changes in feedstock characteristics (i.e. moisture content, dry matter, ash content, and dry bulk density) as influenced by the various operations in the supply chain. By accounting for all equipment that comes in contact with biomass from the point of harvest to the throat of the conversion facility and the change in characteristics, the BLM enables detailed economic costs and energy consumption analysis. As a result of this analysis, high impact areas for improvement (i.e. equipment efficiencies, operational parameters, environmental conditions etc.) can be identified to guide feedstock supply system research and development.

Three feedstock supply system cases are examined for this analysis. The first case is a cob only removal. In this case, the harvester is modified to pull a cart that separates and collects cobs directly from the harvester. The removal rate for cobs is assumed to be around 12% of the total available biomass (Karlen et al., 2012). The second case examines a moderate removal rate

Results and Discussion

Average grain costs and returns are shown in Table 1. There was no significant difference in net returns between CT and NT. However, CT is much more common than NT in Iowa. Only 18% of the area planted to corn in Iowa in 2010 was NT, and over 87% of NT corn was planted into soybean stubble, not corn stubble (USDA-ERS, 2012). This may indicate that producers would need to see clear advantages, economic or otherwise, before they would be willing to shift toward

NT corn production. The NT+Rye treatment had higher production costs than NT Standard due to the added cost of cover crop seed and cover crop planting.

Table 1. 2008-2011 average production costs, grain gross returns, and net returns for each continuous corn treatment

	CT Standard	NT Standard	NT+ Rye
	------------------------------$ ha^{-1} ------------------------------		
Grain gross returns	1975.15	1973.87	1973.87†
Production Cost	842.61	826.57	874.12
Grain Net Return	1132.54	1147.30	1099.75†

†A zero residue harvest treatment was not included for NT+Rye in the study, so grain gross returns and grain net return calculations assume grain yield equal to the NT, Standard treatment.

The difference in grain yields between the cases of CT Standard and NT Standard were insignificant, varying from 9.10 to 9.25 Mg ha^{-1} (dry matter), so the logistics analysis assumed a 9.25 Mg ha^{-1} yield for all analyses. The cost of each of the three logistics supply systems are shown in Table 2. The cob only supply system was more expensive due to the low yields, which increase the radius of farm acres needed to supply the biorefinery, driving up the transportation costs. The high residue removal case was least expensive due to the cheaper harvesting cost by using the flail shredder to cut the stubble and windrow the residue. So, economics tends to drive residue harvest toward higher removal rates.

Table 2: Biomass yield, nutrient replacement (N, P, K) costs, and feedstock logistics costs for the three harvest logistics supply systems, cob only, medium residue removal and high residue removal.

Feedstock	Harvest System	Removal Rate	Dry Biomass Yield	Nutrient Replacement Cost	Logistics Cost
			Mg ha^{-1}	$ Mg^{-1}	$ Mg^{-1}
Corn Cob Only	Cob caddy	12%	1.0	17.28	47.70
Stover	Rake and Bale	50%	4.1	19.11	42.65
Stover	Chop, Rake and Bale	60%	5.2	20.11	39.40

However, the higher removal rates could lead to higher soil erosion and reduce soil organic carbon, and these impacts would be greater under CT than under NT, making the minimum amount of residue needed to sustain the soil resource higher under CT than under NT (Wilhelm et al., 2010). Field research indicated that corn cob only harvest would likely meet the minimum residue retention under CT for Iowa corn production levels. However, rake and bale would often not retain sufficient residue under CT (Johnson et al., 2012). Industry partners working toward commercialization have recognized the economic benefits of higher harvest rates while maintaining minimum residue levels and have shifted from corn cob only harvest to removing more biomass, but short of rake and bale removal levels. Shifting to NT would likely retain sufficient residue to allow for rake and bale harvest, and possible chop, rake, and bale harvest (Johnson et al., 2012). Adding cover crops or perennial crop phases may help ensure that higher removal rates could be sustained (Wilhelm et al., 2010).

Since higher removal rates reduce feedstock costs to the biomass plant, there may be opportunities for economic incentives to adopt NT or NT+Rye, depending on how contracts and payments to producers are structured. Suppose the biorefinery pays all harvest and logistics costs, and, following the assumption used in the Billion-Ton Update (U.S. Department of Energy, 2011), a grower payment of \$33 Mg^{-1} which includes nutrient replacement costs. Net returns for residue harvest would be \$15.72, \$56.95, \$67.03 ha^{-1} for cob only; rake and bale; and chop, rake, and bale, respectively. If sustainable harvest limits CT to cob only, while NT or NT+Rye allow for rake and bale, or chop, rake and bale, shifting to NT or NT+Rye could increase biomass harvest net returns by \$41.23 ha^{-1} to \$51.31 ha^{-1}. This may provide additional incentive for producers to adopt NT and would cover much of the added cost for planting a rye cover crop. In addition, the biorefinery could see reductions in biomass costs of \$5.05 to \$8.30 Mg^{-1}. An important question is whether the higher net returns for NT would be sufficient to substantially increase NT adoption. Also, it is important to note that grower benefits for adopting NT or NT+Rye only occur if the biorefinery does not accept biomass harvested at rates above sustainability limits. However, short-term biomass cost reductions to the biorefinery occur with higher removal rates regardless of whether harvest rates are sustainable, but higher removal rates could drive up costs in the long run through reductions in productivity and increases in production costs.

While this analysis used field research data from Iowa REAP sites, future research will apply the methodology to other regions using field data from other REAP sites.

References

Archer, D. W., and Johnson, J. M. F. 2012. "Evaluating Local Crop Residue Biomass Supply: Economic and Environmental Impacts." *Bioenergy Research*, 5(3):699-712.

Duffy, M. 2011. "Estimated costs of crop production in Iowa - 2012." Iowa State University.

Graham, R. L., English, B. C., and Noon, C. E. 2000. "A Geographic Information System-based modeling system for evaluating the cost of delivered energy crop feedstock." *Biomass and Bioenergy*, 18(4), 309-329.

Hoskinson, R. L., Karlen, D. L., Birrell, S. J., Radtke, C. W., and Wilhelm, W. W. 2007. "Engineering, nutrient removal, and feedstock conversion evaluations of four corn stover harvest scenarios." *Biomass and Bioenergy*, 31, 126-136.

Jacobson, J.J. and Searcy, E.M. 2010. “Uniform-format feedstock supply system design for woody biomass”. American Society of Chemical Engineers, Spring Conference, Orlando, FL.

James, L. K., Swinton, S. M., and Thelen, K. D. 2010. "Profitability analysis of cellulosic energy crops compared with corn." *Agronomy Journal*, 102(2), 675-687.

Johnson, J.M.F., Varvel, G.E., Stott, D.E., Osborne, S., Novak, J.M., Karlen, D.L., Lamb, J.A., and Baker, J. 2012. “Corn stover management effects on soil organic carbon contents from several U.S. locations”. Proceedings Sun Grant Initiative 2012 National Conference, October 2-5, 2012, New Orleans, LA.

Karlen, D.L. 2010. “Corn stover feedstock trials to support predictive modeling.” *GCB Bioenergy,* 2, 235–247.

Karlen, D. L., Birrell, S. J., and Wirt, A.R. 2012. “Corn stover harvest strategy effects on grain yield and soil quality indicators”. *Agrociencia* (in press).

Kurkalova, L. A., Secchi, S., and Gassman, P. W. 2010. “Corn stover harvesting: potential supply and water quality implications.” In Handbook of Bioenergy Economics and Policy, 307–323. Natural Resource Management and Policy. New York: Springer.

NDSU. 2012. “2012 North Dakota Weed Control Guide.” W-253. North Dakota State University.

U.S. Department of Energy. 2011. “U.S. Billion-Ton Update: Biomass Supply for a Bioenergy and Bioproducts Industry.” R.D. Perlack and B.J. Stokes (Leads), ORNL/TM-2011/224. Oak Ridge National Laboratory, Oak Ridge, TN. 227p.

USDA-ERS. 2012. “ARMS farm financial and crop production practices.” USDA Economic Research Service. http://www.ers.usda.gov/data-products/arms-farm-financial-and-crop-production-practices.aspx (accessed August 24, 2012).

USDA-NASS. 2012. “Quick Stats.” USDA National Agricultural Statistics Service. http://quickstats.nass.usda.gov/ (accessed August 24, 2012).

Wilhelm, W. W., Hess, J. R., Karlen, D. L., Johnson, J. M. F., Muth, D. J., Baker, J. M., Gollany, H. T., Novak, J. M., Stott, D.E., and Varvel, G.E. 2010. Balancing limiting factors and economic drivers for sustainable midwestern US agricultural residue feedstock supplies. *Industrial Biotechnology*, 6, 271–287.

4.2
INTEGRATING SOCIAL CAPITAL INTO BIOJET FEEDSTOCK FACILITY SITING DECISIONS

Nicholas Lovrich[1], Wenping Shi[2], Natalie Martinkus[3], Paul Smith[2,], John Pierce[4], Aditi Kulkarni[2], Michael Gaffney[5], Michael Wolcott[3], Shane Brown[3]*

Abstract
Development of aviation biofuels (biojet) from second-generation feedstocks is gaining significant momentum from the market, production, and overall supply chain. Nowhere is this effort more significant than in the Northwest U.S. where alliances have been formed to assess the feasibility of making this goal a reality (safnw.com). To date, much effort has focused on the conversion innovations necessary for producing biojet. However, for these scientific efforts to become truly transformational for society, technologies must be compatible with regional feedstock, environmental, infrastructure, and community assets. At the local community level, siting decisions must be compatible with the existing social and cultural assets. Those assets likely include a capacity for collective action and the ability to adapt to change. Thus, siting decisions that integrate social and cultural assets into a holistic analysis of regional infrastructure and natural/ human resources may optimize site selection in multistate regional projects.

Here we describe empirical measurements for multiple core dimensions used to quantify capacity for collective action – in particular, social capital and creative vitality. These measures, when merged and analyzed via GIS techniques, are used to clarify key biojet feedstock supply chain issues present at the community level. This integrated approach will provide a better understanding of how social and cultural traits influence a community's support for or opposition to various bioeconomy issues--in this case, sustainable economic development initiatives for renewable fuels. This methodology is currently being deployed in (Idaho, Montana, Oregon, and Washington); however, the data are available to apply these concepts to other US regions.

Keywords: Social capital, creative vitality, collective action, biofuels supply chain, GIS, siting decisions

Introduction
The Northwest Advanced Renewables Alliance (NARA) initiative is focused on developing socially acceptable and economically viable biofuel solutions for the U.S. Pacific Northwest (PNW) region. This paper explores the use of various metrics, methods and analyses to identify potential communities in Idaho, Montana, Oregon and Washington that are "physically" and "socially" able to accommodate and accept potential NARA infrastructure/supply chain nodes and biofuel markets. Geographic Information Systems (GIS) screen and visually illustrate the physical assets and county-level social data to facilitate site selection optimization for the region.

Key Social Asset Indicators

[1] *The Thomas S. Foley Institute for Public Policy and Public Service, Washington State University, WA*

[2] *Department of Agricultural and Biological Engineering, The Pennsylvania State University, PA*

[3] *Department of Civil and Environmental Engineering, Washington State University, WA*

[4] *School of Public Affairs and Public Administration, University of Kansas, KS*

[5] *Division of Governmental Studies and Services, Washington State University, WA*

** Corresponding author*

The research literature on local community indicators of collaborative capacity and potential for effective collective action in a number of public policy areas, including the natural resources and environmental protection area, is now quite rich (Lysak, 2006). That literature points to the centrality of two key elements – namely, *social capital* for building upon and enhancing trust-based collective action (Putnam, 2000; Halpern, 2005) and *creative leadership* (Florida, 2002) in coming to win-win solutions to obstacles impeding the production of public goods through purposive collective action. Fortunately, several relevant studies conducted in recent years related to this subject in the NARA area can be drawn upon to support the use of the Rupasingha et al. (2006) social capital datasets and the WESTAF (2010) Creative Vitality Index (CVI) datasets, available for all U.S. counties, for the social asset mapping work reported here. These two sources of local community social assets can be shown to be **retrospectively predictive** – that is, in looking at successful and unsuccessful prior outcomes of collaboration in the NARA region it is evident that a higher presence of these two indicators of social assets is clearly associated with successful collaborative process outcomes, and the obverse is true of failed collaborations.

Table 1. Social Assets Data for Comparative Case Studies in Idaho and Montana

County & State	Archival Collaborative Process Outcomes[a]	CRR 2009[b]	Non-rent-seeking groups score[c]	Mean CVI 2006-2010[d]	Arts & Letters Workforce[e]	Arts-related Businesses[f]
Ada, ID	Successful -- Community Policing	0.82	2.2458	1.0956	234.9188	35.8034
Canyon, ID	Unsuccessful -- Community Policing	0.79	1.5427	0.3736	107.7891	14.3201
Lewis & Clark, MT	Successful -- Health Services Coordination	0.71	5.8215	0.9598	343.0019	44.7992
Lake, MT	Unsuccessful -- Health Services Coordination	0.36	2.3677	0.5032	173.9029	38.8597

a. Successful and unsuccessful collaborations in Idaho and Montana
b. Response rate to annual U.S, Census American Community Survey, 2009 (Rupasingha et al.)
c. Number of Non-rent-seeking Groups (excluding churches) per 1,000 population (Rupasingha et al.)
d. Average CVI score for the period 2006-2010 (WESTAF)
e. Sum of arts & letters occupations indexes, 2002-2010 (WESTAF, Census of Occupations)
f. Ave. business enterprises related to Independent Artists, Writers, and Performers/10k 2002-2010 (WESTAF, Northern American Industry Classification System)

The findings displayed in Table 1 are consistent with our expectations regarding the utility of the Rupasingha et al. and CVI datasets as sources of insight-bearing indicators of the collaborative capacity present in U.S. counties. In both the Ada Co. and Canyon Co. community policing comparison in Idaho (Erp et al., 2009) and the Lewis and Clark Co. and Lake Co. health planning comparison in Montana (Grott, 1999) the successful collaborative outcome counties have higher scores on the social capital indicators derived from the Rupasingha datasets and higher creative vitality scores derived from the CVI datasets. The successful cases took place in counties where the potential for the coproduction of public goods is high as reflected in the surrogate of census survey response rate, where the network of civic and professional associations which bridge across social divisions are strong, and where the CVI elements of arts and letters-related workforce participants and local business enterprises are elevated.

This exercise in retrospective prediction using the Rupasingha et al. datasets and the WESTAF CVI datasets provides a strong basis for making use of these same sources of data to aid in the NARA program's region-wide pilot community selection process. This paper demonstrates how data derived from those two datasets were used to help prioritize sites in the NARA region. A similar process of social asset assessment is likely to be possible elsewhere in the country where comparable pilot site selection challenges must be made relating to the production of renewable energy for the U.S. economic marketplace.

Methodology

Physical Assets

The physical attributes considered for the GIS analysis include: cities (location and population), major road network, railroad network, forest residue data (county-level), refined products pipelines, pipeline terminals, and refineries (Figure 1). Based on the work of Zhang et al. (2011), community physical asset qualification criteria included: town population must be greater than 1,000 to ensure a viable work source; town must be located within one mile of major road and rail to facilitate movement of products; and town must be located in a county that produces a large amount of forest residue annually.

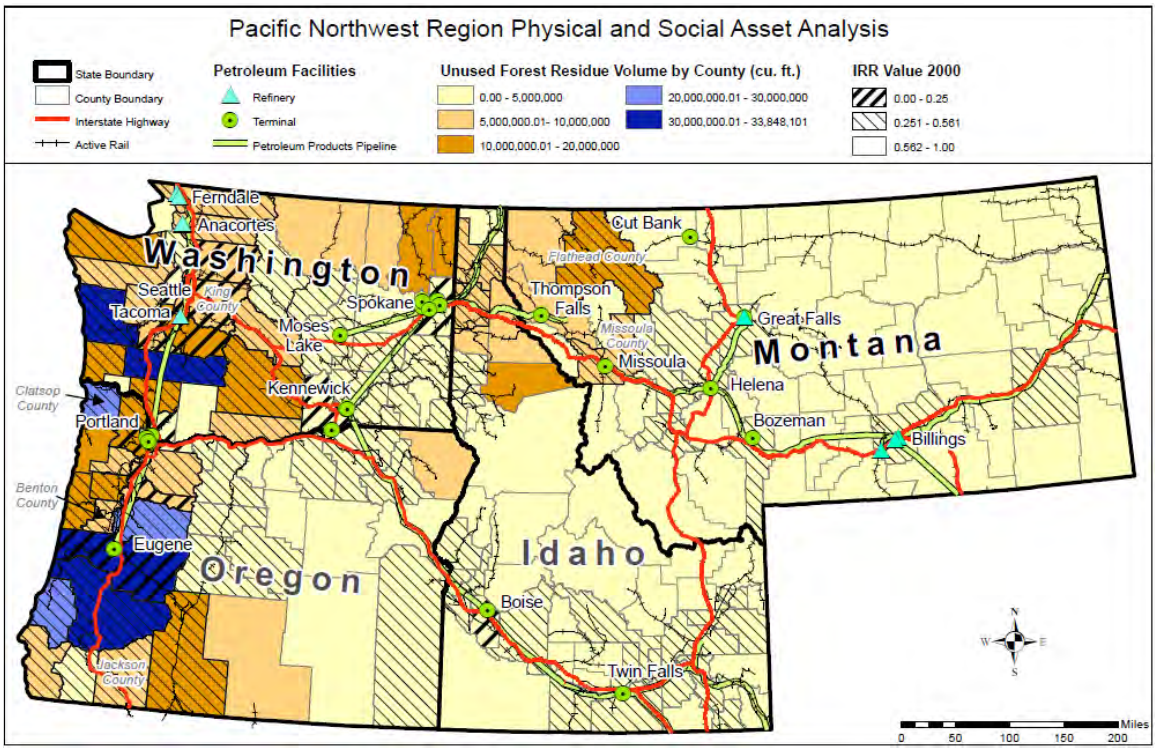

Figure 1. Base Map of NARA Region with Physical Assets and the 36 Counties with more than 5 Million cu. ft. of Forest Residue and Lower 0.561 IRR Score

For this exercise, a spreadsheet of forest residue volume by county was added into GIS and joined to the county shapefile. Forty-eight NARA region counties were determined to have a suitable forest residue volume of over 5 million cu.ft. and were used for subsequent consideration (Figure 1). To assess the degree of "rurality" of a geographical area, the following two measures were used:

Index of Relative Rurality: IRR estimates the degree of rurality of each county, with scores closer to 0 indicating a high level of urbanization and scores closer to 1 representative of high rurality. The IRR is based on four dimensions: population size, density, percentage of urban residents, and distance to the closest metropolitan area (Waldorf 2006). Counties with scores nearer to 0 on this index and featuring high social asset scores AND having spatial proximity to biomass sources and related structural assets will be good candidates for selection as pilot communities.

Metropolitan and Micropolitan Statistical Areas: Metropolitan and Micropolitan statistical areas are geographic entities defined by the Office of Management and Budget for use by Federal agencies in collecting, tabulating, and publishing Federal statistics. A metropolitan area contains a core urban area of 50,000 or more population, and a micropolitan area contains an urban core of at least 10,000 (but less than 50,000) population. Each metro or micro area consists of one or more counties and includes the counties containing the core urban area, as well as any adjacent counties that have a high degree of social and economic integration (as measured by commuting to work) with the urban core (USCB, 2012).

Social Assets

Creative Vitality Index (CVI): The CVI is a measure of the health of the creative economy of a given geographical area compared to a national index (WESTAF, 2010). The CVI is based on two components on a 3:2 ratio that weighs community participation in the arts and concentrations of arts-related employment. Each geographical area is evaluated on these components for the measurement of its CVI score. The national CVI is set at 1.00. This analysis is based on the following county-level CVI measures: (a) average of CVI scores, 2006 to 2010; (b) arts & letters occupations Indexes (mean per capita level for 2002-2010 derived from the U.S. Census of Occupations [SOC]); and, (c) local arts-related business enterprises and entrepreneurial endeavors (mean per capital level for 2002-2010 derived from the North American Industry Classification System [NAICS]). The importance of these arts-related assets to economic development at the *city level* was documented in the work of Florida (2002).

Social Capital: The level of supportive collective action expected from a particular county is measured through the following two measures:

a. **Non-rent-seeking groups score:** The sum of per capita presence of non-rent-seeking groups (those seeking public goods available to all; Krueger, 1974) is multiplied by a constant for all U.S. counties and has been estimated from various public sources (principally U.S. Census-based statistics and derivative governmental research centers) by Rupasingha, Goetz and Freshwater (2000). These data have been used in prior studies to predict community-level adaptation to economic change (Rupasingha et al., 2006).
b. **Census Response Rate (CRR)**: This is the rate of response registered in a county to the annual U.S. Census Bureau's *American Community Survey* involving over 3.4 million households aggregated over a five-year period. CRR serves as a surrogate for the coproduction of public goods by citizens at the express request of their own community and their national government.

High Social Capital and CVI scores reflect communities rich in social capital and creative thinking assets. Less rural counties with high biomass availability and rich in these particular social attributes may be considered as particularly suitable locations for NARA pilot programs. Also, more rural areas that are proximate to relatively larger towns with greater biomass availability may also be considered for the pilot program as potential supply chain "procurement" nodes. The literature on "assets-based community development" is replete with examples of communities that have been able to mobilize their social capital and creative problem solving assets for the promotion of community-based economic development and local institutional sustainability (McKnight and Kretzmann, 1993; Emery et al., 2006).

The social asset analysis using GIS initially involved comparing the IRR values for each county against the highest forest residue-producing counties in the state. Since potential NARA pilot communities must be located in a region with high volumes of biomass, ***the goal is to identify those counties that have high forest residue yields yet also possess suitable human resources to capitalize on the economic development opportunities that may emerge.*** For these communities, we examined the social capital and creative vitality assets. This process leads to geographically-based communities of sufficient size to permit NARA to engage a variety of stakeholder representatives in a collaborative process directed toward collective action related to sustainable biofuel production.

Findings

NARA Region

The NARA region possesses good promise for the selection of communities with high collaborative collective action potential. Table 2 compares the social attributes of the four NARA-region states to corresponding national scores. The CVI scores for Washington and Oregon are higher than the national mean score of 1.00, and Montana scores are close to the national CVI mean score. Idaho lags both the region and nation in this regard. In terms of non-rent-seeking networks and the coproduction surrogate state scores, Montana has high bridging and CVI scores as well as a high co-production of public goods score. In sum, the NARA region has sufficient cases of coincident geobiophysical and social assets to warrant optimism that a number of promising sites for NARA projects are available to serve as NARA pilot communities.

Table 2. Social Asset Scores for the PNW Region

Region	CRR 2009	Non-rent-seeking groups score	Mean CVI 2006-2010	Arts & Letters Workforce	Arts-related Businesses
Idaho	0.695	2.894	0.675	154.536	25.020
MT	0.611	4.675	0.915	169.291	34.779
Oregon	0.718	3.051	1.013	179.035	36.851
Washington	0.713	3.623	1.005	164.484	32.706
National	0.706	2.701	1.000	148.801	20.979

Index of Relative Rurality (IRR)

The initial screening on counties with a forest residue volume over 5 million cu. ft. resulted in 48 counties in the NARA region, among which 36 counties have IRR scores lower than the NARA regional average (0.561) (Figure 1; Table 3). Further, counties classified as “Rural” statistical areas were dropped, leaving 31 candidate counties (Table 3). Those counties with IRR values closer to 0 exhibit relatively higher urbanization and hence are hypothesized to be better suited to support NARA infrastructure/supply chain nodes. The delineation of the metropolitan and micropolitan statistical area is provided along with IRR scores to indicate the county’s workforce diversity and integration capacity. Table 3 displays IRR, scores, forest residue volume, statistical area delineation, and social asset scores.

Table 3. Top 36 Counties Based on Biogeophysical Assets and Corresponding Social Asset Measures Scores

County and State	Forest Resid. (cu. ft.)	IRR 2000	Metro Stat. Area[1]	CRR 2009	Non-rent-seeking groups score	Mean CVI 2006-2010	Arts & Letters Workforce	Arts-related Businesses
King, WA	7,124,616.6	0.1034	1	0.77	2.7069	2.0696	379.2927	71.8670
Jackson, OR	8,854,393.9	0.2714	1	0.75	2.6322	1.6614	230.8279	56.7414
Missoula, MT	8,280,129.2	0.3159	1	0.75	3.6029	1.6168	353.0553	70.5528
Jefferson, WA	5,365,814.7	0.5046	3	0.8	5.0106	1.3298	269.7591	112.0979
Benton, OR	9,626,171.8	0.2701	1	0.8	3.1355	1.1668	446.9898	74.4471
Flathead, MT	11,722,814.6	0.5314	2	0.61	5.4388	1.1098	214.9520	56.1939
Clatsop, OR	26,622,733.3	0.4361	2	0.72	4.7825	1.0688	202.3677	61.6810
Lane, OR	33,000,396.4	0.2466	1	0.77	2.9548	0.9404	258.8892	54.0597
Lincoln, OR	12,428,005.2	0.3901	3	0.7	4.8259	0.8662	189.0391	60.0536
Clackamas, OR	9,628,728.2	0.2635	1	0.78	1.9329	0.8092	229.3760	53.2232
Bonner, ID	8,695,854.0	0.5582	3	0.6	3.7387	0.7670	206.5264	56.2350
Thurston, WA	7,178,085.5	0.2431	1	0.78	2.4955	0.7618	211.2453	33.3049
Whatcom, WA	7,645,444.8	0.2995	1	0.78	3.1767	0.7590	211.0550	46.3014
Marion, OR	6,108,703.5	0.2105	1	0.77	2.2254	0.6512	168.3523	26.3028
WA, OR	12,854,560.0	0.1918	1	0.79	1.7376	0.6480	159.0200	21.7877
Klickitat, WA	7,636,995.1	0.5303	3	0.7	3.6709	0.6432	153.7936	48.4392
Pierce, WA	11,414,511.6	0.1948	1	0.75	1.6848	0.6404	137.7729	22.9530
Clallam, WA	15,175,246.9	0.4647	2	0.81	4.2282	0.6036	189.8213	46.1810
Kootenai, ID	5,216,918.7	0.2915	1	0.77	2.7337	0.5986	144.8493	27.0934
Skagit, WA	8,920,766.2	0.3196	1	0.78	3.0705	0.5778	161.3218	35.1470
Snohomish, WA	6,409,500.2	0.2138	1	0.77	2.5504	0.5466	148.6923	24.4532
Douglas, OR	33,848,101.9	0.4341	2	0.75	2.0625	0.4772	113.8456	18.7945
Klamath, OR	15,334,156.5	0.4455	2	0.67	3.6503	0.4600	147.5446	20.3840
Coos, OR	29,393,8856	0.4556	2	0.78	2.5587	0.4268	140.0185	25.6279
Yamhill, OR	8,513,741.4	0.3502	1	0.78	1.2467	0.4206	157.5698	26.9166
Kittitas, WA	7,135,554.1	0.4635	2	0.67	5.4169	0.4012	202.1425	35.7538
Cowlitz, WA	15,452,587.2	0.3144	1	0.78	2.8624	0.3940	104.1812	17.4401
Curry, OR	6,364,904.6	0.5367	2	0.7	1.4096	0.3800	159.4428	43.3417
Yakima, WA	14,840,579.3	0.2909	1	0.76	2.1528	0.3766	117.8265	12.8905
Pacific, WA	17,508,565.3	0.4939	3	0.56	8.5243	0.3642	120.2464	27.0854
Mason, WA	9,537,375.5	0.5030	2	0.67	3.2338	0.3400	111.9339	23.0972
Grays Harbor, WA	33,196,922.9	0.4175	2	0.74	6.0343	0.3268	105.8904	16.8248
Linn, OR	20,697,657.6	0.3746	2	0.78	3.0936	0.3092	101.8371	16.2576
Lewis, WA	30,711,250.9	0.4782	2	0.74	3.2552	0.3078	105.5540	15.1186
Columbia, OR	13,674,543.6	0.4159	1	0.79	2.0571	0.3000	115.1981	25.4467
Polk, OR	10,431,098.5	0.3339	1	0.79	2.8272	0.2482	101.5438	22.5609
National Ave.	**--**	**--**	**--**	**0.706**	**2.701**	**1.00**	**148.801**	**20.979**

Social Assets

Six counties -- Flathead, MT; Missoula, MT; Clatsop, OR; Benton, OR; Jackson, OR; and King, WA -- have CVI scores higher than the national average score of 1.00, of which Flathead, MT has the lowest coproduction public goods score (CRR=0.61), and Jackson, OR has a below National average score in regard to non-rent-seeking groups score (Table 3). On the other hand, among those six counties, Missoula, MT, Benton, OR and Clatsop, OR are in the top group in regard to both coproduction of public goods (CRR) and the bridging and civic groups (non-rent-seeking groups) social capital score, and Benton, OR, King, WA, and Missoula, MT are in the top group for the arts and letters occupations (Table 3).

Physical Assets

The six counties identified in the social asset screening were then evaluated based on their physical assets relating to the potential to host a biomass conversion facility. Considering there will be multiple conversion facilities located across the PNW region, each state may be evaluated individually for a potential location. Of the three Oregon counties listed, Benton is best situated to host a conversion facility due to its proximity to surrounding counties with high volumes of forest residue, its location along major road and railways, and its proximity to counties with a low rurality rating (meaning a large potential work force). In Washington, King County is well situated near petroleum refineries, high volumes of forest residue, major road and rail, and a major population center. Both counties listed in Montana are located near large reserves of forest residue; however, Missoula County is located along a major roadway (I-90) and has a much larger population than Flathead County, thus giving it preference.

Summary

This paper provides an initial overview of an integrated approach for using data-driven methods to determine optimal biojet supply chain sites at the community level within the 4-state region. The simultaneous consideration of feedstock, transportation and production infrastructure, population density, and social and cultural assets with GIS can indeed help identify suitable conditions to maximize the likelihood of community compatibility with NARA needs and objectives.

The results from the initial GIS analysis indicated that 31 counties in the 4-state NARA region rank high in forest residues and possess favorable human resource assets sufficient to qualify as candidate NARA communities in terms of economic development potential. When considering the results from the social asset analysis, six counties (Flathead, MT; Missoula, MT; Clatsop, OR; Benton, OR; Jackson, OR; and King, WA) emerged as having strong social asset characteristics. After screening these six counties for physical assets, Missoula, MT, Benton, OR and King, WA emerged as the top counties featuring a combination of **both** natural and built environment assets **and** relatively strong social capital and creative vitality social assets. These findings inspire confidence that community engagement efforts to promote aviation biofuel production as a sustainable advanced renewable energy option for communities in the 4-state region will be successful.

Acknowledgement

This work, as part of the NW Advanced Renewables Alliance (NARA), was funded by the Agriculture and Food Research Initiative Competitive Grant no. 2011-68005-30416, USDA National Institute of Food and Agriculture.

References

Emery, Mary, Susan Fey and Cornelia Flora. 2006. Using Community Capitals to Develop Assets for Positive Community Change. *CD Practice*, Issue 13:1-19.

Erp. Michael, Michael Gaffney, John Goldman, Kelsey Gray and Nicholas Lovrich. 2009. *WRICOPS – A Decade of Service, 1997-2007: Brief History, Major Accomplishments, Principal Activities and Prospects for the Future*. Pullman, WA: Division of Governmental Studies and Services, Washington State University.

Florida, Richard. 2002. *The Rise of the Creative Class*. New York: Basic Books.

Grott, Catherine. 1999. *Health Care Reform at the State Level: The Dynamics of Achieving Service Integration at the Local Health Department Level in Montana*. PhD Dissertation. Washington State University.

Halpern, David. 2005. *Social Capital*. Malden, MA: Polity Press.

Krueger, Anne. 1974. The Political Economy of the Rent-Seeking Society. *The American Economic Review*, Vol. 64, No. 3: 291-303.

Lysak, Tetyana. 2006. *Collaborative Policymaking in Watersheds: Understanding Implementation Progress in Washington State*. PhD Dissertation, Washington State University.

McKnight, John L. and John P. Kretzmann. 1993. *Building Communities from the Inside Out: A Path Toward Finding and Mobilizing a Community's Assets*. Chicago: ACTA Publications.

NARA. NorthWest Advanced Renewables Alliance Web. Available online: *http://nararenewables.org/about.*

Putnam, Robert. 2000. *Bowling Alone: The Collapse and Revival of American Community.* New York: Simon and Schuster.

Rupasingha, Anil, Stephen J. Goetz and David Freshwater. 2000. Social Capital and Economic Growth: A County-Level Analysis. *Journal of Agricultural and Applied Economics* 32: 565-572.

Rupasingha, Anil, Stephen J. Goetz and David Freshwater. 2006. The Production of Social Capital in U.S. Counties. *Journal of Socio-Economics* 35(1):83-101.

USCB. 2012. Metropolitan and Micropolitan Statistical Areas Main. United States Census Bureau. Available online: *http://www.census.gov/population/metro/*

Waldorf, Brigitte S., 2006. Continuous Multi-dimensional Measure of Rurality: Moving Beyond Threshold Measures. Department of Agricultural Economics, Purdue University, West Lafayette, IN 47907, USA.

WESTAF, 2010. The Creative Vitality™ Index: An Overview. Western States Arts Federation. Available online: *http://www.westaf.org/publications_and_research/cvi*

Zhang, F, D.M Johnson, and J.W Sutherland. 2011. A GIS-Based Method for Identifying the Optimal Location for a Facility to Convert Forest Biomass to Biofuel. *Biomass and Bioenergy*. 35.9 (2011): 3951-3961.

4.3 ECONOMIC FEASIBILITY OF BIOFUELS CROPS IN FLORIDA AND NEW JERSEY

Z.R. Helsel[1,], J. Alvarez[2], R. Brumfield[3]*

Abstract

Enterprise budgets were developed, sensitivity analyses performed, and the economic feasibility evaluated for sugarcane, energycane, sweet sorghum and switchgrass for bioenergy on southern Florida's marginal lands and similarly for switchgrass grown in New Jersey. Conversion of sugarcane juice to sugar at long term average prices was similar to producing ethanol at market prices of ~$2.20/gal and profitable at average biomass yields or higher. At 2012 sugar prices (~ $0.32/lb), ethanol prices needed to be greater than about $3.40/gal to compete with sugarcane for ethanol production. Breakeven costs of sweet sorghum (juice ethanol), if grown as a plant and ratoon crop and harvested using corn silage custom practices, were significantly higher than for sugarcane; but if grown as one crop in rotation and handled similar to sugarcane, breakeven prices were only nominally greater than for sugarcane. Energycane and switchgrass biomass was considered for cellulosic conversion to ethanol. Breakeven prices were $0.25-0.50 higher for ethanol from energycane than sugarcane over similar yield ranges mainly because of higher processing costs for cellulosic ethanol. Switchgrass was estimated to produce results similar to the energycanes, but may have the advantage of use in livestock operations or conservation plans on marginal lands. In New Jersey when pelletizing switchgrass for direct combustion, breakeven prices were high. Utilization of direct cut harvesting (after maturity and drydown) without pelletizing offered significant cost reductions. Harvesting and handling costs were among the highest of all production practices suggesting detailed analysis of alternatives will be necessary to make these bioenergy crops profitable.

Keywords: switchgrass, Panicum, energycane, sweet sorghum, Saccharum, sugarcane, ethanol

Introduction

Utilizing biomass for energy has captured attention worldwide as fossil fuel based supplies tighten and prices fluctuate. While significant focus has been placed on conversion processes and agronomic production practices, until recently, little attention has been placed on the economic evaluation of these two aspects. We evaluated the economic feasibility of sugarcane (*Saccharum officinarum L.*), energycane (*Saccharum spp*.) sweet sorghum (*Sorghum bicolor (L.) Moench*) and switchgrass (*Panicum virgatum L.*) for bioenergy production primarily on southern Florida's marginal lands. A similar analysis was conducted for switchgrass grown in New Jersey. Enterprise budgets were developed and sensitivity analyses were performed.

Methods

Enterprise budgets were developed with agronomic and cost data, with the objective of estimating production costs and projecting gross and net returns. Data were obtained from several sources. Agronomic performance information came from local research and interviews with producers. Information on prices, including custom rate charges, was provided by local suppliers of agricultural inputs and services.

[1] *Department of Plant Biology and Pathology, Rutgers University, NJ*

[2] *Everglades Research and Education Center, University of Florida, FL*

[3] *Department of Agricultural, Food and Resource Economics, Rutgers University, NJ*

** Corresponding author*

Production of energy crops for this study was assumed to take place on mineral soils (sand lands) in and around the Everglades Agricultural Area (EAA) of South Florida not currently being used for sugarcane or other high-value crops and on non-food crop land in New Jersey. Production potential of these soils is generally lower than the land currently in high value crops. For sugarcane and sweet sorghum, we assumed that each net ton (at field moisture) would yield 19.5 gal and 14.0 gal respectively of ethanol from direct fermentation of expressed juices. We evaluated energycane and switchgrass biomass at 90 and 70 gal ethanol/dry ton from cellulosic conversion processes. The combustion value of switchgrass was assumed to be 7000 Btu/lb (HHV). Specific methodologies can be obtained for each crop and state from applicable literature in the Reference Cited section.

Results and Discussion

A summary of the enterprise budget categories and costs for each crop produced on South Florida sandland is presented in Table 1.

Table 1. Biomass Energy Crop Enterprise Budgets, South Florida Sandlands

Table 1. Biomass Energy Crop Enterprise Budget, South Florida Sandlands ($/A/yr*)						
Activity	Sugar Cane	Energy Cane	Sweet Sorghum (2 cuts)	Sweet Sorghum (1 cut)	Switch Grass (2 cuts)	Switch Grass (1 cut)
Projected Yield (T/A)	32 wet	30 wet	45 wet	30 wet	7 dry	4 dry
Fallow Management	9.50	6.31	--	--	7.60	--
Land Preparation	57.03	37.87	134.11	134.11	20.82	20.88
Planting	83.80	47.34	66.00	66.00	22.88	22.80
Cultural Activities	312.40	309.33	465.80	252.05	271.95	171.15
Miscellaneous	87.57	82.26	66.56	45.22	32.32	21.48
Interest	77.06	72.39	58.60	39.79	28.44	18.90
Harvest & Transport	224.00	255.00	608.24	401.62	227.88	127.40
Variable - Total	851.36	810.50	1,399.34	938.78	611.89	382.54
Overhead	210.00	200.00	221.00	119.80	117.60	77.60
TOTAL	1,061.36	1,010.50	1,620.34	1,058.58	729.49	460.14
Breakeven Price ($/gal or $/T)	2.20	2.60	3.12	3.07	104	115

*All data are $/A/yr. except yield and breakeven price.

In the case of sugarcane, the production of sugar with a long term average price of $0.2234/lb, was similar to producing ethanol valued at about $2.20/gal when biomass yields were at average yields of 32 net T/A or higher. When ethanol prices are at $2.90/gal, the profitability of ethanol production is much higher at all levels of biomass yields evaluated. If current (2012) sugar prices of about $0.32/lb remain, then ethanol prices will need to be atleast $3.35 to $3.45/gal to make producing ethanol from sugarcane more profitable than food sugar.

With sweet sorghum, comparisons were made between two crop systems: a) a plant crop followed by a ratoon crop (ie. two crops per year) and b) a single plant crop assumed to be in rotation with a vegetable or other cash crop within the same year. Two harvest systems, one modeled after corn silage custom harvesting (data presented in table 1) and the other after that used in the sugarcane industry (data not presented), were compared. While gross returns were greater for the two-crop sweet sorghum, breakeven prices for the single crop in rotation were lower. If the single crop could be grown as a rotational crop and harvested and handled similarly to sugarcane (and that should be possible), break-even prices would be even lower (~ $0.50 – 0.55/gal) than those for sweet sorghum using corn silage harvesting custom rates. These breakeven prices are not much greater than those for ethanol from sugarcane, a main difference being reflective of sugarcane's lower ethanol processing costs.

Energycane presents a wide range of outcomes for breakeven prices at biomass yields from 25 to 40 net tons per acre, and two assumed cellulosic ethanol processing costs ($1.07/gal and $1.65/gal). When comparing sugarcane and energycane with the processing cost of ethanol assumed at an average of $1.35/gal for the energycane and $.50/gal for sugarcane, breakeven prices are much lower for ethanol from sugarcane than from energycane mainly because of the processing cost difference, not the production costs. Although switchgrass harvested twice a year in Florida incurred lower costs than energycane harvested once a year, yields of energycane were higher. The one-cut system for switchgrass (used in most of the United States) had production costs that were nearly $275 less than the two-cut system but had a slightly higher breakeven price.

Switchgrass is adapted to a broad area of the United States and has the opportunity to fit in an overall conservation plan and/or livestock enterprise in addition to its potential as a biofuel. In a highly urbanized state like New Jersey there are insufficient contiguous acres to facilitate the establishment of large ethanol processing plants so niche opportunities were considered where biomass could be harvested and processed for heat from combustion. Harvest of switchgrass in the late fall, handled as hay and then pelletized for retail sale was compared to a direct-cut chopped forage for burning directly in a combustion boiler. Results suggested that retail prices of pellets needed to be in excess of $220/T for this harvest and handling system to be profitable even at the highest yield levels and in excess of $280/T at average yields (4T/A). With direct cutting of dried winter-harvested switchgrass, harvest and processing costs were substantially lower. The drawbacks to this system, however, were dry matter losses through the winter period, snow cover at times, and a low density material that limited transport distance.

In comparing production activities for the various crops evaluated, data in Table 1 suggests that cultural activities and harvest and transport represent the highest costs among the enterprises. Within cultural activities, fertilizers, particularly nitrogen, represent the greatest costs. Some reduction could be made if minerals remaining after processing could be returned to the land or allowed to physiologically recycle where possible. It is obvious that closer distances to the processing plant and efficient harvest and handling logistics will be important to the economic success of biomass for energy.

Summary

Although these results are still preliminary, most scenarios analyzed appear to indicate that the potential of the four crops analyzed as biofuel crops will largely depend on fermentable or combustible biomass yields, the market price of the biofuel crop, cost of fertilizer and chemical inputs, and harvest methods including distance from the fields to the processing plant. The competition with sugarcane for food is likely not to be a concern because use for energy would be intended for marginal soils and, if more acres are devoted to it, the amount and price of sugar should not be greatly impacted because Florida is a minor player in the world sweetener market. There is evidence that energycanes, and species like them, may become a potentially useful bioenergy crop on the unmanaged mineral soils in south central Florida. The success of this endeavor will be predicated on the development of new varieties with longer lived stands producing higher biomass yield. More efficient management practices, especially fertilizer nutrient inputs, will also be needed. Improvement of the cellulosic ethanol conversion process to lower per gallon processing costs will make it competitive with current sugarcane juice to ethanol processes. If sweet sorghum can be produced in a rotation with another crop annually(or ratoon yields increased) and use some of the harvest and handling practices developed over time in the sugarcane industry, then it can become profitable as ethanol prices rise. For this potential to be fully realized, however, further research on crop nutrients and other production practices will be needed to reduce energy related input costs and dollar investments in producing sweet sorghum. Switchgrass, with its broad adaptability, has potential for use both as a feedstock for cellulosic ethanol production as well as for direct combustion and other conversion processes. However, harvest and handling logistics need to be optimized and other costs reduced for it to be a profitable bioenergy crop.

Additional detail of these studies and analyses can be found in the following publications:

References

Alvarez, J and Z. R.Helsel. 2011. *Economic Feasibility of Biofuel Crops in Florida:Energycane on Mineral Soils.* University of Florida, Gainesville, FL. IFAS Ext. Pub. #SC089. http://edis.ifas.ufl.edu/SC089.

Alvarez, J and Z. R.Helsel. 2011. *Economic Feasibility of Biofuel Crops in Florida:Sugarcane on Mineral Soils.* University of Florida, Gainesville, FL. IFAS Ext. Pub. #SC090. http://edis.ifas.ufl.edu/SC090.

Brumfield, R. and Z. R. Helsel. 2011. *Switchgrass Bioenergy Budgets.* E331. Rutgers Cooperative Extension, New Brunswick, NJ. http://njaes.rutgers.edu/pubs/publication.asp?pid=E331

Helsel, Z. R. and J.Alvarez. 2011. *Economic Potential of Switchgrass as a Biofuel Crop in Florida.* University of Florida, Gainesville, FL. IFAS Ext. Pub. #FE900. http://edis.ifas.ufl.edu/FE900.

Helsel, Z. R. and J.Alvarez. 2011. *Economic Potential of Sweet Sorghum for Ethanol Production in South Florida.* University of Florida, Gainesville, FL. IFAS Ext. Pub. #FE896. http://edis.ifas.ufl.edu/FE896.

4.4
THE BIOMASS SITE ASSESSMENT TOOL (BIOSAT) INTEGRATED WITH LANDSCAPE SUITABILITY

Timothy M. Young[1,] James H. Perdue[2], Xia Huang[1]*

Abstract

A challenge in the development of renewable energy is the ability to spatially assess the risk of woody cellulosic feedstock supplies to conversion facilities. Policy makers and investors need improved methods to identify the interactions associated with landscape features, socio-economic conditions, ownership patterns, and the influence these variables have on supply curves and the marginal cost (MC) curves of woody cellulosic producers. This study estimates opportunity zones in a spatial context for woody cellulosic feedstocks based on landscape suitability and geo-referenced economic supply using the BioSAT model (www.biosat.net). The study covered 13 southeastern states in the U.S. Population density, farm income, road density, forest land area relative to crop land area, water area, slope, forest ecoregion type, annual net growth-to-removal ratio, and area of lands in public preserves were used to distinguish regions and the suitability for woody cellulosic feedstock supply. BioSAT was used to estimate the MC curves for these regions to further identify highly suitable zones. Highly suitable zones for woody cellulosic feedstocks were located in Central Mississippi, northwest and southeast Alabama, north Arkansas, west Georgia, southeast Oklahoma, Kentucky, Tennessee, and southwest Virginia**.** Softwood and hardwood logging residues MC in these regions ranged from $38 to $41/dry ton. Highly suitable regions for softwood pulpwood occurred in Alabama, Florida, southeast Oklahoma, South Carolina, and Virginia where MC ranged from $46 to $61/dry ton. In highly suitable regions that contained hardwood pulpwood, MC for hardwood pulpwood ranged from $34 to $56/dry ton.

Keywords: Biomass; site assessment; model; spatial analysis; landscape suitability

Introduction

Elbehri (2007) noted replacing petroleum products with cellulosic feedstocks presents several technical, economic, and research challenges, one of which is the availability of cellulosic feedstocks. Elbehri (2007) further noted that high relative costs of production, logistics, and transportation of cellulosic feedstocks are all potential constraints that need to be better understood. Elbehri's thesis provides the rationale for this research, *i.e., provide decision-makers with a better quantitative tool to accurately assess the costs of woody cellulosic supply.* The objective of this study was to estimate the economic availability of woody cellulosic feedstocks in a geo-spatial context.

A plethora of literature exists on the economic availability of biomass (Young *et al.* 1991, Ugarte *et al*. 2000; Biomass Research and Development Board 2008, Western Governors Association 2008, U.S. Dept. of Energy 2011, and others). A recent report concluded that 1.3 billion tons of biomass are available annually for energy production (U.S. Dept. of Energy 2011).

---

[1] The University of Tennessee, Center for Renewable Carbon, TN

[2] U.S. Forest Service Southern Research Station, TN

* Corresponding author

Methods

The methodology had three main components: 1) estimation of forest biomass availability; 2) measurement of landscape suitability for forest biomass; and 3) estimation of producers' supply curves. All records were organized at the U.S. Census Bureau 5-digit ZIP Code Tabulation Area (ZCTA) level. There were 10,016 ZCTAs in the 13-state[3] study region which corresponded to 10,016 potential analytical polygons.[4]

BioSAT Model

The BioSAT model (www.biosat.net) estimated the economic availability of woody cellulose for procurement zones with one-way haul distances ranging in size from 128.8 km to 321.9 km which were not always concentric, *i.e., the shape of such zones rely on the transportation network and corresponding physical biomass supply* (Perdue *et al.* 2011). The supply chain of BioSAT has three main cost components: resource, harvesting, and transportation. Estimates of total biomass, and average annual growth and removals were obtained from the Forest Inventory and Analysis Database (FIADB) version 3.0.

Resource cost data (*e.g., stumpage, mill residue prices, etc*.) were obtained from Timber Mart South (http://www.tmart-south.com/tmart/). The Fuel Reduction Cost Simulator (FRCS) as modified for the Billion Ton Study (Perlack *et al.* 2005, U.S. Dept. of Energy 2011) was used to estimate the costs of harvesting logging residues. Merchantable wood harvesting costs were estimated from the Auburn Harvest Analyzer (Tufts *et al.* 1985) which was expanded for six ecoregions types, five forest types, and five harvesting systems by Baker and Greene (Center for Forest Business, Warnell School of Forestry and Natural Resources, University of Georgia). Transportation costs were based on travel times and distances adapting the truck transportation model of Berwick and Farooq (2003).

Landscape Suitability

The availability of woody cellulosic supply, as well as other forest resources, is physically constrained by a set of factors from the natural and socio-economic environment. Twelve variables were used in this study to determine the suitability of the forest landscape (Table 1). Suitability assumes the presence of harvestable forests, access to abundant forest resource supply, and minimal socio-economic restrictions from human activity (*e.g., urban development, suburban sprawl, national parks, etc*.). Attributes of "*forest land area ratio*," "*slope*," as well as "*suitable ecoregions for forests*" determined the spatial degree of the presence of harvestable forests. The attribute "*timberland annual growth-to-removal ratio*" was an indicator of forest net growth. "*Population density*," "*farm net income*," "*median income*," and "*road density*" were used to estimate socio-economic indicators.

---

[3] Alabama, Arkansas, Florida, Georgia, Kentucky, Louisiana, Mississippi, North Carolina, Oklahoma, South Carolina, Tennessee, Texas, Virginia.

[4] The average area for 5-digit ZCTAs in the 13-state study region was 209.84 km^2.

Table 1. Geographical landscape and socio-economic factors used in study.

Variable	Resolution	Unit	Data Sources
Population Density	5-digit ZCTA	People/mile^2	U.S. Census Bureau (2010) population density in each 5-digit ZCTA.
Farm Net Income	County	Dollar	USDA NASS Census Agriculture (2007) farm net income in each county.
Road Density	5-digit ZCTA	km/km^2	U.S. Census Bureau (2010) road length
Crop Cultivated Land Area Ratio	5-digit ZCTA	percent	U.S. National Land Cover Database (2006)
Forest Land Area Ratio			
Urban Land Area Ratio			
Water Area Ratio			
Slope	5-digit ZCTA	percent	U.S. National Elevation Dataset (1999) NED 1arc second
Ecoregions Level III	Ecoregions	-	U.S. EPA (2011)
Timberland Annual Growth-to-Removal Ratio	County	-	Forest Inventory and Analysis – The Timber Products Tools (TPO) (2009)
Lands in Public Preserves	5-digit ZCTA	-	U.S. Forest Service (2009)

Forest biomass annual growth and removal quantity data were collected at the county level from Forest Inventory and Analysis Database (FIADB) version 3.0 (Figure 1a), and allocation was done for each of the 10,016, 5-digit ZCTAs using geographic information system (GIS) technology. National land cover and digital raster map data were used to identify forestland. In the digital raster map, each pixel represents one particular land cover class, *e.g., water, urban, forest, or cropland, etc*. (Figure 1b). Forest biomass annual growth and removal quantities were proportionally allocated to each 5-digit ZCTA using the county boundary, 5-digit ZCTA, and the land cover image data with GIS spatial overlay techniques. Due to errors between county and 5-digit ZCTA boundaries (*i.e., some 5-digit ZCTAs cross county boundaries*), each forest biomass county was split into multiple area parts via the 5-digit ZCTA area shape, and assigned a unique 5-digit ZCTA identifier. By overlaying each area part with the land cover image layer, the numbers of pixels in all land cover classes within each area were estimated (Figure 1c). By summing up the pixels of deciduous forests, coniferous forests and mixed forests, which together represented forestland in the unit of a county, a forestland pixel ratio for each area part to its belonging county was calculated and the forest biomass quantity in every area part was derived for this pixel ratio (Figure 1d). A summed quantity value for all area parts belonging to the same 5-digit ZCTA were then calculated as the forest biomass quantity in this 5-digit ZCTA.

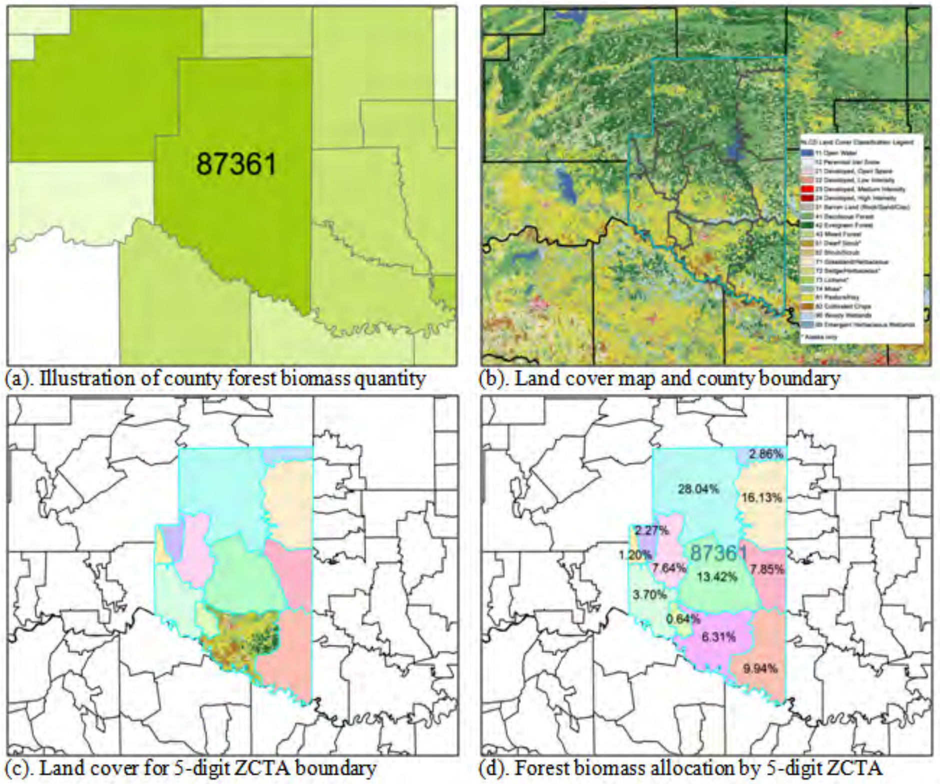

Figure 1. Illustration of forest biomass allocation at the level of a 5-digit ZCTA.

Results

Landscape Suitability

Regions that had forest area ratio greater than 30%, timberland annual growth-to-removal ratios greater than 1.5, ecoregions defined as mostly forestland, slopes less than 10%, and less than 39 people/km^2 were considered areas for highly suitable forest production. Based on these criteria, high suitable opportunity zones for woody cellulosic feedstocks were located along the Central Mississippi, northwest and southeast Alabama, southeast Oklahoma, west Georgia, Kentucky, Tennessee and southwest Virginia (Figure 2). This research supports the conclusions of Butler *et al.* (2010) in identifying forest biomass that is physically constrained by a set of factors from the natural and socio-economic environment. This study also expands the scope of the research by Butler *et al.* (2010) in analyzing the southeastern region of the U.S.

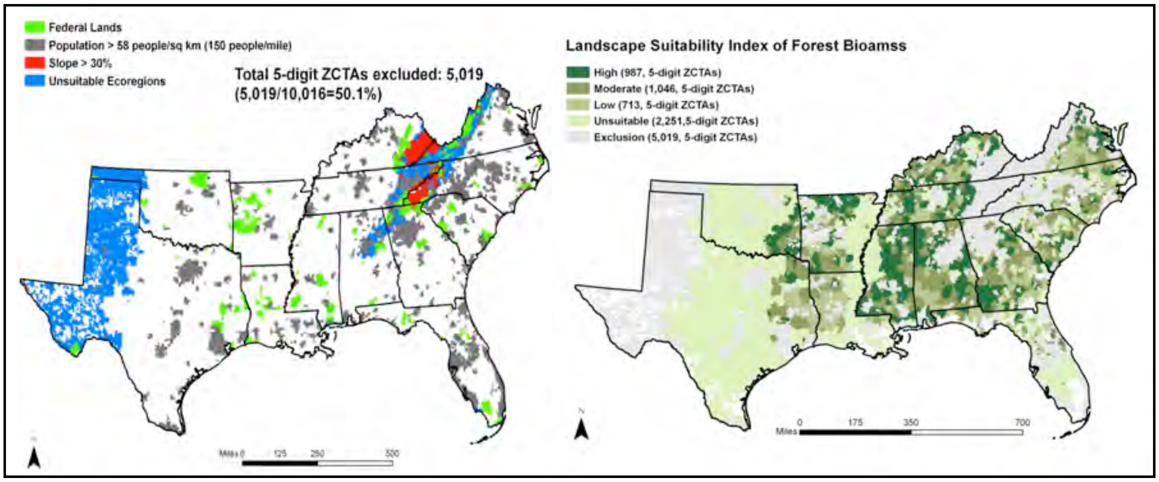

Figure 2. ZCTAs excluded in the 13-state study region (*left figure*) and opportunity zones for woody biomass identified by landscape suitability (*right figure*).

Geo-Referenced Supply Curves from BioSAT

As an illustration, the BioSAT model was used to derive detailed economic information for southern pine pulpwood (*pinus spp*.) for one of the high suitability opportunity zones located in central Mississippi (ZCTA 39090, Kosciusko MS). A 193.1 km haul distance was assumed and the associated supply or marginal cost (MC) curve is displayed in Figure 3. MC increases from approximately $48 to $66/dry ton over a maximum supply of 773,096 dry tons of southern pine pulpwood. The estimates for this illustration in MS and other BioSAT estimates for the southeast are consistent with the results of U.S. Dept. of Energy (2011) but expand upon the research by including geo-referencing and forest suitability at a finer resolution (*i.e., the 5-digit ZCTA*).

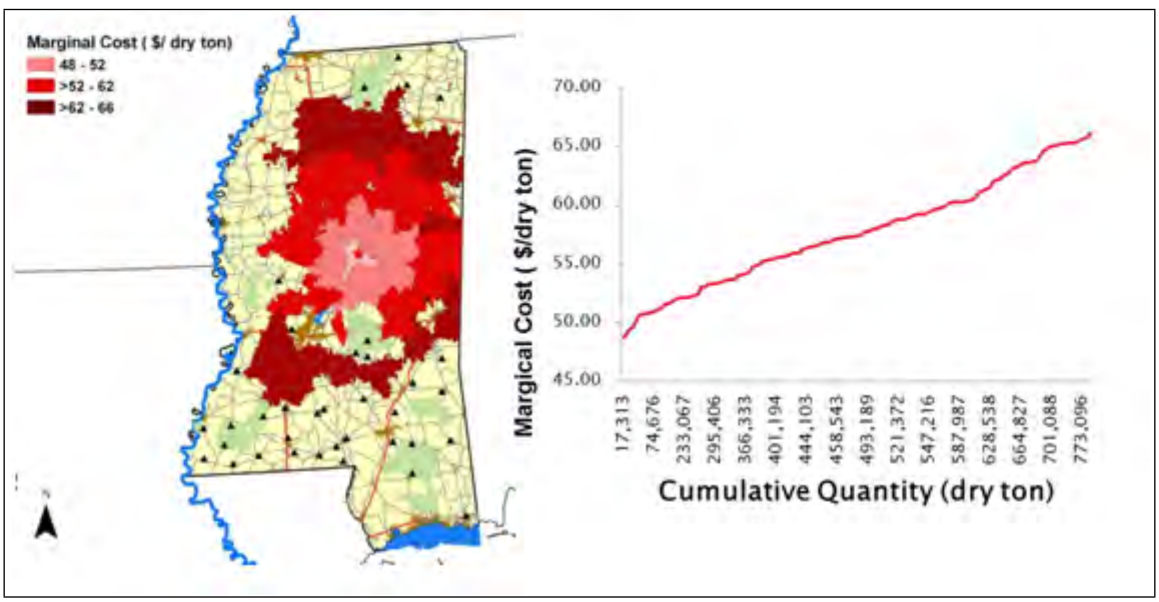

Figure 3. Spatial representation of biobasin for ZCTA 39090 (Kosciusko MS) and associated marginal cost curve for pine pulpwood (*pinus spp.*) from the BioSAT model.

References

Berwick, M. and M. Farooq. 2003. Trucking cost model for transportation managers. Upper Great Plains Transportation Inst., North Dakota State University. Fargo, ND.

Biomass Research and Development Board. 2008. Increasing feedstock production for biofuels economic drivers, environmental implications, and the role of research.

Butler, B.J., Z. Ma, D. Kittredge and P. Catanzro. 2010. Social versus biophysical availability of woody biomass in the Northern United States. Northern Journal of Applied Forestry. 27(4): 151-159

Elbehri, A. 2007. The changing face of the U.S. grain system. Economic Research Service. U.S. Department of Agriculture, Washington, DC.

Perlack, R.D., L.L. Wright, A.F. Turhollow, R.L. Graham, B.J. Stokes and D. C. Erbach. 2005. Biomass as feedstock for a bioenergy and bioproducts industry: the technical feasibility of a billion-ton annual supply. Publication DOE/GO-102995- 2135/ORNL TM-2005/66. Oak Ridge National Laboratory, OAR Ridge, TN. 60p.

Perdue, J.H., T.M. Young and T.G. Rials. 2011. The Biomass Site Assessment Model – BioSAT. Final Report for U.S. Forest Service, Southern Research Station. 282p.

Tufts, R.A., B.L. Lanford, W.D. Greene and J.O. Burrows. 1985. Auburn harvesting analyzer. The Compiler. 3(2):14-15. Forest Res.Syst. Inst., Florence, AL.

Ugarte, D.L.T., G. Daniel and D.E. Ray. 2000. Biomass and bioenergy applications of the POLYSYS modeling framework. Biomass and Bioenergy. 4(3):1-18.

U.S. Department of Energy. 2011. U.S. billion-ton update, biomass supply for a bioenergy and bioproducts industry. R.D. Perlack and B.J. Stokes (Leads), ORNL/TM-2011/224. Oak Ridge National Laboratory, Oak Ridge, TN. 227p.

Western Governor's Association. 2008. Strategic assessment of bioenergy development in the west – spatial analysis and supply curve development. University of California, Davis. 86p.

Young, T.M., D.M. Ostermeier, J.D. Thomas and R.T. Brooks. 1991. The economic availability of woody biomass for the Southeastern United States. Bioresources Technology. 37(1):7-16.

4.5
DEVELOPMENT OF A PROCESS-BASED HERBACEOUS BIOENERGY
CROP MODEL

Yubin Yang[1,], Lloyd Ted Wilson[1], Jiale Lv[1], Jenny Wang[1]*

Abstract

The objectives of this study are: 1) Determine the phenotypic traits that govern bioenergy crop growth and development; 2) Develop an individual-based herbaceous bioenergy crop model that captures the temporal and spatial dynamics of crop growth and development; 3) Conduct comprehensive analysis on the genotype (G) × environment (E) × management (M) interactions to identify site-/genotype-specific management practices for optimal biomass production.

Field experiments were conducted between 2009-2010 to determine major phenotypic traits for three genotypes of biomass sorghum through both in-field observations and multiple destructive samplings. Results for major phenotypic traits were used for model parameter estimation.

The process-based crop model is based on our integrated functional-architectural modeling framework that simulates the temporal and spatial dynamics of plants. The functional component of the system incorporates major physiological processes and simulates the growth and development of individual organs, integrated to an individual plant and a population of plants. The architectural component of the system includes an architecture engine that constructs 3D plants based on the physiological states of its organs. The model will be used to simulate biomass productivity for integrated bioenergy supply chain analysis.

Keywords: Biomass sorghum, energycane, phenotypic traits, crop model, functional-architectural modeling framework

Introduction

Biomass productivity highly depends on agronomic and pest management and site-specific weather and soil conditions. Optimizing biorefinery siting and supply chain operation depends on our ability to accurately predict crop performance, seasonal availability, and associated economic risks. Most existing bioenergy crop models are based on either radiation use efficiency, average plant, or plant population (Kiniry et al., 1996; Kiniry et al., 2005; Corson et al., 2007). Many of these models have limited capability to elucidate the genotype (G) × environment (E) × management (M) interactions and to capture temporal and spatial dynamics of crop growth and development. The objectives of this study are: 1) Determine the phenotypic traits that govern bioenergy crop growth and development; 2) Develop an individual-based herbaceous bioenergy crop model that captures the temporal and spatial dynamics of crop growth and development; 3) Conduct comprehensive analysis on G×E×M interactions to identify site-/genotype-specific management practices for optimal biomass production.

Materials and Methods

Determination of Major Phenotypic Traits

Three high biomass sorghum cultivars (M81-E, Mega Green, and Sugar Graze Ultra) were selected for field experiments. Sorghum seeds were sowed in each of two fields in 2009 (May 22, and July 30) and again in 2010 (May 4 and July 24) at the Texas A&M AgriLife Research and

[1] *Texas A&M University System, AgriLife Research and Extension Center, TX*

* *Corresponding author*

Extension Center in Beaumont, Texas. For each field, seedlings (4-leaf stage) were hand thinned to three densities (5, 10, 20 plants per m-row) one week after emergence. Fields were managed under local production practices. For each cultivar and density, the following data were measured ca. every two weeks using destructive sampling: number of tillers per plant, height, diameter, and number of nodes of each tiller, dry mass of culm, leaf blade and leaf sheath, grain mass, and root length and dry mass. Five to ten representative plants were removed from 2m sections of the middle two rows of each density during each sampling. All samples were placed in separate paper bags, oven-dried for 48 hours at 75ºC, and then weighed.

Model Description

The herbaceous bioenergy crop modeling system is based on our research in developing population- and individual-based crop models for rice (Wu and Wilson, 1998; Yan et al., 2009), cotton (Wilson et al., 1992; Yang et al., 2009), and tomatoes (Wilson et al., 1986). It is designed to provide the capability to simulate plant growth and development at the scales of individual organs, plants, and plant populations. The modeling system integrates a functional and an architectural component (Fig. 1).

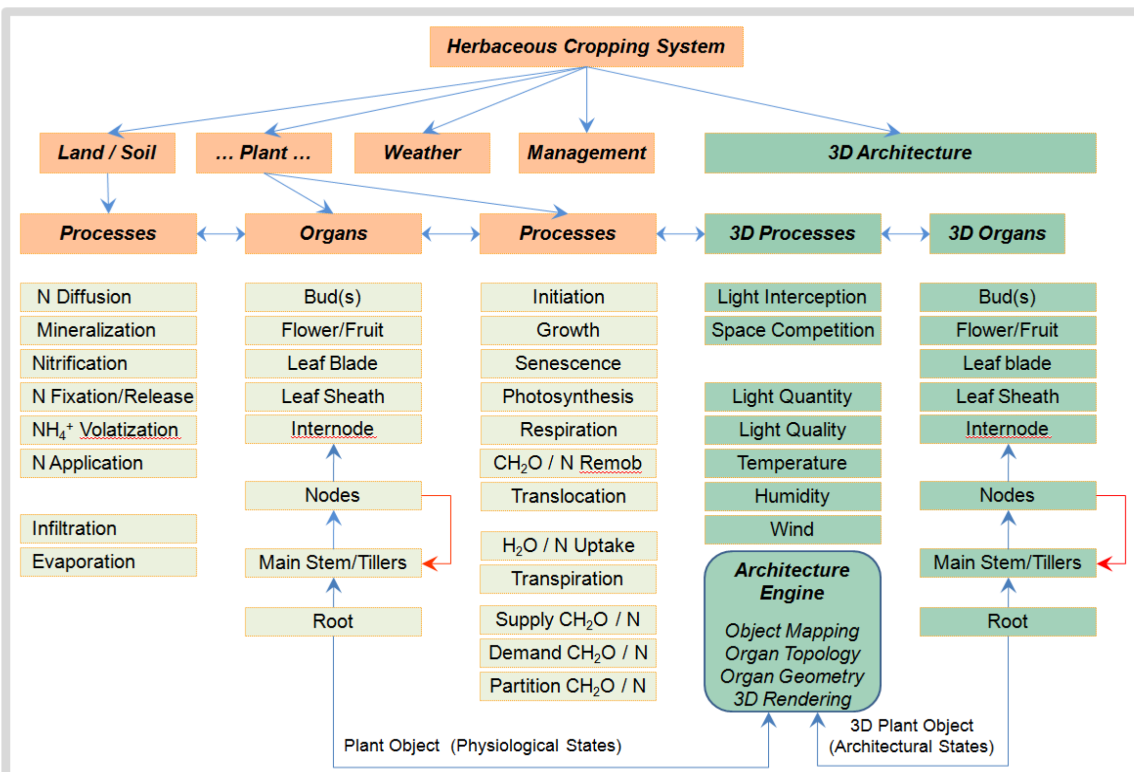

Figure 1. Functional-architectural modeling Framework.

The functional component of the system features an individual-based plant model that incorporates major physiological processes and simulates the growth and development of individual organs (leaf blade, sheath, internode, branch, flower, fruit, and root). Most of the processes are based on the rice population simulation model (RicePSM) (Wu and Wilson, 1998) and are adapted for dry land and organ level processes. We used a multi-tier supply/demand/ allocation scheme to distribute photosynthate and nitrogen: 1) between root and shoot system based on total photosynthate supply, 2) among stem nodes within a tiller (main or sub-tiller) with each node having a separate supply pool, and 3) among organs within a node. The allocation to each organ is based on its demand as determined by its physiological state, allocation priority, distance from multiple supply pools, and light and temperature microenvironment that controls node and branch differentiation.

The architectural component of the system constructs a 3D plant based on the physiological states, geometry (shape, curvature, size), and topology (spatial arrangement), and creates a visual 3D image of the plant (i.e. visualization).

Results and Discussions

The physiological time (effective degree days above threshold $10°C$) required for a single node production ranges from 35 to 45 DD early in the season for each of the 3 sorghum genotypes (Fig. 2). It increased more or less linearly with the progression of the season. Plants at lower density requires less thermal time (data not shown) to complete node production, due to less competition for space and nutrients between plants. The increase in physiological time for node production later in the season is likely due to increased competition and decreased effectiveness of heat units.

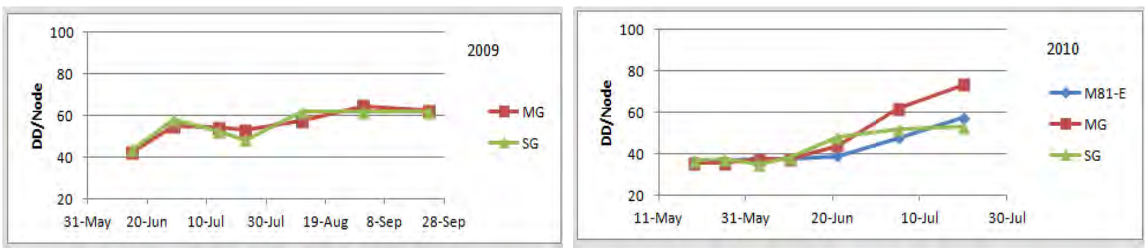

Figure 2. Physiological time for node production (Planting date: May 22, 2009; May 4, 2010)

Organ biomass accumulation over time (e.g. leaf blade, sheath, or culm) follows a sigmoid pattern (Fig. 3). Organ biomass increases with increasing nodal osition and then quickly tapers off towards the final nodes. These patterns are a result of the dynamic competition and interactions between plant organs, in terms of supply, demand, and allocation. In addition to within-plant competition and interactions, competition for light, space and nutrients between adjacent plants also directly affects plant growth and development. Plants at lower densities produce more biomass duo to less competition (Fig. 4).

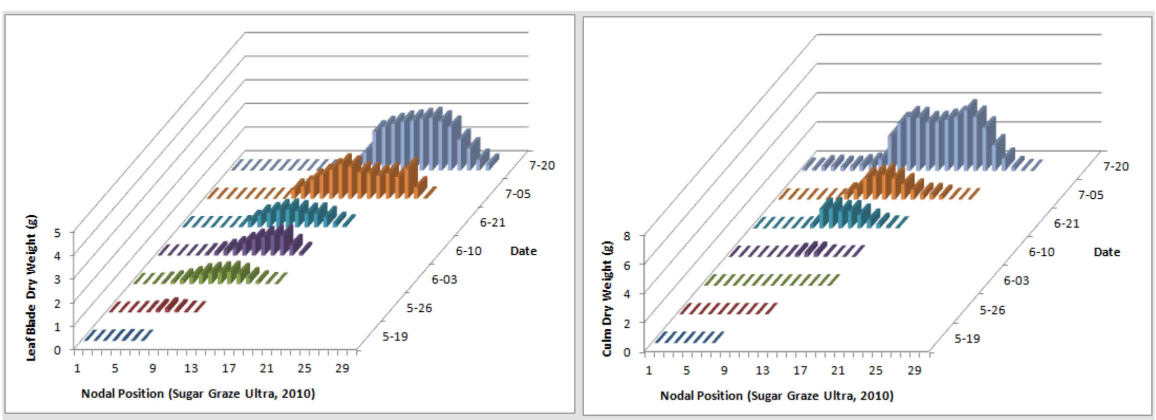

Fig. 3. Observed leaf blade & culm mass vs. nodal position and time (Sugar Graze Ultra, 2010; 5 plants/m-row)

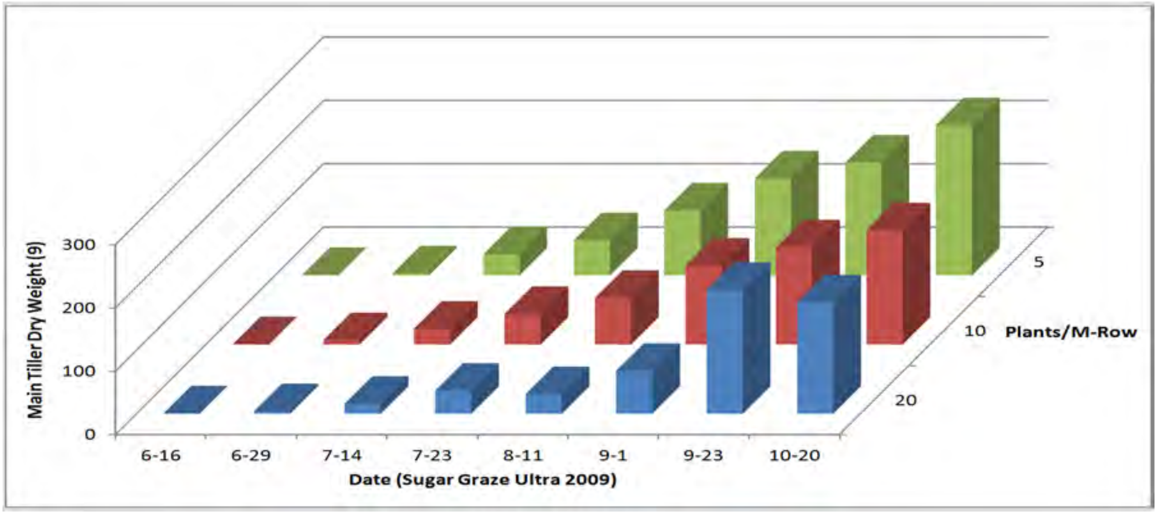

Fig. 4. Main tiller dry weight vs. plant density and time (Sugar Graze Ultra 2010).

The herbaceous crop model has been designed to integrate crop growth characteristics, to capture the temporal and spatial dynamics of crop development, and to maximize biomass production per unit area. Figure 5 shows the simulated leaf blade and culm biomass dynamics of Sugar Graze Ultra, using 2010 weather data in Beaumont, Texas. The simulated dynamics of leaf blade and culm biomass closely matches the observed dynamics (Fig. 3 vs. 5). Fig. 6 shows snap shots of a simulated sorghum plant over the growth season.

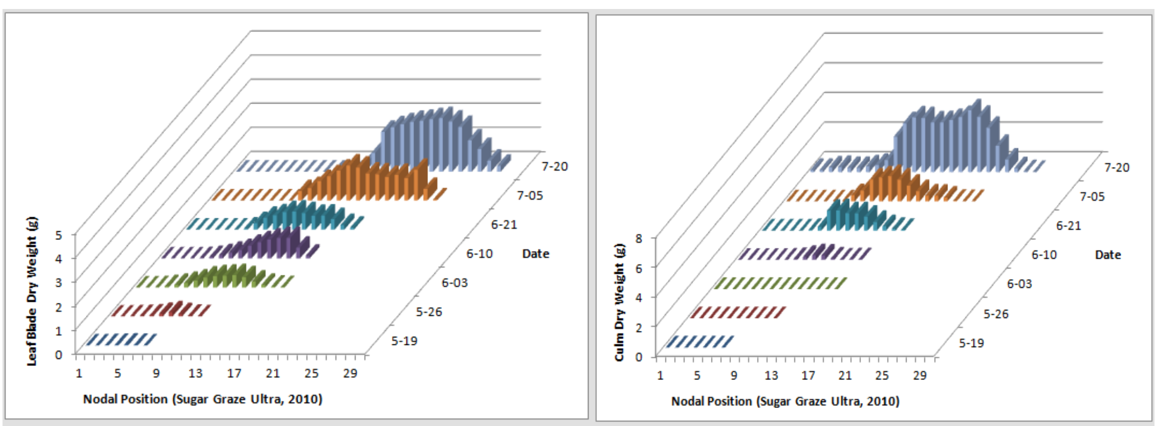

Figure 5. Simulated Leaf blade & culm mass vs. nodal position and time (Sugar Graze Ultra, 2010).

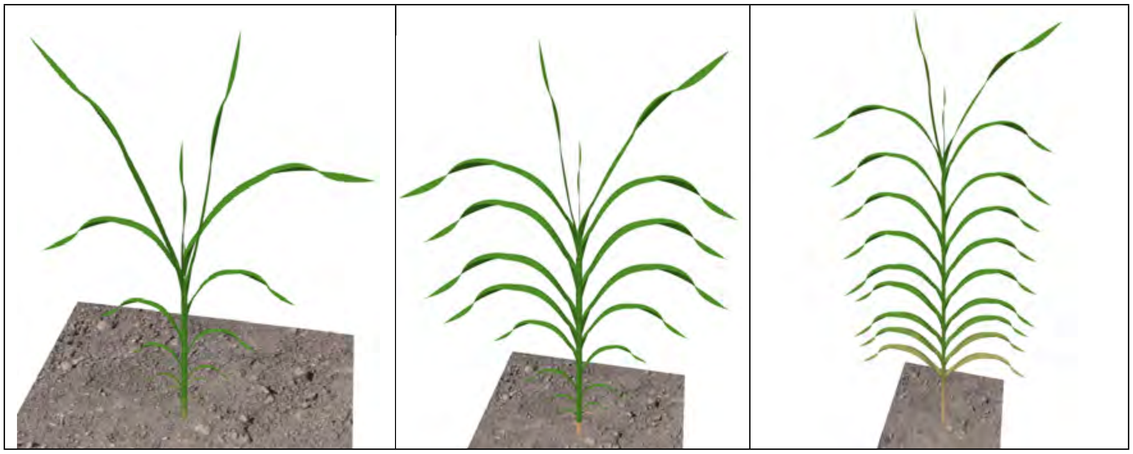

Fig. 6. Snap shots of a simulated sorghum plant over the growth season

Further Work

The model is currently being calibrated and validated using data from the field experiments. It will be further refined to capture the effect of microenvironment data such as light, organ temperature and light quality on plant growth and development, and to incorporate traits that can fully elucidate the genotype (G) × environment (E) × management (M) interactions.

References

Corson, M.S., Rotz, C.A., Skinner, R.H., 2007. Evaluating warm-season grass production in temperate-region pastures: A simulation approach. Agricultural Systems 93, 252-268.

Kiniry, J.R., Cassida, K.A., Hussey, M.A., Muir, J.P., Ocumpaugh, W.R., Read, J.C., Reed, R.L., Sanderson, M.A., Venuto, B.C., Williams, J.R., 2005. Switchgrass simulation by the ALMANAC model at diverse sites in the southern US. Biomass Bioenergy 29, 419-425.

Kiniry, J.R., Sanderson, M.A., Williams, J.R., Tischler, C.R., Hussey, M.A., Ocumpaugh, W.R., Read, J.C., Esbroeck, G.V.v., Reed, R.L., 1996. Simulating Alamo switchgrass with the ALMANAC model. Agronomy Journal 88, 602-606.

Wilson, L.T., Corbett, A., Trichilo, P.J., Kerby, T.A., Plant, R.E., Goodell, P.B., 1992. Strategic and tactical modelling: cotton - spider mite agroecosystem management. Experimental and Applied Acarology 14, 357-370.

Wilson, L.T., Gutierrez, A.P., Tennyson, R., Zalom, F.G., 1986. A physiological based model for processing tomatoes: Crop and pest management. Acta Horticulturae 200, 125-132.

Wu, G.W., Wilson, L.T., 1998. Parameterization, verification, and validation of a physiologically complex age-structured rice simulation model. Agricultural Systems 56, 483-511.

Yan, D., Wilson, L.T., Yang, Y., Koti, S., Medley, J.C., 2009. Development of an integrated rice functional-architectural modeling system. Pp. 55-56. 39th Biological Systems Simulation Conference, May 11 - May 13, 2009. Griffin, Georgia, USA.

Yang, Y., Wilson, L.T., Koti, S., Yan, D., 2009. A Cotton Cropping System Model: Integration from Individual Organs to Whole Plant and Population, 39th Biological Systems Simulation Conference, Griffin, Georgia. Pp. 21-22.

4.6
NATIONWIDE CROP SUITABILITY MODELING OF BIOMASS FEEDSTOCKS

Michael D. Halbleib[1,], Christopher Daly[1], David B. Hannaway[1]*

Abstract
A major objective of the Sun Grant GIS component is to gain an understanding of the spatial distribution of current and potential biofuel/bio-energy feedstock resources across the country. To this end, the Sun Grant Western Region GIS Center (PRISM Climate Group) at Oregon State University has developed, and is applying, an environmental modeling approach (PRISM-EM) for making current and potential national feedstock production maps. PRISM-EM incorporates the important environmental constraints on biomass production, namely climate and soils. This approach, rather than attempting to develop empirical models from existing biomass data, was chosen because nearly all dedicated feedstocks have insufficient information from which to extrapolate yield nationwide. The centerpiece of the environmental model is a semi-monthly FAO-style water balance simulation, which tracks precipitation input, evapotranspiration, and soil moisture depletion. An estimate of monthly relative yield (0-100 percent) is the product of the water stress coefficient and a temperature growth curve. In what is known as a "limiting factor" approach, the final relative yield is the lowest of the modeled yields resulting from the water balance simulation, plant injury curves for summer heat and winter cold, and growth constraints due to soil pH, drainage, and salinity. The crop suitability mapping system is driven by PRISM temperature and precipitation data, prepared at a monthly time step on a regular grid across the US. PRISM is a state-of-the-science climate mapping technology that produces several major spatial climate datasets for the US, including official maps for the US Department of Agriculture.

Keywords: Environmental Mapping, Suitability Mapping, Biomass Yield, PRISM

Introduction
A major objective of the Sun Grant GIS component is to gain an understanding of the spatial distribution of current and potential biofuel/bio-energy feedstock resources across the country. Biofuel crops have become a point of national focus, with several new crops identified as potential feedstocks. Traditional crops such as wheat, corn, and sorghum, provide residues that can serve as biofuel feedstocks, and have long production histories and rich knowledge bases with regard to physiology, production, and spatial distribution. However, many new crops identified as potential feedstocks, such as switchgrass, miscanthus, and energycane, have little production history in the United States. It is not surprising, then, that planners tasked with assessing farming, transportation, processing needs, and infrastructure for new crops are asking the basic question: Where can these new crops be raised successfully and what kind of production can be expected within a given geographic region?

Attempts to estimate the potential spatial distribution and yield of new biofuel feedstocks have taken two main approaches: (1) empirical models based on field data; and (2) application of mechanistic plant growth models (Jager et al. 2010, Nair et al. 2012). Commonly used empirical approaches involve statistical extrapolation of plot/field-level yield data to larger regions and climatic envelope modeling (e.g., Casler et al. 2007, Barney and DiTomaso 2010, Schmer et al., 2009, Araya et al. 2010, Jager et al. 2010, Wullschleger et al. 2010, Tulbure et al. 2011). The main drawback of empirical approaches has been a lack of suitable yield data (Miguez et al. 2011). Attempts to relate yield data to environmental conditions can be confounded by factors other than

[1] *Oregon State University, PRISM Climate Group, OR*

* *Corresponding author*

environment, such as fertilization, cutting rotation, supplemental irrigation, and other management practices (Jager et al. 2010). In addition, yield histories can be as short as a single year, and are thus affected by year-to-year variability in weather conditions. Finally, yield data are typically collected from demonstration plots in areas where the crop is likely to succeed, and thus provide little guidance as to how environmental factors limit production near the edges of the crop's range (Miguez et al. 2011). Despite these shortcomings, empirical approaches provide important assessment tools for planning activities and supply guidance for more mechanistic modeling approaches (Jager et al. 2010).

Plant growth models attempt to simulate the important physiological processes that affect growth, development, and yield. Most plant growth models simulate photosynthesis, carbon allocation, phenology, biomass production, and root/shoot partitioning. Examples of simulation models include EPIC (Williams et al. 1984, Brown et al. 2000), ALMANAC (Kiniry et al. 2008), and MISCANFOR (Hastings et al. 2009, Miguez et al. 2011). A review of plant growth models that have been used for biofuel feedstock assessment is available from Nair et al. (2010). These models have the potential to provide detailed information on crop performance and yield, but do require significant environmental data inputs and detailed knowledge of crop physiology (e.g., Brown et al. 2000). In addition, calibration and validation of models requires detailed plot-level data, which is often scarce or poorly distributed for many new crops. Parameterization of some models to specific crops and locations can make it difficult to generalize results over large areas (e.g., Miguez et al. 2011).

We have developed a modeling system, called PRISM-EM (PRISM Environmental Model), which stems from earlier work to estimate the suitability of US-grown perennial grasses in China (Hannaway et al. 2005). The system draws from both the statistical-empirical and crop growth modeling approaches, while keeping the modeling system very simple and universal so that assessments can be made quickly and easily over large areas. The basic question we seek to answer is: What is the spatial distribution of the major environmental constraints that limit the production of this crop? Our interest here is in general biomass production, rather than a detailed accounting of phenology, flowering, grain development, *etc*.

We begin with gridded climate and soils datasets that describe the environment across the conterminous US (Figure 1). These serve as input to a simple FAO-style model that tracks water balance (Allen et al. 1998) and temperature constraints on growth. Output from the model is in the form of relative yield, ranging from 0 (no production) to 100 (full production). A land use grid can be applied to the relative yield map to screen out land use types that are not suitable for agriculture (e.g., forests). The relative yield map can be transformed into an actual yield map by developing statistical relationships between relative and actual yield using available yield data.

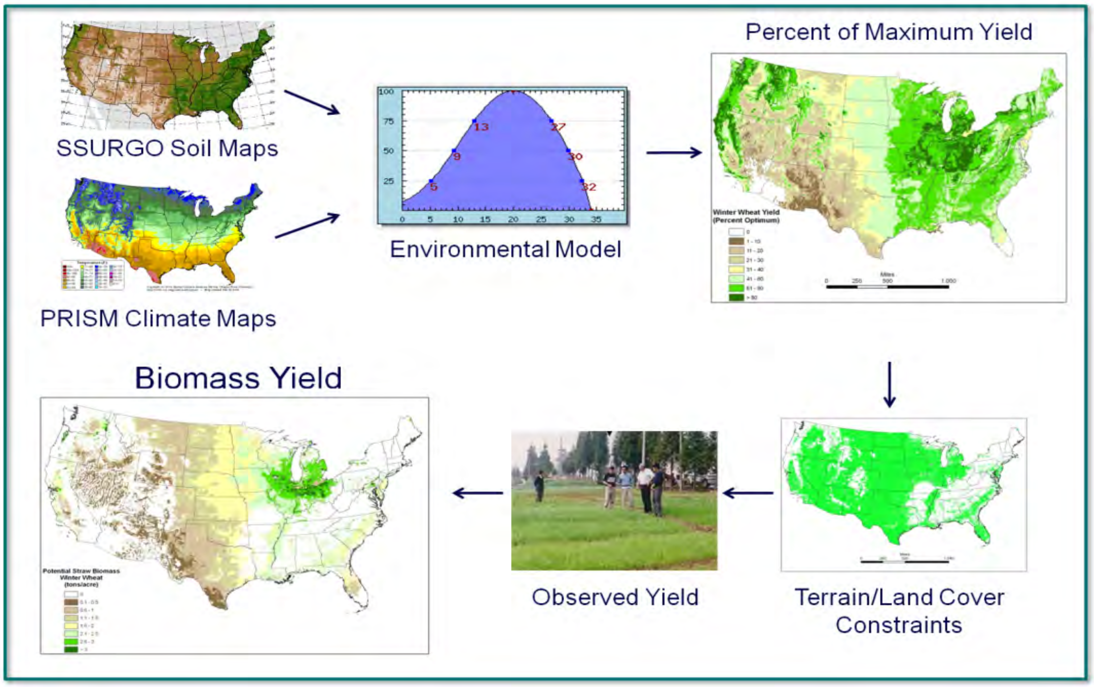

Figure 1. Flow chart of the PRISM-EM modeling approach.

Model Details

Climatological variables used as input are provided by the PRISM Climate Group (Oregon State University) and represent monthly, 30-year averages for the period 1971-2000 (Daly et al. 2008). The climate datasets have values on a regular grid with a grid cell size of approximately 800 meters across the conterminous US (model is currently run at a 4-km resolution, however). Variables used are 1971-2000 mean monthly precipitation and average temperature, mean July maximum temperature, and mean January minimum temperature. Spatial soils data were obtained from the USDA Natural Resources Conservation Service SURRGO dataset, and the necessary spatial data layers extracted from available data. Soil variables utilized in the model are pH, water holding capacity, salinity, and drainage.

The environmental model uses a “limiting factor” approach to estimating relative yield. Relative yield is calculated as the *lowest* yield resulting from any of the factors considered to limit growth. These factors are water balance (deficit), seasonal temperature extremes (winter low temperature and summer high temperature), and soil properties (pH, drainage, and salinity).

Water Balance Model

The water balance model uses mean monthly 30-year average precipitation (*P*), apportioned on a semi-monthly time step, to determine total available water (*TAW*) in the soil profile (Figure 2). Available soil water holding capacity (*AWC*) is estimated from the SURRGO soils data and the depth of the rooting zone (*Droot*) is defined by the user. Monthly average temperature (*T*) is used to estimate potential evapotranspiration (*ETo*). Actual evapotranspiration (*ETa*) is a function of *ETo*, a water stress coefficient (*Ks*), the plant’s water use efficiency (*Kc*, user-defined), and the root zone moisture depletion (*Dr*), which is the difference between the plant’s moisture demand and the soil water supply. *ETa* in a given time interval reduces the next time interval’s soil water supply, which is at least partially replenished by precipitation. At the end of each time interval, *Ks* is calculated as the difference between *TAW* and *Dr*. Relative yield for that interval is the product of *Ks* and a user-defined temperature growth response function, which defines the relationship between temperature and relative production for that crop (Figure 3).

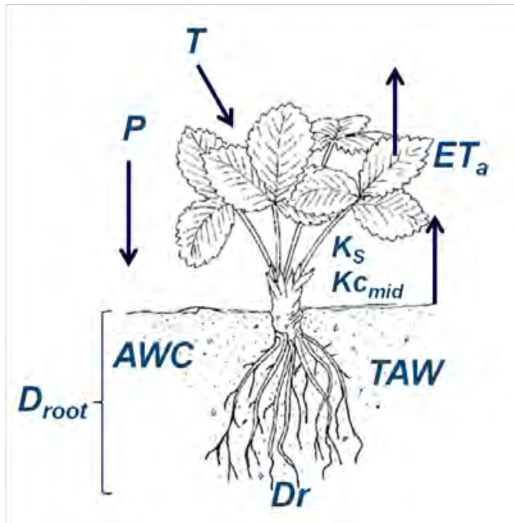

Figure 2. Schematic of water balance model function. See text for definitions of symbols.

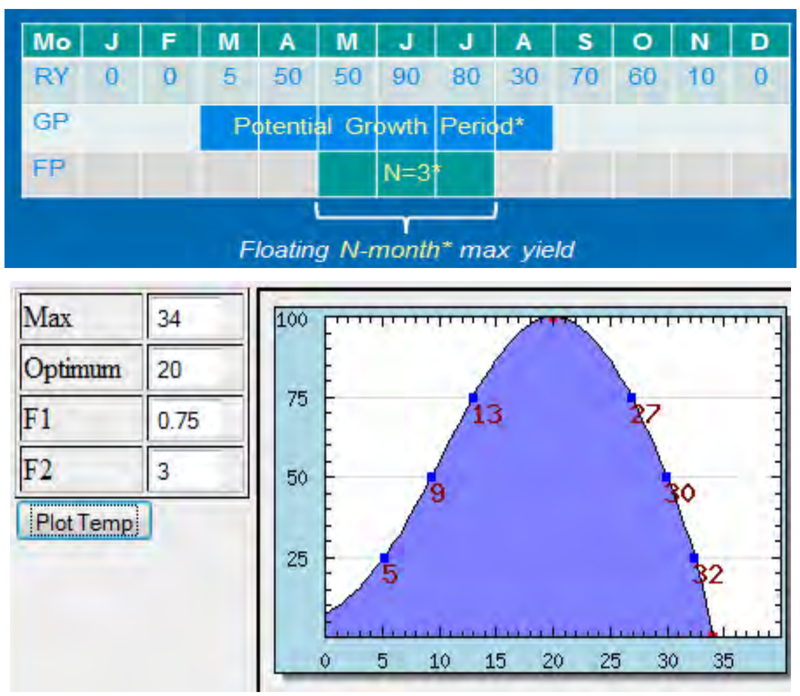

Figure 3. Example of a user-defined temperature growth function from the model interface. The x-axis is mean monthly temperature in degrees C, and the y-axis is relative growth response (0-100 percent).

The output of the water balance model is a relative yield estimate ranging from 0 to 100 for each month (shown, for example, as RY in Figure 4). The user specifies a potential growth period, which is the range of months in which production is likely to occur across the modeling region. In the example in Figure 4, the potential growth period is March – August. The user also specifies the number of sequential months within the potential growth period over which maximum production is likely to occur. RY values are averaged over these months to obtain a final water balance yield. For example, if the period of significant biomass accumulation is typically three months, the user would input N = 3, as shown in Figure 4. This maximum growth period is typically allowed to “float,” meaning the model will use the three-month sequence with the highest average RY as the final water balance yield, to accommodate varying growing season timing under differing climates.

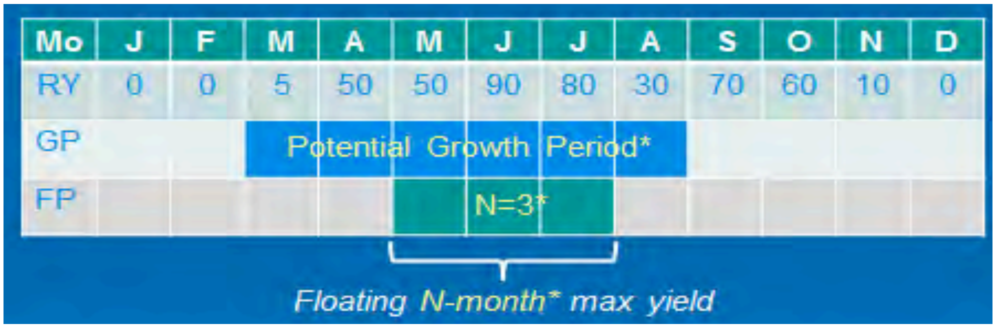

Figure 4. Schematic of the method used to calculate final water balance yield.

Seasonal Temperature Extremes

The winter temperature constraint simulates a perennial crop’s ability to tolerate and survive average winter low temperatures. A single-tailed temperature response function relates the PRISM 30-year average January minimum temperature to expected damage or mortality and resultant loss of production. The summer temperature constraint simulates a crop’s ability to tolerate and survive average summer high temperatures. A single-tailed temperature response function relates the PRISM 30-year average July maximum temperature to expected damage or mortality and resultant loss of production.

Soil Constraints

The soil constraint function for soil pH uses a two-tailed curve similar to that of the temperature growth function (Figure 3) that can be broadened or narrowed based on expected plant response to pH. The soil constraint function for salinity uses a one-tailed curve that represents growth reduction due to increasing soil salinity. The soil constraint function for drainage is based on the seven soil drainage classes as defined by the NRCS, ranging from very poorly drained to excessively drained. The expected plant response for each drainage class can be set individually, ranging from 0 (full constraint) to 100 (no constraint).

Final Yield Calculation

The final relative yield is calculated as the *lowest* yield resulting from any of the constraint functions: water balance, winter low temperature, summer high temperature, soil pH, soil drainage, and soil salinity. Model output is in the form of a regularly spaced grid with an estimate of relative yield from 0 to 100 percent. The output can be imported into most GIS packages for visualization.

Results

Initial PRISM-EM runs were conducted at 4-km resolution on several species of crops that are currently in production throughout the country, specifically winter wheat, corn, and sorghum. “Non-usable” lands, such as forested and urban areas, were masked from the output grids using the National Land Cover Database (NLCD). As a validation exercise, the resulting gridded and masked relative yield estimates were averaged across each county in the conterminous US and compared to ten-year (2000-2009) county average grain yields obtained from the USDA Risk Management Agency (RMA). The RMA requires yield reports from all participants in the federal crop insurance program, resulting in the most comprehensive database of yield information available for the US. To minimize the effects of spurious county averages arising from limited acreage, the "30-30-30" rule was applied: Counties were included in the comparison only if they encompassed at least 30 4-km grid cells, at least 30% of the county was deemed "useable" by the NLCD grid, and a county contained at least 30 yield reports from the RMA database.

Results were promising; a nationwide linear regression analysis relating modeled relative yields against reported average county yields for winter wheat resulted in an R^2 value of 0.69. Examination of some of the outliers revealed several issues. The NRCS database describes pH, drainage, and salinity for native soils, and does not account for alterations that may have been made to increase agricultural productivity, such as liming to increase pH and tiling to improve drainage. An example of a discrepancy attributable to tiling of poorly drained soils can be seen in northwestern Ohio; relative yield is modeled as low because of poor native soil drainage (Figure 5), but the reported county average yield is quite high (Figure 6). A discrepancy caused by liming of acidic soils is seen in New Jersey, where, again, modeled yield is low compared to the reported county average (Figures 5 and 6). In the western US, discrepancies occurred in some very large counties. Here, the reported yields may have applied to only a small part of the county that had been cultivated, while the modeled yield included all area classified as useable.

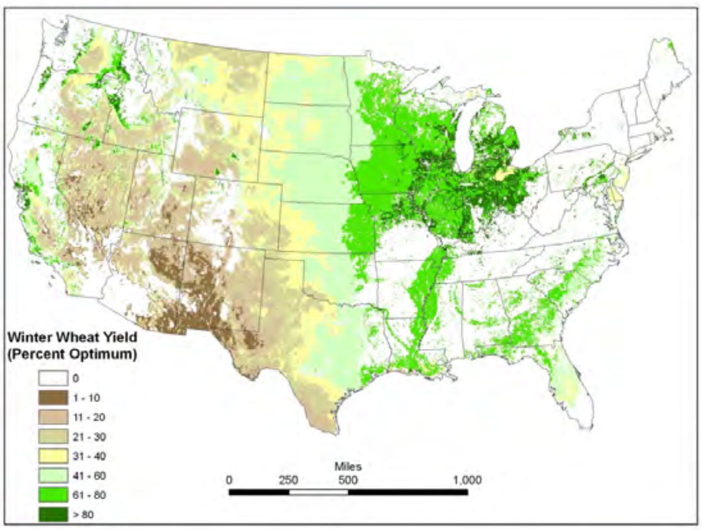

Figure 5. PRISM-EM relative yield map for winter wheat.

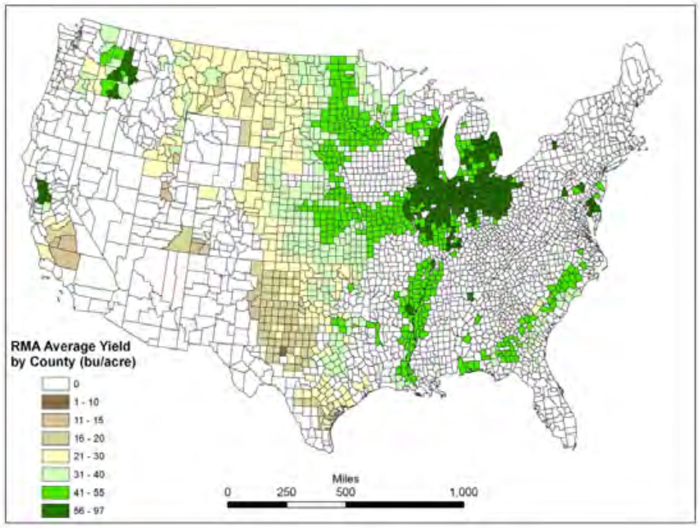

Figure 6. USDA RMA county average reported yields for winter wheat, 2000-2009.

The PRISM-EM relative yield map can be transformed into an actual yield map by assigning a realistic maximum yield to represent 100 percent relative yield and simply scaling the map by this factor. More sophisticated transformations can also be made by developing spatially varying relationships between relative and actual yield, using *in situ* yield data at available locations. In our winter wheat example, the PRISM-EM relative yield map was converted to actual biomass yield by applying the nationwide regression function to transform relative yield into grain yield, then applying a harvest index, which is the proportion of the crop's biomass allocated to grain, to arrive at an estimate of biomass. Using a harvest index of 0.4 for winter wheat, we arrived at the biomass map shown in Figure 7.

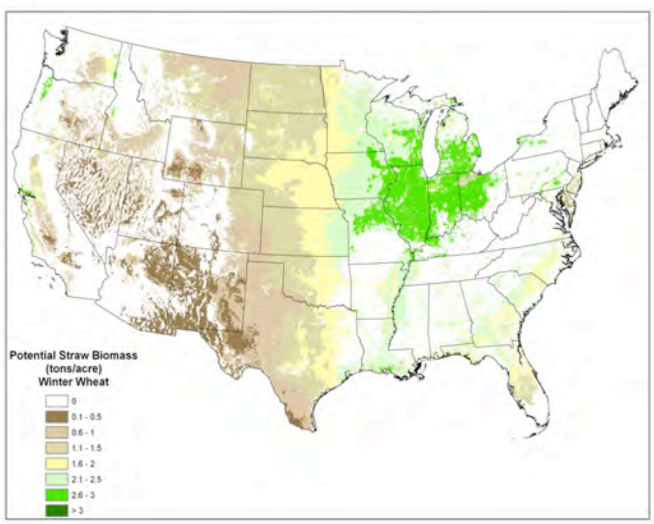

Figure 7. PRISM-EM modeled winter wheat straw yield, using a linear regression function between relative yield (Figure 5) and 2000-2009 average reported yield (Figure 6), and a harvest index of 0.4.

Conclusion and Further Work

Many potential biofuel feedstock crops, such as switchgrass, miscanthus, energycane, willow, and poplar, are sufficiently new that they lack long yield histories, detailed production information, and yield distribution data. This general lack of production information makes it difficult to estimate where the crop might be produced and what yields might be expected. PRISM-EM was designed to produce realistic mapped estimates of relative biomass yield, based on climatological and soils information and a crop's basic tolerances to these factors. These maps can be transformed into actual yield maps by applying a range of statistical functions relating relative to actual yield. The transformation can be as simple as setting 100 percent relative yield to a maximum expected biomass yield and scaling the map accordingly, or as complex as using *in situ* yield reports to develop spatially varying relationships across the country. PRISM-EM maps are meant to be "first guess" maps to guide planning efforts. As more data become available for a given crop, sophisticated crop growth models will likely be used increasingly to provide more detailed and specific crop performance and yield information.

As we have applied PRISM-EM to non-traditional crops, we have found that even the most basic information about optimal temperature, water use efficiency, heat and cold injury, *etc*., are largely unavailable. (Much research is underway to answer these types of questions, but it will take time to develop.) To accommodate this lack of information, we have adopted an environmental continuum approach. Here, we place well-known crops on a multi-dimensional continuum of water use efficiency, optimum temperature, and tolerances to heat stress, cold injury, and soil conditions. These serve as "markers" for which we have reasonably good model parameters. We then place the lesser-known crops on this continuum by comparing what is known about the crops relative to the markers and ranking their tolerances accordingly. This has allowed us to produce initial maps of most nationally important feedstock crops suitable for review.

As these draft maps are shared with local and regional experts and comments are received, we will modify the crop rankings and associated plant response curves, and produce new maps that reflect the expert opinion and experience of the participants.

A major PRISM-EM improvement currently underway is gaining the ability to run the model on individual monthly climate data, rather than on long-term average climate only. The goal is to develop distributions of relative yield, which will provide yield variability information in addition to the average yield. This will allow an assessment of relative production volatility, and identification of areas with an unusually high risk of years with poor production potential.

References

Allen, R.G., Pereira, L.S., Raes, D., Smith, M. (1998). *Crop evapotranspiration - Guidelines for computing crop water requirements*. FAO Irrigation and Drainage Paper 56, Food and Agriculture Organization of the United Nations, Rome, Italy.

Araya, A., Keesstra, S.D., Stroosnijder, L., (2010) A new agro-climatic classification for crop suitability zoning in northern semi-arid Ethiopia. *Agricultural and Forest Meteorology*, 150 (7–8): 1057-1064.

Barney, J.N., and DiTomaso, J.M., (2010) Bioclimatic predictions of habitat suitability for the biofuel switchgrass in North America under current and future climate scenarios. *Biomass and Bioenergy*, 34: 124-133.

Brown, R.A., Rosenberg, N.J., Hays, C.J., Easterling, W.E.; and Mearns, L.O., (2000). Potential Production and Environmental Effects of Switchgrass and Traditional Crops under Current and Greenhouse-Altered Climate in the Central United States: A Simulation Study. *Agriculture, Ecosystems and Environment*, 78: 31-47.

Casler, M. D., Vogel, K. P., Taliaferro, C. M., Ehlke, N. J., Berdahl, J. D., Brummer, E. C., Kallenbach, R. L., West, C. P., Mitchell, R. B. (2007) Latitudinal and Longitudinal Adaptation of Switchgrass Populations. *Crop Sci.* 47: 2249-2260.

Daly, C., Halbleib, M., Smith, J.I., Gibson, W.P., Doggett, M.K., Taylor, G.H., Curtis, J., and Pasteris, P.A. 2008. Physiographically-sensitive mapping of temperature and precipitation across the conterminous United States. *International Journal of Climatology*, 28: 2031-2064.

Hannaway, D.B., Daly, C., Cao, W., Luo, W., Wei, Y., Zhang, W., Xu, A., Lu, C., Shi, X., Li, X. 2005. Forage Species Suitability Mapping for China Using Topographic, Climatic and Soils Spatial Data and Quantitative Plant Tolerances. *Scientia Agricultura Sinica*, 4: 660-667.

Hastings A., Clifton-Brown J., Wattenbach M, Mitchell C. P., Smith P. (2009) The development of MISCANFOR, a new Miscanthus crop growth model: towards more robust yield predictions under different climatic and soil conditions. *Global Change Biology Bioenergy*, 1: 154–170.

Jager, H.I., Baskaran L. M., Brandt C. C., Davis E. B., Gunderson C. A., Wullschleger S. D. (2010). Empirical geographic modeling of switchgrass yields in the United States. *Global Change Biology: Bioenergy*, 2: 248-257.

Kiniry, J.R.; Schmer, M.R., Vogel, K.P., Mitchell, R.B., (2008). Switchgrass Biomass Simulation at Diverse Sites in the Northern Great Plains of the U.S. *Bioenerg. Res.*, 1: 259-264.

Miguez, F.E., Maughan, M., Bollero, G.A., Long, S.P. (2011). Modeling spatial and dynamic variation in growth, yield and yield stability of the bioenergy crops Miscanthus 9 giganteus and Panicum virgatum across the conterminous USA. *GlobalChange Biology: Bioenergy*, doi: 10.1111/j.1757-1707.2011.01150.x.

Tulbure, M.G., Wimberly, M.C., Boe, A., Owens, V.N. (2012). Climatic and genetic controls of yields of switchgrass, a model bioenergy species. *Agriculture, Ecosystems & Environment*: 146: 121-129.

Nair, S. S., King, S., Zhang, X., Miguez, F.E., Izaurralde, R. C., Post, W. M., Dietze, M.C., Lynd, L.R., Wullschleger, S. D. (2012). Bioenergy crop models: descriptions, data requirements, and future challenges. *Global Change Biology: Bioenergy*, doi: 10.1111/j.1757-1707.2012.01166.x

Schmer, M. R., Mitchell, R. B. Vogel, K. P. Schacht, W. H., Marx, D.B., (2009). *Spatial and Temporal Effects on Switchgrass Stands and Yield in the Great Plains.* Publications from USDA-ARS / UNL Faculty. Paper 394.

Williams, J. R., Jones, C. A., Dyke, P.T. (1984). A modeling approach to determining the relationship between erosion and soil productivity. *Transactions of the ASAE*, 27:129-144.

Wullschleger S.D., Davis E.B., Borsuk M.E., Gunderson C.A., Lynd L.R. (2010). Biomass production in switchgrass across the United States: database description and determinants of yield. *Agronomy Journal*, 102: 1158–1168.

4.7
ACCURATELY ASSESSING WOODY BIOMASS POTENTIAL IN NORTH CAROLINA, US

James Jeuck[1], Dennis Hazel[1], Robert Bardon[1]

Abstract
Since 2007, NCSU Extension Forestry has conducted over 50 detailed biomass supply assessments supporting prospective projects on behalf of bio-energy industries and economic developers. These analyses leverage data from numerous sources and scales for gross woody biomass, drain, and net woody biomass distributed spatially across timberland. Described here are details of NCSU *Fiber*Analytics processing techniques for two levels of woody biomass supply assessment offered to clients. The first level results in state-wide, coarse-resolution, gradient maps of net supply based on client feedstock preferences. These are derived from net supply-distance curve coefficients generated through a series of neighborhood functions performed on net supply maps. Web-hosting interactive assessment enables potential industries, policy developers or others to explore scenarios across the state. The second level of supply assessment is performed for clients with identified site locations. For each identified site, supply areas are developed for specified haul distances using road networks. All forms of potential woody biomass are applied to timberland distributed (derived from satellite imagery) throughout each supply area is summed and used to develop supply curves. Estimated demand from facility-specific demand regions for existing and potential competitors are subtracted yielding accurately portrayed net supply based on distance and feedstock type.

Keywoods: biomass supply analysis, ArcGIS, USFS FIA, USFS TPO, USDA NASS, spatial supply modeling,

Introduction
North Carolina State University Extension Forestry has been a major player in woody biomass promotion and policy in NC. We provide outreach and education to potential new biomass industries and economic developers across the state. Part of our efforts led to the development of a service center, *Fiber*Analytics, which provides analytic support and resources for new biomass industries scoping NC. Our analytic support is focused around biomass supply models for both woody and other biomass that utilize our knowledge of the most accurate and current information on biomass supply and demand (drain). This paper briefly outlines the data used, a course-level state-wide model and our detailed model for site specific analysis. This may be useful for other groups wishing to provide similar services across the states.

Data
Data sources used are briefly described below. All county-level tabular data are acquired for NC, VA, TN, GA, and SC as our analysis often crosses state lines. Data not provided in green tons is converted to keep the units the same in our analysis. Summary descriptions are of tabular public data sources and our derived usage are provided in Table 1.

[1] *Extension Forestry, North Carolina State University, NC*

* Corresponding author

Table 1. Sources of county-level data used by NCSU FiberAnalytics for statewide and site specific biomass analysis.

Source: USFS Forest Inventory and Analysis (FIA)	
http://www.fia.fs.fed.us/tools-data/default.asp	
Data description: 2003-2011 running average of annual permanent inventory plot data summarized at the county level	
FIA Data	***Fiber*Analytics Use/ Derivation**
Growing stock sawtimber: 9"+ dbh softwoods (cuft); 11"+ dbh hardwoods (cuft)	same (gT)
Biomass inventory: 1-5" dbh (dT)	same (gT)
Pulpwood inventory: 5-9" dbh softwood (cu ft); 5-11" dbh hardwood (cu ft)	same (gT)
All live stems to 4" top: 5"+ dbh hardwoods, softwoods (cu ft)	Pulpwood volumes in tops of sawtimber stems (gT) Non-growing stock sawtimber volumes (gT)
Total biomass to 1.5" top and branches to 1.5": 5"+ dbh hardwoods, softwoods (cu ft)	Topwood in all merchantable stems (4" to 1.5" tops and branches to 1.5" on all stems) (gT)
Annual pulpwood growth: 5-9" dbh softwood (cu ft), 5-11" dbh hardwood (cu ft)	same (gT)
All merchantable stem growth: 5"+ dbh hardwood, softwood	same (gT)
Source: USFS Timber Products Output (TPO)	
http://srsfia2.fs.fed.us/php/tpo_2009/tpo_rpa_int2.php	
Data description: Average of 1995-2009 county-level summaries of biannual forest products industries surveys describing timber harvest levels by product	
TPO Data	***Fiber*Analytics Use/ Derivation**
Removals: sawtimber, veneer, pulpwood, composite, fuelwood, other - hardwoods, softwoods (gT)	Sawtimber removals: hardwood, softwood (gT) Pulpwood class removals: (combined pulpwood and composite) - hardwood, softwood (gT)
Biomass inventory: 1-5" dbh (dT)	same (gT)
Logging residues: hardwood, softwoods (gT)	same at 65% recovery efficiency (gT)
Other removals: hardwoods, softwoods (gT)	same at 65% recovery efficiency (gT)
Source: USDA National Agricultural Statistics Service (NASS)	
http://www.nass.usda.gov/	
Data description: Average of 2001-2011 county-level summaries of annual surveys by commodity crop	
NASS Data	***Fiber*Analytics Use/ Derivation**
Corn harvested: (bu)	Corn stover: g(T)
Hay harvested: (dT)	Hay as a surrogate for energy crops: (gT)

USFS Forest Inventory and Analysis (FIA)[2] is a national program where each state conducts annual[3] plot-level inventories of forest resources. We use their data summarized to the county level. This rich dataset is used to estimate net[4] current inventory of hardwood and softwood sawtimber, pulpwood, woody biomass from tops and non-merchantable stems, annual growth and removals by supply area[5].

[2] http://www.fia.fs.fed.us/tools-data/default.asp

[3] FIA inventories annually sample only a portion of a state's plots. Complete inventory cycles span across different years according to each state's inventory program. Current NC data spans from 2003-2011.

[4] Net growth and net volumes estimates do not include natural mortality.

[5] We caution our clients on FIA inventory data having high variability (some over 50%) at the county level making it less reliable in smaller supply areas.

USFS Timber Products Output (TPO)[6] provides summaries of biennial surveys to forest industry to estimate county-level timber removals by product class, logging residues[7], and “other removals”[8]. We use a running average of (currently1995-2009[9]) TPO data to smooth market fluctuations.

County-level potential for agricultural residues (i.e., corn stover) or hay production comes from the National Agricultural Statistic Service (NASS)[10]. Currently, corn is the only NC crop with residues large enough to be utilized. Hay is used as a surrogate for energy crops[11] production associated with marginal lands, realizing that energy crops would have 2 to 3 times the yield.

Land cover comes from the 2006 National Land Cover Database (NLCD) provided by the Multi-Resolution Land Class Consortium[12]. This is national 30m X 30m (.223 acre) resolution raster grid dataset classified to 16-land uses. Preserved forest lands are removed from this dataset using the Protected Area Database US 1.1[13] of private and public protected areas. Public forested lands are not removed realizing harvest levels may be lower than on private lands. This used to determine spatial distribution and acreages of hardwood[14], softwoods[15], crop land, and pasture/ hay land. County acreage estimates for these four land cover grids are derived by assignment of Federal Information Processing Standard (FIPS) county codes to each respective land cover[16].

The Environmental System Resource Institute (ESRI) StreetMap Road Network[17] data set provides road networks used to build supply areas using ESRI Network Analyst.

[6] http://srsfia2.fs.fed.us/php/tpo_2009/tpo_rpa_int2.php

[7] We currently suggest using a 65% recovery rate logging residues and other removals in North Carolina.

[8] "The growing-stock volume of trees removed from the inventory by cultural operations such as timber stand improvement, land clearing, and other changes in land use, resulting in the removal of the trees from timberland" (Cooper et al. 2009).

[9] 2009 is the most recent TPO data as of the date of this paper.

[10] http://www.nass.usda.gov/

[11] Currently there are is very little land in North Carolina growing energy crops.

[12] http://www.mrlc.gov/

[13] http://databasin.org/protected-center/features/PAD-US-CBI

[14] Hardwoods combines the NLCD classes "deciduous forest" and "woody wetlands"

[15] Softwoods combines the NLCD classes "conifer forest" and "mixed forest"

[16] Performed using a zonal statistics tool in ArcGIS 10.1

[17] http://www.esri.com/software/arcgis/extensions/streetmap/index.html

Our FiberAnalytics drain database[18] tracks current and potential demand of five major feedstock types[19] in NC and the four surrounding states. These include pulpmills, pellet plants, chip mills and chip export companies, OSB and fiberboard plants, power companies, combined heat and power, and other process steam facilities. This dataset is updated regularly making it the most reliable and complete data source for drain in our region.
Other spatial data used as requested by clients include poultry and swine farms by size, parcels, major powerlines, rail systems and canals, certified forestlands, deferred tax parcels, and corporate lands (TIMOs and REITs).

Statewide, Coarse Resolution Assessment

Clients have requested a statewide view of potential biomass commodities to quickly ascertain potential "hot-spots" in the state based on feedstock mix and travel cost criteria. We provide this analysis through a spatial supply-distance model for each biomass resource type outlined here. The gross supply, drain, and net supply models used for statewide analysis are provided for in Figure 1, using hardwood logging residues and hardwood whole-tree chips as an example.

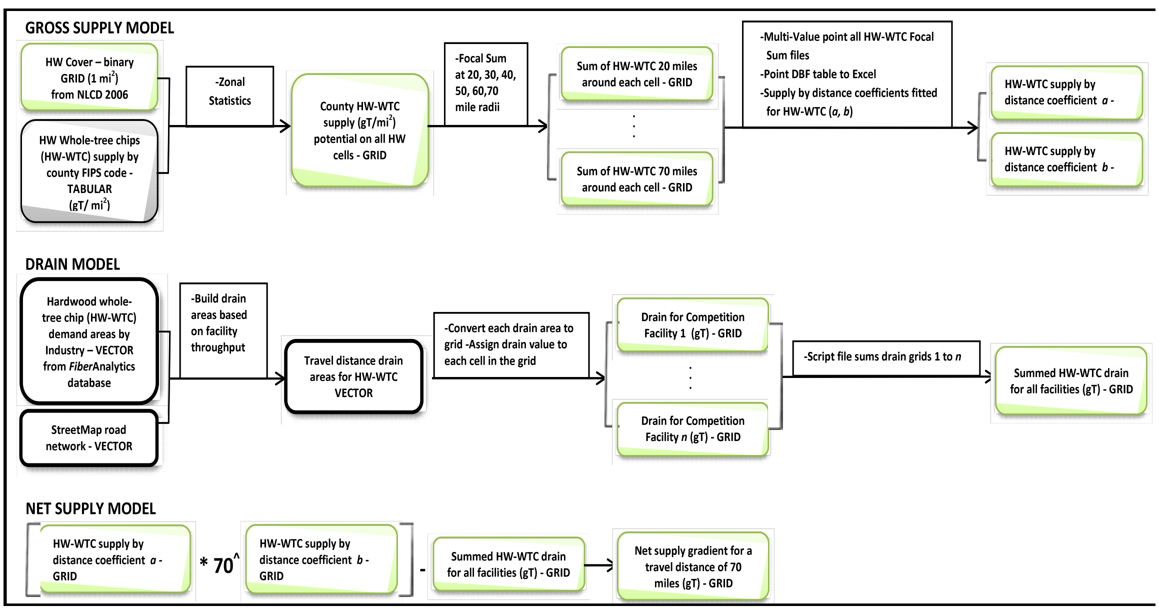

Figure 1. Flow chart for statewide biomass analysis models used by NCSU *Fiber*Analytics. This flow chart example shows the steps for the gross hardwood logging residues supply, drain for whole-tree chips (from logging residues), and the net hardwood logging residue gradient map produced. The net supply model assumes the client wants to know the amount of hardwood logging residues at a 70-mile radius search. These models are currently developed for logging residues, other removals, and pulpwood for hardwoods and softwoods, and for corn stover and hay, but can be modified for many uses.

The NLCD grid is resampled to 1-mi^2 resolution and reclassified into four binary land cover grids (hardwoods, softwoods, crops, and hay/pasture) where "1" is assigned to cells in that land use and

[18] We assume a conservative annual throughput of 90% of the boiler plate specifications, which may tend to overestimate drain for a plant, but we would rather stay on the conservative side of our net supply estimates

[19] These are hardwood pulpwood, softwood pulpwood, hardwood whole-tree chips, softwood whole-tree chips, and fuel or "dirty" chips

"0" to all other cells. County biomass estimates (in gT/mi^2)[20], are assigned to every "1" cell in the associated land cover grids. This equally distributes county-level green ton estimates to every cell in that land cover class and results in eight[21] "biomass supply" layers. Next, to each biomass supply layer, we apply a series of neighborhood functions[22], each designed to sum green ton estimates at 10-mile to 70-mile radii circles around each cell in the layer. Combined[23], these green ton values are used to develop supply curve coefficients for every cell in a given biomass supply layer. The resulting supply curve data are fitted in Excel to the exponential model:

$$gT = ad^b \qquad [1]$$

where, gT = the annual gT potential for each cell its own *d*-radius supply area
d = maximum travel distance around each cell
and *a*,*b* = fitted coefficients apply to each cell.

This yields two raster grids (from *a* and *b,* Eqn. 1) for each biomass resource that are the basis of the spatial model.

The demand grid is developed by: 1) creating drain polygons[24] around each facility location; 2) converting drain polygons to separate 1-mi^2 raster grids, 3) assigning each cell in the grid[25] that facility's feedstock type and annual throughput; and 4) adding up all similar feedstock requirement grids layers. This results in a statewide drain grid[26] for each of the four major feedstock types, accumulating where drain areas overlap.

Given a "prescription" by a client for annual biomass feedstock requirements and a preferred distance, we can apply the model using map algebra. An example may be a pellet mill requiring 600,000 gT annually of hardwood pulpwood. They prefer to purchase within 50-miles of their site and want to account for current demand. The spatial supply model simply becomes:

$$net\ gT_{[hw\ pulp]} = \left(a_{[hw\ pulp]} \times 50^{b_{[hw\ pulp]}}\right) - drain_{[hw\ pulp]} \qquad [2]$$

Where, $gT_{[hw\ pulp]}$ = resulting hardwood pulpwood supply gradient grid
$a_{[hw\ pulp]}$, $b_{[hw\ pulp]}$ = model coefficient grids for hardwood pulpwood
$drain_{[hw\ pulp]}$ = drain grid for hardwood pulpwood

---

20 Based on the county acreage estimates for the four land cover types described earlier

21 These are 1) hw logging residues, 2) hw other removals, 3) hw pulpwood, 4) sw logging residues, 5) sw other removals, 6) sw pulpwood, 7) corn stover, and 8) hay

22 Performed using the Focal Statistics tool in ArcGIS 10.1

23 Performed using the Multi-Value Point" tool in ArcGIS 10.1

24 Described in the next section of this document. These varying in sized based on the facility feedstock throughput from 30-mile to 100-mile travel distances

25 Performed using the "Polygon to Raster" tool in ArcGIS 10.1

26 Performed through Python script that performs adding multiple raster files (~85) for each feedstock demand type

The result is a gradient of net supply potential surrounding every cell in the grid that is modified by the drain for that cell. The gross volume map generated in the parentheses of Eqn. 2 is seen in Figure 3(a), the drain map is seen in Figure 3(b), and resulting net volume map sis seen in Figure 3(c).

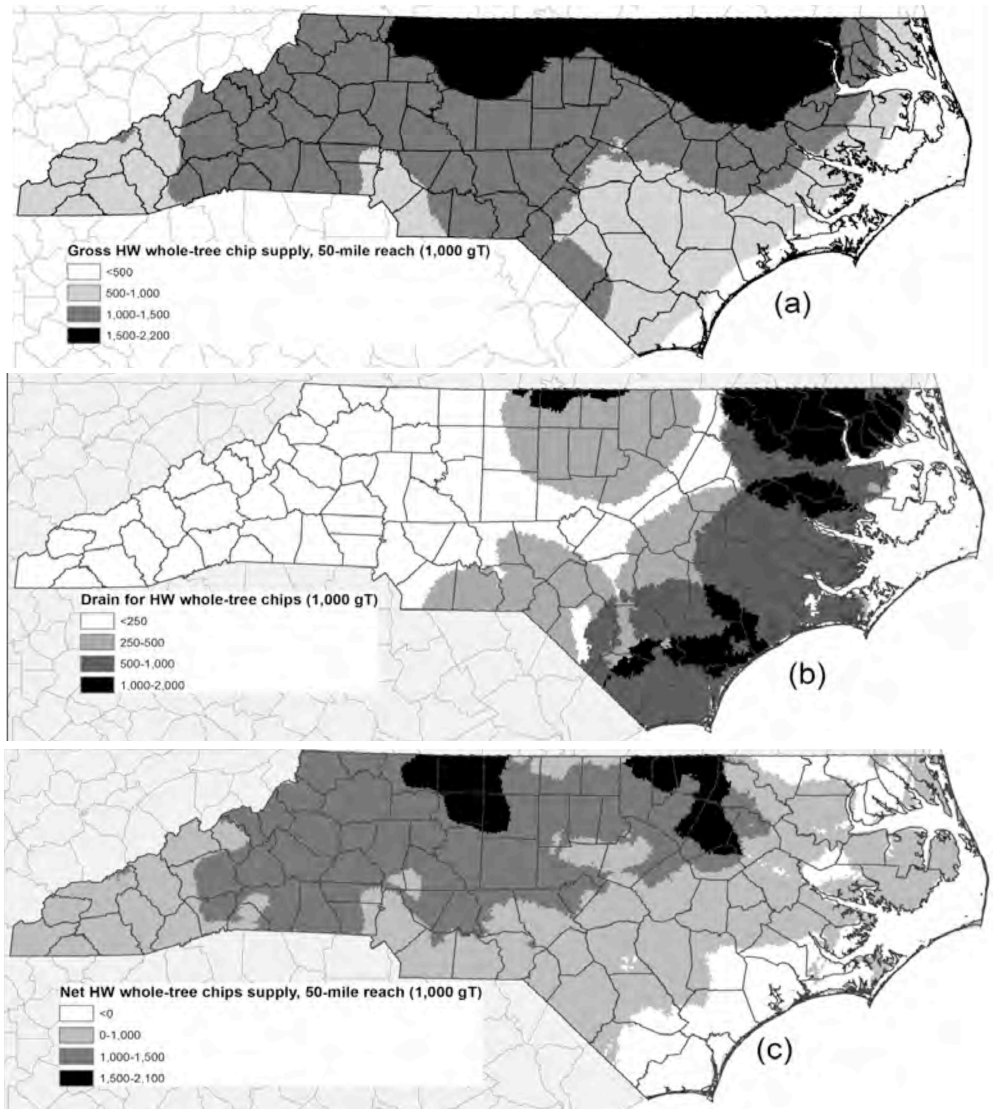

Figure 3. NC statewide biomass estimates for logging residues and other removals (whole-tree chips) in gross supply (a), drain (b), and net supply (c) for a 50-mile reach around every 1-mi^2 raster cell in NC. This provides an overview across the state where the best locations for net HW whole-tree supply exists.

This flexible procedure allows for numerous modifications. For one project we analyzed supply for 70-miles around rail lines to determine the locations of fiber sourcing along the lines (Figure 4). Clients might require a variety of feedstock "recipes" (i.e. 50% corn stover, 50% hardwood logging residues) which can be accommodated by the model.

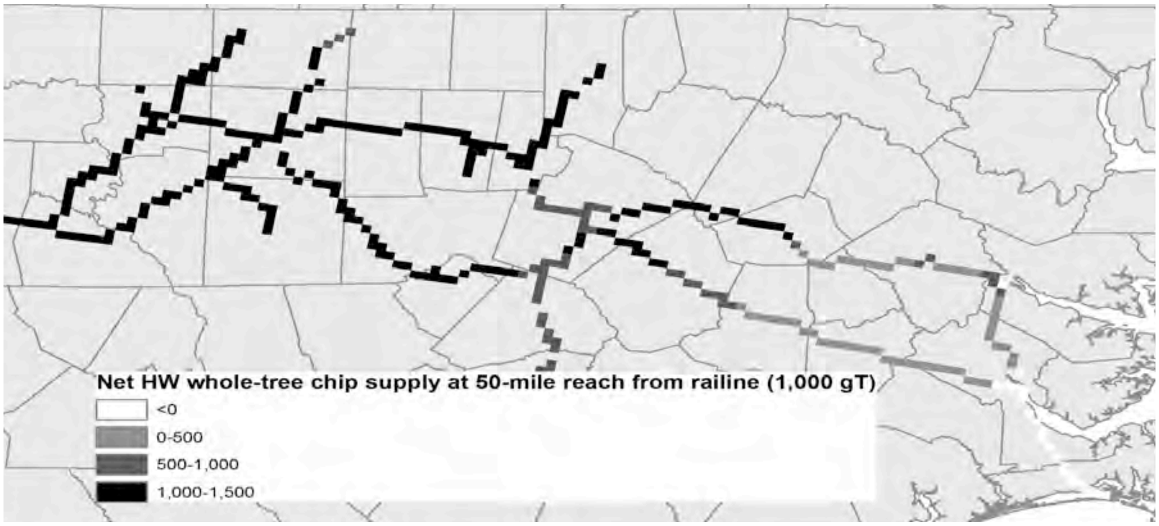

Figure 4. A modification of the statewide analysis shows net whole-tree chip supply for a 50-mile reach around selected NC rail lines, depicted in1-mi^2 raster cells. This shows poor supply near the coast as a result of reduced hardood loggingin that region.

Detailed, Site Specific Analysis

The majority our analysis occurs on regions surrounding predetermined sites. In the past 5 years, we have performed roughly 50 site analyses for clients. We have the ability to tailor any analysis as per a client's needs and continue to improve our methods and services; however, all projects include detailed resource supply-drain analysis described below. The gross supply and drain models for site specific analysis are depicted in Figure 2, using hardwood land cover

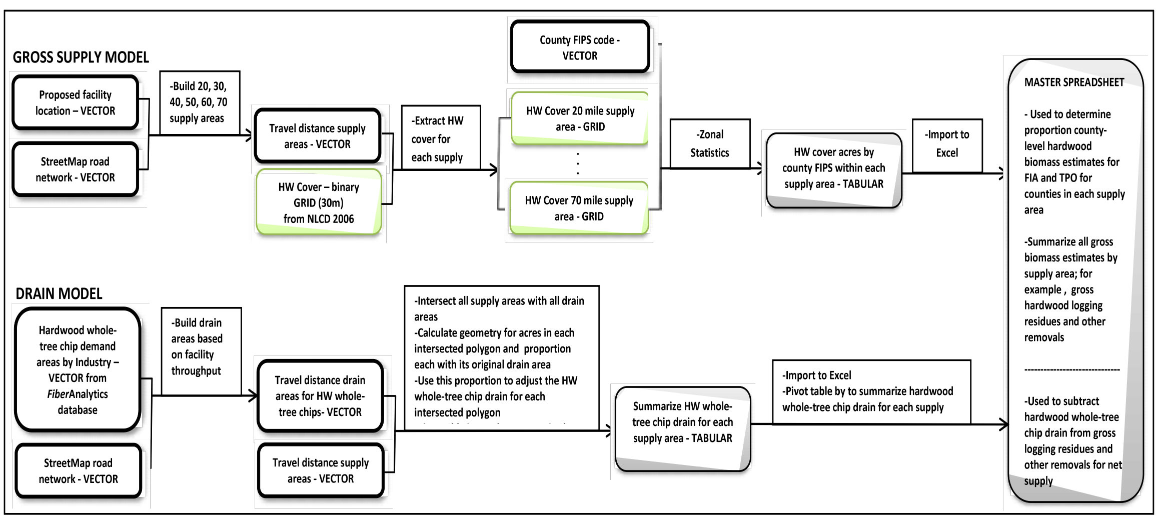

Figure 2. Flow chart for site specific biomass analysis used by NCSU *Fiber*Analytics. This flow chart example shows the steps for how the analysis for gross hardwood biomass and drain would be for a location provided by a client. Net hardwood biomass calculations are completed in the master spreadsheet. Once the acreage data is input into the spreadsheet all data listed in Table 1 are computed and summary reports and graphs are generated.

Gross supply is developed in the following steps. In a master spreadsheet for each client, FIA, TPO, and NASS data are organized by in a county using the unique FIPS number serving as the lookup key. Clients provide us location(s) they are investigating which are loaded into ArcGis 10.1 and have distance-based supply polygons constructed around them using road networks which provide a more accurate estimate of supply area based in road system response to topography[27] (Figure 5). These are built according to client specifications but we suggest a range between 20-mile to 80-mile ranges in 10-mile increments, that provides enough data points to build supply-distance curves. These supply polygons are used in extracting the four land cover types into each service area. If four service areas area required (ranging 20 to 80 miles), then sixteen land cover supply grids are produced.[28] Each resulting grid cell has its county FIPS associated to it,[29] producing tables that summarizing acres of land cover the service area has in each county. County FIPS and associated land cover acres are copied to a lookup table in master spreadsheet. For each land cover type proportions are calculated for supply area acres in the county to total county acres. This proportion is used to adjust the county-level biomass estimates for all FIA, TPO, and NASS data for each county in all supply areas which is then summarized for each supply area.

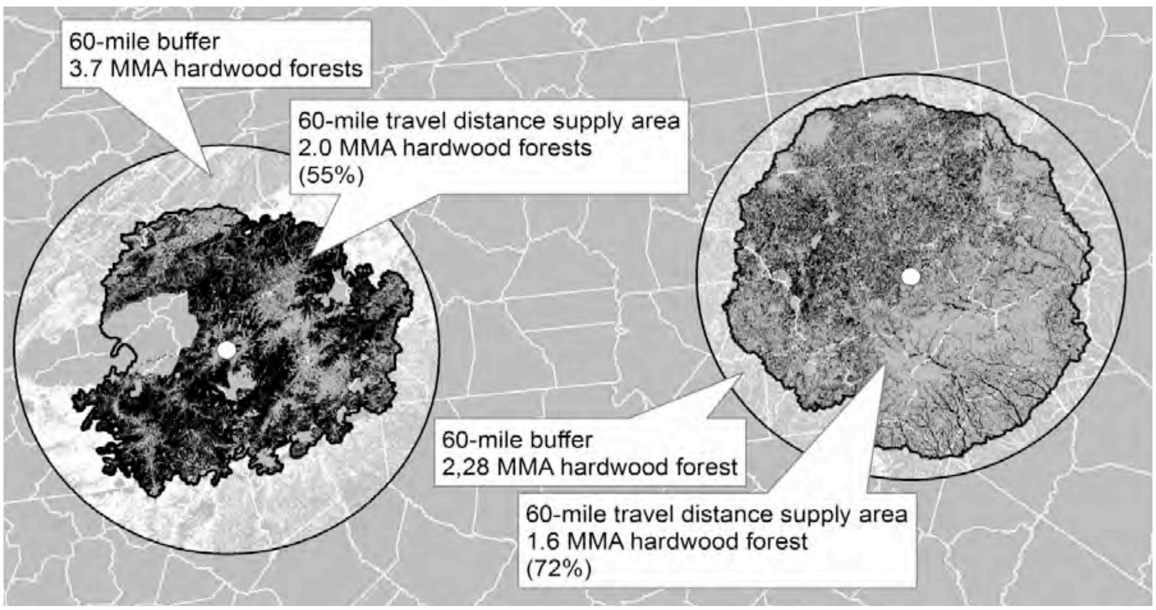

Figure 5. This illustrates the importance of generating hardwood acreage estimates using road networks compared to buffer. Hardwood forests inside 60-mile buffers are in white and hardwood forests inside 60-mile travel distances are in black. Travel distance, and thus supply area varies according to topography, thus the mountain 60-mile supply areas have only 55% of the hardwood forest land as the 60-buffer does. Piedmont road networks are better distributed, but still the 60-mile travel distance based supply area only has 72% of the hardwood forests as the 60-mile buffer.

The spatial drain model is developed from our list of pulpwood and whole-tree chips users. Drain areas are developed using road networks, the travel distance ranging from 30-miles to 100-mile

[27] Performed using the "New Service Area" tool in ArcGIS 10.1. This gives a more realistic supply area than using the Focal Statistics, which only using circles, as in the statewide, coarse resolution analysis.

[28] HW20, HW40, HW60, HW80, SW20,…,SW80, CROP20,…CROP80, PAST20,…PAST80

[29] Performed using the "Zonal Statistics as Table" using a county layer's FIPS code as the summarization attribute

depending of the facility throughput[30]. All drain polygons are then intersected[31] with the supply area polygons and the portion of each facility's drain area lying inside a service area is proportioned to the facility's total drain area. This proportion is used to estimate the amount of drain each facility contributes to each supply area. These are summed in the spreadsheet for total drain by supply area. Net supply (gross supply minus drain) is thus estimated at the supply area level. Figure 6(c) illustrates supply curves generated from the supply region landcover in Figure 6 (a) used with FIA and TPO data and *Fiber*Analytics drain model (Figure 6(c)). This is one of many outputs provided by this service.

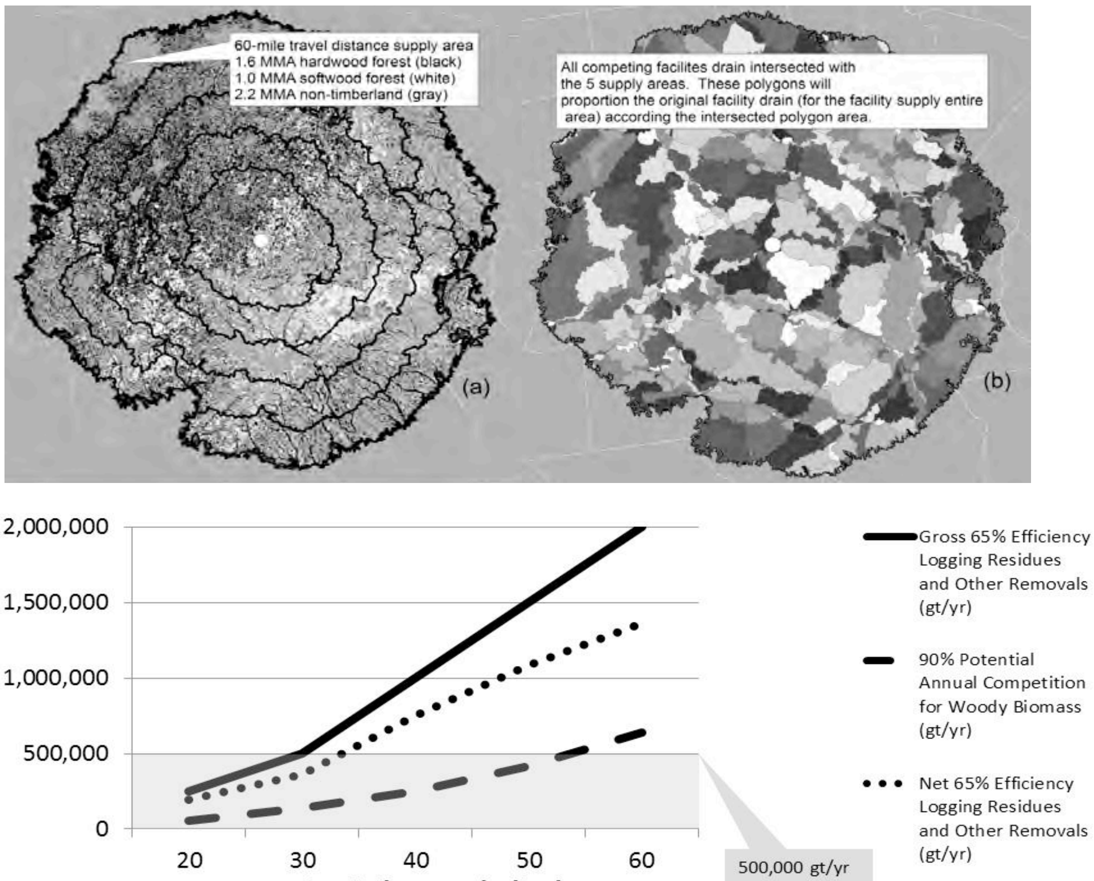

Figure 6. Site specific analysis for clients wishing for complete analysis of biomass resources for a point (center dot). Map (a) shows the spatial distribution of hardwood (black) and softwood (white) forests inside 20-mile to 60-mile travel distance supply areas. This is used in conconjuction with FIA and TPO to determine analyze a wide variety of data on whole-tree chip and pulpwood chip potential. Map (b) is a representation of the FiberAnalytic's drain model after intersection with the supply areas. This is used to derive the amount of drian within each supply region. Graph (c) is a representation of one form of supply curve generated from the analysis showing the gross volume of logging residues and other removals (all species), drain for whole-tree chips, and the net volume after drain. If a client is looking 500,000 gT/yr feedstock, this anlaysis indicates the net volume (dotted line) meets the plant needs at roughly 35 miles.

---

[30] Performed using the "New Service Area" tool in ArcGIS 10.1.

[31] Performed using the "Intersection" tool in ArcGIS 10.1

In effort to continue assisting our stakeholders, continuously provide improvements to our services. For example, we are currently developing an interactive online version of this analysis tool that should be of great value to potential clients in and around NC. Another improvement is the adjustment of forestland volumes found in streamside management zones across the state.

Successful Results

NCSU Extension Forestry FiberAnalytics has leveraged this use of woody biomass analysis in a number of successful projects. We provided data necessary for the development of the southeast's first RPS (Senate Bill 3 2007). One of our clients has two pellet plants in the final planning stages. Analysis provided for regional economic developers resulted in one operating pellet plant and one under construction.

Analysis for another regional economic developer has a major pellet plant and at least one biomass power plant under consideration. A university CHP facility now planning conversion from coal to wood. Two military installations now considering a 25 MW biomass power plant from our work and an energy company has developed several CHP projects and is planning others. These all lead to a strong green economy, job growth, and better management opportunities for landowners across NC.

4.8
COMPARISON OF THREE REMOTE SENSING METHODS TO PREDICT ABOVE GROUND PLANT BIOMASS PRODUCTION

Tucker Porter[1,], Chengci Chen[2], Rick Lawrence[3], Bok Sowell[1]*

Abstract
A quick, accurate, and non-destructive method is needed to estimate the amount of above-ground plant biomass in a pasture or across a landscape. Direct harvesting is currently the most widely used method in determining above-ground plant biomass production. This method, however, is costly, time-consuming, and destructive and only allows individual samples to be measured accurately out of a potentially highly variable sward. Remote sensing of vegetation spectral responses, which tend to be highly responsive to changes in biomass, promises to provide a means for frequent, non-destructive measurements of above-ground plant biomass at management relevant scales. The objective of this study was to compare different remote sensing techniques to determine which is the most accurate in predicting above-ground plant biomass production. Above-ground plant biomass production predicted by (1) the normalized difference vegetation index (NDVI) measurements collected by a ground-based sensor was compared with (2) NDVI and (3) band combination measurements collected by satellite-based imagery. Regression using a combination of near, middle, and thermal infrared bands explained the most variability (78%), followed by NDVI measured from Landsat images (8%), and NDVI measured from the ground-based sensor Crop Circle (3%). When data points containing large amounts of dormant, senesced and dead vegetation were removed, variability explained by Crop Circle improved 74% and Landsat images improved 23%.

Keywords: above-ground plant biomass; remote sensing; normalized difference vegetation index; bandwise regression

Introduction
Direct harvesting is currently the most widely used method in determining above-ground plant biomass production (Harmoney et al. 1997; Flynn et al. 2008). This method, however, is costly, time consuming, destructive and only allows individual samples to be measured accurately out of a potentially highly variable sward (Harmoney et al. 1997; Flynn et al. 2008). Therefore, a quick, accurate, and non-destructive method is needed to estimate the amount of above-ground plant biomass in a pasture or across a landscape (Harmoney et al. 1997).

Remote sensing of vegetation indices, such as normalized difference vegetation index (NDVI) (Rouse et al. 1973) promise to provide a means for inexpensive, frequent, and non-destructive measurements of above-ground plant biomass at management relevant scales (Weiser et al. 1986).

There are several ways to obtain NDVI measurements. Two common approaches are to use satellite-based imagery or a ground-based sensor such as Crop Circle (Holland Scientific 2012). Several factors affect the accuracy of NDVI including: (1) the presence of dormant, senescent, decaying, and dead vegetation (Todd et al. 1998), (2) leaf area index (Weiser et al. 1986), and (3) varying soil conditions and soil types (Todd et al. 1998).

---

[1] *Department of Animal and Range Sciences, Montana State University, MT*

[2] *Central Agricultural Research Center, Montana State University, MT*

[3] *Department of Land Resources and Environmental Sciences, Montana State University, MT*

** Corresponding author*

The ability of the NDVI measurement to accurately predict above-ground plant biomass is in question (Lawrence and Ripple 1998; Maynard et al. 2006). Also, research indicates NDVI is a suboptimal way to relate above-ground dry plant biomass to spectral responses and using bandwise regression (i.e., multiple linear regression with individual spectral bands as potential explanatory variables) is a better method (Lawrence and Ripple 1998; Maynard et al. 2006). Therefore the objectives of this study were to:

1. Compare the accuracy of NDVI measurements taken from the ground-based sensor Crop Circle with NDVI measurements taken from the satellite-based sensor Landsat to determine above-ground dry plant biomass production.
2. Determine the best combination of individual bands from Landsat to predict above-ground dry plant biomass production using bandwise regression and verify if the predicted biomass from the multiple linear regression model equaled actual biomass ($p \leq 0.05$).
3. Compare the regression models from (1) NDVI measurements acquired by the satellite-based sensor Landsat, (2) the ground-based sensor Crop Circle, (3) and the best combination of bands from Landsat in predicting above-ground dry plant biomass production.

Methods

The study was conducted over two growing seasons from 2011 to 2012 on 8.1 ha of Conservation Reserve Program (CRP) pastureland located at Benchland, Montana, near the Montana State University Central Agricultural Research Station (Judith Basin County, 47˚05'21.37" N 110˚00'44.47"W).

The 8.1 ha CRP pasture was divided into nine .81 ha plots. Six 1-m^2 quadrats were randomly selected in each plot. When the plants reached boot stage (May), peak growth (June/July), and dormancy (October), the 1-m^2 quadrats in each plot were scanned by the Crop Circle ACS-470 (Holland Scientific 2012) and the biomass was hand clipped to within 2.5 cm above the soil surface. This resulted in 108, 1-m^2 ground-based NDVI measurements and biomass samples for each year. All biomass samples were dried at 40.6˚ C for 72 hours. Total dry biomass production per 1-m^2 quadrat was then recorded.

Landsat images of the study area were acquired using USGS Global Visualization Viewer. The acquired Landsat images were within 14 days of the corresponding field data collection date (Maynard et al. 2006).

Pixel values for bands one through seven were extracted for all pixels covering the study area and were used to calculate predictor variables used in regression equations (Maynard et al. 2006). Satellite-based NDVI measurements were calculated from the red and near infrared band values from these pixels using the standard formula of: NDVI = (Band 4 – Band 3)/(Band 4 + Band 3) (Maynard et al. 2006).

Multiple linear regression models were used to estimate total above-ground dry plant biomass production. Each model used different independent or predictor variables: (1) NDVI measurements collected by the ground-based sensor Crop Circle, (2) NDVI measurements collected by satellite-based sensors and (3) Landsat bands. When conducting bandwise regression, forward and backward stepwise regression was used with bands one through seven from thematic mapper (TM) and enhanced thematic mapper plus (ETM+) sensors to provide guidance as to which bands might be significant in predicting above-ground dry plant biomass production (Lawrence and Ripple 1998).

To compare the best combination of bands from Landsat to predict biomass production using bandwise regression with field collected biomass samples, 90% of the samples collected were randomly selected to build the predictive model while the remaining randomly selected 10% were used to test the predictive model. A paired *t*-test was used to determine whether there was a statistically significant difference between predicted biomass and actual biomass. A *p*-value less than or equal to 0.05 suggested a statistically significant difference. To determine which remote sensing method best predicted above-ground dry plant biomass production coefficients of determination (R^2) were calculated. The method with the highest R^2 value determined which method best predicted biomass production by accounting for the greatest variability in measured biomass. All statistical analysis was completed using the statistical software R version 2.15.1 or Tibco Spotfire S+ 8.2.

Results

The variability explained by the Crop Circle NDVI linear regression model was 0.3% (Figure 1). The variability explained by the Landsat NDVI linear regression model was 8% (Figure 1). Although the Landsat NDVI linear regression model accounted for more variation than the Crop Circle NDVI linear regression model, neither model is a good predictive model. However, NDVI was intended primarily as a measure of green vegetation and is affected by dormant, senesced, decaying and dead vegetation (Todd et al. 1998). When data points collected during the 2011 dormancy harvest and 2012 peak growth harvest were removed because of large amounts of dormant, senesced and dead vegetation that occurred throughout the study area it resulted in a 74% increase in variability explained by the Crop Circle NDVI linear regression model and 23% increase in the Landsat NDVI linear regression model (Figure 1).

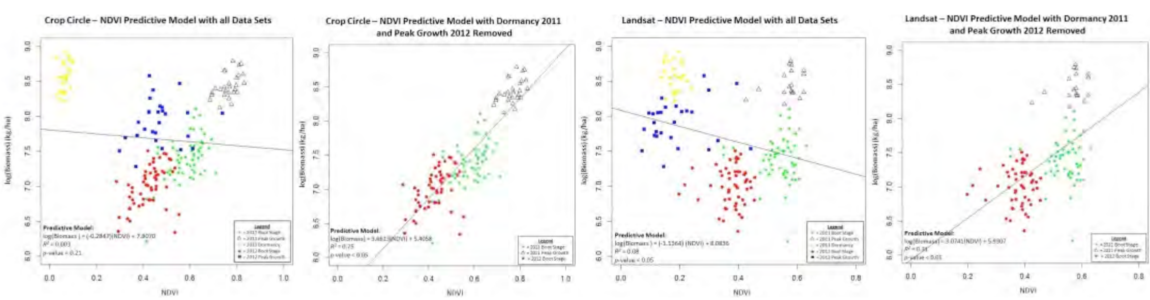

Figure 1. Linear regression models of NDVI measurements acquired by Crop Circle and Landsat satellites.

Bandwise regression determined bands four, five, and six (corresponding to near, middle and thermal infrared, respectively) to be statistically significant (all *p*-values < 0.01) (Lawrence and Ripple 1998), and each band was used in the final linear regression model (Biomass = 27.942 (Band 4) – 53.988 (Band 5) – 100.016 (Band 6) + 16,993.431, R^2 = 0.79). There was no significant difference between predicted above-ground dry plant biomass from bandwise regression and actual above-ground dry plant biomass measurements from withheld validation locations (p = 0.9958) (Figure 2).

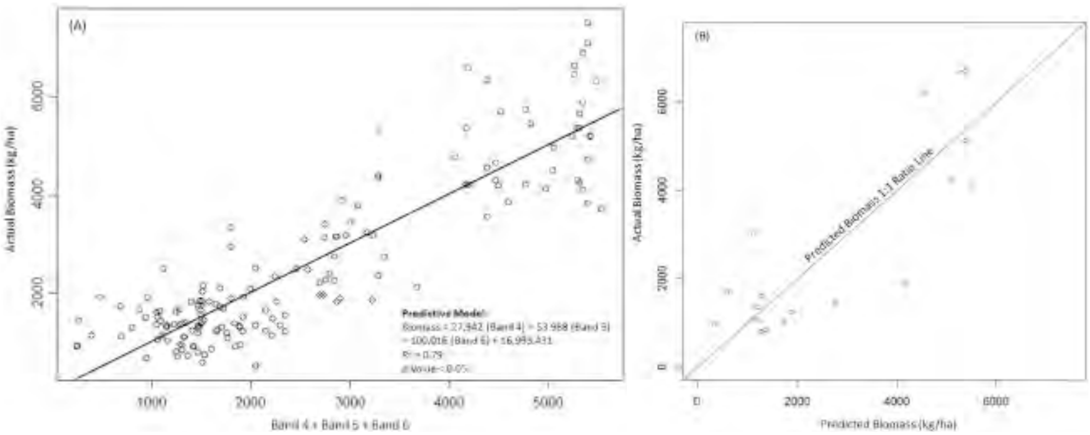

Figure 2. (A) scatter plot and regression line of biomass vs. Band 4, Band 5 and Band 6 using 90% of data samples and (B) scatter plot of actual biomass vs. predicted biomass from withheld validation locations and 1:1 ratio line.

The linear regression model determined by bandwise regression increased the variability explained by 70% over the linear regression model using NDVI measurements from Landsat images (Table 1). In addition, the bandwise regression model increased the variability explained by 75% over the linear regression model using NDVI measurements from Crop Circle (Table 1). The best combination of bands from Landsat determined by bandwise regression is the superior predictive model (Table 1).

Table 1. Linear regression models for NDVI measurements and bandwise regression.

Remote Sensing Technique	Model	Adjusted R^2	*p*-value
NDVI Collected by Crop Circle	Biomass = -1539.6 (NDVI) + 3385.0	0.03	0.01
NDVI Collected by Landsat Imagery	Biomass = -3185.1 (NDVI) + 3813.8	0.08	< 0.05
Bandwise Regression	Biomass = 26.273 (Band 4) – 53.013 (Band 5) – 98.079 (Band 6) + 16828.63	0.78	< 0.05

Discussion

When NDVI measurements were taken when dormant vegetation was present in October 2011 and senesced vegetation was present in June 2012, because of drought conditions, the index did not perform well (Figure 1). These results support previous analyses regarding the limitations of NDVI (Lawrence and Ripple 1998; Maynard et al. 2006). NDVI fails to accurately report biomass production where dry vegetation and living green vegetation coexist within a sward (Todd et al. 1998). This is because in healthy green tissue, NDVI values are higher because red light is absorbed by chlorophyll; while near infrared light is reflected by the internal structure of leaves (Knipling 1970). In the absence of chlorophyll the opposite occurs. Thus, NDVI fails to accurately correlate to biomass because the reflectance patterns of the dead vegetation are more similar to that of soil than to healthy green vegetation (Todd et al. 1998).

The superior performance of bandwise regression over NDVI also supports previous analyses (Lawrence and Ripple 1998; Maynard et al. 2006). Bandwise regression determined that near, middle, and thermal infrared bands were significant. The near infrared portion of the spectrum is sensitive to above-ground plant biomass while the middle infrared portion of the spectrum is known to be sensitive to leaf moisture content and mineral soil content (Knipling 1970; Lawrence and Ripple 1998). The study area can be characterized throughout the growing season as having a heterogeneous mixture of live plants at various stages of phenological development, dead and decaying plant material, bare soil and rocks. Therefore, the inclusion of these bands into the predictive model versus the standard red and near infrared bands, which derive NDVI, allowed bandwise regression to more accurately predict above-ground dry plant biomass production under the conditions that occurred throughout the growing season on the study area.

Based on our research and findings, we make the following conclusions.

1. NDVI is a valuable tool for predicting above-ground dry plant biomass production when measuring live, green, photosynthetically active vegetation.
2. NDVI becomes a less reliable method to predict above-ground dry plant biomass production when exposed to bare soil, rocks, dead, senesced, dormant or decayed vegetation.
3. Linear regression predictive models determined by bandwise regression using individual spectral bands is a superior method to predict above-ground dry plant biomass production over multiple growing seasons on a landscape with heterogeneous mixtures of bare soil, rocks, dead, senesced, dormant, decayed and live photosynthetically active vegetation than NDVI.

References

Flynn, S.E., C.T. Dougherty, and O. Wendroth. 2008. Assessment of pasture biomass with the normalized difference vegetation index from ground-based sensors. *Agronomy Journal* 100: 114-121.

Harmoney, K.R., K.J. Moore, J.R. George, E.C. Brummer, and J.R. Russell. 1997. Determination of pasture biomass using four indirect methods. *Agronomy Journal* 89:665-672.

Holland Scientific. 2012. Holland Scientific©. Available at: http://hollandscientific.com/. Accessed 09 August 2012.

Knipling, E. B. 1970. Physical and physiological basis for the reflectance of visible and near-infrared radiation from vegetation. *Remote Sensing of Environment* 1:155-159.

Lawrence, R.L. and W.J. Ripple. 1998. Comparisons among vegetation indices and bandwise regression in a highly disturbed, heterogeneous landscape: Mount St. Helens, Washington. *Remote Sensing of Environment* 64:91-102.

Maynard, C.L., R.L. Lawrence, G.A. Nielsen and G. Decker. 2006. Modeling vegetation amount using bandwise regression and ecological site descriptions as an alternative to vegetation indices. *GIScience & Remote Sensing* 43:1-14.

Rouse, J.W., R.H. Haas, D.W. Deering, J.A. Schell. 1973. Monitoring the vernal advancement and retrogradation (green wave effect) of natural vegetation. NASA/GSFC progress report RSC 1978-2, Greenbelt, Maryland 20771.

Todd, S.W., R.M. Hoffer, and D.G. Michunas. 1998. Biomass estimation on grazed and ungrazed rangeland using spectral indices. *International Journal of Remote Sensing* 19:427-438.

Weiser, R.L., G. Asrar, G.P. Miller, and E.T. Kanemasu. 1986. Assessing grassland biophysical characteristics from spectral measurements. *Remote Sensing of Environment* 20:141-152.

4.9

ANALYZING THE ECONOMICS OF AN ALTERNATIVE PREPROCESSING TECHNOLOGY IN THE SWITCHGRASS LOGISTICS SYSTEM FOR A BIOREFINERY IN EAST TENNESSEE

T. Edward Yu[1,], James A. Larson[1], Yuan Gao[2], Burton C. English[1]*

Abstract

It is generally believed that preprocessing biomass can reduce the transportation and storage costs of feedstock for biofuel production by condensing feedstock. However, the capital costs of preprocessing could be significant in the feedstock logistics system. Applying a spatial-oriented mixed-integer mathematical programming model, this study evaluates the economic values of an alternative preprocessing technology, stretch-wrap baling, in the biomass feedstock supply chain for a potential commercial-scale switchgrass biorefinery in East Tennessee. Preliminary results suggest that the stretch-wrap baling equipment outperforms the conventional hay harvest methods in terms of total delivered costs. Although the densification process involves additional capital and operation costs, the total delivered costs of switchgrass for a 50-million-gallon per year biorefinery in the preprocessing system is 11% − 16% lower than various logistic methods using conventional hay equipments.

Key words: biomass feedstock, cellulosic biofuel, logistic costs, preprocessing technology

Introduction

Over the past decade, the U.S. government and stakeholders have actively promoted the development of renewable energy to reduce dependence on imported fossil oils and to enhance revenues of agricultural producers. Currently, the main focus of the development of renewable energy is to produce biofuels from lignocellulosic biomass (LCB) feedstocks such as perennial crops, crop residues, and logging residues. The Renewable Fuel Standard (RFS) in the Energy Independence and Security Act of 2007 explicitly mandates the volume of biofuels produced from LCB feedstock to increase from 0.1 billion gallons per year (BGY) in 2010 to 16 BGY by 2022. However, the Environment Protection Agency has revised biofuels production targets downward from the original RFS mandate the past three consecutive years because LCB-based biofuels are currently not cost competitive to petroleum. One of the significant challenges to the economic viability of a biofuels produced from LCB is the substantial costs related to harvest, storage, and transportation of LCB feedstock because of its low density and the potential for dry matter losses during storage. Storage of certain LCB feedstocks may reduce the quantity and quality of LCB and increase the feedstock costs for the biorefinery (Mooney et al. 2012). The estimated costs of transporting, handling and storing LCB feedstock, such as corn stover or switchgrass, can make up more than 32% of total delivered costs (Hess et al. 2009).

The influences of various components in the biomass feedstock logistics system on the cost of feedstock, such as storage method, storage duration, hauling distance between the field and biorefinery, and the capacity of biorefinery have been discussed in the literature. The role of preprocessing facilities for LCB feedstock in the supply chain has gained attention recently given that increasing the density of feedstocks through preprocessing or pretreatment can improve efficiency in feedstock transportation and storage (e.g. Uslu et al. 2008, Sokhansanj and Turhollow 2004, Carolan et al. 2007, Larson et al. 2010). However, preprocessing may have a high capital cost

[1] *Department of Agricultural & Resource Economics, University of Tennessee, TN*

[2] *Strategy, Policy and Review Department, International Monetary Fund, Washington, DC*

* *Corresponding author*

that could potentially offset the cost savings in transportation and storage of delivered LCB feedstock (Yu et al. 2010).

It is apparent that a cost-effective supply chain of LCB feedstocks is crucial to accelerate the development of an economically viable LCB-based biofuels industry to meet the mandates. Therefore, the objective of this study is to evaluate the costs of LCB feedstocks delivered to a commercial-scale biorefinery for alternative feedstock logistic system configurations. Specifically, the economic value of an alternative satellite preprocessing technology in the feedstock supply chain for the biorefinery is analyzed.

Method and Data

This study evaluated the economic potential of satellite preprocessing facilities within a supply chain by minimizing the costs for two potential feedstock supply scenarios. The baseline scenario includes two conventional hay logistics systems for LCB feedstock. LCB feedstocks were assumed to be harvested using either large round or large rectangular balers, stored at the edge of the field with or without tarp, and delivered to the biorefinery as needed throughout the year. The second feedstock supply scenario assumed that LCB was preprocessed using an industrial stretch-wrap baler to condense and wrap feedstock with protective plastic before storage and delivery to the biorefinery. This preprocessing technology was originally developed in Europe for processing garbage and is introduced in the U.S. for agricultural products. The technology can create a 1.5-dry ton condensed and shrink-wrapped bale of switchgrass with about the same dimensions as a conventional large round bale. In the preprocessing scenario, the feedstock was assumed to be harvested by a chopper with rotary header, directly delivered to the preprocessing facility, baled in a more condensed form, wrapped by plastic for protection, stored on the site and delivered to the biorefinery throughout the year.

The value of preprocessing was evaluated by comparing the feedstock logistics costs of the baseline with the optimal case in preprocessing scenario. If the preprocessing system had a lower plant-gate cost than the baseline, then the preprocessing system can potentially enhance the profit of the commercial-scale biorefinery. The optimal location and number of preprocessing facilities will be determined in the analysis. However, if the model does not indicate a lower plant-gate cost for the preprocessing system, the benefit of additional feedstock densification process may be limited. The analysis was applied to a potential switchgrass biorefinery in East Tennessee as a case study. There are total 13 counties included in the study area given their geographical connection with the pilot-scale cellulosic ethanol plant currently operated in Monroe County, Tennessee. Those counties were divided into five square-mile land resource units based on a remote sense data, excluding federal lands.

The analytical engine of this study is a mixed-integer mathematical programming model, Bio-Energy Siting and Technology Assessment (BESTA), incorporating the spatial data generated from a high-resolution GIS model, BioFLAME (Wilson 2009). The integration of the mathematical programming mechanism and GIS data is designed to identify the feedstock harvest area and optimal location of the biorefinery and satellite preprocessing facilities for switchgrass based on the size of biorefinery, throughput of the preprocessing facilities, and the availability of biomass feedstock. The detailed road and rail networks, suitable industrial parks form placement of preprocessing and biorefinery facilities, and other geo-spatial layers were incorporated from the GIS model. The shortest path from every potential land resource unit providing switchgrass along the road network determined and used to generate a least-cost transportation layer. In addition, dry matter loss for storage periods of up to 365 days was modeled for the conventional hay systems following Mooney et al (2012). The parameters for calculating the ownership and operating costs of the equipments used for harvest, storage, preprocess and transportation in both baseline and preprocessing systems can be found in Table III in Larson et al. (2010).

Results

Figure 1 summarizes the preliminary results of baseline and preprocessing scenarios. Two options in the baseline system, large round bale with tarp and pallet protection (RoundTP) and large rectangular bale with tarp and pallet (RectangularTP), were included in the baseline scenario. For a 50-mgy biorefinery, the round bale system has higher delivered costs ($48.8 million or $74 per dry ton), when compared to the rectangular system ($46.3 million or $70 per dry ton). Despite higher production being needed for rectangular bales when compared to round bales to compensate for higher dry matter losses during storage, the economy of harvesting and transportation for rectangular bales make this option more cost effective comparing to round bales.

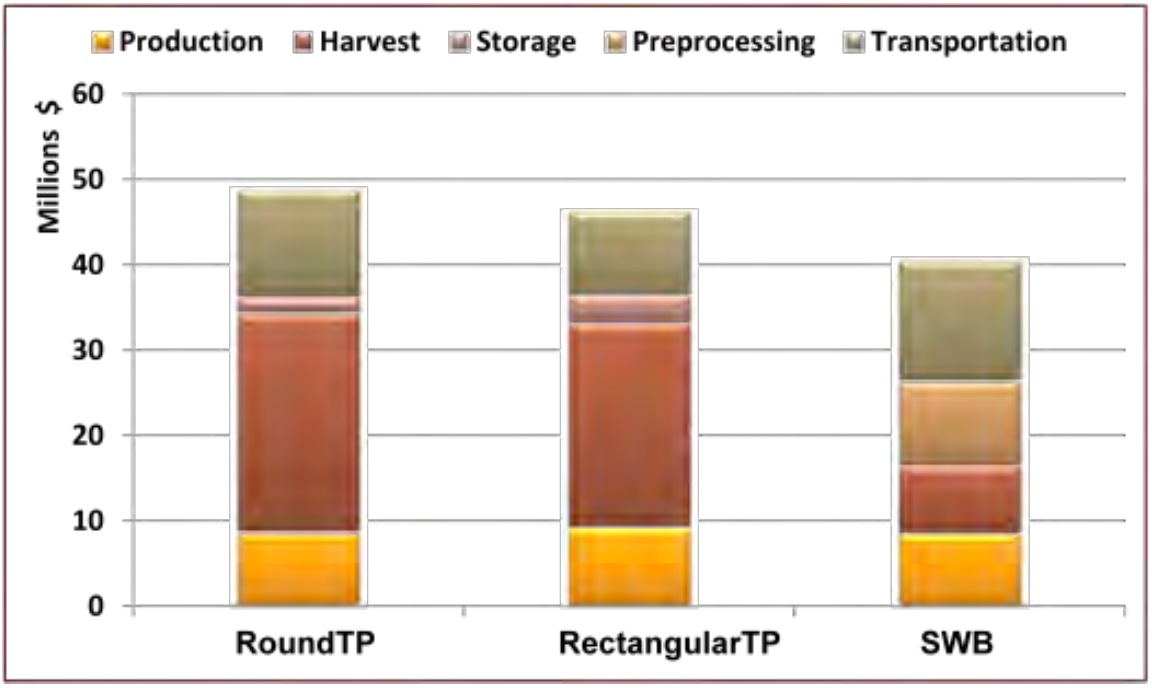

Figure 1. Switchgrass Delivered Cost under Various Harvest and Storage Options

The total delivered cost of the baled/wrapped switchgrass under preprocessing system is $40.5 million or $62 per dry ton. The preprocessing cost ($9.9 million) accounts for about one-quarter of total delivered costs. The transportation cost, including the shipping cost of the chopped switchgrass directly delivered from the field to biorefinery, the cost of chopped switchgrass from the field to preprocessing facilities, and the cost from preprocessing facilities to biorefinery in condensed-wrapped bales, totaled $14.1 million. Applying the single-pass procedure, the harvest cost for about 658,000 tons of chopped switchgrass per year was about $8.0 million.

The delivered cost of switchgrass for a 50-mgy capacity biorefinery in the preprocessing system was about 11% and 16% lower than the protected rectangular bale and protected round bale, respectively, in the baseline scenario. Preprocessing had cost advantages in transportation; however, the total transportation cost of harvested switchgrass including three components (field −biorefinery, field−preprocessing, and preprocessing−biorefinery) in the preprocessing system was still higher than both cases in the baseline scenario. The cost comparison of those cases; however, does not explicitly consider potential differences among management and the associated costs and risks for those cases.

Figure 2 illustrates the feedstock area and the optimal location of preprocessing facilities in the study area. The biorefinery was located in Monroe County, about 20 miles west of the pilot plant in Vonore, Tennessee. Preprocessing facilities were primarily located along with Interstate 75, while the feedstock draw area covered total 10 out of 13 counties. Given the throughput of the stretch-wrap baler, seven units of the preprocessing facility were needed to meet the feedstock demand of biorefinery. Nearly all units of preprocessing facilities operated at full capacity (63,000 tons).

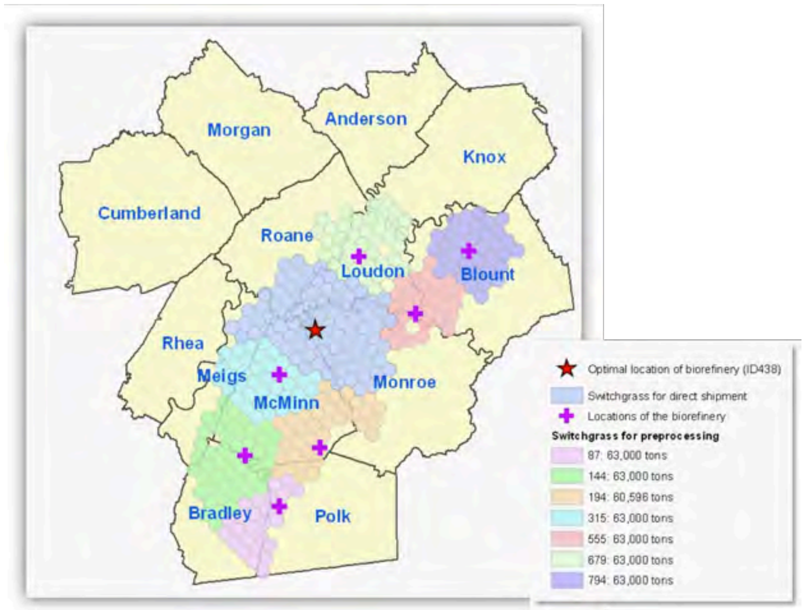

Figure 2. Location of biorefinery, preprocessing facilities and feedstock draw area in the preprocessing system

Conclusions

This study analyzes the economic values of adopting an alternative preprocessing technology in the LCB feedstock supply chain for a potential commercial-scale biorefinery. Despite the capital investment and operation costs, the evaluated preprocessing system still presents advantage over the conventional hay system in terms of the total delivered costs. Comparing two cases under the baseline system with the evaluated preprocessing system, the stretch-wrap baling system improves the switchgrass logistics costs by 11% − 16% under east Tennessee production condition. The advantage of the preprocessing system in the LCB feedstock logistic system may be more significant when the size of biorefinery capacity increases. Additional cost saving is potentially achieved when more switchgrass is harvested and condensed.

Further research should continue to evaluate the dry matter losses or feedstock quality of those condensed-wrapped bales generated from the preprocessing system during storage. Also, exploring various options in harvest, storage, preprocessing and transportation in the LCB feedstock logistic system is necessary for enhancing the profitability of the industry. Particularly, exploring the economic values of combing various pretreatment and preprocessing procedures to generate a more densified feedstock with constant quality will assist the development of a sustainable feedstock supply chain to this emerging industry.

References

Carolan, J.E., S.V. Joshi, and B.E. Dale. 2007. “Technical and Financial Feasibility Analysis of Distributed Bioprocessing Using Regional Biomass Pre-Processing Centers.” *Journal of Agricultural & Food Industrial Organization* 5:1–29.

Hess, J. R., C.T. Wright, K.L. Kenney, and E.M. Searcy. 2009. “Uniform-Format Bioenergy Feedstock Supply System Design Report Series: Commodity-Scale Production of an Infrastructure-Compatible Bulk Solid From Herbaceous Lignocellulosic Biomass”, *Volume A: ‘Uniform-Format’ Vision and Conventional-Bale Supply System*, Table 2.2, NL/EXT-09-17527DRAFT, Idaho National Laboratory.

Larson, J.A., T. Yu, B.C. English, D.F. Mooney, and C. Wang. 2010. “Cost Evaluation of Alternative Switchgrass Producing, Harvesting, Storing, and Transporting Systems and their Logistics in the Southeastern US.” *Agricultural Finance Review* 70:184-200.

Mooney, D.F., J.A. Larson, B.C. English, and D.D. Tyler. 2012. Effect of Dry Matter Loss on Profitability of Outdoor Storage of Switchgrass. *Biomass & Bioenergy* 44:33-41.

Sokhansanj, S., and A.F. Turhollow. 2004. “Biomass Densification – Cubing Operations and Costs for Corn Stover.” *Applied Engineering in Agriculture*, 20: 495-99.

Uslu, A., A. Faaij, and P. Bergman. 2008. “Pre-treatment Technologies and Their Effects on the International Bioenergy Supply Chain Logistics, Techno-economic Evaluation of Torrefaction, Fast Pyrolysis and Pelletisation.” *Energy* 33:1206-1223.

Wilson, B. S. 2009. *Modeling Cellulosic Ethanol Plant Location Using GIS*. M.S. Thesis., The University of Tennessee, Knoxville.

Yu, T., B.C. English, J.A. Larson, and S. Cho. 2011. *Evaluating the Economics of Incorporating Preprocessing Facilities in the Biomass Supply Logistics with an Application in East Tennessee*. Southeastern Sun Grant Center, University of Tennessee, Knoxville, TN.

4.10
PREDICTING BIOMASS YIELD IN BIOENERGY CROP PRODUCTION SYSTEMS USING CANOPY NDVI

A.J. Foster[1], V.G. Kakani[1,], J.Ge[2] J.Mosali[3]*

Abstract
Remote sensing technology has been successful in monitoring crop N status and estimating crop yield in numerous traditional cropping systems. However, there is limited information on the use of remote sensing technology in bioenergy crop production systems. Therefore, the objective of the study was to determine the relationships between biomass yield and canopy height and canopy NDVI under different cropping systems. Variable canopy height was generated by supplying N at different rates (winter legume (hairy vetch (*Vicia villosa* Roth)), 0, 84,168, and 252 kg N ha^{-1}) in two field studies at Stillwater and Woodward, Oklahoma. Fields were planted with switchgrass 'Alamo' (*Panicum virgatum* L.) and mixed grasses (Indian grass (*Sorghastrum nutans)*, big bluestem (*Andropogon gerardii)* and Switchgrass) in a split plot design. Canopy heights, canopy NDVI, LAI and biomass were measured at bi-weekly intervals during the season on an individual plot basis. Regression analysis was done across locations, cropping systems and N treatments. Strong linear relationships were observed between NDVI and LAI (r^2 =0.76) and NDVI and canopy height (r^2 =0.64). However, canopy height alone (r^2 =0.68) was a good predictor of plot biomass yield. The index of NDVI x canopy height (r^2=0.60) did not improve the prediction for biomass yield achieved using height alone, but did for NDVI alone (r^2=0.41). These results suggest that there is great potential for the use of remote sensing in predicting the biomass yield in bioenergy crop production systems.

Keywords: biomass yield; switchgrass; nitrogen fertilizer; Normalize Difference Vegetation Index

Introduction
The goal of the United State is to use biomass to supply 5% of the nation's power, 20% of the transportation fuels, and 25% of its chemicals by 2030 (Perlack et al., 2005). To achieve this goal an annual supply of 907 MMg (1 billion dry tons) of biomass is required and about one-third of this biomass is projected to come from perennial crops such as switchgrass (Sanderson et al., 2006). To meet this demand, projected bio-refineries will require substantially large amount of biomass on a yearly basis (Schmer et al., 2010). Therefore, an accurate estimate feedstock biomass before harvesting will be important to these bio-refineries in developing their operational plan.

Measurement of harvestable biomass in perennial grass production systems has always been a challenge to producers. The most accurate method of measuring harvestable biomass in a grassland system requires clipping of samples, which is laborious and time consuming (Ward et al., 2011; Schmer et al., 2010; Starks and Brown, 2010; Sanderson et al., 1996). It is our perspective that the intense labor and time requirements of this method are a major limitation for producers using this method. A method that is less tedious would be welcomed by most producers. There have been numerous non-destructive approaches investigated for estimating harvestable biomass; however, most are operator dependent, labor intensive, costly, or require calibration for different species (Hanna et al., 1999; Harmoney et al., 1997). In order to

[1] Department of Plant and Soil Sciences, Oklahoma State University, OK

[2] Department of Geography, Oklahoma State University, OK

[3] The Samuel Roberts Noble Foundation, Inc., OK

* Corresponding author

plan the year round operation of bio-refineries effectively, efficient and reliable methods are needed to estimates harvestable biomass in perennial grass systems. Profitability of cellulosic refineries will be dependent on the ability to maintain a reliable supply of feedstock (Schmer et al., 2010).

Bioenergy crops such as switchgrass can grow to over a meter tall. The height of these grassland systems limit the potential methods for estimating the harvestable biomass prior to harvest. Traditionally, harvestable biomass is estimated from regression predictive models developed from establishing mathematical relationships between non-destructive sampling measurements, such as sward height, leaf area index and biomass. Schmer et al. (2010) pointed out that switchgrass is grown for bioenergy will be harvested mechanically. Therefore, estimating the harvestable biomass is more important than estimating the total above ground biomass. Furthermore, recently Schmer, et al. (2010) in an on farm switchgrass study demonstrate the use of the modified Robel pole approach to develop prediction equation for estimating switchgrass harvestable biomass. The prediction model developed from the study showed that elongated leaf height, visual obstruction, and canopy height measurements accounted for greater than 80% of the variation in switchgrass biomass. Harmony et al. (1997) compared the ability of a modified Robel pole, rising plate meter, canopy height stick and Li- Cor LAI 2000 canopy analyzer to determine forage availability in a diverse pasture systems. The prediction models developed showed that the use of the Robel pole (r^2 =0.63), canopy height (r^2=0.60), and rising plate (r^2=0.59) to have the strongest linear relationship with the clipped biomass samples. Strong relationship was also observed between plant height and forage biomass in a few studies. Plant height alone (r^2=0.81) was found to be highly correlated independently of the area the plant occupied with forage biomass in corn plants at growth stage ranging between V8-V10 grown in Oklahoma (Freeman et al., 2007). Ground based remote sensing devices that measure forage reflectance characteristics have been suggested as alternatives or to be used in combination to improve the predictive ability of models developed from these methods.

Spectral reflectance in the red and near infrared (NIR) regions of the spectrum has been shown to be directly related to above ground forage biomass. Mathematical combination of red and NIR spectral waveband measured as vegetative indices take advantage of the plant reflectance in both region of the spectrum(Lusch, 1999). Indices such as NIR: red ratio and normalized difference vegetation index (NDVI) take advantage of reflectance in both NIR and red region reducing measurement variability due to soil type, sunlight intensity and angle of sunlight incidence (Lusch, 1999). NDVI has been reported to be correlated with biomass when the leaf area index (LAI) is less than 3 (Flynn et al., 2008; Serrano et al., 2000; Weiser et al., 1986). However, NDVI alone showed very weak relationship with biomass in corn and mixed tallgrass prairie, but improved in combination with canopy or plant height (Freeman et al., 2007; Olson and Cochran, 1998). The new development of an active, on the go, ground based sensor, the GreenSeeker (Ukiah, CA) for collecting reflectance data and calculating NDVI offers great opportunity for determining harvestable biomass. The sensor can be used day or night without being influenced by current light condition as it emits and record its own light and reflectance. The use of the GreenSeeker sensor for measuring reflectance offers a non-destructive and minimally labor intensive method of sampling herbage biomass. Development of accurate, generalizable models for predicting harvestable biomass in perennial grass bioenergy production systems from reflectance is warranted. Therefore, the objective of the study was to determine the relationships between plant height and canopy NDVI with harvestable biomass yield from perennial grass systems grown for bioenergy.

Materials and Methods

To investigate our objective, field plots were established at two sites during the 2010 growing season, to evaluate the effect of fertilizer N on switchgrass and mix grass yield. The mix grass plots were seeded with composition of 50, 25 and 25 % of switchgrass, Indian grass and big blue stem, respectively. Stand appraisal using visual observation was done in April in Stillwater and May in Woodward. Five different N treatments were applied to plots arranged in a split plot randomized design with three replications to enable varying yield potential. In the split plot design, species was the main plot and fertilizer treatment was the subplot. The characteristics of both sites were different (Table 1). Plant heights, canopy NDVI, leaf area index were measured throughout the growing season on an individual plot basis. Canopy height measurement was taken by vertically placing a canopy height stick, marked in 5-cm increments at level with the soil surface and using the elongated vertical height of uppermost leaf or canopy height which is the height of the flag leaf taken at the flag leaf collar. Three canopy height measurements were taken per plot. Leaf area index readings were taken about the center point of the plots with the Li-Cor LAI 2000 leaf canopy analyzer. Average LAI was determined by the leaf canopy analyzer through measuring the light attenuation difference between the three above canopy and nine below canopy readings. The differences in light attenuation resulted from either the absorption or reflection of incident light by the vegetation. Using the attenuation values obtained, a standard attenuation coefficient was used automatically within the instrument to derive an output resulting in LAI value (Harmoney et al., 1997). Canopy NDVI readings were recorded using a GreenSeeker NDVI hand unit from an area of about 3 to 4 m^2 holding sensor approximately 0.6-1.0 m above the canopy and walking the same speed in each plot. The GreenSeeker Hand Held optical reflectance sensor uses active radiation from red (650 ± 10 nm) and near infrared (770 ± 15 nm) band independent of solar radiations (Freeman et al.,2007). The device uses built-in software to calculate NDVI directly. The NDVI is computed according to the formula.

$$\mathrm{NDVI} = \frac{\rho_{NIR} - \rho_{Red}}{\rho_{NIR} + \rho_{Red}}$$

Where ρ_{NIR} is the fraction of reflected NIR radiation, and ρ_{Red} is the fraction of reflected red radiation. Relationships among biomass yield, plant height, canopy NDVI, and LAI were examined using simple linear regression models.

Table 1. Characteristics of the experimental plots used in this study.

	Plot 1 (Stillwater)	Plot 2 (Woodward)
Location	36.130° N 97.104°W	36.426° N 99.414°W
Soil Type	Easpur loam	Carey silt loam
Annual precipitation, mm (2011)	409.45	335.03
Annual air temperature, °C (2011)	-28.53/43.63 (Min/Max)	-19.35/44.05 (Min/Max)
Plot Size	9 m x 9 m	7.6 m x 9 m

Results and Discussion

There was a strong linear relationship across locations and nitrogen treatments between canopy height and biomass yield for data collected throughout the growing season (June to August). Figure 1 shows a moderately strong relationship between canopy height and biomass (r^2 =0.68). The linear equation Y= 296 + 91*(Height) was found to be a good predictor of biomass yield. Earlier studies by Harmony et al., (1997) and Schmer et al., (2010) also found canopy height alone to be a good predictor of biomass yield in switchgrass. This is important because it indicates that height alone can be used to estimate biomass yield. However, the labor and time required to obtain enough samples to make reliable prediction may deter producers. Remote sensing approach using NDVI alone (Fig.2) accounted for little variability (r^2 = 0.41) in biomass systems across both locations, while the index NDVI x height (Fig.3) did not improve the variability (r^2 = 0.60) achieved using height alone. Likewise, Freeman et al. (2007) in a six year study also found the index NDVI x height to be a good predictor of plant biomass in corn and height alone to be a more accurate predictor. However, in this study a moderately strong relationship was also observed between NDVI and canopy height with r^2 = 0.64 (Fig.4) and a strong relationship between NDVI and LAI with r^2 = 0.76 (Fig.5). This suggests that the measurement of canopy NDVI could be used to predict the canopy height for estimating the biomass yield. Therefore, while NDVI was not a strong predictor of biomass yield it was a good predictor of canopy height. This result indicates that NDVI could be used in model development for biomass yield prediction in perennial grass systems for bioenergy production.

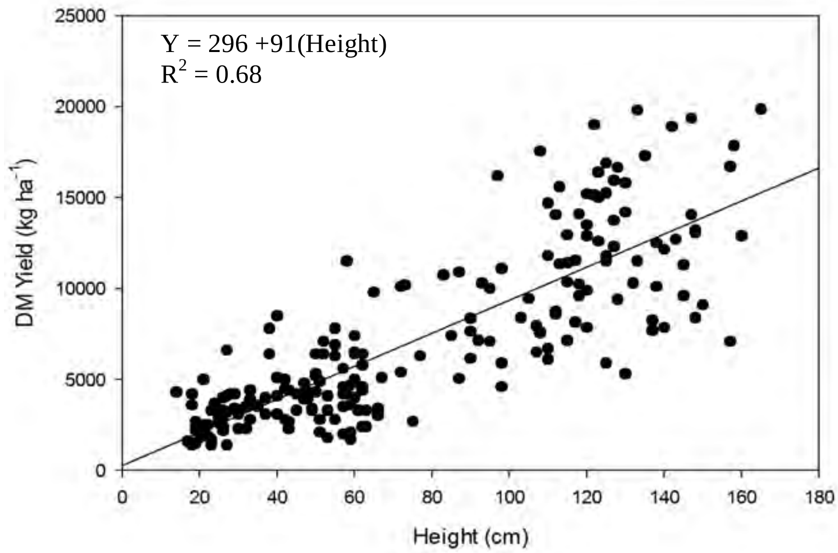

Fig.1. Relationship between canopy height and dry matter yield for switchgrass and mix grass (Indian, Big Bluestem and Switchgrass) biomass production systems at different nitrogen rate across two locations (Woodward and Stillwater) in Oklahoma.

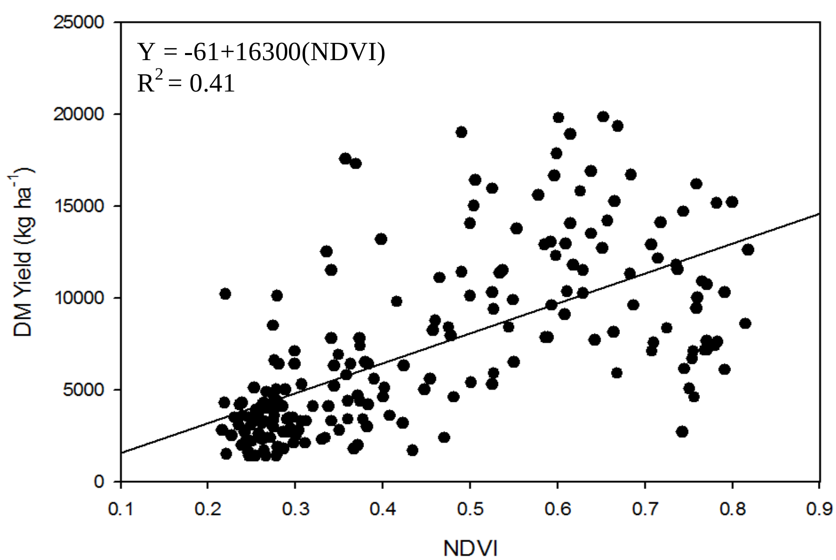

Fig. 2. Relationship between NDVI and dry matter yield for switchgrass and mix grass (Indian, Big Bluestem and Switchgrass) biomass production systems at different nitrogen rate across two locations (Woodward and Stillwater) in Oklahoma.

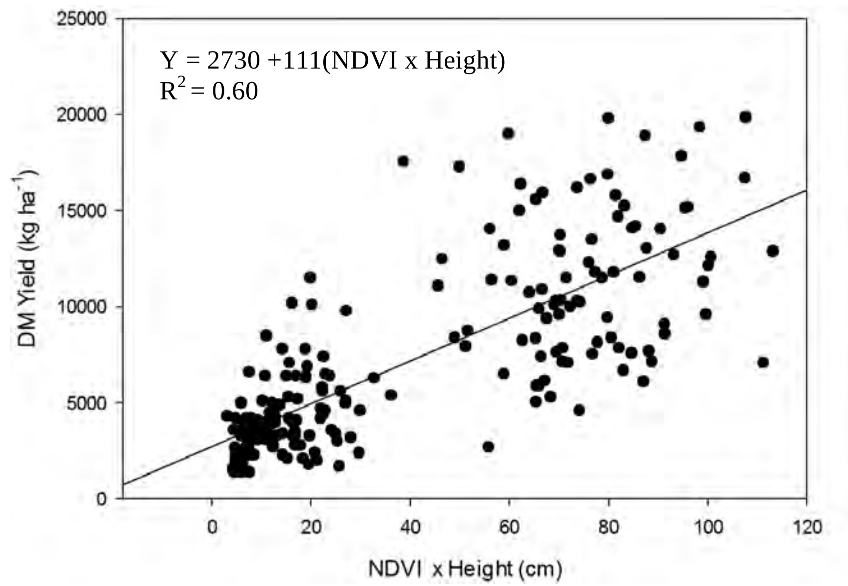

Fig. 3. Relationship between NDVI x height and dry matter yield for switchgrass and mix grass (Indian, Big Bluestem and Switchgrass) biomass production systems at different nitrogen rate across two locations (Woodward and Stillwater) in Oklahoma.

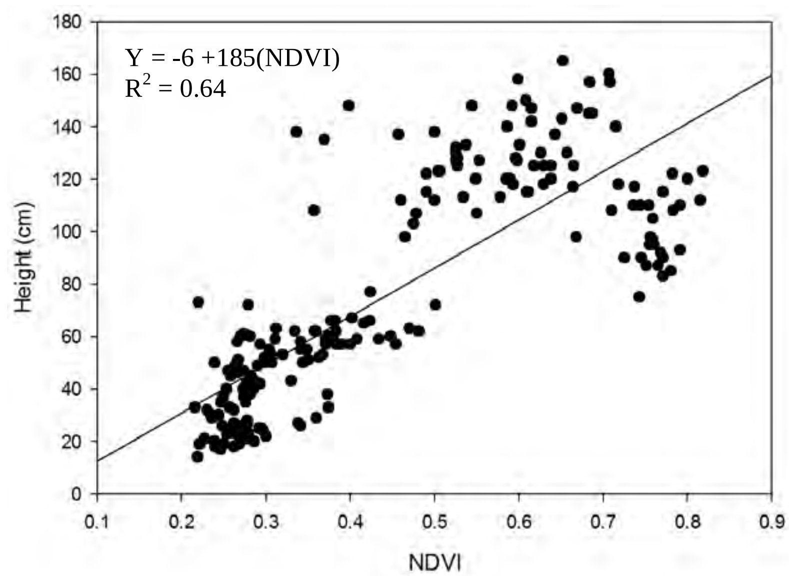

Fig.4. Relationship between NDVI and height for switchgrass and mix grass (Indian, Big Bluestem and Switchgrass) biomass production systems at different nitrogen rate across two locations (Woodward and Stillwater) in Oklahoma.

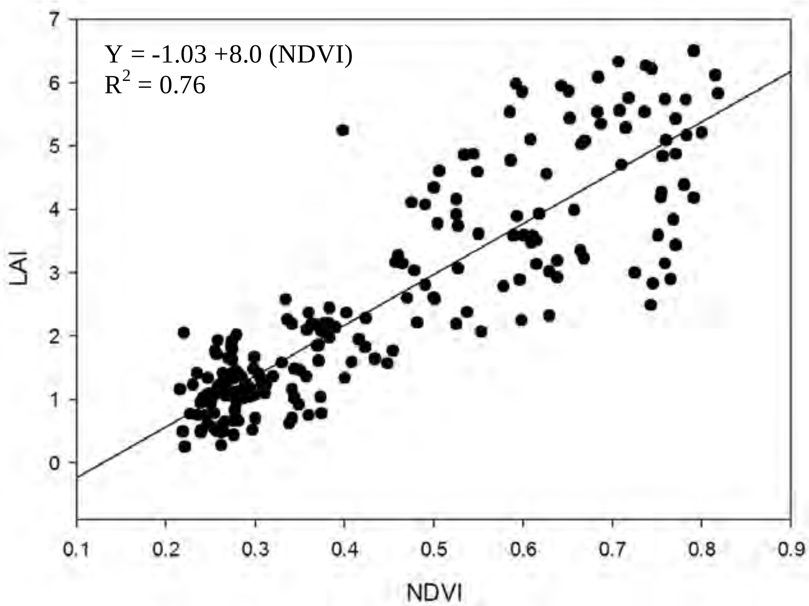

Fig.5. Relationship between NDVI and LAI for switchgrass and mix grass (Indian, Big Bluestem and Switchgrass) biomass production systems at different nitrogen rate across two locations (Woodward and Stillwater) in Oklahoma.

Conclusions

Canopy height was found to be a good predictor of both biomass and NDVI of canopy height across locations, nitrogen treatments, and cropping systems. Clearly, these results suggest that canopy height is an important variable in yield prediction of switchgrass. Therefore, the use of remote sensing approach may offer some potential in the estimation of canopy height that could be used to developed algorithms for estimating biomass yield.

References

Flynn E.S., C.T. Dougherty, O. Wendroth. 2008. Assessment of Pasture Biomass with the Normalized Difference Vegetation Index from Active Ground-Based Sensors. Agron. J. 100:114-121. DOI: 10.2134/agrojnl2006.0363.

Freeman K.W., K.L. Martin, R.K. Teal, W.R. Raun, K. Girma, D.B. Arnall, R.W. Mullen. 2007. By-Plant Prediction of Corn Forage Biomass and Nitrogen Uptake at Various Growth Stages Using Remote Sensing and Plant Height [Electronic Resource]. Agronomy Journal 99:530-536. DOI: http://dx.doi.org/10.2134/agronj2006.0135.

Hanna M.M., D.A. Steyn-Ross, M. Steyn-Ross. 1999. Estimating Biomass for New Zealand Pasture Using Optical Remote Sensing Techniques. Geocarto International 14:89-94. DOI: 10.1080/10106049908542121.

Harmoney K.R., E.C. Brummer, J.R. Russell, K.J. Moore, J.R. George. 1997. Determination of Pasture Biomass Using Four Indirect Methods. Agronomy Journal 89:665-672.

Lusch D.P. 1999. Introduction to Environmental Remote Sensing Center for Remote Sensing and GIS Michigan State University

Olson K.C., R.C. Cochran. 1998. Radiometry for Predicting Tallgrass Prairie Biomass Using Regression and Neural Models. Journal of Range Management 51:186-192.

Perlack R.D. L.W., A.F. Turhollow, R.L. Graham, B.J. Stokes, and D.C. Erbach. 2005. Biomass as a Feedstock for a Bioenergy and Bioproducts Industry: The Technical Feasibility of a Billion-Ton Annual Supply, A joint study sponsored by the US Department of Energy and the US Department of Agriculture [online] Available: http//: http://www1.eere.energy.gov/biomass/pdfs/final_billionton_vision_report2.pdf [2010 Jul.18].

Sanderson M.A., F. Agblevor, M. Collins, D.K. Johnson. 1996. Compositional Analysis of Biomass Feedstocks by near Infrared Reflectance Spectroscopy. Biomass & Bioenergy 11:365-370.

Sanderson M.A., P.R. Adler, A.A. Boateng, M.D. Casler, G. Sarath. 2006. Switchgrass as a Biofuels Feedstock in the USA. Canadian Journal of Plant Science 86:1315-1325.

Schmer M.R., W.H. Schacht, D.B. Marx, R.B. Mitchell, K.P. Vogel. 2010. Efficient Methods of Estimating Switchgrass Biomass Supplies BioEnergy research 3:243-250.

Serrano L., I. Filella, J. Penuelas. 2000. Remote Sensing of Biomass and Yield of Winter Wheat under Different Nitrogen Supplies. Crop Science 40:723-731.

Starks P.J., M.A. Brown. 2010. Prediction of Forage Quality from Remotely Sensed Data: Comparison of Cultivar-Specific and Cultivar-Independent Equations Using Three Methods of Calibration. Crop Sci. 50:2159-2170. DOI: 10.2135/cropsci2009.08.0455.

Ward A., A.L. Nielsen, H. Møller. 2011. Rapid Assessment of Mineral Concentration in Meadow Grasses by near Infrared Reflectance Spectroscopy. Sensors 11:4830-4839.

Weiser R.L., G. Asrar, G.P. Miller, E.T. Kanemasu. 1986. Assessing Grassland Biophysical Characteristics from Spectral Measurements. Remote Sensing of Environment 20:141-152. DOI: 10.1016/0034-4257(86)90019-2.

5 CASE STUDIES

5.1
PRODUCTION SYSTEM OF SUGAR CANE IN SÃO PAULO STATE – BRAZIL: A CONCEPTUAL MODEL

Bruno Oliveira Cardoso[1,], Katia Regina Evaristo de Jesus[2]*

Abstract

The production of sugar cane in Brazil started only 25 years after its discovery in 1500 and is currently one of the main agricultural crops of the country. The sugar cane stands for one of the oldest cultures in Brazil, presently, the cultivation of sugar cane is the third largest planted area in Brazil, mainly because it represents an alternative and renewable source of energy. The most prominent producing region is the South-Central-Southeast with more than 85% of production and the largest national producer is the State of São Paulo with approximately 60% of this production. The production system of sugar cane is complex: the production plants depend on sugarcane growers and capital goods. The products alcohol, sugar and energy are distributed to fuel and electricity distributors, food industry, wholesale and retail, trading and exporting. The environmental and social equity concerns have been strengthened in recent years, especially due to market globalization. As a result of the society awareness that has emerged from the new global posture, the need arises for adjustment of agricultural activities or agro-industrial processes for the entire production system to generate positive impact for the environment and society. This article aims to show the information raised and organized about the of system production sugarcane in the São Paulo State and from that create a proposal of conceptual model of this system. This model will be validated by experts of Sugar Cane Sustainability Area. This work can be the basis for future sustainability assessment of the production of sugar cane.

Keywords: Sugar cane, sustainability agricultural, sustainability assessment, conceptual model

Introduction

Currently, the world is searching for alternative energy less polluting sources to replace fossil fuels, which are a major source of carbon dioxide emissions and it is one of those responsible for climate change today. Thereby, there is great pressure from society and Government to be held in agroenergy production more sustainable bases so less impactful on the environment and society.

Many initiatives for the production of alternative biofuels are being conducted in several countries with different biomasses, but mostly are still used as raw products that are also part of the human diet, causing great impact on food prices. The Brazil has been using sugar cane as main source of sugar to produce ethanol, employed as an alternative to the fuel in cars.

Brazil is in a great position, because it has extensive arable areas, favourable climate and technological knowledge about the production process, and is currently the second largest producer of ethanol, and the world's largest producer of sugar cane.

---

[1] *Embrapa Environment (Brazilian Agricultural Research Corporation), Jaguariúna, SP. Brazil*

[2] *Embrapa Environment, Jaguariúna, SP. Brazil*

* *Corresponding Author*

However, with the increase in demand, it comes a need to expand and improve the production process of sugar cane and to think actions that encourage development is needed information, mechanisms and standards that guided the decision-making processes.
This paper proposes a conceptual model of two main production systems of sugar cane in the State of São Paulo and with potential to support the assessment of sustainability of agroenergetic systems in this State.

Scenario of Sugar Cane in São Paulo

In 2009, according to data of Brazilian Institute of Geography and Statistics (IBGE), the State of São Paulo occupied an area of 4.9 million hectares of sugar cane which represents approximately 51% of the total (IBGE, 2010). Currently in São Paulo, sugarcane is produced by independent producers and by processing plants in partnership, land lease or own land (OLIVEIRA, NACHILUK & TORQUATO, 2010).

The suppliers of sugar cane in Brazil's Center South are organized into 29 associations regionally distributed in the States of São Paulo, Minas Gerais, Goiás and Mato Grosso, represented by the Organization of Cane Planters Sugar Center South (ORPLANA). In the State of São Paulo, which represent 97% of the associated (ORPLANA, 2010). Suppliers are organized into 26 associations in seven regions: Araçatuba, Araraquara, Catanduva, Jaú, Piracicaba, Ribeirão Preto, and Vale do Paranapanema.

The stratification of cane suppliers leads to the conclusion that 89% produce up to 10.000 ton of cane, in areas up to 150 ha and it was responsible for 35% of production, while only 11% of suppliers delivered at 65% to the processing plants (OLIVEIRA, NACHILUK & TORQUATO, 2010).

Neves et al. (2010) says that the agro-industrial system of sugar cane has, by historical feature, tendency to be a vertical system, where the industrial group is the owner of the land, plantation, and the entire machinery etc, so control all the production system.

Neves et al. (2010) says, that there has been a reversal of this trend. The cane from suppliers always fluctuated between 30-40% of total participation and that from the crop of 2000/2001 much of production growth occurred based on suppliers. UNICA database show that, the sugar cane suppliers, in São Paulo, grew 156%, from 40 million ton to 90 million ton. This shows that this aspect of the production system is very important for the analysis of the current production process.

Production System Definition

Production systems consist in the application of a group of interrelated knowledge to obtain a certain product. It is a broad concept on production systems defined by GASTAL (1975) that, in terms of the productive process, apply to various forms of production, since the individual production to those involving the use of an instrumental and more complicated and diverse. In this sense, a system of agricultural production can be described in many ways, depending on the purpose of study.

CAMPOS (1977) says that the agricultural production systems, by their very nature, are quite complex, because it is possible to include a large number of living elements that interact with each other and with the environment, and also because they respond to the influence of socioeconomic factors.

According to MELLO et al. (1978), is regarded as the set of agricultural techniques, practices or management performed in a culture, more or less evenly, by significant groups of producers.

To NEVES et al. (1984), "from an agronomic point of view, a given production system can be seen as a set of agriculture activities and its operations, which reflect a given level of technology”.

ALVES et al. (1978) says that farmers use in conducting their crops a set of practices that sets the technological level of their holdings and this set of recommended practices for each level of technology is the production system.

Building the Conceptual Model

The conceptual model to be presented is the result of a critical analysis of the results of documentary and bibliographic research specializing in issues of sugar cane, productive system, agricultural activity and other issues related, drawing on primary and secondary sources, print or available over the internet. In addition, many of knowledge placed in the model were acquired in workshops, conferences and seminars, as well as meetings with specialist of the production system of sugar cane.

MELLO et al. (1978) considers that the conduct of a culture involves several "activities", each activity involves several "operations", each operation can be performed by various "practices". In every operation of the productive cycle is selected a specific practice, sets of these practices that characterized the conduct of culture since the activity of soil preparation to harvesting, constitute a "technique". The distinction between "activity" and "operation" is of less importance, however, it is essential that the distinction between "practice" and "technique", the latter used as synonymous with the production system.

Based on the system settings and in the knowledge acquired by reading and other activities, was elaborated the conceptual model (table 1) of two Productive Systems of sugar cane. The criteria for the construction was to define what are the main farming techniques used in the sector and from them to separate the two most representative groups of the production system.

Table 1. Conceptual Model of the Productive System of sugar cane in São Paulo.

<table>
<tr><td></td><td>Productive System I</td><td colspan="3">Productive System II</td></tr>
<tr><td>Type of Producer</td><td>Supplier</td><td colspan="3">Processing Plant</td></tr>
<tr><td>Land</td><td>Owner</td><td>Leased</td><td>Partnership</td><td>Owner</td></tr>
<tr><td>Size of Land</td><td>Small (until 150 ha)</td><td colspan="3">Medium and Lager (over 150 ha)</td></tr>
<tr><td>Representation on the State of São Paulo</td><td>89%</td><td colspan="3">11%</td></tr>
<tr><td>Soil preparation</td><td>Rudimentary way and with low technology. Is not the correct preparation of the plots.</td><td colspan="3">Planting fields properly sized for mechanized harvesting.</td></tr>
<tr><td>Soil conservation</td><td>Non-existent or without technical knowledge. There is little soil analysis..</td><td colspan="3">Very well planned and performed frequently. Analyses are performed.</td></tr>
<tr><td>Sugar cane Seedling</td><td>Produced by the producers themselves, without concern for the quality and variety. The times, cooperatives Act to publicize the importance of plant nurseries, plant health and the use of improved varieties. When used varieties, are not the most suitable.</td><td colspan="3">Structure of plant nurseries or acquired in nurseries of good quality. Use of improved varieties is intense and with new varieties. Use of "pellets".</td></tr>
<tr><td>Planting</td><td>Manual</td><td colspan="3">Manual / mechanic</td></tr>
<tr><td>Agricultural Tracts</td><td>Liming and fertilization are performed with some guidance of cooperatives</td><td colspan="3">There is no infrastructure for application of vinasse. Pest permitted substances. Some with biological control.</td></tr>
<tr><td>Use of Fire</td><td>Allowed and common.</td><td colspan="3">Little / use in areas where it is still permitted.</td></tr>
<tr><td>Mechanization</td><td>When is performed by Plant or through rural condos.</td><td colspan="3">Good infrastructure of tractors and agricultural implements. Precision agriculture in its majority. Use of telemetry or similar technology in field activities.</td></tr>
<tr><td>Harvest</td><td>Manual and mechanized sometimes.</td><td colspan="3">Mechanized.</td></tr>
<tr><td>Transport</td><td>Provided by the plant, always to the nearest.</td><td colspan="3">Provided by the plant, always to the nearest.</td></tr>
<tr><td>Rotation of crops</td><td>Little or non-existent</td><td colspan="3">Made with soy, peanut, always in the area reform. Sorghum between two harvest.</td></tr>
<tr><td>Legislação Ambiental</td><td>Low suitability</td><td colspan="3">Producers subscribers of "agro-environmental Protocol." Respect for environmental legislation.</td></tr>
<tr><td>Worker labor</td><td>Familiar and contracted (informally) during periods of higher demand. There is no improvement. There is no control of the use of PPE.</td><td colspan="3">Length of labor legislation. Improvements are made, mainly due to mechanization. Producers subscribers of "Social Protocol-renewal"</td></tr>
<tr><td>Technological Contribution</td><td>Little or non-exixtent</td><td colspan="3">Medium or high</td></tr>
<tr><td>Cost management</td><td>Rudimentary / non-existent</td><td colspan="3">Agricultural economic management with a history and held plot by plot</td></tr>
</table>

This model served as a basis for the survey of indicators of power ranges, which will be used in the evaluation methodology will be developed. To do this, the model will be evaluated by experts in the field in question.

Some authors adopt the technological level as differentiator of systems, but as OLIVEIRA et al. (2010) says thay was not very pronounced differences among the highlighted regions, however, the relationship of the suppliers and the plant is what differentiates the way of producing sugar cane. In regions where there is a greater number of small producers, it was recorded more manual operations performed by plants, demonstrating that for small properties the mechanization is infeasible. That is, from the point of view of the producer of the size of the area does not justify the acquisition of Harvester, likewise the plant sees no advantage in spending to perform mechanical harvesting (OLIVEIRA, NACHILUK & TORQUATO, 2010).

Results and Discussion

Conceptual Model of Production System of Sugar Cane

Based on that Nair says, formerly the productive system of sugar cane was dominated by the owners of agribusinesses, but this situation has changed. Therefore, searched in the model to highlight and differentiate well these two participants of the production system.

This point of view, allows you to observe the two contrasting sides of the production system of sugarcane and thus assist better decision making and evaluation of the productive process.

In addition, the first column represents the main activities used in the production process of sugar cane and the lines show the techniques used by different systems found in São Paulo.

References Cited

Alves, Hélio A. et al. Coffee production systems in sul de Minas: a new methodological approach. Journal of Rural Economics, Brasilia, 16 (4): 105-26, Oct./dez. 1978

Brazilian Institute of Geography and Statistics (IBGE). Aggregated database. Available at: <http://www.sidra.ibge.gov.br/bda/tabela/protabl.asp?c=1618&z=t&o=1&i=P>. Access in: 28 Aug. 2012

Campos, Miguel P. Introducion. In: TECHNICAL ADVISORY COUNCIL ROUNDTABLE, 22, 1977. Agricultural system _ produccion. Santo Domingo, UCA, 1977. p. 5-9.

Gastal, Edmundo. Production system of agricultural research programming. Brasília, EMBRAPA, 1975

Mello, Nilda T. Cardoso; Cézar, Sérgio A. G.; Arruda, Silvia T.; Mascarenhas, Marli Dias; Proposed new methodology of cost of production of the Instituto de Economia Agrícola. São Paulo, Secretaria da Agricultura, IEA, 1978. 13 p. (research report, 14/88)

Neves, Evaristo. M. & Azevedo, A. J. B. V. Agricultural production systems. Changes in government policies and their effect on cost estimates. The soil, Piracicaba, 76 (1): 3138, Jan. 1984/jun..

Oliveira, Marli Dias Mascarenhas; Nachiluk, Katia; Torquato, Sergio. Alves Production systems and arrays of technical coefficients of culture of sugarcane in São Paulo State Economic Information, São Paulo, v. 40, no. 6, p. 68-91, June 2010.

ORGANIZATION OF CANE PLANTERS OF THE CENTER-SOUTH REGION OF BRAZIL-ORPLANA. Available at: <http://www.orplana.com.br>. Access in: Aug. 2012.

5.2
FEEDSTOCK COSTS AND TRANSPORTATION EMISSIONS AND THEIR IMPACT ON THE SITE SELECTION OF A SWITCHGRASS-BASED BIOREFINERY: A CASE STUDY OF TENNESSEE

T. Edward Yu[3,], Joshua S. Fu[4], James A. Larson[1], Burton C. English[1]*

Abstract
This study evaluates the potential sites of switchgrass-based biorefineries in Tennessee by examining the plant-gate cost and truck emissions of delivering feedstock to biofuel production. Applying a spatial-oriented mixed-integer mathematical programming model using GIS data, we first estimate feedstock cost and identify the location of a single-feedstock biorefinery with the least cost in three different regions of the state, i.e. east, middle and west Tennessee. Given the feedstock draw area and the road links for hauling feedstock to the biorefinery in each region, US Environment Protection Agency's Mobile Vehicle Emission Simulator (MOVES) model is used to estimate the emissions generated from hauling feedstock in the study region. Results show that feedstock costs and transportation emissions are affected by the degree of feedstock draw area dispersion and topography of the draw area around the biorefinery site. Based on feedstock costs and transportation emissions, the biorefinery is suggested to be located in Bedford County in middle Tennessee. In addition, when the capacity of biorefinery is expanded, the enlarged feedstock draw area creates higher vehicle travel miles, resulting in more transportation costs and hauling emissions of feedstock. This implies that the improved production efficiency of the larger facility (i.e. economies of scale) needs to make up for the additional transportation cost.

Keywords: switchgrass, feedstock transportation, truck emissions, cost minimization, site selection

Introduction
Developing a commercialized cellulosic biofuels sector generated from dedicated energy crops, crop residues, and forest residues has become an important energy program in many states of the U.S. over the past few years. The Tennessee Biofuels Initiative (TBI) is a state sponsored program committing $70 million in 2007 to develop a bioenergy sector using lignocellulosic biomass (LCB) feedstocks in Tennessee. Given the progress of conversion technologies for cellulosic biofuel production and feedstock development under TBI, the potential of establishing a commercial-scale biomass-based energy sector in Tennessee in the near future has been discussed (Brass 2011).

In order to expedite the commercialization of the LCB biofuel industry, several technical hurdles still need to be overcome. Currently, the high cost of the feedstock supply system, including production, harvest, storage and transportation, has been recognized as one major barrier to make large-scale production of cellulosic biofuel (Larson et al. 2010). The amount of LCB feedstocks needed to supply a commercial-scale biorefinery will be significant as LCB feedstocks generally have low density. Also, most of the potential lands for LCB feedstock production in Tennessee are currently idled or are used for less transportation-intensive traditional crop activities. Converting those lands to LCB feedstock production implies increased traffic on roadways that link the fields and the biorefinery, which will generate additional vehicle emissions from hauling feedstock to the biorefinery. As road transport is considered one of the main sources of air pollution, the environmental impacts of increased traffic induced by LCB feedstock shipments

[3] *Department of Agricultural & Resource Economics, University of Tennessee, TN*

[4] *Department of Civil and Environmental Engineering, University of Tennessee, TN*

* *Corresponding author*

have receiving increasing attention in recent literature (e.g. Kumar et al. 2006, Jäppinen et al. 2011).

Given the potential for developing a cellulosic biofuel industry in Tennessee, the objective of this study is to explore the potential site for the biorefinery through examination of plant-gate costs and hauling emissions of feedstock from the field to the biorefinery in different regions in Tennessee. Switchgrass is a native perennial grass that can fit the humid subtropical climate of Tennessee and the U.S. southeast, and has high yields on marginal soils commonly found in many areas of the region (Wright, 2007). In addition, standard hay equipment used in the region can be applied to the harvest of switchgrass (Mooney et al. 2012). Therefore, this study evaluates switchgrass as the feedstock for biofuel production in Tennessee.

Methods and Data

To meet the study objective, we first apply a spatially-oriented, mixed-integer mathematical programming model, the Bio-Energy Site and Technology Assessment (BESTA) model, to identify the feedstock draw area and location of commercial-scale biorefineries in three Grand Divisions in Tennessee (eastern, middle, and western) by minimizing feedstock plant-gate costs. Each region, excluding the federal land, is disaggregated into a vector of database of contiguous 5 square-mile crop zones to represent potential feedstock supply areas. The cost-minimization also identifies the most efficient road links within the feedstock draw area to the biorefinery based on the real road network for each region. A complete description of the BESTA model is available in Gao (2011). Based on the output of feedstock flows on the road networks in BESTA, existing traffic emissions in the study area and the additional emissions produced from feedstock transportation are estimated using the U.S. Environmental Protection Agency's Mobile Vehicle Emission Simulator (MOVES) model (USEPA 2010).

The biorefinery considered in this study is a single-feedstock conversion facility. Two potential capacities of biorefinery, 50 million gallons per year (MGY) and 75 MGY, are evaluated to compare the feedstock plant-gate costs. Plant-gate costs are estimated for large square bale harvest, storage, and transportation systems commonly used for the harvest and storage of hay and can also be used for switchgrass in Tennessee. The potential feedstock supply area assumed in the analysis includes Tennessee and a buffer area within 50 miles adjoining the state border. The potential location for the biorefineries is assumed to be limited to feasible industrial parks with access to water, power, and roads, as well as sufficient storage space in each region. Feedstock supply system cost data are obtained from Larson et al. (2010) and Gao (2011). GIS data are from the BioFLAME model (Wilson 2009).

Results

Table 1 presents the total plant-gate cost of feedstock for the optimal site of the biorefinery of 50-MGY and 75-MGY in each region and associated feedstock hauling emissions. The optimal sites of the 50-MGY biorefineries in east, middle and west Tennessee are located in McMinn County, Bedford County and Lawrence County, respectively. When the capacity increased by 50%, the optimal location of the biorefinery in east and west Tennessee changed to Greene County and Obion County, respectively, while Bedford County is still the optimal choice for the 75-MGY biorefinery. As expected, the number of counties supplying feedstock (i.e. the feedstock draw area) for the 75-MGY biorefinery is much larger than the counties for the 50-MGY biorefinery. The average slope of the roads in east Tennessee is higher than the road slope in the west region due to the Appalachian Mountains, which potentially affected feedstock transportation emissions by region. The cost presented in Table 1 reflects the most efficient storage method for the large square bales of switchgrass by setting switchgrass on woody pallets with a tarp (Mooney et al. 2012).

Table 1. Total Plant-gate Costs and Hauling Emissions of Switchgrass to Biorefinery Using the Large Square Bale Harvest and Logistic System in Tennessee

	50-MGY				75-MGY		
	East	Middle	West		East	Middle	West
Biorefinery location	McMinn	Bedford	Weakley		Greene	Bedford	Obion
Number of supply counties	13	10	16		15	13	21
Average road slope (%)	3.48	2.28	1.78		4.31	2.08	1.56
Total feedstock cost (million $)	$46.3	$45.9	$47.7		$71.1	$69.9	$72.9
Production	$9.2	$9.2	$9.3		$14.2	$13.8	$13.9
Harvest	$23.9	$23.9	$24.0		$36.5	$35.9	$36.1
Storage	$3.3	$3.3	$3.3		$5.0	$5.0	$5.0
Transportation	$9.9	$9.5	$11.1		$15.4	$15.2	$17.9
Hauling distance & emissions							
VMT (1,000 miles)	1,846	1,540	2,445		3,039	2,888	4,194
CO_2 (tons)	5,003	4,180	6,351		8,939	7,794	10,496
NO_x (tons)	45.8	38.2	57.3		81.0	71.3	95.6
PM_{10} (tons)	2.8	2.4	3.5		5.1	4.4	5.6
$PM_{2.5}$ (tons)	2.5	2.1	3.1		4.6	3.9	5.0

Feedstock cost and Transportation Emissions for the 50-MGY Biorefinery

For a 50-MGY biorefinery, the total cost for supplying about 658,000 tons of large square bales of switchgrass per year is similar among the least-cost sites in the three regions, ranging between $45.9 million and $47.7 million (or $69-$72 per dry ton). The least cost site of biorefinery is found in middle Tennessee. When decomposing the total cost by operation, harvesting is found to make up a majority of the total cost (>50%), followed by transportation costs and production cost. Transportation cost for the site in middle Tennessee is lower than the other two regions because the feedstock draw area in the middle Tennessee region is relatively compact (10 counties) than that in the east and west Tennessee (13+ counties).

The total feedstock draw area is influenced by the yield of switchgrass in each crop zone and the availability of the cheaper traditional crops or grasses. As the opportunity cost of converting hay land to switchgrass production is the least among all crops in Tennessee, the available hay land in each crop zone determines the density of switchgrass produced in that spatial unit. Also, the yield of switchgrass in a crop zone also affects the harvests of switchgrass. Hence, the density of switchgrass production in some crop zones in the middle Tennessee is higher than other crop zones given more available hay area and better yield. Agricultural lands in west Tennessee are primarily used for grains, oilseeds, and cotton, thus the opportunity costs of converting those high value crops for switchgrass production are too high.

Switchgrass hauling to the optimal site in west Tennessee generated more the most vehicle miles traveled (VMT), whereas the VMT associated with feedstock hauling to the biorefinery site in middle Tennessee is the least (about 1.5 million miles) because of the differences in feedstock supply draw area. Given that the least amount of miles traveled by the trucks and the flattest gradient of road networks in middle Tennessee, the biorefinery in Bedford County generated the least traffic emissions when comparing to the optimal sites in the other two regions.

Feedstock cost and Transportation Emissions for the 75-MGY Biorefinery

When biorefinery capacity is expanded by 50% to 75 million gallons of biofuels per year, the total feedstock plant-gate costs for supplying nearly 987,000 tons of switchgrass increase to \$69.9–\$72.9 million (\$71–\$74 per dry ton). Again, the biorefinery using large square bales of switchgrass in middle Tennessee has the lowest plant-gate cost. Compared to the cost associated with the 50-MGY biorefinery, all components except for transportation cost increases by about 50%. The transportation cost increases more substantially (54%–61%) since the draw area of feedstock extends considerably to meet the feedstock demand. It is expected that the transportation cost will rapidly rise when the capacity of the biorefinery expands further, which implies that the economies of scale for the larger biorefinery has to counterbalance the increase in transportation cost or the biorefinery would need to adopt alternative feedstock supply systems to lower the transportation cost.

Given by the much larger feedstock draw area in west Tennessee (21 counties), the VMT for hauling switchgrass to the biorefinery in Obion County in west Tennessee is the highest (nearly 4.2 million miles). The miles traveled for hauling switchgrass to the biorefinery in east and middle Tennessee are similar (3.0 vs. 2.9 million miles). However, the average road grade in related counties in middle Tennessee is lower than road grades in east Tennessee, making the hauling emissions to the biorefinery in the Bedford County to be less than one in the east region.

Conclusions

Our analysis suggests that the feedstock cost and transportation emissions are affected by degree of feedstock draw area dispersion and topography of draw area around the biorefinery site. Although the differences in the plant-gate cost of switchgrass among all three regions are small, the emissions produced from delivering feedstock to the biorefinery in the middle region are clearly lower than that for the other two regions. Thus, the biorefinery using switchgrass as feedstock located in middle Tennessee (Bedford County) is found to be the most sustainable with the least economic costs and hauling emissions of feedstock.

References

Brass, J. 2011. "East Tennessee Farmers' First Switchgrass; Harvest Ready to Turn Into Biofuel." Checkbiotech.http://bioenergy.checkbiotech.org/news/east_tenn_farmers_first_switchgrass_harvest_ready_turn_biofuel (accessed on March 9, 2011).

Gao, Y. 2011. Evaluation of Pre-processing and Storage Options in Biomass Supply Logistics: A Case Study in East Tennessee. M.S. Thesis, The University of Tennessee, Knoxville.

Jäppinen, E., O.J. Korpinen, and T. Ranta. 2011. Effects of Local Biomass Availability and Road Network Properties on the Greenhouse Gas Emissions of Biomass Supply Chain. *ISRN Renewable Energy* 2011: 6.

Kumar, A., S. Sokhansanj, and P.C. Flynn. 2006. Development of a Multicriteria Assessment Model for Ranking Biomass Feedstock Collection and Transportation Systems. *Applied Biochemistry and Biotechnology* 129:71–87.

Larson, J.A., T. Yu, B.C. English, D.F. Mooney, and C. Wang. 2010. Cost Evaluation of Alternative Switchgrass Producing, Harvesting, Storing, and Transporting Systems and their Logistics in the Southeastern US. *Agricultural Finance Review* 70:184-200.

Mooney, D.F., J.A. Larson, B.C. English, and D.D. Tyler. 2012. Effect of Dry Matter Loss on Profitability of Outdoor Storage of Switchgrass. *Biomass & Bioenergy* 44:33-41.

U.S. Environmental Protection Agency. 2010. Motor Vehicle Emission Simulator. http://www.epa.gov/otaq/models/moves/index.htm. (accessed on June 02, 2011).

Wilson, B. S. 2009. Modeling Cellulosic Ethanol Plant Location Using GIS. M.S. Thesis., The University of Tennessee, Knoxville.

Wright, L. 2007. *Historical Perspective on How and Why Switchgrass was Selected as a "Model" High-Potential Energy Crop*. ORNL: Oak Ridge, TN. http://info.ornl.gov/sites/publications/files/Pub7047.pdf.

5.3 FEEDSTOCK OPPORTUNITIES IN THE NORTH CENTRAL REGION FOR DROP IN FUELS

Kevin D. Kephart[1,], Robert J. Nelson[2]*

Abstract

The bio-fuels industry is well established in the North Central region of the United States. Corn-based (*Zea mays* L.) ethanol production has evolved since the late 1970s and biodiesel production has been underway since the mid-1990s. Companies in this region will expand or launch new facilities for commercial cellulosic ethanol production. Land-grant universities in the region have helped establish these new industries through technological developments, research on feedstocks, testing of co-products, work force development, and public education. The North Central region exhibits a range of crop productivities, including marginal lands with climates suitable for production of oilseed crops. Using existing technologies, vegetable oils, animal fats, and food wastes can be converted into green diesel and jet fuels with high energy density, very low oxygen content, and winter performance equivalent to petroleum counterparts. Development of oilseed crops that are optimized for energy or industrial uses will benefit the agricultural community by having more cropping system options to maintain or improve soil quality, while also providing disease and pest control. The region currently produces oilseed crops that are used in feed and industrial applications. Intensifying research focus on oilseed crops will significantly benefit future renewable fuel yields produced on marginal lands. The purpose of this presentation is to identify feedstocks that can be deployed in the Northern Great Plains region.

Keywords: Oilseed feedstocks, drop-in fuels

Introduction

The current renewable bio-fuels industry is well established in the North Central region of the United States. Corn-based (*Zea mays* L.) ethanol production has evolved since the late 1970s and biodiesel production has been underway since the mid-1990s. Land-grant universities in the region have helped establish these new industries through technological developments, feedstock research, testing of co-products, work force development, and public education.

The North Central region exhibits a range of cropping conditions, including marginal lands with climates suitable for production of oilseed crops. Vegetable oils can be converted into diesel and jet fuels that have high energy density, contain no oxygen, and improved winter performance relative to biodiesel. Development of oilseed crops that are optimized for energy or industrial uses will provide more cropping system options to maintain or improve soil quality while also providing disease and pest control. The North Central Sun Grant region currently produces oilseed crops that are used in feed and industrial applications. Intensifying research focus on oilseed crops will significantly benefit future renewable fuel yields produced on marginal lands.

This paper identifies crops that can be developed for feedstock production in the Northern Great Plains region and concludes that oilseed crops and the existing corn-ethanol industry in the North Central region can produce much of the Navy's expected needs. Additionally, the North Central region has the production capacity to serve future energy needs for the commercial aviation industry.

[1] South Dakota State University, SD

[2] Private consultant, SD

* Corresponding author

Oilseed Feedstock Production

There are several species that producers are already familiar with and the region has experienced periodic increases and decreases in acreages committed to oilseed production based on market fluctuations and introduction of new agricultural production technologies. The most prevalent species under cultivation or of interest include camelina (*Camelina spp.*), flaxseed (*Linum usitatissimum* L.), sunflower (*Helianthus annuus* L.), safflower (*Carthamus tinctorius* L.), crambe (*Crambe spp.*), rapeseeds (*Brassica spp*.), and canola (*Brassica napu*s L. and *B. rapa* L.). This region could respond rapidly if market demands for oilseed production were to increase. Eastern Montana, North Dakota and South Dakota have significant acreages committed to oilseeds. The species differ in yield potential and in their potentials for oil production (Table 1 and Table 2)

Table 1: Harvested acres in 2007 for oilseed crops in South Dakota (SD), North Dakota (ND), and Montana (MT) [1].

ACRES HARVESTED Species	SD	ND	MT
Camelina			20,400
Crambe		7,481	4,839
Flaxseed	6,837	315,807	20,236
Canola	242	1,067,764	7,872
Other Rapeseed			14,200
Sunflower	380,313	894,159	3,410
Safflower	9,641	39,531	37,188

[1] USDA National Agricultural Statistics Service 2007.

Distillers Oil from Ethanol Production

Corn oil is currently being extracted post-fermentation at many corn-ethanol facilities and is being supplied to biodiesel manufacturers. Most corn oil derived from ethanol facilities is not suitable for human food use. The process in wide use utilizes centrifugation of the syrup before applying the solubles to the wet cake before drying.

Yield of distiller’s oil varies, but is a minimum of about 35% of the available oil ICM Co.). Therefore, the approximate total available corn oil supply is around 30-40 million gallons per year in South Dakota and 400 to 500 million gallons for the United States. This oil is more suitable for hydrorefining to green diesel than for conversion to biodiesel because of a high proportion of free fatty acids.

Table 2: Crop yields in 2007 and calculated oil yield for selected oilseed crops in South Dakota (SD), North Dakota (ND), and Montana (MT) [1].

		CROP YIELD			OIL YIELD		
		----------- lbs per acre ----------			-------- lbs oil per acre --------		
Species		SD	ND	MT	SD	ND	MT
Camelina				600			240
Crambe			1,000	1,200		300	360
Flaxseed		730	1,000	520	260	370	190
Canola		410	1,200	1,200	160	490	470
Other Rapeseed				450			180
Sunflower		1,500	1,400	1,100	610	580	440
Safflower		570	940	850	110	190	170

[1] USDA National Agricultural Statistics Service 2007.

Table 3: Oilseed composition and fatty acid chain lengths for oilseed crops grown in the Northern Great Plains Region.

Oilseed Species	%oil in seed	C_{16} Palmitic Acid	C_{18} Linolenic, linoleic, oleic and Stearic acids	C_{20} Arachidic & eicosanoic acid	C_{22} Erucic & brassidic acid	C_{24} Tetracosanoic & nervonic
Camelina[1]	~35-40%		73%	12%	2.5%	
Canola[1, 2]	40%	5%	95%	2%	0-2%	
Rapeseed[1, 2]	40-45%	~5%	~60	10%	23-50%	
Flax[3]	34-37%	~6%	~90%			
Sunflower[4, 2]	40-50%	~7%	90+%			
Safflower[5, 6]	~20-40%		75-90%			
Crambe[1, 7]	~26-38%	2%	30%		50-60%	2%
Corn[8]	~3-6%*	11-13%	87-89%			

[1]Sun Grant Bioweb, [2]Downey 1990, [3]Duke 1983, [4]Janick and Whipkey 2002, [5]Kephart *et al.* 1990, [6]Magness *et al.* 1971, [7]Lessman 1990, [8]Corn Refiners Association 2006.

Fatty Acid Composition and Potential Fuel Production

In addition to variations in yield and oil concentration, oilseed species differ in fatty acid composition (Table 3). The relative composition of fatty acids in feedstocks will influence carbon chain lengths for the resulting fuels. Manipulation of the proportions of the chain lengths can be used to adjust fuel specifications. Crambe oil is particularly well suited as a feedstock with long fatty acid chain lengths. Corn oil has a greater proportion of relatively shorter chain lengths. All of the fatty acid profiles are suitable for green diesel and green jet fuel production.

Based on oilseed crop production statistics from the 2007 USDA Census of Agriculture (Table 1 and 2), and oil concentrations for these crops (Table 3), an estimated 130 million gallons of green diesel can be produced from oilseed crops in existing farming systems in the Northern Great Plains (Table 4). The region's existing oilseed capabilities could potentially provide 58% of the

Navy's expected needs in 2020. The region's production capacity can be increased significantly through increased agronomic research, plant breeding, and integration of biotechnology.

The existing corn-based ethanol industry can provide distillers oil from existing cropping systems and energy production industry. In South Dakota alone, 30 million gal of corn oil can be accessed to produce 22.5 million gal of green diesel. Nationally, the corn ethanol industry can produce 400 million gal of corn oil, yielding 300 million gal of green diesel. The corn and oilseed-based industries have a great potential to produce domestic fuels for both the nation's military and commercial aviation industries.

Table 4: Estimates of green diesel production from oilseed crops grown in South Dakota (SD), North Dakota (ND), and Montana (MT) [1].

Species	SD	ND	MT	Total
	---------------------------------- Gal Green Diesel ----------------------------------			
Camelina			450,432	450,432
Crambe		206,475	160,267	366,742
Flaxseed	165,113	10,677,435	349,071	11,191,619
Canola	3,506	47,889,215	342,195	48,234,916
Other Rapeseed			235,172	235,172
Sunflower	21,255,694	47,506,668	138,821	68,901,183
Safflower	99,784	681,909	590,174	1,371,867
Total	21,524,097	106,961,702	2,266,132	130,751,931

[1] USDA Census of Agriculture 2007

Of the green diesel produced from hydrorefining, final processing would be expected to yield 50% fungible diesel fuel and 50% jet fuel. The North Central region oilseed crop could produce 65 million gal of both fuel types, whereas corn oil could be used to produce 150 million gal of both fuel types.

Future Crop Development Opportunities

There are short-, mid-, and long-term strategies to be implemented in order to have a sustainable bio-fuels industry to support military and commercial aviation. As a short-term opportunity, distiller's corn oil should be evaluated. This resource is currently available in substantial quantities and would not entail major changes in cropping systems or land use.

Mid-term efforts should be directed toward expansion of oilseed production and crushing capacity in arid and semi-arid areas of the North Central region. Expansion of oilseeds would diversify small grains cropping systems and would in turn support more sustainable crop production. Limitations in infrastructure must be addressed to support production of these crops, however. Immediate needs include capital investment in crushing facilities and a logistics infrastructure, establishing a seed industry and supporting plant breeding programs.

As a long-term strategy, development of technologies to produce green diesel and jet fuel from cellulosic feedstocks will need to be expanded. Research and development is currently underway to employ thermochemical processes that contribute to improved logistics of the feedstocks and subsequent production of drop-in fuels.

All regions of the U.S. have opportunities to provide drop-in fuels for military and commercial aviation. Developing these resources will diversify our sources for energy production and will in turn enhance the nation's energy security.

References

Corn Refiners Association. 2006. http://www.corn.org/wp-content/uploads/2009/12/CornOil.pdf. accessed 11 March, 2011

Downey, R.K. 1990. Canola: A quality brassica oilseed. p. 211-217. In: J. Janick and J.E. Simon (eds.), Advances in new crops. Timber Press, Portland, OR; http://www.hort.purdue.edu/newcrop/proceedings1990/V1-211.html#Table 3. accessed 11 March, 2011

Duke, James A. 1983. Handbook of Energy Crops. http://www.hort.purdue.edu/newcrop/duke_energy/. accessed February 2011.

ICM Company. "ICM Oil Extraction Technology — highest proven yield" http://www.icminc.com/services/oil_extraction/. accessed February 2011.

Janick, J., and A. Whipkey (eds.). 2002. Trends in new crops and new uses. ASHS Press, Alexandria, VA.

Kephart, Kenneth D., Glen A. Murray, and Dick L. Auld. 1990. Alternate Crops for Dryland Production Systems in Northern Idaho. http://www.hort.purdue.edu/newcrop/proceedings1990/V1-062.html#Sunflowers. accessed February 2011.

Lessman, K.J. 1990. "Crambe: A new industrial crop in limbo". p. 217-222. In: J. Janick and J.E. Simon (eds.), Advances in new crops. Timber Press, Portland, OR. http://www.hort.purdue.edu/newcrop/proceedings1990/V1-217.html. accessed February 2011.

Magness, J.R., G.M. Markle, C.C. Compton. 1971. Food and feed crops of the United States. Interregional Research Project IR-4, IR Bul. 1 (Bul. 828 New Jersey Agr. Expt. Sta.).; http://www.hort.purdue.edu/newcrop/Crops/Safflower_seed_oil.html. accessed 11 March, 2011.

Sun Grant Bioweb. 2011. http://bioweb.sungrant.org/Technical/Biomass+Resources/Agricultural+Resources/New+Crops/Oilseeds/. accessed 8 March, 2011

USDA National Agricultural Statistics Service. 2007 Census of Agriculture. http://www.agcensus.usda.gov/Publications/2007/Full_Report/Volume_1,_Chapter_1_State_Level/index.asp. accessed 8 March 2011.

5.4
INVESTIGATING THE VIABILITY OF CAMELINA SATIVA AS AN ENERGY CROP IN CENTRAL MONTANA

Chengci Chen[1,], Anton Bekkerman[2]*

Abstract

Camelina sativa has been identified as an oilseed bioenergy feedstock, but a sustainable production for this energy crop has not yet been well developed. Moreover, there is a major concern about bioenergy feedstock production directly competing for land use with food crops. One potential resolution is using camelina as a rotation crop to grow in traditional fallow periods in wheat-based production systems, resulting in a complementarity, rather than substitution, to food crops. This study investigates the impact of using camelina as a rotation crop on winter wheat yields and system profitability. A replicated rotation study with each crop appearing in each year was conducted from 2008 to 2011, and the performance of the camelina-winter wheat rotation was compared to fallow-winter wheat, barley-winter wheat, and canola-winter wheat rotations. Average winter wheat yields were 2401, 2331, and 1858 kg/ha following camelina, canola, and barley, respectively, representing a 13.2%, 15.7% and 32.8% winter wheat yield reduction relative to the fallow-winter wheat rotation (2766 kg/ha). Winter wheat production decreases were offset in the cropping systems by 907 kg/ha camelina 594 kg/ha canola, and 1779 kg/ha barley. The current winter wheat-fallow rotation practice provides more net return to producers due to substantially low total cost incurred in the cropping system. To attract producers to include canola and camelina in the cropping system requires either a higher grain price and/or improving the yield potential of these crops. Although winter wheat-fallow resulted in better net return to producers, the sustainability of this practice should be evaluated with long term experiments.

Key Words: Camelina, Cropping Systems, Economic Analysis

Introduction

Oilseeds have been identified as one of the seven bioenergy feedstocks by USDA and DOE. Camelina (*Camelina sativa)*, a member of the plant family Brassicaceae, is an ancient crop that originated in northern Europe (Schultze-Motel 1979). Since 2003, this crop has been evaluated by scientists in Montana, Wyoming, and Washington for its adaption. It is found that camelina can adapted to the semi-arid region of the Northern Great Plains (McVay and Lamb. 2008). Recent studies have shown that non-food oilseed camelina is a superior feedstock for biodiesel and jet fuel, based fuel performance based during commercial airline and military fighter jet testing (http://www.susoils.com/flights.php).

An economically and environmentally sustainable cropping system is the key to the success of camelina feedstock production. There was concern about biofuel feedstock production directly competing for land use with food crops. One potential resolution is to use camelina as a rotational crop to grow in traditional fallow periods in wheat-based production systems, resulting in integrated camelina production, rather than being a substitute on food crop land. Traditionally

[1] *Montana State University Central Agricultural Research Center, MT*

[2] *Montana State University Department of Ag Economics and Economics*

* *Corresponding author: cchen@montana.edu*

farmers in the Northern Great Plains adopted winter wheat-summer fallow system to reduce the risk of crop failure. This traditional dryland wheat-fallow production system and associated conventional tillage for weed control during the fallow period causes depletion of soil organic matter, declining soil fertility, soil erosion, and inefficient water use (Bowman et al., 1999; Peterson et al., 1998). Replacing fallow with camelina feedstock could increase returns and profitability of wheat-fallow based systems in the NGP region.

In recent years, adoption of reduced tillage and no-till has allowed for increased cropping intensity across many regions in the NGP (Nielsen et al., 2011). As an energy crop, camelina has a potential as a rotation crop to eliminate the fallow period. Growing camelina in the fallow period will avoid direct competition for land use with food crops in wheat-based production systems. An expected net economic return largely determines what crops farmers choose to grow (Stanger et al., 2008). Pea and lentil, for example, had increased from less than 50,000 acres in 2003 to 500,000 acres in 2011 in Montana. The reason for this rapid increase was higher net returns of pea and lentil as rotation crops with wheat, compared with traditional fallow-wheat system (Chen et al., 2012).

It is not clear how camelina will affect winter wheat yield when replacing camelina with fallow in wheat-based production system. The objective of this study was to investigate the impact of using camelina as a rotation crop on winter wheat yields and system profitability.

Materials and Methods

This experiment was carried out at the Central Agricultural Research Center (47^0 03’ N, 109^{0}57’W; 1400 m elevation) near Moccasin, MT from 2008 to 2011. The soil was classified as a Judith clay loam (fine –loamy, carbonatic, frigid Typic Calciustolls). Soil water holding capacity is limited by gravel content and shallow soil profile. The 20-yr average annual precipitation and air temperature were 373 mm and 7^{0}C, respectively. The experiment was in a randomized complete block design with four replications and plot size of 15.24 m by 3.66 m. Treatments were winter wheat-fallow (WW-FAL), winter wheat-barely (WW-BAR), winter wheat-canola (WW-CAN) and winter wheat-camelina (WW-CAM) rotations. Fertilizers were applied based on soil test result as recommended by Jacobsen et al., (2003). The varieties used were Yellowstone winter wheat, Haxbery barley, Hyola 357 RR canola, and Blaine Creek camelina, respectively. Crops were directly seeded using a ConservaPak no-till drill (ConservaPak, Indian Head, SK, Canada) at recommended seeding rates. Herbicides, namely, glyphosate, bronate, quizalofop (assure II) and pendimethalin were used according to recommendation to control weeds. In order to determine grain yield, crops were harvested using a Wintersteiger plot combine (Wintersteiger Inc., Salt Lake City, UT). Grain nitrogen content of winter wheat was determined to calculate protein content following the procedure described by Chen et al. (2011).

Data were statistically analyzed using SAS (SAS 9.3 version) computer software and economic analysis was performed using enterprise budgets to estimate costs, gross incomes and net returns. Crop prices and protein premiums for winter wheat were derived from expected local cash prices at planting time based on future prices and historic basis in Montana’s largest wheat production regions. The detailed costs of inputs and prices of outputs to calculate total costs, gross incomes and net returns are well described in Chen et al. (2012).

Results and Discussion

Agronomic Viability

As shown in Table 1, winter wheat yield changed from year to year duo to the variation in precipitation. Averaged over three years, the grain yield of winter wheat obtained following camelina, canola, and barley was 2401, 2331, and 1858 kg/ha, respectively, representing 13.2%, 15.7% and 32.8% yield reduction from the traditional fallow-winter wheat (FAL-WW) system

(2766 kg/ha). Winter wheat grain protein ranged from 132 to 137 g/kg and did not affected by crop rotation. Winter wheat following barley reduced the grain yield the most (32.8%). This substantial reduction in grain yield was due to the cereal following cereal rotation resulting in the buildup of grassy weed and certain diseases. The agronomic benefits of using different crops in a rotation have been well documented (Chen et al., 2012; Miller et al., 2003; Tanaka et al., 2005).

Table 1. Crop rotation effect on agronomic benefits in terms of cumulative grain yield of various crops from 2008 - 2011 at Central Agricultural Research Center, MT. Results are mean for four replications.

	Winter Wheat Yield (kg/ha)	Winter Wheat Protein (g/kg)	Camelina Yield (kg/ha)	Canola Yield (kg/ha)	Barley Yield (kg/ha)
WW-CAM	2401b	137a	907		
WW-CAN	2331b	132a		594	
WW-BAR	1858c	135a			1779
WW-FAL	2766a	137a			
2009	1934	165	1087	686	2107
2010	3084	119	1204	1006	2145
2011	1998	121	431	90	1083

WW=Winter wheat, CAM=Camelina, CAN=Canola, FAL=Fallow, BAR=Barley; Mean grain yield of winter wheat for each treatment in a column followed by a common letter are not statistically different from each other at 5% LSD value.

Similar to winter wheat, camelina and canola yields also varied from year to year. Averaged over three years, camelina grain yield in the winter wheat-camelina (WW-CAM) rotation was 907 kg/ha, compared to 594 kg/ha of canola grain yield in the winter wheat-canola rotation (Table 1). This suggests that camelina is a more adaptable alternative rotational oil crop than canola for this part of the state.

Economic Benefits

Despite potential agronomic benefits of camelina production, widespread adoption of camelina systems depends on sufficient economic incentives associated with producing systems. In this study, economic incentives are evaluated by investigating net returns of alternative systems. Specifically, system enterprise budgets were developed and used to assess production costs and market returns during the period 2008-2011. These budgets were used to compare the returns of WW-CAM system with WW-FAL, WW-BAR, and WW-CAN systems.

Results indicate that the system yielding the highest average net return is WW-FAL, primarily due to the significantly lower production costs. That is, although additional market returns are obtained in systems that have continuous crop production (observed in higher market revenues for those systems), these returns are not sufficiently high to offset the additional production costs associated with the production of those crops. Furthermore, although the 4-year average net returns for the WW-CAM rotation are higher than the WW-BAR system, these outcomes must be interpreted with caution because camelina market prices were temporarily higher in 2008 and 2009.

As demand for camelina decreased significantly in 2010 and 2011, resulting in a substantial drop in market prices, the net return for the WW-CAM system was no longer sufficient to incentivize the crop's production. We conducted an analysis to understand market conditions necessary for camelina production to be adopted using scenario analyses. Table 2 presents net returns ratios of the camelina system relative to the other systems. When the ratio is less than one, then the camelina system will result in lower net returns than the alternative system. For example, using actual 2008-2011 market prices, the ratio of WW-CAM to WW-CAN net return is 2.07, implying that the WW-CAM system yields a higher net return than the WW-CAN rotation. The table also shows various scenarios associated with different camelina market prices, assuming that production costs and market prices of other commodities do not change. The scenario analyses indicate that the WW-CAM system is most preferable when camelina prices $0.375/kg. Otherwise, camelina rotation is not as profitable as at least one other alternative.

Table 2. Net returns of camelina rotation relative to alternative systems

		Camelina Prices Scenarios ($/kg)			
	2008-2011 Prices	0.110	0.199	0.287	0.375
WW-CAN	2.07	-0.10	0.90	1.90	2.89
WW-CAM	1.00	1.00	1.00	1.00	1.00
WW-BAR	1.25	-0.06	0.54	1.14	1.74
WW-FAL	0.81	-0.04	0.35	0.74	1.13

WW=Winter wheat, CAM=Camelina, CAN=Canola, FAL=Fallow, BAR=Barley

The scenario analyses provide insights about market conditions when camelina can be part of a profitable system. It is necessary to note that although current conditions make camelina system adoption unlikely, substantial changes in market demands for camelina could sufficiently increase prices. Furthermore, indirect economic benefits of camelina exist. For example, repeated use of the WW-FAL rotation can result in soil nutrient depletion through plant uptake, soil erosion and decrease of soil organic matter during fallow period (Machado, 2011; Papendick, 1996) and hinder crop diversification, aggravate labor and machinery demand during peak season and promote disease and pest incidence. In addition, co-products development from camelina meal will increase camelina value.

Conclusion

The current winter wheat-fallow rotation practice provides more net return to producers due to substantially low total cost incurred in the cropping system. To attract producers to include canola and camelina in the cropping system requires either a higher grain yield price and/or improving the yield potential of these crops. Although winter wheat-fallow resulted in better net return to producers, the sustainability of this practice should be evaluated with long term experiments.

References

Bowman R.A., M. F. Vigil, D. C. Nielsen, and R. L. Anderson. 1999. Soil organic matter changes in intensively cropped dryland Systems. Soil Sci. Soc. Am. J. 63:186-191.

Chen C., G. Han, H. He and M. Westcott. 2011. Yield, protein and remobilization of water soluble carbohydrate and nitrogen of three spring wheat cultivars as influenced by nitrogen input. Agron. J. 103:786-795.

Chen C., K. Neill, M. Burgess, A. Bekkerman. 2012. Agronomic benefits and economic potential of introducing fall-seeded pea and lentil into conventional wheat-based crop rotations. Agron. J. 104:215-224.

Jacobson J., G. Jackson and C. Jones. 2003. Fertilizer guidelines for Montana crops. Publ. EB161. Montana State University, Ext. Serv., Bozeman.

Machado, S. 2011. Soil organic carbon dynamics in the Pendleton long-term experiments: Implications for biofuel production in Pacific Northwest. Agron. J. 103:253–260.

McVay K.A. and P.F. Lamb. 2008. Camelina Production in Montana. A self-learning resource from MSU extension. Available at http://msuextension.org/publications/AgandNaturalResources/MT200701AG.pdf; Accessed Aug. 9, 2012.

Miller P. R., Y. Gan, B.G. McConkey, and C.L. McDonald. 2003. Pulse crops for the northen Great Plains. I. Cropping sequence effects on cereal, oilseed and pulse crops. Agron. J. 95:980-986.

Nielsen, D.C., M. F. Vigil, and J.G. Benjamin. 2011. Evaluating decision rules for dryland rotation crop selection. Field Crops. Res. 120:254-261.

Papendick, R.I. 1996. Farming systems and conservation needs in the northwest wheat region. Am. J. Altern. Agric. 11:52–57.

Peterson, G.A., A.J. Schlegel, D.L. Tanaka, and D.R. Jones. 1996. Precipitation use efficiency as affected by cropping and tillage systems. J. Prod. Agric. 9:180–186.

Stanger, T.F., J.G. Lauer, and J.P. Chavas. 2008. The profitability and risk of long-term cropping systems featuring different rotations and nitrogen rates. Agron. J. 100:105-113.

Tanaka D.L., R.L. Anderson and S.C. Rao. 2005. Crop sequencing to improve use of precipitation and synergize crop growth. Agron. J. 97:385-390.

5.5
ENERGY BEETS AS A BIOENERGY FEEDSTOCK IN SOUTHERN GREAT PLAINS

Vijaya Gopal Kakani[1,], Chad B. Godsey[1], Pradeep Wagle[1], Anserd J. Foster[1], Aparna Kakani[1], Raghuveer Sripathi[1], Arjun Pandey[1]*

Abstract
Sugar feedstocks are easy to convert and efficient for biofuel production. Energy beets (Beta vulgaris L.) were not evaluated in Southern Great Plains of USA and have the potential to replicate ethanol yields of sugarcane in Brazil. The objective of this study was to evaluate energy beet for sugar and biomass yield and finally ethanol production. Five energy beet lines of BetaSeed Inc. were evaluated during 2010 and 2011 winter and 2011 summer in Stillwater, OK. Winter crop was planted on 28 Sept in 2010 and 2011 and 14 April/18 May in summer 2011. Monthly root samples were collected. Juice was extracted with commercial fruit juice extractor. Genotypes differed significantly in their root yield and year x genotype interaction was also observed. The winter 2010 and 2011 planted crop survived the winters. The final root weight for the winter 2010 and 2011 planted crop ranged between 42 and 65 wet Mg ha^{-1} and 70 and 95 wet Mg ha^{-1}, respectively. The brix was 15 to 18% and 13 to 18% for the winter crop harvested in June 2011 and 2012, respectively. Based on genotype, yield and percent brix, the theoretical ethanol yield potential ranged from 3700 to 8300 L ha^{-1} or 450 to 890 gallons ac^{-1}. Among the genotypes studies, EFC 174 produced the highest potential ethanol yields. In conclusion, energy beets can be grown during the winter and summers of Southern Great Plains in rotation with other traditional crops.

Keywords: biomass, biofuel, ethanol, energy beet, sugar, root, winter

Introduction
Global demand for non-renewable fuels threatens the environment, global climate, and our Nation's energy and agricultural security. Worldwide energy consumption is projected to increase by 57 percent between 2004 and 2030 (EIA 2007). The recently released National Biofuels Action Plan (NBAP) supports energy supply through biofuels that are clean, affordable and renewable (BRDI 2008a). According to the Energy Independence and Security Act (EISA) of 2007, renewable fuel production should reach 36 billion gallons by 2022. As corn-based ethanol production is reaching the targets set by the federal Renewable Fuel Standards, ethanol from sugar-based or cellulosic feedstocks can help bridge the gap.

Advanced biofuels based on non-food feedstocks are generating much interest (BRDI 2008b). Feedstocks that could be grown on marginal land with reduced inputs are of particular interest. However, biofuels that rely on other sources of biomass, including agricultural wastes, municipal solid waste, and dedicated non-food energy crops such as perennial grasses, fast-growing trees, and algae are still years from commercial production. Nonetheless, this interest has led to proposals to support and/or mandate biofuels produced from feedstocks other than corn starch through explicit requirements, research, development and extension funding, and/or tax incentives. Non-corn biofuels could include fuels produced from cellulosic material (such as perennial grasses), ethanol produced from sugarcane or sugar beets, and biodiesel or renewable diesel produced from vegetable or animal oils. The RFS2 requires that an increasing amount of the biofuel mandate be met through the use of "advanced biofuels" — biofuels produced from feedstocks other than corn starch. In the 2008 farm bill (Capehart *et al*. 2008), Section 9010:

[1] *Department of Plant and Soil Sciences, Oklahoma State University, OK*

** Corresponding author*

Feedstock Flexibility Program for Bioenergy Producers subsidizes the use of sugar for ethanol production through federal purchases of surplus sugar for sale to ethanol producers. These provisions in the farm bill require studies to promote sugar crops as potential sources for ethanol production. Ethanol produced by countries other than the United States use sugar crops as primary feedstocks (Shapouri and Salassi 2006). Sugarcane is widely used, although several countries use sugar beets. Crops high in sugar content (sugarcane and sugarbeets) are easier to process into ethanol than starch crops since the sugar required by fermentation is already present. Fermenting and distilling ethanol from these crops is also well established.

Sugar beet is a lost crop of the Southern Great Plains and can bring diversity to biofuel feedstocks of this region. It can be revived as a potential biofuel feedstock due to suitability of the region for its production. Historical data (NASS-USDA 2007) show that the crop was grown in both Texas and Kansas under irrigation with yields as high as 70 Mg ha^{-1}. As of today, sugar beets are grown primarily in the upper Midwest. Current conversion technologies yield 5,500 L ha^{-1} of beet ethanol, which is close to the sugar cane ethanol yield of 5,900 L ha^{-1} (Shapouri and Salassi 2006). Sugar crops that are not staple food sources could help start the ethanol industry while the renewable fuels transitions to a cellulosic ethanol industry. In addition, it would also provide diversity and continuous feedstock supply to the ethanol industry as most of the currently proposed cellulosic feedstocks (switchgrass and sorghum) are summer crops. Recent advances in genetics are resulting in high yields of 100 Mg ha^{-1} and recent deregulation of Roundup Ready (RR) beets enables easy crop management. Reports on the success of RR sugar beets with increased yield and sugar content and reduced input costs suggest it as a profitable feedstock for ethanol production (http://www.isaaa.org/resources /publications/briefs/39/executivesummary/default.html). Hence, the objectives of the study were to (1) determine the yield potential of new varieties of energy beets in Oklahoma and Kansas and (2) estimate the quantity of sugar and ethanol potential of energy beet varieties.

Materials and Methods

Three separate field studies were conducted, two during winter of 2010-11 and 2011-12 and one during summer of 2011 at Stillwater, OK. The soil at the location was Easpur loam, 0 to 1 percent slopes at the Agronomy Farm, Stillwater, OK. In addition, energy beets were evaluated during winter of 2011 for yield and brix at Fort Cobb and Chickasha, OK. Seeds of energy beet cultivars EAC 113, 114, 174, 183 and 184, were sown with a Monosem planter on 28 September 2010 and 2011 for the winter crop, and 14 April/15 May 2011 for the summer crop. Rows were spaced 0.76 m apart and oriented in a north–south direction and seeds were planted 15 cm apart. Excess seedlings were thinned to maintain a plant to plant spacing of 15 cm.

The experimental design was a randomized complete block with four replications. Plot size was 6.1 m wide and 7.6 m long. Monthly samples were collected from December to June for winter crop and from October to December for the summer crop. A shovel was used to dig roots from a 1 m row at each sampling interval. Number of bolts that emerged were counted and chopped. Plants were separated into roots and leaves. Fresh weight of leaves and roots was measured. The roots were washed clear of the soil, cut into pieces, and passed through a commercial fruit juice extractor to separate the juice and bagasse. The leaves and bagasse were dried at 70°C for 5 days. The volume and weight of the expressed juice was measured and a 50 ml juice sample was stored at -20°C for brix (%) measurement and further analysis. The brix was measured using a portable refractometer Refracto 30GS (Metler-Toledo, Columbus, OH). The potential ethanol yield was calculated using the following equation.

$$\text{Potential Ethanol yield (L ha}^{-1}\text{)} = \text{Wet root weight (kg ha}^{-1}\text{) x juice expression (\%) x brix (\%) x 10 x 0.511 / 720 (g L}^{-1}\text{ of ethanol)}$$

where, 0.511 is the potential sugar to ethanol conversion efficiency and 10 is the multiplier for brix (%) to grams sugar per liter.

The data was subjected to analysis of variance (ANOVA) as a randomized complete block design with years and varieties as main factors. Mean values were compared with the least significant difference (LSD) test at $P<0.05$. Statistical analysis was carried out with the SAS statistical package.

Results and Discussion

Weather and Crop

The energy beets were subjected to extreme weathers during the winters of 2010 and 2011. The average mean monthly growing conditions are presented in Table 1. The crop survived the winters of 2010 and 2011 and began to grow after mid-February (Fig.1). At Stillwater, the winter of 2010-11 was extremely cold with a record minimum temperature of -28.5°C, while the crop was exposed to temperatures as high as 38.6 during the summer months. The 2011-12 growing season had a mild winter with the lowest temperature of only 10.2°C, while the summer maximum was 39.7°C. The observed growth temperatures were greater during the latter part of the growing season when compared an optimum temperature of 17-24°C for root growth (Terry 1968). The total rainfall received during the 2010-11 and 2011-12 growing seasons were 370.5 mm and 565.8 mm, respectively. The seasonal water use for a good summer beet crop is northern parts of US is about 750 mm (Schneekloth and Andales, 2009). Therefore the 2010-11 energy beet crops received only 50% of the requirement while the 2011-12 crop received about 75% of the seasonal water use.

Table 1. Mean monthly maximum (Tmax) and minimum (Tmin) tempeatures, solar radiation, and total montly rainfall at Stillwater, OK during the energy beet growing seasons of 2010-11 and 2011-12.

Month	2010-11				2011-12			
	Mean Tmax (°C)	Mean Tmax (°C)	Rainfall (mm)	Solar Radiation (MJ m^{-2} d^{-1})	Mean Tmax (°C)	Mean Tmax (°C)	Rainfall (mm)	Solar Radiation (MJ m^{-2} d^{-1})
Oct	12.4	0.0	73	15.6	24.9	8.4	58.5	15.7
Nov	23.0	9.2	98	10.1	17.1	2.9	48.5	11.2
Dec	24.1	11.9	154	7.6	10.2	-2.6	13.3	8.2
Jan	29.1	16.4	28	11.5	8.1	-6.3	8.0	10.2
Feb	32.3	19.4	54	11.1	11.2	-4.0	46.8	12.5
Mar	38.3	23.2	2	16.5	17.4	4.8	20.8	14.0
Apr	29.1	13.2	0	18.0	24.7	9.1	49.5	20.1
May	24.2	8.8	15	24.0	24.7	9.1	97.8	21.8
Jun	16.3	3.0	66	24.9	26.3	14.1	42.8	26.8

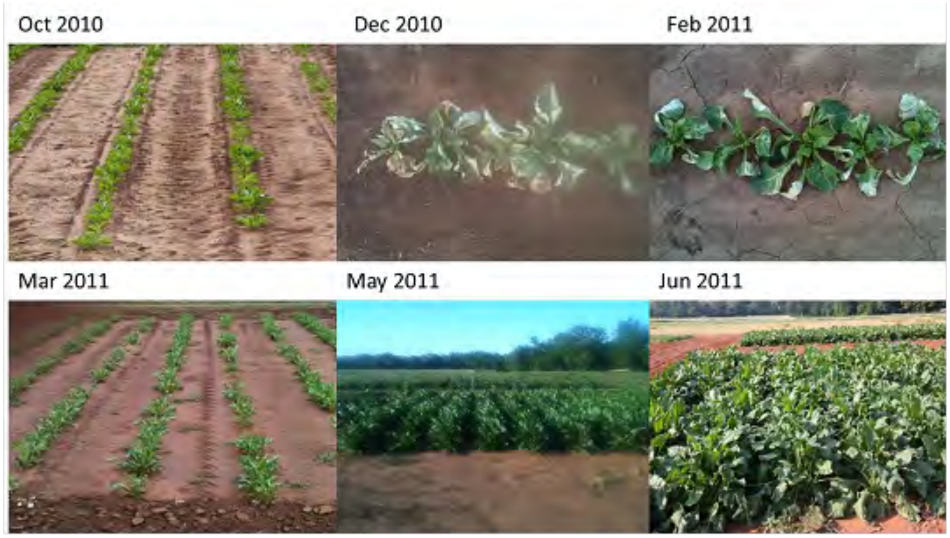

Fig. 1. Progress in energy beet crop growth during the 2010-11 growing season at Stillwater, OK.

Biomass Yield

The economical part of energy beet is root. Wet root weights of energy beets were between 38 and 65 Mg ha^{-1} in the crop harvested in June 2011, while the root yield was between 56 and 87.5 Mg ha^{-1} for the crop harvested in June 2012 (Fig. 2). Among the genotypes tested, EFC174 and EGC183 recorded the lowest yield of about 38 wet Mg ha^{-1} in 2011. The same genotype produced 80.7 and 78.5 wet Mg ha^{-1}, respectively during 2012. These results suggest that EFC174 and EGC183 were most sensitive to cold winters of Stillwater, OK. Except for EAC113, most of the genotypes tested produced higher root yields during the 2011-12 growing season. The high yield of genotypes in 2011-12 can be attributed to mild winter conditions of 2011. The crop required less time to recover from cold stress and was able to initiate rapid growth during the spring months. The energy beet yields obtained are on par with that of the national average yields of sugar beets (NASS-USDA, 2007). The yields obtained are similar or better than the yields that were recorded between 1940 and 1990 in Kansas and Texas (NASS-USDA, 2007).

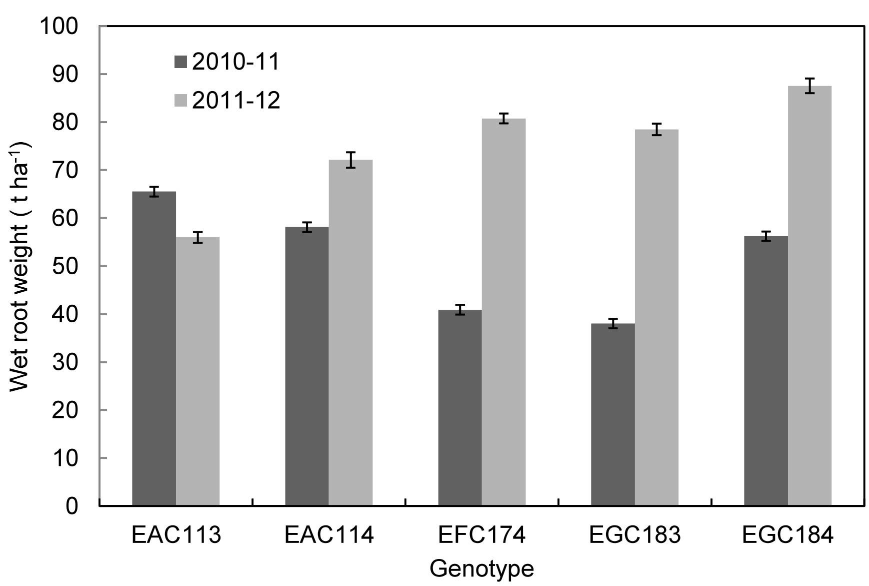

Fig. 2. Wet root weights of five energy beet genotypes grown in winter of 2010 and 2011 at Stillwater, OK.

Brix

Brix is a measure of sugar content in an aqueous solution. The mean brix values ranged between 13.7 and 17.4% (Fig. 3). Among the genotypes tested EFC 174 had the highest brix values followed by EAC114, EAC113, EGC183 and EGC184. Among the years 2010-11 had slightly higher brix values that 2011-12. Genotypes that produced lower root yield had higher brix values suggesting the trade-off between root yield and sugar content.

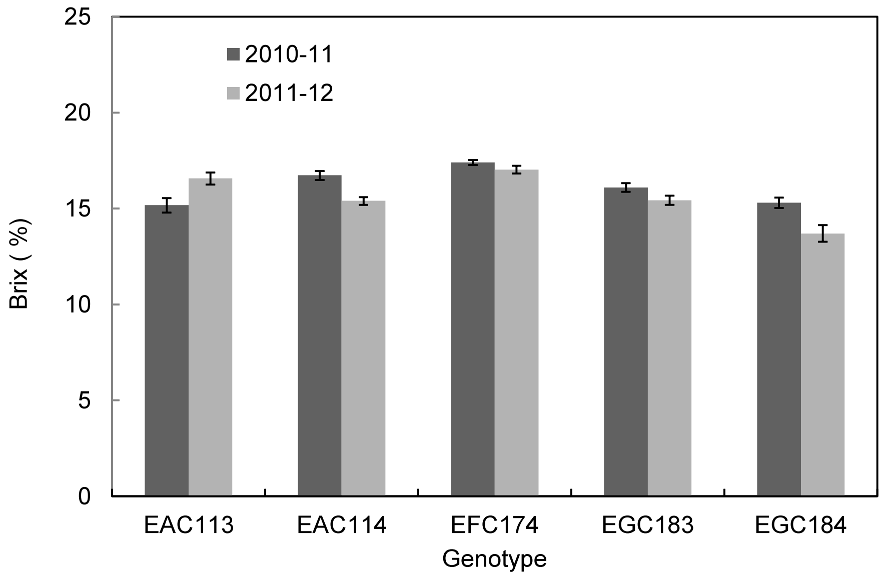

Fig. 3. Percent brix of five energy beet genotypes grown in winter of 2010 and 2011 at Stillwater, OK.

Potential Ethanol Yield

Ethanol is the final fuel product derived from fermentation of the sugars in the energy beet juice. Based on the brix in expressed juice and theoretical conversion efficiency, the ethanol production efficiency is 0.97 to 0.123 L of ethanol per liter of juice. The potential ethanol yield ranged between 3692 and 6002 L ha^{-1} from the 2010-11 energy beet crop, while it was between 5602 and 8294 L ha^{-1} for 2011-12 energy beet crop (Fig. 4). These ethanol yields are on par or higher than those of sugar beet and sugarcane as reported by Shapouri and Salassi (2006). The potential ethanol yields from energy beets in Oklahoma are 100% higher than those reported for sweet sorghum (Zegada-Lizarazu and Monti, 2012).

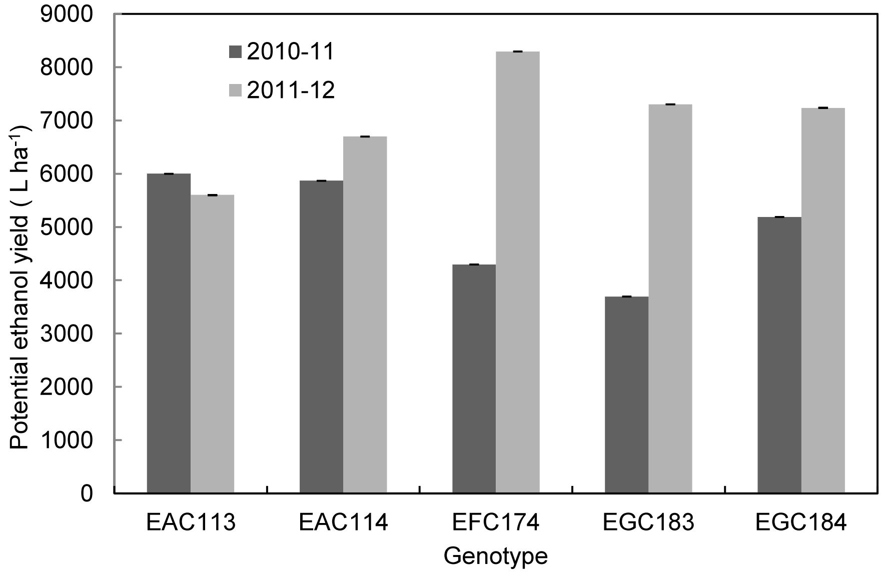

Fig. 4. Potential ethanol yield of five energy beet genotypes grown in winter of 2010 and 2011 at Stillwater, OK.

Conclusions

The energy beets grown during winter of 2010 and 2011 demonstrated the winter survival and yield potential in Oklahoma that is located at the northern edge of the Southern Great Plains. As a winter crop, the energy beets can fit into rotation with other winter crops such as wheat and canola. The crop can also be grown in sequence with sweet sorghum to enhance ethanol yields per unit land area.

References

BRDI. 2008a. Increasing Feedstock Production for Biofuels: Economic Drivers, Environmental Implications and the Role of Research. Available at www.brdisolutions.com, verified on March 20, 2009.

BRDI. 2008b. National Biofuels Action Plan. Available at www.brdisolutions.com, verified on March 20, 2009.

Capehart, T., Schnepf, R. and Yacobucci, B.D. 2008. Biofuels provisions in the 2007 Energy Bill and the 2008 Farm Bill: A side by side comparison. CRS Report for Congress, prepared for members and committees of Congress. CRS Report RL34239.

EIA, 2007. International Energy Outlook 2007. Avalilabe at ftp://tonto.eia.doe.gov/forecasting/0484(2007).pdf. DOE/EIA-0484(2007), Washington D.C., May 2007. Verified on August 31, 2012.

NASS-USDA, 2007. Available at http://www.nass.usda.gov/, verified on March 20, 2009.

Report3.pdf. verified on August 31, 2012..

Shapouri, H. and Salassi, M. 2006. The economic feasibility of ethanol production from sugar in the United States. Available at http://www.usda.gov/oce/reports/energy/EthanolSugarFeasibility. Verified on August 31, 2012.

Schneekloth, J. and A. Andales. 2009. Seasonal Water Needs and Opportunities for Limited Irrigation for Colorado Crops. Colorado State Fact Sheet 4.718.

Terry N. 1968. Developmental Physiology of Sugar Beet: I. The influence of light and temperature on growth. Journal of Experimental Botany 19:795-811.

Zegada-Lizarazu W., Monti A. 2012. Are we ready to cultivate sweet sorghum as a bioenergy feedstock? A review on field management practices. Biomass and Bioenergy 40:1-12. DOI: 10.1016/j.biombioe.2012.01.048.

5.6
SOCIAL ACCEPTABILITY OF BIOENERGY IN THE U.S. SOUTH

John Schelhas[1,], Sarah Hitchner[2]*

Abstract

In the U.S. South, a wide range of bioenergy technologies are now in various stages of development, and a comprehensive and dynamic understanding of the social acceptability of bioenergy is critical as the bioenergy industry expands in this region. Because of the multiple values and perspectives at play across the Southern landscape, we must analyze bioenergy development broadly, taking into account diverse values, governance processes, and equity concerns. Many ideas, facts, and opinions contribute to people's perceptions of bioenergy, and conducting content analysis using a cultural models approach will enable us to understand how different people and groups see bioenergy development, how they frame the issues, where value conflicts and compatibilities lie, and how values influence behavior. In this paper, we focus on identifying key conventional discourses that people reference when they talk about bioenergy in different contexts, including public media, policy and management discussions, outreach programs, and among landowners and within communities. We hope that our research, which aims to elucidate these conventional discourses related to bioenergy, will help guide managers and policy makers by showing the beliefs and values that underlie public opinion, clarifying tradeoffs and synergies, and suggesting language-based ways to negotiate this social complexity.

Keywords: bioenergy, biomass, social acceptability, cultural models, discourse, U.S. South

Introduction

Southern forests have the potential to supply woody biomass feedstocks for a range of energy products, from electricity to pellets and liquid fuels. The American public generally supports increased production of renewable energy from domestic sources. However, there are also strong societal concerns about the impacts of increased woody biomass harvesting on ecosystems and rural communities. As bioenergy development proceeds, it is important to understand how people view and react to both the opportunities presented by bioenergy markets and the significant changes in economies and landscapes these entail.

Using an integrative analytical framework designed to illuminate different perspectives and trade-offs (McShane *et al*. 2011), we are examining the social context of biofuels and emerging bioenergy projects and options in the southeastern U.S. (Hitchner and Schelhas 2012). This work addresses the socio-economic impacts of biofuels on rural communities and will enable a comprehensive and dynamic understanding of social acceptability, which is critical as the bioenergy industry develops in this region.

We are using content analysis to examine the narratives and related cultural models that guide bioenergy discourse in different contexts, such as the public media, policy and management discussions, outreach programs, as well as among landowners and within communities. This discursive analysis will allow identification of diverse values, stakeholders, equity concerns, and governance processes that are shaping conversations, awareness, and decisions about bioenergy. We are also engaged in field research, guided by this larger analytical framework and rooted in comparative ethnography, in a set of research sites selected to represent a variety of types and

---

[1] *Southern Research Station, USDA Forest Service, GA*

[2] *Center for Integrative Conservation Research, University of Georgia, GA*

* *Corresponding author*

stages of bioenergy development in different socio-economic contexts across the U.S. Southeast (preliminary results presented in Hitchner and Schelhas 2012). In this paper, we identify several major conventional discourses that are recurring themes in discussions regarding biofuels and provide examples from public bioenergy conferences we have attended and private conversations we have had with people in our field sites. We further describe how these same conventional discourses are referenced by both proponents and opponents of biofuels.

Bioenergy Discourses

Bioenergy development will bring about changes in regional economies and landscapes, particularly in the areas immediately surrounding biofuels plants. One way of understanding beliefs and values, who holds them, and how they operate is through content analysis of what people say and write (Quinn 2005). This approach complements, not replaces, scientific analysis by other disciplines, for example, of forest cover change or economic impact. Content analysis using cultural models, with attention to stakeholders and scale, enables us to understand how different people and groups see bioenergy development, how they frame the issues, where value conflicts and compatibilities lie, and how values influence behavior. This approach has been used to understand a variety of environmental and social issues. Kempton *et al*. (1995) analyzed American environmental values at the national level, showing shared and divergent values. Paolisso and Dery (2010) explored value differences across stakeholder groups around the Chesapeake Bay and discussed implications for regional planning. Firestone and Kempton (2007) examined the social acceptability of offshore wind power by clarifying public values, attitudes, and beliefs about wind power and how these relate to larger societal discourses and scientific narratives. Schelhas and Pfeffer (2008) discussed how national park neighbors' conservation narratives are influenced both by major societal discourses and by their own social position and livelihoods, as well as how values and discourses influence behaviors.

Conventional discourse analysis is an extension of the cultural models approach. Strauss (2012) analyzed conventional discourses in the United States about immigration and social programs to understand the complexities of public opinion on these topics. She noted that ideas, words, and phrases are shared freely among people within fairly coherent "opinion communities." These shared words and phrases constitute "conventional discourses," and use of them invokes a set of assumptions about what a speaker thinks and values. Everyone belongs to multiple opinion communities and thus uses and combines conventional discourses in unique ways. The ways people deal with conflicting discourses--compartmentalization, true ambivalence, and integration —are particularly instructive (Strauss 2012: 27). Conventional discourses reveal the cultural standing of beliefs and values; for example, we can compare professional and elite discourses to those found in segments of the general population.

In our research, we are applying conventional discourse analysis to ask questions such as: What various outcomes do different stakeholders expect from bioenergy development? How are the expressed values influenced by social position and livelihoods? What are the major biofuels-related discourses circulating in the public sphere, and how are the values and narratives of landowners and community members related to bioenergy shaped by larger public discourses? What behaviors have landowners and community members taken or plan to take, and how are these influenced by societal and local discourses?

Preliminary Results and Discussion

In this paper we can only provide a small sample of our work. The process involves careful examination of notes and transcriptions from interviews, focus groups, workshops, and conferences, as well as text from web pages and publications, in order to identify the major conventional discourses. We group these discourses by general topic, and provide examples of typical rhetoric (see Table 1; which follows Strauss 2012). Note that the language used may range from highly metaphorical to more prosaic, with both being useful and interesting.

Table 1. Selected bioenergy-related discourses (for typical rhetoric, sources are indicated by quotes for written texts or transcripts, and lack of quotes for field notes).

Topic	Conventional Discourse	Typical Rhetoric
Forests	Environmental benefits	"Southern forests are one of the world's environmental jewels. … they house a wide variety of species, unique forested ecosystems, and provide economic and aesthetic values …. [as well as] an abundance of plant and animal diversity and pristine watersheds."
	Useless and wasted trees	I don't know who wouldn't want to find some use for those trash trees.
Rural development	Rural development	"There's no more important opportunity for rural America than bioenergy."
	Family farms	"We can … take care of family farmers. I want farmers to make money."
Subsidies	Bloated government subsidies	"Companies across America are lining up to feed at the government trough."
	Level playing field	"Government shouldn't pick winners and losers."
	Government investment	From Apollo to the computer, the government can be powerful. It's a driver for the diffusion of technology. The government will spend $6.2 billion on a ship, and $2 billion is needed for innovation in cellulosic technologies. This is a good investment for the American people.
Oil and gas	Ethanol ruins engines	75% of all our repairs on farm equipment are because of ethanol. It destroys engines from the inside out. I just wanted to say that I think ethanol stinks.
	Reduce foreign oil	"We buy oil from people who would harm us."
	Need energy development	We have oil and gas if we can drill for it. It's been a long time since we have built a nuclear reactor, or a refinery.
	Fossil fuel addiction	"We need to wean ourselves from fossil fuel addiction."

Once we have identified a range of discourses (Table 1 only presents selected examples), we can look at larger chunks of texts that come from known sources and identify the ways that these conventional discourses are used rhetorically as shortcuts to collectively understood sets of values and then strategically deployed to influence people. For example, here are two texts, reflecting an anti-biofuel and a pro-biofuel narrative (respectively):

> "Most of these arguments do not hold water when put to the real test and, ultimately, we are sacrificing our forests [ENVIRONMENTAL BENEFITS], communities and quality of life [RURAL DEVELOPMENT, FAMILY FARMS] for at best a short-sighted failed investment [GOVERNMENT INVESTMENT] and at worst an environmental tragedy [ENVIRONMENTAL BENEFITS]. We agree that we need to wean ourselves from our fossil fuel addiction [FOSSIL FUEL ADDICTION] and seek

> out alternatives that allow us to maintain our quality of life. But, our forests and communities cannot afford this false solution and it is vital that we find a better way." (Quaranda 2008.)
>
> America needs an energy policy that will adequately address the growing challenges of the 21st century. Advanced biofuels will help provide economic [RURAL DEVELOPMENT] and energy security [NEED ENERGY DEVELOPMENT] in an environmentally sustainable way [ENVIRONMENTAL BENEFITS] by creating jobs [RURAL DEVELOPMENT], lowering carbon emissions [CLIMATE CHANGE], and reducing our dependence on foreign oil [REDUCE FOREIGN OIL]. (Advanced Biofuels Association 2012).

Conclusion

This brief paper represents a preliminary effort to identify the major conventional discourses that appear in discussions of bioenergy. We plan to follow this initial investigation with careful analysis of a variety of texts that differ in type and context. Such detailed analysis will allow us to examine the nuances within broad generalizations, for example by documenting how people talk about bioenergy and emphasizing overlap and differentiation across stakeholder groups. We hope that our research will help guide managers and policy makers by showing the beliefs and values that underlie public opinion, clarifying tradeoffs and synergies, and suggesting language-based ways to negotiate this social complexity.

References

Advanced Biofuels Association web site. http://www.advancedbiofuelsassociation.comh/section.php?sid=1). Accessed: 24 August 2012.

Firestone, J., and W. Kempton. 2007. Public opinion about large offshore wind power: Underlying factors. *Energy Policy* 35: 1584-1598.

Hitchner, S., and J. Schelhas. Social acceptability of biofuels among small-scale forest landowners in the U.S. South. In *Proceedings of the IUFRO 3.08.00 2012 Small-scale Forestry Conference,* September 24-27, 2012, University of Massachusetts, Amherst, MA.

Kempton, W., J.S. Boster, and J.A. Hartley. 1995. *Environmental Values in American Culture*. Cambridge: MIT Press.

McShane, T.O., P.D. Hirsch, T. C. Trung, A.N. Songorwa, A. Kinzig, B. Monteferri, D. Mutekanga, H.V. Thang, J.L. Dammert, M. Pulgar-Vidal, M. Welch-Devine, J.P. Brosius, P. Coppolollo, and S. O'Connor. 2011. Hard choices: Making trade-offs between biodiversity conservation and human well-being. *Biological Conservation* 144(3): 966-972.

Paolisso, M. and N. Dery. 2010. A cultural model assessment of oyster restoration alternatives for the Chesapeake Bay. *Human Organization* 69(2): 169-179.

Quaranda, S. 2008. Don't log the forests for the fuel: a position paper on the potential environmental and economic impacts of the cellulosic ethanol industry in the southern United States. Asheville, NC: Dogwood Alliance.

Quinn, N., editor. 2005. *Finding Culture in Talk: A Collection of Methods*. New York: Palgrave MacMillan.

Schelhas, J., and M.J. Pfeffer. 2008. *Saving Forests, Protecting People? Environmental Conservation in Central America.* (Globalization and Environment Series.) Walnut Creek, CA: AltaMira Press.

Strauss, C. 2012. *Making Sense of Public Opinion: American Discourses about Immigration and Social Programs*. Cambridge: Cambridge University Press.

5.7
ECONOMIC COMPETITIVENESS OF ETHANOL P4RODUCTION FROM CELLULOSIC FEEDSTOCK IN TENNESSEE

*Ankit Bansal[1], Prabodh Illukpitiya[1, *], Surendra P. Singh[1], Fisseha Tegegne[1]*

Abstract

Transformation of the renewable and abundant biomass resources into a cost competitive, high performance biofuel can reduce Tennessee's dependence on fossil fuel and enhance energy security. This study evaluates the economic feasibility of selected bioenergy crops for Tennessee and compares their cost competitiveness. The selected lignocellulosic feedstock consists of switchgrass and *Miscanthus*. Financial analysis was used to select feasible feedstock for biofuel production. For each feedstock, net return, feedstock cost per Btu, feedstock cost per gallon of ethanol, breakeven price of feedstock and breakeven price of ethanol were calculated. The analysis focused feedstock for biofuel production over 25 year project period. Preliminary research shows positive annual equivalent net returns from ethanol production form both feedstock. Sensitivity analysis showed that the feedstock cost for a gallon of ethanol and the breakeven price of ethanol from switchgrass and miscanthus were within a promising range. The results generated here are preliminary and should interpret with caution.

Key words: discount rate; Miscanthus, and switchgrass as feedstock; breakeven price; benefit-cost; sensitivity analysis, Tennessee

Introduction

The growing concern with rising oil prices and global warming and its consequences are the immediate justification for reducing dependence on fossil fuels. Next generation of biofuel feedstock will be composed of cellulose-rich organic materials, which are harvested for their total biomass (World Watch Institute, 2006). Ethanol producing nations like the USA continue to produce ethanol from corn grain rather from cellulosic stalk because of the low ethanol production cost. The US Department of Energy aims to lower the production cost of cellulosic ethanol to $1.07/gallon by 2012 (Goldemberg, 2007).

Biofuels offer alternative benefits on several fronts. These include energy benefits, environmental benefits (McLaughlin et al., 1998), and industrial growth and employment opportunities. In the short to medium term, renewable energy can help diversify energy sources, thus improving the security of energy supply necessary for sustainable economic development.

Since cellulose ethanol production is at relatively early stages, there is information gap in feedstock production as well as processing. For example, producers are concerned about risk and uncertainty associated with feedstock production and marketing. Producers need to have credible information on feedstock selection, various costs associated with production. Specifically information on reliable benefit-cost estimation is essential to attract growers to produce energy crops.

[1] *Department of Agricultural and Environmental Sciences, Tennessee State University, TN*

* *Corresponding Author*

Rationale and Significance

Per capita energy consumption goal in Tennessee for 2012 was 284.3 million Btu, out of that 28 percent account for transportation sector which is the second largest energy-consuming sector of the State's economy (EPA, 2005). This dependency makes Tennessee's economy very vulnerable to price fluctuations and shortages in petroleum production. However, the State's energy security could improve with diversification of renewable energy sources. Local production of biofuel would not only improve Tennessee' economic security but also provide employment opportunities in Tennessee. The paper compares the preliminary economic analysis of feedstock production from switchgrass and Miscanthus under Tennessee's growing condition.

Data Sources and Analytical Framework

In biofuel feedstock production, the cost of producing each feedstock includes commonly used cost categories from land preparation to harvesting. The analysis assumes that feedstock production is on non-prime land under rain fed conditions hence irrigation was not considered.

From an economic point of view, the overall approach is to estimate average annual costs and returns over the entire economic life of the crop, which allows for direct comparison among different crops. To calculate costs and revenues in annual equivalent terms, the present values of all costs and revenues over the useful life of the crop were transformed into an equivalent annuity.

The cost of production data for switchgrass was based on University of Tennessee Extension and production costs of *Miscanthus* were based on data from University of Illinois at Urbana-Champaign (khanna et al., 2008) and Mississippi State University (MSU). The dry matter yield of switch grass and *Miscanthus* were based on Ugarte et al., 2007 and Busby et al., 2007 respectively. Price per ton of dry matter was based on Ugarte et al., 2007. Accordingly, four different price scenarios were used for sensitivity analysis for net return from feedstock production. Processing cost per gallon of ethanol for cellulostic biomass is based on Frosch et al., 2008. The wholesale price of ethanol is based on historical price of Energy Information Administration (EIA). Prices were inflated to reflect current prices in Tennessee using appropriate inflation rates.

Preliminary Results

Net returns of the bioenergy crops investigated, *Miscanthus* shows a positive net return per acre (see table1 for details). Annualized net returns after conversion to ethanol show that only *Miscanthus* production is having positive net returns from ethanol production. This is due to the crop's high energy yield (conversion to ethanol). However, it should be noted that conversion costs to ethanol from cellulosic feedstock is still under investigation and hence the results should be interpreted with caution. Profitability is sensitive to price paid by the ethanol producers. When the different price and conversion scenarios were introduced, the ethanol production from grass species varies.

Table 1. Feedstock and Ethanol Production, Costs and Revenues: Switchgrass and *Miscanthus* (preliminary results)

Cost items	**Unit**	**Switchgrass**	***Miscanthus***
A. Feedstock Production			
Total costs	$/acre	$428.32	$638.66
Primary production	tons/acre	8.23	14.47
Gross revenue	$/acre	$298.86-$521.42	$511.57-$892-53
Net revenue	$/year	-$93.05- -$101.33	$297.17- -$18.78
B. Production of Ethanol			
Total processing cost	$/acre	$557.91-$768-79	$980.58-$1188
Total production cost	$/acre	$986.28-$1197.16	$1619.23-$1826.65
Gross revenue (ethanol)	$/acre	$1114.78-$1325.78	$1959.33-$2330.19
Tax credit	$/acre	$234.32-$283.89	$411.84-$498.96
Net revenue (ethanol)	$/acre	$362.82-$412.52	$751.93-$1002.49
Feedstock cost of ethanol	$/1000 Btu	$0.01	$0.02
Feedstock cost of ethanol	$/gallon	$0.52--$0.78	$0.44-$0.66
Break- even price of feedstock	$/MT	$52.05	$44.15
Break- even price of ethanol	$/gallon	$1.53-$1.79	$1.41-$1.67

Figure 1 shows the changes in annualized net returns form feedstock production under different price scenarios. Under present per acre dry matter yield of switchgrass, net return from feedstock production is not profitable under price range between $47-$82. However, given present dry matter yield scenario, *Miscanthus* is profitable even under $47/ton price scenario.

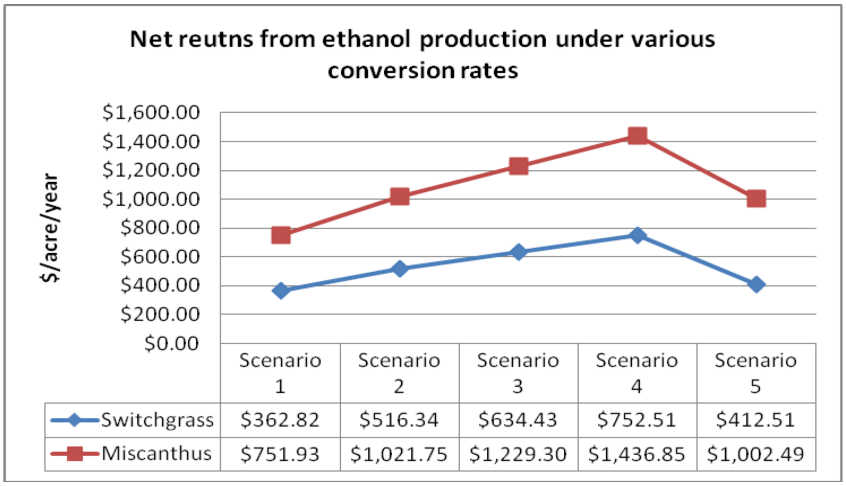

Scenario 1: Conversion rate of ethanol per ton of dry matter = 67 gallons
Scenario 2: Conversion rate of ethanol per ton of dry matter = 80 gallons
Scenario 3: Conversion rate of ethanol per ton of dry matter = 100 gallons
Scenario 4: Variable conversion rates of ethanol per ton of dry matter over time
For 1-5 years (67/65 gallons), for 6-10 years (80 gallons), for 11-15 years (90 gallons), for 16-20 years (100 gallons), for 21-25 years (110 gallons)

Figure 1. Sensitivity of annualize net returns to changing feedstock prices

Annualized net return from ethanol production is profitable even at lower conversion rates (see Figure 2) for both Switchgras and *Miscanthus*. However the value of net return is significantly higher for *Miscanthus* compared to Switchgrass.

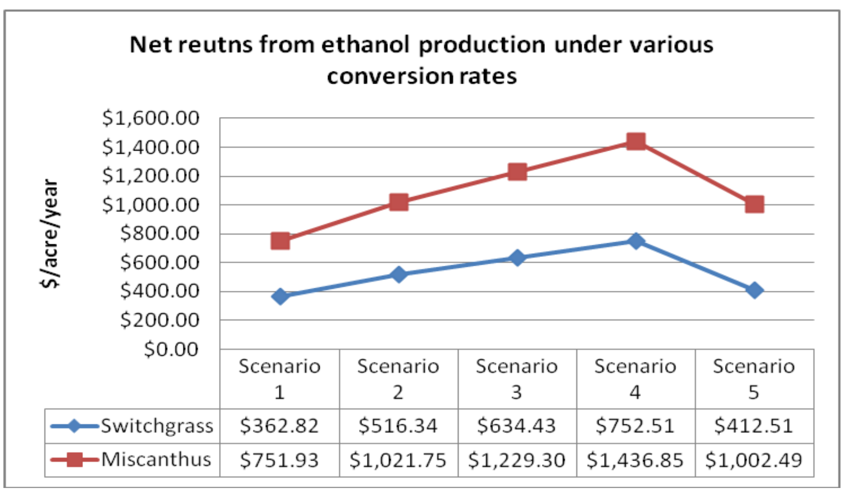

Figure 2. Sensitivity of annualize net returns from ethanol to conversion technology

Figure 3 shows the feedstock costs for gallon of ethanol under various conversion rates. For both switchgrass and *Miscanthus*, feedstock costs per gallon of ethanol is under $1.00 even at lower conversion rate of 67 gallons/dry ton. For switchgrass feedstock cost per gallon of ethanol ranges from $0.52-$0.78 while for *Miscanthus* it ranges from $0.44-$0.66 in conversion rate of 67 gallons/dry ton and above.

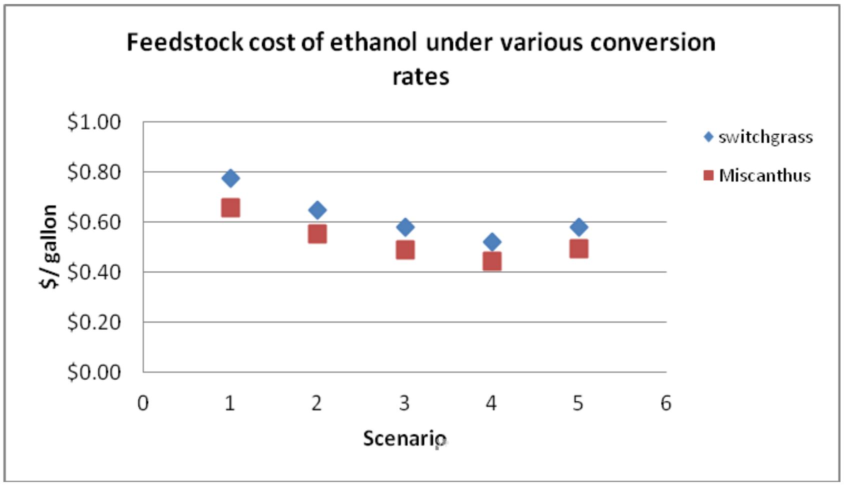

Figure 3. Chaning feedstock costs of ethanol to conversion technology

Ethanol from *Miscanthus* can be priced at $1.67 at conversion rate of 67 galllons/dry ton but it can be priced as low as $1.41 for higher conversion rates. The, breakeven price of ethanol from switchgrass ranges from $1.53-$1.79/gallon.

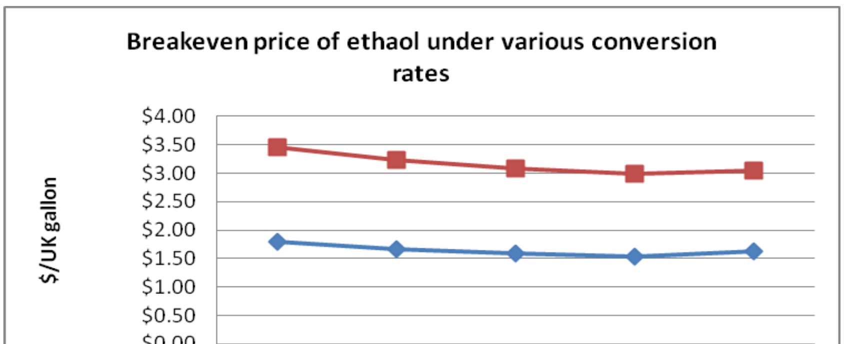

	Scenario 1	Scenario 2	Scenario 3	Scenario 4	Scenario 5
Miscanthus	$1.67	$1.56	$1.50	$1.45	$1.41
Switchgrass	$1.79	$1.66	$1.59	$1.53	$1.63

Figure 4. Breakeven price of ethaol under various conversion rates

Conclusion

The net returns analysis shows that there is potential for *Miscanthus* as bioenergy crop since it showed a positive net return for either case (i.e., when the price of *Miscanthus* is measured as a feedstock or in terms of ethanol). Production of switchgrass showed negative net returns due to low yields. When different price scenarios were considered, a positive net return was observed for both switchgrass and *Miscanthus* in producing ethanol. Also under higher conversion rates, ethanol production from both crops is economical. The lack of accounting all impacts of a biofuel project is a limitation of the analysis. Hence, physical, environmental and socio-economic impacts should be accounted for to evaluate regional impacts of a future biofuel project. The results generated here are preliminary and should interpret with caution.

References

Busby, D., R.D. Little, S. Shaik, A. Martins, F. Epplin, S. Hwang, B.S. Baldwin, and C.M. Taliaferro. 2007. Yield and Production Costs for Three Potential Dedicated Energy Crops in Mississippi and Oklahoma Environments. Paper prepared for Southern Agricultural Economics Association Meeting, Mobile, Alabama.

Energy policy act of 2005. Available [online] http://www.gpo.gov/fdsys/pkg/PLAW-109publ58/pdf/PLAW-109publ58.pdf (Accessed May 31, 2012).

Frosch, Brian J., Roland J. Fumasi, James W. Richardson, Joe L. Outlaw, Brian K. Herbst. 2008. Integration of Agriculture and Energy Systems Conference, Atlanta, GA. Farm Foundation.

Goldemberg J. Ethanol for a sustainable future. *Science;* 315 (5813): 808-10; 2007.

Khanna, Madhu, Basanta Dhungana, John Clifton-Brown. 2008. Costs of producing *Miscanthus* and switchgrass for bioenergy in Illinois. Biomass and Bioenergy 32: 482 – 493.

McLaughlin, S.B and M.E. Walsh. 1998. Evaluating environmental consequences of producing herbaceous crops for bio-energy. *Biomass and Bioenergy*, 14 (4): 317-324.

Mississippi State University. Giant *Miscanthus* budget (working paper). Available [online] http://www.agecon.msstate.edu/what/policy/bioenergy/pdf/*Miscanthus*%20Enterprise%20Budgets.pdf (Accessed on March 15, 2012).

Ugarte, Daniel G. De La Torre, Burton C. English, Kim L Jensen, Chad M. Hellwinckel and R. Jamey Menard. 2007. Expanding the role of biofuels in America's energy portfolio: analysis of the 25x'25 vision. Biofuels, Food & Feed Tradeoffs. Proceedings of a conference April 12-13, 2007, in St. Louis, Missouri.

World Watch Institute. 2006. Biofuels for transportation. Global potential and implications for sustainable agriculture and energy in the 21st century. Extended Summary. A report prepared by the World Watch Institute for the German Federal Ministry of Food, Agriculture and Consumer Protection.

5.8 FARMERS' WILLINGNESS TO PRODUCE ALTERNATIVE CELLULOSIC BIOFUEL FEEDSTOCKS IN KANSAS USING STATE CHOICE EXPERIMENTS

Jason S. Bergtold[1,], Jason Fewell[2], Jeffrey Williams[3]*

Abstract

Many studies have assessed the technical feasibility of producing bioenergy crops on agricultural lands. However, while it is possible to produce large quantities of agricultural biomass for bioenergy from lignocellulosic feedstocks, very few of these studies have assessed farmers' willingness to produce these crops under different contracting arrangements. The purpose of this paper is to examine farmers' willingness to produce alternative cellulosic biofuel feedstocks under different contractual, market, and harvesting arrangements. This is accomplished by using enumerated field surveys in Kansas with stated choice experiments eliciting farmers' willingness to produce corn stover, sweet sorghum and switch grass under different contractual conditions. Using a random utility framework to model the farmers' decisions, the paper examines the contractual attributes most likely to increase the likelihood of feedstock enterprise adoption. Results indicate that net returns above the next best alternative use of the land, contract length, cost-share, financial incentives, insurance, and custom harvest options are all important contract attributes. Farmers' willingness to adopt and their willingness-to-pay for alternative contract attributes vary by region.

Keywords: Adoption, Biofuels, Cellulosic Feedstocks, Contract, Corn Stover, Sweet Sorghum, Stated Choice, Switchgrass, Willingness-to-Pay

Introduction

Despite yearly standards set by the Environmental Protection Agency (EPA), the production of biofuels from cellulosic biofuel feedstocks continues to fall short of projected levels, the majority of which are mandated to be from biomass-based diesel, advanced biofuels, and total renewable fuels. The Energy Information Administration (EIA) in conjunction with the EPA, projects that 8.65 million gallons of cellulosic biofuel will be produced in 2012, which is approximately 1/60 of the 0.50 billion gallon biofuel production goal set for this year(U.S. EPA 2011). According to the "EPA Finalized 2012 Renewable Fuel Standards" the original target levels may still be attainable (U.S. EPA 2011); and as per the standards set by the Energy Independence and Security Act of 2007, any new biofuels produced after 2016 must originate from cellulosic feedstocks (U.S. Congress, House of Representatives 2007).

A growing body of research concerning the production of biofuels has focused on the technical and economic feasibility, as well as the potential supply of alternative sources of cellulosic biofuel feedstocks (see Babcock *et al*. 2007; Bangsund *et al*. 2008; De la Torre Ugarte *et al*. 2007; Gallagher *et al*. 2003; Graham *et al*. 2007; Larson *et al*. 2005; Larson *et al*. 2008; Mapemba and Epplin 2004; Nelson *et al*. 2010; Perlack *et al*. 2005; Perrin *et al*. 2008; Propheter *et al*. 2010; and Walsh *et al*. 2003). These studies establish the feasibility of a market, but do not examine the

---

[1] *Department of Agricultural Economics, Kansas State University, KS*

[2] *Department of Agricultural Economics, Kansas State University, KS*

[3] *Department of Agricultural Economics, Kansas State University, KS*

** Corresponding Author*

necessary market and institutional conditions for a market to develop (Rajagopal *et al*. 2007). Rajagopal and Zilberman (2007) indicate that their still exists a need to understand the factors that lead to the adoption of biofuel technologies by farmers.

Research examining the adoption of alternative cellulosic feedstocks is limited (see Bransby 1998; Hipple and Duffy 2002; Jensen *et al*. 2007; Kelsey and Franke 2009; Paulrud and Laitila 2010; and Sherrington *et al*. 2008). It is likely that farmers will supply cellulosic feedstocks only if a contract is offered by processors (Rajagopal *et al*. 2007). Contractual arrangements will be affected by many factors, such as contract pricing, timeframe, acreage commitments, risk, timing of harvest, yield variability, feedstock quality, harvest responsibilities (*e.g.* custom harvesting), nutrient replacement, location of biorefineries, available cropping choices, technology, and conservation considerations (Altman *et al*. 2007; Epplin *et al*. 2007; Glassner *et al*. 1998; Larson *et al*. 2007; Stricker *et al*. 2000; Wilhelm *et al*. 2004). Contractual arrangements with individuals or groups of producers (*e.g.* via a cooperative) is likely necessary to ensure an adequate supply of feedstocks in the long-term (Rajagopal *et al*. 2007; Epplin *et al*. 2007).

The purpose of this study is to examine farmers' willingness to produce alternative cellulosic biofuel feedstocks under alternative contractual arrangements. Specifically, the study focuses on three feedstocks: corn stover, sweet sorghum and switchgrass, to examine a value-added option, a dedicated annual bioenergy crop, and dedicated perennial energy crop suitable to the Great Palins region. Farmers' willingness to produce under different contractual arrangements is assessed using an enumerated field survey with stated choice techniques. The survey examines what contractual features farmers' prefer and their impact on the potential likelihood of a farmer adopting a biomass feedstock enterprise. A stated choice approach following Louviere et al. (2000) is used to assess farmers' willingness to adopt and survey results are analyzed using a conditional logistic regression model with error components (Bhat 1998; Greene 2007).

Data and Methods

Survey

A survey was administered from November 2010 to February 2011 by Kansas State University and the USDA, National Agricultural Statistics Service (NASS) to assess farmers' willingness to produce cellulosic biomass in the form of corn stover, sweet sorghum, and switchgrass for bioenergy production under different contractual arrangements. A total of 485 farmers where contacted in northeastern, south central, and western Kansas to participate in the survey. These areas of Kansas were selected based on the number of farms growing corn and sorghum; differences in climatic conditions; and use of irrigation. In each area, a random sample of approximately 160 farms over 260 acres in size and $50,000 in gross farm sales were selected from USDA-NASS's farmer list. The stated choice component of the survey was field tested with focus groups at an annual extension conference and then the entire survey was tested using face-to-face interviews with farmers in the targeted study areas.

Potential participants were mailed a four page flier asking for their participation in the survey and providing information about cellulosic biofuel feedstock production on-farm one week prior to being contacted by USDA-NASS enumerators. USDA-NASS enumerators then scheduled one hour interviews with the farmers to complete the survey and stated choice experiments. Interviews, on average took 57 minutes to complete. Upon completion of the survey and receipt at the USDA-NASS office in Topeka, farmers were compensated for their time with a $15 gift card. Of the 485 farmers contacted, 290 completed the survey and 38 were out-of-business, did not farm, or could not be located, giving a response rate of 65 percent. Farmers were asked about their farming operation; willingness to produce feedstocks under contract; biofuel feedstock production preferences and perceptions; conservation on-farm; risk management practices and perceptions; crop marketing practices; and demographics.

Farmer demographics taken from the 2007 U.S. Census of Agriculture (NASS 2009) were used to determine whether the survey respondents are representative of Kansas farmers. Table 1compares some of the demographics as reported by farmers in the survey to statewide numbers as recorded in the 2007 Census of Ag. Farms in the survey are slightly larger in size on average, due to the selection criteria used.

Table 1. Comparison of Kansas Farmer Demographics to Survey Respondents

	2007 Census of Agriculture[a]	Survey
Age	57.7 years	55.1 years
Average size of farm	707 acres	2172 acres
Average amount of rented land on farm	863 acres	1271 acres
Average amount of owned land on farm	381 acres	900 acres
Average amount of permanent pasture land on farm	398 acres	594 acres
Average market value of agricultural products	$219,944	$200,000 to $399,999[b]

[a] *Source*: National Agricultural Statistics Service, USDA, 2007
[b] Category represents the one chosen with the highest frequency by respondents.

Stated Choice Experiments

A stated choice experiment was designed to assess farmers' willingness to enter into a contract with a bio-refinery or other biomass processor for producing corn stover, sweet sorghum and switchgrass following Louviere *et al*. (2000) and Roe *et al*. (2004). Farmers where presented with information about the production of each feedstock and potential contract attributes before answering the stated choice questions. Survey participants where then asked to consider 5 independent choice scenarios, where they were asked to select between two biomass contracts or an "opt out" option (see Figure 1 for an example scenario for each feedstock). The contract attributes, descriptions and levels used to develop the stated choice scenarios are provided in Table 2.

Corn Stover Scenario:

		Contract A	Contract B	Option C
Contract Features	**Net Returns**	$0/acre/year	$30/acre/year	Do Not Adopt
	Contract Length	2 years	2 years	
	Biorefinery Harvest	Yes	No	
	Nutrient Replacement	No	Yes	
	Your Ranking (1-3)	2003	2004	2005

Sweet Sorghum Scenario:

		Contract A	Contract B	Option C
Contract Features	**Net Return Above Sorghum/ Corn Production (Base: $50/ac)**	45% Higher/year	0% Higher/year	Do Not Adopt
	Contract Length	5 Years	2 Years	
	Biorefinery Harvest	Yes	No	
	Insurance Availability	No	No	
	Gov. Incentive Payment	None	25%	
	Your Ranking (1-3)	2048	2049	2050

Switchgrass Scenario:

		Contract A	Contract B	Option C
Contract Features	**Net Return Above Hay Production/CRP Rental Rates (Base: $40/ac)**	35% Higher/year	35% Higher/year	Do Not Adopt
	Contract Length	7 Years	16 Years	
	Biorefinery Harvest	Yes	Yes	
	Insurance Available	No	Yes	
	Seed/Establishment Cost-Share	70%	None	
	Your Ranking (1-3)	2069	2070	2071

Figure 1: Example Choice Scenarios/Questions for Stated Choice Experiments

Table 2: Contract Attributes and Levels for State Choice Experiments for Corn Stover, Sweet Sorghum and Switchgrass

Contract Attribute	Description	Levels
Net Returns (for all features of the contract except cost-share and government payments)	*For Corn Stover*: Represents the ***average annual expected net return*** above variable costs under the contract to the farmer on a per acre basis. This amount is received after all expenses are paid, including harvest and nutrient replacement. *For Sweet Sorghum and* Switchgrass: Represents the expected ***percentage*** gain under the contract ***above*** net returns associated with corn/sorghum production for sweet sorghum and hay production and/ or CRP rental payments for switchgrass on a farmers operation. As a reference point, on average, returns from corn/sorghum production are expected to be $50 per acre and hay production or income from land in CRP are expected to be around $40 per acre in Kansas.	*For Corn Stover:* $0, $10, $20 and $30 *For Sweet Sorghum*: 0%, 15%, 30% and 45% *For Switch-grass*: 5%, 20% and 35%
Contract Length	Represents the time commitment in consecutive years of the contractual agreement.	*For Corn Stover and Sweet Sorghum*: 2,5 and 8 years *For Switch-grass:* 7 and 16 years
Biorefinery Harvest	"Yes" indicates the bio-refinery will harvest the biomass at their expense, and "No" means the farmer is responsible for harvest (including cutting, raking, baling and transportation to the bio-refinery). Harvest charges are included in the percentage net return. That is, the charges are considered paid regardless of who harvests the biomass.	Yes or No
Insurance Availability (Sweet Sorghum and Switchgrass Only)	"Yes" indicates crop insurance is available, and "No" otherwise.	Yes or No
Nutrient Replacement (Corn Stover Only)	"Yes" indicates the bio-refinery will provide the farmer a negotiated amount for lost nutrients (N, P and K) from biomass removal, and "No" otherwise. This amount is assumed to be included in the annual expected net returns. In other words, a "Yes" includes net returns with nutrient replacement costs accounted for.	Yes or No
Government Incentive Payment (Sweet Sorghum Only)	This incentive payment is provided at two levels for production of cellulosic biofuel feedstocks delivered to a bio-refinery. The incentive levels are either none (0) or 25 percent of the price per dry ton of biomass delivered to the refinery. The incentive received is in addition to the net returns above production.	0% and 25%
Seed/Establishment Cost Share (Switchgrass Only)	Indicates a percentage of seed/establishment costs are covered or cost-shared by the biorefinery or processor during the first two years of production or after planting due to lower yields during the establishment period. Establishment costs can range from $150 to $200 per acre. This will be provided every time the crop is replanted. This cost-share is provided in addition to the net returns indicated above.	0%, 35% and 70%

Following Louviere *et al*. (2000), a $(2^3 \times 3 \times 4)^3$ fractional factorial experimental design was used to develop 90 random choice scenarios to be able to identify all main effects and potential interaction effects between attributes and levels. The choice sets were then randomly assigned into 18 blocks, so that each respondent was faced with 5 choice scenarios for each feedstock alternative. Thus, there were 18 versions of the survey. Of the 290 surveys completed, 12 to 20 of each version were completed.

Model

Following Roe *et al*. (2004), we assume that producers want to maximize expected discounted utility when choosing to adopt a contract to produce a cellulosic feedstock. Let producer's *j*'s expected discounted utility for contract option *i* be given by:

$$V_{j,i} = V\left(\Delta R_i, B_i, S_i, C_i, G_i, E_{j,i}\right) + \varepsilon_{j,i}\ , \qquad (1)$$

where ΔR_i is the net returns above the next best alternative enterprise over time; B_i is a variable indicating if a biomass harvest option is part of contract *i*,; S_i is a variable indicating if crop insurance is available; C_i is the length of the contract in years; G_i is the level of government incentive payment, cost share or nutrient replacement; and $E_{j,i}$ is a vector of error components included to account for choice situation invariant variation. It is assumed that all $E_{j,i}$ are mean zero with variance equal to one (Greene 2007). The error term, $\varepsilon_{j,i}$ represents the nonsystematic part of expected utility that is unobserved by the modeler and is distributed type I extreme value (Louviere *et al*. 2000).

The econometric model is based upon a main effects model with error components following Bhat (1998). Focusing on the reduced-form representation of expected utility for equation (1) (see Roe *et al*. 2004), for producer *j* and contract *i*:

$$V_{j,i} = \beta_0 + \beta_1 \Delta R_i + \beta_2 C_i + \beta_3 B_i + \beta_4 S_i + \beta_5 G_i + \textstyle\sum_i \theta_j E_{j,i} + \varepsilon_{j,i}, \text{ for } j = A, B \text{ or } C, \qquad (2)$$

where θ_i represents the standard deviation of the error component or random effect associated with $E_{j,i}$. The error components allow the model to capture correlations among contract or choice alternatives in the model (Greene 2007). For the "opt out" option in each choice scenario, $\boldsymbol{\beta} = 0$, making $V_{C,i} = \theta_C E_{C,i} + \varepsilon_{j,i}$. Models are estimated using NLOGIT 4.0 using simulated maximum likelihood with 1000 Halton draws using the BFGS Quasi-Newton Algorithm (Greene 2007).

Results

Under favorable contractual conditions, survey results indicate that 56.6, 84.9 and 83 percent of farmers would be willing to adopt a value-added feedstock enterprise, such as corn stover, in western, central and northeastern Kansas, respectively. For a dedicated annual bioenergy crop, such as sweet sorghum, 60.6, 68.8 and 61.1 percent of farmers would be willing to adopt in western, central and northeastern Kansas, respectively. Finally, 36.4, 54.3 and 45.3 of farmers would be willing to adopt a perennial bioenergy crop option, such as switchgrass, in western, central and northeastern Kansas, respectively. Thus, adoption of these options does vary by region and the difference in adoption rates between alternative feedstocks likely indicates the differences in how farmers view each of these feedstock options. For example, corn stover is a value-added enterprise, sweet sorghum can be rotated with traditional cash crops, and switchgrass is a perennial option that may be grown on marginal lands.

Table 3 shows the econometric modeling results and select willingness-to-pay measures for the conditional error component logistic regression models estimated for corn stover, sweet sorghum and switchgrass. The McFadden Pseudo-R^2 values indicate a relatively good fit for the models to the data. Two dummy variables (for the northeast and central regions) to capture differences across regions were included in each model. While the northeastern dummy variable was not statistically significant, the central dummy variable was significant in all the models, indicating farmers in the central region of Kansas were more likely to adopt than farmers in western Kansas.

Coefficient estimates in Table 3 indicate, as expected, that as net returns per acre under the contract increase (relative to the next best alternative) the likelihood of producing a feedstock will increase. Furthermore, as the length of a contract increases, the likelihood of production for each feedstock decreases, indicating farmers find longer contracts undesirable, possibly due to reduced management flexibility for the farmer. Having a biorefinery harvest option increases the likelihood of producing all of the feedstocks, providing more flexibility for timing of farming operations. The availability of insurance increases the likelihood of farmers producing both sweet sorghum and switchgrass, reducing the potential risks faced by farmers under contract. For corn stover, nutrient replacement is a significant concern (Wilhelm *et al*. 1986); and farmers are more likely to harvest corn stover if the nutrients are replaced. Incentive payments and establishment cost share both increase the likelihood of producing sweet sorghum and switchgrass, respectively. Given the 2 to 3 year period needed to establish switchgrass, biomass revenues during this time may be substantially reduced, necessitating the need for cost-share to entice farmers to adopt (Gunther 2011).

Farmers may be willing to give up or require more net returns, depending on the favorability of the contract negotiated. Results in Table 3 indicate that farmers may be willing to reduce the level of net returns by $1 to $2 per acre under contract for each year taken off the contract. If the biorefinery or biomass process is not willing to harvest the biomass, then farmers will require $2 to $11 in additional net returns per acre under contract, depending on the crop option selected. For corn stover, if a nutrient replacement option is not provided, the farmer would require an additional $11 in net returns per acre under contract. For sweet sorghum and switchgrass, the availability of insurance would reduce the needed net return per acre under contract by $1.50 to $5.

Table 3: Conditional Error Component Logistic Regression Results and Willingness-to-Pay Estimates for Selected Attributes for Corn Stover, Sweet Sorghum and Switchgrass

Variable (Attribute)[c]	Corn Stover			Sweet Sorghum			Switchgrass	
	Coefficient Estimate (Standard Error)[a]	Willingness-to-Pay[b]		Coefficient Estimate (Standard Error)[a]	Willingness-to-Pay[b]		Coefficient Estimate (Standard Error)[a]	Willingness-to-Pay[b]
Intercept	-5.84** (0.37)	---		-3.75** (0.37)	---		-4.68** (0.051)	---
Northeast[d]	0.12 (0.36)	---		-0.52 (0.42)	---		-0.77 (0.51)	---
Central[d]	1.21** (0.37)	---		1.23** (0.43)	---		1.28* (0.55)	---
Net Returns	0.13** (0.0085)	---		0.14** (0.0084)	---		0.16** (0.018)	---
Contract Length	-0.20** (0.031)	-$1.55		-0.31** (0.026)	-$2.15		-0.17** (0.016)	$-1.02
Biorefinery Harvest Option	1.41** (0.15)	$10.69		1.02** (0.15)	$7.05		0.34** (0.078)	$2.09
Insurance Availability	---	---		0.73** (0.15)	$5.06		0.24** (0.087)	$1.48
Nutrient Replacement	1.47** (0.14)	$11.20		---	---		---	---
Government Incentive Payment	---	---		0.041** (0.0067)	---		---	---
Seed/Est-ablishment Cost Share	---	---		---	---		0.025** (0.0029)	---
McFadden Pseudo R^2	0.52			0.45			0.56	

[a] ** indicates statistical significance at the 0.01 level and * indicates statistical significance at the 0.05 level.
[b] Willingness-to-Pay for an attribute is calculated as the attribute coefficient divided by the *net returns* attribute coefficient following Hensher et al. (2005).
[c] All binary attributes are all effects coded for model estimation. Estimates of the error components are not shown and are available from the authors upon request. The error components were statistically significant.
[d] *Northeast* and *Central* are fixed effects to capture differences in the three regions surveyed in Kansas. The intercept term captures the western region.

Conclusions

The paper examines farmers' willingness to produce alternative cellulosic biofuel feedstocks under alternative contractual arrangements. The study finds that the level of net returns above the next best alternative enterprise, contract length, having a biorefinery harvest option, availability of insurance, and having monetary incentives/cost-share are important contract attributes. In addition, the adoption of different feedstock varieties varies by location and by feedstock type. Bio-refineries looking to establish facilities and a local market should take these considerations into account when trying to locate their facilities and negotiate contracts with farmers.

Acknowledgements

Funding for the primary portion of this project came from the South Central Sun Grant Initiative and Department of Transportation (Award No. DTOS59-07-G-00053), with additional funds from the National Science Foundation, EPSCoR Division, Research Infrastructure Improvement (Award No. 0903806).

References

Altman, I., C.R. Boessen and D.R. Sanders. "Contracting for Biomass: Supply Chain Strategies for Renewable Energy." Paper presented at the Southern Agricultural Economics Association Annual Meeting, Mobile, Alabama, February 3 – 6, 2007. Online. Available at: http://ageconsearch.umn.edu/bitstream/34907/1/sp07al01.pdf (accessed August 30, 2012).

Babcock, Bruce A, Philip W Gassman, Manoj Jha, and Catherine L Kling. 2007.*Adoption Subsidies and Environmental Impacts of Alternative Energy Crops.* Briefing Paper 07-BP 50, Center for Agricultural and Rural Development, Iowa State University, Agricultural Marketing Resource Center, 2007.

Bangsund, Dean A, Eric A DeVuyst, and F Larry Leistritz. 2008. *Evaluation of Breakeven Farmgate Switchgrass Prices in South Central North Dakota.* Agribusiness and Applied Economics Report No. 632, Dept. of Agribusiness and Applied Economics, North Dakota State University.

Bhat, C.R. 1998. "Accommodating Flexible Substitution Patterns in Multidimensional Choice Modeling: Formulation and Application to Travel Mode and Departure Time Choice", *Transportation Research Part B* 7: 455-466.

Bransby, D.I. "Interest Among Alabama Farmers in Growing Switchgrass for Energy." Paper presented at BioEnergy '98: Expanding Bioenergy Partnerships, Madison, Wisconsin, October 4 – 8, 1998. Online. Available at: http://bioenergy.ornl.gov/papers/bioen98/bransby1.html (accessed August 30, 2012).

De La Torre Ugarte, Daniel G, Burton C English, and Kim Jensen. 2007. "Sixty Billion Gallons by 2030: Economic and Agricultural Impacts of Ethanol and Biodiesel Expansion." *American Journal of Agricultural Economics* 89: 1290-1295.

Epplin, F.M., C.D. Clark, R.K. Roberts and S. Hwang. 2007. "Challenges to the Development of a Dedicated Energy Crop." *American Journal of Agricultural Economics* 89: 1296 – 1302.

Gallagher, P.W., M. Dikeman, J. Fritz, E. Wailes, W. Gauthier and H. Shapouri. 2003. "Supply and Social Cost Estimates for Biomass from Crop Residues in the United States." *Environmental and Resource Economics* 24: 335 – 358.

Graham, R L, R Nelson, J Sheehan, R D Perlack, and L L Wright. 2007. "Current and Potential U.S. Corn Stover Supplies." *Agronomy Journal* 99: 1-11.

Glassner, D.A., J.R. Hettenhaus and T.M. Schechinger. "Corn Stover Collection Project." Paper presented at BioEnergy '98: Expanding Bioenergy Partnerships, Madison, Wisconsin, October 4 – 8, 1998. Available at: http://ergosphere.files.wordpress.com/2007/04/bio98_corn_stover.pdf (accessed August 30, 2012).

Greene, W.H. 2007. *NLOGIT Version 4.0: Reference Guide*. Plainview, NY: Econometric Software, Inc.

Gunther, T.P. "Establishment of Swtichgrass in Corn Across a Landscape Gradient: Establishment, Yield and Quality of Biomass Feedstock." M.S. Thesis, Iowa State University. Available at: http://lib.dr.iastate.edu/etd/10464 (accessed August 30, 2011).

Hensher, D.A., J.M. Rose, and W.H. Greene. 2005. *Applied Choice Analysis: A Primer*. Cambridge UK: Cambridge University Press.

Hipple, P.C. and M.D. Duffy. "Farmers' Motivations for Adoption of Switchgrass." In: *Trends in New Crops and New Uses*, eds. J. Janich and A. Whipkey, 252 – 266. Alexandria, VA: ASHA Press.

Jensen, K., C.D. Clark, P. Ellis, B. English, J. Menard, M. Walsh and D. de la Torre Ugarte. 2007. "Farmer Willingness to Grow Switchgrass for Energy Production." *Biomass and Bioenergy* 31: 773 – 781.

Kelsey, K.D. and T.C. Franke. 2009. "The Producers' Stake in the Bioeconomy: A Survey of Oklahoma Producers' Knowledge and Willingness to Grow Dedicated Biofuel Crops." *Journal of Extension*. 47: http://www.joe.org/Joe/2009february/pdf/JOE_v47_1rb5.pdf (accessed August 30, 2012).

Larson, James A, Burton C English, Chad Hellwinkel, Daniel G De La Torre Ugarte, and Marie Walsh. "A Farm-Level Evaluation of Conditions Under Which Farmers will Supply Biomass Feedstocks for Energy Production." Paper presented at American Agricultural Economics Association Annual Meeting, Providence, RI, July 24 – 27, 2005.

Larson, J.A., B.C. English and L. Lambert. "Economic Analysis of the Conditions for Which Farmers Will Supply Biomass Feedstocks for Energy Production." Final Report for Agricultural Marketing Center Special Projects Grant 412-30-54, Agricultural Marketing Resource Center, University of Tennessee, 2007. Available at: http://www.agmrc.org/media/cms/2007UTennProjDeliverable_9BDDFC4C2F4E5.pdf (accessed August 30, 2012).

Larson, James A, Burton C English, and Lixia He. "Risk and Return for Bioenergy Crops Under Alternative Contracting Arrangements." Paper presented at the Southern Agricultural Economics Association Annual Meeting, Dallas, TX, February 2-6, 2008.

Louviere, J.J., D.A. Hensher and J.D. Swait. 2000. *Stated Choice Methods: Analysis and Application*. Cambridge, UK: Cambridge University Press.

Mapemba, Lawrence, and Francis M Epplin. "Lignocellulosic Biomass Harvest and Delivery Cost." Paper presented at the Southern Agricultural Economics Association Annual Meetings, Tulsa, OK, February 14-18, 2004.

National Agricultural Statistics Service. *2007 Census Publication.* USDA National Agricultural Statistics Service, Available at: http://www.agcensus.usda.gov/Publications/2007/index.php (accessed February 3, 2009).

Nelson, R., M. Langemeier, J. Williams, C. Rice, S. Staggenborg, P. Pfromm, D. Rogers, D. Wang, and J. Nippert. "Kansas Biomass Resource Assessment: Assessment and Supply of Select Biomass-based Resources." Research report prepared for the Kansas Bioscience Authority, Olathe, KS, September 2010.

Paulrud, Susanne, and Thomas Laitila. 2010. "Farmers' Attitudes About Growing Energy Crops: A Choice Experiment Approach." *Biomass and Bioenergy* 34: 1-10.

Perlack, R.D., L.L. Wright, A.F. Turhollow, R.L. Graham, B.J. Stokes and D.C. Erbach. *Biomass as Feedstock for a Bioenergy and Bioproducts Industry: The Technical Feasibility of a Billion-Ton Annual Supply*. Washington, DC: U.S. Department of Agriculture and U.S. Department of Energy, 2005.

Perrin, R K, K P Vogel, M Schmer, and R B Mitchell. *Farm-Scale Production Cost of Switchgrass for Biomass.* Agronomy-Faculty Publications, Agronomy and Horticulture Department, University of Nebraska-Lincoln, 2008.

Propheter, J L, S A Staggenborg, S Wu, and D Wang. 2010. "Performance of Annual and Perennial Biofuel Crops: Yields During the First Two Years." *Agronomy Journal* 102: 806-814.

Rajagopal, D., S.E. Sexton, D. Roland-Holst and D. Zilberman. “Challenge of Biofuel: Filling the Tank without Emptying the Stomach?” *Environmental Research Letters*. 2: http://www.iop.org/EJ/article/1748-9326/2/4/044004/erl7_4_044004.html (accessed August 30, 2012).

Rajagopal, D. and D. Zilberman. “Review of Environmental, Economic and Policy Aspects of Biofuels.” Policy Research Working Paper No. 4341. Sustainable Rural and Urban Development Team, Development Research Group, The World Bank. 2007. Available at: http://www.wilsoncenter.org/news/docs/worldbankSept.2007.pdf (accessed August 30, 2012).

Roe, B., T.L. .Sporleder and B. Belleville. 2004. “Hog Producer Preferences for Marketing Contract Attributes,” *American Journal of Agricultural Economics* 86: 115 – 123.

Sherrington, Chris, Justin Bartley, and Dominic Moran. 2008. "Farm-Level Constraints on the Domestic Supply of Perennial Energy Crops in the UK." *Energy Policy* 36: 2504-2512.

Stricker, J.A., S.A. Segrest, D.L. Rockwood and G.M. Prine. “Model Fuel Contract – Co-Firing Biomass with Coal.” Paper presented at the Soil and Crop Science Society of Florida and Florida Nematology Forum, 60th Annual Meeting, Tallahassee, Florida, September 20 – 22, 2000.

U.S. Environmental Protection Agency (EPA). *Regulatory Announcement: EPA Finalizes 2012 Renewable Fuel Standards.* EPA-420-F11-044, U.S. Office of Transportation and Air Quality December, 2011.

U.S. Congress, House of Representatives. *Energy Independence and Security Act of 2007. Title II-Energy Security Through Increased Production of Biofuels; Subtitle A -Renewable Fuel Standard.* Government Printing Office December, 2007.

Walsh, M.E., D.G. de la Torre Ugarte, H. Shapouri and S.P. Slinsky. 2003. “Bionergy Crop Production in the United States.” *Environmental and Resource Economics*. 24: 313 – 333.

Wilhelm, W.W., J.W. Doran, and J.F. Power. 1986. “Corn and Soybean Yield Response to Crop Residue Management Under No-tillage Production Systems. *Agronomy Journal* 78:184-189.

Wilhelm, W.W., J.M.F. Johnson, J.L. Hatfield, W.B. Voorhees and D.R. Linden. 2004. “Crop and Soil Productivity Response to Corn Residue Removal: A Literature Review.” *Agronomy Journal*. 96: 1 – 17.

5.9
ASSESSMENT OF POTENTIAL CAPACITY INCREASES AT COMBINED HEAT AND POWER FACILITIES IN MISSISSIPPI BASED ON AVAILABLE CORN STOVER AND FOREST LOGGING RESIDUE

Joel O. Paz[1,], Selvarani Radhakrishnan[1], Fei Yu[1], Sandra Eksioglu[2], Donald L. Grebner[3]*

Abstract
Biomass materials, such as corn stover and forestry residues, are potential sources for renewable energy for combined heat and power (CHP) production. In this study, we collected and analyzed 10 years of corn stover data (2001-2010) and 3 years of forest logging residue data (1995, 1999, and 2002) in each county in Mississippi to determine the potential of these feedstocks for sustainable CHP energy production. We identified six counties, namely: Amite, Copiah, Clarke, Wayne, Wilkinson and Rankin, that have available forest logging residue to sustain a CHP facility with a range of capacity between 8,044 kW to 9,766 kW. Using corn stover alone, Yazoo and Washington counties can produce 13,430 kW and 13,497 kW of energy, respectively. Considering both feedstocks and based on a conservative amount of 30% available forest logging residue and 33% corn stover, we found that 20 counties have adequate supply for a CHP facility with a capacity of 8,257 kW to 19,564 kW. We found that the 5,000 kW capacity CHP plant in Washington county can be operated with just 13% utilization level of corn stover (CS). The 1,000 kW capacity CHP plant in Scott county can be operated with 7% utilization level of forest logging residue within the county. It was possible to increase the capacity of the CHP plant in Washington county from 5,000 kW to 13,497 kW by using a sustainable CS utilization level of 33%. Similarly in Scott county, a 30% FLR utilization level could potentially increase the capacity of the CHP plant from 1,000 kW to 4,717 kW. The capacities of CHP plants in Scott and Washington counties could increase to 5,193 kW and 14,922 kW, respectively, by combining both types of feedstock.

Keywords. Combined heat and power, sustainability, corn stover, forest logging residue, GIS

Introduction
Combined heat and power is the concurrent process in which heat and power produce in a single process, usually electricity. CHP can produce heat from any fuel source such as natural gas, biomass, biogas and coal. CHP can be applicable for various types of existing technologies for the generating electricity, power, and waste-heat recovery for heating, cooling and thermal applications (Hinnells, 2008). CHP is an efficient and clean way to producing power and thermal energy from a single fuel source. The total CHP system efficiencies are from 60 to 80 percent for producing electricity and thermal energy, which are higher than the average efficiency of conventional power plants (33%) in the United States. These CHP efficiency gains improve the economics, as well as have other environmental benefits (EPA-CHP, 2007).

Forestry is the biggest source of revenue for Mississippi's economy (Munn and Tilley, 2005). About 4 million dry tons of woody biomass is available for energy production, distributed into four major types namely, logging residue (70%), small diameter trees (20%), urban waste (7%), and mill residue (3%) (Perez-Verdin *et al*., 2009). In addition to forest residue, Mississippi has other types of biomass feedstock

[1] Department of Agricultural and Biological Engineering, Mississippi State University, MS

[2] Department of Industrial and Systems Engineering, Mississippi State University, MS

[3] Department of Forestry, Mississippi State University, MS

* Corresponding author

such as corn that can be used for CHP production. Corn production in Mississippi increased significantly from 35,750,000 bushels in 2006 to 134,680,000 bushels in 2007 (NASS, 2012).

The main objectives of this study were to a) determine the potential capacity of CHP plants that can run with available biomass, and b) quantify the sustainable amount of feedstock that can support two biomass based CHP facilities in Mississippi.

Materials and Methods

Available Biomass

Ten years of corn production data (2001-2010) in each county in Mississippi were collected and analyzed to determine the potential of this feedstock for sustainable CHP energy production. Corn production values were obtained by averaging the county production of corn in terms of total bushels produced for the years 2001-2010 (NASS, 2010). Corn production was summed across all Mississippi counties and converted from bushels to tons. Dry weight of corn grain is 56 pounds per bushel (Perlack *et al*., 2002). For this study, one ton of corn stover was produced for every ton of harvested corn grain, based on values reported by Perlack *et al*. (2002). A conservative value of 33% collection rate of stover was used in this study, similar to the value used by (Perlack *et al*., 2002). The moisture content of corn stover was assumed to be 47 percent (Frear *et al*., 2005). The available corn for energy production was calculated using equation 1:

$$\text{Corn stover (dry tons)} = \text{Corn production (in wet tons)} \times 0.33 \times 0.53 \qquad [1]$$

County level dry logging residue data from 1995, 1999, and 2002 were obtained from the Department of Forestry at Mississippi State Univesity. The data were part of an inventory conducted by Periz-Verdin *et al*. (2009) who drew from two main sources, namely, the Mississippi Institute for Forestry Inventory (MIFI) satellite imagery-based data, and Forestry Inventory Analysis (FIA) Timber Products Output database (TPO) forest inventory data. The quantity of logging residues was based on the FIA -TPO forest inventory data as reported by the Southern Research Station. Periz-Verdin *et al*. (2009) converted the average volume of logging residues into dry tons using density values for pine and hardwoods were 0.507 and 0.61 dry tons m^{-3}, respectively of each county. The density values were obtained from a previous study by (Gan and Smith, 2006). According to Perlack *et al*. (2005), not all logging residues are available for bioenergy conversion. Based on this study, it was assumed 65% logging residues are removed during the harvest of conventional products.

Biomass Conversion

The analysis of available biomass feedstock for CHP application focused on existing CHP facilities or plants in Mississippi. There are 22 CHP facilities in the state of Mississippi that generate a total of 570,382 kW (EEA-Inc., 2012). The applications of these units range from dairy facilities with a capacity of 50 kW to oil refineries with a capacity up to 146,900 kW. There are 8 CHP facilities with lower capacities (< 5,000 kW) that are fueled by either wood, wood waste or other biomass sources. Two biomass based CHP plants in Mississippi were selected for this study. The capacity of CHP plants in Scott county and Washington county is 1,000 kW and 5,000 kW, respectively.

Different percentages of available corn stover and forest logging residue for CHP use were evaluated. Several CS and FLR utilization rates ranging from 2 to 33 percent were considered in this study (Figures 1.2 and 1.3). The maximum rates for available corn stover and forest logging residue were 33% and 30%, respectively. High Energy Heating Values (HHV) for corn stover and logging residue were set at 7,560 BTU/lb (dry) and 8,570 BTU/lb (dry), respectively (EPA-CHP, 2012; ANTARES Group Inc., 2008). The energy produced using corn stover and forest logging residue was calculated for each county. For this study, the CHP plants in Scott and Washington counties were assumed to be in operation 24 hours a day, 340 days a year and 8160 hours per year. These values were slightly higher than the operational hours reported by Viana *et al*. (2010). The total CHP energy efficiency was assumed at 70% (EPA-CHP, 2012).

The CHP power rating based on the energy content of feedstock (corn stover or forest logging residue) was calculated using equation [2]:

$$\text{Power Rating} = \text{Feedstock Quantity} * \text{Energy Content of feedstock} * \text{CHP efficiency} \quad [2]$$

One dry ton per day of logging residue and corn stover can produce CHP energy of 146.51 kW and 129.24 kW, respectively.

Results and Discussion

CHP Capacity Based On Available Forest Logging Residue and Corn Stover

The top five Mississippi counties in terms of available forest logging residue are listed in Table 1.1. Each of the 5 counties is covered by forest area that is 80 to 86% of the county area (MIFI, 2005). Thus, these 5 counties are predominately covered by forest and the high percentage of forest land is reflected in the logging residue available in these counties. The top 5 counties can each produce at least 8,257 kW of CHP power from utilizing 30% of available forest logging residue (Table 1.1). The available logging residue tons ranged from 188 tons per day to 222 tons per day. The potential CHP capacities based on available corn stover in the top five Mississippi counties range from 8,021kW to 13,497kW (Table 1.2). These counties are located in the Delta region, which has a predominantly agricultural land cover.

The CHP facility in Washington county has an existing capacity of 5,000 kW. In this study, we found that the CHP plant in Washington county can be operated with just 13% utilization level of corn stover. The 1,000 kW capacity CHP plant in Scott county can be operated with 7% utilization level of forest logging residue within the count, but would require using corn stover at 7% utilization level from adjacent 4 counties. In Washington county, it was possible to increase the capacity of the CHP plant from 5,000 kW to 13,497 kW by using a sustainable CS utilization level of 33%. Similarly in Scott county, a 30% FLR utilization level could potentially increase the capacity of the CHP plant from 1,000 kW to 4,717 kW. The capacities of CHP plants in Scott and Washington counties could increase to 5,193 kW and 14,922 kW, respectively, by combining both types of feedstock (Table 1.3).

Table 1.1. Top 5 Mississippi counties in terms of available forest logging residue and their potential CHP capacities.

County	FLR (ton/day)	County (ton/day)	FLR (kW)
Amite	222	67	9,766
Copiah	219	66	9,617
Clarke	218	66	9,598
Wayne	212	64	9,316
Wilkinson	188	56	8,257

* Forest Logging Residue (FLR), utilization rate (UR)

Table 1.2. Top 5 Mississippi counties in terms of corn stover availability and their potential CHP capacities.

County	CS (ton/day)	County UR at 33% (ton/day)	CS UR at 33% (kW)
Washington	597	197	13,497
Yazoo	594	196	13,430
Sunflower	396	131	8,954
Leflore	393	130	8,878
Sharkey	355	117	8,021

* Available Corn Stover (CS), Utilization Rate (UR)

Table 1.3. Potential capacities of CHP plants in Washington and Scott based on higher utilization rates of corn stover and forest logging residue feedstock.

CHP plant capacity (kW)	CS CHP capacity (kW)	FLR CHP capacity (kW)	CS & FLR CHP capacity (kW)
Washington(5,000)	13,497	1,425	14,922
Scott (1,000)	477	4,717	5,193

*Based on 30% utilization of FLR and 33% utilization of CS

Conclusions

The potential increase in CHP capacity was assessed based on a sustainable utilization rate of available corn stover and forest logging residue in Mississippi. The results show that the available corn stover is 2,048,985 tons/year, and forest logging residues is 2,763,231 tons/year. The total amount of available biomass feedstock is 4,812,216 tons/year, which represents a significant amount of renewable resource that can be utilized for CHP production in Mississippi. In this study, a sustainable corn stover utilization rate of 33% can produce up to 126.9 MW and sustainable forest logging residue utilization rate of 30% can produce 332.7 MW of power using CHP. Mississippi Delta region is the main source for corn stover, while the southwest region of Mississippi has more forested areas, which can be tapped for energy production.

References

ANTARES Group Inc. (2008). "Combined heat and power potential using Texas agricultural wastes", *Report*.

EEA. (2012). Combined Heat and Power Units located in Mississippi; http://www.eea-inc.com/chpdata/States/MS.html. Accessed in May, 2012.

EPA-CHP. (2012). "Catalogue of CHP technologies, Washington DC:" Environmental Protection Agency; http://www.epa.gov/chp/basic/catalog.html. Accessed in May, 2012.

Frear, C., Zhao, B., Fu, G., Richardson, M., Chen, S., & Fuchs, M. R. (2005). Biomass Inventory and Bioenergy Assessment: An Evaluation of Organic Material Resources for Bioenergy Production in Washington State. *Washington State Department of Ecology*.

Gan, J., & Smith, C. T. (2006). Availability of logging residues and potential for electricity production and carbon displacement in the USA. Biomass and Bioenergy, 30(12), 1011–1020.

Hinnells, M. (2008). Combined heat and power in industry and buildings. *Energy Policy*, 36(12), 4522–4526.

McNeil Technologies Inc. (2003). Biomass resource assessment and utilization options for three counties in eastern Oregon. *Report*.

MIFI. (2007). Mississippi Institute for Forest Inventory: Unpublished forest cover classification from Landsat and MODIS composite images. *Report.*

Munn, I. A., & Tilley, B. K. (2005). "Forestry in Mississippi:" The Impact of the Forest Products Industry on the Mississippi Economy: an Input-output Analysis. *Forest and Wildlife Research Center*, Mississippi State University.

Perez-Verdin, G., Grebner, D. L., Sun, C., Munn, I. A., Schultz, E. B., & Matney, T. G. (2009). Woody biomass availability for bioethanol conversion in Mississippi. *Biomass and Bioenergy*, 33(3), 492–503.

Perlack, R. D., & Turhollow, A. F. (2002). Assessment of options for the collection, handling, and transport of corn stover. *Oak Ridge National Laboratory, Oak Ridge, Tennessee, USA, 29.*

Perlack, R. D., Wright, L. L., Turhollow, A. F., Graham, R. L., Stokes, B. J., & Erbach, D. C. (2005). Biomass as feedstock for a bioenergy and bio products industry: *the technical feasibility of a billion-ton annual supply. DTIC Document.*

USDA-NASS. (2012). National Agricultural Statistics Service: http://quickstats.nass.usda.gov. Accessed in May, 2012.

Viana, H., Cohen, W. B., Lopes, D., & Aranha, J. (2010). Assessment of forest biomass for use as energy. GIS-based analysis of geographical availability and locations of wood-fired power plants in Portugal. *Applied Energy*, 87(8), 2551–2560.

5.10 BIOENERGY FROM RESERVE PRAIRIES IN MINNESOTA: MEASURING HARVEST AND MONITORING WILDLIFE

Shelby Williams[1,], Jacob Jungers[1], Kevin Johnson[2], Colleen Satyshur[2], Melissa DonCarlos[2], Robert Dunlap[3], Troy Mielke[2], Joe Schaffer[4], David Tilman[1], Donald Wyse[5], Roger Moon[6], Todd Arnold[3], Clarence Lehman[1]*

Abstract

Conservation of land is valued by society and nurtured by policy that should be informed by science and technology. Over 1.5 million acres are in the Conservation Reserve Program in Minnesota alone. This and similar programs provide ecosystem services, but as prices of commodity crops increase, along with costs of farm operations, many reserve lands may revert to cropland, potentially reducing quality of soil, water, climate, and habitat.

In this study we investigated whether reserve lands could reliably be harvested to yield high quality renewable bioenergy while concurrently preserving resident wildlife populations. Implications can inform policy on earning opportunities from harvested bioenergy while maintaining or expanding conservation lands.

This paper broadly outlines our ongoing, six-year study on production-level harvesting of over 1000 acres of re-established Minnesota prairie. It and its on-line supplementary material (www.cbs.umn.edu/wildlife) focus on protocols, methods, and management practices that have emerged. Results and statistical analyses from this study will be reported in subsequent publications. We describe the logistics of managing a landscape-scale bioenergy research program, with emphasis on harvesting, sampling, and coordination with land managers. In addition, in supplementary material we offer specific protocols to survey small mammals, birds, reptiles, amphibians, and invertebrates. These protocols are intended for researchers to assess whether wildlife populations are affected by various harvesting regimes for bioenergy, and the quality and quantity of bioenergy that can be expected.

The pursuit of principles integrating conservation biology, ecology, agronomy, and energy production, as described here, is an intrinsic part of establishing a viable domestic bio-based economy.

Introduction

Minnesota grasslands continually produce biomass that largely goes untapped. A properly restored and managed field of mixed grasses, legumes, and other flowering plants offers key ecosystem services including carbon sequestration, enhanced water quality, biodiversity, and wildlife habitat (Foley *et al*. 2005). It also offers flexibility for use as animal feed or forage (Sanderson and Adler 2008). In general, contemporary

[1] Department of Ecology, Evolution, and Behavior, University of Minnesota, MN

[2] Cedar Creek Ecosystem Science Reserve, MN

[3] Department of Fisheries, Wildlife, and Conservation Biology, University of Minnesota, MN

[4] Minnesota Native Landscapes, MN

[5] Department of Agronomy and Plant Genetics, University of Minnesota, MN

[6] Department of Entomology, University of Minnesota, MN

* Corresponding author

energy crop fields, such as soybean and corn, and some other feedstocks such as miscanthus and switchgrass, support lower levels of wildlife than do diverse grasslands (Robertson e*t al*. 2010; Meehan *et al*. 2010; Gardiner *et al*. 2010). Suitable wildlife habitat in such cases may be reduced by simplification of the landscape, complete harvest of all cover, wetland drainage, chemical application, mechanical injury, and other causes.

But what of restored native grasslands? Can they be harvested sustainably and still provide suitable wildlife habitat? We considered principles of wildlife ecology to design an experiment testing the effects of harvest patterns, edges, and unharvested refuges on production-scale fields within restored native grasslands. We surveyed birds, small mammals, reptiles, amphibians, and invertebrates, including insects and spiders. We also conducted several specialized pilot surveys. This paper outlines the project thus far, five years into a six-year study, to summarize lessons learned. Detailed results and statistical analyses from this study will be reported in subsequent publications.

Site Selection and Logisitics

A common criticism of biomass production is that it uses land that might otherwise be used for food production, leading to increased greenhouse gases, among other outcomes (Fargione *et al.* 2008; Searchinger *et al*. 2008). However, mixed grassland biomass is an exception in that it can be established or restored on marginal land that is either not suitable for typical crop production (Cai *et al.* 2011), or as is more often the case, has been taken out of production because of low yields. For this study, we selected three regions of representative climate, soil, and wildlife composition in western Minnesota spanning the state's latitudinal gradient (Figure 1). These were re-established prairies, restored no less than five years earlier, held in federal, state, or private conservation under fire and weed management appropriate for their region.

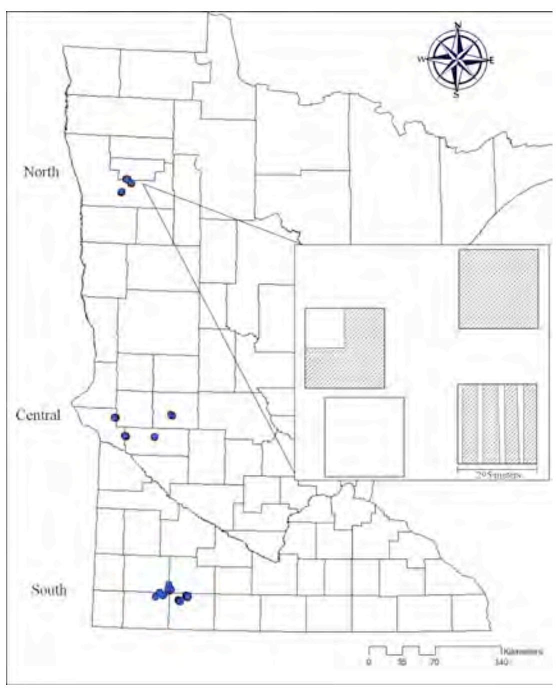

Fig. 1. Three regions in Minnesota where restored grasslands were studied to evaluate effects of biomass harvesting on grassland wildlife. Inset shows one block of four 20-acre plots with one unharvested control and three different harvest plans.

Locating landscapes with enough contiguous, re-established prairie to establish replicated, consistently-sized production scale plots was challenging. We were able to accomplish this goal with plots averaging 20 acres each, organized into study blocks of an average three-mile radius. The blocks within a region were close enough for harvesting efficiency and delivery to potential biomass consumers. This also kept the soil and climate within each region similar enough to support a randomized block design. We chose plots using detailed maps that included soil and elevation parameters, wetland delineation, and land cover from aerial images, then visited potential locations to determine plot suitability.

Plot distributions within fields required detailed attention. Removing bales would become difficult and expensive if plots were further into fields and away from roads. Wetness and slope were considered as well, especially since the fields used in this study did not have drain tiles. We recognized these as challenges in using marginal agricultural or non-agricultural land for harvesting. Given those constraints, sufficient land for this study was located and partnerships with federal, state, and local agencies and private entities were secured largely within the first year of the project, but required some care and effort.

Wildlife

We evaluated wildlife with biological field crews surveying birds, small mammals, reptiles, amphibians, and invertebrates. Each of these taxa required distinct protocols, detailed in supplementary material (www.cbs.umn.edu/wildlife). Any single survey does not define the response of the landscape to bioenergy harvest, but together these surveys characterize outcomes of harvest management. We identified wildlife to species level where possible, but several taxa were only identified to order, family, or genus (*e.g.* invertebrates, some genera of small mammals).

Invertebrate sampling techniques included sweep nets, pitfalls, and bee bowls. We also developed a new quantitative invertebrate sampling technique (QuIST) to collect all invertebrates within a grassland canopy and calibrate conventional sweep net measurements. Our measurements of invertebrates examine their important roles as food for wildlife and as beneficial predators and pollinators. Small mammals were surveyed because they occupy a central role in grassland ecosystems, consuming invertebrates and plants lower in the food web and in turn becoming food for larger predators. We conducted small mammal surveys in late summer using Sherman live-traps. Reptiles and amphibians are sensitive and susceptible to environmental disturbances and therefore are important indicators. We surveyed them throughout summer using funnel and pitfall live-traps. Grassland birds are of widespread interest, not only for activities such as bird-watching and hunting, but because their populations have declined more precipitously than any other bird guild. We used area-based search methods to survey birds throughout the entire plot, using both auditory and visual cues.

In addition to the wildlife surveys, we conducted vegetation surveys throughout the growing season. These surveys tracked the presence and absence of a variety of plants, percent cover at randomly placed quadrats, and also which plants were blooming and providing resources for pollinators. Other surveys were piloted for special purposes, including winter pellet surveys for deer, artificial nest and predator surveys using trail cameras, snow depth measurements, and nesting waterfowl surveys.

Harvesting

Biomass harvesting was organized in six treatment patterns: 50% harvest in strips, 50% harvest in blocks, 75% harvest in strips, 75% harvest in blocks, 100% harvest, and 0% harvest. Patterns were designed to test for the importance of unharvested areas in providing wildlife refuges, connectivity, edges, and landscape complexity. Harvesting was guided by semi-permanent bamboo poles placed in the plots. Following harvest, we traced the edges on all-terrain vehicles using global positioning systems (GPS) to record actual harvested areas, which occasionally differed from the plan due to temporary wetlands or other obstructions. We collected sample cores from biomass bales and analyzed them for minerals and other factors (Jungers *et al.* 2011).

We did not employ custom equipment for harvesting. A discbine with multiple small spinning heads was used for all cutting. After the biomass was cut, it was roller-conditioned and dispensed to form windrows. The discbine head worked well for cutting the various plant types in the project and cut both wet and dry material. It also allowed greater ground speed. However, it can be expensive to repair if damaged by rocks or other debris, which can occur on marginal lands targeted for this study.

During the first harvest season (2009), the discbine head was mounted on a two-wheel-drive, self-propelled, swathe-type cutter, but this was suboptimal because the unit was difficult to transport between plots, and it got stuck in wet ground. Accordingly, in 2010 and later, we mounted the discbine on a four-wheel drive tractor, which solved the transportation problem and also provided the versatility of another tractor on site. A high capacity wheel V-rake worked well to combine two windrows of cut biomass into one windrow and also to flip the material to speed drying. If conditions were dry, the biomass did not have to be raked.

We tested both round and square balers. Both produced large bales of similar size. In 2009, the large square baler produced 4'x 4' x 8' twine-tied bales weighing around 1,000 pounds at 15% moisture. They stacked, hauled, and transported well—better than round bales—and had no tendency to roll on slopes. However, they were not as resistant to rain. The square baler was effective but heavy for its tire size and difficult to load for transport. In 2010, we switched to a round baler, which produced a 4' wide by 6' high bale wrapped with plastic net. That size allowed easy hauling by truck to final destinations. Round, net-wrapped bales can be left outdoors for up to three years or more without cover, allowing storage in the field, where costs are lower.

Available time windows for harvesting were relatively short, due in part to regulations of land managers, but also to weather conditions. For example, many wildlife management areas by regulation cannot be harvested before November 1, sometimes leaving little available time before snowfall. Occasionally, wet conditions or snow prevented a complete fall harvest. Where possible, harvesting was then completed the following spring. The best method for transporting bales from the field was tractors with front and rear-mounted bale spikes. With these, bales can be placed a safe distance from the roadside for future transport or loaded directly onto trucks.

A practical consideration for geographically broad studies like this is preventing the spread of weeds, so for this project transportation equipment carried on-board air compressors to clean machinery before departing any plot.

Public Involvement

Ultimately policy flows from the public, and with that in mind we dedicated part of the project to meetings and demonstrations for agencies, landowners, news media, and the general public. During multiple fall harvest seasons, we advertised in local media and moved a representative set of harvesting equipment to one of our 20-acre plots that was close to a roadway with safe parking nearby. We presented the ideas of ecosystem services from multiple concurrent uses of land and conducted discussion and feedback sessions. Conditions permitting, we demonstrated the harvesting process to those not familiar with issues of harvesting non-agricultural land. Attendance was good and responses were enthusiastic, though more people interested in land management and wildlife attended than those interested purely in bioenergy. These sessions were then distributed more broadly through news reports and photos in local newspapers.

Discussion

With proper planning, diverse, re-established grasslands can provide multiple benefits to conservation lands and to agricultural lands used for bioenergy (Tilman *et al.* 2006). Harvesting can provide an easier and less expensive management alternative to prescribed burning on conservation lands. As riparian buffers, prairies can be planted and subsequently harvested alongside waterways, with bioenergy revenues potentially making such buffers profitable and allowing them to be wider than they otherwise could be. Wet and mesic prairies could be established to catch drain-tile runoff of food-crop fields and remove nitrogen and other nutrients before they reach natural watersheds, increasing bioenergy yields in the process. Integrating animal production for food onto grassland bioenergy fields may offer further opportunities for managing a multifunctional system. For example, if grazers use mixed-species grasslands in the spring and consume cool-season grasses, that could maximize the growth of warm-season grasses and bring higher bioenergy yields. Lower potential yields than heavily managed monoculture grasses are offset by putting to use land that is not suitable for heavy management, and providing broad conservation services to society across the landscape.

References

Cai, X., Zhang, X., Wang, D. (2011). "*Land availability for biofuel production*." *Environmental Science & Technology,* **45**(1), 334–339.

Fargione, J., Hill, J., Tilman, D., Polasky, S., Hawthorne, P. (2008). "*Land clearing and the biofuel carbon debt*." *Science,* **319**,1235-1238.

Foley, J.A., DeFries, R., Asner, G.P., Barford, C., Bonan, G., *et al*. (2005). "*Global consequences of land use*." *Science,* **309,** 570-574.

Gardiner, M.A., Tuell, J.K., Isaacs, R., Gibbs, J., Ascher, J.S., *et al*. (2010). "*Implications of three biofuel crops for beneficial arthropods in agricultural landscapes*." *Bioenergy Research,* **3**, 6–19.

Jungers, J.M., Lehman, C.L., Sheaffer, C.C., Wyse, D.L. (2011). "*Characterizing grassland biomass for energy production and habitat in Minnesota*." *Proc. of the 22nd N. Amer. Prairie Conf.,* 168–171.

Meehan, T.D., Hurlbert, A.H., Gratton, C. (2010). "*Bird communities in future bioenergy landscapes of the Upper Midwest.*" *PNAS,* **107**, 18533–18538.

Robertson, B.A., Doran, P.J., Loomis, L.R., Robertson, J.R., Schemske, D.W. (2010). "*Perennial biomass feedstocks enhance avian diversity*." *GCB Bioenergy,* **3**, 235-246.

Sanderson, M.A., Adler, P.R. (2008). "*Perennial forages as second generation bioenergy crops*." *International Journal of Molecular Sciences,* **9**, 768–788.

Searchinger, T., Heimlich, R., Houghton, R., Dong, F., *et al.* (2008). "*Use of US croplands for biofuels increases greenhouse gases through emissions from land-use change.*" *Science,* **319**, 1238–1240.

Tilman, D., Hill, J., Lehman, C. (2006). "*Carbon-negative biofuels from low-input high-diversity grassland biomass.*" *Science,* **314**, 1598-1600.

This project was supported in part by financial awards from the Minnesota Environmental and Natural Resources Trust Fund, the USDA Natural Resources Conservation Service, the National Fish and Wildlife Foundation, and the University of Minnesota's College of Biological Sciences, by land-use grants from the Minnesota Department of Natural Resources, the US Fish and Wildlife Service, and generous private landowners, and by logistical support from the Cedar Creek Ecosystem Science Reserve. We are also grateful to Linda Meschke and Jill Sackett for orchestrating the public involvement and to dozens of dedicated undergraduate researchers who conducted the field surveys each summer.

6 EXTENSION AND EDUCATION

6.1 TRANSFORMATIVE REGIONAL APPROACHES FOR NORTHEAST WOOD ENERGY

Michael Jacobson[1,], Daniel Ciolkosz[2]*

Abstract

An important component of research on biomass feedstock production and utilization is transferring that information to stakeholders across the supply chain. To that end, a recent Sun Grant project focused on developing a variety of extension-related materials for states in the Northeast. These include: a) series of educational publications designed to be easily adapted to any state in the region, b) a "Northeast Wood Energy Webinar Series", a collection of monthly webinars focused on topics of interest and concern for the wood energy community, c) workshops and short courses where stakeholders meet to develop expertise and discuss important developments in wood energy, and d) a book entitled "Wood Based Energy in the Northern Forests", to be published by Springer in 2013. This collection of resources provides a comprehensive set of information and educational tools to assist the sustainable and effective development of wood energy in the region. Another central aspect of this effort is to develop linkages and networks. One example is the launch of a USDA regional project group entitled "NEERA 1005 - Sustainable Wood Energy", to promote cross-institutional collaboration between land grant institutions in the region. A variety of evaluation tools including focus groups, post-workshop and -webinar surveys, and interviews with university extension personnel in the region were carried out to gage needs and effectiveness of the extension materials. The degree to which the dissemination of this information has contributed to knowledge, visibility, and growth of woody biomass use in the Northeast is discussed.

Keywords: extension, wood energy, Northeast

Need for Collaboration

In recent years, especially since the global recession of 2007/2008, wood-based energy has become an expanding and topical research area. Driven by concerns over climate change, energy independence and local economic development, a number of initiatives are underway across the US and world to develop sustainable wood energy systems. Universities are carrying out research, and state and federal government is providing incentives to industry. The extent of the activities in wood energy is broad. It ranges from determining feedstock availability to production, processing and end-uses. As the design and implementation of wood-energy projects grows there is more need for collaboration within regions that have common ecology, land use, and economic systems. It is helpful to discuss this topic within a regional context because of the forest types and markets that are unique to different regions. For example, the Northeast US is rich in slow growing mixed hardwood forests, with forest land use dominated by large numbers of small-plot private landowners. Harvest for timber dominates the wood economy in this region, with a relatively limited low-use wood market.

[1] *The Pennsylvania State University, Department of Ecosystem Science and Management, PA*

[2] *The Pennsylvania State University, Department of Agricultural and biological Engineering, PA*

** Corresponding author*

As projects ramp up and new technologies are developed it is critical for policy makers and practitioners to have access to science based knowledge and resources. Working together across states within the Northeast region allows uniform access to the best information available, while building the regional community of wood energy extension specialists and retaining local responsiveness to issues and needs within the region. University based extension is critically poised to play a key role to facilitate such collaboration, and stands to benefit from it as well, since limited support of extension has made it extremely difficult to maintain a critical mass of wood energy educators in any one state.

The Northeast Wood Energy Program

This project was designed to develop a critical collection of extension-oriented information on wood-based energy in the Northeast United States, for utilization throughout the region. Three main components were envisioned for this effort: 1) a website portal for information access, 2) a series of fact sheets that could be easily configured to address individual states' unique characteristics, and 3) a webinar series that provides timely instruction and commentary on contemporary issues facing the wood energy sector in the region. These three components were intended to work in a complementary fashion, with fact sheets springing from the content of webinars, and the website serving to showcase both webinars and fact sheets. Ideally, this effort would draw together extension educators and specialists throughout the region, and help foster collaborative efforts at extending and expanding the current project. The end impact of this effort would be an educated and equipped community of extension personnel providing critical assistance within their local wood energy communities. The content topics of the project were designed to avoid focusing on one small portion of the wood energy economy, but rather to work "across the supply chain", allowing educators and stakeholders to better understand the broader ramifications of wood energy decisions and actions.

Key Efforts to Date

To start the collaborative process an online survey was sent to over one hundred extension educators and researchers across the Northeast. The survey was carried out by e-mail using Survey Monkey. The survey was divided into categories of wood bioenergy, namely 1) Forest production, harvesting and management (including short rotation woody crops and environmental issues), 2) Logistics and supply chains: Biomass to power, heat or liquid fuels, and 3) Federal, state and local policies and incentives (including economic and social issues). Within these categories respondents were asked to note the most important topics. They were also asked to list other important topics, not fitting in those three categories. Finally, they were asked to list the 3 most important facts sheets and webinars that should be developed and presented.

There were 20 responses from 11 states. The distribution of responses by employment was 48% government, 33% academic and 19% private sector. Given the broad range of issues and audiences in dealing with wood energy there was no clear critical priority areas that stood out, but the comments provided some initial ideas to develop the first set of fact sheets, short courses, and webinars. Table 1 shows some examples of what respondents suggested that extension materials address.

Table 1. Selected comments from survey of extension material needs

Forest production, harvesting and management	Logistics and supply chains	Federal, state and local policies and incentives
• Harvesting techniques, costs and BMPs • Biomass availability • Biomass yields and economics • Database of available resource professionals	• Case studies of successful projects • Transportation thresholds • Project scale • Procurement strategies • Different end markets • Specifications for wood biomass	• Financing and access to funds • Air quality issues • Compatibility with local ordinances and regulations • Comparative economics with other fuels

1. Web site development

A website was designed to provide resources, clearinghouse and one stop shop for woody biomass extension information in the Northeast. http://extension.psu.edu/energy/ne-wood-energy

2. Print literature development

To date the following fact sheets related to bioenergy were produced:

- A Bioenergy Primer for the Forestry Community;
- A Bioenergy Primer for Forest Landowners;
- Green Buildings and Bioenergy; and
- Is Biomass Heat Right for You?

These fact sheets are written with a Pennsylvania-focus, but are designed to be easily adapted to other states in the region with minimal modification.

3. Webinar series

Using expertise from across the region, to date, ten webinars have been aired and stored at the website, with the following titles:

- The Bumpy Road from Coal to Wood;
- Heating the Northeast - Reflections from the Conference;
- Biomass Harvesting Guidelines: Forest Management Issues ;
- Forest Biomass and Bioenergy: Opportunities and Constraints in the Northeastern United States;
- Short Rotation Woody Crops in the Northeast;
- Wood Chip and Pellet Supply and Trends in the Market: Thoughts from Vermont;
- Woody Biomass in Minnesota; Opportunities for Income and Environmental Benefits;
- Biomass Carbon Accounting: Implications for Policy and Climate; and
- Why Wood Energy?

To bring stakeholders together to discuss wood energy a short course was held at Penn State in Nov 2011. Over 30 participants from across the Northeast discussed wood energy with a practical focus of developing successful wood energy projects. The course included hands-on project assessment of converting from fossil fuels to wood energy for heat and electricity. The book publisher Springer has contracted the course organizers to develop a book based on the short course that will be forthcoming in 2013. The book with be a state of the art review of wood energy in the Northeast.

4. Development of NEERA 1005 Sustainable Wood Energy

NEERA 1005: Sustainable Wood Energy is a regional agricultural experimental station project that was developed as part of this effort. NEERA 1005 provides a forum for university researchers and extension educators to discuss wood energy issues. A description of this project is at http://nimss.umd.edu/homepages/home.cfm?trackID=13676. Annual meetings of the group serve to draw together project participants for collaborative planning of extension, research, and educational programs focused on wood energy.

Needs and Future Directions

The material developed to date was in part funded by a Sun Grant extension project. That project is a spring board for continuing extension activities in the region. All the above mentioned materials and activities will continue to be utilized and expanded. Enhancement of the website, facts sheets and webinars will continue. Recently funded projects including a Sun Grant on genetic improvement of shrub willow have substantial extension components that spring in part from this project.

It is perhaps too early to evaluate the usefulness of these materials and whether these efforts are leading to transformative changes in wood energy development across the region. There is still much work needed in developing partnerships and facilitating collaborative learning, but informal feedback from extension educators and researchers in the region indicate that not only is this a significant need, but that the projects efforts to date have been valuable and are generating positive impacts within the region.

6.2
DEVELOPMENT AND DISSEMINATION OF BIOENERGY EDUCATIONAL CURRICULUM FOR CHILDREN

Scott D. Scheer[1,] Dennis Hall[2], Jane Wright[3]*

Abstract
It is important for the field of bioenergy that future consumers, policy makers, and taxpayers develop knowledge and awareness of bioenergy. Current resources to promote bioenergy usually target youth in grades 6-12. Research indicates that to effectively impact youth knowledge, skills, and abilities, they should be reached at earlier ages for long-term developmental outcomes. Therefore, educational resources for children are needed to increase bioenergy knowledge, appreciation, and career interest. This bioenergy curriculum for children (K-2) contributes to the national science education standards content areas of life sciences and science as inquiry. The educational material is designed to inform and educate future consumers to gain knowledge and appreciation of bioenergy. The bioenergy curriculum follows the developmentally appropriate practice guidelines for primary grades as established by the National Association for the Education of Young Children Three bioenergy curriculum pieces (each with 9-10 activities) were developed in the content areas of: 1) Bioenergy Sources (e.g., grasses & algae); 2) Bioenergy Conversion (e.g., combustion, fermentation); and 3) Bioproducts (e.g., wood, biodiesel).

Keywords: bioenergy education, children, curriculum, experiential learning

Introduction
It is significant for the field of bioenergy that future consumers, policy makers, and taxpayers develop knowledge and awareness of bioenergy. In addition, the demand to fill bioenergy-related jobs is expected to increase in the long-term (White and Walsh 2008) which will require today's youth to become interested in pursuing bioenergy careers.

Minimal research exists about youth awareness and knowledge of bioenergy. However a recent Finnish study examining bioenergy and youth (9th graders) in relation to school, home, and media reported that youth were positive towards learning about bioenergy, but less enthusiastic for utilizing bioenergy (Halder et al. 2011). In addition, the youth indicated a positive attitude about bioenergy but lacked an understanding and knowledge of bioenergy. These results suggest that both positive attitudes and sufficient knowledge of bioenergy are needed to improve the utilization of bioenergy.

Existing material to promote bioenergy knowledge, awareness, and career aspirations usually targets youth from about 6th through 12th grades. Research implies that to effectively impact youth knowledge, skills, and abilities, they should be reached at earlier ages for long-term developmental outcomes (Bronfenbrenner 2005; Enver et al. 2008). Therefore, educational resources for children are needed to increase bioenergy knowledge, appreciation, and future career interest.

---

[1] *Department of Agricultural Communication, Education, and Leadership and OSU Extension, The Ohio State University, OH*

[2] *Ohio BioProducts Innovative Center, OH*

[3] *4-H Youth Development, OSU Extension, OH*

**Corresponding author*

Outcome-Based Objectives

This project for developing and implementing a bioenergy education curriculum for children (K-2) is directly related to the Sun Grant priority area of education, extension, and economic development outreach by providing Extension educators curriculum to utilize with 4-H and school science education programs. The project is structured to leverage existing systems and educational opportunities.

The objectives are to:

1. develop a bioenergy educational curriculum for children;
2. connect curriculum to contribute to the national science education standards in the K-4 content areas of life sciences and science as inquiry;
3. disseminate and evaluate the curriculum initially in a state 4-H Extension system (Ohio) for use with elementary-aged children (focus on K-2);
4. inform and educate future consumers to gain knowledge and appreciation of bioenergy, plus consider careers in this field.

Procedures

All too often educational material, regardless of content area is reduced in complexity or transposed for lower grade levels. Such an approach can be especially problematic since the key to effective educational programs is that it is developmentally appropriate. Therefore, it is critical the curriculum is age-appropriate to create bioenergy excitement and interest.

The bioenergy curriculum follows the developmentally appropriate practice guidelines for primary grades as established by the National Association for the Education of Young Children (Copple and Bredekamp 2009). Some of the key features include: creating a positive climate for learning; responding to individual and cultural variation; and using a developmentally appropriate curriculum to enhance motivation and guidance.

In addition, the bioenergy educational curriculum incorporates the experiential learning model (Kolb 1984) which involves the phases of 1) experience/do, 2) share, 3) process, 4) generalize, and 5) apply. The curriculum also follows Ohio's programming parameters for young children developed by the PI and used in Extension systems throughout the United States (Scheer 1997; Trutner and Scheer 2005). Program parameters include: cooperative-learning centered, activity based, noncompetitive, and success oriented.

Successful educational programs exist in this area and were examined for building upon and expanding their work. Although most of these programs target youth in middle and high schools, the content base is informative. These programs include:

1. Cornell's Biofuels Race to the Pumps game (Dr. Larry Walker and colleagues) and Biomass to Sugars Lab Kit (Dr. Rutzke and colleagues); and
2. Ohio BioProducts Innovative Center's (OBIC) employs a variety of educational engagement activities including bio-foam and "shrink-wrap" demonstrations (Dennis Hall and colleagues).

In addition, Dennis Hall, Co-PI of this project collaborates with Dr. Rutzke's Northeast Bioenergy and Bioproducts (NBB) educational program for providing teachers (grades 8 - 16) with training, tools, and in class-support. Part of the effort consisted of five master teacher training mirror sites; one includes OBIC (Columbus, Ohio). The PI participated in the week-long training through OBIC to gain additional content knowledge for developing the K-2 educational material.

An experiential learning model was incorporated for developing three bioenergy curriculum pieces. Each curriculum piece consists of about nine to ten developmentally appropriate activities. The curriculum pieces contain the content areas of:

1. **Bioenergy Sources** (focus on sources of woody crops, grasses, oil seed crops, food processing wastes, algae, etc.);
2. **Bioenergy Conversion** (combustion, biochemical, physical methods, fermentation, digestion, etc.);
3. **Bioproducts** (wood pellets, biodiesel, charcoal, biogas, bioethanol, etc.).

Examples of the leader-directed activities in the three content areas are as follows:
1) bioenergy sources (Bioenergy and saving the planet: Environmental sustainability, Bioenergy and biomass: Having fun together, and Our sun: The ultimate bioenergy generator), 2) bioenergy conversion (Bioenergy combustion: Fire as fuel, Don't pass gas: Convert that biomass, and Fermentation: Sugar to Fuel), 3) bioproducts (Bio-based lubricants: Feels slippery to me, Bio-based insulation, and Fueling the future).

The national science education standards (National Research Council 1996) in the K-4 content areas of life sciences and science of inquiry were supported through the learning activities across the three curriculum areas of bioenergy sources, conversion, and bioproducts. For developing learner understanding for the life science content standard of "organisms and environments" the bioenergy activities help children become familiar with how plants harness energy from the sun and through various processes (e.g., fermentation, combustion) as this energy is converted into bioenergy products such as biofuel. These activities follow a science of inquiry approach (e.g., ask questions, plan/conduct a simple investigation, use simple tools to gather data).

Implementation and Evaluation

Pilot testing has begun with the curriculum, plus content review. The bioenergy curriculum was evaluated for content accuracy (by co-PI, Dennis Hall, Assistant Director for the Ohio BioProducts Innovation Center), developmentally appropriate practice-structure (by PI Scott Scheer, Professor and State Extension specialists) and education delivery and design (by Extension educators who focus on child development and education).

The pilot-test was conducted to collect feedback from adult leaders to assess the curriculum in about 10 Ohio counties. Specific aspects of curriculum assessment include ease of use, maintains learner interest, and clarity of content.

A workshop was held for Extension professionals in those counties that are pilot testing the curriculum. During the workshop participants learned about the curriculum objectives and background on bioenergy. In addition, there were six stations for them to conduct and teach each other bioenergy activities. Initially the overall feedback has been positive, however, there were some concerns that a few of the activities maybe too complicated for children in grades K-2.
Once the pilot test is complete, the curriculum will be revised. The bioenergy curriculum would be available for use not only in Ohio, but in other states via web access.

Conclusions

For long-term bioenergy growth and understanding, today's children must be part of bioenergy education and extension strategies. This project developed three curriculum pieces (bioenergy sources, conversion, and bioproducts) to promote bioenergy knowledge, awareness, and career aspirations. In addition, the educational curriculum helps children begin to understand the concept of environmental sustainability and the significant role of bioenergy for providing long-term solutions to bring authentic environmental sustainability for future generations.

Acknowledgement

This project was funded by the Northeast Regional Sun Grant Initiative, with a grant from the U.S. Department of Transportation: US DOT Assistance #DTOS59-07-G-00052.

References

Bronfenbrenner, U. (Ed.). (2005). *Making human beings human: Bioecological perspectives on human development*. Thousand Oaks, CA: Sage.

Copple, C. and Bredekamp S. (Eds.). (2009). *Developmentally appropriate practice in early childhood programs* (3rd ed.). Washington, DC: NAEYC.

Enver, A., Partridge, M. D., and Clark, J. K. (2008). *Growth and change: Closing Ohio's knowledge gap to build a 21st century economy.* The Swank Program in Rural-Urban Policy and Exurban Change Project Summary Report. Columbus, OH: The Ohio State University.

Halder, P., Havu-Nuutinen, S., Pietarinen, J., and Pelkonen, P. (2011). Bio-energy and youth: Analyzing the role of school, home, and media from the future policy perspectives. *Appl. Energ.*, 80, 1233-1240.

Kolb, D. A. (1984) *Experiential Learning*, Englewood Cliffs, NJ.: Prentice Hall.

National Research Council (1996). *National Science Education Standards*. Washington, D.C.: National Academies Press.

Scheer, S. D. (1997). Programming parameters for five to eight year-old youth in 4-H. *J. Extension* [On-line serial] *35*(4). Available URL address: http://www.joe.org

Trutner, S., and Scheer, S. D. (2005). *4-H Cloverbud volunteer guidebook.* Columbus OH: The Ohio State University Extension publications.

White, S., and Walsh, J. (2008). *Greener pathways: Jobs and workforce development in the clean energy economy.* Center on Wisconsin Strategy, Workforce Alliance, Apollo Alliance. Available URL address: http://www.cows.org/greenerpathways

6.3
BIOENERGY EDUCATION AND OUTREACH THROUGH EXTENSION.ORG

Susan Hawkins[1,], Jason de Koff [2], Zane Helsel[3]*

Abstract

The eXtension Farm Energy Community of Practice (CoP) provides an on-line environment where Land Grant University personnel and their colleagues collaborate to develop objective, researched-based outreach materials. www.eXtension.org/ag+energy hosts a wide variety of resources, from fact sheets to decision tools to multimedia, to promote a practical understanding of bioenergy issues. Topics range from feedstocks, through logistics and processing to the use of bioenergy and are targeted to the agricultural professional. Through a Sun Grant project, the eXtension Farm Energy CoP is developing an online library of multimedia resources, with an emphasis on those generated by Sun Grant investigators. Join us to see what is available for you to use – such as bioenergy curriculum, articles and webinars. Find out how to contribute your own energy resources to this eXtension archive, whether it is an image, video, research summary, case study or fact sheet.

Keywords: eXtension, farm energy, community of practice, bioenergy, multimedia, curriculum

Introduction

The use of the internet for learning purposes has been important since its inception. For farmers, this access has been limited but is becoming an increasingly more viable option. According to the USDA National Agricultural Statistics Service (2011), 62% of U.S. farms now have internet access, which is an increase from around 50% access in 2005 (USDA, 2011). The internet has become an important source of information for farmers in areas like marketing (Bamka, 2000) and business management (Roth et al., 2009). In one study, 73% of farmers from focus groups in Louisiana, Tennessee, and Virginia preferred the use of the internet for learning purposes (Franz et al., 2010). According to Franz et al. (2010), in addition to being experts, Extension professionals need to be able to provide the proper learning environment to farmers.

The eXtension Farm Energy Community of Practice (CoP) provides an online learning environment that connects experts from universities with peers and farmers in need of technical advice. A number of learning tools are available including Frequently Asked Questions (FAQs), Ask an Expert (AaE), a bioenergy curriculum, articles, and webinars to enhance the learning experience. In addition, an online library of multimedia resources is being developed through a SunGrant project with an emphasis on those resources generated by SunGrant investigators.

Who We Are

Currently the Farm Energy CoP (a.k.a Sustainable Ag Energy CoP) is made up of 225 members from universities across the country. Our website www.eXtension.org/ag+energy contains over 150 articles on topics that range from energy efficiency on the farm to switchgrass for bioenergy. Within the Farm Energy CoP there are individual groups that are focused around specific topics like feedstocks, conversion processes, and biodiesel. All content is developed for the website by

---

[1] *University of Vermont Extension, VT*

[2] *Department of Agricultural and Environmental Sciences, Tennessee State University, TN*

[3] *Department of Plant Biology & Pathology, Foran Hall/ Cook Campus, NJ*

* *Corresponding Author*

experts and reviewed by peers prior to publication. In order to minimize duplication, links to other existing material from other Extension and partner sources are provided.

- Sign up for an eXtension ID: http://about.extension.org/get-an-id/
- Join the Sustainable Ag Energy CoP (Fig. 1) www.extension.org/people/communities/25

Figure 1.

What We Do

The Farm Energy CoP engages its stakeholders and audience through a variety of resource types. While we continue to provide the traditional Extension Fact Sheet, we also provide interactive resources that address different learning styles and needs, and that make best use of internet technology.

Ask an Expert

Ask an Expert (AaE) (Fig. 2) is a tool for the public to get information directly from experts. This is particularly helpful for users with specific questions about a given situation. Members of the Farm Energy CoP can sign up as "experts" and questions are routed directly to their email accounts if the questions meet particular constraints the expert has identified (i.e. region, topic, etc.).

- Sign up as an Expert - http://www.extension.org/aae/prefs/expertise

Figure 2. Ask an Expert

Frequently Asked Questions

These are questions with answers that are related to the content developed by the Farm Energy CoP. Questions are created by eXtension authors or posed to experts through AaE. These question/answer sequences are edited by other experts before publication to the website.

- http://www.extension.org/ag_energy/faqs

Webinars

Live webinars are regularly available on a range of energy-related topics, and can also be viewed anytime through archived media. A monthly series called "BioEnergy Fridays" is co-hosted with the University of Nebraska on the last Friday of each month. Available archived series include topics like energy efficiency, cellulosic biofuels, biogas and anaerobic digesters, and wind energy.

- Live webinars posted at https://learn.extension.org/events/tag/ag%20energy
- Archived webinars http://farmenergymedia.extension.org/videos?type=webinar

Multimedia Archive

Through a SunGrant funded project, we have developed our Farm Energy Media site which provides instructional and stock video, webinars and images. This system provides self-service for sharing, both posting and viewing the media, without passwords. The site allows the flexibility of embedding from YouTube and Vimeo, linking directly, or uploading media.

- Partner projects can showcase their educational materials together with other research-based providers
- Constituents will find valuable farm energy multimedia resources all on "one site" with a useful search tool
- This "one site" is actually a reference site, and can therefore gather resources from many suitable sites
- Engagement of specialists, practitioners and producers in an easy to use system
- Each multimedia resource has an information page associated with it, to be used for full description, transcript for accessibility, links to additional reference, etc

➢ Go to http://farmenergymedia.extension.org/ to use or contribute media (Fig. 3)

Figure 3. Farm Energy Media site

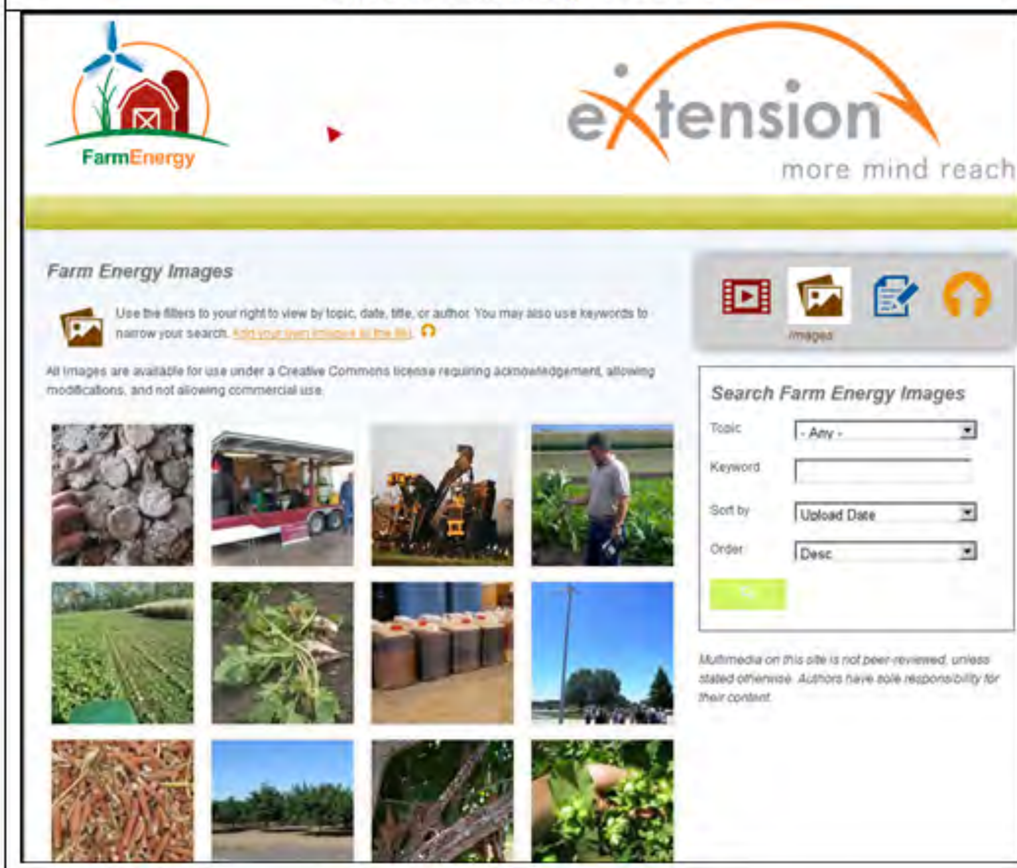

Curriculum

The bioenergy curriculum featured on the Farm Energy CoP website was developed by the Bioenergy Training Center and over 40 specialists for use in educating stakeholders about different issues related to bioenergy. The online course is broken up into four different modules (Intro to Bioenergy, Bioenergy Crop Production & Harvesting, Water Resources: Issues & Opportunities, and Community Economic Development). Each module is separated into units with questions and answers related to the material within each unit. Additional courses on Anaerobic Digestion and On-Farm Energy Conservation and Efficiency are in development.

- http://www.extension.org/pages/63365/bioenergy-curriculum

Analytics

The most recent website analytics data (Fig. 4) shows that the Farm Energy CoP received 6,200 unique visits for the month and 68,000 over a year, with average time on page at almost 3 minutes. Our most popular articles are New Uses for Crude Glycerin from Biodiesel Production, Miscanthus for Biofuel, Algae for Biofuel, Biodiesel Cloud Point and Cold Weather Issues, and Reactors for Biodiesel Production, showing us that the biodiesel team led by U. of Idaho Biodiesel Education Center is successful with their PR efforts, and that in-depth articles and obscure topics are in demand.

Figure 4. Google Analytics for Farm Energy CoP webpages

Participation

The Farm Energy CoP continues to seek specialists, and others interested, for content development and leadership, editing, answering questions from stakeholders, webinar presentation, etc. Your participation will help us delve more deeply into these topic areas: feedstocks, conversion processes, biomass handling and logistics, anaerobic digestion, biodiesel, biomass combustion, sustainability, solar, and wind energy. If you are interested in being involved in these or any other agricultural energy topics, please contact Susan.Hawkins@uvm.edu.

References

Bamka, W.J. (2000). “Using the internet as a farm-marketing tool,” *Journal of Extension* 38(2): 2TOT1.

Franz, N.K., F. Piercy, J. Donaldson, J. Westbrook, and R. Richard. (2010). “Farmer, agent, and specialist perspectives on preferences for learning among today’s farmers,” Journal of Extension 48(3):3RIB1.

Roth, S., J. Hyde, and E.H. Vranich. (2009). “Internet strategies to improve farm business management. The National e-Commerce Extension Initiative, Southern Rural Development Center, Available at: http://srdc.msstate.edu/ecommerce/curricula/farm_mgmt/module1_1.htm

USDA. (2011). “Farm computer usage and ownership,” *USDA National Agricultural Statistics Service* Sp Sy 9 (11).

6.4
EDUCATION AT THE SPEED OF RESEARCH: COMMUNICATING THE SCIENCE OF BIOFUELS

R. Justin Hougham, Jennifer A. Schon, Karla B. Eitel, Steven J. Hollenhorst

Abstract
Overcoming key obstacles that prevent wood-based jet fuel and petrochemical substitutes from being economically viable is the focus of the Northwest Advanced Renewables Alliance (NARA). The NARA Education Initiative, or GreenSTEM, includes an imaginative suite of programs that seamlessly link an array of educational and training programs with our university and commercial partners in order to meet the region's most compelling energy development needs. The overarching goal of the GreenSTEM is to increase the capacity of the region for a transition to biofuels. GreenSTEM K-12 is a program whereby energy and biofuel curricula are developed and field-tested at the award winning McCall Outdoor Science School (MOSS), annually reaching 2,500 K-12 students and 150 teachers. K-12 education and teacher education will work to educate/train our future bio-energy workforce and provide a conduit to transfer science/technology of biofuels and co-products. This approach is an exciting and tangible way to address a very important concept that can engage learners in many modalities. This work introduces, deepens, and reinforces elements of chemistry, earth physics, biology and developing skills around the nature of science. It is pertinent and timely that science curriculum address the basic components of this concept in secondary education, in-service teacher training and pre-service teacher coursework in order to prepare science-literate students for the changing environments and economies of the twenty-first century. This is a foundation for conversations pertaining to bio-fuels, food security, and energy security- ultimately supporting biofuel workforce and economies while addressing sustainability and environmental outcomes in this growing industry.

Keywords: Education, outreach, place-based education

Contact information: College of Natural Resources, McCall Outdoor Science School, 1000 University Lane, McCall, ID 83638; *Corresponding author: rhougham@uidaho.edu

Energy Literacy for Tomorrow
Around 8% of U.S. energy comes from renewable sources. In addition to growth in the use of renewable energy, efficient technologies have been applied to household uses that has led to a decrease in energy use between '78 and '05- even as houses have grown in size. There is increasing innovation and enthusiasm surrounding the idea that the US would benefit from reducing its dependence on foreign oil and developing alternative sources of energy and fuel. But each potential source has tradeoffs for the economy and the environment. Examples of alternative energy include solar, biomass, wind, geothermal, and hydro. Alternative energy is proposed as clean, abundant, competitive, and secure approaches to our nation's energy profile. How can we use inquiry in *GreenSTEM* to problem-solve in this area?

In the United States Department of Agriculture (USDA) funded Northwest Advanced Renewables Alliance (NARA) project, the GreenSTEM Education Team at the McCall Outdoor Science School (MOSS) has worked closely with other teams in the project to use the exciting efforts found in research and industry efforts to move bio-fuels forward. The Education Team's efforts to communicate energy literacy were designed to reach the public at many levels—in-service teachers, k-12 students, and online to the public. Included here are descriptions of three efforts that build towards an improved, systemic approach to supporting energy literacy and public understanding of biofuels. This includes a lesson for high school students -*Carbon in the Forest: Value of a Tree*, in-service teacher trainings in energy literacy -*Idaho Science, Technology, Engineering and Math (ISTEM) Summer Institute* and a web-based educational resource that can serve teachers, researchers, media and public interests *Northwest Advanced Renewables Alliance (NARA) Energy Literacy*

Principles Matrix. These three efforts can be used independent of each other, or they can be seen as nested efforts.

Carbon in the Forest: The Value of a Tree

Energy issues and literacy are increasingly a point of conversation, policy debate, media attention, and economic impact in the United States and worldwide. While there are contested dimensions of the impact and interpretation of energy sources as well as carbon sequestration and cycling, there are fundamental elements of this concept that apply basic chemistry, ecology, and field measurement skills. It is pertinent and timely that science curriculum address the basic components of this concept in secondary education in order to prepare science- literate students for the changing environments and economies of the twenty-first century. This is a foundation for conversations pertaining to bio-fuels, food security, and energy security.

Carbon cycles can be a difficult concept for students to learn for many reasons. First, science curriculum that puts all of the pieces of the puzzle together is developing, but not yet common. Second, this concept – carbon cycling- can remain fairly abstract until a hands on application of field measurements better imply scale and interpret the landscape. Third, due to politicized and media driven debate, this concept may be confusing for the many perspectives on the matter and avoided altogether in instruction for this reason. This lab is an exciting and tangible way to address a very important concept that can engage learners in many modalities. This lab can be designed to introduce, deepen, or reinforce elements of chemistry, earth physics, biology and developing skills around the nature of science.

Carbon and carbon dioxide are important parts of understanding energy literacy. This set of exercises offers a methodology for estimating the carbon sequestered in a forest stand, making tangible and accessible an important part of the conversation of climate science. Estimates such as this can begin further inquiry and instruction in areas such as land conversion, carbon sequestration, carbon credits, and carbon footprint. This lab has also been adapted for use on grassland/prairie, agricultural landscapes and arid steppe.

The Carbon in the Forest lab can be completed using a diameter tape, clinometer, 100ft tape (or chain), calculator, cruise tool/prism, field notebook, pen, camera/video, increment borer. Many of these tools can be checked out form county extension offices, as well as very economically reconstructed in applied math exercises (ex. a clinometer can be crafted from a protractor and a plumb line). The entire lesson can be downloaded here http://adventurelearningat.com/wpcontent/uploads/2012/08/ValueofaTree_5EHS.pdf

Teacher Training

In early 2012, a core group of 5 teachers worked with the McCall Outdoor Science School to design the professional development experience that was delivered to their peers at the 2012 Idaho Science, Technology, Engineering and Math (ISTEM) Summer Institute. They were posed with the problem of educating their peers on water resources in a changing climate, biofuels, Adventure Learning and Problem-based Learning. These teachers had been given a stipend for their work. The product of their work was the co-delivery, along with MOSS faculty, of a strand at the 2012 ISTEM institute.

Teachers participating in the strand at the summer institute will learned about problem-based learning, Adventure Learning, water resources in a changing climate and biofuels by engaging in a problem-based workshop that will use Adventure Learning as a curricular support. These teachers received a stipend and will be invited to participate in follow-up activities at the MOSS campus in which they will gain skills to coach a team to develop a project for the Imagine Tomorrow competition at Washington State University; those who choose to complete follow-up activities will receive an additional stipend. Finally, workshop participants were asked to recruit one or two colleagues to “follow” their participation in the workshop through an online Adventure Learning environment, and these colleagues received a stipend for participating as distance learners. Teacher stipends are provided through grants from the National Science Foundation (NSF) and the U.S. Department of Agriculture (USDA).

In this project's efforts, teachers explored sub questions, such as: What are the negative impacts of our current energy practices? How much of our current fuel comes from renewable sources, and how much from nonrenewable sources? How is biofuel made from wood waste? What are the barriers (technological, social, economic, infrastructure) to large-scale implementation of a biofuel program? What are the tradeoffs (environmental, economic, social) of a large-scale biofuel program? How would a large-scale biofuel program impact our community?

To investigate these problems, participants were guided through a series of activities that gave them some tools to start asking questions and solving problems. Investigation of each problem will use a similar format. Strand facilitators modeled the role that teachers will take if they apply this approach in their classroom, i.e. they will facilitate activities, help participants to form questions and connect them with experts who can inform their thinking. Learning activities included:

1. Hands-on investigation of some aspect of the issue (an in-class lab and possible field trip). For alternative energy, this will be an inquiry lab that explores the amount of carbon in a tree, along with exploration of data in Google Public Data Explorer – per capita emissions, total emissions, emissions by sector, etc., and a field trip to a forest
2. Research in expert groups to investigate the implications of this issue on the ecology and economy of the community using a modified Jigsaw technique for cooperative learning.
3. Interviews with experts (economists, engineers, hydrologists, biologists) who are working on this issue
4. Collaboration with their colleagues to brainstorm solutions for the issues, as well as ways to teach about the issues.
5. Communication with colleagues off site who are following their learning expedition. Participants will communicate about what they are learning as well as how they see themselves using it in their classroom

NARA Energy Literacy Principles

The NARA Energy Literacy Principles Matrix was developed as part of the USDA funded Northwest Advanced Renewables Alliance (NARA) project to create a resource for science teachers to organize and locate curriculum about energy literacy- and specifically biofuels. Energy literacy can be found in a variety of topic areas in schools and alterative energy can be challenging to teach in the classroom. Energy Literacy is complex and holistic, and draws from all the major sciences: biology, ecology, chemistry, physics, math, Earth science, and environmental science. Scientists and educators have developed literally thousands of resources for teachers, however it can be difficult to understand how resources can be used to teach different components of the energy issues that cut across curricular and disciplinary lines. Find out more at http://energyliteracyprinciples.org/

The NARA Energy Literacy Principles Matrix resource serves three primary functions. (1) It lays out the fundamental concepts (or building blocks) of energy literacy in an organized, logical way. (2) It organizes, classifies, describes, and cross-references resources to both the fundamental concepts AND to state science standards. (3) It makes it easy for teachers to find what they are looking for and both contribute to the Matrix and evaluate resources found there. Key terms for using the NARA Energy Literacy Principles Matrix include Topic, Subtopic, Resource, and Cross Reference. Interface within the website includes Basic Search, Advanced Search and Browse.

Topic: A modified list of key climate concepts, based on Department of Energy materials
http://www1.eere.energy.gov/education/energy_literacy.html
Example- *"Biological processes depend on energy flow through the Earth system"*

Subtopic: ‘Building blocks’ that break the Topic into smaller, essential concepts.
Example- *“The sun is the major source of energy for organisms and ecosystems of which they are a part.”*

Resource: A document, data set, or media element that has been linked to Topics and Subtopics to help teach climate concepts.
Example- *The Value of a Tree* lesson was developed by the NARA Education Team and is found here:
http://adventurelearningat.com/wpcontent/uploads/2012/08/ValueofaTree_5EHS.pdf

Cross reference: If you download a resource, you can later go back and search in the Matrix for other concepts that the resource addressed. Alternately, you can see how the concepts relate across topics and subtopics.

Basic Search: This function allows you search the Matrix using a word or key term. It will only pull up results that are from words in the Topics, Subtopics, and Resource descriptions

Advanced Search: This function allows you to search the Matrix by words or terms too, but adds the use of drop-down boxes of Topics and Subtopics to better refine the results. You can also search by Resource Type.

Browser: This function allows you to see the organization of the Matrix, and browse Subtopics by scrolling over them. This interface most resembles the ‘matrix’ concept that we used to organize the project.

Education at the Speed of Research

Fundamentally, integrated approaches to energy literacy must be developed to effectively cross disciplines, include all stakeholders and situate energy literacy into the consciousness of learners of all ages. Meaningful approaches to this challenge address education at all levels- students, teachers, and public. These efforts found in the NARA GreenSTEM project communicate the exciting research in biofuels, while enriching the greater public understanding of energy literacy. Addressing many entry points into the education system while supporting an online collection of materials supports learners and provides the infrastructure for education at the speed of research.

SunGrant
INITIATIVE

www.sungrant.org